

***Preparation and biological evaluation
of new triterpene derivatives of ursolic
and oleanolic acids***

Dissertation presented to the Faculty of Pharmacy, University of Coimbra, to obtain the
degree of Doctor of Philosophy in Pharmacy in the speciality of Pharmaceutical
Chemistry.



**Faculdade de Farmácia
Universidade de Coimbra
2012**

Ana Sofia Mendes Leal

*Preparation and biological evaluation of new
triterpene derivatives of ursolic and oleanolic acids*

Work developed under the scientific supervision of:

Professor Doctor Jorge António Ribeiro Salvador

Laboratory of Pharmaceutical Chemistry, Faculty of Pharmacy

University of Coimbra

With the collaboration of:

Doctor Yongkui Jing

Division of Hematology/Oncology, The Tisch Cancer Institute,

Mount Sinai School of Medicine, New York, USA

This thesis was supported by

Fundação para a Ciência e a Tecnologia

Under the programme POCI 2010

SFRH / BD / 41566 / 2007



GOVERNO DA REPÚBLICA
PORTUGUESA



UNIÃO EUROPEIA
Fundo Social Europeu

Aos meus pais e irmã

Aos meus avós

Aos restantes familiares e amigos

Agradecimentos/ Acknowledgements

Ao Professor Doutor Jorge António Ribeiro Salvador, expresso aqui o meu agradecimento pela confiança que depositou e continua a depositar em mim e que culminou com a apresentação desta dissertação. Presto ainda o meu reconhecimento pelo modo optimista, empenho e disponibilidade que demonstrou ao longo deste trabalho e que foram determinantes para a conclusão do mesmo. Por fim, agradeço as sugestões e a revisão do presente texto.

À Professora Doutora Maria Luísa Sá e Melo, à data do início do projeto Directora do Laboratório de Química Farmacêutica da Faculdade de Farmácia da Universidade de Coimbra, agradeço o acolhimento neste Laboratório e os ensinamentos de química farmacêutica transmitidos ao longo dos anos.

I would like to thank Doctor Yongkui Jing (Ph.D.) for welcoming me in his lab and providing all the conditions needed for the work I developed at the Division of Hematology/Oncology, The Tisch Cancer Institute, Mount Sinai School of Medicine, New York, USA, and also for his supervision, continuous support and enthusiasm with this work. His intrinsic know-how and clear vision of cancer biology and medicinal chemistry provided me a much broader experience.

Ao Professor Doutor António José Paixão e à Doutora Ana Matos Beja Alte de Veiga, do CEMDRX, Departamento de Física da Faculdade de Ciências e Tecnologia da Universidade de Coimbra, agradeço a disponibilidade e apoio prestados no trabalho de difracção de raios-X deste projecto.

A todos os docentes e funcionários do Laboratório de Química Farmacêutica da Faculdade de Farmácia da Universidade de Coimbra, o meu agradecimento pela convivência, e pelos ensinamentos científicos e de vida.

Agradeço também à Fátima Nunes e ao Pedro Cruz pela amizade e paciente trabalho técnico desenvolvido de elucidação estrutural das minhas inúmeras amostras, no IPN e L-RMN, respectivamente.

Aos colegas de laboratório, que foram uma peça essencial para a realização deste trabalho, pela disponibilidade que sempre demonstraram em ajudar e pelo apoio prestado mesmo nas situações mais caricatas. Agradeço, também a amizade, o interesse e preocupação pelo trabalho desenvolvido, assim como a importante troca de ideias.

I thank Rui, Hao and Lixuan in Doctor Jing's lab for their assistance and friendship. I also thank all the floor colleagues and friends who worked on the same floor for their support. With them I felt true friendship and personal concern, which was the main reason for my pleasant stay in New York.

Aos Funcionários da biblioteca da Faculdade de Farmácia da Universidade de Coimbra, agradeço também todo o apoio e disponibilidade.

À Fundação para a Ciência e a Tecnologia, agradeço o apoio financeiro sob a forma de uma bolsa de doutoramento (SFRH / BD / 41566 / 2007).

Aos meus pais e à minha irmã, agradeço o apoio incondicional e a paciência infinita durante o desenvolvimento deste trabalho, pois sem eles não teria chegado a bom porto. Agradeço lhes também a compreensão pelas minhas longas ausências, e pelos valores e educação que me inculcaram.

Aos meus avós, já falecidos, agradeço o carinho com que sempre me trataram e a preocupação que sempre nutriram pelo meu percurso académico, que em muito contribuíram para que chegasse até aqui. À minha avó Conceição agradeço a preocupação e o olhar sempre atento durante esta fase atribulada.

À minha madrinha Maria e aos meus primos Nuno, Sónia e Saul agradeço a amabilidade com que receberam em Nova Iorque na sua casa, e o apoio e carinho incondicional com que me presentearam durante a minha estadia nos Estados Unidos.

À minha restante família agradeço o apoio incondicional nas escolhas que foi fazendo ao longo da minha vida, e que sem dúvida fizeram de mim uma melhor cientista e pessoa.

Aos amigos pelos momentos de partilha e por compreenderem as minhas incontáveis ausências.

I thank all the friends that I left behind in the USA for their friendship, happy moments lived and support.

A todos os que de alguma forma contribuíram para a execução deste trabalho o meu muito obrigado.

Contents

| | |
|--|--------------|
| <i>Resumo</i> | <i>I</i> |
| <i>Abstract</i> | <i>III</i> |
| <i>List of abbreviations</i> | <i>V</i> |
| <i>List of tables</i> | <i>IX</i> |
| <i>List of figures</i> | <i>XV</i> |
| <i>List of schemes</i> | <i>XXIII</i> |
| <i>Thesis organization</i> | <i>XXV</i> |
| | |
| 1. Introduction | 1 |
| 1.1. Cancer | 3 |
| 1.1.1. Biology of cancer..... | 4 |
| 1.1.1.1. Targeting the cell cycle in cancer treatment | 6 |
| 1.1.1.2. Targeting apoptosis in cancer treatment | 8 |
| 1.2. Natural products in medicinal chemistry | 10 |
| 1.2.1. Natural products and treatment of cancer..... | 13 |
| 1.3. Terpenoids | 19 |
| 1.3.1. General dispositions | 19 |
| 1.3.2. Biosynthetic diversity of triterpenoids | 20 |
| 1.3.3. Ursolic acid..... | 21 |
| 1.3.3.1. General activities | 23 |
| 1.3.3.2. Antitumor activity..... | 29 |
| 1.3.3.3. Semisynthetic derivatives with antitumor activity | 44 |
| 1.3.4. Oleanolic acid..... | 58 |
| 1.3.4.1. General activities | 59 |
| 1.3.4.2. Antitumor activity..... | 65 |
| 1.3.4.3. Semisynthetic derivatives with antitumor activity | 72 |
| 1.4. General objectives of this thesis | 85 |

2. Ursolic acid derivatives: synthetic routes, structural elucidation, biological evaluation and SAR studies 87

| | |
|---|------------|
| 2.1. Intermediates synthesis | 90 |
| 2.2. Heterocyclic derivatives | 95 |
| 2.2.1. Introduction..... | 95 |
| 2.2.2. Results and Discussion..... | 97 |
| 2.2.2.1. Chemistry..... | 97 |
| 2.2.2.1.1. Imidazole derivatives | 97 |
| 2.2.2.1.2. Methylimidazole derivatives..... | 110 |
| 2.2.2.1.3. Triazole derivatives | 121 |
| 2.2.2.2. Biological evaluation..... | 126 |
| 2.2.3. Conclusions..... | 132 |
| 2.3. Fluorolactones and fluorine derivatives | 133 |
| 2.3.1. Introduction..... | 133 |
| 2.3.2. Results and Discussion..... | 136 |
| 2.3.2.1. Chemistry..... | 136 |
| 2.3.2.1.1. Fluorolactones | 136 |
| 2.3.2.1.2. Acyl fluorides | 150 |
| 2.3.2.2. Biological evaluation..... | 152 |
| 2.3.3. Conclusions..... | 160 |
| 2.4. Experimental section..... | 161 |
| 2.4.1. Chemical | 161 |
| 2.4.2. Biological activity assays | 201 |

3. Oleanolic acid derivatives: synthetic routes, structural elucidation, biological evaluation and SAR studies 203

| | |
|--|------------|
| 3.1. Intermediates synthesis | 206 |
| 3.2. Heterocyclic and fluorine derivatives..... | 213 |
| 3.2.1. Introduction..... | 213 |
| 3.2.2. Results and Discussion..... | 214 |
| 3.2.2.1. Chemistry..... | 214 |
| 3.2.2.1.1. Imidazole derivatives | 214 |
| 3.2.2.1.2. Methylimidazole derivatives..... | 227 |

| | |
|---|------------|
| 3.2.2.1.3. Triazole derivatives..... | 237 |
| 3.2.2.1.4. Fluorine derivatives..... | 241 |
| 3.2.2.2. Biological evaluation | 246 |
| 3.2.3. Conclusions | 252 |
| 3.3. Experimental section..... | 253 |
| 3.3.1. Chemical | 253 |
| 3.3.2. Biological activity assays | 282 |
| | |
| 4. Concluding remarks | 283 |
| | |
| 5. References | 289 |

Resumo

O cancro é uma das causas de morte mais comuns. Nos Estados Unidos, uma em cada quatro mortes é devida ao cancro. A Organização Mundial de Saúde prevê que em 2030, 30 milhões de mortes serão devidas a cancro. Estes dados remetem para a urgência na pesquisa de novas moléculas capazes de melhorar o tratamento e prevenção da doença oncológica.

Os triterpenóides representam um grupo de compostos abundante e diversificado, que pode ser encontrado em plantas, frutas e vegetais. As plantas medicinais contendo triterpenóides tem constituído ao longo dos séculos uma base para a medicina tradicional no tratamento de diversas doenças. Triterpenóides como o ácido ursólico, o ácido oleanólico, a betulina, o ácido betulínico, o ácido maslínico e o ácido glicirretínico, foram isolados de extratos de plantas, demonstrando ter várias actividades biológicas, incluindo a anti-tumoral. O potencial interesse em derivados de triterpenóides extraídos de plantas com actividade anti-tumoral está bem patente no crescente número de publicações nesse domínio científico. Uma análise das publicações enquadrando os triterpenóides com actividade anti-tumoral revelou um aumento exponencial no número de artigos e patentes na referida área científica. Estes factos têm impulsionado a comunidade científica para a síntese de novos derivados triterpénicos com melhorada actividade anti-tumoral.

Com o objectivo de melhorar a actividade anti-tumoral dos ácidos ursólico e oleanólico, novos derivados semissintéticos heterocíclicos (compostos **2.18-2.58** e **3.15-3.50**) e fluorados (compostos **2.59-2.82** e **3.51-3.58**) foram sintetizados e caracterizados através de técnicas de espectrometria de massa, espectroscopia de infravermelhos e ressonância magnética nuclear, e por fim avaliados através do uso de MTT para a inibição do crescimento de linhas celulares tumorais e para os mecanismos de acção relevantes para a actividade anti-tumoral. A actividade antiproliferativa dos compostos estudados na linha tumoral do pâncreas AsPC-1 foi usada para estabelecer a relação estrutura-actividade entre os compostos.

Todos os 61 novos compostos derivados do ácido ursólico, compostos **2.18-2.82**, demonstraram uma boa actividade antiproliferativa nas células tumorais pancreáticas AsPC-1, vários dos novos compostos apresentaram melhor actividade antiproliferativa do que o ácido ursólico **2.1**, e alguns apresentaram mesmo um IC₅₀ inferior a 1 µM. Os compostos com resultados mais promissores foram também avaliados para a sua actividade antiproliferativa em linhas celulares tumorais de mama, fígado, pulmão, e próstata. O derivado heterocíclico **2.57** revelou ser o mais activo neste grupo, tendo sido usado para avaliar o mecanismo de acção responsável pelos efeitos antiproliferativos nas células AsPC-1: este composto, induz o aumento dos níveis de p53 o que leva ao aumento dos níveis de NOXA e p21^{waf1}, conduzindo à activação das caspases 9 e 3 induzindo a apoptose nas células AsPC-1 tratadas. O composto fluorado **2.72** revelou ser o mais activo a inibir de forma efectiva o crescimento da linha celular tumoral pancreática através da inibição do ciclo celular na fase G1 a 1 µM e aumento dos níveis de p21^{waf1} e indução da apoptose a 8 µM, com aumento dos níveis de NOXA e diminuição dos níveis de c-FLIP.

Os 42 novos derivados do ácido oleanólico **3.15-3.17** e **3.19-3.58** e o composto **3.18**, já descrito, apresentaram uma actividade antiproliferativa superior ao ácido oleanólico **3.1** nas células AsPC-1. Os compostos **3.27**, **3.39** e **3.49**, que apresentaram os valores de IC₅₀ mais baixos nas células tumorais AsPC-1, viram a sua actividade antiproliferativa estudada em linhas celulares tumorais de mama, próstata, fígado e pulmão. Os estudos revelaram que os compostos têm boa actividade antiproliferativa, com IC₅₀ mais baixos que 5 µM. Os compostos **3.27** e **3.39** induziram apoptose nas células AsPC-1, quando estas foram tratadas durante 24 h a uma concentração de 1.5 µM.

Os novos compostos sintetizados derivados dos ácidos ursólico e oleanólico e avaliados na sua actividade antiproliferativa representam um novo grupo de moléculas com potencialidade para o tratamento de tumores sólidos malignos.

Abstract

Cancer is one of the most common causes of death. In the United States alone, one in four deaths is the consequence of cancer. The World Health Organization (WHO) estimates that 30 million deaths will be related to cancer in the year 2030. These data demonstrate that research aimed at the identification of new molecules that can improve the treatment and prevention of cancer is urgent.

Triterpenoids are a large and diverse group of compounds that can be found in medicinal plants, fruits and vegetables. Medicinal plants containing triterpenoids have been used for centuries in traditional medicine for the treatment of various diseases. Triterpenoids, such as ursolic acid, oleanolic acid, betulin, betulinic acid, maslinic acid, and glycyrrhetic acid purified from plant extracts, have diverse biological activities, including antitumor activity. The potential interest of plant-derived triterpenoids as antineoplastic agents is reflected in the large number of scientific papers appearing in the field. Analysis of the publications concerning antineoplastic triterpenoids abstracted in available the online databases over the past few years revealed an exponential increase in the number of papers and patents in this area of research. These facts prompted the scientific community to pursue the synthesis of new, improved derivatives of the triterpenoids available.

With the aim of improving the antitumor activity of ursolic and oleanolic acids, a series of new heterocyclic (compounds **2.18-2.58** and **3.15-3.50**) and fluorine (compounds **2.59-2.82** and **3.51-3.58**) derivatives were synthesized, fully characterized using MS, IR and NMR techniques and evaluated for their antiproliferative activity via an MTT assay, as well as for their mechanisms of antitumor action. The antiproliferative activity against the AsPC-1 pancreatic cancer cell line was used to establish the structure activity relationship (SAR) between compounds.

The new 61 ursolic acid derivatives **2.18-2.82** showed a good antiproliferative activity against AsPC-1 cells, several of the newly synthesized compounds were more

active than that of ursolic acid **2.1** and some presented IC_{50s} lower than 1 μ M. The most promising compounds were evaluated further for their antiproliferative activity in breast, hepatic, lung and prostate cancer cell lines. The best heterocyclic derivative, compound **2.57**, was evaluated for its mechanisms of action in AsPC-1 cells: it induced the upregulation of p53, leading to the upregulation of NOXA and p21^{waf1}, these events culminated with the upregulation of caspases 9 and 3, thus inducing apoptosis in AsPC-1 cells. The fluorine derivative **2.72** exhibited the most effective inhibitory activity against pancreatic cancer cell growth, as it arrested the cell cycle at the G1 phase at 1 μ M and upregulated p21^{waf1} and induced apoptosis at 8 μ M, with the upregulation of NOXA and the downregulation of c-FLIP.

The new 42 oleanane derivatives **3.15-3.17** and **3.19-3.58** and the already described derivative **3.18** had better antiproliferative profile than oleanolic acid **3.1** against AsPC-1 cancer cells. Compounds **3.27**, **3.39** and **3.49**, which had the lowest IC_{50s} in AsPC-1 cancer cells, were studied further for their antiproliferative activity in breast, prostate, liver and lung cancer cell lines. It was found that these compounds also had an excellent antiproliferative activity, with IC_{50s} lower than 5 μ M. Compounds **3.27** and **3.39** induced apoptosis in AsPC-1 cells treated for 24 h at a concentration of 1.5 μ M.

The novel ursane- and oleanane-type triterpenoids synthesized and evaluated for their antiproliferative activity represent a new group of valuable molecules for the treatment of solid cancers.

List of abbreviations

| | |
|---------------|--|
| ACF | aberrant crypt foci |
| AChE | acetylcholinesterase |
| AD | Alzheimer disease |
| AI | androgen-insensitive |
| AIF | apoptosis inducing factor |
| ALT | alanine aminotransferase |
| AP | alkaline phosphatase |
| Apaf-1 | apoptotic protease-activating factor-1 |
| AR | aldose reductase |
| AST | aspartase aminotransferase |
| ATP | adenosine triphosphate |
| Bcl-2 | B-cell lymphoma gene-2 |
| bFGF | basic fibroblast growth factor |
| BH | Bcl-2-homologous domain |
| BSA | bovin serum albumin |
| CAM | cell adhesion molecule |
| cAMP | cyclic adenosine monophosphate |
| CARD | caspase recruitment domain |
| CBMI | 1,1'-carbonylbis(2'methylimidazole) |
| CDI | 1,1'-carbonyldiimidazole |
| CDK | cyclin dependent kinase |
| CdkI | CDK inhibitor |
| CDT | 1,1'-carbonyl-di(1,2,4-triazole) |
| ChAT | coline acetyltransferase |
| CNS | central nervous system |
| compd | compound |
| COSY | 2D homonuclear correlation spectroscopy |
| COX | cyclooxygenase |
| CRP | C-reactive protein |
| d | doublet |
| DAST | diethylaminosulfur trifluoride |
| dd | doublet of doublets |
| DDQ | 2,3-dichloro-5,6-dicyanobenzoquinone |
| DED | death effector domain |
| DEN | diethylnitrosamine |
| DEPT | distortioneless enhancement by polarization transfer |
| DISC | death-inducing signal complex |
| DMAP | 4-(dimethylamino)-pyridine |
| DMAPP | dimethylallyl diphosphate |
| DMBA | dimethylbenz[α]anthracene |

| | |
|------------------------|---|
| DMF | dimethylformamide |
| DMSO | dimethylsulfoxide |
| DNA | deoxyribonucleic acid |
| DR | death receptor |
| E2F | transcription factor activating adenovirus E2 gene |
| EC | effective concentration at 50% |
| ECM | extracellular matrix |
| EGFR | epidermal growth factor receptor |
| EI-MS | electron impact mass spectrometry |
| ERK | extracellular signal regulated kinase |
| EtOAc | ethyl acetate |
| FACS | fluorescence activated cell sorter |
| FADD | Fas-associated death domain protein |
| FAS | fatty acid synthase |
| FasL | ligand of Fas death receptor |
| FBS | fetal bovine serum |
| FCC | flash column chromatography |
| FLICE | FADD-like interleukin-1 β -converting enzyme inhibitory protein |
| FLIP | FLICE-inhibitory protein |
| GPx | glutathione peroxidase |
| GSH | glutathione |
| HFD | high fat diet |
| HIF | hypoxia inducible transcription factor |
| HIV | human immunodeficiency virus |
| HMBC | 2D heteronuclear multiple bond correlation spectroscopy |
| HMGB1 | high mobility group box protein 1 |
| HMQC | 2D heteronuclear multiple quantum correlation spectroscopy |
| HPLC | high pressure liquid chromatography |
| HSC | hepatic stellate cell |
| HUVECs | human umbilical vein endothelial cells |
| IAP | inhibitor of apoptosis |
| IC₅₀ | concentration required to obtain 50% inhibition |
| ICAM | intercellular adhesion molecule |
| ID₅₀ | dose required to obtain 50% inhibition |
| IKB | inhibitor of NF- κ B |
| IKK | IKB kinase |
| IL | interleukin |
| IPP | isopentenylallyl diphosphate |
| IR | infra-red spectroscopy |
| IUPAC | International Union for Pure and Applied Chemistry |
| J | coupling constant |
| JNK | c-Jun N-terminal kinase |
| LOX-1 | low density lipoprotein receptor-1 |

| | |
|----------------------|--|
| m | multiplet |
| m/z | ion mass/charge ratio |
| M⁺ | molecular ion |
| MAP | mitogen activated protein |
| m-CPBA | <i>meta</i> -chloroperbenzoic acid |
| MDR | multi drug resistance |
| MEK | MAPK/Erk kinase |
| MIC | minimum inhibitory concentration |
| MIF | migration inhibitory factor |
| MKP | MAP kinase phosphatase |
| MMP | metalloproteinase |
| MMPP | magnesium bis(monoperoxyphthalate) hexahydrate |
| mp | melting point |
| mRNA | messenger ribonucleic acid |
| MS | mass spectrometry |
| MT | metallothionein |
| mTOR | mammalian target of rapamycin |
| MTT | 3-(4,5-dimethylthiazol-2-yl)-2,5-diphenyltetrazolium bromide |
| NaOMe | sodium methoxide |
| NFAT | nuclear factor of activated T cells |
| NFκB | nuclear factor κB |
| NMR | nuclear magnetic resonance spectroscopy |
| NO | nitric oxide |
| NOESY | nuclear overhauser effect |
| NOS | nitric oxide synthase |
| ODC | ornithine decarboxylase |
| ORTEP | oak ridge thermal ellipsoid plot program |
| p | phosphate |
| PARP | poly-(ADP-ribose)-polymerase |
| PCNA | proliferative cell nuclear antigen |
| Pgp | p-glycoprotein |
| PI3K | phosphatidylinositol 3-kinase |
| PKC | protein kinase C |
| PMSF | phenylmethylsulfonyl fluoride |
| PPAR-α | peroxisome proliferator activated receptor |
| PTEN | phosphatase and tesar homolog deleted on Chromosome 10 |
| r.t. | room temperature |
| Rb | retinoblastoma protein |
| ROS | reactive oxygen species |
| RT | reverse transcriptase |
| s | singlet |
| SAR | structure activity relationship |
| SDH | sorbitol dehydrogenase |
| SDS | sodium dodecyl sulfate |

| | |
|----------------------|--|
| Smac | second mitochondria-derived activator of caspase |
| SMC | smooth muscle cells |
| STAT | signal transducer and activator of transcription |
| t | triplet |
| <i>t</i>-Bu | tert-butyl |
| <i>t</i>-BuOH | tert-butyroxy |
| TGF | transforming growth factor |
| THF | tetrahydrofuran |
| TI | therapeutic index |
| TLC | thin layer chromatography |
| TNF | tumor necrosis factor |
| TPA | 12-O-tetradecanoylphorbol-13-acetate |
| TRAIL | TNF-related apoptosis-inducing ligand |
| TRP | tyrosinase related protein |
| uPA | urokinase type plasminogen activator |
| VCAM-1 | vascular cell adhesion molecule-1 |
| VEGF | vascular endothelial growth factor |
| VSMC | vascular smooth muscle cells |
| WHO | World Health Organization |
| XIAP | X-chromosome-linked inhibitor of apoptosis |
| δ | chemical shift (NMR) |

List of tables

| | |
|--|----|
| Table 1.2.1. Some examples of natural products and natural product derivatives currently in clinical use. | 12 |
| Table 1.3.1. Some sources of ursolic acid in Nature. | 22 |
| Table 1.3.2. Minimum inhibitory concentration (MIC) of ursolic acid for several bacterial species. | 23 |
| Table 1.3.3. <i>In vitro</i> determination of the IC ₅₀ (μM) of ursolic acid for several strains of leishmania. | 24 |
| Table 1.3.4. IC ₅₀ (μM) for ursolic acid in oral, stomach and esophageal cancer cell lines. | 29 |
| Table 1.3.5. IC ₅₀ (μM) for ursolic acid in colorectal cancer cell lines. | 31 |
| Table 1.3.6. IC ₅₀ (μM) for ursolic acid in several hepatic cancer cell lines. | 33 |
| Table 1.3.7. IC ₅₀ (μM) for ursolic acid in uterine cervix, ovary and breast carcinoma cell lines. | 35 |
| Table 1.3.8. IC ₅₀ (μM) for ursolic acid in prostate carcinoma cell lines. | 37 |
| Table 1.3.9. IC ₅₀ (μM) for ursolic acid in lung and skin cancer cell lines. | 39 |
| Table 1.3.10. IC ₅₀ (μM) for ursolic acid in leukemia and lymphoma cancer cell lines. .. | 41 |
| Table 1.3.11. IC ₅₀ (μM) for ursolic acid in several cancer cell lines. | 42 |
| Table 1.3.12. Cytotoxic effects of ursolic acid in nontumoral cell lines, represented as IC ₅₀ (μM). | 44 |
| Table 1.3.13. IC ₅₀ (μM) of ursolic acid derivatives for the inhibition of the production of NO in mouse macrophages. | 45 |
| Table 1.3.14. IC ₅₀ (μM) of the ursolic acid derivatives 1.16-1.21 and 5-fluorouracil in Hep G2 cancer cells. | 47 |

| | |
|---|----|
| Table 1.3.15. IC ₅₀ (μM) for compounds 1.27-1.33 in ovary SKOV3 and stomach BGC-823 cancer cell lines. | 49 |
| Table 1.3.16. IC ₅₀ (μM) for compounds 1.6, 1.34 and 1.35 in bladder and pancreatic cancer cell lines. | 49 |
| Table 1.3.17. IC ₅₀ (μM) for compounds 1.36-1.55 in colon (HT-29), liver (Hep G2), stomach (BGC-823), bladder (NTUB1), neuroblastoma (SH-SY5Y) and cervix (HeLa) cancer cell lines, and in two nontumorigenic cell lines (HELFL and GES-1). | 51 |
| Table 1.3.18. IC ₅₀ (μM) for compounds 1.56-1.77 in ovary (SKOV3), liver (Hep G2), stomach (BGC-823), neuroblastoma (SH-SY5Y) and cervix (HeLa) cancer cell lines, and in a nontumorigenic cell line (HELFL). | 54 |
| Table 1.3.19. IC ₅₀ (μM) for compounds 1.78-1.83 in bladder (NTUB1) and colorectal (HT-29) tumor cancer cells. | 55 |
| Table 1.3.20. Values of MIC (μg/mL) for oleanolic acid against several strains of bacteria. | 60 |
| Table 1.3.21. Protective effects of oleanolic acid in five models of gastric ulceration in the mouse. | 61 |
| Table 1.3.22. IC ₅₀ (μM) for oleanolic acid in oral, esophageal, liver and colorectal carcinomas cell lines. | 67 |
| Table 1.3.23. IC ₅₀ (μM) for oleanolic acid in ovary and breast carcinoma cell lines. | 68 |
| Table 1.3.24. IC ₅₀ (μM) for oleanolic acid in osteosarcoma, lung and skin cancer cell lines. | 69 |
| Table 1.3.25. IC ₅₀ (μM) for oleanolic acid in leukemia, lymphoma and neuroblastoma cancer cell lines. | 70 |
| Table 1.3.26. IC ₅₀ (μM) of oleanolic acid derivatives for the inhibition of the production of NO in mouse macrophages. | 72 |
| Table 1.3.27. IC ₅₀ (μM) of oleanolic acid derivatives for the inhibition of the production of NO in mouse macrophages. | 74 |

| | |
|---|-----|
| Table 1.3.28. IC _{50s} (μM) for compound 1.100 in several cell lines..... | 76 |
| Table 1.3.29. Cell viability of B16 cells treated with compounds 1.173-1.186 relative to the control (100% of cell viability)..... | 80 |
| Table 2.2.1. NMR data for compound 2.21 | 103 |
| Table 2.2.2. Selected ¹ H and ¹³ C NMR data from the backbone of compounds 2.20, 2.25 and 2.26 | 108 |
| Table 2.2.3. Selected ¹ H and ¹³ C NMR data from the backbone of compounds 2.43-2.45 | 120 |
| Table 2.2.4. Selected ¹ H and ¹³ C NMR data from the backbone of compounds 2.46 and 2.54 | 124 |
| Table 2.2.5. The IC ₅₀ (μM) of ursolic acid intermediates in the inhibition of AsPC-1 cell growth..... | 126 |
| Table 2.2.6. The IC ₅₀ (μM) of ursolic acid heterocyclic derivatives in the inhibition of AsPC-1 cell growth..... | 127 |
| Table 2.2.7. The IC ₅₀ (μM) of ursolic acid heterocyclic derivatives in the inhibition of the growth of pancreatic (PANC-1 and MIA PaCa 2), breast (MCF-7), prostate (PC-3), hepatic (Hep G2) and lung (A549) cancer cell lines. | 129 |
| Table 2.3.1. Selected ¹ H and ¹³ C NMR data from the backbone of compounds 2.63 and 2.73 | 147 |
| Table 2.3.2. Selected ¹ H and ¹³ C NMR data from the backbone of compounds 2.75 and 2.79 | 149 |
| Table 2.3.3. The IC ₅₀ (μM) of ursolic acid intermediates in the inhibition of AsPC-1 cell growth..... | 152 |
| Table 2.3.4. The IC ₅₀ (μM) of ursolic acid fluorolactone derivatives in the inhibition of AsPC-1 cell growth..... | 153 |
| Table 2.3.5. The IC ₅₀ (μM) of ursolic acid fluorolactones in the inhibition of the growth of three pancreatic cancer cell lines. | 154 |

| | |
|---|-----|
| Table 2.3.6. The IC ₅₀ (μM) of ursolic acid fluorolactones in the inhibition of the growth of breast (MCF-7), prostate (PC-3), hepatic (Hep G2) and lung (A549) cancer cell lines.. | 156 |
| Table 3.2.1. Selected ¹ H and ¹³ C NMR data from the backbone of compounds 3.15 and 3.18 | 217 |
| Table 3.2.2. Selected ¹ H and ¹³ C NMR data of the backbone for compounds 3.21 and 3.22 | 222 |
| Table 3.2.3. Selected ¹ H and ¹³ C NMR data from the backbone of compounds 3.27-3.29 | 226 |
| Table 3.2.4. Selected ¹ H and ¹³ C NMR data from the backbone of compounds 3.30 and 3.34 | 230 |
| Table 3.2.5. Selected ¹ H and ¹³ C NMR data of the backbone of compound 3.37 | 232 |
| Table 3.2.6. Selected ¹ H and ¹³ C NMR data from the backbone of compounds 3.40 and 3.41 | 236 |
| Table 3.2.7. Selected ¹ H and ¹³ C NMR data from the backbone of compounds 3.42 and 3.43 | 238 |
| Table 3.2.8. Selected ¹ H and ¹³ C NMR data from the backbone of compounds 3.45 and 3.48 | 240 |
| Table 3.2.9. Selected ¹ H and ¹³ C NMR data of the backbone of compounds 3.51 and 3.52 | 245 |
| Table 3.2.10. The IC ₅₀ (μM) of oleanolic acid heterocyclic derivatives to inhibit AsPC-1 cell growth..... | 247 |
| Table 3.2.11. The IC ₅₀ (μM) of oleanolic acid fluorine derivatives to inhibit AsPC-1 cell growth. | 249 |
| Table 3.2.12. The IC ₅₀ (μM) of oleanolic acid heterocyclic derivatives to inhibit growth of pancreatic (PANC-1 and MIA PaCa 2), breast (MCF-7), prostate (PC-3), hepatic (Hep G2) and lung (A549) cancer cell lines..... | 251 |

Table 3.2.13. Results of FACS analyses for AsPC-1 cells treated with compounds **3.27**, **3.39** and **3.49** for 24 h at the indicated concentrations. The results represent the percentage of the number of cells in the indicated phase of the cell cycle, mean \pm SD of three independent experiments. 252

List of figures

| | |
|---|----|
| Figure 1.1.1. Estimated new cases of the three major cancers in women and men in Europe in 2006. | 3 |
| Figure 1.1.2. Estimated cancer-related death incidence for women and men in Europe in 2007. | 4 |
| Figure 1.1.3. Cancer hallmarks. Adapted from the literature. ⁶ | 5 |
| Figure 1.1.4. Cell cycle progression and regulation..... | 7 |
| Figure 1.1.5. Simplified apoptotic pathways in mammalian cells. | 9 |
| Figure 1.2.1. Sources of small molecules in clinical use for 1981-2006. S) Totally synthetic molecule; ND) natural product derived molecule; N) natural product; S*) from total synthesis, but the pharmacophore is from a natural product. Adapted from the literature. ³⁷ | 11 |
| Figure 1.2.2. Representation of some vinca alkaloids..... | 14 |
| Figure 1.2.3. Representation of podophyllotoxin and some derivatives..... | 15 |
| Figure 1.2.4. Representation of naturally occurring paclitaxel and its semisynthetic derivatives..... | 16 |
| Figure 1.2.5. Representation of quinine alkaloids..... | 17 |
| Figure 1.2.6. Representation of the porphyrins currently used in clinical setting as chemosensitizers. | 17 |
| Figure 1.2.7. Chemopreventive drugs currently in clinical use..... | 18 |
| Figure 1.2.8. Natural products with chemopreventive activity in clinical studies. | 18 |
| Figure 1.3.1. Simplified scheme of the origin of the diverse biosynthetic plant terpene classes. | 19 |
| Figure 1.3.2. Simplified scheme of the origin of some triterpenoids..... | 20 |

| | |
|--|----|
| Figure 1.3.3. Ursolic acid and naturally occurring analogues..... | 21 |
| Figure 1.3.4. Schematic representation of compounds 1.8-1.15 | 46 |
| Figure 1.3.5. Schematic representation of compounds 1.22-1.26 | 48 |
| Figure 1.3.6. Schematic representation of compounds 1.27-1.33 | 48 |
| Figure 1.3.7. Schematic representation of esters 1.36-1.55 of ursolic acid..... | 50 |
| Figure 1.3.8. Schematic representation of ursolic acid amide derivatives 1.56-1.71 | 52 |
| Figure 1.3.9. Schematic representation of ursolic acid amide derivatives 1.72 and 1.73 which have an α,β unsaturated ketone in ring C. | 53 |
| Figure 1.3.10. Schematic representation of ursolic acid amide derivatives 1.74-1.77 | 53 |
| Figure 1.3.11. Schematic representation of anhydride derivatives of ursolic acid..... | 55 |
| Figure 1.3.12. Schematic representation of ursolic acid derivatives with an open ring A..... | 56 |
| Figure 1.3.13. Schematic representation of compounds 1.92-1.96 | 57 |
| Figure 1.3.14. Schematic representation of compound 1.97 and oxaliplatin 1.98 | 58 |
| Figure 1.3.15. Oleanolic acid and some of its natural analogues. | 58 |
| Figure 1.3.16. Schematic representation of compounds 1.137-1.154 | 77 |
| Figure 1.3.17. Schematic representation of compounds 1.155-1.163 | 78 |
| Figure 1.3.18. Schematic representation of compound 1.164 | 79 |
| Figure 1.3.19. Schematic representation of compounds 1.165-1.172 | 79 |
| Figure 1.3.20. Schematic representation of compounds 1.187-1.191 | 81 |
| Figure 1.3.21. Schematic representation of compounds 1.192-1.194 | 82 |
| Figure 1.3.22. Schematic representation of oleanolic acid derivatives 1.195-1.198 with an open ring A..... | 83 |

| | |
|---|-----|
| Figure 1.3.23. Schematic representation of oleanolic acid derivatives 1.199-1.205 with indole-fused ring | 84 |
| Figure 2.1.1. ¹ H NMR spectrum of compound 2.2 | 93 |
| Figure 2.1.2. ¹³ C NMR spectrum of compound 2.2 | 94 |
| Figure 2.2.1. Schematic representation of the reagents 1,1'-carbonyldiimidazole (CDI), 1,1'-carbonyl-di(1,2,4-triazole) (CDT) and 1,1'-carbonylbis(2'-methylimidazole) (CBMI). | 95 |
| Figure 2.2.2. Reaction mechanism of triterpenoids with CDI for the formation of carbamates..... | 96 |
| Figure 2.2.3. Reaction mechanism of CDI with triterpenoids for the formation of <i>N</i> -alkylimidazoles (A) and <i>N</i> -acylimidazoles (B)..... | 97 |
| Figure 2.2.4. IR spectrum of compound 2.19 | 99 |
| Figure 2.2.5. ¹ H NMR spectrum of compound 2.21 | 100 |
| Figure 2.2.6. ¹³ C NMR spectrum of compound 2.21 | 100 |
| Figure 2.2.7. HMQC spectrum of compound 2.21 | 101 |
| Figure 2.2.8. HMQC spectrum detail of compound 2.21 , with incidence in the imidazole ring signals..... | 101 |
| Figure 2.2.9. HMBC spectrum of compound 2.21 | 102 |
| Figure 2.2.10. ¹ H NMR spectrum of compound 2.24 | 105 |
| Figure 2.2.11. ¹³ C NMR spectrum of compound 2.24 | 105 |
| Figure 2.2.12. Detail of the HMBC spectrum of compound 2.24 . The correlations between proton H12 and carbons C9, C14 and C18 are highlighted. | 106 |
| Figure 2.2.13. Some HMBC correlations for compound 2.24 | 107 |
| Figure 2.2.14. IR spectrum of compound 2.34 | 110 |

| | |
|---|-----|
| Figure 2.2.15. IR spectrum of compound 2.38 | 112 |
| Figure 2.2.16. ¹ H NMR spectrum of compound 2.42 | 114 |
| Figure 2.2.17. ¹³ C NMR spectrum of compound 2.42 | 115 |
| Figure 2.2.18. HMQC spectrum of compound 2.42 , showing the correlations between protons and carbons of the methylimidazole ring (blue), C3 (red) and C12 (green). | 115 |
| Figure 2.2.19. Selected HMBC correlations for compound 2.42 | 116 |
| Figure 2.2.20. ¹ H NMR spectrum of compound 2.44 | 118 |
| Figure 2.2.21. ¹³ C NMR spectrum of compound 2.44 | 119 |
| Figure 2.2.22. HMBC spectrum of compound 2.44 | 119 |
| Figure 2.2.23. ¹ H NMR spectrum of compound 2.46 | 122 |
| Figure 2.2.24. ¹³ C NMR spectrum of compound 2.46 | 122 |
| Figure 2.2.25. Graphical representation of the SAR relationship between ursolic acid 2.1 and novel semisynthetic derivatives with modification at C2 of the ursane structure. Comparisons were based on the IC _{50s} of compounds against the AsPC-1 cell line. Compound 2.57 , which was the most active of these series, was 4-fold more active than the original intermediate 2.13 and 7-fold more active than ursolic acid 2.1 . Compound 2.43 was 4-fold more active than compound 2.12 and 6-fold more active than ursolic acid 2.1 . Compound 2.58 was 3-fold more active than compound 2.16 and ursolic acid 2.1 | 128 |
| Figure 2.2.26. Cell cycle arrest and apoptosis induction of compound 2.57 in AsPC-1 cells. (A) Cell cycle analysis of AsPC-1 cells treated with compound 2.57 . The results shown are means ± SE of three independent experiments. (B) Representative FACS analyses of cell cycle of AsPC-1 cells treated with compound 2.57 at the indicated concentrations for 24 h. The sub-G1 phase (apoptotic cells) of AsPC-1 cells was detected only in cells treated with compound 2.57 at 10 μM. The cell cycle was determined by FACS after staining with PI. | 130 |
| Figure 2.2.27. Compound 2.57 increased the levels of p21 ^{waf1} , NOXA and p53 protein in AsPC-1 cells. AsPC-1 cells were treated with compound 2.57 at the indicated | |

| | |
|---|-----|
| concentrations for 24 h. The relative levels of indicated proteins were determined by Western blot analysis. GAPDH was used as a loading control..... | 131 |
| Figure 2.3.1. Examples of nucleophilic (DAST and Deoxofluor) and electrophilic (Selectfluor and Accfluor) fluorine reagents. | 133 |
| Figure 2.3.2. Some examples of fluorinated drugs used in medical settings. | 134 |
| Figure 2.3.3. Anticancer fluorinated drugs. | 135 |
| Figure 2.3.4. IR spectrum of compound 2.59 | 141 |
| Figure 2.3.5. ¹ H NMR spectrum of compound 2.73 | 142 |
| Figure 2.3.6. ¹ H NMR spectrum of compound 2.72 | 142 |
| Figure 2.3.7. ¹³ C NMR of compound 2.73 | 143 |
| Figure 2.3.8. HMBC of compound 2.73 | 144 |
| Figure 2.3.9. NOESY spectrum of compound 2.73 | 145 |
| Figure 2.3.10. Detail of the NOESY spectrum of compound 2.73 . Correlation of proton H12 with the methyl group at C27 (green) and correlation of proton H12 with proton H9 (red)..... | 145 |
| Figure 2.3.11. ORTEP diagram of compound 2.66 (50% probability level, H atoms of arbitrary sizes)..... | 146 |
| Figure 2.3.12. Some HMBC (black) and NOESY (red) correlations for compound 2.79 .148 | |
| Figure 2.3.13. IR spectrum of compound 2.81 | 151 |
| Figure 2.3.14. ¹³ C NMR spectrum of compound 2.82 | 151 |
| Figure 2.3.15. Structure activity relationships (SAR) among several synthetic derivatives of ursolic acid 2.1 . The comparison was made based on their IC _{50s} in the inhibition of AsPC-1 cell growth. Compound 2.60 was 5-fold more potent than compound 2.4 , and compound 2.61 was 2-fold more potent than compound 2.5 | 155 |

Figure 2.3.16. Structure activity relationships (SAR) among several synthetic derivatives of ursolic acid **2.1**. The comparison was made based on their IC_{50s} in the inhibition of AsPC-1 cell growth. Compound **2.71** was 5- fold more potent than ursolic acid **2.1**. Compounds **2.72** and **2.73** were 19-fold more potent than ursolic acid **2.1**, 4-fold more potent than compound **2.71** and 26-fold more potent than compound **2.59**. Compounds **2.78** and **2.79** were 11-fold more potent than ursolic acid **2.1**, 2-fold more potent than compound **2.71**, and 17-fold more potent than compound **2.59**. Compound **2.66** was 11-fold more potent than ursolic acid **2.1** and 15-fold more potent than compound **2.59**. Compound **2.65** was 6-fold more potent than ursolic acid **2.1** and 8-fold more potent than compound **2.59**.
 157

Figure 2.3.17. Cell cycle arrest and apoptosis induction by compound **2.72** in AsPC-1 cells. (A) Cell-cycle analysis of AsPC-1 cells treated with compound **2.72**. (B) Representative FACS analyses of G1 phase arrest in AsPC-1 cells treated with compound **2.72** at 1 μM for 24 h. (C) Representative FACS analyses of induction of sub-G1 phase (apoptotic cells) in AsPC-1 cells treated with compound **2.72** at 8 μM for 24 h. (D) Relative levels of apoptosis- and cycle-related proteins in AsPC-1 cells treated with a variety of concentrations of compound **2.72** for 24 h. The cell cycle was determined by FACS after staining with PI. The relative protein levels were determined by Western blot analysis. GAPDH was used as a loading control. 158

Figure 2.3.18. Relative levels of apoptosis- and cycle-related proteins in (A) MIA PaCa 2 and (B) PANC-1 cells. Cells were treated with compound **2.72** at 8 μM for 24 h. Relative protein levels were assessed by Western blot analysis. GAPDH was used as a loading control. 160

Figure 3.1.1. ¹H NMR spectrum of compound **3.5**. 208

Figure 3.1.2. ORTEP diagram of compound **3.5** (50% probability level, H atoms of arbitrary sizes). The asymmetric unit also contains a molecule of acetonitrile..... 208

Figure 3.1.3. ¹³C NMR spectrum of compound **3.7**. 210

Figure 3.1.4. ORTEP diagram of compound **3.9** (50% probability level, H atoms of arbitrary sizes)..... 210

Figure 3.1.5. ¹H NMR spectrum of compound **3.13**. 212

| | |
|---|-----|
| Figure 3.2.1. IR spectrum of compound 3.15 | 214 |
| Figure 3.2.2. ^1H NMR spectrum of compound 3.15 | 216 |
| Figure 3.2.3. ^{13}C NMR spectrum of compound 3.15 | 216 |
| Figure 3.2.4. Selected HMBC correlations for compound 3.21 | 219 |
| Figure 3.2.5. ^1H NMR spectrum of compound 3.22 | 219 |
| Figure 3.2.6. ^{13}C NMR spectrum of compound 3.22 | 220 |
| Figure 3.2.7. HMQC spectrum of compound 3.22 , with the correlations between protons and carbons of imidazole ring (red) and at position C12 (green)..... | 220 |
| Figure 3.2.8. HMBC spectrum of compound 3.22 . Correlations between proton H12 and carbonyl carbon, carbon C13, and carbons C9 and C11, are highlighted in red, green and blue, respectively. | 221 |
| Figure 3.2.9. Selected HMBC correlations for compound 3.27 | 224 |
| Figure 3.2.10. IR spectrum of compound 3.29 | 225 |
| Figure 3.2.11. Selected HMBC correlations for compound 3.34 | 229 |
| Figure 3.2.12. ^1H NMR spectrum of compound 3.40 | 233 |
| Figure 3.2.13. ^{13}C NMR spectrum of compound 3.40 | 234 |
| Figure 3.2.14. HMQC spectrum of compound 3.40 , with the correlations between protons and carbons of methylimidazole ring (red), C2 (green), C12 (blue), methyl group at C28 (yellow) and methyl group at the methylimidazole ring (purple). | 234 |
| Figure 3.2.15. HMBC spectrum of compound 3.40 | 235 |
| Figure 3.2.16. ^1H NMR spectrum of compound 3.52 | 243 |
| Figure 3.2.17. ^{13}C NMR spectrum of compound 3.52 | 243 |
| Figure 3.2.18. Detail of the NOESY spectrum of compound 3.52 . The correlation between H12 and the methyl group at C26 is marked in red. | 244 |

Figure 3.2.19. Selected HMBC correlations for compound **3.52**..... 244

Figure 3.2.20. Structure activity relationships (SAR) among several synthetic derivatives of oleanolic acid **3.1**. The comparison was made based on their IC_{50} s in the inhibition of AsPC-1 cell growth, considering IC_{50} of oleanolic acid **3.1** as 100 μ M. Compound **3.30** is 31- fold more potent than oleanolic acid **3.1**. Compound **3.23** is 23-fold more potent than oleanolic acid **3.1**. Compound **3.21** is 29- fold more potent than oleanolic acid **3.1**. Compound **3.39** is 143-fold more potent than oleanolic acid **3.1**. 250

List of schemes

| | |
|---|-----|
| Scheme 2.1.1. Synthesis of derivatives 2.2-2.9 | 90 |
| Scheme 2.1.2. Synthesis of derivatives 2.10-2.13 | 91 |
| Scheme 2.1.3. Synthesis of derivatives 2.14 and 2.15 | 92 |
| Scheme 2.1.4. Synthesis of derivatives 2.16 and 2.17 | 93 |
| Scheme 2.2.1. Synthesis of derivatives 2.18-2.23 | 98 |
| Scheme 2.2.2. Synthesis of derivatives 2.24-2.28 | 104 |
| Scheme 2.2.3. Synthesis of derivatives 2.29-2.31 | 109 |
| Scheme 2.2.4. Synthesis of derivatives 2.32-2.37 | 111 |
| Scheme 2.2.5. Synthesis of derivatives 2.38-2.42 | 113 |
| Scheme 2.2.6. Synthesis of derivatives 2.43-2.45 | 117 |
| Scheme 2.2.7. Synthesis of derivatives 2.46-2.50 | 121 |
| Scheme 2.2.8. Synthesis of derivatives 2.51-2.55 | 123 |
| Scheme 2.2.9. Synthesis of derivatives 2.56-2.58 | 125 |
| Scheme 2.3.1. Synthesis of derivatives 2.59-2.62 | 137 |
| Scheme 2.3.2. Synthesis of derivative 2.63 | 137 |
| Scheme 2.3.3. Synthesis of derivatives 2.64-2.67 | 138 |
| Scheme 2.3.4. Synthesis of derivatives 2.72 and 2.73 | 139 |
| Scheme 2.3.5. Synthesis of derivatives 2.74-2.80 | 140 |
| Scheme 2.3.6. Synthesis of derivatives 2.81 and 2.82 | 150 |
| Scheme 3.1.1. Synthesis of derivatives 3.2-3.4 | 206 |

| | |
|--|-----|
| Scheme 3.1.2. Synthesis of derivatives 3.5 and 3.6 | 207 |
| Scheme 3.1.3. Synthesis of derivatives 3.7-3.10 | 209 |
| Scheme 3.1.4. Synthesis of derivatives 3.11-3.13 | 211 |
| Scheme 3.1.5. Synthesis of derivative 3.14 | 212 |
| Scheme 3.2.1. Synthesis of derivatives 3.15-3.19 | 215 |
| Scheme 3.2.2. Synthesis of derivatives 3.20-3.22 | 218 |
| Scheme 3.2.3. Synthesis of derivatives 3.23-3.26 | 223 |
| Scheme 3.2.4. Synthesis of derivatives 3.27 and 3.28 | 224 |
| Scheme 3.2.5. Synthesis of derivative 3.29 | 225 |
| Scheme 3.2.6. Synthesis of derivatives 3.30-3.33 | 227 |
| Scheme 3.2.7. Synthesis of derivative 3.34 | 228 |
| Scheme 3.2.8. Synthesis of derivatives 3.35-3.38 | 231 |
| Scheme 3.2.9. Synthesis of derivatives 3.39 and 3.40 | 233 |
| Scheme 3.2.10. Synthesis of derivative 3.41 | 235 |
| Scheme 3.2.11. Synthesis of derivatives 3.42-3.44 | 237 |
| Scheme 3.2.12. Synthesis of derivatives 3.45-3.48 | 239 |
| Scheme 3.2.13. Synthesis of derivative 3.49 | 241 |
| Scheme 3.2.14. Synthesis of derivative 3.50 | 241 |
| Scheme 3.2.15. Synthesis of derivatives 3.51-3.56 | 242 |
| Scheme 3.2.16. Synthesis of derivatives 3.57 and 3.58 | 246 |

Thesis organization

This dissertation is divided in five chapters. The first section comprehends a general introduction, the second and third sections relate all the experimental work developed, the results, the discussion and experimental procedures and the last two chapters are dedicated to the concluding remarks and the supporting references used in this work.

The first chapter of this thesis presents the state-of-the-art relative to medicinal chemistry and natural products, focusing on the therapeutic potential of natural products, particularly of ursolic and oleanolic acids. The chemotherapeutic properties of ursolic and oleanolic acids are described. This chapter also focuses on the reported derivatives of ursolic and oleanolic acids and their antitumor activities.

The second chapter is devoted to the synthesis and biological evaluation of ursolic acid intermediates, heterocyclic and fluorine derivatives. The synthesis of intermediates is described, as well as the experimental procedures used in that synthesis. The subsections dedicated to the heterocyclic and fluorine derivatives are composed of a general introduction describing the state-of-the-art related to the topic, chemical results and discussion with selected aspects of the structural elucidation of the new compounds, and biological results and discussion with establishment of the SAR findings and mechanisms of action, the subsections end with conclusions. The experimental procedures are described in the end of the chapter.

The third chapter of this work comprises the synthesis and evaluation of new oleanolic acid derivatives and has been divided in two major subsections: the synthesis of intermediates and the synthesis and evaluation of new oleanolic derivatives. The synthesis of new olenane-type compounds is described and some details regarding the structural elucidation and biological evaluation of the antiproliferative activity of compounds are provided. This chapter ends with conclusions and experimental procedures.

Chapter 4 states the major findings and conclusions of this work. The last chapter provides the supporting references used in this dissertation.

The nomenclature of natural products and related compounds followed the guidelines established by the IUPAC-IUB Joint Commission on Biochemical Nomenclature, as published by P. M. Giles Jr in *Pure & Applied Chemistry*, **1999**, 71, 587-643, and reviewed by H. A. Favre in *Pure & Applied Chemistry*, **2004**, 76, 1283-1292. However, some compounds have been designated using their trivial name. Reference indexation was made following the guidelines of the *American Chemical Society: Style Guide*. Several databases were used for bibliographic research; however, the ISI Web of Knowledge (Thompson Reuters) was preferred. SciFinder tools to search the CAS database were used to check the novelty of the compounds obtained in this work.

In Chapters 1-3, ursane- and oleanane-type substrates and products were numbered sequentially. Compound numbering includes the chapter number.

1.

Introduction

1.1. Cancer

Cancer is a complex group of diseases characterized by the unregulated growth and spread of abnormal cells. The abnormal cells result from a series of missteps in the genome that lead to anomalies in the control of cell fate. The genomic alterations can be due to external factors or internal failures that were not duly corrected. Malignant tumors result from the spread of abnormal cells to adjacent tissues. They can invade other tissues and form new colonies, called metastases.^{1,2}

In the year 2007, cancer was the second cause of death worldwide.³ In Europe, it is expected that, in 2015, 23% of the deaths will be due to cancer among the population older than 65 years.⁴

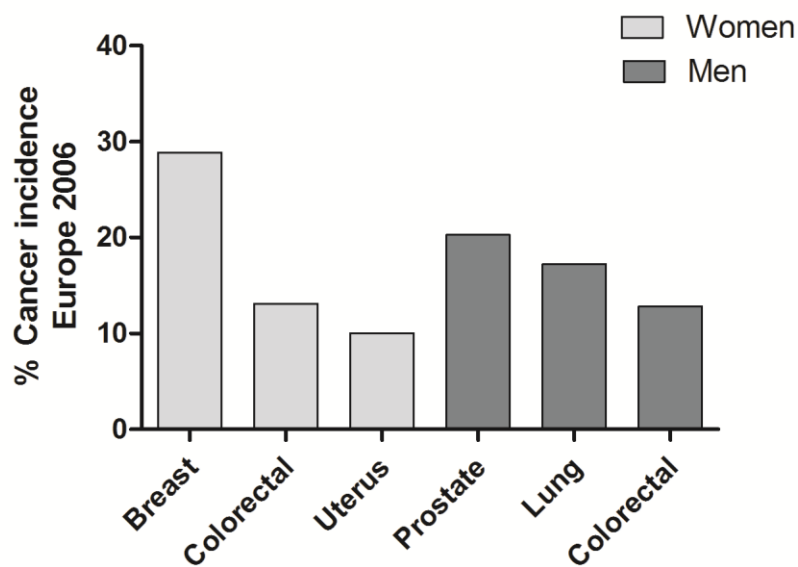


Figure 1.1.1. Estimated new cases of the three major cancers in women and men in Europe in 2006.

The incidence of cancer in women and men is different regarding the type of cancer. Breast and prostate cancers have greater incidence in women and men, respectively (Figures 1.1.1 and 1.1.2).^{3,4}

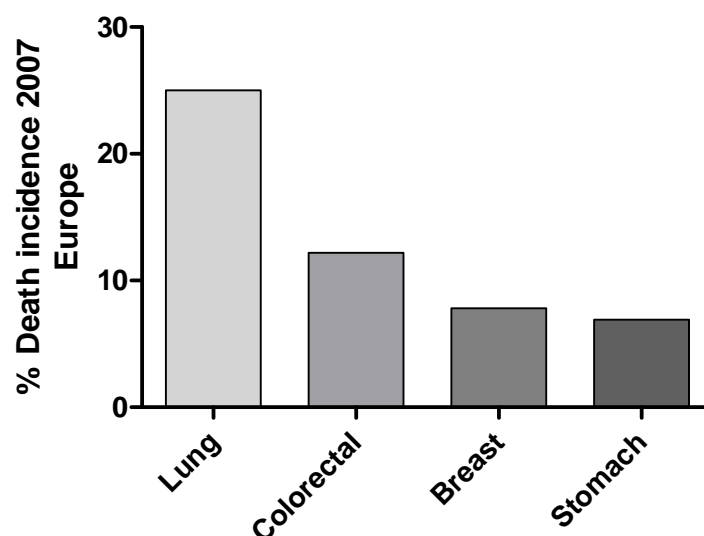


Figure 1.1.2. Estimated cancer-related death incidence for women and men in Europe in 2007.

Cancer-related death is changing with modifications in the social and economic behavior of the populations. In 2011, in the USA, deaths by cancer will most likely be primarily due to lung and bronchus cancer, in both men and women.⁵

1.1.1. Biology of cancer

Normal cells evolve to the neoplastic state progressively, in a multistep process, acquiring a series of successive hallmark capacities that allow them to become tumorigenic and, finally, malignant (Figure 1.1.3). Tumors are complex tissues composed of different cell types, with a very singular microenvironment.⁶⁻⁸

One of the first hallmarks acquired by cancer cells is the ability to auto-sustain a proliferative signaling output that allows proliferation for an undetermined amount of time without dependence on exogenous growth stimulation and avoiding the negative feedback mechanisms that attenuate proliferation and evade growth suppressors. Programmed cell death (apoptosis, autophagy or necrosis) is a mechanism via which organisms control the number of cells in a population. Cancer cells acquire the ability to resist cell death via several mechanisms. In addition to programmed cell death, cancer cells have the ability to avoid destruction by the immune system. Changes in telomeres,

telomerases, DNA polymerases and in the entire machinery that controls and regulates DNA replication, genetic instability and mutated DNA are also hallmarks of cancer cells.^{6, 8}

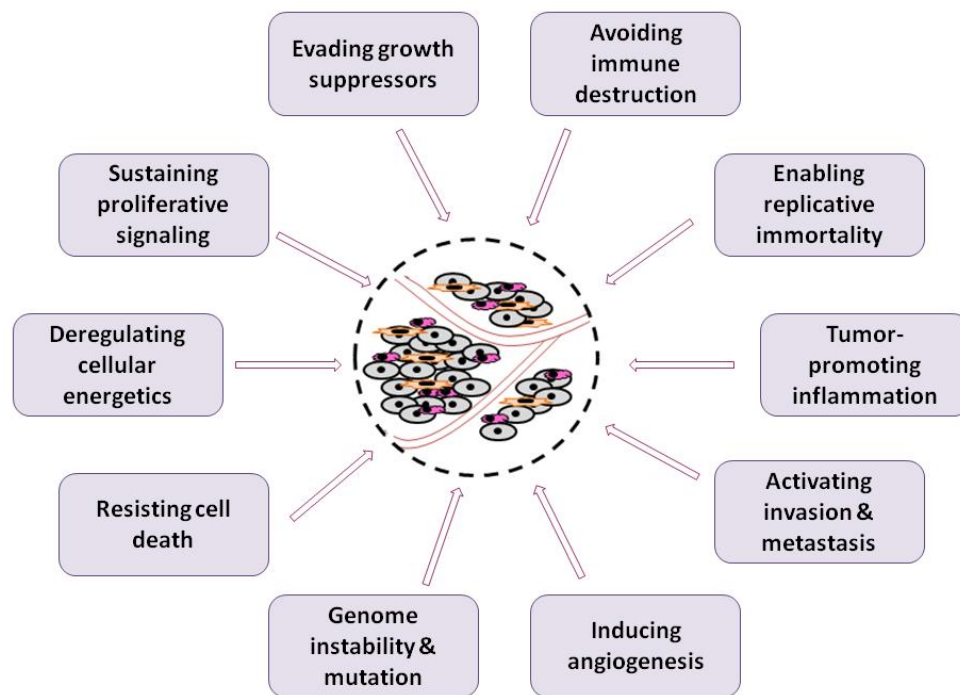


Figure 1.1.3. Cancer hallmarks. Adapted from the literature.⁶

After a certain stage, cancer cells start to require additional nutrients and oxygen, which the normal vascularization of the tissue does not provide. Cancer cells have the ability to induce angiogenesis, i.e., the creation of new blood vessels, producing a series of angiogenic and inflammatory factors, which enhance tumorigenesis. One of the last stages in tumor progression is the invasion of surrounding tissues and metastasis to other parts of the organism.^{6, 7, 9}

Cancer is a complex group of diseases and, with the evolution of knowledge in biology, biochemistry and genomics, more layers of complexity are expected. Treatment and chemoprevention are far from the ideal solution for this disease and additional,

improved drugs targeting known and recently discovered proteins and genes are still needed.

1.1.1.1. Targeting the cell cycle in cancer treatment

The cell cycle is an ubiquitous and complex process that is involved in the growth and proliferation of cells, organism development, in the regulation of DNA damage repair and in diseases such as cancer. The cell cycle involves numerous regulatory proteins that direct the cell through a specific sequence of events culminating in mitosis, with production of two daughter cells.¹⁰

The cell cycle is a sequence of four stages: the G1, S, G2 and M phases. The duplication of the genetic material of the cell occurs in the S phase and the physical separation of the cellular material for the two new cells and mitosis occur in the M phase. The G1 and G2 phases are gaps for the control and preparation of the subsequent phases.¹⁰ The progression of the cell cycle is closely regulated by cyclins and cyclin-dependent kinases (CDKs).¹¹ The binding of a CDK to the correspondent cyclin induces conformational changes, leading to the exposure of the active site on the CDK. CDKs are constitutively expressed in the cell; after adequate stimulation, such as DNA damage, CDK inhibitors (CdkIs; p16^{ink4a}, p15^{INK4B}, p18^{INK4C}, p19^{INK4D}, p21^{Cip1}, p27^{Kip1} and p57^{Kip2}) interact with CDKs and change their conformation, creating an inactive form (Figure 1.1.4).^{1, 2}

Cyclin D, the first cyclin to be expressed, allows entrance into the G1 phase of the cell cycle.¹² Synthesis of cyclin D is stimulated by integrins, nutrients, G coupled-proteins and tyrosine kinase receptors. Cell cycle progression is accompanied by the synthesis of cyclins E, A and B, in that order. After a complete cell cycle, cells can undergo a new cell cycle or enter the G0 phase, which is a quiescent state.

The restriction point (R point) represents a mark for the progression of the cell cycle from the G1 phase to the S phase and is controlled by the nuclear Rb protein. This protein regulates the activity of the E2F family of transcription factors, which is critical for the expression of the genes that are necessary for the entrance of cells into the S phase. CyclinD/CDK4/6 phosphorylates the Rb protein. This form is further phosphorylated by the cyclinE/CDK2 complex, producing an Rb-hyperphosphorylated form, which releases the E2F transcription factor (Figure 1.1.4).^{1, 2, 13}

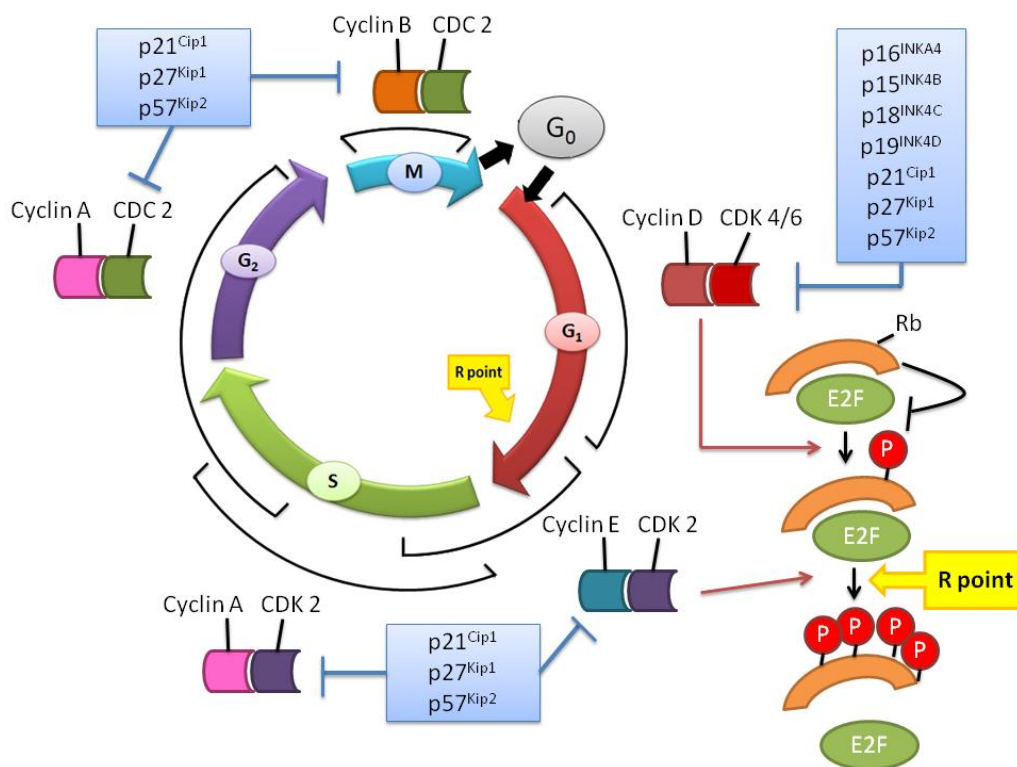


Figure 1.1.4. Cell cycle progression and regulation.

During cell cycle progression several checkpoints impose control and ensure that the cell cycle is properly completed. The checkpoints at the end of the G₁ and S phases do not allow cell cycle progression if the DNA is damaged. At the end of the G₂ phase, the cell cycle can be blocked if DNA replication is not completed. The M phase also has a control checkpoint: the cell cycle does not progress if the chromatids do not assemble in the correct form at the mitotic spindle.

In normal cells, DNA damage triggers a series of responses that culminate in cell cycle arrest or induction of cell death. Each type of DNA damage involves a different set of cellular machinery components, which are tightly regulated. Cancer cells are able to elude several cell cycle checkpoints and complete a cell division successfully.^{11, 12, 14}

Cancer cells often have mutated genes that encode cell cycle regulators, overexpress cyclins and CDKs or delete and inhibit the expression of CdkI.^{13, 15} Tumor cells have the ability to overcome the G₂ and M phase checkpoints, generating cells with more mutations than the parental cells, increasing tumorigenesis.¹³

Targeting components of the cell cycle is an option in the treatment of cancer.^{13, 14}

1.1.1.2. Targeting apoptosis in cancer treatment

Programmed cell death controls morphogenesis and cell population, eliminates damaged cells and maintains homeostasis.¹⁶ Programmed cell death can be achieved by apoptosis, autophagy or necrosis. Apoptosis is morphologically distinct from the other types of cell death, presenting cell shrinkage, cytoplasmic condensation, nuclear fragmentation, cytoplasmic membrane blebbing and formation of apoptotic bodies. In addition it is restrict to one cell without an inflammatory process.¹⁷⁻²²

Apoptosis can be initiated by two major pathways: the extrinsic pathway, which culminates in the activation of caspase 8, and the intrinsic pathway, with the activation of caspase 9 (Figure 1.1.5). Recently, other pathways for the activation of apoptosis were described: the granzyme B pathway, which is a caspase-independent pathway, and the endoplasmic reticulum stress-induced pathway.^{17, 22-24}

The extrinsic pathway of apoptosis is activated at the cell surface when a specific ligand binds to its corresponding death receptor (DR); this leads to the oligomerization of the receptor and promotes the recruitment of adapter proteins, such as the Fas associated death domain protein (FADD). The adapter proteins connect to several pro-caspase 8 molecules via the death effector domains (DED), forming the death-inducing signaling complex (DISC). Because of the high concentration of pro-caspase 8, the mutual activation of caspase 8 takes place, leading to the activation of downstream executioner caspases.^{16, 21, 23-26}

The intrinsic pathway of apoptosis is correlated to mitochondria. After an apoptotic stimulus, proapoptotic Bcl-2 members (Bax/Bak) alter the permeability of the mitochondrial membrane because of the interaction between BH3-only proteins, such as PUMA, NOXA and Bim, with anti-apoptotic proteins (Mcl-1, Bcl-2 and Bcl-xL). This alteration in permeability is due to the formation of permeability transition pore complexes, leading to changes in mitochondrial membrane potential, cytochrome c release and production of reactive oxygen species (ROS). The presence of cytochrome c in the cytosol allows the interaction between the caspase recruitment domain (CARD)-containing adapter protein Apaf-1, ATP, and pro-caspase 9, which results in the

formation of the apoptosome. Pro-caspase 9 is then activated and activates downstream executioner caspases.^{16, 21, 22, 26, 27}

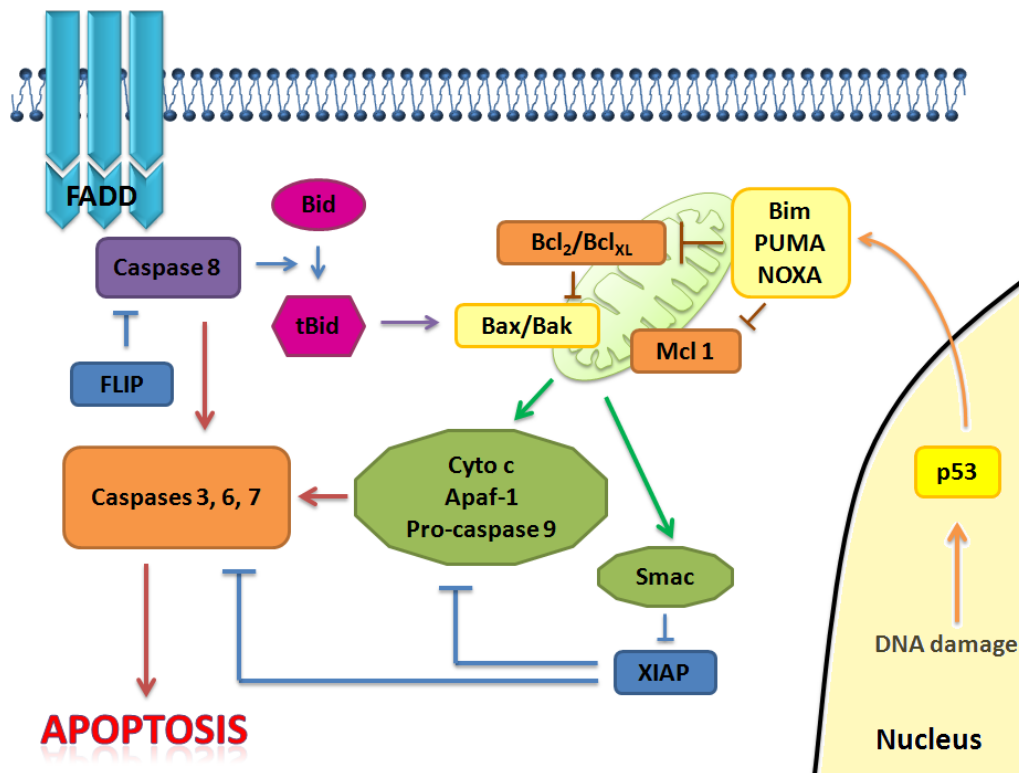


Figure 1.1.5. Simplified apoptotic pathways in mammalian cells.

The extrinsic and intrinsic pathways converge in the activation of the effector caspases, caspases 3, 6 and 7, leading to the cleavage of DNA, proteins and enzymes. The extrinsic and intrinsic pathways exhibit cross talk once caspase 8 has activated Bid via the formation of truncated Bid, *tBid*. This BH3-only protein translocates from the cytosol to mitochondria, thus activating the intrinsic apoptotic pathway.^{22, 25, 28}

Apoptosis is a highly regulated mechanism; thus, several inhibitory and regulatory mechanisms are present in cells. FADD-like interleukin-1 β converting enzyme (FLICE) inhibitory proteins (FLIPs) are caspase 8 homologues that compete for the binding of DED regions in the DISC complex, leading to the inhibition of this complex and inhibition of apoptosis.^{18, 22} The intrinsic pathway can be inhibited by a family of inhibitors of apoptosis (IAPs), the best-known of which is XIAP. XIAP has the ability to inhibit both initiator (caspase 9) and effector caspases. Smac is released from

mitochondria simultaneously with cytochrome c and has the ability to inhibit the activity of XIAP.^{16, 22, 23, 26}

The extrinsic and intrinsic apoptotic pathways are regulated by proteins such as p53, the nuclear factor κ B (NF κ B), the ubiquitin proteasome system and the PI3K/Akt pathway. p53 is a regulator of gene transcription, controlling genes that are important for the cell cycle, DNA repair and apoptosis. NF κ B regulates a large series of genes involved in apoptosis, tumorigenesis and inflammation. The ubiquitin/proteasome system is responsible for the degradation of the intracellular proteins and regulates cell growth and apoptosis. The PI3K/Akt pathway controls many signaling pathways that are important for cell survival, proliferation, mobility and tissue neovascularization.^{21, 23, 25}

Defects in the apoptosis mechanism play an important role in tumor pathogenesis, as they allow the survival of neoplastic cells beyond their normal life span, subvert the need for exogenous survival factors, provide protection from hypoxia and oxidative stress as the tumor mass expands and allow the accumulation of genetic alterations that deregulate cell proliferation, interfere with differentiation, promote angiogenesis and increase cell mobility and invasiveness during tumor progression.^{23, 29} Several genes that encode components of the apoptotic machinery are directly targeted by genetic lesions on cancer cells, leading to the overexpression of proapoptotic proteins, such as Bcl-2, XIAP and FLIP, and the downregulation of anti-apoptotic proteins, such as DR, Bax and Bad.^{28, 30}

Most of the cancer therapeutic drugs promote cancer cell apoptosis. The targeting of the apoptotic pathway is also responsible for the side effects of these drugs. Mutations in apoptotic programs can lead to chemoresistance to cancer therapy.^{17, 20, 22}

1.2. Natural products in medicinal chemistry

Natural products have been the source of medicines for mankind for thousands of years. The first written records of the use of plants as a source of medicine date from 2600 BC in Mesopotamia. Quinine was the first isolated natural compound to be commercialized by Caventou.³¹ According to the WHO, the primary health care of 80%

of the world's population is based on traditional medicinal treatments derived from natural sources.³²⁻³⁴

In modern pharmaceutical research on new drugs, natural sources (such as plants and microorganisms) have been explored to identify novel lead compounds. From the pharmaceutical entities approved worldwide between 1981 and 2006, 5.7% were natural products and 27.6% were natural-product derived molecules, whereas from 2005 to 2010, seven natural products and 12 natural product derivatives were approved for use in clinical practice (Figure 1.2.1).³⁵⁻³⁹

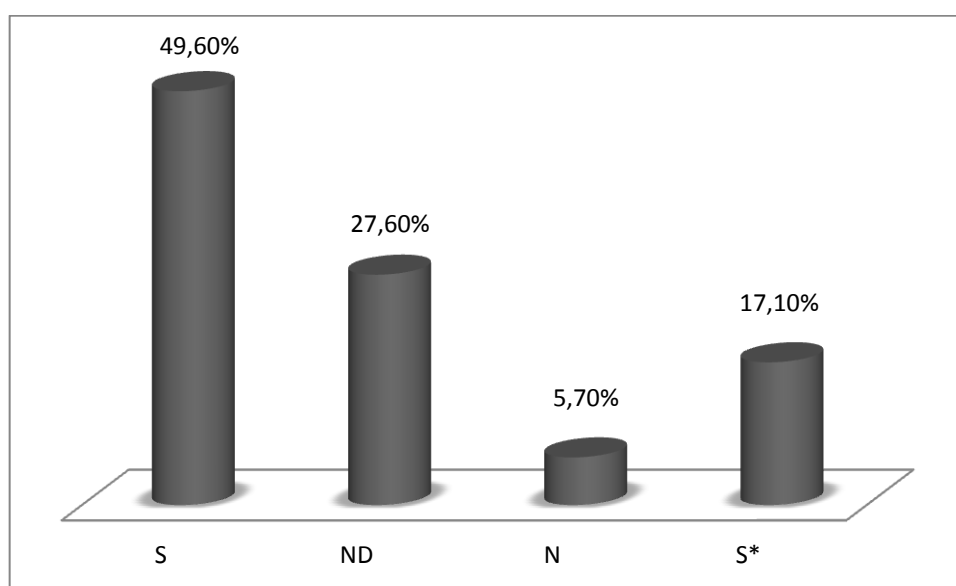


Figure 1.2.1. Sources of small molecules in clinical use for 1981-2006. S) Totally synthetic molecule; ND) natural product derived molecule; N) natural product; S*) from total synthesis, but the pharmacophore is from a natural product. Adapted from the literature.³⁷

Natural products have been major sources of lead compounds in the discovery of new drugs for the treatment of infectious diseases, lipid disorders, neurological diseases, cardiovascular and metabolic diseases, immunological, inflammatory and related diseases, and oncologic diseases (Table 1.2.1).⁴⁰⁻⁴⁴

Despite promising data, pharmaceutical companies have invested less in the discovery and research at natural products over the last decade, which can be explained by the development of combinatorial chemistry.^{34, 45, 46} Natural products can also present difficulties regarding access and supply, which discourage pursuit of research into this

type of compounds by pharmaceutical companies.⁴⁷ Another factor that may have contributed to the lack of interest of pharmaceutical companies in natural products was the introduction of high-throughput screening assays for several defined molecular targets. There are few libraries of natural products, or the existent libraries compile mixtures of compounds with different activities and concentrations. These obstacles to the screening and research of natural products are being solved with the introduction of better separation techniques, such as high-pressure liquid chromatography (HPLC) coupled with mass spectrometry (MS) and improved and more potent nuclear magnetic resonance (NMR) techniques.^{43, 45, 47-54}

Table 1.2.1. Some examples of natural products and natural product derivatives currently in clinical use.

| Entry | Disease area | Generic name (Trade name) | Lead compound | Year |
|-------|---------------------|---|-------------------|------|
| 1 | Antibacterial | Doripenem (Finibax/Doribax [®]) | Thienamycin | 2005 |
| 2 | Antiparasitic | Fumagillin (Flisint [®]) | Fumagillin | 2005 |
| 3 | Oncology | Romidepsin (Istodax [®]) | Romidepsin | 2009 |
| 4 | Alzheimer's disease | Galantamine (Reminyl [®]) | Galantamine | 2002 |
| 5 | Immunosuppression | Mycophenolate sodium (Myfortic [®]) | Mycophenolic acid | 2003 |
| 6 | Dyslipidemia | Rosuvastatin (Crestor [®]) | Mevastatin | 2003 |
| 7 | Pain | Capsaicin (Istodax [®]) | Capsaicin | 2009 |
| 8 | Diabetes | Exenatide(Byetta [®]) | Exenatide | 2006 |

Natural products are derived from the phenomenon of biodiversity in which the interactions between organisms and their environment formulate diverse complex chemical entities.^{34, 35} Natural products typically have more stereogenic centres and more architectural complexity (aromatic rings, complex ring systems, and higher degree of molecule saturation) than do synthetic molecules fashioned by medicinal chemists.^{36, 55}

Natural products contain relatively more carbon, hydrogen and oxygen, and less nitrogen and other elements than do synthetic medicinal agents.⁴⁹ Natural products often have a molecular masses greater than 500 da and high polarity (greater water solubility).⁴⁴ Most classical small molecules obtained from nature are secondary metabolites-products from conditional pathways that are turned on in a particular context or situation, making them more likely to hit a molecular target.³⁶

Despite all this knowledge only, 10% of the world's biodiversity has been explored for possible new biologically active natural compounds. New sources of natural products are now being explored, such as marine microorganisms and small organisms.^{36, 48, 51, 53, 54, 56}

1.2.1. Natural products and treatment of cancer

Natural products represented around 50% of the entire pool of drugs between 2003-2005 in clinical use for the treatment of cancer.^{38, 39} Novel natural compounds with diverse structures that were isolated from plant sources have been considered as prototypes, leads or heads of series, and structural modifications have provided extraordinary therapeutic possibilities to compounds. In 2007, more than 30 compounds of natural origin were in different phases of clinical study for the treatment of various types of cancer.⁵⁷

Secondary metabolites are directly involved in the regulation of the growth of organisms; therefore, many serve as templates for the modulation of tumor development.⁵⁸ Cancers are highly dependent on oncogene activation for the maintenance of their malignant phenotype. Multitarget agents and combination therapies may be required to prevent salvage or escape mechanisms and to enhance the efficacy of the therapy in cancer treatment. The promiscuous character of natural products has been associated with dirty drugs, in contrast to high-affinity single-target drugs; however in the face of the new knowledge on cancer mechanisms, the ability of natural compounds to hit several targets can be advantageous in cancer treatment.⁵⁸

Currently, several natural products are in clinical use for cancer treatment; the most common can be divided into five major classes: vinca alkaloids, epipodophyllotoxins, taxanes, camptothecins and photosensitizers. Nevertheless, a series of new compounds

with different chemical structures and targets are being explored.^{58, 59} From these groups several derivatives were synthesized with the aim of improving the activity and reducing the side effects of the original products.

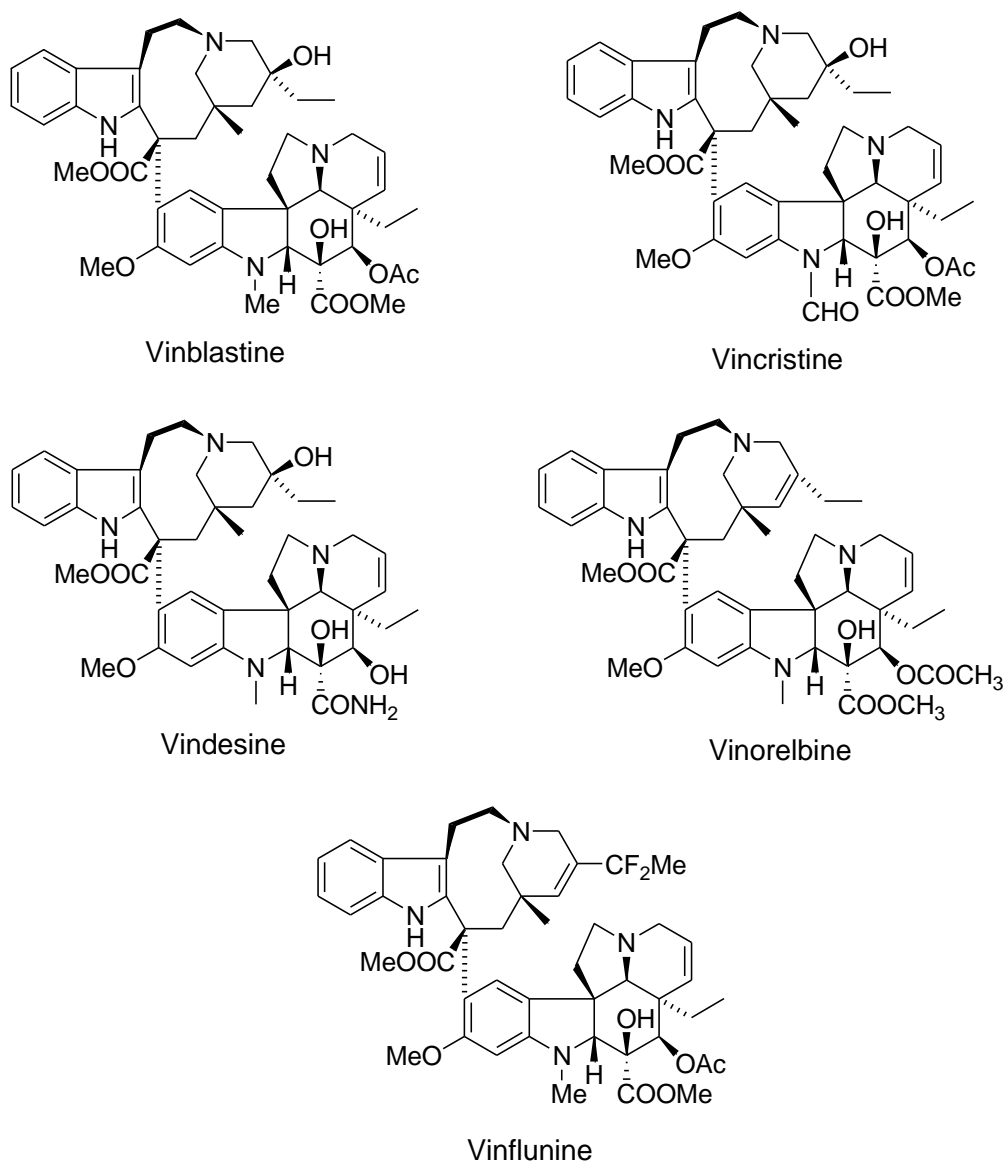


Figure 1.2.2. Representation of some vinca alkaloids.

Vinka alkaloids are isolated from *Catharanthus roseus*. Vinblastine and vincristine were the first plant constituents to be used as antineoplastic agents, in the 1950s. Vinka alkaloids inhibit the growth of cancer cells, preventing mitosis by disrupting microtubules and consequently dissolving cell mitotic spindles. Cancer cells treated with vinka

these derivatives as it presents better bioavailability and better activity against a variety of drug-resistant cancers compared with the parent compound (Figure 1.2.4).^{31, 57}

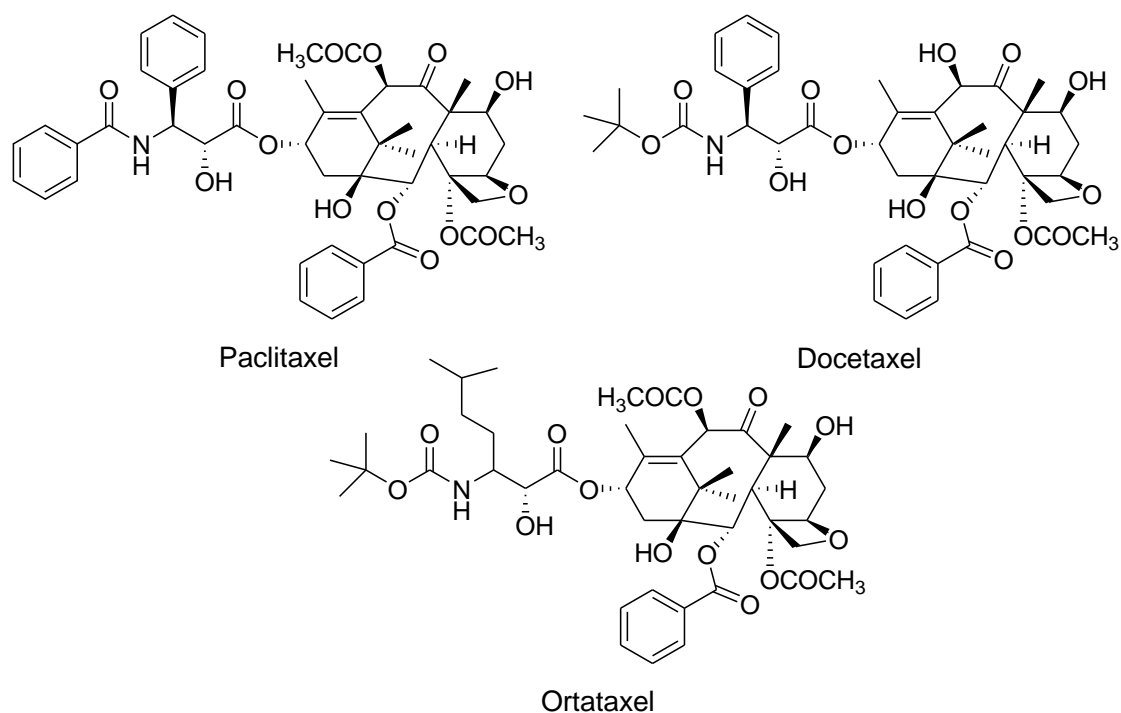


Figure 1.2.4. Representation of naturally occurring paclitaxel and its semisynthetic derivatives.

Camptothecin is a quinoline alkaloid discovered in *Camptotheca acuminata*. This compound presents solubility and toxicity problems and was never used in clinical trials. Camptothecin has a different mode of action when compared with taxanes: it inhibits topoisomerase I by stabilizing intermediate complexes produced during DNA synthesis. The semisynthetic derivatives topotecan and irinotecan were prepared to overcome these problems associated to the use of camptothecin (Figure 1.2.5).^{57, 61}

Photodynamic therapy is a promising new cancer treatment approach that was first described in 1903 by Von Tappeiner and Jesionek. Photosensitizing compounds have a low cytotoxicity in the dark however, when subjected to radiation, produce highly reactive and toxic species. Porphyrins are the most extensively used group of sensitizer/tumor-selective compounds. Photofrin was the first sensitizer to be used in clinical settings; hypericin has been studied in recent years as a naturally occurring

photosensitizer that exhibits high affinity for tumors by triggering necrosis or apoptosis, depending on the level of oxidative stress produced (Figure 1.2.6).³¹

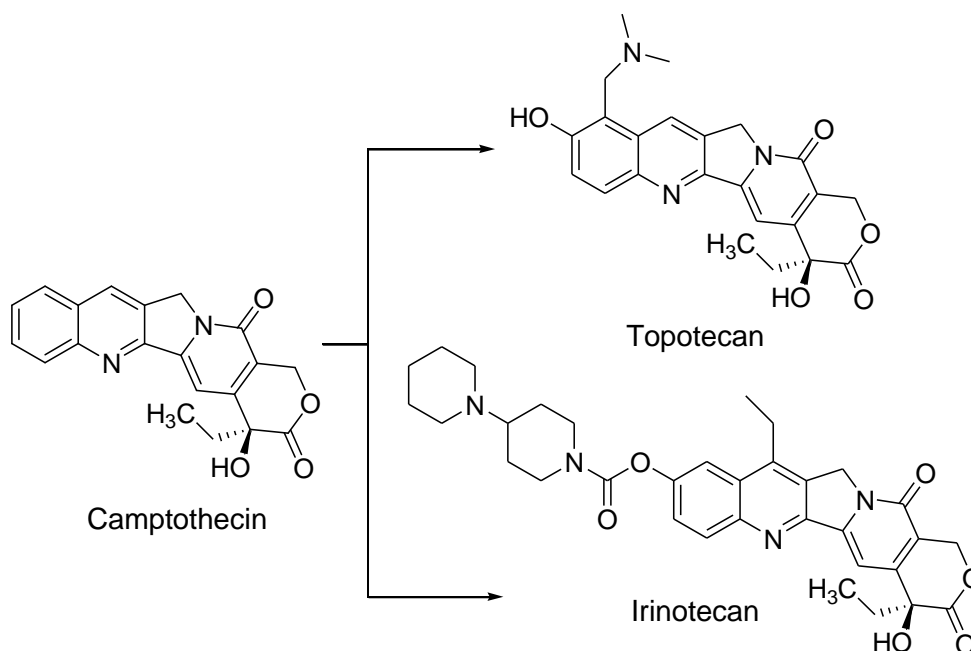


Figure 1.2.5. Representation of quinoline alkaloids.

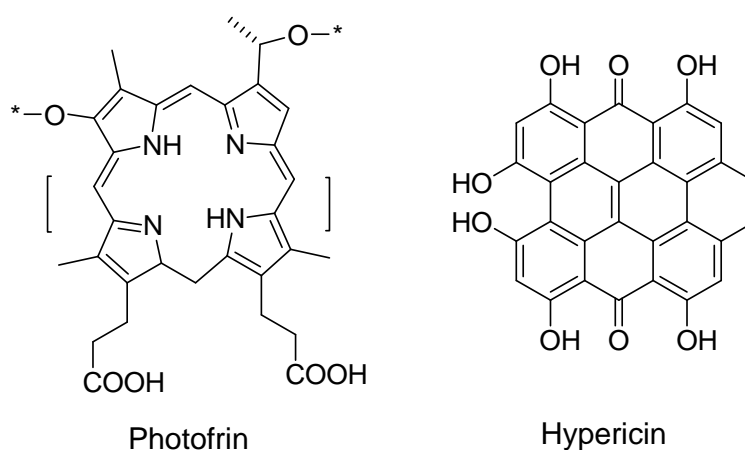


Figure 1.2.6. Representation of the porphyrins currently used in clinical setting as chemosensitizers.

Preventing disease is highly preferable to treatment. Chemoprevention was defined by Sporn M. B. and collaborators as a strategy for cancer control via the administration or

ingestion of synthetic or natural compounds that act to retard or suppress the process of carcinogenesis.^{62, 63} These compounds can be classified as blocking or suppressing agents depending on the stage of carcinogenesis at which they act.

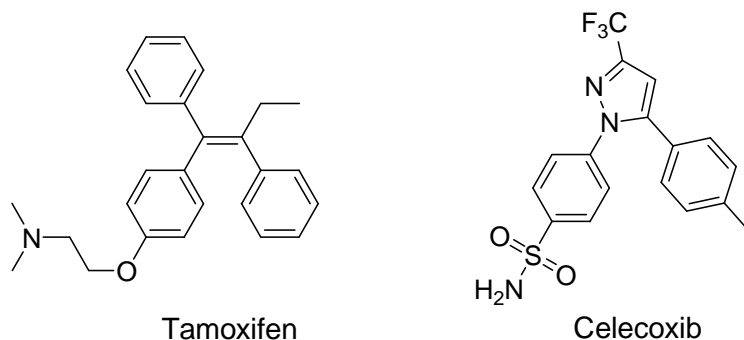


Figure 1.2.7. Chemopreventive drugs currently in clinical use.

The FDA has approved tamoxifen for the prevention of breast cancer and celecoxib for the prevention of colon cancer in patients with family history of polyposis (Figure 1.2.7). Curcumin and resveratrol are the most promising natural compounds for chemoprevention and also increase the sensitivity of cancer cells to traditional chemotherapeutic agents (Figure 1.2.8).^{31, 55, 64-66} Curcumin inhibits the action of several carcinogens, induces apoptosis and has antiangiogenic effects in cancer cells.^{67, 68} Resveratrol inhibits several steps of carcinogenesis *in vitro* and *in vivo* via several mechanisms.⁶⁹

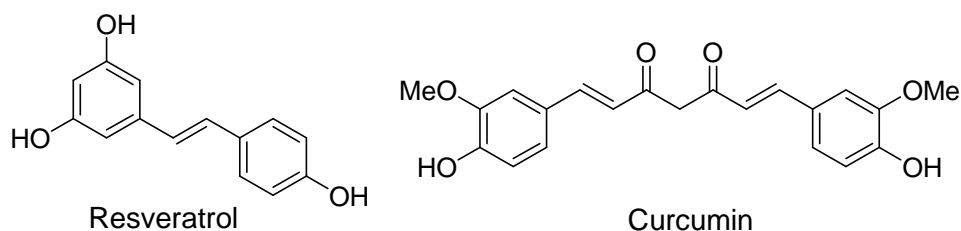


Figure 1.2.8. Natural products with chemopreventive activity in clinical studies.

1.3. Terpenoids

Natural products are characterized by structural diversity, which is mainly due to the initial formation of building blocks with the arrangement of diverse carbon-carbon bonds, carbocations and electrophilic additions. Terpenoids are a diverse family of secondary plant metabolites that are minor but ubiquitous components of the human diet and are considered relatively nontoxic.

1.3.1. General dispositions

Terpenes have their primary origin in the condensation of a unit of isopentenylallyl diphosphate (IPP) and dimethylallyl diphosphate (DMAPP). Until 1990, the IPP and DMAPP building blocks of terpene were assigned to the mevalonate pathway; however, isotope experiments revealed a coexistent pathway called the non-mevalonate pathway. These two pathways coexist and metabolites from both pathways can be mutually exchanged.^{70, 71}

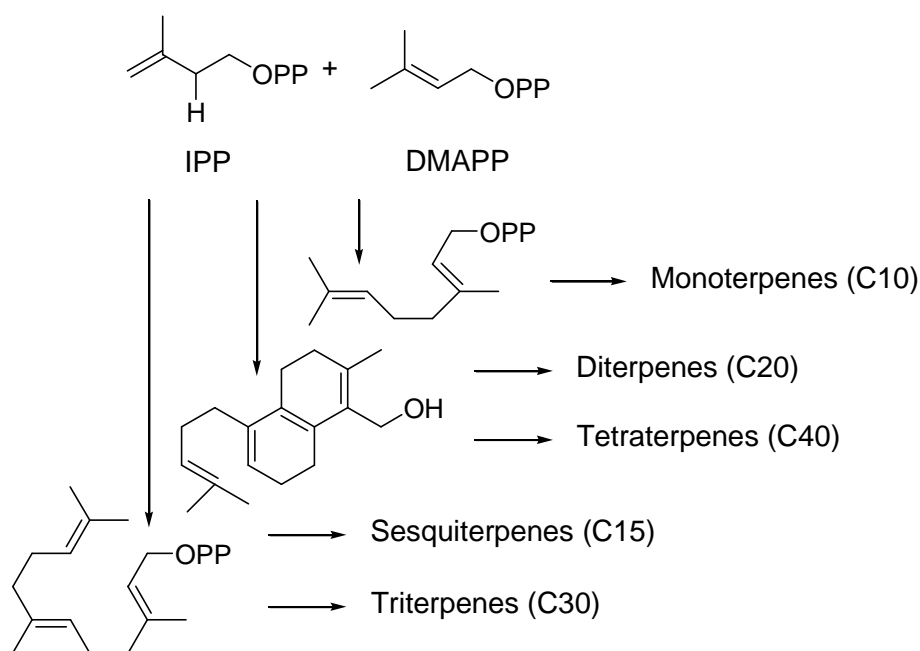


Figure 1.3.1. Simplified scheme of the origin of the diverse biosynthetic plant terpene classes.

Despite the knowledge of the synthetic pathway involved in the synthesis of terpenes, these compounds are traditionally known as derivatives of isoprene, a five-carbon acyclic chain (C_5H_8). Based on the number of building blocks, terpenes are commonly classified as monoterpenes (C_{10}), sesquiterpenes (C_{15}), diterpenes (C_{20}), triterpenes (C_{30}) and tetraterpenes (C_{40}) (Figure 1.3.1).

1.3.2. Biosynthetic diversity of triterpenoids

Triterpenes are a diverse group of natural products derived from squalene or related acyclic 30-carbon precursors. As a general mechanism, these precursors can be activated by a cationic attack and, via a cascade of cation–olefin cyclizations, generate a cyclic carbocation that can rearrange and cyclize further. These reactions are catalyzed by a group of enzymes generally known as triterpene synthases, which can be classified as squalene cyclases and oxidosqualene cyclases.⁷²⁻⁷⁵

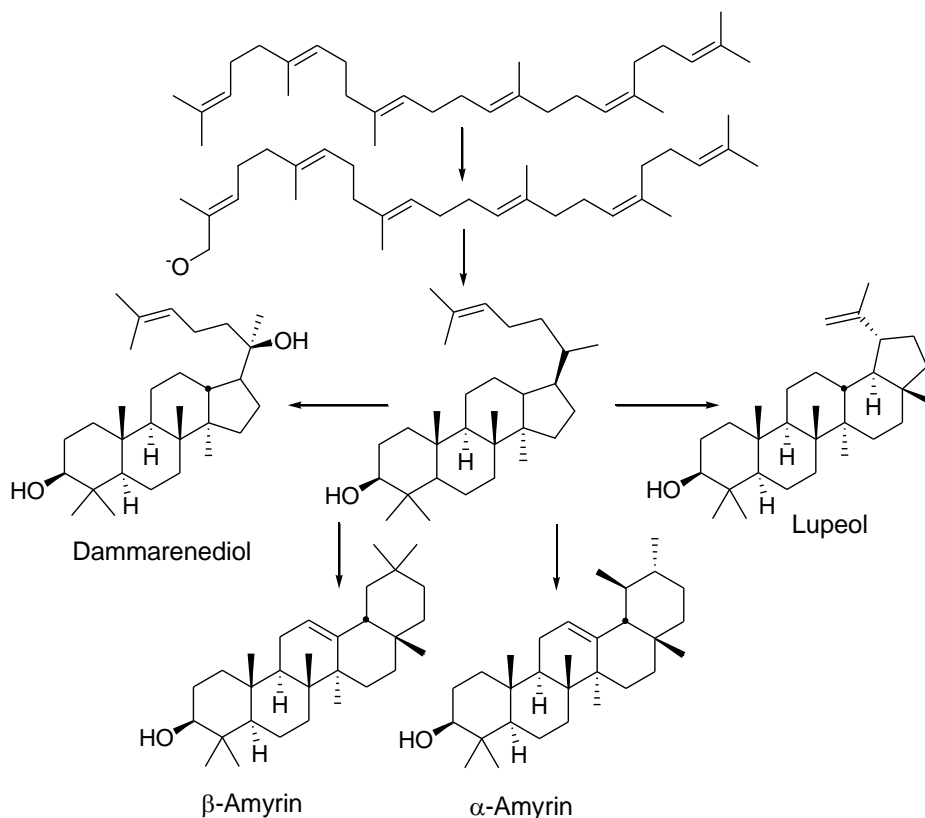


Figure 1.3.2. Simplified scheme of the origin of some triterpenoids.

Oxidosqualene is probably the precursor of most 3β -OH-triterpenoids; however, squalene cyclization followed by oxidation of the hydroxyl group at C3 is also plausible. Oxidosqualene is the precursor for β -amyrin, α -amyrin, lupeol and dammarenediol (Figure 1.3.2). β -Amyrin gives origin to oleanane triterpenoids, α -amyrin to ursane type triterpenoids and lupeol to lupane triterpenoids.⁷² From a biological point of view, the most important triterpenoid structures are oleanane, ursane, lupane and dammarane-euphane triterpenoids.⁷⁶

1.3.3. Ursolic acid

Ursolic acid (3 β -hydroxy-urs-12-en-28-oic acid) and analogues (Figure 1.3.3) are present in several plants, vegetables and fruits, (Table 1.3.1) in the free form or conjugated with glycosides.^{77,78}

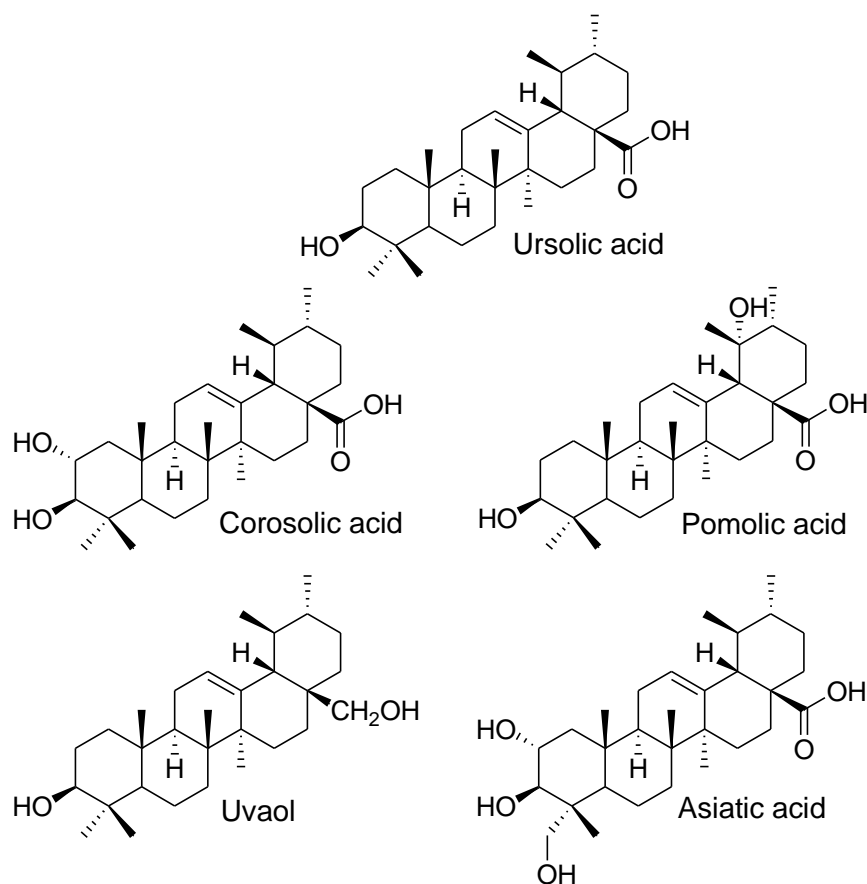


Figure 1.3.3. Ursolic acid and naturally occurring analogues.

Table 1.3.1. Some sources of ursolic acid in Nature.

| Entry | Specie | Activity | Ref. |
|-------|--------------------------------|--|--------|
| 1 | <i>D. dendo</i> | Antimicrobial | 79 |
| 2 | <i>Quinchamalium majus</i> | Antitubercular | 80 |
| 3 | <i>Rosmarinus officinalis</i> | Tripanocidal | 81 |
| 4 | <i>Gardenia saxatilis</i> | Antiplasmodial | 82 |
| 5 | <i>Pourouma guianensis</i> | Antileishmanial | 83 |
| 6 | <i>Geum japonicum</i> | Anti-HIV | 84 |
| 7 | <i>Actinidia arguta</i> | Lipolytic | 85 |
| 8 | <i>Lycopus lucidus</i> | Antiatherosclerotic | 86 |
| 9 | <i>Origanum majorana</i> | Anti-alzheimer | 87, 88 |
| 10 | <i>Eucalyptus tereticornis</i> | Hepatoprotector | 89 |
| 11 | <i>Nepeta sibthorpii</i> | Analgesic | 90 |
| 12 | <i>Salvia officinalis</i> | Anti-inflammatory and antimicrobial | 91, 92 |
| 13 | <i>Perilla frutescens</i> | Anti-inflammatory and antitumor | 93 |
| 14 | <i>Prunella vulgaris</i> | Anti-inflammatory and antiallergic | 94 |
| 15 | <i>Plantago major</i> | Anti-inflammatory | 95 |
| 16 | <i>Ugni molinae</i> | Anti-inflammatory | 96 |
| 17 | <i>Cussonia bancoensis</i> | Anti-inflammatory and anti-nociceptive | 97 |
| 18 | <i>Vaccinium macrocarpon</i> | Anti-inflammatory | 98 |
| 19 | <i>Calluna vulgaris</i> | Antitumor | 99 |
| 20 | <i>Prunus mume</i> | Antitumor | 100 |

Ursolic acid has several biological activities, such as antibacterial, antiprotozoal, anti-HIV, antiosteoporotic, cardioprotector, antiobesity, antiatherosclerotic, antidiabetic, immunomodulator, analgesic, hepatoprotector, anti-inflammatory and anticarcinogenic.

1.3.3.1. General activities

Resistant bacterial infections are a common problem in hospitals and immunosuppressed individuals. Ursolic acid has been tested in several strains of bacteria (Table 1.3.2).

Table 1.3.2. Minimum inhibitory concentration (MIC) of ursolic acid for several bacterial species.

| Entry | Bacteria | MIC ($\mu\text{g/mL}$) | | Ref. |
|-------|---|--------------------------|----------------------|------|
| | | Ursolic acid | Reference antibiotic | |
| 1 | <i>M. tuberculosis</i> H ₃₇ Ra | 50 | 0.06 ^a | 101 |
| 2 | <i>M. tuberculosis</i> H ₃₇ Rv | 31 | 0.03 ^b | 80 |
| 3 | <i>E. faecium</i> FN-1 | 4 | 128 ^c | 92 |
| 4 | <i>E. faecium</i> BM4147 | 4 | 32 ^c | 92 |
| 5 | <i>E. faecalis</i> FA2-2 | 4 | 4 ^c | 92 |
| 6 | <i>E. faecalis</i> NCTC 12201 | 4 | 4 ^c | 92 |
| 7 | <i>S. aureus</i> OM481 | 8 | 64 ^c | 92 |
| 8 | <i>S. aureus</i> OM584 | 8 | 64 ^c | 92 |
| 9 | <i>S. pneumonia</i> R6 | 8 | 0.06 ^c | 92 |
| 10 | <i>E. coli</i> K12 | >128 | n.t. | 92 |
| 11 | <i>P. aeruginosa</i> PAO1 | >128 | n.t. | 92 |
| 12 | <i>S. marcescens</i> NUSM8905 | >128 | n.t. | 92 |
| 13 | <i>E. coli</i> ATCC 25922 | >256 | 4 ^d | 102 |
| 14 | <i>S. aureus</i> ATCC 25923 | 8 | <1 ^e | 102 |
| 15 | <i>S. aureus</i> ATCC 29213 | 8 | <1 ^e | 102 |
| 16 | <i>E. faecalis</i> ATCC 29212 | 4 | <1 ^f | 102 |
| 17 | <i>P. aeruginosa</i> ATCC 27858 | 256 | 16 ^g | 102 |
| 18 | Penicillinase-producing <i>E. coli</i> | >256 | >256 ^d | 102 |
| 19 | MRSA (<i>mecA</i> gene) | >256 | 256 ^e | 102 |
| 20 | <i>E. faecium</i> (<i>vanB</i> gene) | >256 | 64 ^f | 102 |
| 21 | <i>E. faecalis</i> (<i>vanA</i> gene) | >256 | 256 ^g | 102 |
| 22 | <i>P. aeruginosa</i> | >256 | 64 ^g | 102 |

a) Isoniazid; b) Rifampin; c) Ampicillin; d) Amoxicillin; e) Oxacillin; f) Vancomycin; g) Ticarcilin.

Biofilm formation in bacterial infections is a common cause of the reoccurrence of symptoms and treatment failure. Bacterial cells involved in a biofilm, a polysaccharide matrix, often have lower metabolism and oxygen consumption, which renders them resistant to antibiotics. Ursolic acid is a biofilm formation inhibitor.⁷⁹

Protazoan parasites affect 3 billion people worldwide, with malaria and trypanosomatid parasites causing the greatest morbidity.¹⁰³ Ursolic acid was shown to suppress parasitemia in mice infected with *Plasmodium berghei* and was also reported to reduce the *in vitro* proliferation of *P. falciparum* 3D7, W2 and K1 strains.^{82, 104-106} Leishmaniasis is an insect-borne protozoan infection for there is no effective vaccine. Ursolic acid can inhibit the growth of two species of *Leishmania* in the form of promastigotes or amastigotes (Table 1.3.3) because of the activation of nitric oxide (NO) intermediates by macrophages.^{83, 107}

Table 1.3.3. *In vitro* determination of the IC₅₀ (μM) of ursolic acid for several strains of leishmania.

| Entry | Species | IC ₅₀ (μM) | Ref. |
|-------|-------------------------------------|-----------------------|------|
| 1 | <i>L. amazonensis</i> promastigotes | 20 | 83 |
| 2 | <i>L. infantum</i> promastigotes | >25 | 83 |
| 3 | <i>L. amazonensis</i> promastigotes | 11 | 107 |
| 4 | <i>L. amazonensis</i> amastigotes | 24 | 107 |

Betulinic acid has been the triterpenoid most used for the study of anti-HIV activity.^{108, 109} Ursolic acid was found to have anti-HIV activity, with a low therapeutic index because of its toxicity (TI = 3.3).¹¹⁰ This triterpenoid acts via inhibitory effects on HIV reverse transcriptase (RT; 28% inhibition at 100 μM), inhibition of the dimerization of RT^{84, 111} and inhibition of the gp120-CD4 interaction, which is required for the entry of the virus into lymphocytes.^{112, 113}

Osteoporosis is the most common consequence of the imbalance between bone resorption by osteoclasts and bone formation by osteoblasts.^{114, 115} An *in vitro* study showed that ursolic acid stimulated osteoblast differentiation and mineralization through the activation of mitogen-activated protein (MAP)-kinases (JNK and p38) and

transcription factors (NF- κ B and AP-1), with a mechanism of action that is different from that of the drugs currently used.^{116, 117}

Cardio-related diseases are the number one cause of death worldwide.¹¹⁸ The administration of ursolic acid to a Dahl salt-sensitive, insulin-resistant rat model of hypertension prevented the development of severe hypertension via antihyperlipidemic, antioxidant, diuretic, salturetic and natriuretic effects.¹¹⁹ Treatment of arrhythmic Wistar rats with ursolic acid has vasodepressor and bradycardic effects that can be attributed to a β -blocker activity and inhibition of a Na⁺/H⁺ exchanger.¹²⁰ In two different rat models of heart injury, ursolic acid exhibited antioxidative activity, protecting the heart from further damage by decreasing the lipid peroxidation and increasing the activity ROS scavenging activities;^{121, 122} these effects were also verified in isolated mitochondria.¹²³ Treatment of rats with isoproterenol-induced myocardial infarction with ursolic acid prevents the increase of the activity of creatine kinase-MB, lipid peroxidase markers, DNA fragmentation and several markers of apoptosis in plasma and heart tissues; and the decrease of the activity of enzymatic antioxidants.¹²⁴

Obesity is a global health problem and a risk factor for the development of metabolic disorders, dislipidemia, atherosclerosis and type 2 diabetes.^{125, 126} Ursolic acid decreases the levels of triacylglycerol in the plasma via the inhibition of pancreatic lipase (IC₅₀ 15.83 μ M) and by stimulating lipolysis in adipocytes.^{85, 127} Ursolic acid has the ability to reduce the levels of plasma total cholesterol, free fatty acids and triglycerides in diabetic mice.¹²⁸ Fatty acid synthase (FAS) is a key enzyme in the synthesis of long-chain fatty acids, which are a target in the treatment of obesity; ursolic acid inhibits FAS with an IC₅₀ of 6.0 μ g/mL by changing the conformation of the enzyme.¹²⁹ Ursolic acid has the ability to activate the peroxisome proliferator-activated receptor (PPAR)- α in Hep G2 cells, leading to a reduction in the cellular content of triglycerides and cholesterol by increasing fatty acid uptake and oxidation and by inhibiting fatty acid synthesis.¹³⁰

Atherosclerosis is considered a chronic inflammatory disease.^{131, 132} Vascular smooth muscle cells (VSMCs) treated with ursolic acid exhibit inhibition of chemotaxis, reduction in the expression of the proliferative cell nuclear antigen (PCNA) and a

disorganization of β -tubulin.¹³³ C-reactive protein (CRP) is an acute response protein that acts as a direct regulator of the development of atherosclerosis.¹³⁴⁻¹³⁶ Ursolic acid decreases the synthesis of CRP, leading to the reduction of the vascular cell adhesion molecule 1 (VCAM-1) and of the low-density lipoprotein receptor-1 (LOX-1) in the endothelium.¹³⁷

Diabetes and diabetic complications are responsible for a significant amount of hospital admissions and expenses in health care.¹³⁸ The antidiabetic and glycativere-reducing stress activity of ursolic acid are well documented. Ursolic acid has an insulin-sensitizing effect *in vitro*^{139, 140} and *in vivo*.^{128, 141, 142} In diabetic mice, the supplement of the diet with ursolic acid leads to improvement of glucose plasma levels, lower intolerance to glucose, increases sensitivity to insulin, improvement of the immune response by stimulating T-cell activation;¹⁴¹ reduction of the activities of aldose reductase (AR) and sorbitol dehydrogenase (SDH), leading to the reduction of oxidative stress, and augmentation of the activity of glucokinase and glycogen content in the liver.¹²⁸ Ursolic acid also reduces the activities of AR and SDH in the polyol pathway in the kidney, contributing to the decrease and prevention of glycation, which is associated with renal diseases.¹⁴²

Diabetes increases the risk of developing mild cognitive impairment, which is usually associated with brain inflammation and insulin resistance.¹⁴³⁻¹⁴⁵ Mice on a high-fat diet (HFD) ultimately develop type 2 diabetes with a pronounced insulin resistance in the hippocampus, culminating in cognitive impairment. Ursolic acid reverses the cognitive impairment via the inhibition of endoplasmic reticulum stress, inhibition of the NF- κ B (I κ B) kinase (IKK)- β /NF- κ B-mediated inflammatory signaling pathway, and activation of the PI3K/Akt/mTOR pathway in the mouse hippocampus.¹⁴⁶

Alzheimer's disease (AD) is characterized by selective neuronal loss and neurofibrillary and extracellular deposits of insoluble amyloid protein.¹⁴⁷ Oxidative stress contributes to the formation of amyloid plaques, which can be a source of oxidative species by themselves. An *in vitro* study showed that ursolic acid inhibits the formation of ROS from amyloid plaques, thus improving cell viability by decreasing neurotoxicity.⁸⁷ The decrease in choline acetyltransferase (ChAT) and

acetylcholinesterase (AChE) activity is correlated with dementia.¹⁴⁸ Ursolic acid inhibits AChE in a dose-dependent and competitive/non competitive way.⁸⁸

Mice treated with ursolic acid exhibited an increase in bone marrow cellularity and α -esterase-positive cells. The same mice treated simultaneously with an antigen and ursolic acid show an increase in specific antibody titre and in the number of plaque-forming cells in the spleen. These effects contribute to the immunomodulator effect of ursolic acid.¹⁴⁹

Ursolic acid presents some analgesic effects in mice. It increased the response time in the hot plate test and produced some results in the acetic acid-induced writhing test assay,^{90, 97} which were reversed by naloxone, suggesting an involvement of opioid receptors in this process.⁹⁰

Ursolic acid is known being hepatoprotective against several toxins.^{89, 150-152} In isolated rat hepatocytes, incubation with ethanol increases the levels of aspartate aminotransferase (AST), alanine aminotransferase (ALT) and alkaline phosphatase (AP), which are markers of hepatic function, and decreases cell viability; co-treatment of cells with ursolic acid leads to preservation of cell viability and reversal of the induction of AST, ALT and AP.⁸⁹ These effects were also observed in an *in vivo* assay.¹⁵⁰ Toxins, such as galactosamine, thioacetamide and carbon tetrachloride, are used to induce liver injuries in animal models. Pretreatment with ursolic acid grants a protection against the alterations of several biochemical markers of liver damage.¹⁵² Metallothionein (MT) enzymes are liver enzymes that are required for the homeostasis of essential metals.¹⁵³ Ursolic acid induces the hepatic expression of MT in murine hepatic cells via the induction of the tumor necrosis factor (TNF)- α and interleukin (IL)-6.¹⁵⁴

Liver fibrosis is a consequence of chronic liver damage and is caused by xenobiotic damage, viral infection and certain genetic diseases.¹⁵⁵ The induction of cell death in hepatic stellate cells (HSCs) can lead to the recovery from established experimental fibrosis.¹⁵⁶ In culture activated HSCs, ursolic acid induces apoptosis through the activation of the NF- κ B and Akt pathways, which leads to mitochondrial permeability

and activation of downstream caspases. Treatment of Wistar rats with liver fibrosis with one single injection of ursolic acid led to the reversal of the induced liver fibrosis.^{157, 158}

Anti-inflammatory effects of ursolic acid were detected in *in vitro* cell culture systems and *in vivo* experiments. *In vitro* experiments have shown that the anti-inflammatory activity of ursolic acid is due to its ability to repress the activity of several pro-inflammatory enzymes, such as lipoxygenase,^{99, 159, 160} cyclooxygenase-2 (COX-2, an inductive cyclooxygenase with an IC₅₀ value of 130 μM),^{95, 161} matrix metalloproteinase-9 (MMP-9, by stimulating the nuclear translocation of glucocorticoid receptor),^{162, 163} and inducible nitric oxide synthase (iNOS, with an IC₅₀ of 17 μM in RAW 264.7 cells).^{94, 164, 165} Ursolic acid reportedly attenuates the effect of NF-κB; however, contradicting results have been published. You *et al* reported an induction of iNO and TNF-α via NF-κB activation, implying that the effects of this triterpenoid are dependent on the biological status of macrophages.^{166, 167}

Adhesion molecules, such as endothelial (E)-selectin, VCAM-1 and intercellular adhesion molecule (ICAM)-1, are expressed on the surface of endothelial cells at an early stage of inflammation. Expression of E-selectin is induced by NF-κB activation. Pretreatment of human umbilical vein endothelial cells (HUVECs) with ursolic acid reduced the expression E-selectin, in parallel to the inhibition of the NF-κB signaling pathway.¹⁶⁸ RAW264.7 mouse macrophages treated with ursolic acid exhibit a decrease in intracellular migration inhibitory factor (MIF), which occurs through extracellular signal-regulated kinase 2 (ERK2) activation.¹⁶⁹

Mucus in the airway epithelium plays a pivotal role in defensive mechanisms against airborne chemicals, particles and microorganisms. Ursolic acid regulates mucin secretion by acting directly on the airway mucin-secreting cells.¹⁷⁰

In vivo studies of the use of ursolic acid as an anti-inflammatory agent were performed in mice, with inflammation induced by 12-*O*-tetradecanoylphorbol-13-acetate (TPA), croton oil (in the mice ear), and dimethylbenz[α]anthracene (DMBA). Ursolic acid (ID₅₀ 0.1 mg/ear) had a better effect than indomethacin (ID₅₀ 0.3 mg/ear), but its effect was not better than that of hydrocortisone (ID₅₀ 0.03 mg/ear) on a TPA model.⁹³ Ursolic acid reduced the oedema in mouse ears treated with croton oil, by 84% (ID₅₀ 0.14 μM/cm²), which is an effect that is two-fold more potent than that of indomethacin (ID₅₀

0.26 $\mu\text{M}/\text{cm}^2$).⁹¹ Mouse skin treated with DMBA exhibits an increase in the mRNA levels of TNF- α , COX-1 and iNOS; the application of ursolic acid decreased these levels by several fold.¹⁷¹

Some signaling pathways of the inflammatory process are closely related with the promotion, progression and invasion of cancer.^{1, 9, 163, 165, 171}

1.3.3.2. Antitumor activity

Cancer treatment and/or prevention should target tumor microenvironment, promotion, progression, angiogenesis, invasion and metastasis, as well as the immune response and chronic inflammation. Natural compounds supply a vast range of options for cancer treatment and prevention. Ursolic acid can target several steps of cancer development, thus representing a promising tool for the treatment and chemoprevention of cancer.^{77, 172-178}

Table 1.3.4. IC₅₀ (μM) for ursolic acid in oral, stomach and esophageal cancer cell lines.

| Entry | Cell line | IC ₅₀ (μM) | Assay | Time (h) | Ref. |
|-----------------------------|-----------|------------------------------------|----------------|----------|------|
| <i>Oral carcinoma</i> | | | | | |
| 1 | HSC-2 | 63.4 | MTT | 24 | 179 |
| 2 | HSG | 105.1 | MTT | 24 | 179 |
| 3 | KB | 8.2 | Methylene blue | 72 | 180 |
| 4 | Ca9-22 | 12.9 | MTT | - | 181 |
| <i>Stomach carcinoma</i> | | | | | |
| 5 | HGT | 20.0 | MTT | 24 | 99 |
| 6 | | 117.6 | SRB | 48 | 182 |
| 7 | | >10 | MTT | 96 | 183 |
| 8 | BCG-823 | 66.38 | MTT | 24 | 184 |
| 9 | | >10 | MTT | 72 | 185 |
| 10 | | 22.96 | MTT | 24-72 | 186 |
| 11 | NUGC-3 | 30.0 | MTT | 48 | 112 |
| <i>Esophageal carcinoma</i> | | | | | |
| 12 | YES-2 | 10-25 | WST-8 | 48 | 100 |
| 13 | Eca-109 | 40.0 | MTT | 48 | 187 |

Stomach and esophageal cancers are responsible for 2.4% of new cases of cancer in the USA.^{3, 5} Ursolic acid has demonstrated antiproliferative activity against several oral, stomach and esophageal cancer cells (Table 1.3.4). Ursolic acid is a well known inhibitor of inflammation. Its activity against stomach cancer HGT cells is based on its activity as an inhibitor of 15-lipoxygenase, an important inflammatory enzyme (Table 1.3.4, entry 5).⁹⁹

DNA polymerase and DNA topoisomerase are enzymes that are critical for DNA replication, repair and recombination and are ideal targets for anticancer agents. Ursolic acid inhibits DNA polymerases α and β with an IC_{50} of 38 and 42 μ M, respectively, and topoisomerase II with an IC_{50} of 150 μ M, inhibiting the growth of NUGC-3 stomach cancer cells via cell cycle arrest at the S phase (Table 1.3.4, entry 11).¹¹²

The combination of ursolic acid with 5-fluorouracil has synergistic effects in esophageal cancer cells, because these two compounds target and arrest the cell cycle in two different phases.¹⁰⁰ The combination of ursolic acid with 5-fluorouracil exhibits adjuvant antiproliferative effects in Eca-109 cells, as it induces cell cycle arrest at the G1 phase through the increase in p27^{kip1} and apoptosis, with a decrease in the ratio of Bel-2:Bax. Similar results were obtained in an *in vivo* mouse model of esophageal cancer treated with ursolic acid.^{187, 188}

The incidence of colorectal cancer is increasing, mainly because of modifications in eating habits.³ In an *in vivo* model of the formation of aberrant crypt foci (ACF) induced by azoxymethane, which is a model of colorectal cancer, ursolic acid had a chemopreventive effect on the initiation phase of the formation of ACF, which was correlated with the increase of neutral shingomyelinase, an enzyme that is downregulated in cancer cells.¹⁸⁹ Ursolic acid reduced the formation of ACF induced by 1,2-dimethylhydrazine.¹⁹⁰

Ursolic acid is active against several colorectal cancer cell lines (Table 1.3.5). In HT-29 cells, ursolic acid induces apoptosis through the activation of caspases 8 and 9, as a consequence of the increase in the levels of DNA-histone complexes¹⁹¹ and in the activity of alkaline sphingomyelinase.¹⁹² Shan *et al* reported that HT-29 cells treated with ursolic acid undergo apoptosis via suppression of the phosphorylation of the epidermal growth factor receptor (EGFR), downregulation of ERK1/2, p38 MAP kinase and JNK and

increase in the expression of Bcl-2 and Bcl-xL, with consequent activation of caspases 9 and 3.¹⁹³

Several pathways are altered in colorectal cancer. COX-2, an inducible enzyme that is present in 90% of colorectal cancers, plays an essential role in tumorigenesis and chemoresistance.^{194, 195} HCT15 cells overexpress COX-2, which is in contrast with HCT116 cells, which do not express this enzyme, rendering HCT116 cells more sensitive to treatment with ursolic acid. In HT-29 cells with ursolic acid-induced apoptosis, COX-2 was overexpressed via the activation of the p38 MAP kinase pathway as a mechanism of apoptosis resistance.¹⁹⁶

Table 1.3.5. IC₅₀ (μM) for ursolic acid in colorectal cancer cell lines.

| Entry | Cell line | IC ₅₀ (μM) | Assay | Time (h) | Ref. |
|-------|-----------|-----------------------|----------------|----------|------|
| 1 | | 30.0 | Crystal violet | 3 | 197 |
| 2 | | 20.0-40 | WST-1 | 24 | 191 |
| 3 | HT-29 | 26.0/20.0/18.0 | MTT | 24/48/72 | 193 |
| 4 | | 4.7 | Methylene blue | 72 | 180 |
| 5 | | 26.31 | MTT | 24-72 | 186 |
| 6 | | 25.0 | Trypan blue | 48 | 196 |
| 7 | | 30.0 | MTT | 72 | 198 |
| 8 | | 2.5-4 | MTT | 48 | 199 |
| 9 | HCT15 | 10.7 | SRB | 48 | 200 |
| 10 | | 7.2 | - | - | 201 |
| 11 | | 17.5 | SRB | 48 | 202 |
| 12 | | 9.6 | - | 48 | 203 |
| 13 | CO115 | 5-10 | MTT | 48 | 199 |
| 14 | Caco-2 | >50 | MTT | 48 | 204 |
| 15 | | 34.4 | MTS | 96 | 205 |
| 16 | SW480 | 20 | MTT | 72 | 206 |
| 17 | SW620 | 38 | MTT | 72 | 206 |

The TNF-related apoptosis-inducing ligand (TRAIL) is a promising anticancer agent, as it binds to DR4 and DR5 and induces apoptosis; however, resistance to TRAIL is often seen in cancer.²⁰⁷ HCT116 cells are moderately sensitive to ursolic acid and TRAIL;

nevertheless, pretreatment with ursolic acid before treatment with TRAIL enhances the cytotoxicity of the latter. Ursolic acid enhances the protein levels of DR4 and DR5 in HCT116 and HT-29 colorectal cancer cells, which is accompanied by a decrease in the expression of Bcl-xL, survivin and XIAP; these results were confirmed in an *in vivo* model.²⁰⁸ Treatment of SW480 colorectal cancer cells sensitive to TRAIL with ursolic acid induces apoptosis via the downregulation of Bcl-xL, Bcl-2 and survivin.²⁰⁶

The HCT15 and CO115 colorectal cancer cell lines have mutations in KRAS and BRAF, respectively. Ursolic acid inhibits the growth of HCT15^{198, 199, 209} and CO115^{199, 209} cells in a time- and concentration-dependent manner, with inhibition of PI3K activity and decrease in the levels of p-Akt in CO115 cells.^{199, 209} Ursolic acid enhances synergistically the apoptotic effects of 5-fluorouracil in HCT15 cells, with an increase in autophagosomes and a decrease in mutant p53 and phosphor-mammalian target of rapamycin (p-mTOR).²¹⁰ DNA damage is one of the causes of induction of tumorigenesis. Oxygen peroxide (H₂O₂) can induce DNA damage; ursolic acid protects Caco-2 cells from H₂O₂ damage by increasing incision activity for DNA repair.²⁰⁴

Hepatocellular carcinoma is one of the most deadly cancers, with poor chemotherapeutic options.^{3, 211} Treatment of different hepatic cancer cell lines with low doses of ursolic acid (Table 1.3.6, entries 8, 16, 17 and 19) induces apoptosis through an increase in DNA fragmentation and in the activity of caspases 3 and 8, decrease in membrane potential and in the activity of Na⁺-K⁺-ATPase, and suppression of vascular endothelial growth factor (VEGF) and ICAM-1 which are two molecules that are important for angiogenesis and invasion in cancer.²¹² Caspase activation and DNA fragmentation were observed by others in Hep G2 cells.²¹³⁻²¹⁵ The induction of apoptosis and of the cell cycle arrest by ursolic acid in Hep G2 cells is due to the downregulation of the PI3K/Akt pathway, with consequent downregulation of survivin²¹³ and upregulation of p53, leading to the downregulation of Bcl-2 and Bcl-xL, upregulation of Bax and p21^{waf1} ^{213, 214} and inhibition of topoisomerase I and replication protein A.²¹⁴ Pretreatment with ursolic acid has chemoprotective effects in Hep G2 cells treated with *t*-butyl hydroperoxide, via DNA repair.²¹⁶

MDR is one of the main causes of failure of chemotherapeutic drugs. The expression of Pgp, which encodes a membrane transporter, is associated with MDR. Doxorubicin is

one of the main combinational therapeutic options for the treatment of hepatic cancer, although its application is limited because of drug resistance induced by Pgp.²¹⁷ Doxorubicin resistant Hep G2 cells (R-Hep G2) (Table 1.3.6, entries 12 and 13) are sensitive to ursolic acid treatment. These results were confirmed *in vivo* in xenographic nude mice.^{218, 219} Ursolic acid can circumvent the effects of Pgp, as it is not a substrate of this pump.²¹⁸ Ursolic acid induces apoptosis in R-Hep G2 cells through the activation of the extrinsic and intrinsic death pathways, with increase in the levels of the ligand of the Fas death receptor (FasL) and *t*Bid and increase in apoptosis inducing factor (AIF).^{218, 219}

Table 1.3.6. IC₅₀ (μM) for ursolic acid in several hepatic cancer cell lines.

| Entry | Cell line | IC ₅₀ (μM) | Assay | Time (h) | Ref. |
|-------|-----------|-----------------------|-------------|----------|----------|
| 1 | | 21.10 | MTT | - | 220 |
| 2 | | 53.42 | MTT | 24-72 | 186 |
| 3 | | 68.82 | MTT | 24 | 184 |
| 4 | | 37.0 | MTT | 48 | 218 |
| 5 | | 33.96 | MTT | 48 | 219 |
| 6 | Hep G2 | 31.54/26.65 | MTT | 48/72 | 213 |
| 7 | | 20-30 | MTT | 48 | 214 |
| 8 | | 4-8 | MTT | - | 212 |
| 9 | | 30-40 | MTT | 72 | 216 |
| 10 | | 20 | Trypan Blue | 72 | 215 |
| 11 | | 87.4 | MTS | 96 | 205, 221 |
| 12 | R-Hep G2 | 20.0 | MTT | 48 | 218 |
| 13 | R-Hep G2 | 21.3 | MTT | 48 | 219 |
| 14 | Bel-7402 | 98.5 | SRB | 48 | 182 |
| 15 | SMMC-7721 | 45.72 | MTT | 24 | 222 |
| 16 | Hep3B | 4-8 | MTT | - | 212 |
| 17 | HuH7 | >8 | MTT | - | 212 |
| 18 | HuH7 | 75 | MTT | 24 | 223 |
| 19 | HA22T | 8.0 | MTT | - | 212 |

Ursolic acid induces apoptosis in a dose-dependent way in the SMMC-7721 and HuH7 cell lines (Table 1.3.6, entries 15, 17 and 18), with induction of Bax and downregulation of Bcl-2.^{222, 223} In SMMC-7721 cells, ursolic acid induces p53, thus

modifying the expression of GDF15, SOD2, ATF3 and *fos*.²²² HuH7 cells treated with ursolic acid exhibit a downregulation of NF- κ B, leading to the downregulation of XIAP.²²³

Diethylnitrosamine (DEN) is known as a chemical carcinogenic agent that is present mainly in tobacco smoke. Hepatocarcinogenesis induced by DEN in mice and promoted by phenobarbital is characterized by high levels of lipid peroxidation and carbonyl proteins. Oral administration of ursolic acid reduces the levels of lipid peroxidation and protein carbonyls, restoring membrane integrity.²²⁴

Cancers of the uterine cervix, uterine corpus and ovaries are responsible for 5% of all cancers diagnosed in women, with a death incidence of 4.9%.^{3, 5} Ursolic acid is active against cervical cancer cells, inducing cell death (Table 1.3.7, entries 1-4). Cervix cancer HeLa cells treated with ursolic acid exhibit accumulation in the sub-G1 phase (apoptosis) as a result of the activation of caspase 8. Calpain and CDK5 are also upregulated by ursolic acid in HeLa cells and may play an important role in apoptosis induction.²²⁵

Mutations of the tumor suppressor PTEN are found in 30-50% of all human endometrial cancers. PTEN blocks G1 cell cycle progression, induces apoptosis and regulates the PI3K/Akt cell survival pathways.^{226, 227} Exposure of SNG-II and HEC108 endometrial cancer cells to ursolic acid reduce the levels of p-Akt, PI3K and downstream targets, MAP kinase and p-P44/42, inducing apoptosis.²²⁸

Ursolic acid inhibits the proliferation of CAOV3 ovary cancer cells, with an IC₅₀ higher than 40 μ M (Table 1.3.7, entry 9). ERK plays an important role in cell growth, development, division, death and malignant transformation. Ursolic acid decreases ERK and its phosphorylation in CAOV3 cells and inhibits MAP kinase phosphatase (MKP)-1, an enzyme that regulates the expression of ERK via its degradation. Ursolic acid also increases the levels of Bax and decreases the levels of Bcl-2 in CAOV3 cells, inducing apoptosis.²²⁹

Breast cancer is the number one cause of death by cancer in women.^{3-5, 230} Ursolic acid has chemopreventive effects in mammary carcinoma.²³¹ Ursolic acid prevents the induction of COX-2 and the synthesis of prostaglandin E₂ in human mammary epithelial cells treated with phorbol 12-myristate-13-acetate, by activating ERK1/2, JNK and p38

MAP kinase.¹⁶¹ Ursolic acid was ineffective in the inhibition of the mammary tumorigenesis induced by DMBA in rats.²³²

Table 1.3.7. IC₅₀ (μM) for ursolic acid in uterine cervix, ovary and breast carcinoma cell lines.

| Entry | Cell line | IC ₅₀ (μM) | Assay | Time (h) | Ref. |
|-------------------------|------------|-----------------------|-------|----------|----------|
| <i>Cervix carcinoma</i> | | | | | |
| 1 | | >10 | MTT | 72 | 185 |
| 2 | HeLa | 108.0 | SRB | 48 | 182 |
| 3 | | 33.12 | MTT | 24 | 184 |
| 4 | UIISO | 7.0 | - | - | 201 |
| <i>Ovary carcinoma</i> | | | | | |
| 5 | | >10 | MTT | 72 | 185 |
| 6 | SKOV3 | >10 | MTT | 96 | 183 |
| 7 | | 7.9 | - | 48 | 203 |
| 8 | | 9.6 | SRB | 48 | 200 |
| 9 | CAOV3 | >40 | MTT | 48 | 229 |
| 10 | OVCAR-5 | 7.0 | - | - | 201 |
| 11 | A2780 | 20.8 | - | - | 233 |
| <i>Breast carcinoma</i> | | | | | |
| 12 | MCF-7/wt | 30 | MTT | 72 | 206 |
| 13 | MCF-7/ADR | 40 | MTT | 72 | 206 |
| 14 | BT-20 | 48 | MTT | 48 | 234 |
| 15 | | 53 | MTT | 48 | 235 |
| 16 | | 178.0 | MTT | 72 | 236 |
| 17 | MCF-7 | 10.3 | MTT | 72 | 237 |
| 18 | | 18.2 | MTS | 96 | 205, 221 |
| 19 | | 17.5 | SRB | 48 | 202 |
| 20 | | 3.3 | MTT | 72 | 237 |
| 21 | MDA-MB-231 | 40 | MTT | 24/48 | 238 |
| 22 | | 25-50 | SRB | 24 | 239 |

Breast cancer is known to be influenced by several hormones, more specifically, estrogen and progesterone. Aromatase plays an important role in the production of

estrogen. Triterpenoids, such as ursolic acid, have a structure that is similar to that of steroids, rendering them good leading molecules for hormonal-related therapy.²⁴⁰ Ursolic acid is an inhibitor of aromatase, with an IC₅₀ of 32 μM.²⁴¹

Ursolic acid inhibits the proliferative activity of MCF-7 cells (Table 1.3.7, entries 15-19) via the induction of the intrinsic mitochondrial apoptotic pathway, with poly ADP-ribose polymerase (PARP) cleavage and downregulation of Bcl-2 proteins. In these cells ursolic acid was shown to modulate glucocorticoid receptor content.²³⁵

Treatment of the highly metastatic MDA-MB-231 cancer cells with ursolic acid leads to a decrease in cell viability (Table 1.3.7, entries 20-21). Ursolic acid induces apoptosis through both intrinsic and extrinsic pathways, with downregulation of Bcl-2, upregulation of Bax, release of cytochrome c, decrease of mitochondrial membrane potential and induction of the Fas receptor.²³⁸ Ursolic acid has the ability to inhibit the migration and invasion of MDA-MB-231 cells via the inhibition of the Akt/mTOR and NF-κB signaling pathways, which results in the inhibition of MMP-2 and the urokinase-type plasminogen activator (uPA).²³⁹

Prostate cancer is the leading cause of cancer-related death in men.³⁻⁵ In the initial stages of prostate cancer, cells are dependent of androgens for growth, but progression to an androgen-independent growth can occur, leading to the most lethal phenotypes of the disease.²⁴²

The androgen-sensitive cells LNCaP undergo apoptosis when treated with ursolic acid (Table 1.3.8, entries 6-8).²⁴³⁻²⁴⁵ In the LNCaP and LNCaP-AI (androgen insensitive) cell lines, ursolic acid has the ability to disturb the ratio of Bcl-2:Bax, inducing apoptosis through the intrinsic pathway.^{243, 244} The decrease in Bcl-2 is due to its phosphorylation and consequent degradation by the activation of a JNK-mediated pathway.²⁴⁴ LNCaP cells treated with ursolic acid present a decrease in the phosphorylation of IKK, thus preventing the activation of NF-κB, a decrease in the phosphorylation of signal transducer and activator of transcription (STAT) 3 (which is related to the decrease of IL-6) and a decrease in p-Akt, culminating in apoptosis.²⁴⁵

Ursolic acid can inhibit the proliferation of hormone refractory prostate cancer cells PC-3 (Table 1.3.8, entries 10-13).^{243, 246, 247} PC-3 cells treated with ursolic acid exhibit a decrease in Bcl-2, which is related to the activation of the JNK pathway.^{243, 246} Treatment

of PC-3 cells with ursolic acid leads to the inhibition of the Akt pathway, subsequently increasing the expression of FasL, inducing the extrinsic apoptotic pathway, reducing MMP-9 expression and inhibiting invasion to adjacent tissues.²⁴⁶ The reduction of p-Akt through the disruption of the mTOR pathway is correlated with the induction of autophagy in PC-3 cells treated with ursolic acid. The activation of autophagy is correlated with G1 cell cycle arrest, with upregulation of p21^{waf1} and p27 and downregulation of cyclins D1 and D3 and CDK4.²⁴⁷

Table 1.3.8. IC₅₀ (μM) for ursolic acid in prostate carcinoma cell lines.

| Entry | Cell line | IC ₅₀ (μM) | Assay | Time (h) | Ref. |
|-------|---------------|-----------------------|-------|----------|------|
| 1 | | >100 | MTT | 24 | 234 |
| 2 | | 25-50 | MTT | 72 | 245 |
| 3 | DU145 | >50 | MTT | 24 | 248 |
| 4 | | 20-30 | MTT | 24 | 247 |
| 5 | | 50 | MTT | 72 | 249 |
| 6 | | 20-25 | MTT | 72 | 245 |
| 7 | LNCaP | 15.7 | MTT | 48 | 243 |
| 8 | | 20-50 | MTT | 48 | 244 |
| 9 | LNCaP-AI | 20-50 | MTT | 48 | 244 |
| 10 | | >40 | MTT | 24 | 247 |
| 11 | PC-3 | 40-80 | MTT | 72 | 246 |
| 12 | | 32.6 | MTT | 48 | 243 |
| 13 | | 30.5 | SRB | 48 | 202 |
| 14 | RC-58T/h/SA#4 | 10-20 | SRB | 72 | 250 |

Ursolic acid inhibits growth in the DU145 prostate cancer cell lines, which is an androgen-independent cell line (Table 1.3.8, entries 1-5). DU145 cells treated with ursolic acid undergo apoptosis via the downregulation of Bcl-2, due to the activation of the JNK signaling pathway, which induces phosphorylation of Bcl-2 and its consequent degradation.²⁴⁹ DU145 cells treated with ursolic acid exhibit a decrease in the phosphorylation of IKK, which impairs the activation of NF-κB; there is also a decrease

in p-STAT 3. The downregulation of the NF- κ B and STAT 3 pathways was also observed in a xenograft mouse model of DU145 prostate cancer cells.²⁴⁵

CXCR4 and CXCL12 are chemokine receptors that are involved in tumor proliferation, invasion and metastasis. Ursolic acid has the ability to reduce the mRNA expression of these receptors in DU145 and PC-3 prostate cancer cells. This downregulation is enabled by the suppression of NF- κ B. In a transgenic model of prostate cancer, ursolic acid also decreased the expression of CXCR4, which correlated with the decrease of metastasis to the lung, liver and gastro-intestinal tract.²⁴⁸

Ursolic acid induced apoptosis in a primary cell line of prostate cancer, RC-58T/h/SA#4, through activation of caspases 8 and 9, with a decrease in Bcl-2 levels.²⁵⁰

Lung cancer is one of the deadliest cancers, representing 27% of the deaths by cancer worldwide.³⁻⁵ Ursolic acid can induce cell cycle arrest, inhibit proliferation and inhibit invasion and migration in A549 human non-small lung cancer cells (Table 1.3.9, entries 1-6).^{251, 252} Ursolic acid induces cell cycle arrest at the G1 phase and apoptosis in A549 lung cancer cells because of the increase in p21^{waf1} expression in a p53-dependent manner, decrease in cyclins and CDKs, increase in the expression of I κ B- α (leading to a decrease in the expression of NF- κ B), increase in the apoptotic proteins Bax and FasL and decrease in the anti-apoptotic proteins Bcl-2 and Bcl-xL.²⁵¹ Alterations in NF- κ B expression were also observed in H1299 and ASTC-a-1 lung cancer cells.^{165, 253}

Ursolic acid treatment can prevent the invasion and migration of A549, H3255 and Calu-6 lung cancer cells through a decrease in the production of VEGF and transforming growth factor (TGF)- β 1 and suppression of the expression of ICAM-1, fibronectin and MMP-9 and -2.²⁵² Suppression of MMP-9 is observed in H1299 lung cancer cells.¹⁶⁵ H460 lung cancer cells treated with ursolic acid exhibit an increase in the expression of the MMP-1, -2, -3, -9 and -10 genes, which is correlated with the induction of apoptosis.²⁵⁴

Ursolic acid sensitizes ASTC-a-1 cells to paclitaxel and cisplatin, reducing the need of high doses of these two chemotherapeutic drugs. The combination of paclitaxel or cisplatin with ursolic acid induces apoptosis through the activation of the intrinsic pathway, via overexpression of *t*Bid and activation of the Fas/FasL-caspase 8 pathway; inhibition of NF- κ B was also observed.²⁵³

Skin cancer is one of the most common types of cancer and is responsible for nearly half of the diagnosed cancers in the Caucasian population.^{3, 5} Melanoma is the deadliest of the skin cancers, once it affects deeper layers of the skin, and has the ability to spread to other tissues.²⁵⁵ Ursolic acid is well known to inhibit TPA-induced skin tumorigenesis in mice,^{171, 256-258} with increased levels of mRNA expression for COX-1, COX-2, and TNF- α .¹⁷¹

Table 1.3.9. IC₅₀ (μ M) for ursolic acid in lung and skin cancer cell lines.

| Entry | Cell line | IC ₅₀ (μ M) | Assay | Time (h) | Ref. |
|-----------------------|-----------|-----------------------------|-------------|----------|------|
| <i>Lung carcinoma</i> | | | | | |
| <i>1</i> | | 4-8 | MTT | 48 | 252 |
| <i>2</i> | | 40 | XTT | 48 | 251 |
| <i>3</i> | A549 | 9.4 | SRB | 48 | 200 |
| <i>4</i> | | 42.5 | MTT | 72 | 237 |
| <i>5</i> | | >100 | MTT | 24 | 234 |
| <i>6</i> | | 9.2 | - | 48 | 203 |
| <i>7</i> | H3255 | 8-16 | MTT | 48 | 252 |
| <i>8</i> | Calu-6 | 8-16 | MTT | 48 | 252 |
| <i>9</i> | H460 | 10 | Trypan Blue | 24 | 254 |
| <i>Skin carcinoma</i> | | | | | |
| <i>10</i> | B16 2F2 | 4.8 | - | 72 | 259 |
| <i>11</i> | B16 F0 | 10-12.5 | Trypan Blue | 48 | 260 |
| <i>12</i> | | 10 | SRB | 48 | 200 |
| <i>13</i> | B16 F10 | 50 | MTT | 24 | 261 |
| <i>14</i> | B16 | 10 | MTT | 96 | 262 |
| <i>15</i> | M4Beu | 12.5-15.0 | Trypan Blue | 48 | 263 |
| <i>16</i> | A431 | 50 | MTT | 48 | 264 |
| <i>17</i> | A375 | 8.0 | Microscopy | 72 | 265 |
| <i>18</i> | SK-MEL-2 | 10.8 | SRB | 48 | 200 |
| <i>19</i> | SK-MEL-3 | 10.1 | - | 48 | 203 |

Treatment of mouse melanoma B16 cells with ursolic acid induces an increase in the number of cells at the G1 phase of the cell cycle, and increased concentrations of the triterpenoid induce apoptosis (Table 1.3.9, entry 14).²⁶² Ursolic acid induces apoptosis in

B16 F10 cells, with induction of the p53 gene and downregulation of Bcl-2 through the inhibition of NF- κ B.²⁶¹ In M4Beu cancer cells, ursolic acid treatment induces apoptosis with activation of caspase 3 through the intrinsic mitochondrial pathway, with a decrease in Bcl-2 levels and increase in Bax levels.^{263, 266} Activation of caspase 3 with induction of apoptosis are observed in A431²⁶⁴ and HaCaT^{266, 267} cancer cells treated with ursolic acid. Ursolic acid has the ability to inhibit reverse transcriptase in A371 cancer melanoma cells, with consequent induction of apoptosis and differentiation.²⁶⁵

Melanoma is well known to being resistant to chemotherapeutic drugs. Ursolic acid can overcome this feature by inducing apoptosis in B16 F0 melanoma chemoresistant cells via the repression of tyrosinase-related protein (TRP)-2, an enzyme that is involved in melanogenesis (Table 1.3.9, entries 11 and 12).^{260, 268}

Several proteases, such as urokinase and cathepsins, play an important role in the invasion and metastasis of cancers.²⁶⁹ Ursolic acid is an inhibitor of the activity of urokinase (IC₅₀ 12 μ M) and cathepsin (IC₅₀ 10 μ M); the inhibition of these two enzymes is associated with the reduction of the number of lung metastasis in mice bearing B16 melanoma cancer.²⁷⁰

Ursolic acid increases the cell mediated immune response against B16 F10 metastatic tumors in mice via activation of natural-killer cell activity and increase in antibody-dependent cell-mediated cytotoxicity and antibody-dependent complement-mediated cytotoxicity.²⁷¹

Leukemia, a blood cancer, is responsible for 2.8% of the new cases of cancer diagnosed every year.^{3, 5} Treatment of different leukemia cell lines with ursolic acid has antiproliferative effects (Table 1.3.10, entries 1-16). The induction of apoptosis by ursolic acid in HL60 cancer cells is associated with increased levels of intracellular Ca²⁺²⁷² and with induction of the inhibitory effects of c-AMP.²⁷³ In a more recent study, ursolic acid was shown to induce HL60 monocytic differentiation through the activation of the ERK pathway.²⁷⁴ Its ability to induce cell death was observed in the MDR cancer cells, HL60/ADR and K562/ADR, although this required higher doses of ursolic acid (Table 1.3.10, entries 8 and 16).²⁰⁶ In K562 cancer cells, ursolic acid induces apoptosis through the downregulation of Bcl-xL and upregulation of p-JNK.²⁷⁵ In KBM-5 cancer cells,

ursolic acid inhibits NF- κ B-DNA binding, deregulating this pathway; it also suppress the TNF-mediated induction of cyclin D1, COX-2 and MMP-9.¹⁶⁵

In L1210, K562 and HL60 leukemia cells treated with oxygen peroxide, ursolic acid pretreatment inhibits DNA damage, via the impairment of the generation of ROS species.²⁷⁶ The combination of ursolic acid and doxorubicin results in an antagonistic effect, decreasing the apoptotic effects of doxorubicin in L1210 and HL60 cells and its differentiation effects in K562 cancer cells. The antagonistic effects of ursolic acid are likely due to its antioxidant properties by modulating glutathione (GSH) metabolism.²⁷⁷

Table 1.3.10. IC₅₀ (μ M) for ursolic acid in leukemia and lymphoma cancer cell lines.

| Entry | Cell line | IC ₅₀ (μ M) | Assay | Time (h) | Ref. |
|-----------------|-----------|-----------------------------|-----------------|----------|------|
| <i>Leukemia</i> | | | | | |
| 1 | | 32.6 | NBT | 120 | 274 |
| 2 | | 5-10 | MTT | - | 272 |
| 3 | | 10.9 | Trypan Blue | 24 | 277 |
| 4 | | 17.0 ^a | TB exclusion | 24 | 276 |
| | HL60 | | Twentyman | | |
| 5 | | 157.6 | and Luscombe | 48 | 182 |
| 6 | | 29.0 | MTT | 72 | 206 |
| 7 | | 19.0 | MTT | - | 181 |
| 8 | HL60/ADR | 32.0 | MTT | 72 | 206 |
| 9 | | 14.6 | Trypan Blue | 24 | 277 |
| 10 | L1210 | 12.0 ^a | TB exclusion | 24 | 276 |
| 11 | | 8.8 | XTT | 48 | 278 |
| 12 | | 17.0 ^a | TB exclusion | 24 | 276 |
| 13 | | 33.0 | MTT | 72 | 206 |
| 14 | K562 | 17.2 | SRB | 48 | 202 |
| 15 | | 38.9 | XTT | 72 | 279 |
| 16 | K562/ADR | 43.0 | MTT | 72 | 206 |
| <i>Lymphoma</i> | | | | | |
| 17 | P3HR1 | 5.5 | XTT | 72 | 279 |

a) Value for IC₈₀

Ursolic acid has the ability to suppress the activation of STAT 3, which is constitutively activated in multiple myeloma, by suppressing its nuclear translocation and DNA-binding activity, leading to the downregulation of cyclin D1, survivin, Bcl-2, Bcl-xL and Mcl-1. Ursolic acid also potentiates the effects of the proteasome inhibitor bortezomib and of the TNF inhibitor thalidomide, which are used currently in the treatment of multiple myeloma.²⁸⁰

C6 glioma cells treated with ursolic acid have less invasive potential. Ursolic acid inhibits directly the interaction of ZIP/p65 with protein kinase C (PKC)- ζ , which leads to the blockage of the NF- κ B-dependent pathway induced by IL-1 β or TNF- α . This sequence of events permits the decrease in activity and levels of expression of MMP-9, which is a key enzyme for the invasion of C6 glioma cells.²⁸¹ The downregulation of MMP-9 was observed in HT1080 fibrosarcoma cells.^{162, 163}

Table 1.3.11. IC₅₀ (μ M) for ursolic acid in several cancer cell lines.

| Entry | Cell line | IC ₅₀ (μ M) | Assay | Time (h) | Ref. |
|-----------------------------|-----------|-----------------------------|------------|----------|------|
| <i>Glioma</i> | | | | | |
| 1 | U87 | >100 | MTT | 24 | 234 |
| 2 | | 9.0 | Microscopy | 72 | 265 |
| 3 | C6 | 48.0 | MTT | 24 | 281 |
| <i>Neuroblastoma</i> | | | | | |
| 4 | U251 | 15.1 | SRB | 48 | 202 |
| 5 | XF498 | 10.7 | SRB | 48 | 200 |
| 6 | | 9.9 | - | 48 | 203 |
| 7 | SH-SY5Y | 54.6 | MTT | 24 | 184 |
| <i>Pancreatic carcinoma</i> | | | | | |
| 8 | AsPC-1 | >100 | MTT | 24 | 234 |
| <i>Bladder carcinoma</i> | | | | | |
| 9 | NTUB1 | 29.4 | MTT | 72 | 282 |
| <i>Thyroid carcinoma</i> | | | | | |
| 10 | ARO | 7.0 | Microscopy | 72 | 265 |

Ursolic acid inhibits the differentiation of U87 glioblastoma cells and ARO thyroid carcinoma cells through the inhibition of endogenous reverse transcriptase (Table 1.3.11, entries 1, 2 and 10).²⁶⁵

Angiogenesis consists in the formation of new capillaries from pre-existing vessels and is essential for tumor progression. Angiogenesis comprises several steps, which include the stimulation of endothelial cells by growth factors (such as VEGF), the release of proteolytic enzymes (such as MMPs), the subsequent degradation of the extracellular matrix (ECM) followed by invasion through ECM, migration and proliferation of endothelial cells and, finally, the formation of new capillary tubes.²⁸³ Ursolic acid inhibits endothelial cell proliferation with an IC_{50} of 5 μ M and has inhibitory effects on the angiogenic process in chorioallantoic membranes of the chick embryo, with an ID_{50} of 10 nmol/egg.^{284, 285}

High concentrations of ursolic acid promote angiogenesis through the formation of capillary-network-like structures with activation of the PI3K-Akt pathway in HUVECs cultured in serum-free medium. These effects, however, were not observed in HUVECs treated with low concentrations of ursolic acid and were contradictory with those obtained with HUVECs cultured in medium supplemented with serum.²⁸⁶ These observations suggest that the effects of ursolic acid on the angiogenic process are dependent on the concentrations and cell culture medium used.

The antiangiogenic effects of ursolic acid were specifically observed in mice bearing melanoma B16 F10 cells, with decrease in the levels of VEGF, MMP-2, MMP-9 and NO;²⁸⁷ in colorectal cancer cells, in a dose-dependent manner;²⁸⁸ and in hepatoma cell lines, with decrease of the mRNA expression of the hypoxia-inducible transcription factor (HIF)-1 α , VEGF, IL-8 and uPA and in the production of ROS and NO.²⁸⁹

Chemotherapy and radiotherapy often produce detrimental side effects. Ursolic acid has no proven cytotoxic effects *in vitro* (Table 1.3.12 and references cited therein) and in *in vivo* models.^{77, 133, 234} Ursolic acid reduces the mutagenicity of doxorubicin in mice,²⁹⁰ enhances hematopoietic recovery after radiation treatment of sarcoma in mice²⁹¹ and reduces lipid oxidation and DNA damage after UVB radiation in human lymphocytes.²⁹²

Table 1.3.12. Cytotoxic effects of ursolic acid in nontumoral cell lines, represented as IC₅₀ (μM).

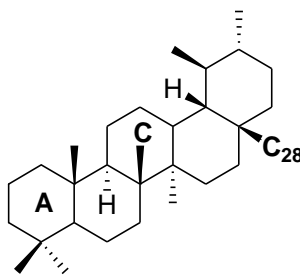
| Entry | Cell line | Cell type | IC ₅₀ (μM) | Assay | Time (h) | Ref. |
|-------|-----------|----------------------|-----------------------|------------|----------|------|
| 1 | L-02 | Liver | >8 | MTT | - | 212 |
| 2 | HFLF | Lung fibroblast | 21.28 | MTT | 24 | 184 |
| 3 | GES-1 | Gastric epithelium | 93.83 | MTT | 48 | 186 |
| 4 | HSF | Gingival fibroblasts | 54.7 | MTT | 24 | 179 |
| 5 | MEF | Fibroblast | >50 | MTT | 24 | 248 |
| 6 | WI38 | Fibroblast | 160.0 | Microscopy | 72 | 265 |

The proven effects of ursolic acid in several targets of cancer cells and its effects in animal models render this triterpenoid a potential lead for use in the chemoprevention and chemotherapeutic treatment of cancer.

1.3.3.3. Semisynthetic derivatives with antitumor activity

Ursolic acid has been modified with the aim of improving the pre-existent antitumor activity. The main sites of modification were located at carbons C2, C3, C11 and C28 of the ursane backbone, generating several derivatives.

Ursolic acid was first investigated for its anti-inflammatory properties, which are related with its ability to inhibit NO production and COX activation.^{159, 164} The induction of NO synthase is also observed in cancer, with production of high levels of NO in cancerous cells. Honda *et al* synthesized a series of new ursolic acid derivatives that can inhibit the production of NO in mouse macrophages. Most of the synthetic derivatives presented better activity compared with that of ursolic acid, as ursolic acid is toxic above 10 μM and is inactive below 10 μM in mouse macrophages (Table 1.3.13).²⁹³⁻²⁹⁵

Table 1.3.13. IC₅₀ (μM) of ursolic acid derivatives for the inhibition of the production of NO in mouse macrophages.

| Entry | Compd | Ring A | Ring C | C28 | IC ₅₀ (μM) |
|-------|--------------|--------|--------|-------|-----------------------|
| 1 | 1.1 | | | COOH | 5.1 |
| 2 | 1.2 | | | COOH | 17.6 |
| 3 | 1.3 | | | COOMe | 8.9 |
| 4 | 1.4 | | | COOMe | 0.1 |
| 5 | 1.5 | | | COOH | 0.8 |
| 6 | 1.6 | | | COOMe | 5.1 |
| 7 | 1.7 | | | COOH | 6.2 |
| 8 | Ursolic acid | - | - | - | Toxic |

Kwon *et al* synthesized a series of new ursane derivatives, **1.8-1.15** (Figure 1.3.4) that can inhibit the synthesis and production of NO in RAW247 cells, with better activity

than that of the parental compound, ursolic acid. Compound **1.14** at 20 μM was the best compound identified, with an NO inhibition of 93.7%.²⁹⁶

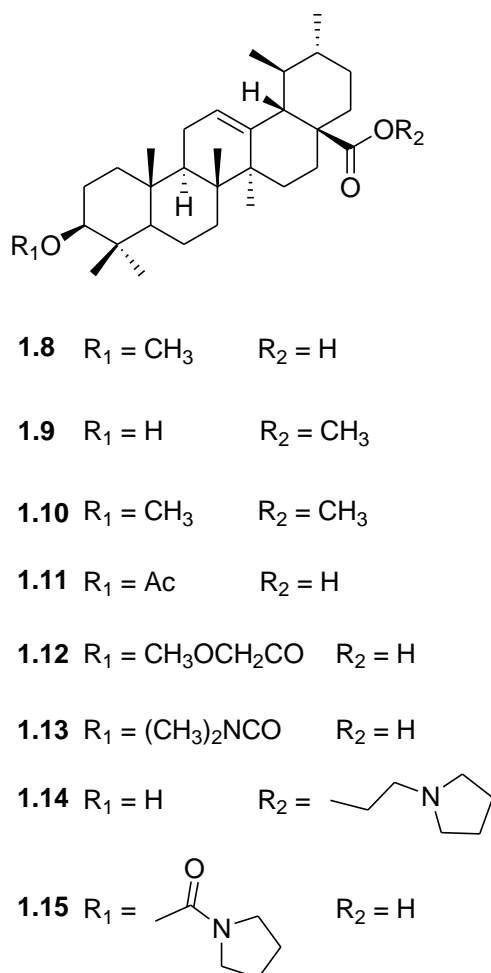
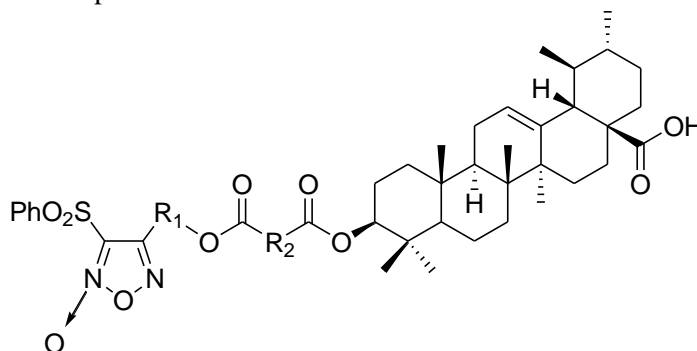
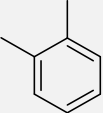
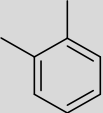


Figure 1.3.4. Schematic representation of compounds **1.8-1.15**.

High concentrations of NO can be cytotoxic, induce apoptosis in tumor cells, prevent metastasization and assist macrophage killing tumor cells.^{297, 298} NO can be generated by synthetic NO-donors, such as furoxan, nitrate and diazeniumdiolate.^{299, 300} A series of furoxan NO-donating derivatives of ursolic acid (at carbon C3), derivatives **1.16-1.21**, were synthesized and evaluated for their cytotoxic activity against Hep G2 cancer cells (Table 1.3.14, entries 1-6). Compounds **1.16-1.19** and **1.21** have been proven to be more active than ursolic acid (Table 1.3.14, entry 7) and 5-fluorouracil (Table 1.3.14, entry 8) in the inhibition of Hep G2 cell growth.²²⁰

Table 1.3.14. IC₅₀ (μM) of the ursolic acid derivatives **1.16-1.21** and 5-fluorouracil in Hep G2 cancer cells.

| Entry | Compd | R ₁ | R ₂ | IC ₅₀ (μM) |
|-------|----------------|---|--|-----------------------|
| 1 | 1.16 | O(CH ₂) ₂ | O(CH ₂) ₂ | 3.20 |
| 2 | 1.17 | O(CH ₂) ₃ | O(CH ₂) ₂ | 10.74 |
| 3 | 1.18 | O(CH ₂) ₂ (CH ₃)CH | O(CH ₂) ₂ | 5.42 |
| 4 | 1.19 | O(CH ₂) ₄ | O(CH ₂) ₂ | 4.93 |
| 5 | 1.20 | O(CH ₂) ₄ |  | 51.36 |
| 6 | 1.21 | O(CH ₂) ₂ (CH ₃)CH |  | 9.76 |
| 7 | Ursolic acid | - | - | 21.10 |
| 8 | 5-Fluorouracil | - | - | 15.96 |

The cytotoxic activity of triterpenoids seems to be strongly correlated with their hydrophilicity. Compounds **1.22-1.26** (Figure 1.3.5), which are highly polar quaternary salts of ursolic acid, were prepared and evaluated for their cytotoxic activity against CEM T-lymphoblastic leukemia cells. Compound **1.24** was the best compound identified with an IC₅₀ of 4.1 μM.³⁰¹

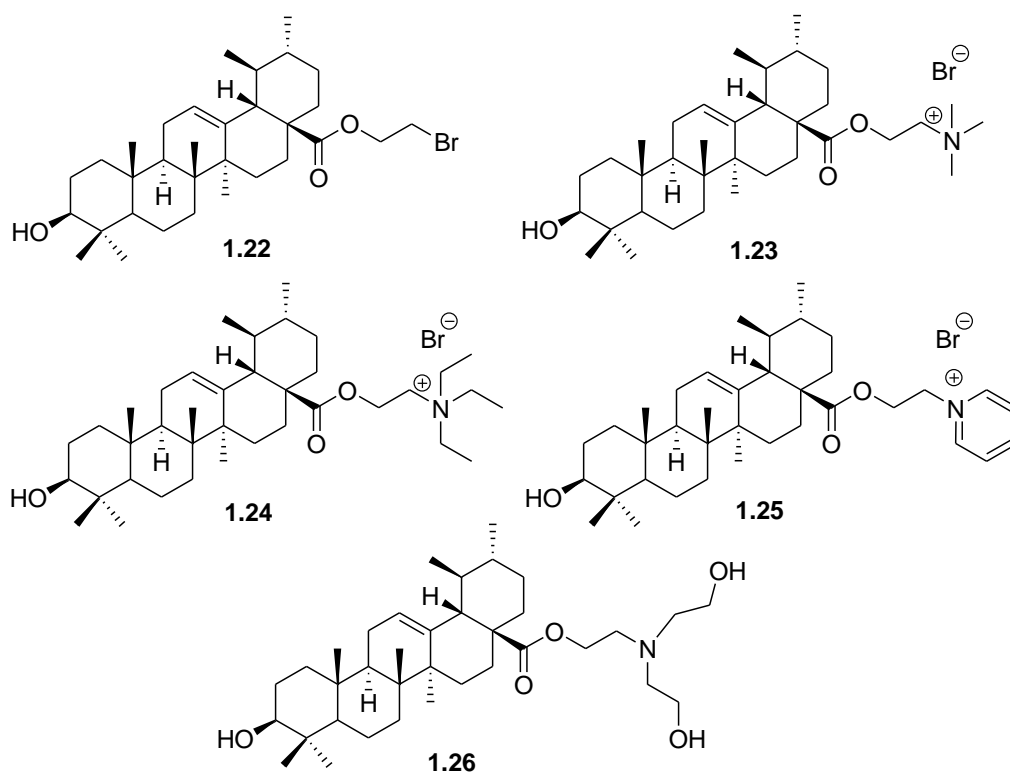


Figure 1.3.5. Schematic representation of compounds 1.22-1.26.

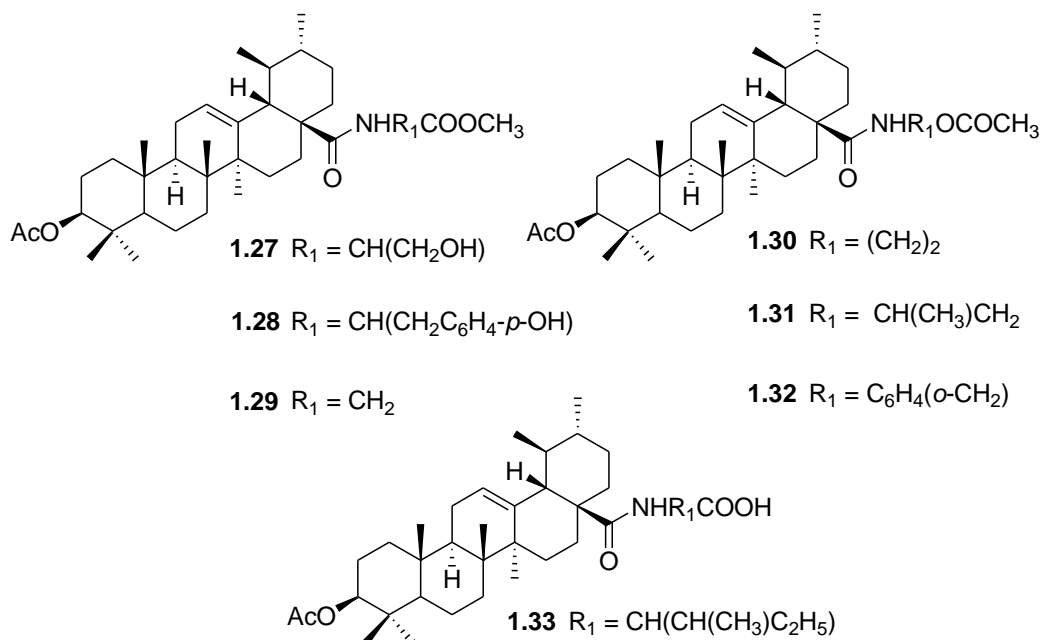


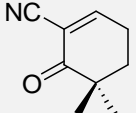
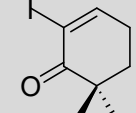
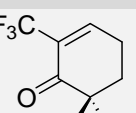
Figure 1.3.6. Schematic representation of compounds 1.27-1.33.

Esterification at carbon C3 and the introduction of an amino group at carbon C28 in the ursolic acid backbone allowed the synthesis of compounds **1.27-1.33** (Figure 1.3.6), which exhibited good cytotoxic activity in ovary SKOV3 and stomach BGC-823 cancer cell lines (Table 1.3.15). Compound **1.31** was the best compound identified.¹⁸³

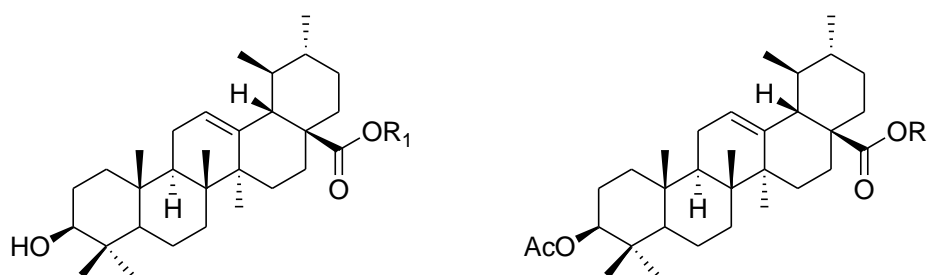
Table 1.3.15. IC₅₀ (μM) for compounds **1.27-1.33** in ovary SKOV3 and stomach BGC-823 cancer cell lines.

| Entry | Compd | IC ₅₀ (μM) | |
|-------|-------|-----------------------|---------|
| | | SKOV3 | BGC-823 |
| 1 | 1.27 | - | >10 |
| 2 | 1.28 | - | >10 |
| 3 | 1.29 | - | >10 |
| 4 | 1.30 | 6.1 | >10 |
| 5 | 1.31 | 2.2 | 8.3 |
| 6 | 1.32 | >10 | >10 |
| 7 | 1.33 | >10 | - |

Table 1.3.16. IC₅₀ (μM) for compounds **1.6, 1.34** and **1.35** in bladder and pancreatic cancer cell lines.

| Entry | Compd | Ring A | IC ₅₀ (μM) | | | |
|-------|-------|---|-----------------------|------|--------|---------|
| | | | 253JB-V | KU7 | PANC-1 | PANC-28 |
| 1 | 1.6 |  | 0.17 | 0.30 | 0.53 | 0.97 |
| 2 | 1.34 |  | 4.9 | 6.02 | 6.91 | 13.49 |
| 3 | 1.35 |  | 0.17 | 0.47 | 0.65 | 1.13 |

Modifications at carbon C2 of the ursane triterpenoid originated compounds **1.4-1.7** (Table 1.3.13, entries 4-7), which were the most active against NO production in macrophages. With the aim of studying the effects of different substituents at carbon C2, compounds **1.6**, **1.34** and **1.35** were evaluated against two bladder (KU7 and 253JB-V) and two pancreatic (PANC-1 and PANC-28) cancer cell lines. Compound **1.6** was the best compound tested (Table 1.3.16, entry 1).³⁰²



1.36 $R_1 = \text{CH}_2\text{CH}(\text{OH})\text{CH}_2\text{OH}$

1.37 $R_1 = \text{CH}_3$

1.38 $R_1 = \text{CH}_2\text{CH}_3$

1.39 $R_1 = \text{CH}_2\text{CH}_2\text{CH}_3$

1.40 $R_1 = \text{CH}(\text{CH}_3)_2$

1.41 $R_1 = \text{CH}_2\text{CH}_2\text{CH}_2\text{CH}_3$

1.42 $R_1 = \text{CH}_2\text{CH}_2\text{CH}_2\text{CH}_2\text{CH}_3$

1.43 $R_1 = \text{CH}_2\text{CH}_2\text{CH}_2\text{CH}_2\text{CH}_2\text{CH}_3$

1.44 $R_1 = \text{CH}_2\text{CH}_2\text{CH}(\text{CH}_3)_2$

1.45 $R_1 = \text{CH}_2\text{CH}_2\text{OH}$

1.46 $R_1 = \text{CH}_2\text{COOC}(\text{CH}_3)_3$

1.47 $R_1 = (\text{CH}_2)_2\text{ONO}_2$

1.48 $R_1 = (\text{CH}_2)_3\text{ONO}_2$

1.49 $R_1 = (\text{CH}_2)_4\text{ONO}_2$

1.50 $R_1 = \text{H}$

1.51 $R_1 = \text{CH}_2\text{CH}_3$

1.52 $R_1 = \text{CH}_2\text{CH}_2\text{CH}_3$

1.53 $R_1 = \text{CH}_2\text{CH}_2\text{CH}_2\text{CH}_3$

1.54 $R_1 = \text{CH}_2\text{CH}(\text{OH})\text{CH}_2\text{OH}$

1.55 $R_1 = \text{CH}_2\text{CH}_2\text{OH}$

Figure 1.3.7. Schematic representation of esters **1.36-1.55** of ursolic acid.

A series of ursane esters, compounds **1.36-1.55** (Figure 1.3.7), were prepared from ursolic acid and evaluated for their cytotoxic activity in several cells lines (Table 1.3.17).^{182, 184, 186, 282}

Table 1.3.17. IC₅₀ (μM) for compounds **1.36-1.55** in colon (HT-29), liver (Hep G2), stomach (BGC-823), bladder (NTUB1), neuroblastoma (SH-SY5Y) and cervix (HeLa) cancer cell lines, and in two nontumorigenic cell lines (HELFL and GES-1).

| Entry | Compd | Cell line | | | | | | | |
|-------|-------|-----------|--------|---------|-------|---------|-------|-------|-------|
| | | HT-29 | Hep G2 | BGC-823 | NTUB1 | SH-SY5Y | HeLa | HELFL | GES-1 |
| 1 | 1.36 | - | 44.23 | 20.51 | - | - | - | - | 154.3 |
| 2 | 1.37 | - | - | 54.1 | 37.13 | - | 51.8 | - | - |
| 3 | 1.38 | - | 70.77 | 69.32 | 13.45 | 66.28 | 29.18 | 81.92 | - |
| 4 | 1.39 | - | 89.11 | 79.68 | 18.28 | 92.52 | 48.03 | >100 | - |
| 5 | 1.40 | - | - | - | 7.97 | - | - | - | - |
| 6 | 1.41 | - | >100 | >100 | 15.64 | >100 | 63.24 | >100 | - |
| 7 | 1.42 | - | - | - | 27.79 | - | - | - | - |
| 8 | 1.43 | - | - | - | 26.16 | - | - | - | - |
| 9 | 1.44 | - | - | - | 10.93 | - | - | - | - |
| 10 | 1.45 | - | - | - | 19.53 | - | - | - | - |
| 11 | 1.46 | - | - | - | >30 | - | - | - | - |
| 12 | 1.47 | - | 79.58 | 84.24 | - | 71.07 | 36.21 | 68.06 | - |
| 13 | 1.48 | - | 87.44 | 98.28 | - | 89.57 | 69.39 | 82.56 | - |
| 14 | 1.49 | - | >100 | >100 | - | >100 | >100 | >100 | - |
| 15 | 1.50 | - | - | 100.0 | 14.27 | - | 50.0 | - | - |
| 16 | 1.51 | - | >100 | >100 | - | >100 | >100 | >100 | - |
| 17 | 1.52 | - | >100 | >100 | - | >100 | >100 | >100 | - |
| 18 | 1.53 | - | >100 | >100 | - | >100 | >100 | >100 | - |
| 19 | 1.54 | 18.43 | 27.46 | 15.66 | - | - | - | - | 155.4 |
| 20 | 1.55 | 23.56 | 29.83 | 17.22 | - | - | - | - | 137.2 |

The exposure of the bladder cancer cell line NTUB1 to 40 μM of compound **1.40** for 24 h increased the production of ROS. This increase in ROS was accompanied by an

increase in the number of cells in the G1 phase and in apoptosis induction.²⁸² BGC-823 stomach cancer cells treated with compound **1.54** showed an accumulation of cells in the sub-G1 phase, upregulation of caspase 3 and downregulation of Bcl-2 and survivin, leading to the induction of the intrinsic apoptotic pathway. Compound **1.54** was tested in a mouse model, in which it led to a reduction in tumor growth with low toxicity to the hosts.¹⁸⁶

The cytotoxicity of compounds **1.56-1.77**, which are C28 amide derivatives of ursolic acid (Figures 1.3.8-1.3.10), was tested against several cancer cell lines and nontumorigenic cell lines (Table 1.3.18).^{184, 185}

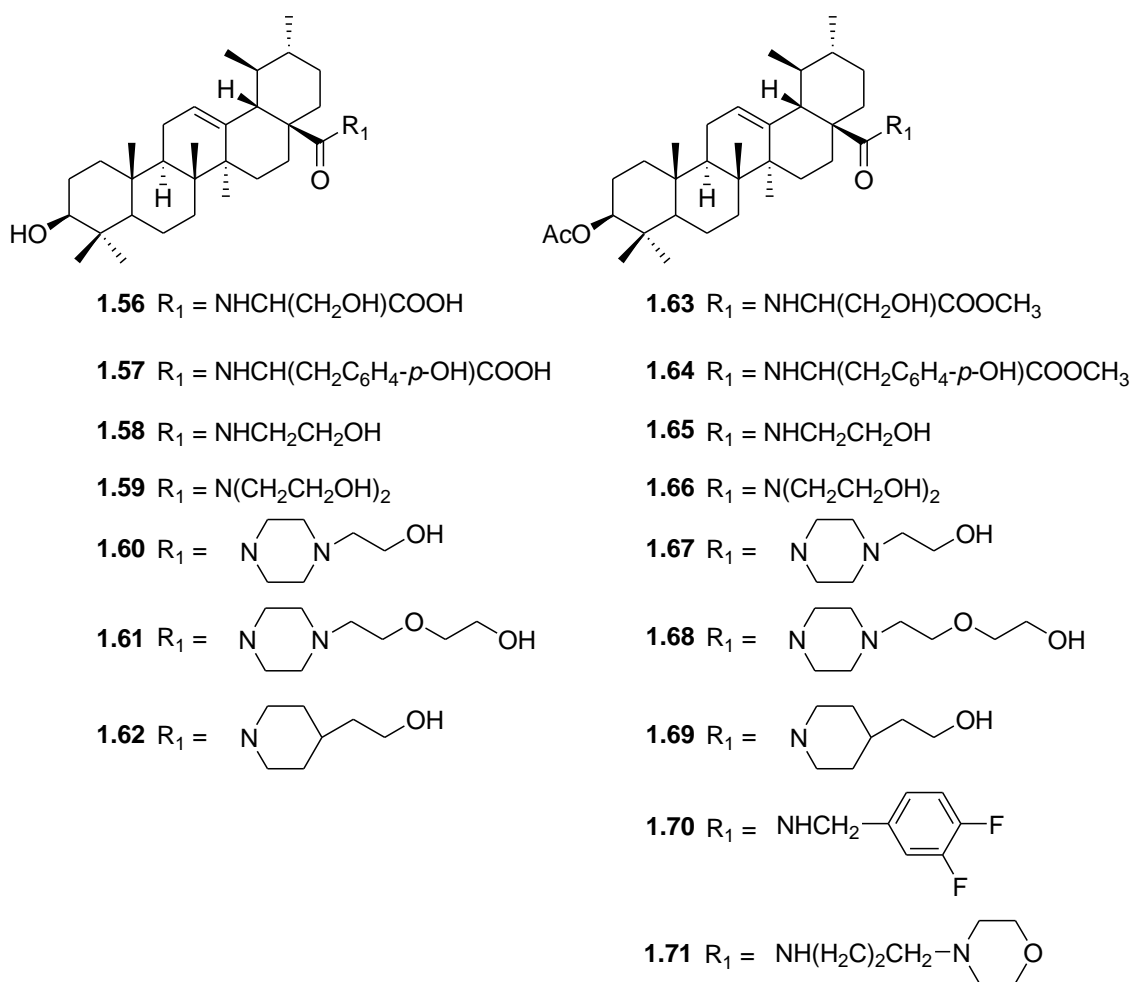


Figure 1.3.8. Schematic representation of ursolic acid amide derivatives **1.56-1.71**.

Compound **1.66** induced apoptosis and cell cycle arrest at the S phase in Hep G2 cancer cells in a time- and dose-dependent manner, with increase in the activity of caspase 3. Compared with the control group, an anti-tumor effect as observed in Kunming mice treated with compound **1.66**.¹⁸⁴

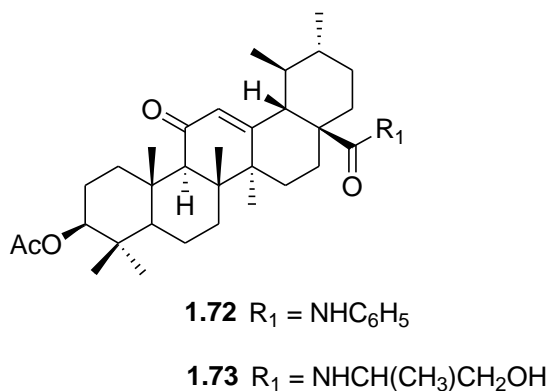


Figure 1.3.9. Schematic representation of ursolic acid amide derivatives **1.72** and **1.73** which have an α,β unsaturated ketone in ring C.

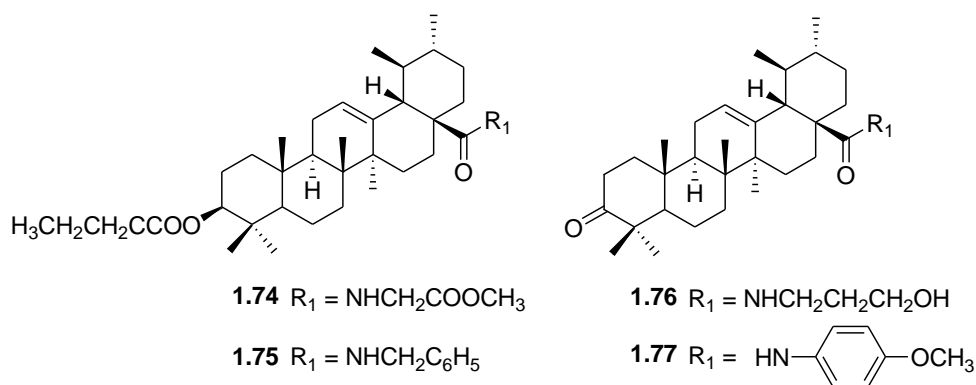


Figure 1.3.10. Schematic representation of ursolic acid amide derivatives **1.74-1.77**.

Table 1.3.18. IC₅₀ (μM) for compounds **1.56-1.77** in ovary (SKOV3), liver (Hep G2), stomach (BGC-823), neuroblastoma (SH-SY5Y) and cervix (HeLa) cancer cell lines, and in a nontumorigenic cell line (HELFL).

| Entry | Compd | Cell lines | | | | | |
|-----------|-------------|------------|--------|---------|---------|-------|-------|
| | | SKOV3 | Hep G2 | BGC-823 | SH-SY5Y | HeLa | HELFL |
| <i>1</i> | 1.56 | - | 83.03 | 79.30 | 72.21 | 41.65 | 60.33 |
| <i>2</i> | 1.57 | - | >100 | >100 | >100 | >100 | >100 |
| <i>3</i> | 1.58 | - | 82.36 | 78.26 | 65.01 | 32.33 | 52.75 |
| <i>4</i> | 1.59 | - | 35.66 | 39.27 | 21.38 | 14.36 | 36.92 |
| <i>5</i> | 1.60 | - | >100 | 98.26 | >100 | 52.33 | 32.75 |
| <i>6</i> | 1.61 | - | 36.71 | 35.04 | 30.28 | 23.78 | 28.06 |
| <i>7</i> | 1.62 | - | >100 | >100 | >100 | 67.29 | >100 |
| <i>8</i> | 1.63 | - | 35.36 | 29.01 | 37.18 | 20.61 | 22.34 |
| <i>9</i> | 1.64 | - | >100 | 82.95 | >100 | 66.67 | 35.81 |
| <i>10</i> | 1.65 | - | 46.62 | 48.47 | 49.41 | 16.27 | 27.82 |
| <i>11</i> | 1.66 | - | 20.25 | 15.52 | 13.24 | 10.87 | 38.06 |
| <i>12</i> | 1.67 | - | 20.46 | 13.86 | 11.70 | 7.24 | 31.04 |
| <i>13</i> | 1.68 | - | 15.26 | 12.83 | 9.51 | 6.28 | 38.92 |
| <i>14</i> | 1.69 | - | 59.38 | 51.34 | 40.12 | 12.43 | 30.02 |
| <i>15</i> | 1.70 | >10 | - | >10 | - | >10 | - |
| <i>16</i> | 1.71 | 7.40 | - | 4.46 | - | 2.71 | - |
| <i>17</i> | 1.72 | >10 | - | >10 | - | >10 | - |
| <i>18</i> | 1.73 | >10 | - | >10 | - | >10 | - |
| <i>19</i> | 1.74 | - | - | 5.63 | - | >10 | - |
| <i>20</i> | 1.75 | >10 | - | >10 | - | >10 | - |
| <i>21</i> | 1.76 | >10 | - | >10 | - | >10 | - |
| <i>22</i> | 1.77 | >10 | - | >10 | - | >10 | - |

Compounds **1.78-1.83**, with modifications at carbon C3 (Figure 1.3.11), have diverse cytotoxic activities (Table 1.3.19).^{197, 282} Compound **1.82** was the most active in inhibiting the growth of bladder cancer cells.²⁸²

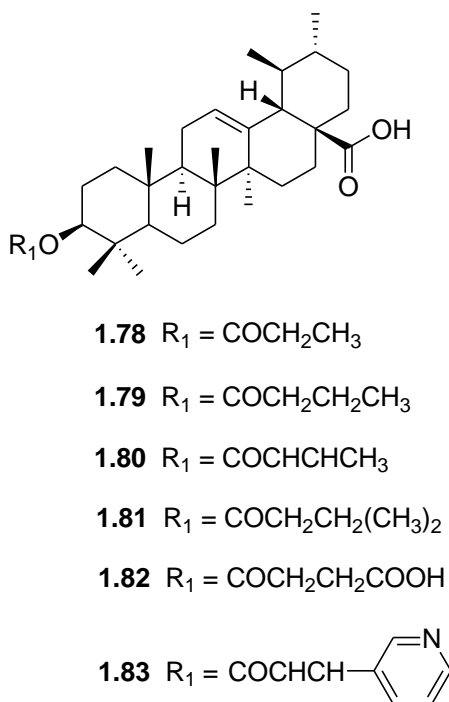


Figure 1.3.11. Schematic representation of derivatives of ursolic acid.

Table 1.3.19. IC_{50} (μM) for compounds **1.78-1.83** in bladder (NTUB1) and colorectal (HT-29) tumor cancer cells.

| Entry | Compd | Cell line | |
|-------|-------|-----------|-------|
| | | NTUB1 | HT-29 |
| 1 | 1.78 | >30 | - |
| 2 | 1.79 | >30 | - |
| 3 | 1.80 | 11.94 | - |
| 4 | 1.81 | 30.98 | - |
| 5 | 1.82 | 8.65 | - |
| 6 | 1.83 | - | 45 |

Some researchers have synthesized a series of new ursolic acid derivatives with an open and modified ring A (Figure 1.3.12). The cytotoxicity of compounds **1.85-1.87** and **1.91** was tested against NRP.152 prostate cells. Compounds **1.85** and **1.86** had an IC_{50} greater than $5.0 \mu\text{M}$ and compounds **1.87** and **1.91** had an IC_{50} of $2.4 \mu\text{M}$ and $0.3 \mu\text{M}$, respectively.³⁰³

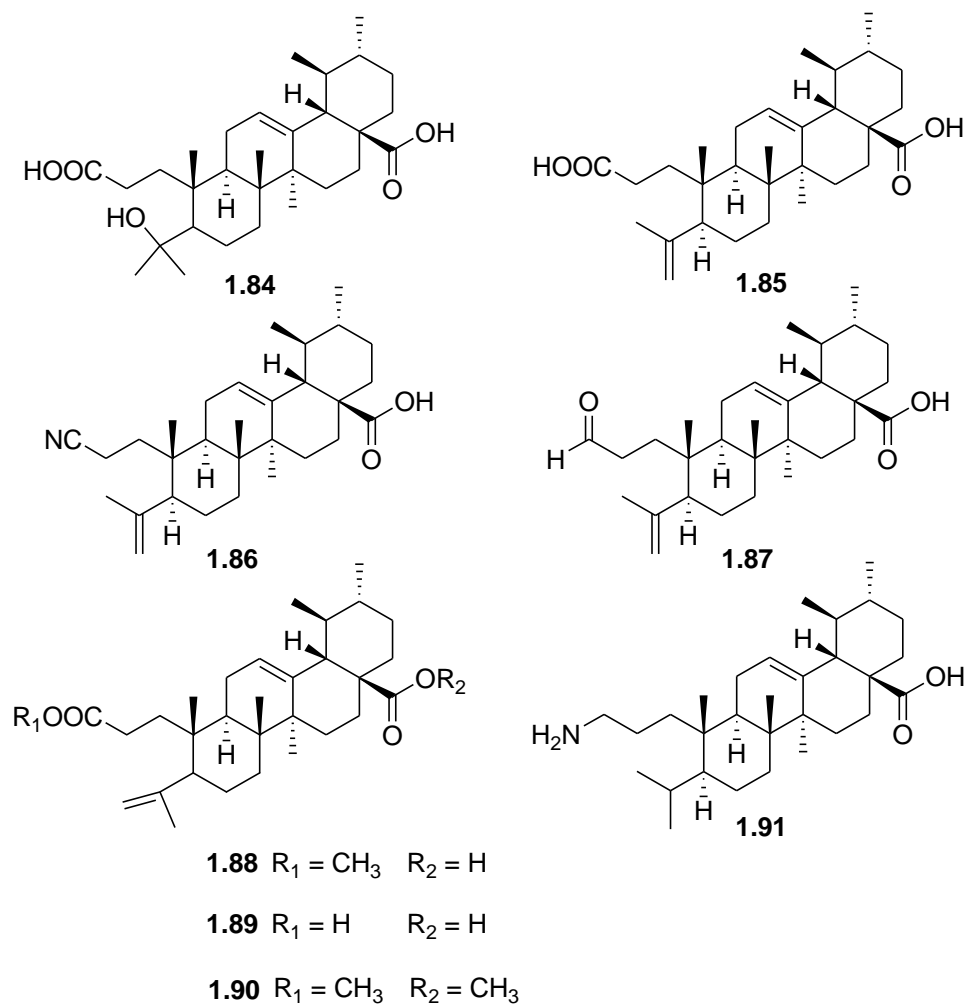


Figure 1.3.12. Schematic representation of ursolic acid derivatives with an open ring A.

The cytotoxicity of compounds **1.84** and **1.88-1.90** (Figure 1.3.12) was tested against NTBU1 bladder cancer cells. Compounds **1.84** and **1.88** presented an IC_{50} greater than $30 \mu\text{M}$ and compounds **1.89** and **1.90** presented an IC_{50} of 25.49 and $15.63 \mu\text{M}$, respectively. Compound **1.89** induced apoptosis and cell cycle arrest at the G2/M phase through the increase of ROS production.²⁸²

Aromatase is a key enzyme for the development of breast and prostate hormone-dependent cancers. Ursolic acid inhibits this enzyme (IC_{50} 32 μ M). Compounds **1.86** (Figure 1.3.12) and **1.92-1.96** (Figure 1.3.13) were tested for the inhibition of aromatase, which revealed an IC_{50} around 500 μ M for these compounds.²⁴¹

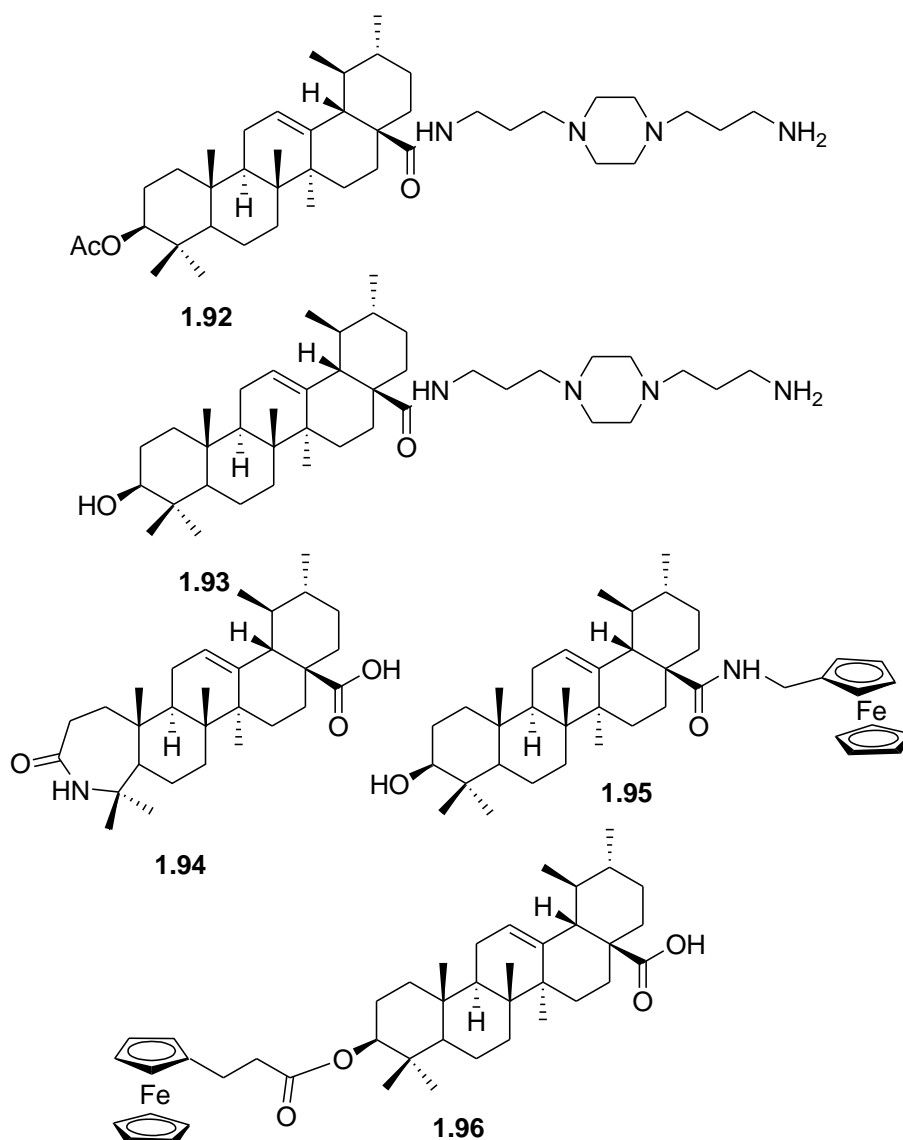


Figure 1.3.13. Schematic representation of compounds **1.92-1.96**.

The combination of ursolic acid with oxaliplatin (compound **1.97**), a chemotherapeutic drug in clinical use, exhibited cytotoxic activity against HT-29 cancer cells (Figure 1.3.14).³⁰⁴

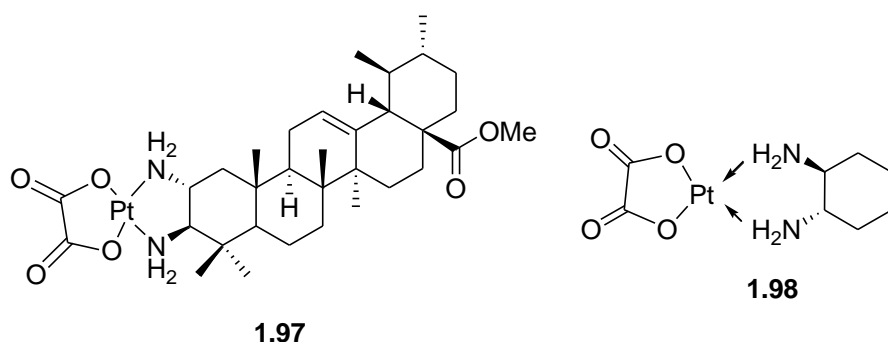


Figure 1.3.14. Schematic representation of compound **1.97** and oxaliplatin **1.98**.

1.3.4. Oleanolic acid

Oleanolic acid is a pentacyclic triterpenoid that can be found in the form of free acid or aglycones in various medicinal plants and fruits.^{77, 175} Oleanane triterpenoids are a wide group that is present in nature and includes oleanolic acid (3 β -hydroxy-olean-12-en-28-oic acid), maslinic acid (2 α ,3 β -dihydroxyolean-12-en-28-oic acid), morolic acid (3 β -hydroxyolean-18-en-28-oic acid), moronic acid (3-oxoolean-18-en-28-oic acid) and others (Figure 1.3.15).

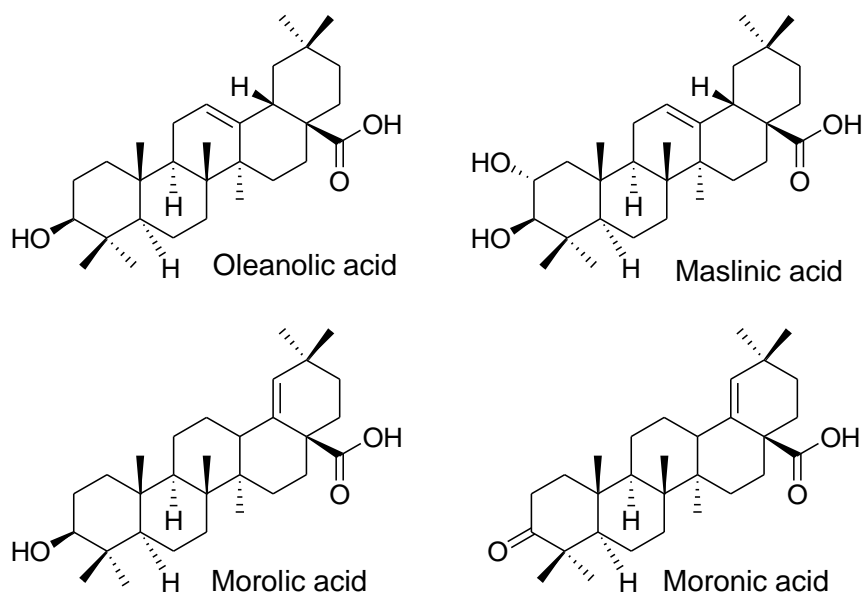


Figure 1.3.15. Oleanolic acid and some of its natural analogues.

Oleanolic acid was first considered inactive; however, in the past two decades it attracted interest because of its pharmacological effects combined with a low toxicity.^{173, 305} Oleanolic acid has demonstrated antibacterial, antiparasitic, antiosteoporotic, antifertility, antihypertensive, antihyperlipidemic, diuretic, antidiabetic, immunomodulator, anti-inflammatory, inhibitory of complement pathway, antinociceptive, gastroprotective, hepatoprotective and anti-HIV activities.

1.3.4.1. General activities

Nosocomial infections, which are caused by resistant or multiple-resistant bacteria, are a serious public health problem. Oleanolic acid has demonstrated activity against some bacteria that are responsible for these infections (Table 1.3.20).^{92, 102, 306} Tuberculosis is responsible for a high number of deaths. Oleanolic acid was tested against *Mycobacterium tuberculosis* H₃₇Ra and *M. tuberculosis* H₃₇Rv and exhibited a MIC of 50 µg/mL and 30 µg/mL, respectively.^{80, 101} Oleanolic acid was also active against *Streptococcus mutans* (MIC 625 µg/mL) and *Porphyromonas gingivalis* (MIC 488 µg/mL), two strains that are responsible for caries and periodontal disease.³⁰⁷

Leishmaniasis affects millions of people worldwide and its treatment is based in pentavalent antimonials, which are toxic and prone to drug resistance.⁸³ Oleanolic acid has the ability to inhibit the promastigote and amastigote growth of *Leishmania amazonis* with an IC₅₀ of 10 µg/mL and 27 µg/mL, respectively, because of a direct effect on *L. amazonis*.⁸³ The anti-parasitic activity of oleanolic acid against promastigotes of *L. infantum* and *L. amazonensis* was higher than 25 µg/mL.¹⁰⁷

Several diseases are transmitted by insects and are responsible for losses in cereal and vegetable cultures despite the current use of insecticides. Oleanolic acid has insecticidal and anti-feedant effects on *Stiphilus oryzae* insects.³⁰⁸

The therapeutic approach for the treatment of HIV includes nucleoside analogue HIV RT inhibitors, non-nucleoside RT inhibitors and protease inhibitors. Oleanolic acid inhibits HIV replication with an EC₅₀ of 3.7 µM and a therapeutic index (IC₅₀/EC₅₀) of 12.8.^{110, 309, 310} The anti-HIV activity of oleanolic acid is due to its activity as an inhibitor of HIV protease.^{111, 311} Oleanolic acid was also shown to have inhibitory activity (with

and IC₅₀ of 56.5 μ M) on the hepatitis C viral protease, which is an important enzyme for the maturation of the virus and for the progression of hepatitis C.^{312, 313}

Table 1.3.20. Values of MIC (μ g/mL) for oleanolic acid against several strains of bacteria.

| Entry | Bacteria | MIC (μ g/mL) | | Ref. |
|-------|---|-------------------|----------------------|----------|
| | | Oleanolic acid | Reference antibiotic | |
| 1 | <i>E.coli</i> ATCC 25922 | >256/95 | 4 ^a /- | 102, 306 |
| 2 | <i>S.aureus</i> ATCC 25923 | 8/95 | <1 ^b /- | 102, 306 |
| 3 | <i>S.aureus</i> ATCC 29213 | 8/>95 | <1 ^b /- | 102, 306 |
| 4 | <i>E.fecalis</i> ATCC 29212 | 4 | <1 ^c | 102 |
| 5 | <i>P.aeruginosa</i> ATCC 27853 | 256 | 16 ^d | 102 |
| 6 | Penicillinase-producing <i>E.coli</i> | >256 | >256 ^a | 102 |
| 7 | MRSA (<i>mecA</i> gene) | >256 | 256 ^b | 102 |
| 8 | <i>E.faecium</i> (<i>vanB</i> gene) | >256 | 64 ^c | 102 |
| 9 | <i>E.fecalis</i> (<i>vanA</i> gene) | >256 | 256 ^c | 102 |
| 10 | <i>P.aeruginosa</i> (overexpression of efflux pumps) | >256 | 64 ^d | 102 |
| 11 | <i>E.faecium</i> FN-1 | 8 | 128 ^e | 92 |
| 12 | <i>E.faecium</i> BM4147 | 8 | 32 ^e | 92 |
| 13 | <i>E.faecalis</i> NCTC 12201 | 8 | 4 ^e | 92 |
| 14 | <i>E.faecalis</i> FA2-2 | 8 | 4 ^e | 92 |
| 15 | <i>S.pneumoniae</i> R6 | 16 | 0.06 ^e | 92 |
| 16 | <i>S.aureus</i> OM481 | 16 | 64 ^e | 92 |
| 17 | <i>S. aureus</i> OM584 | 16 | 64 ^e | 92 |
| 18 | <i>E.coli</i> K12 | >128 | - | 92 |
| 19 | <i>P.aeruginosa</i> PAO1 | >128 | - | 92 |
| 20 | <i>S.marcescens</i> NUSM8905 | >128 | - | 92 |
| 21 | <i>Salmonella typhimurium</i> | 65 | - | 306 |

a) Amoxicillin; b) Oxacillin; c) Vancomycin; d) Ticarcillin; e) Ampicillin.

Osteoporosis is a disease that is characterized by low bone mineral density and structural deterioration of bone tissue.¹¹⁶ The anti-osteoporotic effect of oleanolic acid is

related with its inhibitory capacity regarding the formation of osteoclast-like multinucleated cells (OCLs), with a 27.6% inhibition relative to the control.³¹⁴

The anti-fertility activity of oleanolic acid was evaluated in male albino rats. Its administration for 60 days decreased the fertilizing capacity of the animals via the arrest of spermatogenesis, without significant side effects.³¹⁵

The gastroprotective effects of oleanolic acid were tested in five induced gastric ulceration mouse models (Table 1.3.21).³¹⁶⁻³¹⁸

Table 1.3.21. Protective effects of oleanolic acid in five models of gastric ulceration in the mouse.

| Entry | Ulceration model | Control | | Oleanolic acid | | Ref. |
|-------|------------------|-----------------|-------------------------------------|----------------|-------------------------------------|------|
| | | Dose (mg/kg) | Ulceration index (mm ²) | Dose (mg/kg) | Ulceration index (mm ²) | |
| 1 | Aspirin | 50 ^a | 35.8 | 50 | 40.7 | 316 |
| 2 | Ethanol | 50 ^b | 60.0 | 50 | 86.2 | 318 |
| 3 | | 20 ^b | 40.6 | 50 | 60.6 | 316 |
| 4 | Indometacin | 20 ^b | 0.3 | 50 | 14.0 | 318 |
| 5 | Acetic acid | 50 ^a | 6.9 | 50 | 17.8 | 317 |
| 6 | Pylorus ligature | 50 ^a | 50.2 | 50 | 62.0 | 316 |

a) Ranitidine; b) Omeprazol.

The lesions caused by acetic acid were analyzed histologically, which showed that oleanolic acid leads to the regeneration of the lesions and produces an increase in gastric mucosal thickness.³¹⁷ The gastroprotective activity of oleanolic acid can be due to its ability to accelerate cell proliferation in MRC-5 fibroblasts and to increase the content of prostaglandins.³¹⁹

Oleanolic acid has cardiovascular protective and regulatory effects in *in vitro* and *in vivo* models. An *in vitro* study showed that oleanolic acid was able to improve the balance of vasodilator/anti-aggregant vs. vasoconstrictor/prothrombotic eicosanoids in human coronary smooth muscle cells (SMCs) via the activation of the MAPK/Erk kinase (MEK) 1/2 and p38 MAPK pathways, leading to an increase in the activity of COX-2, which results in an increase in prostaglandin I₂ release.³²⁰

Oleanolic acid prevents the development of severe hypertension through a potent diuretic-natriuretic-saluretic activity, the decrease in heart rate, an anti-hyperlipidemic effect, an antioxidant effect via increase of glutathione peroxidase (GPx) and superoxide dismutase activities and hypoglycemic activity in Dahl salt-sensitive rats.¹¹⁹ Oleanolic acid also displays dose-dependent vasodepressor and an anti-dysrhythmic effects.¹²⁰ Oleanolic acid exhibits a moderate diuretic effect compared with furosemide, which is a diuretic used clinically for the treatment of hypertension.³²¹ Oleanolic acid induces arterial vasorelaxation through a calcium-independent pathway, with activation of the PI3K/Akt pathway, which leads to the phosphorylation of endothelial NO synthase and production of NO.³²²

Oxygen-derived free radicals are involved in the pathogenesis of myocardial ischemia-reperfusion (I-R) injury.³²³ Pretreatment of rats with oleanolic acid conferred cardioprotection against I-R injury through the increase of GSH status in mitochondria and stimulation of the synthesis and regeneration of GSH and α -tocopherol.³²⁴

Atherosclerosis remains the main cause of cardiovascular diseases. Oxidative stress is a characteristic of atherosclerosis and is responsible for the migration, proliferation and apoptosis of VSMCs. Treatment of VSMCs with oleanolic acid led to the upregulation of hemo oxygenase-1 through the activation of the Nrf2 pathway via the PI3K/Akt and ERK pathways.³²⁵ Apolipoprotein E knockout (ApoE^{-/-}) mice treated with oleanolic acid exhibit a decrease in plaque formation.^{326, 327}

Type 2 diabetes is associated with disorders of glucose metabolism. An ideal antidiabetic agent should be able to lower blood glucose in both the fed and fast states.³²⁸ Several enzymes are involved in the regulation of glucose blood levels. Glycogen phosphorylase is the enzyme that is responsible for glycogen breakdown, to produce

energy.³²⁹ Oleanolic acid is a natural inhibitor of glycogen phosphorylase (IC₅₀ 14 μM).³²⁸⁻³³⁰ Tyrosine phosphatase 1B is involved in the process of dephosphorylation of the insulin receptor; as it regulates the insulin pathway, oleanolic acid is a competitive inhibitor of this enzyme, with an IC₅₀ of 3.4 μM.³³¹ α-Glucosidase hydrolyses the cleavage of glucose from disaccharides and oligosaccharides; the inhibition of this enzyme delays carbohydrate digestion, causing a reduction in the postprandial rise in blood glucose. Oleanolic acid inhibits this enzyme with an IC₅₀ of 11.2 μM.³³²

Oleanolic acid can reduce the levels of blood glucose in alloxan- and streptozotocin-induced diabetes in animal models.³³³⁻³³⁵ The antiglycative effects of oleanolic acid in streptozotocin-induced diabetic mice are accompanied by a beneficial effect on kidney function.^{142, 336} Diabetic streptozotocin-induced mice transplanted with Balb/c islets for the treatment of diabetes and treated simultaneously with oleanolic acid have a faster improvement of glucose levels and a decrease in pro-inflammatory cytokines, thus delaying the immune responses against the islets.³³⁷

Obesity is a global concern as it can increase the predisposition to several diseases.^{125, 126} Oleanolic acid treatment in high-fat fed mice decreased the levels of serum glucose, insulin, cholesterol and triglycerides and the accumulation of visceral fat.^{338, 339} The reduction in the accumulation of visceral fat can be due to the decrease of ghrelin, a hormone that is secreted in the stomach and has appetite-stimulating activity, and the increase in leptin secretion, a hormone that suppresses food intake.³³⁸ Oleanolic acid is an agonist of TGR5 and, when stimulated, leads to an increase in energy expenditure, thus preventing the development of insulin resistance and the accumulation of visceral fat.³³⁹

Ischemic stroke can result from a transient or permanent reduction in cerebral blood flow.^{340, 341} Oleanolic acid protects neuronal cells from induced death by oxygen peroxide via a reduction in the intracellular levels of Ca²⁺ and ROS, thus having a neuroprotector effect.³⁴² In a mouse model, oleanolic acid reduced cerebral ischemic damage as it reduced the infarcted area and the cerebral edema, prolonging the survival time of the animals. *In vitro* studies have demonstrated that oleanolic acid reduces the oxidative damage induced by treatment with oxygen peroxide in PC12 cells.³⁴³

Multiple sclerosis is an autoimmune/inflammatory degenerative disease of the central nervous system (CNS).³⁴⁴ Oleanolic acid is able to ameliorate the neurological signs of multiple sclerosis by inhibiting the action of the inflammatory and humoral components of the disease in an experimental allergic encephalomyelitis mouse model.³⁴⁵

Oleanolic acid has the capacity to modulate the immune system. Its administration to Balb/c mice increased the total number of white blood cells, bone marrow cells and α -esterase cells, as well as the production of specific antibodies and the percentage of plaque-forming cells in the spleen and inhibited the delayed-type hypersensitive reaction by 88%.¹⁴⁹ The transcription factor “nuclear factor of activated T cells” (NFAT) is excessively activated in immunopathological reactions, including autoimmune diseases.³⁴⁶ Oleanolic acid has the ability to inhibit NFAT with an IC_{50} greater than 50 μ M.³⁴⁷

The antinociceptive effect of oleanolic acid was evaluated in acute nociception induced by intraplantar injection of capsaicin and intracolonic injection of mustard oil in mice. Oleanolic acid exerts its antinociceptive action through an opioid mechanism involving NO production and activation of ATP-gated K^+ channels.^{348, 349}

Oleanolic acid protects against the hepatotoxicity of carbon tetrachloride in mice, in a dose-dependent manner.³⁵⁰⁻³⁵² Oleanolic acid pretreatment induces an increase in ALT levels and in GSH regeneration capacity.³⁵³ It also decreases the levels of lactic dehydrogenase, cytochrome P450 2E1-dependent *p*-nitrophenol hydroxylation, aniline hydroxylation³⁵⁴ and γ -glutamyltransferase, while maintaining the levels of glutathione reductase, catalase, superoxide dismutase, glutathione S-transferase and GPx.³⁵⁵ Pretreatment of rats and mice with oleanolic acid decreases serum transaminase, aminopyrine *N*-demethylase and aniline hydroxylase.³⁵⁵ Hepatic MT is responsible for the acute response to hepatotoxicants and is increased during the pretreatment with oleanolic acid in mouse models.^{351, 352}

Oleanolic acid has protective effects on the hepatotoxicity caused by acetaminophen, bromobenzene, thioacetamide, furosemide, phalloidin, colchicines, D-galactosamine, endotoxin and cadmium.^{350, 352} Pretreatment with oleanolic acid in a mouse model with hepatotoxicity induced by acetaminophen leads to a decrease in the liver injury.³⁵⁶

Oleanolic acid treatment facilitates Nrf2 accumulation, which contributes to the hepatoprotection against acetaminophen, carbon tetrachloride, cadmium and bromobenzene.^{352, 357}

Cadmium liver injury is reduced in mice pretreated with oleanolic acid, with decreased levels of ALT and SDH and increased levels of MT.^{352, 358} In a model of toxicity induced by *t*-butyl hydroperoxide in QZG human liver cells, oleanolic acid decreases toxicity through the activation of the JNK and ERK pathways.³⁵⁹ Mice treated with oleanolic acid and 1-chloro-2,4-dinitrobenzene presented modification in several enzymes related with liver function.³⁶⁰

The anti-inflammatory activity of oleanolic acid was determined using *in vitro* and *in vivo* assays. Oleanolic acid has inhibitory effects on TPA-induced inflammation in the ear of mice. This effect was also observed in carrageenan, 12-deoxyphorbol-13-phenylacetate and dextran rat models.^{93, 305, 361-363} Inflammation is mediated by several enzymes; oleanolic acid has the capacity to inhibit COX-1 and COX-2, which are enzymes that are related with inflammatory states, at 295 and 380 μM , respectively.⁹⁵ Secretory phospholipase A₂ (sPA₂) is a main enzyme in the mediation of inflammation; oleanolic acid inhibits sPA₂ with an IC₅₀ from 3.08 to 7.78 μM .³⁶⁴

High mobility group box protein 1 (HMGB1) is a potent pro-inflammatory mediator.³⁶⁵ In HUVECs, oleanolic acid inhibits the lipopolysaccharide-mediated HMGB1 release and the HMGB1-mediated vascular permeabilization through the inhibition of CAM expression and reduction in monocyte adhesion and migration.³⁶⁶

The classical pathway of the complement system is part of the inflammatory process. Oleanolic acid has the capacity to inhibit the complement pathway with an IC₅₀ of 72.3 μM .^{367, 368} C3-convertase is one of the enzymes involved in the classical complement pathway; oleanolic acid inhibits this enzyme at 219 μM .³⁶⁹

1.3.4.2. Antitumor activity

The main studied activities of oleanolic acid are its antitumoral and chemopreventive activities. Because of them, oleanolic acid has been described in pharmaceutical

preparations for the treatment of nonlymphatic leukemia and is recommended in Japan for use in skin cancer therapy.³⁷⁰

Oral and esophageal cancers represent 3.5% of the estimated new cases of cancer in 2011.⁵ Oleanolic acid is cytotoxic against oral and esophageal cancers (Table 1.3.22, entries 1-3). Co-treatment of YES-2 cancer cells with oleanolic acid and 5-fluorouracil or cisplatin has additive or antagonist effects, respectively.¹⁰⁰

Hepatocellular carcinoma lacks chemotherapeutic options; thus, the demand for new chemotherapeutic drugs is a reality. Oleanolic acid has cytotoxic activity in several hepatocarcinoma cell lines (Table 1.3.22, entries 4-10). Oleanolic acid has been proven to induce the activation of caspases 8 and 3 in Hep G2, Hep3B, Huh7 and HA22T cells,^{212, 215, 223} with a consequent increase in the number of cells in the G1 phase of the cell cycle,²¹⁵ loss of mitochondrial membrane potential,²¹² downregulation of XIAP and Bcl-2 and upregulation of Bax.²²³

Colorectal cancer is the third most common cancer in both men and women.⁵ Chemoprevention has the aim of blocking, inhibiting or reversing some aspects of carcinogenesis. ACF induced by azoxymethane are considered as preneoplastic lesions and biomarkers of colon cancer. Oleanolic acid has the ability to reduce the incidence of azoxymethane-induced ACF in F344 rats.^{371, 372} The reduction of the incidence of ACF by oleanolic acid was correlated with the inhibition of COX-2 and iNOS³⁷¹ and a decrease of cells in the S phase.³⁷² Oleanolic acid has the ability to reduce the incidence of 1,2-dimethyl-hydrazine-induced ACF in rats.¹⁹⁰

Oleanolic acid has demonstrated cytotoxic activity *in vitro* against colorectal cancer cells (Table 1.3.22, entries 11-15). In HT-29 cancer cells, oleanolic acid induces apoptosis, with the activation of the intrinsic pathway through the production of ROS.^{373, 374} The induction of cell death by oleanolic acid is observed in HCT15 colorectal cancer cells, with a decrease of cells in the S phase and an increase of cells in the G0/G1 phase.¹⁹⁸

AKR1B10 is an aldo-keto reductase that is overexpressed in several carcinomas and, when silenced in xenograph mouse models, leads to a reduction in the growth of the

tumor.^{375, 376} It has been suggested that the AKR1B10 enzyme is involved in the development of mitomycin C resistance in human colorectal cancers.³⁷⁷ Oleanolic acid inhibits AKR1B10 with an IC₅₀ of 0.09 μ M by binding to the substrate site of the enzyme in a selective manner.³⁷⁸

Table 1.3.22. IC₅₀ (μ M) for oleanolic acid in oral, esophageal, liver and colorectal carcinomas cell lines.

| Entry | Cell line | IC ₅₀ (μ M) | Assay | Time (h) | Ref. |
|-----------------------------|-----------------------------------|-----------------------------|-------------|----------|------|
| <i>Oral carcinoma</i> | | | | | |
| 1 | HSC-2 | 285.0 | MTT | 24 | 179 |
| 2 | HSG | 503.6 | MTT | 24 | 179 |
| <i>Esophageal carcinoma</i> | | | | | |
| 3 | YES-2 | 100-125 | WST-8 | 48 | 100 |
| <i>Liver carcinoma</i> | | | | | |
| 4 | HuH7 | 100 | MTT | 24 | 223 |
| 5 | | >8 | MTT | 48 | 212 |
| 6 | Hep G2 | 17.5 | MTT | 72 | 237 |
| 7 | | 70 | Trypan Blue | 72 | 215 |
| 8 | | 4-8 | MTT | 48 | 212 |
| 9 | | H22T | 4-8 | MTT | 48 |
| 10 | Hep3B | >8 | MTT | 48 | 212 |
| <i>Colorectal carcinoma</i> | | | | | |
| 11 | HT-29 | 26.6 | Sytox-Green | 72 | 374 |
| 12 | | 160 | Sytox-Green | 72 | 373 |
| 13 | HCT15 | 26.5 | - | 48 | 203 |
| 14 | | 60 | MTT | 72 | 198 |
| 15 | HT-29 mitomycin C-resistant | 180 | Trypan Blue | 96 | 378 |

Breast cancer is the most common cancer in women and is responsible for the greatest number of cancer-related deaths.^{4, 5} Oleanolic acid can induce cell death in breast cancer cells lines (Table 1.3.23, entries 3-10), including breast cancer multi-drug resistant cells (Table 1.3.23, entries 8 and 9). Oleanolic acid induction of cell death in MCF-7

breast cancer cells is related with the inhibition of cell cycle progression at the G0/G1 checkpoint, with inhibition of DNA replication.³⁷⁹

Table 1.3.23. IC₅₀ (μM) for oleanolic acid in ovary and breast carcinoma cell lines.

| Entry | Cell line | IC ₅₀ (μM) | Assay | Time (h) | Ref. |
|-------------------------|------------|-----------------------|-------|----------|------|
| <i>Ovary carcinoma</i> | | | | | |
| 1 | SK-OV-3 | 27.2 | - | 48 | 203 |
| 2 | A2780 | 23.4 | - | - | 233 |
| <i>Breast carcinoma</i> | | | | | |
| 3 | | 28 | MTT | 72 | 206 |
| 4 | | >100 | XTT | 24 | 379 |
| 5 | MCF-7 | 263 | MTT | 72 | 236 |
| 6 | | 213 | MTT | 72 | 380 |
| 7 | | 5.38 | MTT | - | 381 |
| 8 | MCF-7/ADR | 44 | MTT | 72 | 206 |
| 9 | | 37.02 | MTT | - | 381 |
| 10 | MDA-MB-231 | >50 | SRB | 24 | 239 |

Breast cancer cells without expression of estrogen and prostagen receptors and amplified expression of HER2 are less differentiated, more aggressive and do not respond to the available therapies. Oleanolic acid has the ability to target specifically and effectively estrogen-receptor-negative breast cancer cells. In MCF-7, Hs578T and MDA-MB-231 cells, oleanolic acid disrupts the cholesterol synthetic pathway, interfering with the lipid rafts and leading to the decrease in the activity of mTOR complex 1 and mTOR complex 2, thus inhibiting the Akt pathway.³⁸²

The cytotoxic effects of oleanolic acid treatment in MG63 and Saos-2 osteosarcoma cells (Table 1.3.24, entries 1 and 2) are due to the downregulation of mTOR complex 1 and mTOR complex 2, with cell cycle arrest at the G1 phase and downregulation of cyclin D1.³⁸³

Lung cancer is the number one cause of cancer-related deaths; therefore, new chemotherapeutic agents are needed for this disease.⁵ Oleanolic acid has cytotoxic effects

against non-small lung cancer cells (Table 1.3.24, entries 4-8). SPC-A-1 cells treated with oleanolic acid present a decrease in the levels of Bcl-2 and an increase in the levels of Bax and Bad proteins, with induction of apoptosis.³⁸⁴ Lung cancer is characterized by the presence of MDR proteins that contribute to the poor outcome of this cancer.^{385, 386} Oleanolic acid induces apoptosis in A549 and H460 lung cancer cells, overcoming the natural MDR in these cell lines. Oleanolic acid leads to the downregulation of survivin and VEGF and to the upregulation of Bax, but does not inhibit the proteins that are responsible for drug resistance.³⁸⁷

Table 1.3.24. IC₅₀ (μM) for oleanolic acid in osteosarcoma, lung and skin cancer cell lines.

| Entry | Cell line | IC ₅₀ (μM) | Assay | Time (h) | Ref. |
|-----------------------|-----------|-----------------------|-------|----------|------|
| <i>Osteosarcoma</i> | | | | | |
| 1 | MG63 | 75 | MTT | 72 | 383 |
| 2 | Saos-2 | 50 | MTT | 72 | 383 |
| 3 | LM-8 | >100 | MTT | 48 | 388 |
| <i>Lung carcinoma</i> | | | | | |
| 4 | | 35.9 | - | 48 | 203 |
| 5 | A549 | >100 | MTT | 48 | 389 |
| 6 | | 88-100 | MTT | 48 | 387 |
| 7 | SPC-A-1 | 16-32 | MTT | 48 | 384 |
| 8 | H460 | 55-88 | MTT | 48 | 387 |
| <i>Skin carcinoma</i> | | | | | |
| 9 | SK-MEL-3 | 40.5 | - | 48 | 203 |
| 10 | B16 F10 | >100 | MTT | 48 | 390 |
| 11 | B16 2F2 | 3.1 | - | 72 | 259 |

TPA is a well know skin tumor inducer in animal models. The topical application of TPA induces a series of proteins and genes related with tumor induction and promotion, such as ornithine decarboxylase (ODC), MT, *c-fos* and *c-jun*. Oleanolic acid prevents tumor induction by TPA in mice^{257, 391, 392} through the inhibition of the induction of ODC, MT and *c-fos*.³⁹¹ Oleanolic acid also inhibited tumor growth in a xenograph mouse model of melanoma cancer³⁹³ and reduced the development of lung metastasis in an *in vivo* model of melanoma cancer.³⁸⁷

Oleanolic acid has cytotoxic properties towards skin cancer cells (Table 1.3.24, entries 9-11). Oleanolic acid induces apoptosis in B16 F10 cells via the activation of p53 and consequent upregulation of Bax, p21 and p27 and inhibition of the NF- κ B-induced Bcl-2 pathway.³⁹⁰

Table 1.3.25. IC₅₀ (μ M) for oleanolic acid in leukemia, lymphoma and neuroblastoma cancer cell lines.

| Entry | Cell line | IC ₅₀ (μ M) | Assay | Time (h) | Ref. | |
|----------------------|----------------|-----------------------------|------------------------------------|-------------|------|-----|
| <i>Leukemia</i> | | | | | | |
| 1 | K562 | 33 | MTT | 72 | 206 | |
| 2 | | 100 ^a | TB | 24 | 276 | |
| 3 | K562/ADR | 43 | MTT | 72 | 206 | |
| 4 | HL60 | 30 | MTT | 72 | 206 | |
| 5 | | 8.9 | NBT | 72 | 394 | |
| 6 | | 70.6 | Trypan blue | 24 | 277 | |
| 7 | | 40 ^a | TB | 24 | 276 | |
| 8 | | 237.4 | XTT | 72 | 279 | |
| 9 | | HL60/ADR | 32 | MTT | 72 | 206 |
| 10 | | 27.6 | XTT | 48 | 278 | |
| 11 | | L1210 | 32.3 | Trypan blue | 24 | 277 |
| 12 | 8 ^a | TB | 24 | 276 | | |
| <i>Lymphoma</i> | | | | | | |
| 13 | P3HR1 | 58.6 | XTT | 72 | 279 | |
| 14 | U937 | 80.3 | XTT | 72 | 279 | |
| <i>Neuroblastoma</i> | | | | | | |
| 15 | XF498 | >60 | - | 48 | 203 | |
| 16 | 1321N1 | 25 | [³ H] thymidine uptake | 24 | 395 | |

a) Value for IC₈₀

Oleanolic acid induces cell death in leukemic and lymphatic cells, in a dose-dependent manner (Table 1.3.25, entries 1-14). Oleanolic acid can induce apoptosis and cell cycle arrest at the G2/M phase in L1210 leukemic cells, and G0/G1 cell cycle arrest in HL60 cancer cells with induction of apoptosis.³⁹⁶ The combination of oleanolic acid

and doxorubicin increases synergistically the effects on the differentiation of L120 and HL60 cells lines.²⁷⁷ The differentiation effects of oleanolic acid were observed in the M1 leukemia cell line.³⁹⁷ Oleanolic acid induces an increase in apoptosis in the K562 cell line and in the Lucena 1 cell line, a vincristine-resistant cell line, overcoming the overexpression of the Pgp protein.³⁹⁸ Oleanolic acid inhibits the multidrug resistance protein (ABCC1), but has no effect on the Pgp protein.³⁹⁹ The cytotoxic effect of oleanolic acid in multi-drug resistant cell lines was verified in HL60/ADR and K562/ADR cancer cells (Table 1.3.25, entries 3 and 9).²⁰⁶

Oleanolic acid has the ability to induce cytotoxicity and apoptosis in several neuroblastoma cells (Table 1.3.25, entries 15 and 16). The induction of apoptosis in 1321N1 cancer cells by oleanolic acid is due to the generation of ROS, disruption of the mitochondrial membrane potential and cytoskeleton alterations.³⁹⁵ Oleanolic acid inhibits the proliferation of U373 human glioma cells through the inhibition of the activation of STAT 3.⁴⁰⁰

Chemotherapeutic drugs that are DNA damaging agents are used currently in clinical practice. DNA polymerase β is a key enzyme involved in DNA repair and is responsible for some resistance to chemotherapeutic drugs that induce DNA damage.^{401, 402} Oleanolic acid is an inhibitor of DNA polymerase β in the presence or absence of bovine serum albumin (BSA), with an IC_{50} of 7.5 μ M and 3.7 μ M, respectively.^{403, 404} The activity of DNA polymerase β can be divided in lyase and polymerase activities, oleanolic acid can inhibit both of the two activities with IC_{50s} of 26.25 μ M and 24.98 μ M, respectively.³⁸⁹

DNA ligase is responsible for the joining of single-stranded breaks in double-stranded DNA and is involved in DNA replication, repair and recombination.^{405, 406} Oleanolic acid inhibits DNA ligase with an IC_{50} of 216 μ M.⁴⁰⁷

Oleanolic acid has antimutagenic activity in γ irradiation-, doxorubicin- and oxygen peroxide-induced toxicity in the mouse hematopoietic system and leukemic cells.^{276, 290, 291} This antimutagenic effect of oleanolic acid is probably due to its antioxidant effect.^{276, 408} Oleanolic acid can, therefore, be used as a chemopreventive agent, to reduce the severe side effects of common chemotherapeutic drugs.

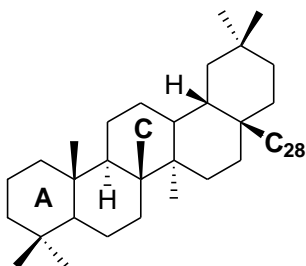
Angiogenesis is the basis of solid tumor growth and dissemination and results from several steps, each one representing a potential target for antiangiogenic drugs. Oleanolic acid inhibits angiogenesis in a dose-dependent manner, as it has inhibitory effects on embryonic angiogenesis in chick embryo chorioallantoic membranes and on the proliferation of vascular endothelial cells.²⁸⁴ Angiogenesis is regulated by several factors, such as VEGF, IL-8, HIF-1 α , ROS, NO, uPA and the basic fibroblast growth factor (bFGF). Hepatic cancer cells Hep3B, Huh7 and HA22T treated with lower concentrations of oleanolic exhibit suppression of the expression of HIF-1 α , VEGF, IL-8 and uPA and lower levels of ROS and NO production, leading to a decrease in the invasion and migration potential of these cells.²⁸⁹

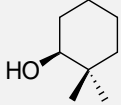
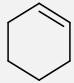
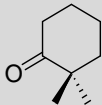
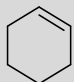
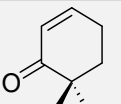
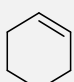
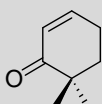
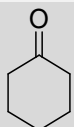
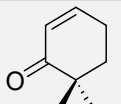
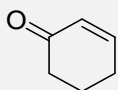
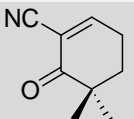
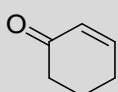
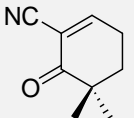
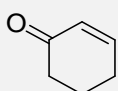
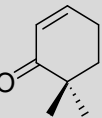
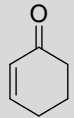
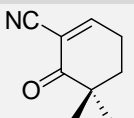
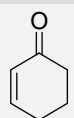
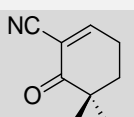
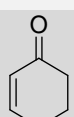
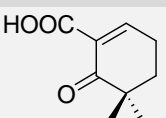
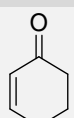
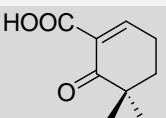
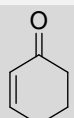
1.3.4.3. Semisynthetic derivatives with antitumor activity

Several semisynthetic derivatives of oleanolic acid have been described. The chemical modifications made in the oleanane structure are located mainly at carbons C2, C3, C11, C12 and C28.

Honda *et al* first synthesized a series of oleanolic acid derivatives (some are represented in Table 1.3.26) and evaluated their inhibitory action on the production of NO by mouse macrophages.^{293-295, 409, 410} NO is an important molecule in physiological and pathological processes. At low concentrations, it promotes tumor growth, as it mediates DNA repair, angiogenesis and stimulates prosurvival pathways; at higher concentrations, it promotes tumor death and regression, as it stimulates DNA damage and apoptosis.^{411, 412}

Table 1.3.26. IC₅₀ (μ M) of oleanolic acid derivatives for the inhibition of the production of NO in mouse macrophages.

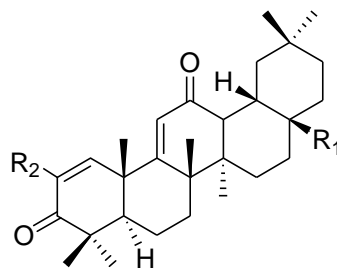


| Entry | Compd | Ring A | Ring C | C28 | IC ₅₀ (μM) |
|-------|-------|---|---|-------|-----------------------|
| 1 | 1.99 |  |  | COOH | >40 |
| 2 | 1.100 |  |  | COOH | 37.1 |
| 3 | 1.101 |  |  | COOH | 5.6 |
| 4 | 1.102 |  |  | COOH | 3.3 |
| 5 | 1.103 |  |  | COOH | 1.4 |
| 6 | 1.104 |  |  | COOMe | 0.2 |
| 7 | 1.105 |  |  | COOH | 0.02 |
| 8 | 1.106 |  |  | COOH | 0.04 |
| 9 | 1.107 |  |  | COOH | 0.0002 |
| 10 | 1.108 |  |  | COOMe | 0.0001 |
| 11 | 1.109 |  |  | COOMe | 0.0008 |
| 12 | 1.110 |  |  | COOH | 0.2 |

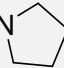
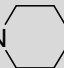
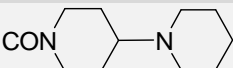
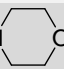
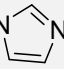
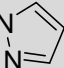
From the first series of oleanolic acid derivatives evaluated, the following structure activity relationships were concluded: a) in ring A, a 1-en-3-one functionality combined with an electron-withdrawing group, such as the carbonyl or nitrile at C2, increases activity; b) in ring C, the 9-en-12-one functionality increases the activity of these compounds the most; c) the influence of the group at C28 is unclear, as only a free carbonyl and a methoxy groups were tested.

To elucidate the influence of the substituent at carbon C28, a series of new compounds were synthesized, following the previous SAR conclusions and using compound **1.107** as an outline model (Table 1.3.27).⁴¹³

Table 1.3.27. IC₅₀ (μM) of oleanolic acid derivatives for the inhibition of the production of NO in mouse macrophages.



| Entry | Compd | R ₁ | R ₂ | IC ₅₀ (nM) |
|-------|-------|---|----------------|-----------------------|
| 1 | 1.111 | CN | CN | 0.0035 |
| 2 | 1.112 | CN | COOH | 1.68 |
| 3 | 1.113 | COOEt | CN | 0.8 |
| 4 | 1.114 | COOEt | COOH | 7.93 |
| 5 | 1.115 | CHO ₂ CH ₂ CH=CH ₂ | CN | 1.33 |
| 6 | 1.116 | CO ₂ (CH ₂) ₃ CH ₃ | CN | 6.65 |
| 7 | 1.117 | | CN | 4.45 |
| 8 | 1.118 | CO ₂ CH ₂ Ph | CN | 4.35 |
| 9 | 1.119 | CO ₂ (CH ₂) ₇ CH ₃ | CN | 60.4 |
| 10 | 1.120 | CO-D-Gluc(OAc) ₄ | CN | 0.07 |
| 11 | 1.121 | CO-D-Gluc | CN | 10.1 |
| 12 | 1.122 | CONH ₂ | CN | 0.098 |
| 13 | 1.123 | CONHNH ₂ | CN | 0.26 |

| | | | | |
|----|-------|---|----|-------|
| 14 | 1.124 | CONHMe | CN | 0.58 |
| 15 | 1.125 | CONH(CH ₂) ₂ CH ₃ | CN | 1.5 |
| 16 | 1.126 | CONH(CH ₂) ₅ CH ₃ | CN | 14.9 |
| 17 | 1.127 | CONHPh | CN | 28.6 |
| 18 | 1.128 | CONHCH ₂ Ph | CN | 9.2 |
| 19 | 1.129 | CONMe ₂ | CN | 1.55 |
| 20 | 1.130 | CON(n-Pr) ₂ | CN | 32.9 |
| 21 | 1.131 | CON  | CN | 0.8 |
| 22 | 1.132 | CON  | CN | 0.95 |
| 23 | 1.133 | CON  | CN | 1.0 |
| 24 | 1.134 | CON  | CN | 2.4 |
| 25 | 1.135 | CON  | CN | 0.014 |
| 26 | 1.136 | CON  | CN | 12.0 |

Among the compounds synthesized, CDDO **1.107** (Table 1.3.26, entry 9), CDDO-Me **1.108** (Table 1.3.26, entry 10), CDDO-CN **1.111** (Table 1.3.27, entry 1) and CDDO-Im **1.135** (Table 1.3.27, entry 25) were the most studied.^{172, 414, 415} CDDO-Me **1.108** is currently in phase II of a clinical trial for the treatment of chronic renal inflammation in patients with type 2 diabetes.⁴¹⁶

Compound **1.100** was evaluated further in other cell lines (Table 1.3.28).^{303, 417} This compound presents a good *in vitro* cytotoxic activity. *In vivo*, it was specifically cytotoxic in a melanoma model; this effect was probably due to the induction of differentiation of melanoma cells through an increase in the production of melanin and by the inhibition of topoisomerase I.⁴¹⁷

Table 1.3.28. IC_{50s} (μM) for compound **1.100** in several cell lines.

| Entry | Cell line | Cell type | IC ₅₀ (μM) |
|-----------|----------------|--|-----------------------|
| <i>1</i> | Ketr-3 | Human renal carcinoma | 37.1 |
| <i>2</i> | B16 BL6 | Highly metastatic mouse melanoma | 23.7 |
| <i>3</i> | KB | Human mouth squamous carcinoma | 14.3 |
| <i>4</i> | KB/V | Viscristin- human mouth squamous carcinoma | 25.5 |
| <i>5</i> | HCT-8 | Human intestine ileocecal adenocarcinoma | 11.6 |
| <i>6</i> | PC-3M | Human prostate carcinoma (highly metastatic) | 42.8 |
| <i>7</i> | A549 | Human lung carcinoma | 6.1 |
| <i>8</i> | B3T3 | Mouse fibroblast cells | 39.3 |
| <i>9</i> | HELF | Human embryonic lung fibroblast cells | 37.7 |
| <i>10</i> | NRP.152 | Mouse prostate | >5 |

With the aim of stimulating NO production in cancer cells, several derivatives of oleanolic acid were synthesized. The activity of compounds **1.137-1.154** (Figure 1.3.16) in preventing Fas-mediated apoptosis induction were evaluated in Hep G2 cells; however, only compounds **1.138** and **1.140-1.143** were effective. This activity is due to the production of small amounts of NO in a p53-independent manner.⁴¹⁸

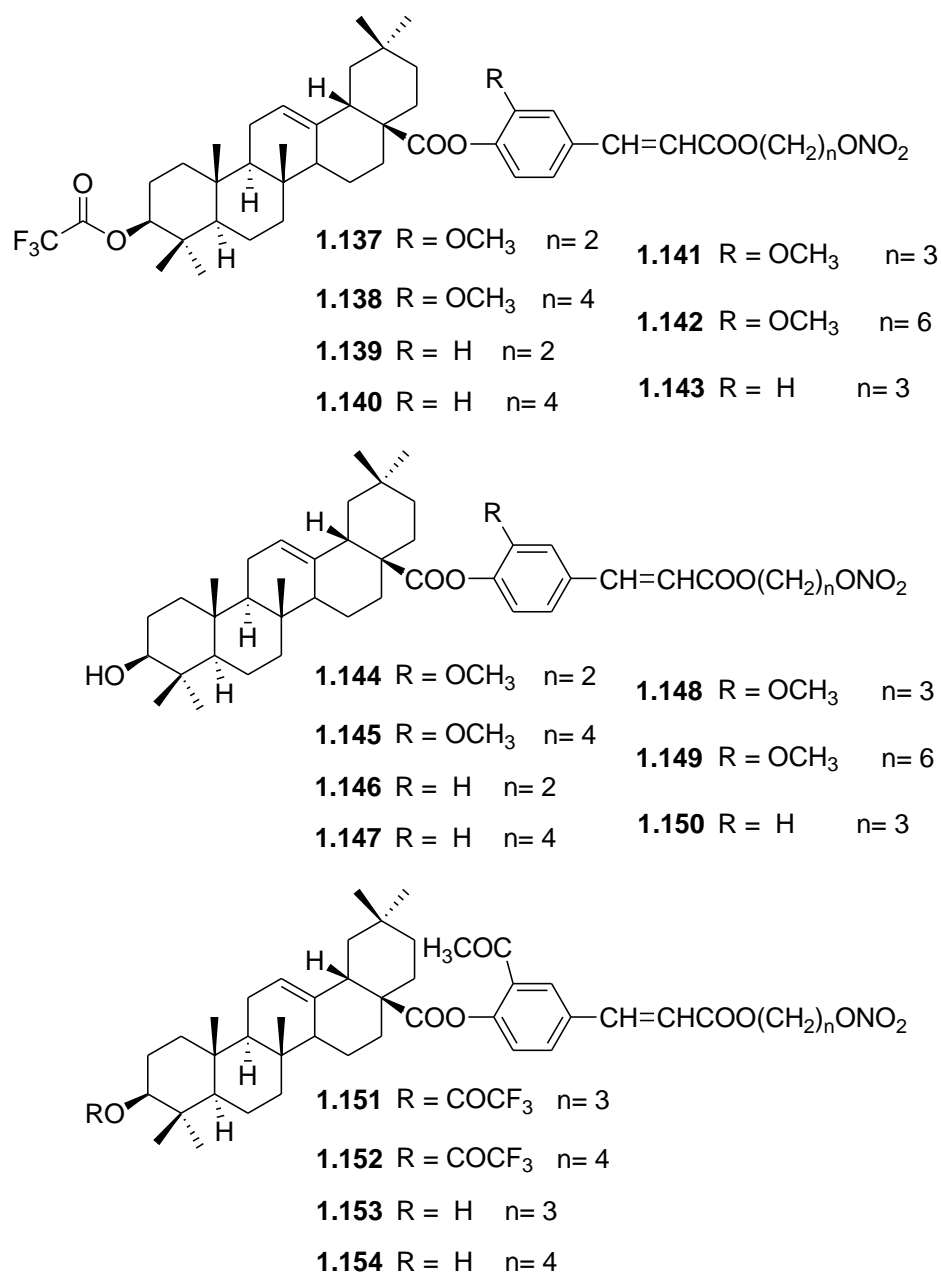


Figure 1.3.16. Schematic representation of compounds **1.137-1.154**.

The cytotoxic activity of compounds **1.155-1.163** (Figure 1.3.17) was evaluated in Hep G2, Hep3b, HeLa, PC-3, MCF-7 and HEK 293 cell lines. Only compounds **1.155-1.159** and **1.162** presented cytotoxic activity against Hep G2 and Hep3b liver cancer cells.⁴¹⁹ Compound **1.156** exhibited an IC₅₀ of 1.37, 4.78 and 14.5 μM against Hep G2, SMMC-7721 and BEL-7402 hepatic carcinoma cell lines, respectively.⁴²⁰

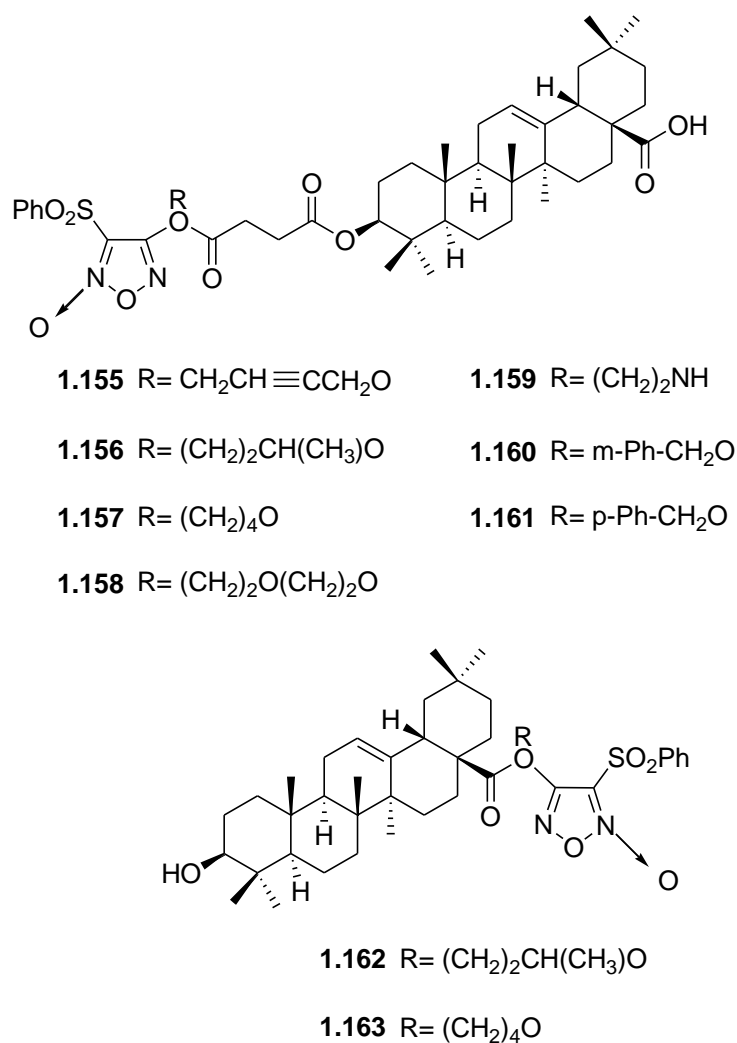


Figure 1.3.17. Schematic representation of compounds **1.155-1.163**.

Compounds **1.155-1.159** and **1.162** promoted high levels of NO in hepatocellular carcinoma cells *in vitro*, in a selective manner. This increase in NO concentration is likely to be responsible for the cytotoxicity of these compounds. In a mouse model of hepatocellular carcinoma, treatment with compounds **1.156** and **1.162** led to a decrease in the volume of tumors.⁴¹⁹

Compound **1.156** presented some restrictions regarding *in vivo* administration. With the aim of facilitating the administration of compound **1.156**, a galactosyl derivative, compound **1.64**, was synthesized (Figure 1.3.18).⁴²⁰

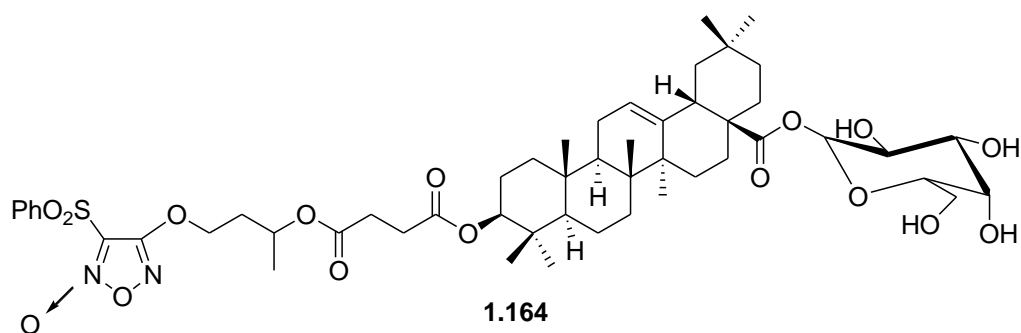
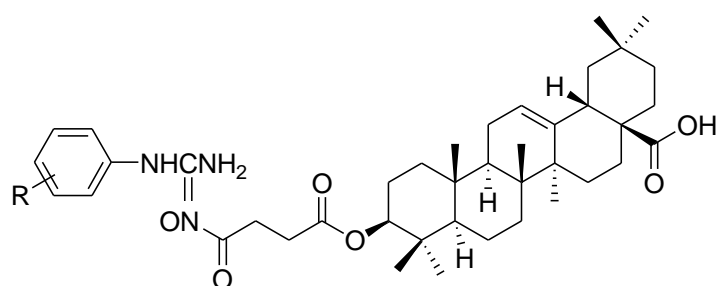


Figure 1.3.18. Schematic representation of compound **1.164**.

Compound **1.164** had better solubility than compound **1.156** and was specific and strongly cytotoxic against hepatocellular carcinoma. Compound **1.164** presented an IC_{50} of 2.13, 1.18 and 2.96 μM for Hep G2, SMMC-7721 and BEL-7402 cell lines, respectively. This compound also presented *in vivo* activity by reducing the volume of tumors in a mouse model of hepatocellular carcinoma.⁴²⁰

N-aryl-*N'*-hydroxyguanidine-based oleanolic acid derivatives, compounds **1.165-1.172**, presented strong selective cytotoxic activity for SMMC-7721 cells, which was related with their ability to produce high amounts of NO (Figure 1.3.19).⁴²¹



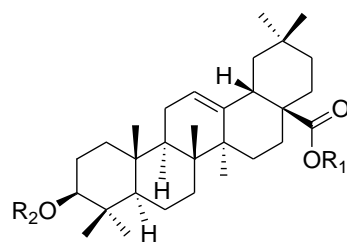
1.165 R= 2-CH₃ **1.169** R= 4-F

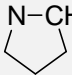
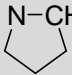
1.166 R= 4-CH₃ **1.170** R= 4-Br

1.167 R= 2-Cl **1.171** R= 2,4-diF

1.168 R= 3-Cl **1.172** R= 3,4-diCl

Figure 1.3.19. Schematic representation of compounds **1.165-1.172**.

Table 1.3.29. Cell viability of B16 cells treated with compounds **1.173-1.186** relative to the control (100% of cell viability).

| Entry | Compd | R ₁ | R ₂ | Cell viability (%) |
|-------|-------|---|----------------|--------------------|
| 1 | 1.173 | HNCH ₂ COOH | H | 87.2 |
| 2 | 1.174 | HNCH(CH ₃)COOH | H | 82.6 |
| 3 | 1.175 | HNCH(CH(CH ₃) ₂)COOH | H | 80.9 |
| 4 | 1.176 | HNCH(CH(CH ₂ CH ₃)CH ₃)COOH | H | 81.0 |
| 5 | 1.177 | HNCH(CH ₂ CH(CH ₃) ₂)COOH | H | 81.4 |
| 6 | 1.178 | HNCH(CH ₂ Ph)COOH | H | 76.4 |
| 7 | 1.179 |  | H | 84.6 |
| 8 | 1.180 | HNCH ₂ COOH | Ac | 39.6 |
| 9 | 1.181 | HNCH(CH ₃)COOH | Ac | 67.8 |
| 10 | 1.182 | HNCH(CH(CH ₃) ₂)COOH | Ac | 80.5 |
| 11 | 1.183 | HNCH(CH(CH ₂ CH ₃)CH ₃)COOH | Ac | 77.5 |
| 12 | 1.184 | HNCH(CH ₂ CH(CH ₃) ₂)COOH | Ac | 73.0 |
| 13 | 1.185 | HNCH(CH ₂ Ph)COOH | Ac | 57.8 |
| 14 | 1.186 |  | Ac | 72.3 |

The cytotoxicity of a series of oleanolic acid derivatives conjugated with amino acids was evaluated in B16 mouse melanoma cells (Table 1.3.29). Among the compounds with an amino methyl ester and an acetoxy group at carbon C3 (compounds **1.180-1.186**), compound **1.180** was the most active found.³⁹³ *In vitro*, compound **1.180** increased the number of cells in the G0/G1 phase and decreased the number of cells in the S phase, with a decrease in the levels of cyclin D1 and CDK4 and an increase in the levels of p15. Compound **1.180** had the ability to inhibit tumor growth in a mouse model, prolonging survival time.³⁹³

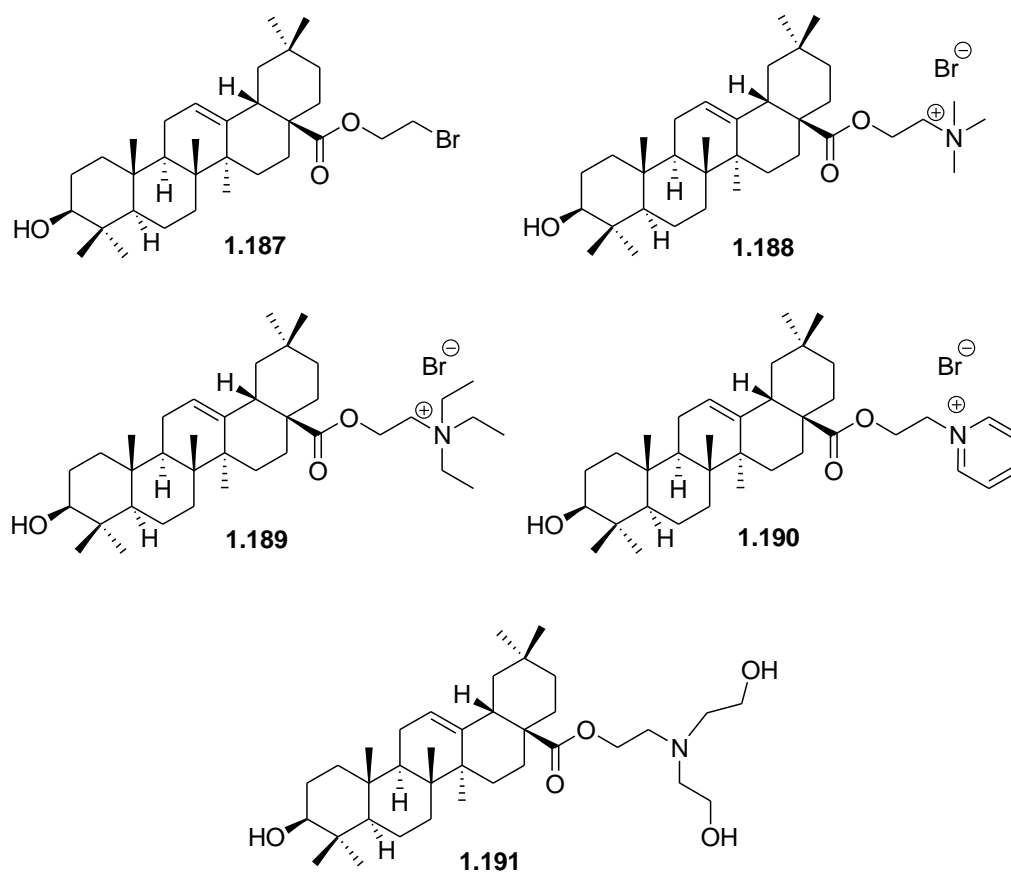


Figure 1.3.20. Schematic representation of compounds **1.187-1.191**.

Oleanolic acid is a hydrophobic compound. This property can hamper reaching the active concentrations needed to overcome this difficulty, a series of quaternary ammonium salts of oleanolic acid were synthesized (compounds **1.187-1.191**, Figure 1.3.20). The cytotoxic activity of these compounds was tested in CEM T-lymphoblastic

leukemia cells: compound **1.190** was the most active derivative found, with an IC_{50} of $10.7 \mu\text{M}$.³⁰¹

Compound **1.192** (Figure 1.3.21) was cytotoxic against MCF-7, MCF-7/ADR, CCRF-CEM, CCRF-VCR100 and MCF10A cell lines, with an IC_{50} of 4.53, 3.77, 1.69, 1.56 and $18.36 \mu\text{M}$, respectively. The normal cell line MCF10A was more resistant to this compound than were the tumor cell lines.³⁸¹

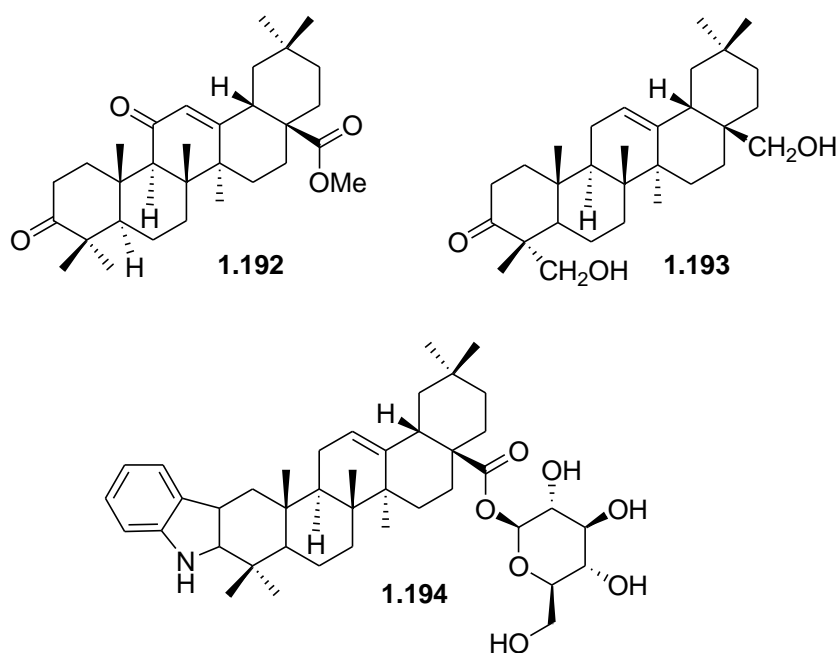


Figure 1.3.21. Schematic representation of compounds **1.192-1.194**.

Compound **1.193** (Figure 1.3.21) inhibited the growth of HT-29 cells with an IC_{50} of $40 \mu\text{M}$, via the inhibition of COX-2 and iNOS, which resulted in apoptosis. In azoxymethane-induced ACF rats, treatment with compound **1.193** inhibited the formation of ACF by 48% at low concentrations.³⁷¹

A dextrose-oleanolic acid derivative, compound **1.194**, was evaluated for its action in osteosarcoma cell lines. It inhibited cell proliferation and induced apoptosis in MG-63, U2-OS, HOS and LM-8 cells. This compound also inhibited tumor growth in the C3H and LM-8 mouse models of osteosarcoma tumors.³⁸⁸

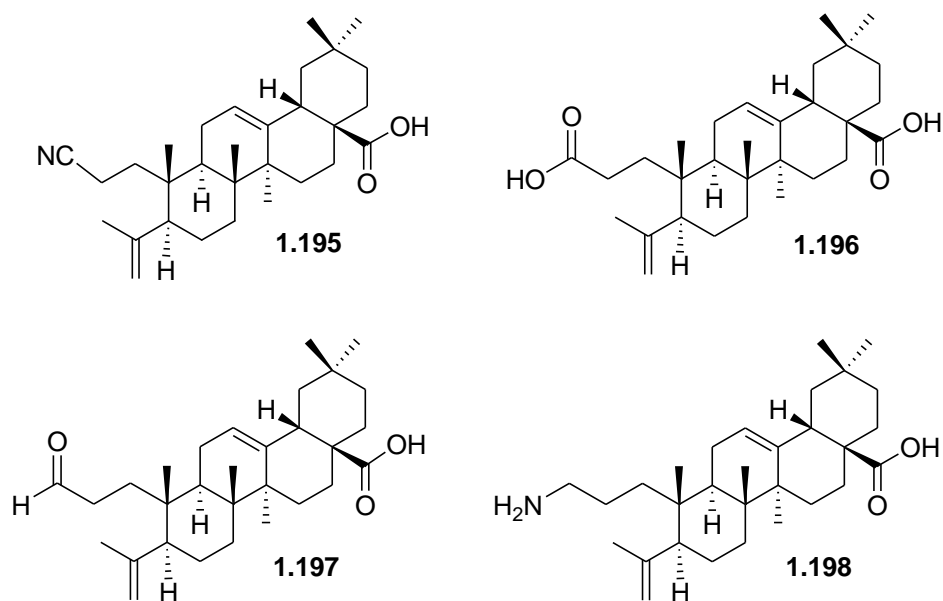


Figure 1.3.22. Schematic representation of oleanolic acid derivatives **1.195-1.198** with an open ring A.

A series of oleanolic acid derivatives with an open ring A (Figure 1.3.22) and indole-fused rings in ring A (Figure 1.3.23) were synthesized. These compounds were evaluated for their ability to inhibit the growth of premalignant NRP.152 prostate cells.^{303, 422} Among the series of open ring A derivatives, compound **1.198** was the more active, with an IC_{50} of 0.7 μ M.³⁰³ The indole-fused ring derivatives of oleanolic acid **1.200** and **1.201** were the only ones that exhibited some activity against NRP.152 cells ($IC_{50} < 5 \mu$ M); the remaining compounds were considered inactive ($IC_{50} > 5 \mu$ M).⁴²²

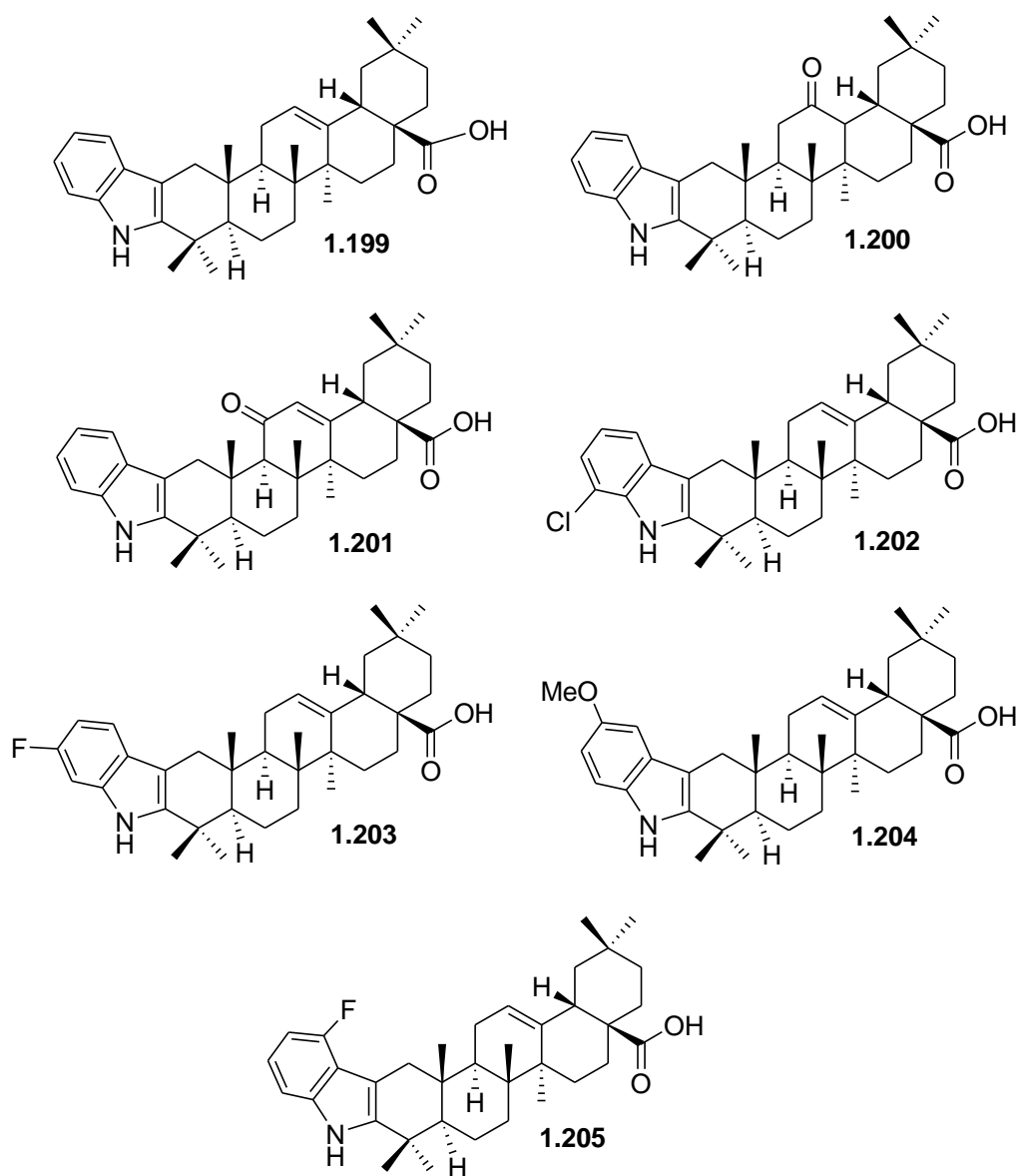


Figure 1.3.23. Schematic representation of oleanolic acid derivatives **1.199-1.205** with indole-fused ring

1.4. General objectives of this thesis

Cancer is the second leading cause of death worldwide, despite the progress in drug discovery. The layers of complexity in the biology of cancer and the drug resistance often found make the need for new chemotherapeutic drugs with different mechanisms of action a current reality.

The recognition of natural triterpenoids, in particular ursane and oleanane type pentacyclic triterpenoids, as lead molecules for the design and synthesis of more efficient and effective antitumor derivatives propped us to the preparation of new ursolic and oleanolic acid derivatives, with better antiproliferative activity than the parental compounds.

The introduction of fluorine and heteroaryl rings into the backbone structure of biological active molecules has proven to further improve the pre-existent biological activity.

With the goal to obtain new pentacyclic triterpene derivatives two synthetic strategies were projected. The reaction of alcohols and carboxylic acids with *N*, *N'*-carbonyldiazole type reagents was used aiming the preparation of carbamates, *N*-acylimidazoles and *N*-alkylimidazoles. The reaction of ursane and oleanane type triterpenoids with electrophilic and nucleophilic fluorination reagents was made with the purpose to synthesize new fluorine derivatives.

The structural elucidation of the new prepared compounds should be achieved through MS, IR and NMR techniques.

The new semisynthetic compounds should be tested for at least one solid tumor cancer cell line, in order to establish an IC_{50} and to define the structure relationship activity correlation between the different compounds. Based on the SAR findings the best compounds should be tested for other cancer cell lines in order to further prove their antiproliferative activity.

The best compound of each series should be tested for basic mechanisms of antitumor activity through the use of FACS and western blot techniques, aiming the study of perturbations on the cell cycle and apoptosis. These techniques should shed some light in the mechanisms of action of the most active compounds found for each series.

2.

**Ursolic acid derivatives:
synthetic routes,
structural elucidation,
biological evaluation
and SAR studies**

A series of new 41 heterocyclic, 14 fluorine, and 6 fluorine-heterocyclic derivatives of ursolic acid **2.1** were synthesized and fully characterized using IR, MS and 1D and 2D NMR. All new compounds were tested for their antiproliferative activity against AsPC-1 pancreatic cancer cells.

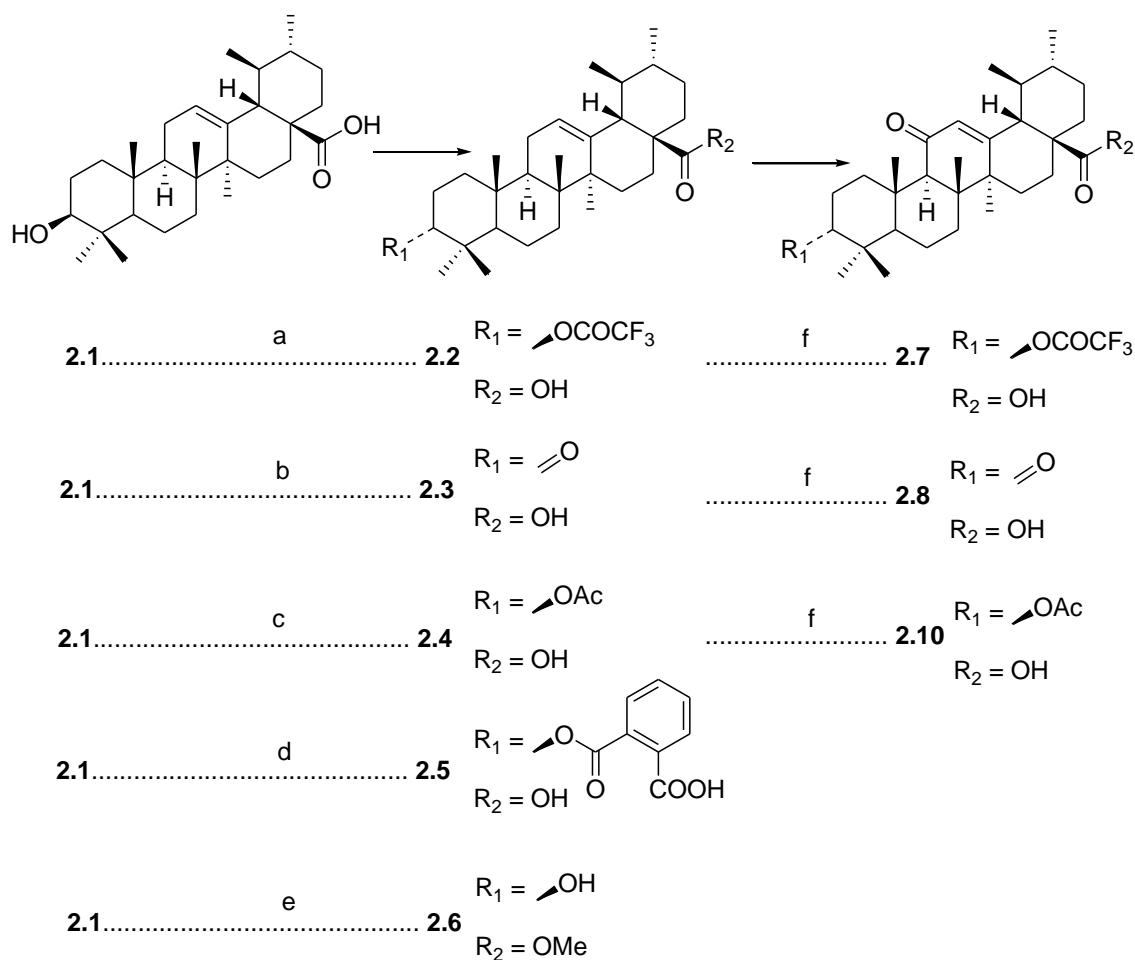
The intermediates were synthesized based on the literature, with some procedural modifications. In addition, these compounds were characterized, and some were evaluated for their antiproliferative activity against AsPC-1 cancer cells. These intermediates served as starting material in synthetic routes to obtain new ursolic acid derivatives.

The heterocyclic derivatives of ursolic acid **2.1** were obtained via the reaction of commercially available heterocyclic reagents. Most of the compounds tested exhibited better antiproliferative activity compared with ursolic acid **2.1** in AsPC-1 pancreatic cancer cells. The best compounds found were tested further for their antiproliferative activity in other pancreatic, breast, lung, prostate and hepatic cancer cell lines. Compound **2.57** was the most active, inducing apoptosis in AsPC-1 cells.

Ursolic acid fluorine derivatives were synthesized via the reaction of ursolic acid **2.1** or intermediates with selectfluor or deoxofluor. These compounds were evaluated for their inhibitory action on the growth of AsPC-1 cells, and the most active were selected and evaluated further for their antiproliferative activity in other cell lines. The most active compound, fluorolactone **2.72**, induced cell cycle arrest at low concentrations and apoptosis at higher concentrations.

2.1. Intermediates synthesis

Scheme 2.1.1.^a Synthesis of derivatives 2.2-2.9.



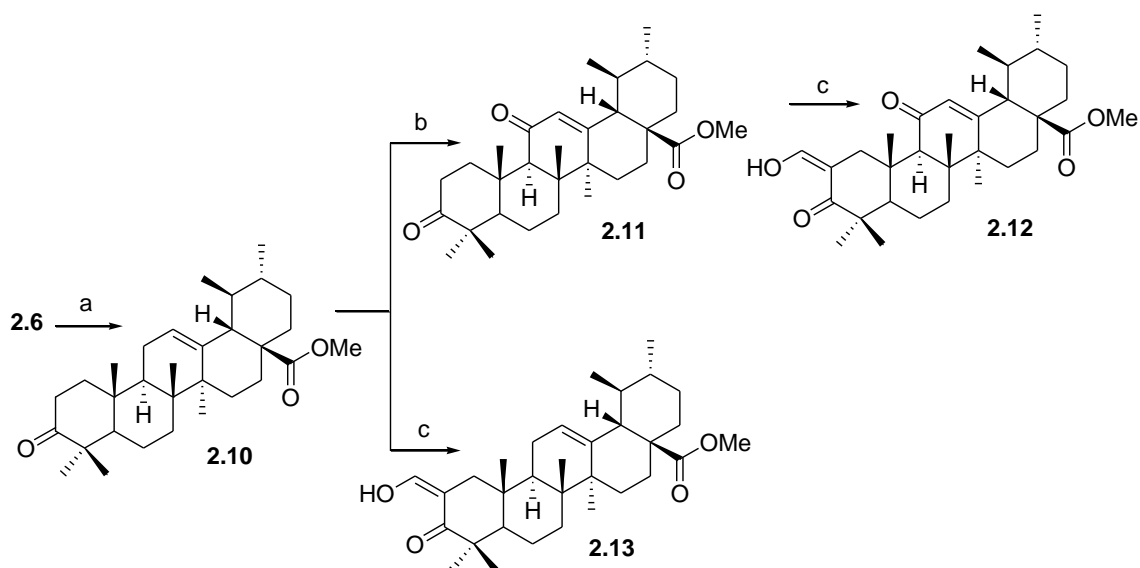
^aReagents: (a) Trifluoroacetic anhydride, DMAP, THF, r.t.; (b) Jones reagent, acetone, ice; (c) Acetic anhydride, DMAP, THF, r.t.; (d) Phthalic anhydride, DMAP, pyridine, 115 °C; (e) CH_3I , K_2CO_3 , DMF, N_2 , r.t.; (f) KMnO_4 , $\text{Fe}_2(\text{SO}_4)_3 \cdot n\text{H}_2\text{O}$, *t*-BuOH, H_2O , CH_2Cl_2 .

Conventionally, anhydrides are obtained via the reaction of the substrate with the adequate anhydride in pyridine in the presence of 4-(dimethylamino)-pyridine (DMAP, catalyst).^{309, 423} To avoid the use of pyridine as a solvent in these reactions, some researchers started to use tetrahydrofuran (THF) in the preparation of the anhydride derivative, with good yields.¹⁸³ Anhydrides **2.2** and **2.4** were prepared in good yields from ursolic acid **2.1** using trifluoroacetic anhydride and acetic anhydride, respectively

(Scheme 2.1.1). Ursolic acid phthalate **2.5** was prepared in reflux of pyridine and with an excess of reagents, to achieve the completion of the reaction (Scheme 2.1.1).^{331, 424}

The oxidation of the 3 β -hydroxyl group of ursolic acid **2.1** was achieved via Jones oxidation (Schemes 2.1.1 and 2.1.2). Some authors have described the advantage of the presence of a carbonyl group in ring C of triterpenoids for their biological activity;²⁹³ however, in ursolic acid **2.1**, the presence of a methyl group at position C19 increases the steric hindrance around position C12, thus rendering the functionalization of ring C more difficult.⁴²⁵ The oxidative mixture of potassium permanganate and copper sulfate is described for the allylic oxidation of oleanolic acid, although this mixture allows not only the preparation of the allylic oxidation, but also the co-preparation of other products.³⁰⁶ The reaction of compounds **2.2-2.4** and **2.10** with a mixture of potassium permanganate and iron sulfate ($\text{Fe}_2(\text{SO}_4)_3 \cdot n\text{H}_2\text{O}$) afforded **2.7-2.9** and **2.11** with a carbonyl group at C11 (Schemes 2.1.1 and 2.1.2). This oxidative mixture is used for the preparation of epoxides in the case of unsaturated steroids;⁴²⁶ however, in the case of ursane triterpenoids, the reaction afforded α,β -unsaturated ketones in ring C, with yields greater than 80%.

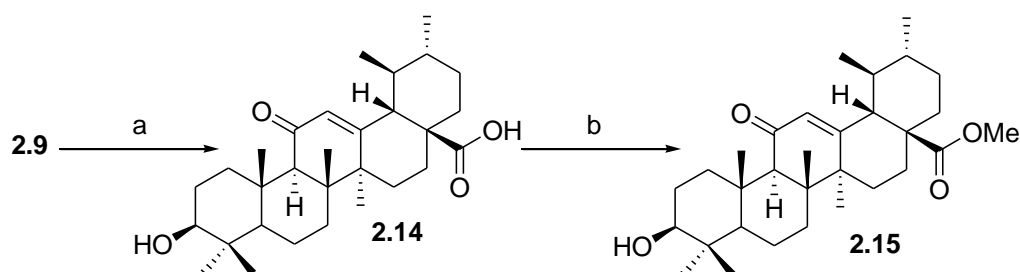
Scheme 2.1.2.^a Synthesis of derivatives **2.10-2.13**.



^aReagents: (a) Jones reagent, acetone, ice; (b) KMnO_4 , $\text{Fe}_2(\text{SO}_4)_3 \cdot n\text{H}_2\text{O}$, *t*-BuOH, H_2O , CH_2Cl_2 ; (c) Ethyl formate, benzene, NaOMe, r.t.

The methylation of the free acid in ursolic acid **2.1** is commonly achieved using diazomethane.⁴²⁷ Lee *et al* described the methylation of carboxylic acid in triterpenoids using a mixture of potassium carbonate and methyl iodide in dry DMF, with quantitative yields (Schemes 2.1.1 and 2.1.3).^{428, 429} The reaction of compounds **2.3**, **2.10** and **2.11** with ethyl formate and sodium methoxide allows the preparation of derivatives with an unsaturated exocyclic double bond in ring A (Schemes 2.1.2 and 2.1.4).^{330, 430, 431} The reaction of compound **2.16** with hydroxylamine leads to the obtention of the pyrazol ursane derivative **2.17** (Scheme 2.1.4).²⁹⁵

Scheme 2.1.3.^a Synthesis of derivatives **2.14** and **2.15**.



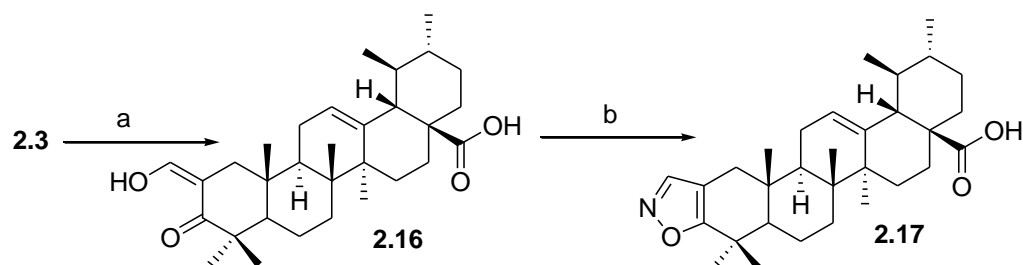
^aReagents: (a) KOH, MeOH, reflux; (b) CH₃I, K₂CO₃, DMF, N₂, r.t.

The compounds synthesized were characterized using IR, MS and 1D NMR. Ursane compounds are characterized by the presence of the H12 proton signal at around δ 5.23 ppm. Compounds **2.2**, **2.4**, **2.5**, **2.7** and **2.9** exhibited a signal in the ¹H NMR spectrum at a δ around 4.7 ppm, corresponding to proton H3 (Figure 2.1.1). The carbonyl carbon of the anhydride moiety was present at a δ around 170 ppm in the ¹³C NMR spectrum; however, in the presence of a trifluoroacetoxy group, this signal became lower and presented as a doublet at δ 157.36 ppm, with a coupling constant of 47 Hz (Figure 2.1.2).

The presence of the α,β -unsaturated carbonyl group in ring C was confirmed by the presence of a band at around 1660 cm⁻¹ in the IR spectra (which is characteristic of the carbonyl group of the α,β -unsaturated ketone), by the presence of the signal for proton H12 at approximately δ 5.6 ppm in the ¹H NMR spectrum (which is slightly higher than that observed for compounds without the carbonyl group at C11), and by the presence of an extra δ signal for a carbonyl group in the ¹³C NMR spectrum. In compounds with a

carbonyl group at C11, the δ values for carbons C12 and C13 in the ^{13}C NMR spectrum were higher than those observed for compounds without the carbonyl group in ring C.

Scheme 2.1.4.^a Synthesis of derivatives **2.16** and **2.17**.



^aReagents: (a) Ethyl formate, benzene, NaOMe, r.t.; (b) $\text{NH}_2\text{OH}\cdot\text{HCl}$, H_2O , EtOH, reflux.

The methylation of the carboxylic acid of ursolic acid **2.1** could be tracked based on the decrease in the δ signal of carbon C28 in the ^{13}C NMR spectrum, because the methylation of this group led to a decrease in the signal of around 8 ppm.

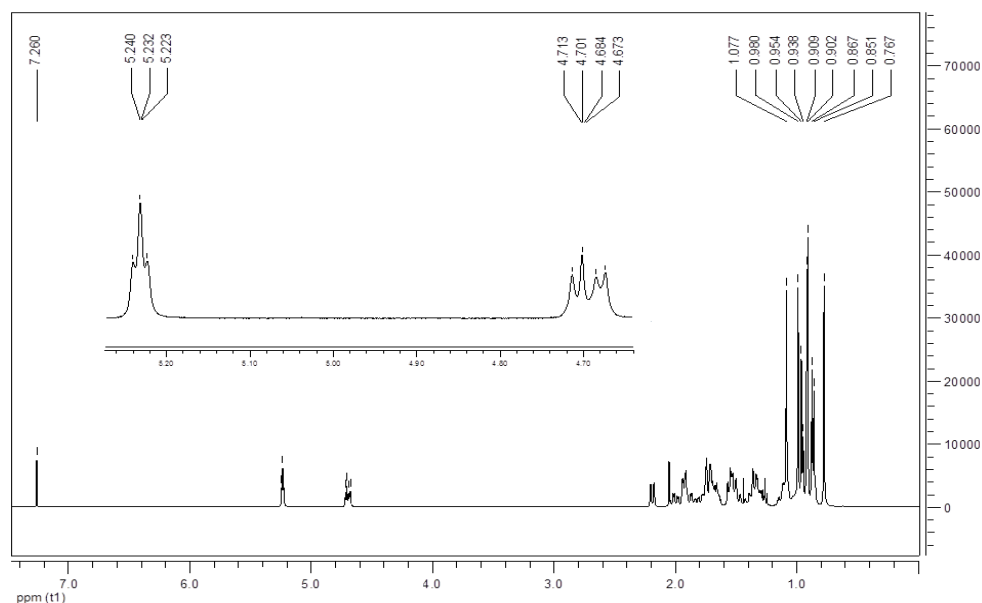


Figure 2.1.1. ^1H NMR spectrum of compound **2.2**.

In compounds **2.12**, **2.13** and **2.16**, the signal at around δ 7.8 ppm corresponded to the proton of the exocyclic double bond at C2 in the ^1H NMR spectrum. In the ^{13}C NMR

spectrum, the presence of this functionality was confirmed by the δ signal around 131 ppm, and the signal for C2 appeared around a δ of 123 ppm.

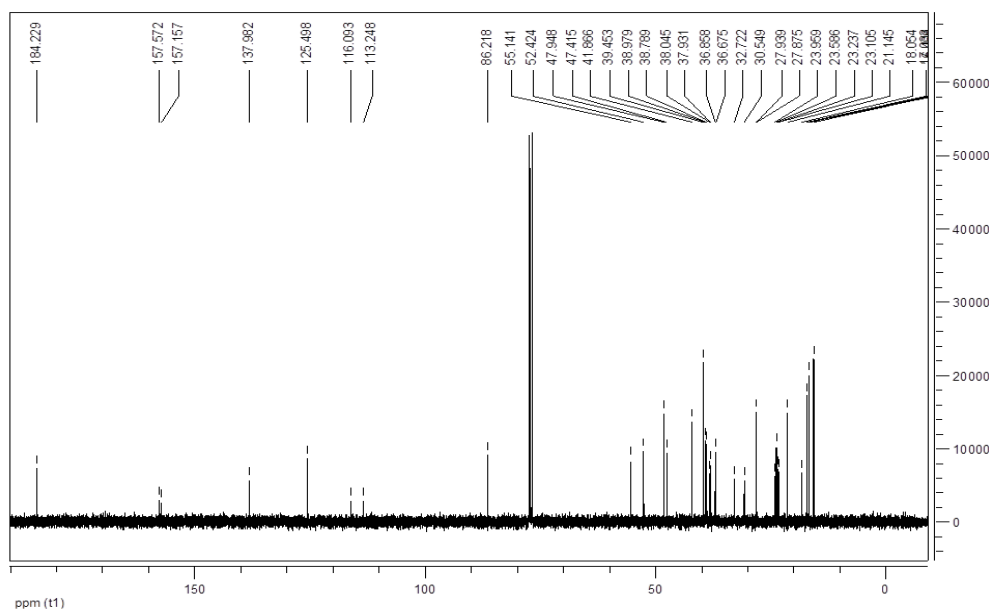


Figure 2.1.2. ¹³C NMR spectrum of compound 2.2.

2.2. Heterocyclic derivatives

2.2.1. Introduction

Heteroaryl groups are present in a variety of biologically active molecules, including several classes of derivatives, such as fungicides and anticancer agents.⁴³²⁻⁴³⁶

In this section, the introduction of different heteroaryl groups into the ursolic acid **2.1** backbone was achieved using the commercially available reagents 1,1'-carbonyldiimidazole (CDI), 1,1'-carbonyl-di(1,2,4-triazole) (CDT) and 1,1'-carbonylbis(2'-methylimidazole) (CBMI) (Figure 2.2.1).

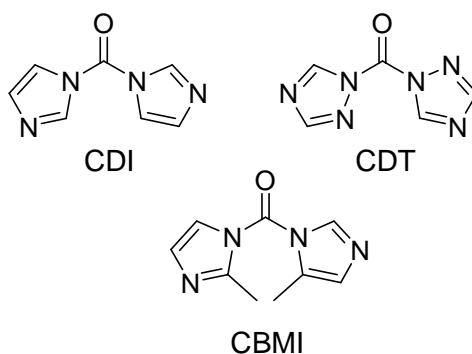


Figure 2.2.1. Schematic representation of the reagents 1,1'-carbonyldiimidazole (CDI), 1,1'-carbonyl-di(1,2,4-triazole) (CDT) and 1,1'-carbonylbis(2'-methylimidazole) (CBMI).

The introduction of a heterocyclic ring(s) in the structure of triterpenoids is a modification that has been performed in betulinic acid and betulin, affording several derivatives. Most of these new compounds presented better cytotoxic activity compared with that of the parental compounds.^{433, 434, 437} The introduction of the heterocyclic ring was made via the reaction of an alcohol, a carboxylic acid or an aldehyde with CDI, CBMI or CDT in reflux of THF under an inert atmosphere, affording *N*-alkylimidazoles,⁴³⁸⁻⁴⁴⁰ imidazole carboxylic esters (carbamates),^{433, 434, 441} or *N*-acylimidazoles.⁴⁴²

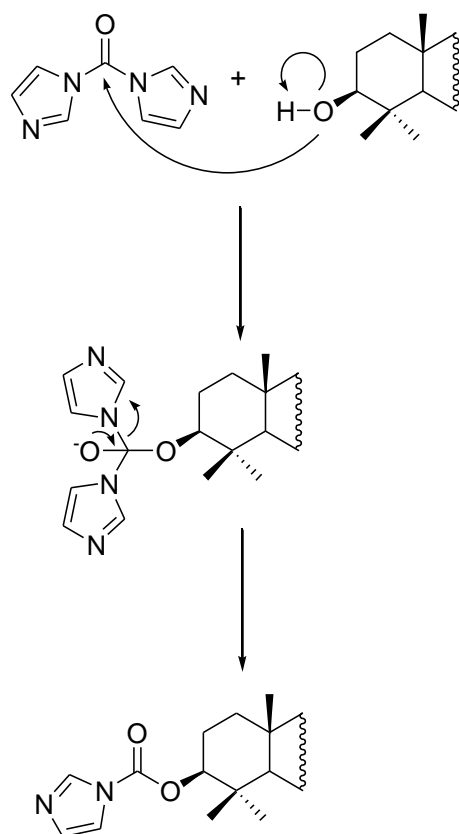


Figure 2.2.2. Reaction mechanism of triterpenoids with CDI for the formation of carbamates.

The formation of carbamates (Figure 2.2.2.), *N*-acylimidazoles or *N*-alkylimidazoles (Figure 2.2.3.) depends on the nature of the reactive group and on the reaction conditions used. Both products are achieved through nucleophilic attack of the alcohol on the carbonyl group of the heteroaryl reagent.^{438, 440, 442}

With the aim of improving the antitumor activity of ursolic acid **2.1** and intermediates, imidazole, methylimidazole or triazole rings were introduced in ursolic acid **2.1** and intermediates at different positions of the structure.

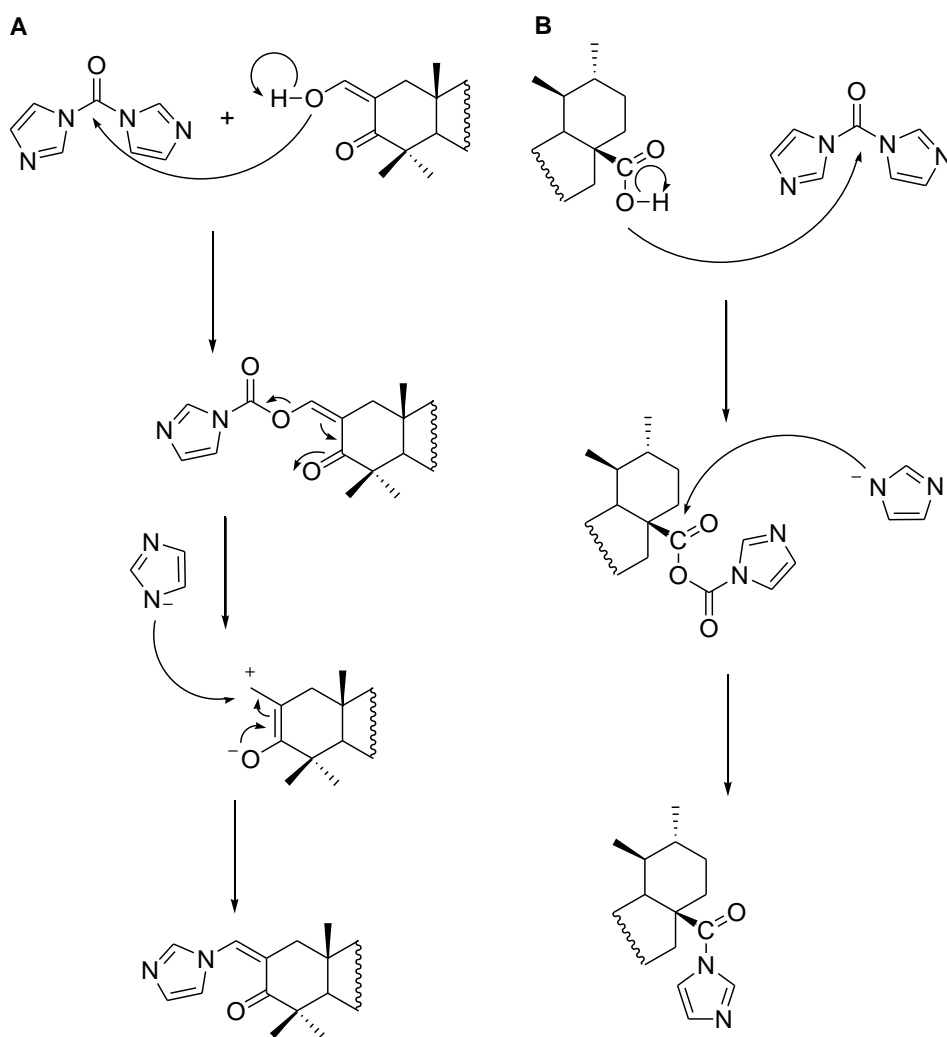


Figure 2.2.3. Reaction mechanism of CDI with triterpenoids for the formation of *N*-alkylimidazoles (A) and *N*-acylimidazoles (B).

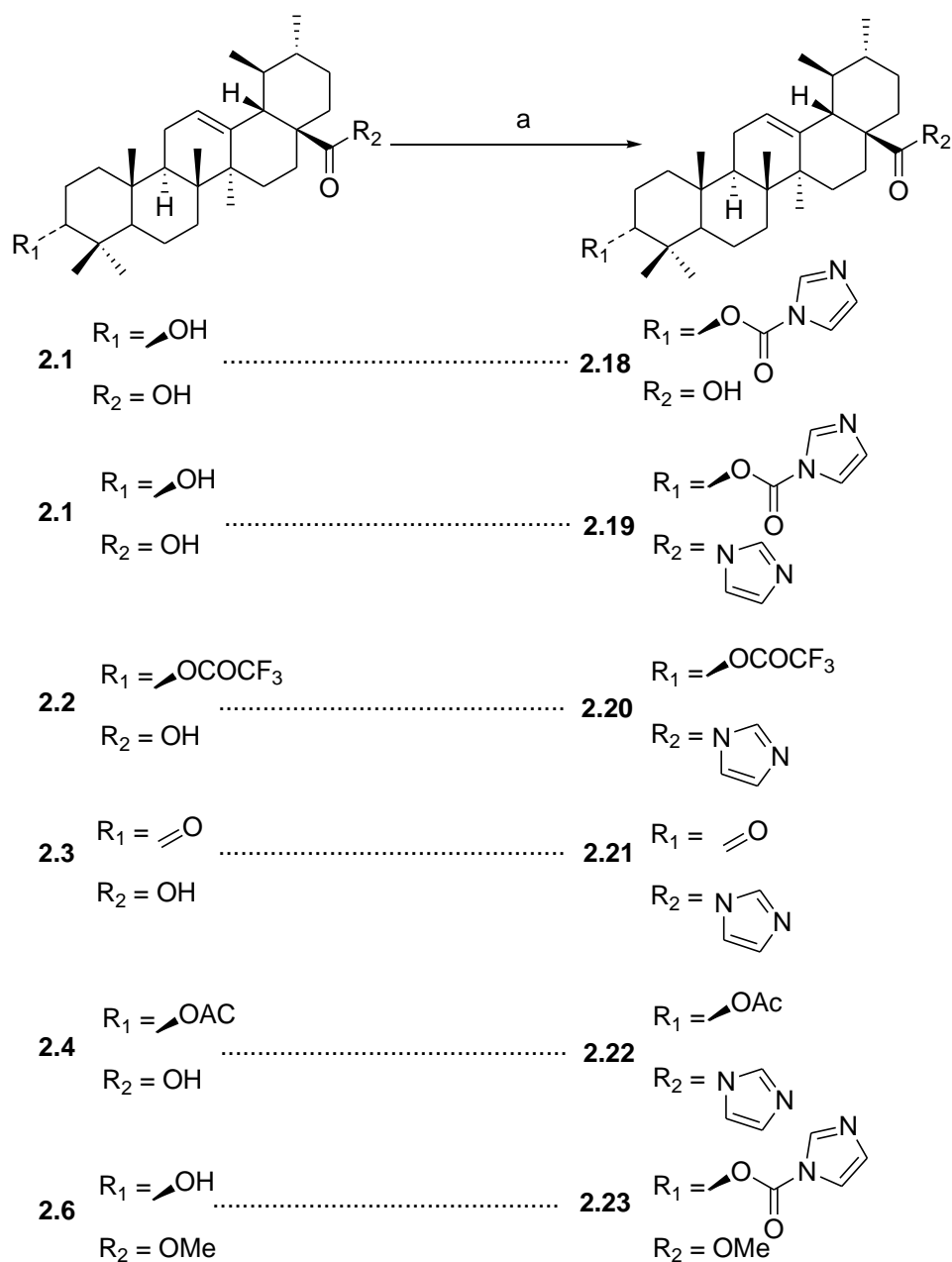
2.2.2. Results and Discussion

2.2.2.1. Chemistry

2.2.2.1.1. Imidazole derivatives

The reaction of ursolic acid **2.1** and intermediates with CDI in THF under an inert atmosphere afforded *N*-acylimidazoles (Schemes 2.2.1 and 2.2.2), carbamates (Schemes 2.2.1 and 2.2.2) and *N*-alkylimidazoles (Scheme 2.2.3).

Scheme 2.2.1.^a Synthesis of derivatives **2.18-2.23**.



^aReagents: (a) CDI, THF, N_2 , reflux.

Carbamates **2.18**, **2.19**, **2.23**, **2.24** and **2.28** (Schemes 2.2.1 and 2.2.2) were characterized by the presence of a band in the IR at around 1750 cm^{-1} , corresponding to the carbonyl group of the ester, a value that was higher than that obtained for carboxylic acids (1700 cm^{-1}) or amides **2.20-2.22** and **2.25-2.27** (1726 cm^{-1}) (Schemes 2.2.1 and 2.2.2). The imidazole group did not stand in the IR spectra as an isolated band: C–N bands were present at around 1400 cm^{-1} and the unsaturated bonds of the ring were sometimes visualized as small bands, at around 3100 cm^{-1} (Figure 2.2.4).

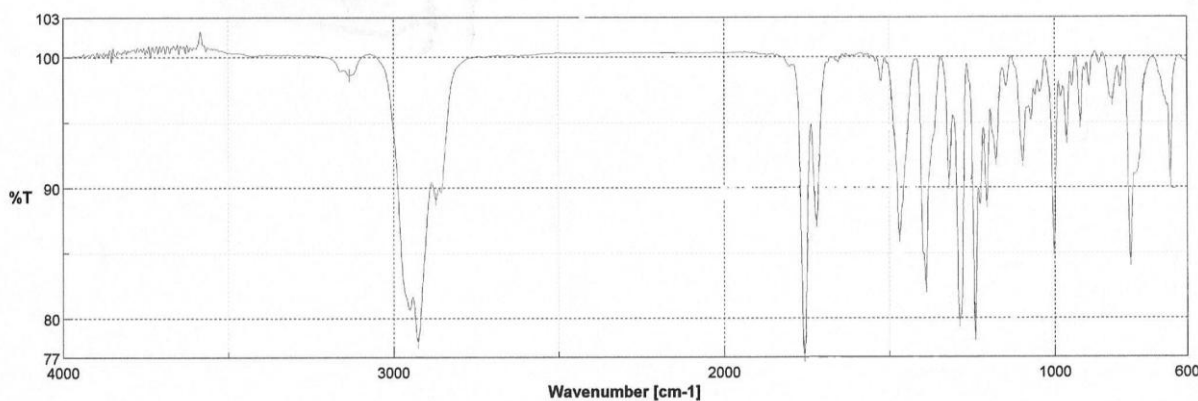


Figure 2.2.4. IR spectrum of compound **2.19**.

In the ^1H NMR spectrum, *N*-alcyimidazole **2.21** presented three signals at δ 8.46, 7.56 and 7.11 ppm that corresponded to the imidazole ring (Figure 2.2.5). In the ^{13}C NMR spectrum, the imidazole ring signals corresponded to δ at 136.69, 117.79 and 127.97 ppm (Figures 2.2.6 to 2.2.8). Proton H12 was detected as a triplet in the ^1H NMR spectrum, with a signal at δ 5.25 ppm, the corresponded carbon (C12) has a δ signal at 126.55 ppm. Proton H12 correlated with carbon C18, which allowed the identification of the signal at δ 54.22 ppm in the ^{13}C NMR spectrum as corresponding to carbon C18 (Figure 2.2.9). Protons of the C29 methyl group (δ 0.91 ppm) also correlated with carbon C18 and carbon C19 (δ 39.22 ppm). The identification of a methyl group at C29 allowed the identification of a signal at δ 1.00 ppm that corresponded to the methyl group at C30. The signals of the methyl groups at C29 and C30 were usually observed as doublets in the ^1H NMR spectrum, as the protons in the methyl group were coupled with the geminal protons at C19 and C20, respectively.

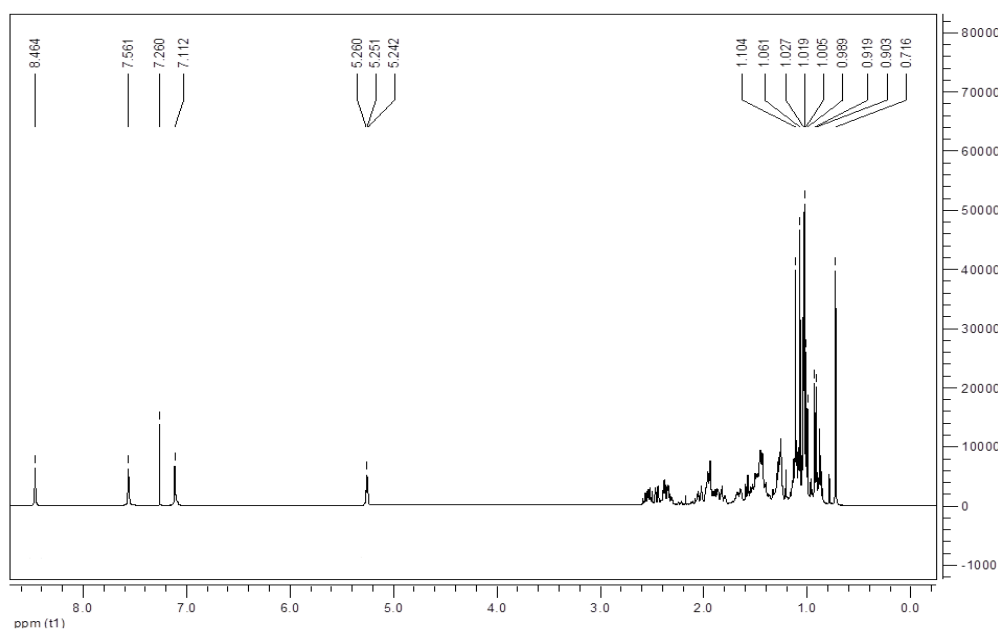


Figure 2.2.5. ^1H NMR spectrum of compound 2.21.

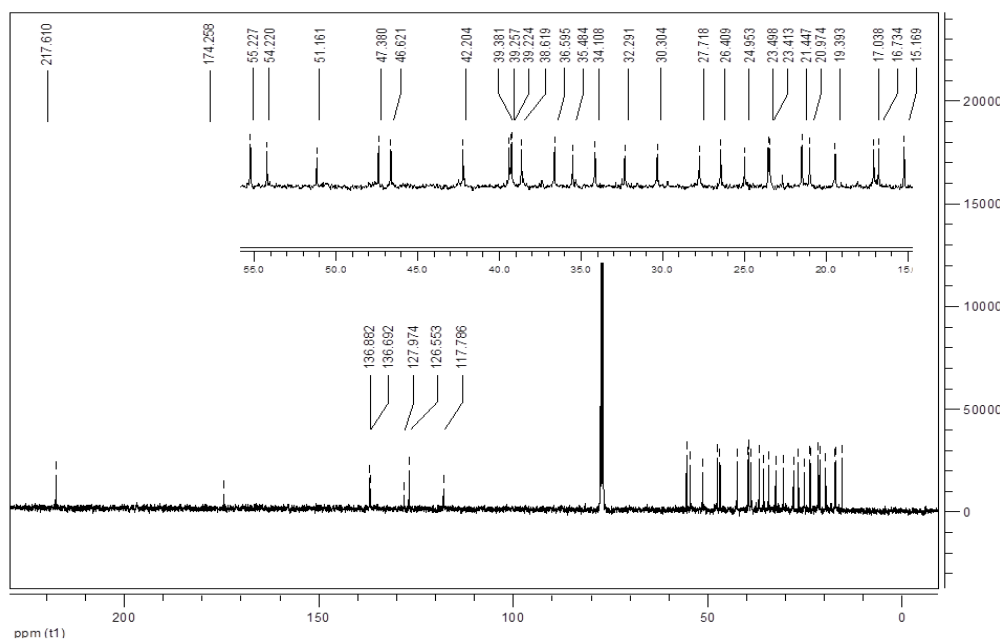


Figure 2.2.6. ^{13}C NMR spectrum of compound 2.21.

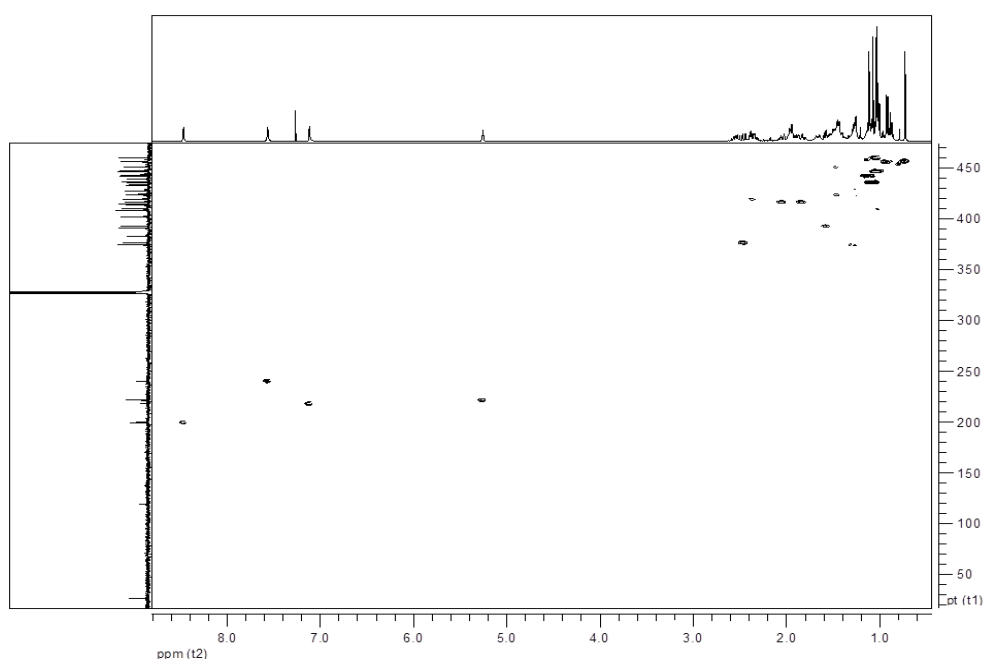


Figure 2.2.7. HMQC spectrum of compound **2.21**.

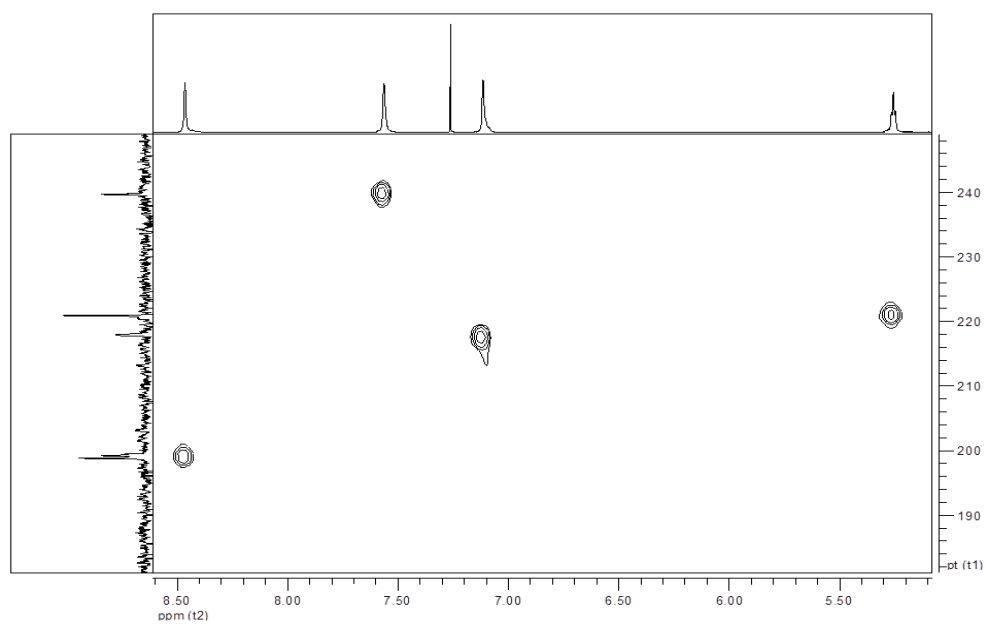


Figure 2.2.8. HMQC spectrum detail of compound **2.21**, with incidence in the imidazole ring signals.

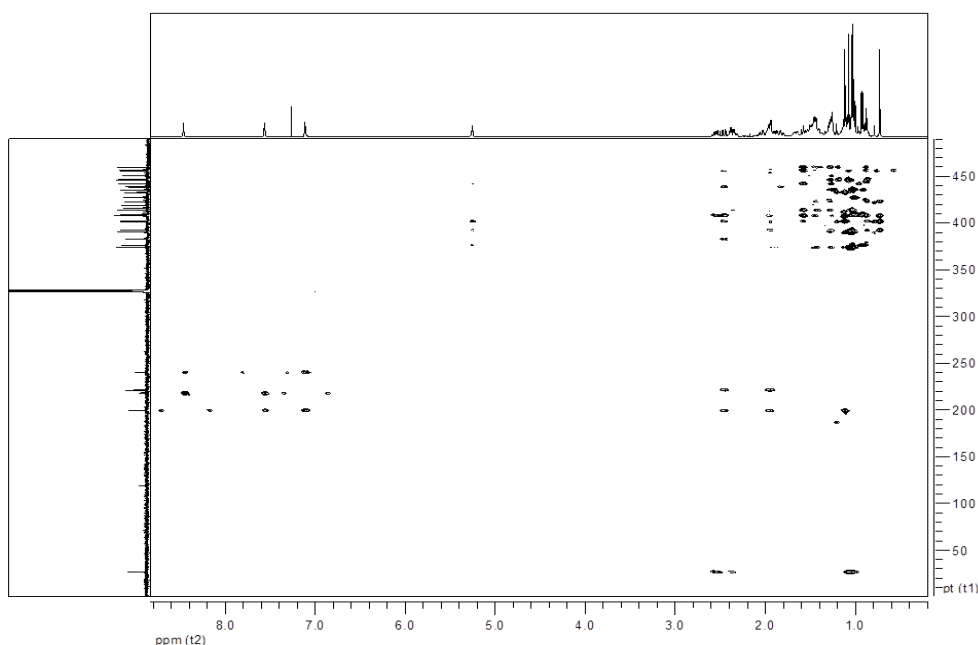
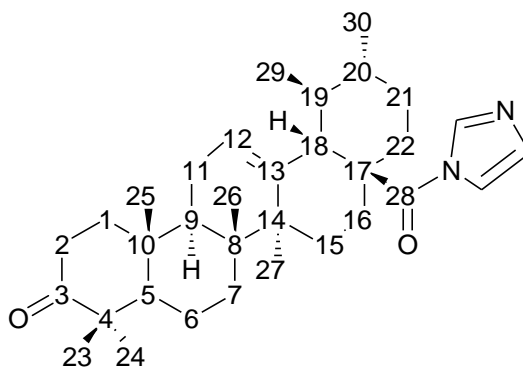


Figure 2.2.9. HMBC spectrum of compound **2.21**.

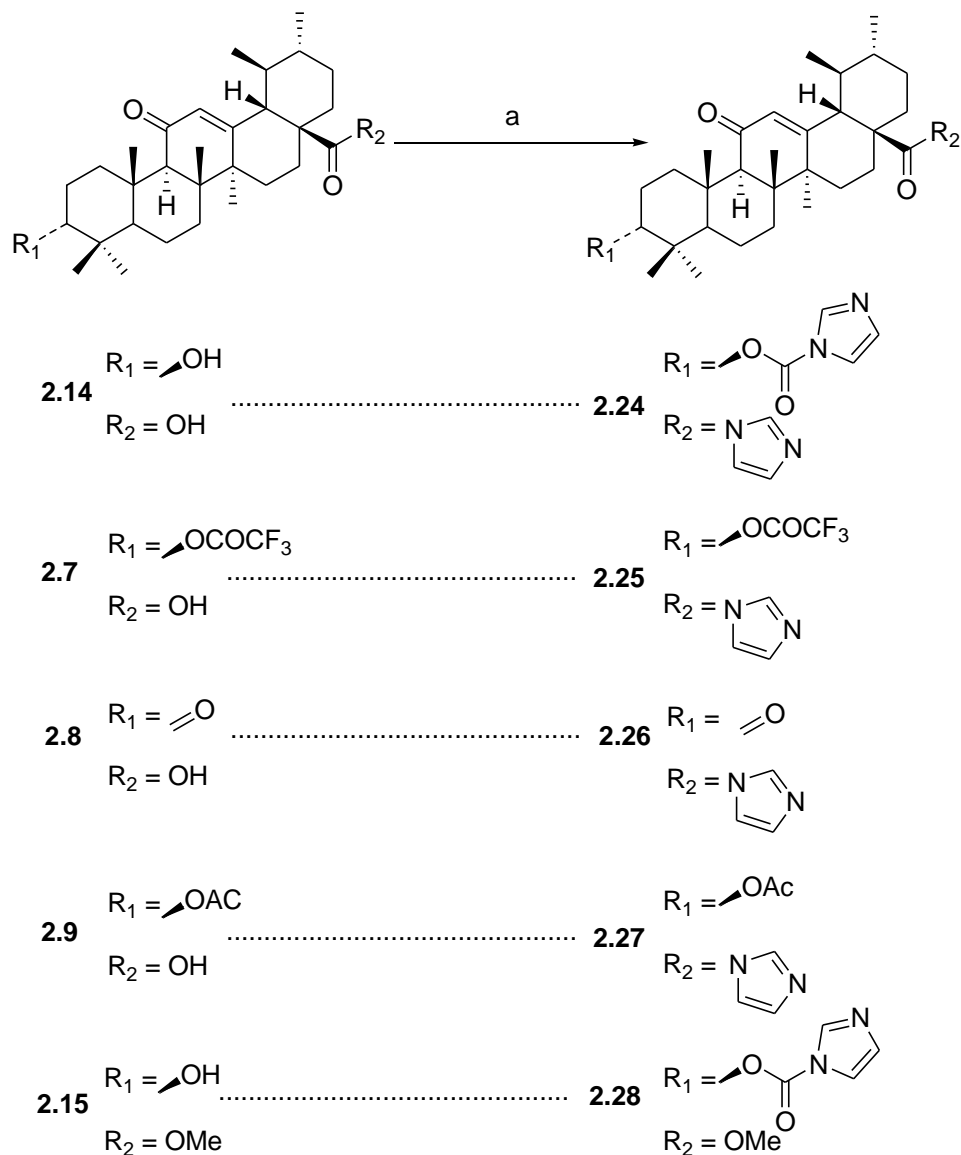
The signal at δ 136.88 ppm corresponded to carbon C13, as this signal was not present in the DETP spectrum of compound **2.21**. The protons of the methyl group at C27 (δ 1.10 ppm) correlated with carbon C13. The identification of the methyl group at C27 allowed the attribution of the δ signals to carbons C8 (39.38 ppm), C9 (46.62 ppm) and C26 (16.73 ppm) in the ^{13}C NMR spectrum.

Carbon C3 of compound **2.21**, with a signal at δ 217.61 ppm, correlated with the methyl groups at C23 and C24; however, because both groups were located at a geminal carbon (C4), it was not possible to identify these carbons specifically. In the ^1H NMR spectrum, the δ signals at 1.06 and 1.03 ppm corresponded to the methyl groups at C23 or C24.

The correlations observed on HMBC and HMQC permitted the identification of several ^{13}C and ^1H NMR δ signals, which are presented in Table 2.2.1.

Table 2.2.1. NMR data for compound **2.21**.

| Entry | Position | δ ^1H NMR | δ ^{13}C NMR |
|-----------|-----------|---------------------------|------------------------------|
| 1 | 3 | - | 217.61 |
| 2 | 4 | - | 47.38 |
| 3 | 5 | - | 55.22 |
| 4 | 7 | - | 32.29 |
| 5 | 8 | - | 39.38 |
| 6 | 9 | - | 46.62 |
| 7 | 10 | - | 36.60 |
| 8 | 12 | 5.25 ($J= 7.32$) | 126.55 |
| 9 | 13 | - | 136.88 |
| 10 | 14 | - | 42.20 |
| 11 | 15 | - | 27.72 |
| 12 | 17 | - | 51.16 |
| 13 | 18 | - | 54.22 |
| 14 | 19 | - | 39.22 |
| 15 | 20 | - | 38.62 |
| 16 | 21 | - | 30.30 |
| 17 | 25 | 1.02 | 15.17 |
| 18 | 26 | 0.72 | 16.73 |
| 19 | 27 | 1.10 | 23.50 |
| 20 | 28 | - | 174.26 |
| 21 | 29 | 0.91 ($J= 6.46$) | 17.04 |
| 22 | 30 | 1.00 ($J= 6.32$) | - |

Scheme 2.2.2.^a Synthesis of derivatives 2.24-2.28.

^aReagents: (a) CDI, THF, N₂, reflux.

Compound **2.24**, a carbamate at C3 with an *N*-acylimidazole group located at C28, has two imidazole groups in its structure, which corresponded to five signals in the ¹H NMR spectrum, as the signal at δ 7.05 ppm corresponded to two protons (Figure 2.2.10). On the ¹³C NMR spectrum, the signals of the imidazole rings were observed at δ signal of 136.95, 136.89, 130.48, 130.11, 117.25 and 116.98 ppm (Figure 2.2.11).

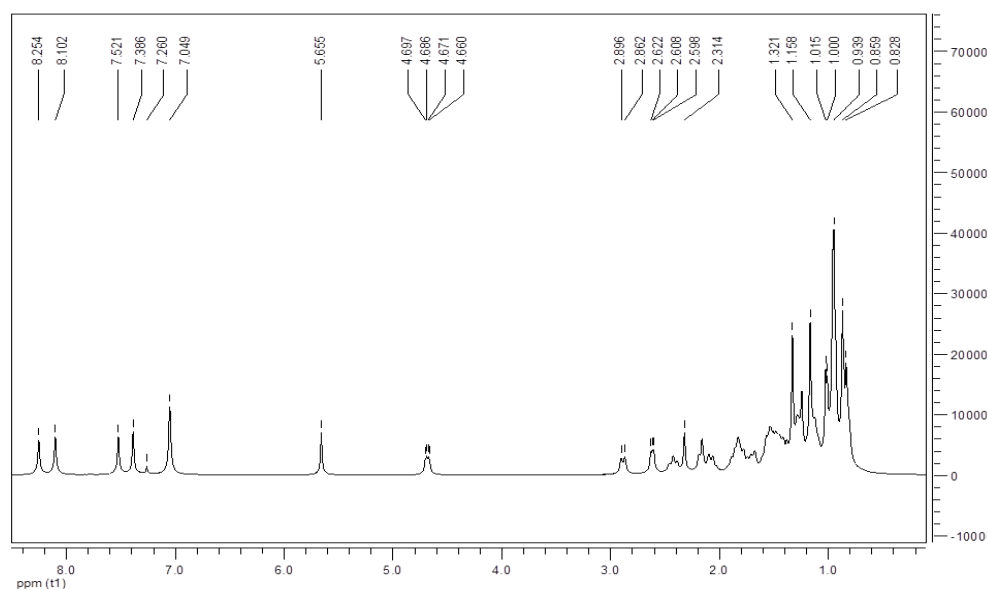


Figure 2.2.10. ^1H NMR spectrum of compound **2.24**.

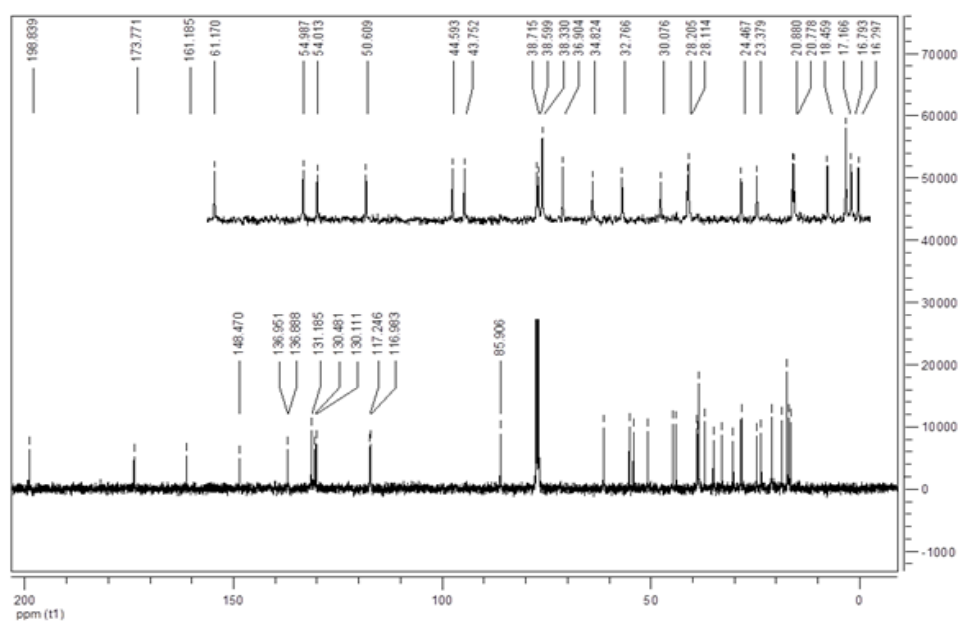


Figure 2.2.11. ^{13}C NMR spectrum of compound **2.24**.

The carbamate group at C3 in compound **2.24** exhibited a signal at δ 85.91 ppm in the ^{13}C NMR spectrum, which corresponded to carbon C3. Proton H3 in the ^1H NMR spectrum appeared as a double doublet with a signal at δ 4.68 ppm. The carbonyl group appeared in the ^{13}C NMR spectrum as a signal at δ 148.47 ppm. Proton H12 was detected as a singlet at δ 5.66 ppm and was correlated with carbons C9 (61.17 ppm), C14 (43.75

ppm) and C18 (54.01 ppm), thus allowing their identification in the ^{13}C NMR spectrum (Figure 2.2.12). Proton H18 (2.61 ppm) allowed the identification of the quaternary carbon C17 (50.61 ppm) and carbon C19 (38.33 ppm). The methyl group signals of carbons C29 (17.17 ppm) and C30 (20.78 ppm) appeared as doublets in the ^1H NMR spectrum, with signals at δ 0.94 and δ 1.01 ppm, respectively.

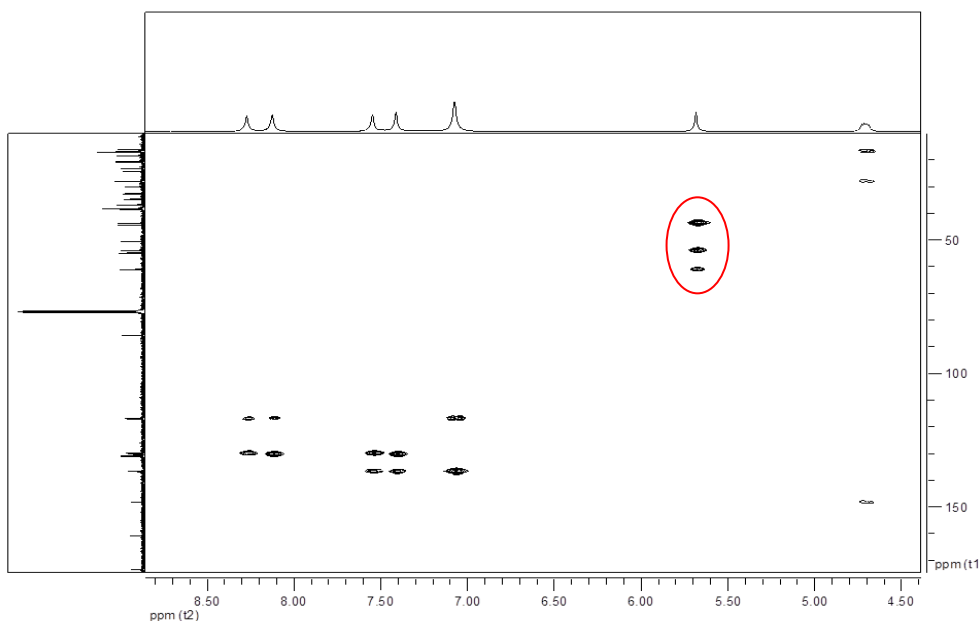


Figure 2.2.12. Detail of the HMBC spectrum of compound **2.24**. The correlations between proton H12 and carbons C9, C14 and C18 are highlighted.

In the ^1H NMR spectrum of compound **2.24**, the signal at δ 2.31 ppm was identified as proton H9, which allowed the attribution of δ signals at 198.84, 44.59 and 36.90 ppm to carbons C11, C8 and C10, respectively. The identification of carbon C10 allowed the attribution of the signal in the ^1H NMR spectrum at δ 1.16 ppm to the methyl group at C25, and the signal at δ 16.30 ppm in the ^{13}C NMR spectrum to C25.

Some of the correlations discussed previously for compound **2.24** are presented in Figure 2.2.13. In addition, other correlations were observed and allowed the identification of other δ signals in the ^{13}C NMR spectrum, as presented in experimental section 2.4.1.

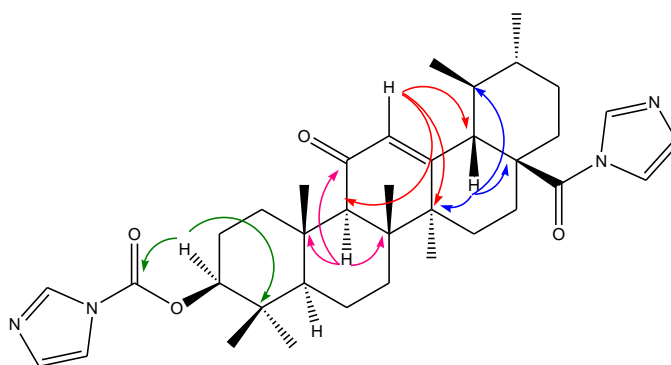


Figure 2.2.13. Some HMBC correlations for compound **2.24**.

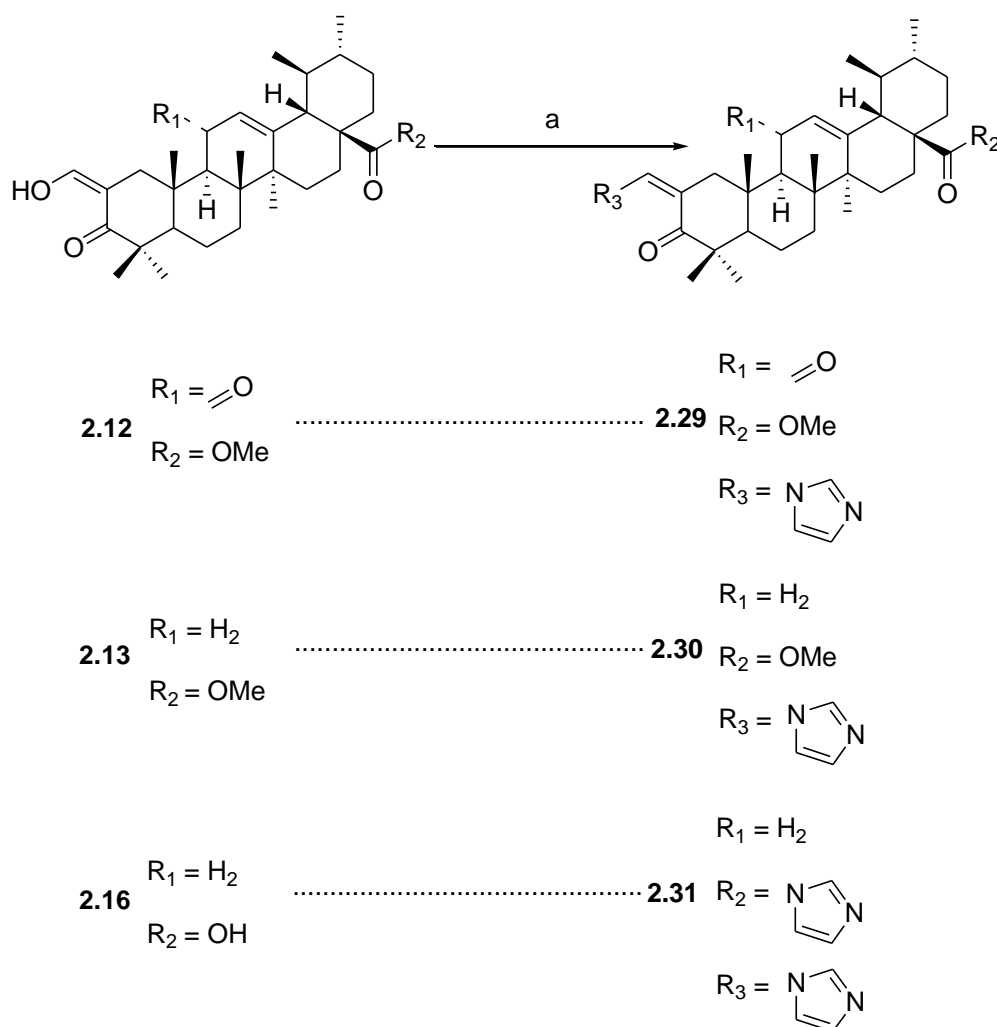
Compounds **2.20**, **2.25** and **2.26** were also analyzed using 1D and 2D NMR. Some of the data obtained in the ^1H NMR and ^{13}C NMR analyses are presented in Table 2.2.2.

Table 2.2.2. Selected ^1H and ^{13}C NMR data from the backbone of compounds **2.20**, **2.25** and **2.26**.

| Entry | Position | 2.20 | | 2.25 | | 2.26 | |
|-------|-----------------|-----------------------|--------------------------|-----------------------|--------------------------|-----------------------|------------|
| | | δ H | δ C | δ H | δ C | δ H | δ C |
| 1 | 1 | - | 38.05 | - | 38.54 | - | 39.76 |
| 2 | 3 | 4.67 ($J=15.50$) | 86.14 | 4.68 ($J=16.08$) | 85.85 | - | 216.91 |
| 3 | 4 | - | 37.88 | - | 38.18 | - | 47.69 |
| 4 | 5 | 0.82 ($J=11.24$) | 55.12 | 0.77 ($J=11.51$) | 54.88 | - | 55.44 |
| 5 | 7 | - | 32.62 | - | 32.74 | - | 32.33 |
| 6 | 8 | - | 39.39 | - | 44.59 | - | 44.47 |
| 7 | 9 | 1.51 | 47.33 | 2.30 | 61.15 | 2.37 | 60.68 |
| 8 | 10 | - | 36.75 | - | 36.88 | - | 36.73 |
| 9 | 11 | - | - | - | 198.91 | - | 198.55 |
| 10 | 12 | 5.23 | 126.30 | 5.66 | 131.17 | 5.68 | 131.21 |
| 11 | 13 | - | 137.01 | - | 161.29 | - | 161.40 |
| 12 | 14 | - | 42.06 | - | 43.74 | - | 43.86 |
| 13 | 15 | - | 27.70 | - | 28.19 | - | 28.29 |
| 14 | 17 | - | 50.87 | - | 50.59 | - | 50.65 |
| 15 | 18 | 2.45 ($J=11.03$) | 54.10 | 2.61 ($J=11.10$) | 53.99 | 2.63 ($J=10.67$) | 54.06 |
| 16 | 19 | - | 39.22 | - | 38.72 | - | - |
| 17 | 20 | - | 38.66 | - | 38.34 | - | 38.78 |
| 18 | 21 | - | 30.35 | - | 30.08 | - | 38.37 |
| 19 | 25 | 0.94 | 15.47 | 1.15 | 16.35 | 1.24 | 15.59 |
| 20 | 26 | 0.68 | 16.70 | 0.86 | 18.43 | 0.89 | 18.36 |
| 21 | 27 | 1.10 | 23.56 | 1.32 | 20.87 | 1.32 | 20.80 |
| 22 | 28 | - | 174.70 | - | 173.79 | - | 173.82 |
| 23 | 29 | 0.91 ($J=6.54$) | 17.08 | 0.93 ($J=6.22$) | 17.20 | 0.93 ($J=6.20$) | 17.18 |
| 24 | 30 | 1.00 ($J=6.15$) | 21.02 | 1.01 ($J=6.09$) | 20.82 | - | - |
| 25 | OCO | - | 157.34 ($J=41.77$) | - | 157.31 ($J=41.52$) | - | - |
| 26 | CF ₃ | - | 114.62 ($J=286.24$) | - | 114.60 ($J=286.28$) | - | - |

Scheme 2.2.3 represents the synthesis of amines **2.29-2.31**. These amines had an α,β unsaturated ketone in ring A, which was confirmed by the presence of a signal around δ 7.8-7.7 ppm, corresponding to the proton in the exocyclic double bond at C2 in the ^1H NMR spectrum. In the ^{13}C NMR spectrum, the presence of this functionality was confirmed by the presence of a signal around δ 131 ppm, correspondent to the carbon of the exocyclic double bond at C2. The signal for carbon C2 appeared at around δ 123 ppm and the signal for C3 appeared at δ 200 ppm. The signals of the imidazole ring were similar to that described for compounds **2.21** and **2.24**.

Scheme 2.2.3.^a Synthesis of derivatives **2.29-2.31**.



^aReagents: (a) CDI, THF, N_2 , reflux.

2.2.2.1.2. Methylimidazole derivatives

The synthesis of the ursolic acid methylimidazole derivatives **2.32-2.45** was achieved via the dissolution of the respective substrate in dry THF under an inert atmosphere and via the addition of CBMI. In some cases, the reaction proceeded slowly because CBMI is a bulky reagent and various substrates can present a slight sterical impairment for the reaction, affording lower yields. These reaction conditions allowed the synthesis of *N*-acylimidazoles **2.34-2.36** and **2.39-2.41** (Schemes 2.2.4 and 2.2.5), *N*-alkylimidazoles **2.43-2.45** (Scheme 2.2.6) and carbamates **2.32**, **2.33**, **2.37**, **2.38** and **2.42** (Schemes 2.2.4 and 2.2.5).

Compound **2.34** has a trifluoroacetoxy moiety at carbon C3. In the IR spectrum, the C–F stretching vibration occurred at around 1100 cm^{-1} , the stretching vibration for the carbonyl group of the anhydride appeared at around 1780 cm^{-1} , whereas the carbonyl group of the amide was present at lower values (1710 cm^{-1}) (Figure 2.2.14).

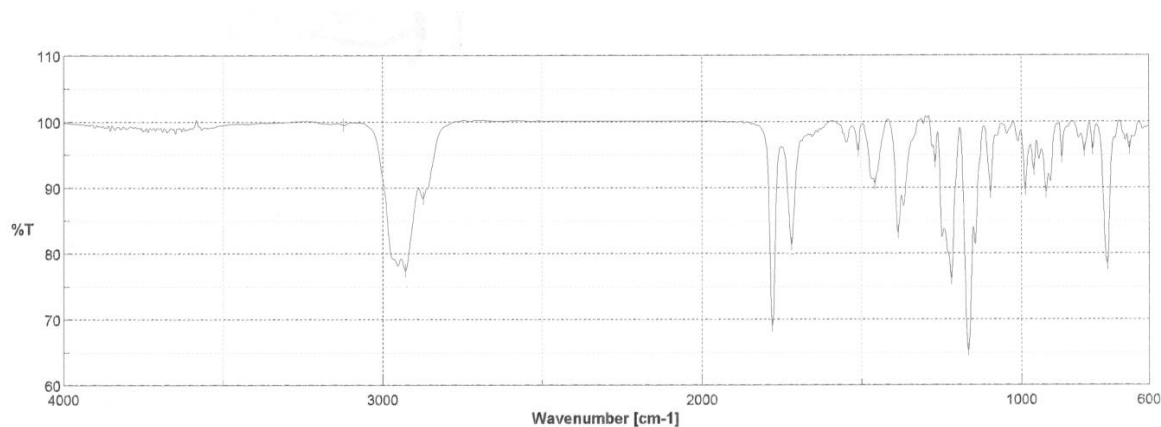
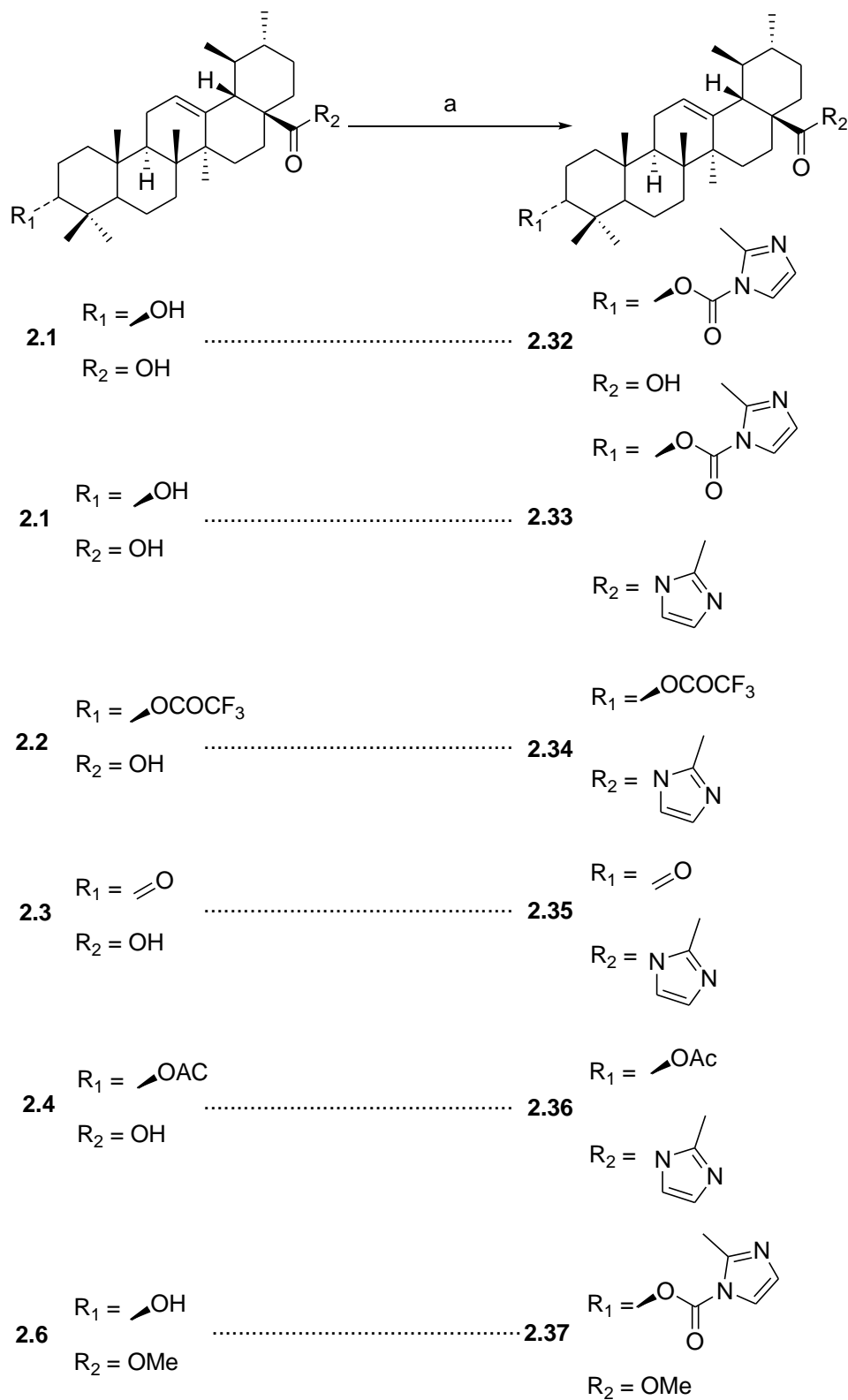


Figure 2.2.14. IR spectrum of compound **2.34**.

Scheme 2.2.4.^a Synthesis of derivatives 2.32-2.37.

^aReagents: (a) CBMI, THF, N₂, reflux.

Compounds **2.38-2.42** have an α,β unsaturated ketone in ring C of the ursane backbone. The stretching vibration of this carbonyl group occurred at 1660 cm^{-1} , which was a lower frequency than that of the anhydride carbonyl group (1780 cm^{-1}) or the amide carbonyl group (1710 cm^{-1}) (Figure 2.2.15). The IR spectra revealed the presence of weak signals at around 3120 cm^{-1} or higher; these signals were due to the C=C stretching vibration of the methylimidazole ring double bonds and the Δ^{12} bond.

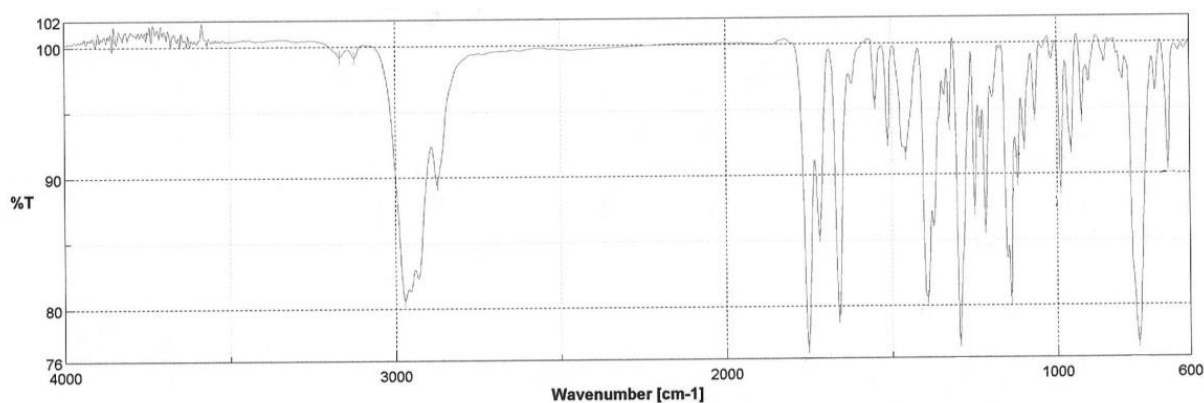
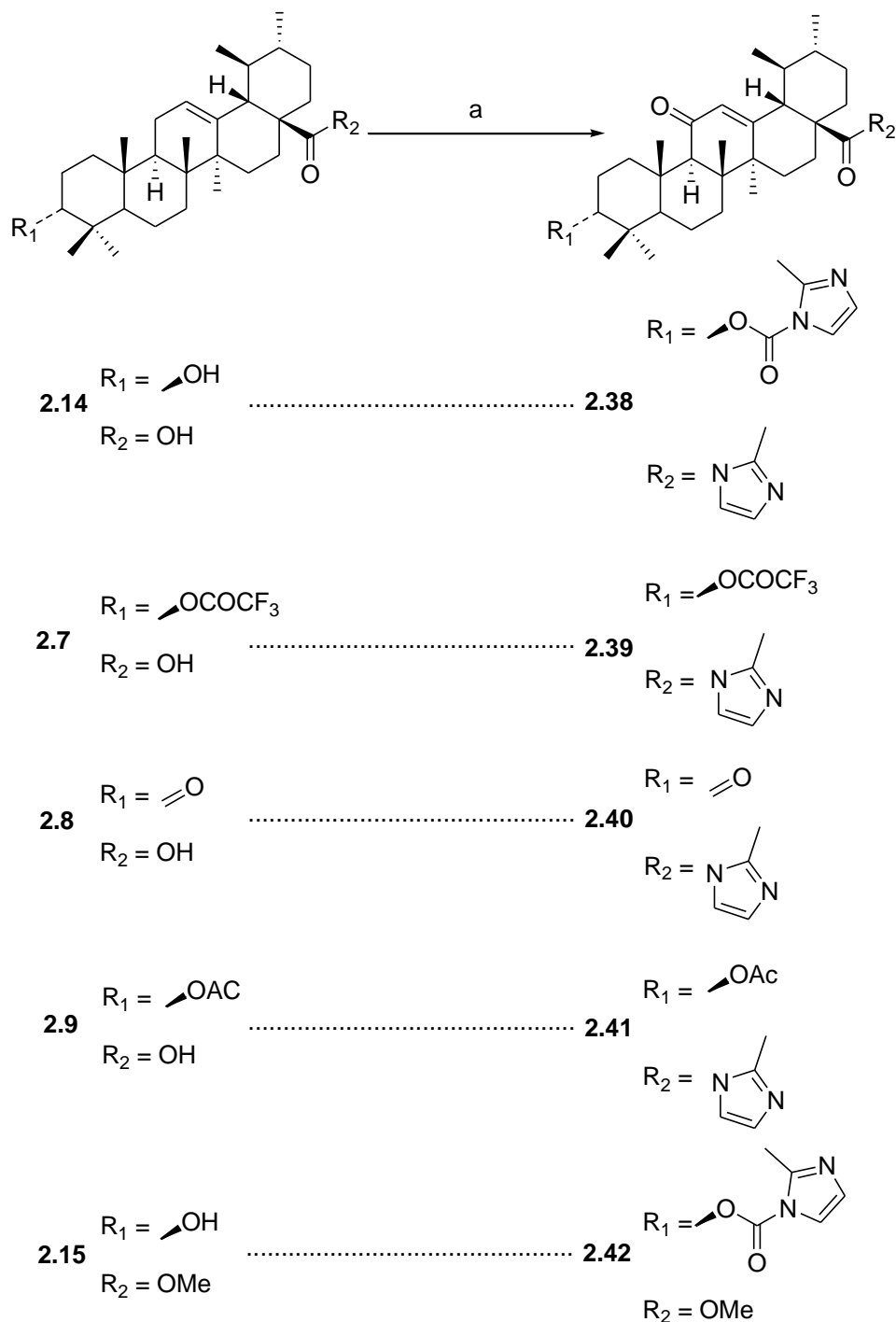


Figure 2.2.15. IR spectrum of compound **2.38**.

The introduction of the methylimidazole ring in the ursane backbone was confirmed by the analysis of the NMR spectra of the compounds prepared. The ^1H NMR signals of the methylimidazole ring occurred as two singlets or doublets for the two protons, with δ signals higher than 6.80 ppm, whereas the methyl group appeared as a singlet at around δ 2.5 ppm. The ^{13}C NMR spectrum of these compounds was characterized by the presence of three additional δ signals greater than 116 ppm and a δ signal between 13 and 17 ppm, which corresponded to the methyl group of the methylimidazole ring.

Scheme 2.2.5.^a Synthesis of derivatives 2.38-2.42.

^aReagents: (a) CBMI, THF, N₂, reflux.

Ursolic acid **2.1** has been well characterized using NMR techniques.⁴⁴³ Proton H₁₂ is usually present as a triplet at around δ 5.23 ppm. Because of the presence of an α,β

unsaturated ketone in ring C, the signal of proton H12 in compound **2.42** appeared at δ 5.61 ppm. Proton H3 in ursolic acid **2.1** was characterized previously.⁴⁴³ The presence of a carbamate at C3 in compound **2.42** resulted in a higher signal in the ^1H NMR spectrum for proton H3 (δ 4.67 ppm), which appeared as a double doublet, similar to what was observed for ursolic acid **2.1** (Figure 2.2.16). In the ^{13}C NMR spectrum, signals at δ 163.09, 130.54 and 85.76 ppm correlated with carbons C13, C12 and C3, respectively (Figures 2.2.17 and 2.2.18).

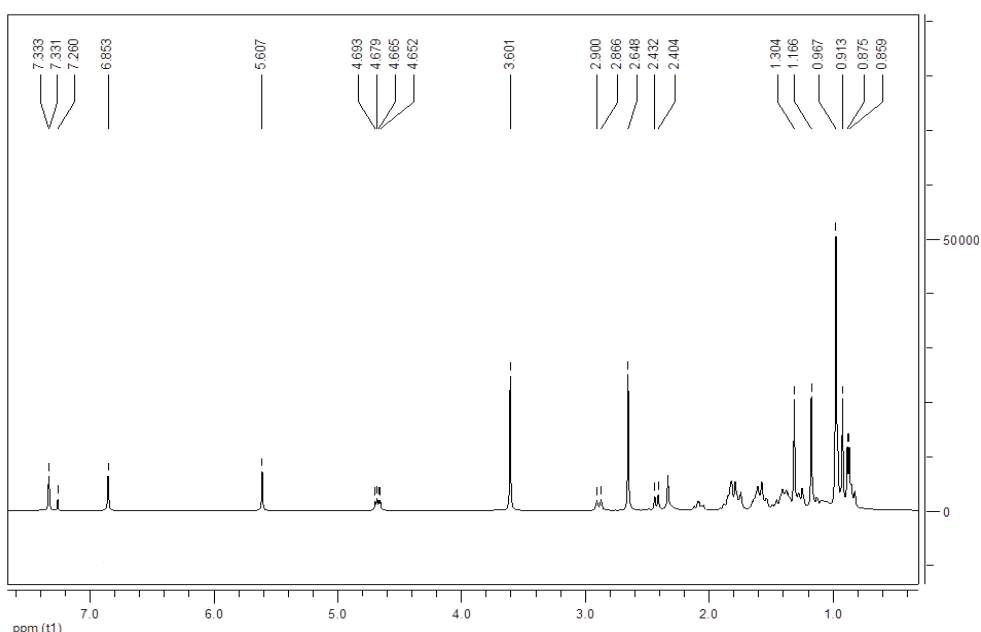


Figure 2.2.16. ^1H NMR spectrum of compound **2.42**.

Proton H18 of compound **2.42** appeared as a doublet at δ 2.42 ppm in the ^1H NMR spectrum and correlated with carbons C13, C14 and C12 in the HMBC spectrum, which were attributed to the δ signals observed at 163.09, 143.72 and 130.54 ppm, respectively. The singlet signal observed at δ 2.33 ppm was attributed to proton H9; the correlation of this proton with the δ signals at 199.44, 44.60 and 36.93 ppm in the HMBC spectrum allowed the identification of carbons C11, C8 and C10, respectively.

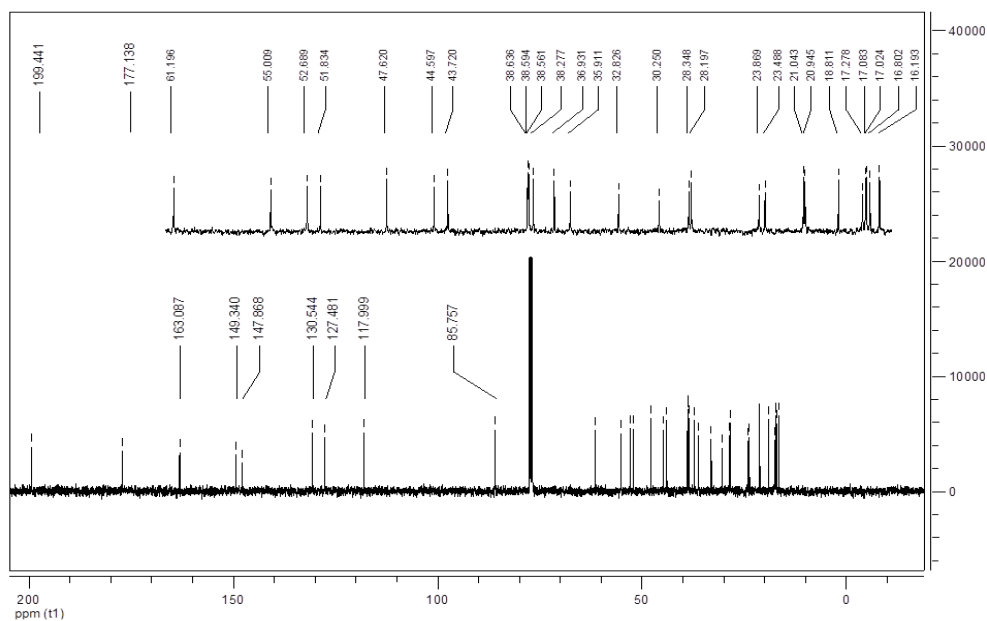


Figure 2.2.17. ^{13}C NMR spectrum of compound **2.42**.

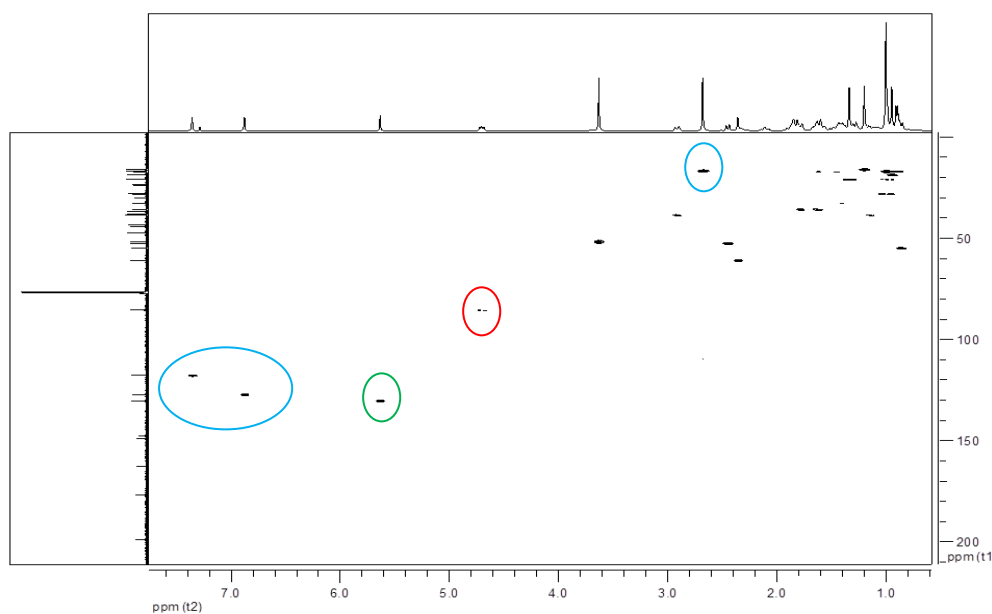


Figure 2.2.18. HMQC spectrum of compound **2.42**, showing the correlations between protons and carbons of the methylimidazole ring (blue), C3 (red) and C12 (green).

The δ signal at 1.17 ppm in the ^1H NMR spectrum of compound **2.42** was identified as the methyl group at C25. This group correlated with carbons C9, C5 and C1, which were identified as the δ signals at 61.20, 55.01 and 38.64 ppm in the ^{13}C NMR spectrum,

respectively. Proton H3 correlated with the carbonyl group of the carbamate, and the methyl group at C27 correlated with carbons C13 and C15.

Other correlations were also observed in the HMBC spectrum of compound **2.42**, allowing the attribution of several δ signals in the ^1H and ^{13}C NMR spectra. Some of the HMBC correlations are illustrated in Figure 2.2.19.

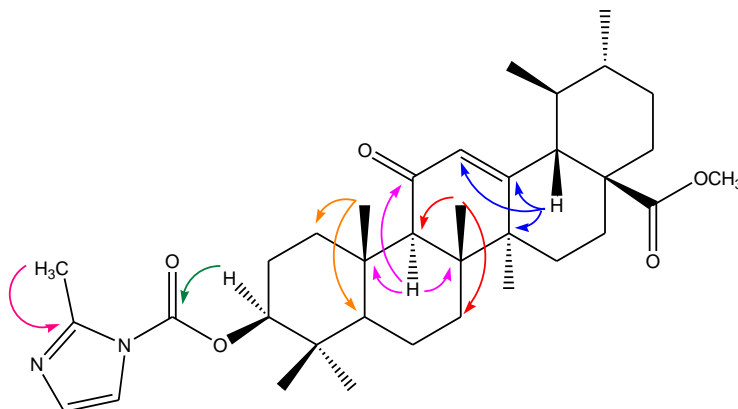
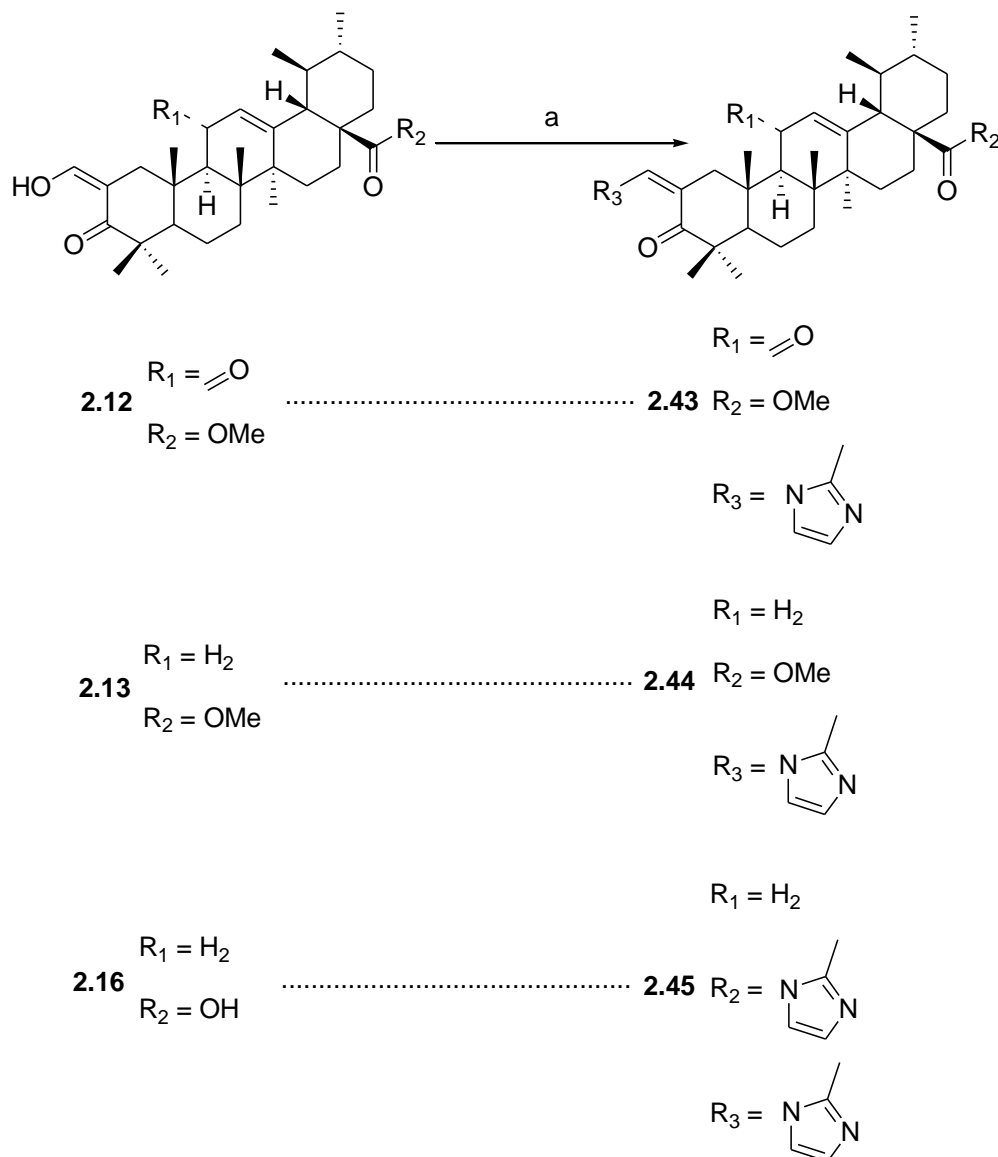


Figure 2.2.19. Selected HMBC correlations for compound **2.42**.

Amines **2.43-2.45** (Scheme 2.2.6) were fully characterized by NMR. These amines have an exocyclic double bond in ring A conjugated with a ketone at C3, affording an α,β unsaturated ketone in ring A. The α,β unsaturated ketone moiety was detected in the ^1H NMR spectrum by the occurrence of a δ signal at 7.6-7.7 ppm, which corresponded to the proton on the exocyclic double bond. In the ^{13}C NMR spectrum, the identification of this moiety in compound **2.44** was due to the occurrence of the δ signals at 206.63, 123.60 and 130.38 ppm, which corresponded to carbons C3, C2 and the exocyclic double bond, respectively (Figures 2.2.20 and 2.2.21).

Scheme 2.2.6.^a Synthesis of derivatives 2.43-2.45.

^aReagents: (a) CBMI, THF, N₂, reflux.

The presence of the α,β unsaturated ketone in ring A of the ursane backbone allows the attribution of ¹³C NMR δ signals to the methylimidazole ring due to the correlations between the exocyclic unsaturated double bond and the heterocyclic ring. In compound **2.44**, the proton observed at 7.66 ppm, which corresponded to the proton in the exocyclic unsaturated bond, correlated with carbon C5' (118.19 ppm) of the heterocyclic ring. Carbon C2' (147.31 ppm) was identified by the fact that it had a methyl group attached and was a quaternary carbon. Carbon C4' (128.57 ppm) was identified by exclusion.

Other correlations in the ursane backbone were observed in the HMBC spectrum; the integration of this information with the data from HMQC, DEPT, ^{13}C and ^1H NMR spectra led to the attribution of additional δ signals to several carbons and respective protons (Table 2.2.3).

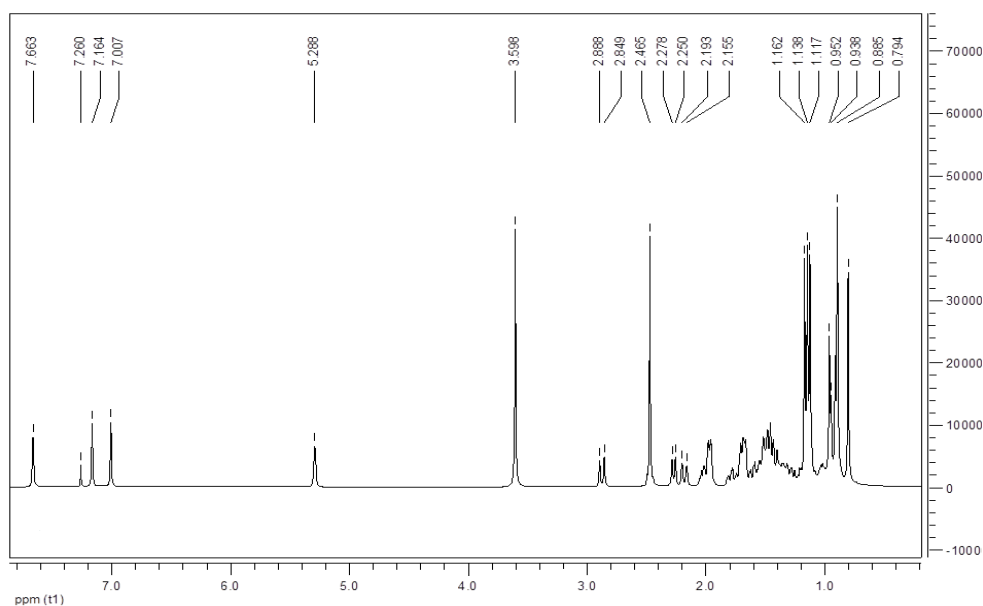


Figure 2.2.20. ^1H NMR spectrum of compound **2.44**.

In compound **2.44**, proton H12 appeared as a δ signal at 5.29 ppm and correlated with carbons C9, C14 and C18, with δ signals at 45.28, 42.21 and 53.01 ppm on the ^{13}C NMR spectrum, respectively. The attribution of carbon C9 allowed the identification of carbon C8 as the δ signal at 39.38 ppm, and carbon C10 as the δ signal at 36.12 ppm on the ^{13}C NMR spectrum (Figure 2.2.22).

The doublet at δ 2.26 ppm in the ^1H NMR spectrum of compound **2.44** was identified as proton H18, which correlated with carbon C17 (48.14 ppm) and carbon C19 (38.83 ppm). Other correlations were found and allowed the identification of the majority of the signals in the ^{13}C NMR spectrum of compound **2.44**. The same procedure was used for compounds **2.43** and **2.45** (Table 2.2.3).

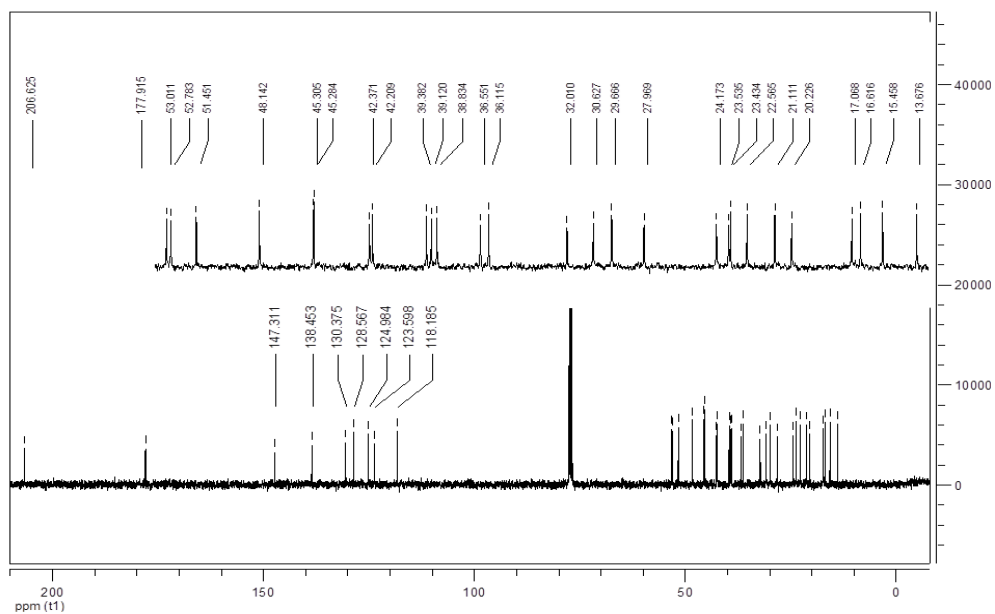


Figure 2.2.21. ^{13}C NMR spectrum of compound 2.44.

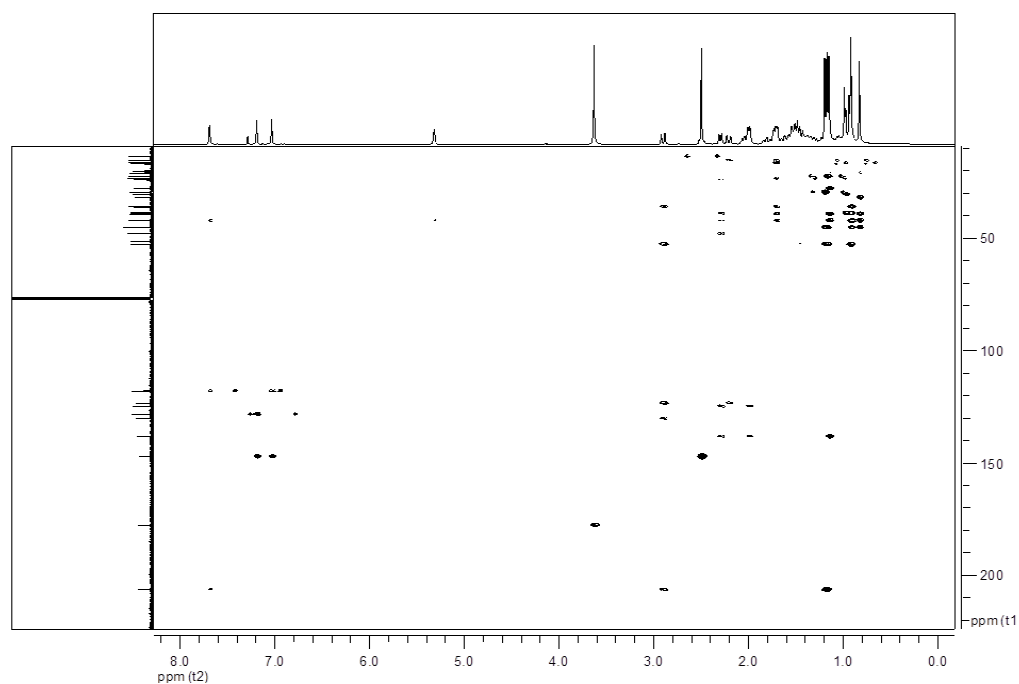


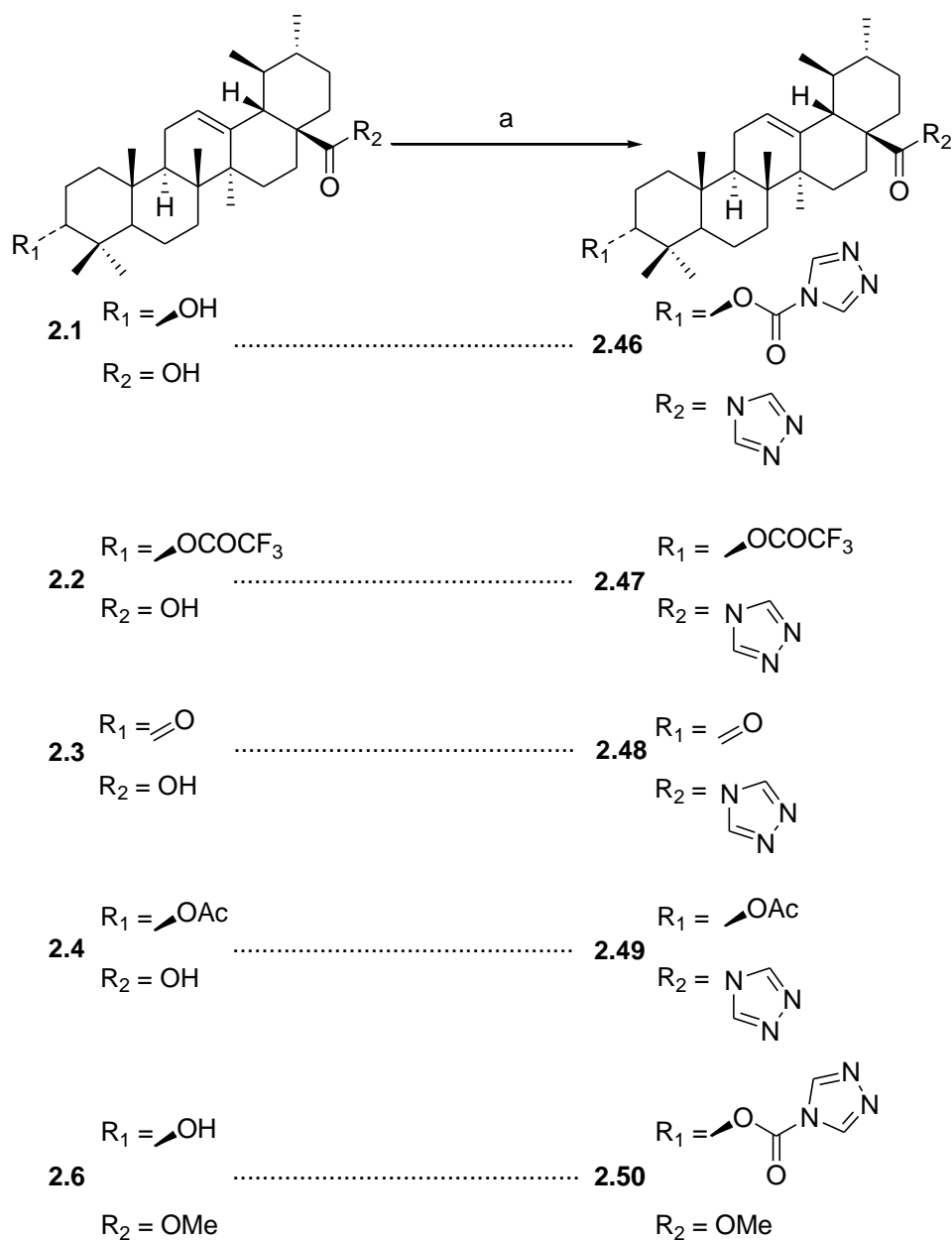
Figure 2.2.22. HMBC spectrum of compound 2.44.

Table 2.2.3. Selected ^1H and ^{13}C NMR data from the backbone of compounds 2.43-2.45.

| Entry | Position | 2.43 | | 2.44 | | 2.45 | |
|-------|--|----------------------|------------|-----------------------|------------|----------------------|------------|
| | | δ H | δ C | δ H | δ C | δ H | δ C |
| 1 | 1 | - | 42.51 | - | 42.37 | - | 42.36 |
| 2 | 2 | - | 122.98 | - | 123.60 | - | 123.07 |
| 3 | 3 | - | 206.36 | - | 206.23 | - | 206.50 |
| 4 | 4 | - | 45.39 | - | 45.31 | - | 45.20 |
| 5 | 5 | - | 53.02 | - | 52.78 | 1.43 | 52.64 |
| 6 | 7 | - | 31.65 | - | 32.01 | - | 31.78 |
| 7 | 8 | - | 44.19 | - | 39.38 | - | 39.39 |
| 8 | 9 | 2.45 | 58.90 | - | 45.28 | - | 45.15 |
| 9 | 10 | - | 36.07 | - | 36.12 | - | 36.03 |
| 10 | 11 | - | 198.71 | - | - | - | 35.43 |
| 11 | 12 | 5.67 | 130.53 | 5.29 | 124.98 | 5.28 | 125.87 |
| 12 | 13 | - | 163.99 | - | 138.45 | - | 137.37 |
| 13 | 14 | - | 43.86 | - | 42.21 | - | 42.40 |
| 14 | 15 | - | 28.47 | - | 27.97 | - | - |
| 15 | 17 | - | 47.64 | - | 48.14 | - | 51.84 |
| 16 | 18 | 2.45 | 52.80 | 2.26 ($J=11.27$) | 53.01 | 2.54 | 54.16 |
| 17 | 19 | - | 38.59 | - | 38.83 | - | 39.55 |
| 18 | 20 | - | 38.72 | - | 39.12 | - | 38.59 |
| 19 | 21 | - | - | - | 30.63 | - | 30.42 |
| 20 | 25 | 1.12 | 15.39 | 0.89 | 15.46 | 0.87 | 15.51 |
| 21 | 26 | 0.94 | 18.26 | 0.79 | 16.62 | 0.77 | 16.90 |
| 22 | 27 | 1.33 | 21.00 | 1.12 | 23.43 | 1.15 | 23.28 |
| 23 | 28 | - | 177.11 | - | 177.92 | - | 176.52 |
| 24 | 29 | 0.89 ($J=6.22$) | 17.19 | 0.89 | 17.07 | 0.95 ($J=6.13$) | 17.24 |
| 25 | 30 | 0.97 ($J=6.28$) | 20.94 | 0.95 ($J=5.85$) | 21.11 | 1.00 ($J=6.13$) | 21.07 |
| 26 | <u>COCH₃</u> | 3.61 | 51.87 | 3.60 | 51.45 | - | - |
| 27 | <u>C2CH</u> | 7.62 | 129.69 | 7.66 | 130.38 | 7.67 | 130.50 |
| 28 | <u>C2'</u> | - | 147.23 | - | 147.31 | - | 147.39 |
| 29 | <u>C2''</u> | - | - | - | - | - | 149.35 |
| 30 | <u>C4'</u> | 7.32 | 128.38 | 7.01 | 128.57 | 7.00 | 128.68 |
| 31 | <u>C5'</u> | 6.99 | 118.24 | 7.16 | 118.19 | 7.16 | 118.11 |
| 32 | <u>C2'CH₃</u> imidazole | 2.49 | 13.66 | 2.47 | 13.68 | 2.47 | 13.75 |
| 33 | <u>C2''CH₃</u> imidazole | - | - | - | - | 2.54 | 17.93 |

2.2.2.1.3. Triazole derivatives

The reaction of ursolic acid **2.1** and intermediates with CDT afforded carbamates **2.46**, **2.50**, **2.51** and **2.55** (Schemes 2.2.7. and 2.2.8), *N*-acyltriazoles **2.47-2.49** and **2.52-2.54** (Schemes 2.2.7 and 2.2.8) and *N*-alkyltriazoles **2.56-2.58** (Scheme 2.2.9).

Scheme 2.2.7.^a Synthesis of derivatives **2.46-2.50**.

^aReagents: (a) CDT, THF, N₂, reflux.

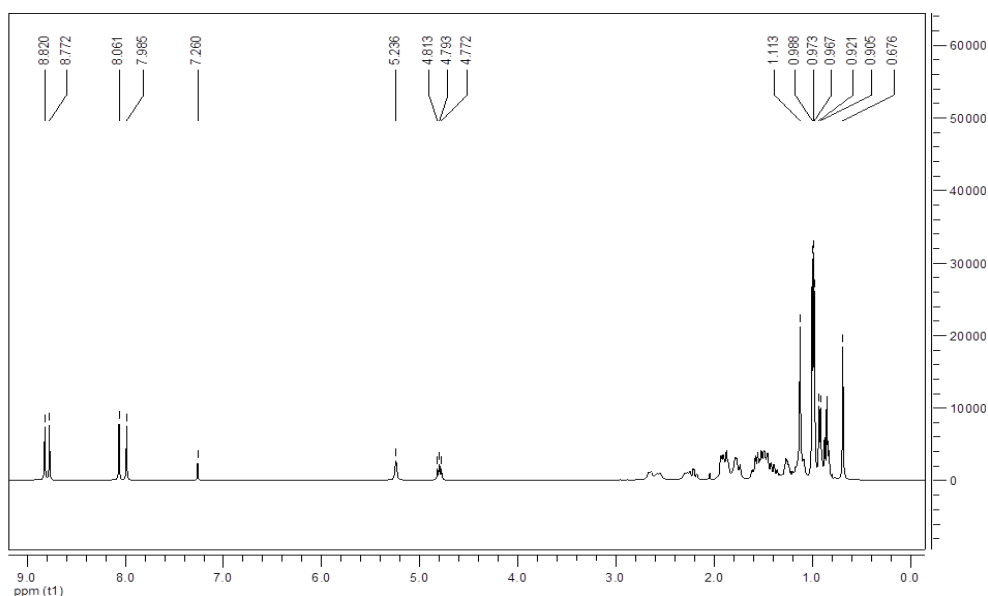


Figure 2.2.23. ^1H NMR spectrum of compound **2.46**.

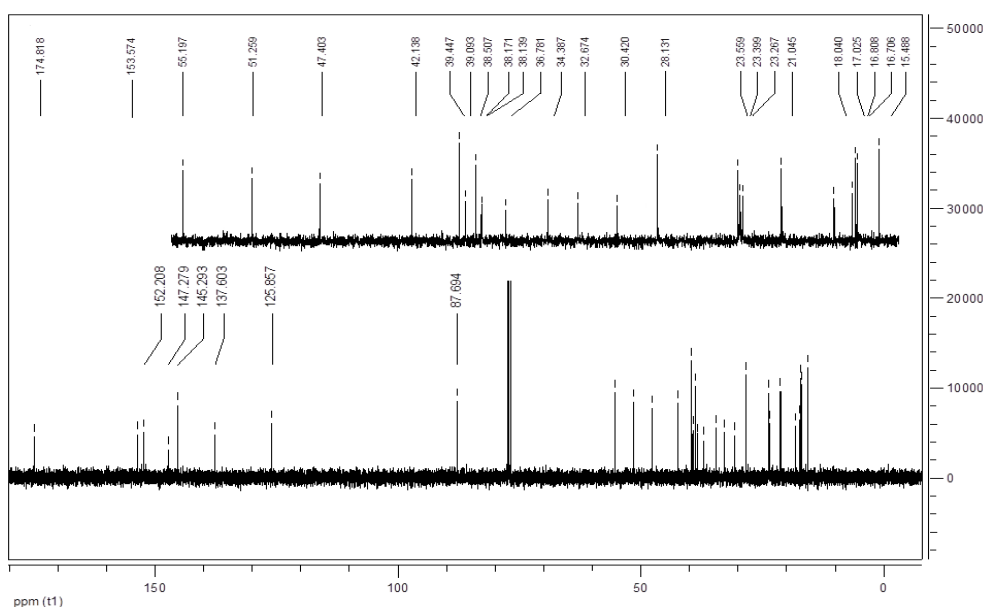
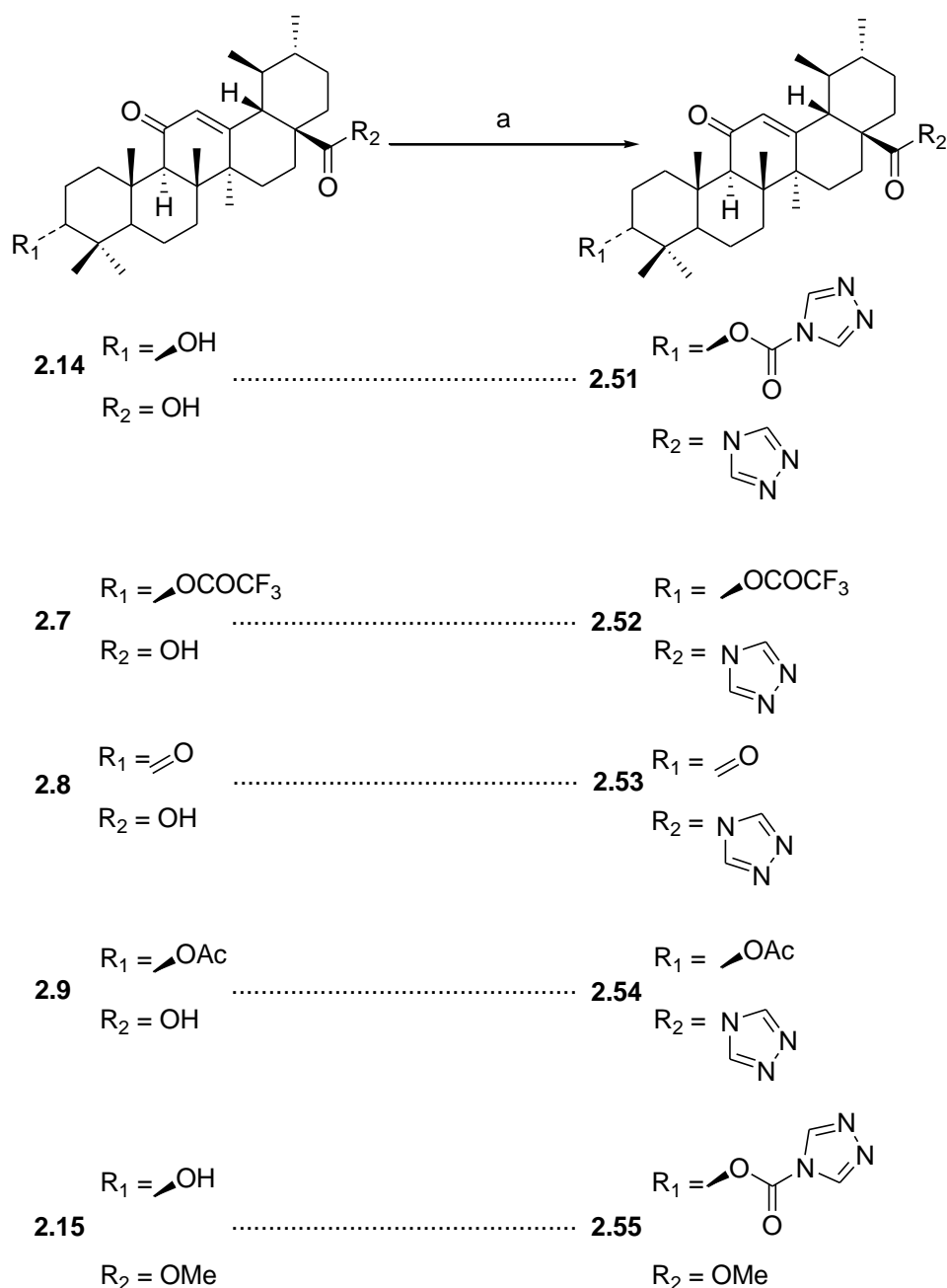


Figure 2.2.24. ^{13}C NMR spectrum of compound **2.46**.

The presence of a triazole heterocyclic ring was confirmed in the ^1H and ^{13}C NMR spectra, because the protons of this ring had a δ signal higher than 8 ppm in the ^1H NMR spectrum and the carbons had a δ signal higher than 145 ppm in the ^{13}C NMR spectrum. For compound **2.46**, with two triazole groups, the δ signals in the ^1H NMR spectrum for the heterocyclic ring on the carbamate moiety were 8.06 and 8.77 ppm, and for the C28

amide moiety, they were 7.98 and 8.82 ppm. In the ^{13}C NMR spectrum, the δ signals were 153.57 and 145.29 ppm, and 152.21 and 145.29 ppm, respectively (Figures 2.2.23 and 2.2.24).

Scheme 2.2.8.^a Synthesis of derivatives 2.51-2.55.



^aReagents: (a) CDT, THF, N_2 , reflux.

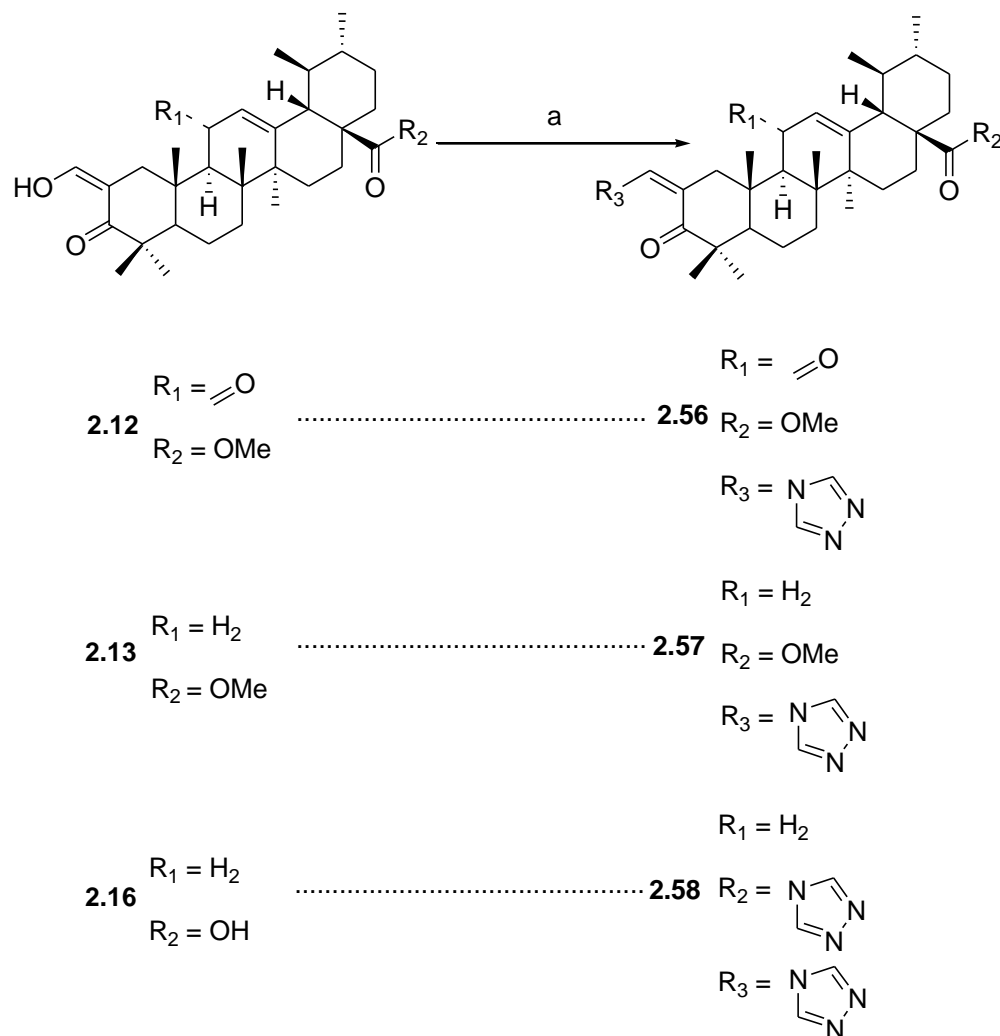
Table 2.2.4. Selected ^1H and ^{13}C NMR data from the backbone of compounds **2.46** and **2.54**.

| Entry | Position | 2.46 | | 2.54 | |
|-----------|--------------------------|-----------------------------|------------|-----------------------------|------------|
| | | δ H | δ C | δ H | δ C |
| <i>I</i> | 1 | - | - | - | 38.80 |
| <i>2</i> | 3 | 4.79 (<i>J</i> = 16.50) | 87.69 | 4.49 (<i>J</i> = 16.28) | 80.53 |
| <i>3</i> | 4 | - | 38.17 | - | 37.97 |
| <i>4</i> | 5 | - | 55.20 | 0.75 (<i>J</i> = 11.55) | 55.02 |
| <i>5</i> | 7 | - | 32.67 | - | 32.86 |
| <i>6</i> | 8 | - | 39.45 | - | 44.65 |
| <i>7</i> | 9 | - | 47.40 | 2.31 | 61.34 |
| <i>8</i> | 10 | - | 36.78 | - | 36.96 |
| <i>9</i> | 11 | - | - | - | 199.33 |
| <i>10</i> | 12 | 5.24 | 125.86 | 5.64 | 131.05 |
| <i>11</i> | 13 | - | 137.60 | - | 161.72 |
| <i>12</i> | 14 | - | 42.19 | - | 43.81 |
| <i>13</i> | 15 | - | - | - | 28.60 |
| <i>14</i> | 17 | - | 51.26 | - | 50.99 |
| <i>15</i> | 18 | - | - | - | 53.97 |
| <i>16</i> | 21 | - | - | - | 30.13 |
| <i>17</i> | 25 | 0.97 | 15.49 | 1.12 | 16.33 |
| <i>18</i> | 26 | 0.68 | 16.71 | 0.83 | 18.53 |
| <i>19</i> | 27 | 1.11 | 23.56 | 1.32 | 20.89 |
| <i>20</i> | 28 | - | 174.82 | - | 174.12 |
| <i>21</i> | 29 | 0.91 (<i>J</i> = 6.35) | 17.03 | 0.93 (<i>J</i> = 6.36) | 17.14 |
| <i>22</i> | 30 | 0.97 | 21.05 | 1.00 (<i>J</i> = 6.29) | 20.87 |
| <i>23</i> | OCO | - | 147.28 | - | 170.97 |
| <i>24</i> | OCOCH₃ | - | - | 2.03 | 21.27 |

The presence of the *N*-acyltriazo, carbamate or *N*-alkyltriazole moieties was studied in a manner similar to that used for the imidazole and methylimidazole derivatives. Some

^1H and ^{13}C NMR δ signals attributed to compounds **2.46** and **2.54** are presented in Table 2.2.4; these were attributed based on the analysis of the 1D and 2D NMR experiments.

Scheme 2.2.9.^a Synthesis of derivatives **2.56-2.58**.



^aReagents: (a) CDT, THF, N_2 , reflux.

The reaction of compounds **2.12**, **2.13** and **2.16** with a vinyl alcohol at position C2 afforded amines **2.56-2.58** with good yield (Scheme 2.2.9). The structural elucidation of the compounds was achieved via MS, IR and 1D and 2D NMR experiments, the results of which are described in experimental section 2.4.1.

2.2.2.2. Biological evaluation

The antiproliferative activity of the new semisynthetic compounds was evaluated via the determination of the IC_{50} (μM) against AsPC-1 cells, a pancreatic cancer cell line, using a MTT assay. Overall, the new semisynthetic compounds exhibited better antiproliferative activity against this cell line compared with the intermediates and ursolic acid **2.1** (Tables 2.2.5 and 2.2.6). Compounds **2.33** and **2.47**, in which the introduction of heterocyclic rings at positions C3 and C28 simultaneously resulted in the decrease of antiproliferative activity compared with ursolic acid **2.1**, probably because of the volume of the substituents, which sterically impaired the interaction with the biological targets. Compounds **2.25**, **2.28**, **2.37** and **2.47** presented an IC_{50} higher than 30 μM . Compounds **2.29-2.31**, **2.43-2.45** and **2.56-2.58**, with a heterocyclic ring conjugated with an α,β unsaturated ketone in ring A, exhibited the best antiproliferative activity in this cell line (Table 2.2.6).

Table 2.2.5. The IC_{50} (μM) of ursolic acid intermediates in the inhibition of AsPC-1 cell growth.

| Compd | AsPC-1 | Compd | AsPC-1 |
|------------|-----------------|-------------|-----------------|
| 2.1 | 12.6 \pm 0.03 | 2.9 | 33.5 \pm 0.05 |
| 2.2 | 10.9 \pm 0.04 | 2.12 | 9.0 \pm 0.04 |
| 2.3 | 24.5 \pm 0.1 | 2.13 | 7.2 \pm 0.02 |
| 2.4 | 71.0 \pm 0.06 | 2.14 | 45.7 \pm 0.06 |
| 2.6 | 17.7 \pm 0.06 | 2.15 | 34.2 \pm 0.04 |
| 2.7 | 84.2 \pm 0.09 | 2.16 | 13.4 \pm 0.03 |
| 2.8 | 54.9 \pm 0.03 | - | - |

AsPC-1 cells were treated with the indicated compounds at varying concentrations for 72 h. The antiproliferative effects were determined using a MTT assay and the IC_{50} was calculated. The results shown are means \pm SE of three independent experiments.

SAR based on the antiproliferative activity against AsPC-1 cell line for ursolic acid **2.1** and compounds **2.12**, **2.13**, **2.16**, **2.29-2.31**, **2.43-2.45** and **2.56-2.58** is represented in Figure 2.2.25, once compounds with an α,β unsaturated ketone in ring A, represent the most active derivatives in these series. Herein compounds **2.29**, **2.43**, **2.44** and **2.57** have

the best antiproliferative activity against AsPC-1 cancer cells. The heterocyclic ring present at C2 position influences the antiproliferative activities, depending on the initial scaffold. Triazole substituent with an α,β unsaturated ketone in ring A appears to generate the most active compounds. Compound **2.57** is the most active compound. It is 7-fold more potent than ursolic acid **2.1**, and 4-fold more potent than compound **2.13** (Figure 2.2.25).

Table 2.2.6. The IC_{50} (μM) of ursolic acid heterocyclic derivatives in the inhibition of AsPC-1 cell growth.

| Compd | IC_{50} (μM) | Compd | IC_{50} (μM) | Compd | IC_{50} (μM) |
|-------------|-----------------------|-------------|-----------------------|-------------|-----------------------|
| 2.18 | 11.7 \pm 0.02 | 2.32 | >100 | - | - |
| 2.19 | 13.2 \pm 0.07 | 2.33 | 53.8 \pm 0.3 | 2.46 | 50.4 \pm 0.04 |
| 2.20 | 42.4 \pm 0.01 | 2.34 | 12.2 \pm 0.03 | 2.47 | 35.7 \pm 0.02 |
| 2.21 | 15.2 \pm 0.03 | 2.35 | 19.6 \pm 0.02 | 2.48 | 19.2 \pm 0.07 |
| 2.22 | 15.2 \pm 0.03 | 2.36 | 20.2 \pm 0.06 | 2.49 | 23.3 \pm 0.05 |
| 2.23 | 8.0 \pm 0.04 | 2.37 | 40.3 \pm 0.05 | 2.50 | 28.4 \pm 0.02 |
| 2.24 | 9.1 \pm 0.05 | 2.38 | 7.3 \pm 0.03 | 2.51 | 10.4 \pm 0.04 |
| 2.25 | 48.3 \pm 0.1 | 2.39 | 26.1 \pm 0.02 | 2.52 | 12.9 \pm 0.02 |
| 2.26 | 11.7 \pm 0.05 | 2.40 | 5.1 \pm 0.03 | 2.53 | 9.9 \pm 0.03 |
| 2.27 | 13.9 \pm 0.04 | 2.41 | 15.3 \pm 0.06 | 2.54 | 10.2 \pm 0.02 |
| 2.28 | 50.8 \pm 0.3 | 2.42 | 19.0 \pm 0.1 | 2.55 | 11.4 \pm 0.04 |
| 2.29 | 2.3 \pm 0.02 | 2.43 | 2.1 \pm 0.01 | 2.56 | 8.1 \pm 0.02 |
| 2.30 | 5.8 \pm 0.05 | 2.44 | 2.1 \pm 0.02 | 2.57 | 1.9 \pm 0.02 |
| 2.31 | 5.1 \pm 0.02 | 2.45 | 11.3 \pm 0.02 | 2.58 | 3.9 \pm 0.04 |

AsPC-1 cells were treated with the indicated compounds at varying concentrations for 72 h. The antiproliferative effects were determined using a MTT assay and the IC_{50} was calculated. The results shown are means \pm SE of three independent experiments.

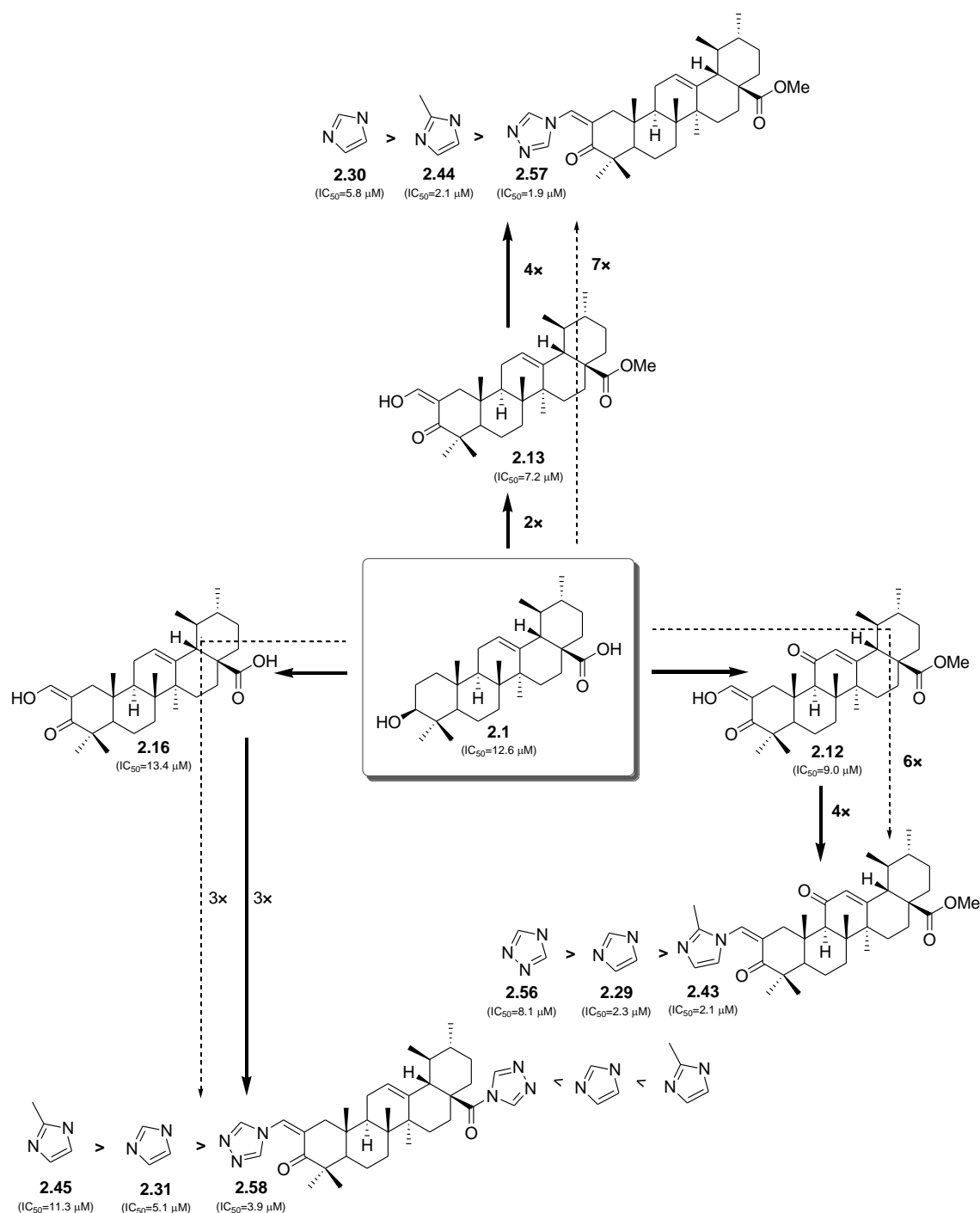


Figure 2.25. Graphical representation of the SAR relationship between ursolic acid **2.1** and novel semisynthetic derivatives with modification at C2 of the ursane structure. Comparisons were based on the IC_{50} of compounds against the AsPC-1 cell line. Compound **2.57**, which was the most active of these series, was 4-fold more active than the original intermediate **2.13** and 7-fold more active than ursolic acid **2.1**. Compound **2.43** was 4-fold more active than compound **2.12** and 6-fold more active than ursolic acid **2.1**. Compound **2.58** was 3-fold more active than compound **2.16** and ursolic acid **2.1**.

Among compounds **2.29-2.31**, **2.43-2.45** and **2.56-2.58**, which were tested for antiproliferative activity in AsPC-1 cells, compounds **2.29**, **2.30**, **2.43**, **2.44**, **2.56** and **2.57** were studied further in other pancreatic (PANC-1 and MIA PaCa 2), hepatic (Hep G2), breast (MCF-7), lung (A549) and prostate (PC-3) cancer cell lines (Table 2.2.7). Compound **2.57**, an *N*-alkyltriazole, exhibited consistent antiproliferative activity in all the tested cell lines, with IC₅₀ values ranging from 1.9 to 4.9 μM. The presence of the *N*-alkyltriazole in ring A conjugated with an α,β unsaturated ketone afforded a greater Michael acceptor compared with compounds **2.30** and **2.44**, allowing a better interaction with the biological target(s).⁴⁴⁴ The nature of the substituent at C2 in compounds with the same ursane backbone may be the reason for the differences observed in antiproliferative activity.

Table 2.2.7. The IC₅₀ (μM) of ursolic acid heterocyclic derivatives in the inhibition of the growth of pancreatic (PANC-1 and MIA PaCa 2), breast (MCF-7), prostate (PC-3), hepatic (Hep G2) and lung (A549) cancer cell lines.

| Compd | PANC-1 | MIA PaCa 2 | Hep G2 | MCF-7 | A549 | PC-3 |
|-------------|-----------|------------|-----------|-----------|-----------|-----------|
| 2.1 | 14.9±0.04 | 10.4±1.0 | 15.0±0.09 | 12.3±0.02 | 11.4±0.03 | 20.8±0.01 |
| 2.29 | 18.2±0.06 | 24.3±0.03 | 27.6±0.05 | 9.4±0.05 | 12.2±0.08 | 12.9±0.05 |
| 2.30 | 5.1±0.04 | 7.3±0.04 | 2.0±0.03 | 5.3±0.02 | 5.6±0.05 | 6.8±0.02 |
| 2.43 | 14.4±0.04 | 8.3±0.02 | 8.5±0.06 | 3.5±0.05 | 18.7±0.03 | 5.7±0.02 |
| 2.44 | 5.6±0.04 | 5.6±0.01 | 4.0±0.01 | 2.2±0.03 | 5.3±0.02 | 3.5±0.02 |
| 2.56 | 12.1±0.2 | 7.8±0.03 | 7.9±0.03 | 12.5±0.06 | 12.9±0.02 | 9.5±0.03 |
| 2.57 | 3.5±0.03 | 4.0±0.05 | 3.2±0.03 | 2.3±0.02 | 4.9±0.01 | 3.0±0.01 |

PANC-1, MIA PaCa 2, MCF-7, PC-3, Hep G2 and A549 cells were treated with the indicated compounds at varying concentrations for 72 h. The antiproliferative effects were determined using an MTT assay and the IC₅₀ was calculated. The results shown are means ± SE of three independent experiments.

Pancreatic cancer AsPC-1 cells are the most susceptible to these compounds and compound **2.57** is the most active one. AsPC-1 cells were used to study the underlying antiproliferative mechanisms of compound **2.57**. AsPC-1 cells were treated with 2-10 μM of compound **2.57** for 24 h.

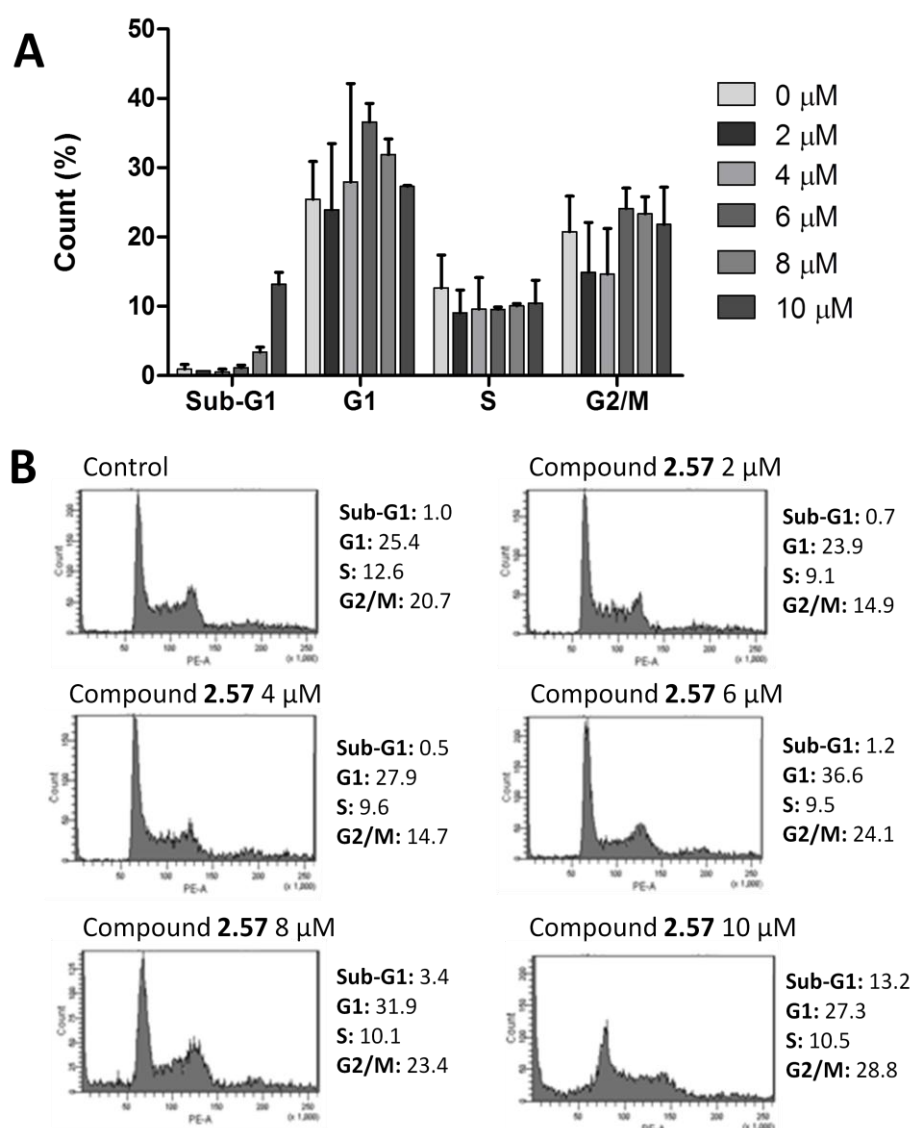


Figure 2.2.26. Cell cycle arrest and apoptosis induction of compound **2.57** in AsPC-1 cells. (A) Cell cycle analysis of AsPC-1 cells treated with compound **2.57**. The results shown are means \pm SE of three independent experiments. (B) Representative FACS analyses of cell cycle of AsPC-1 cells treated with compound **2.57** at the indicated concentrations for 24 h. The sub-G1 phase (apoptotic cells) of AsPC-1 cells was detected only in cells treated with compound **2.57** at 10 μ M. The cell cycle was determined by FACS after staining with PI.

Compound **2.57** induced cell cycle arrest at G1 phase at the concentration of 6 μ M and the population of cells at sub-G1 phase was increased after treatment with compound **2.57** at higher concentrations (Figure 2.2.26), implying that the antiproliferative effects of this compound are due to cell cycle arrest and induction of apoptosis. The levels of a few of cell cycle and apoptosis related proteins were determined (Figure 2.2.27). p21^{waf1} is a cell cycle regulator of G1 phase which is not expressed in pancreatic cancer cells.⁴⁴⁵

NOXA is a BH3 protein responsible for the regulation of anti-apoptotic protein Mcl-1. The levels of p21^{waf1} and NOXA were increased significantly in AsPC-1 cells treated with compound **2.57** at concentrations higher than 6 μ M. Unlike other triterpenoid derivatives which decreased the levels of Mcl-1,²⁸⁰ compound **2.57** did not decrease the levels of Mcl-1. This result suggests that this compound has a new mechanism of action. The apoptosis induction may rely on the induction of NOXA which antagonize the function of Mcl-1 and then lead to apoptosis via activation of caspases 9 and 3. NOXA and p21^{waf1} are regulated by p53 and compound **2.57** increased the levels of p53 protein. The role of p53 in compound **2.57**-mediated cell cycle arrest and apoptosis induction as well as the mechanism of compound **2.57** to increase p53 level need to be studied further.

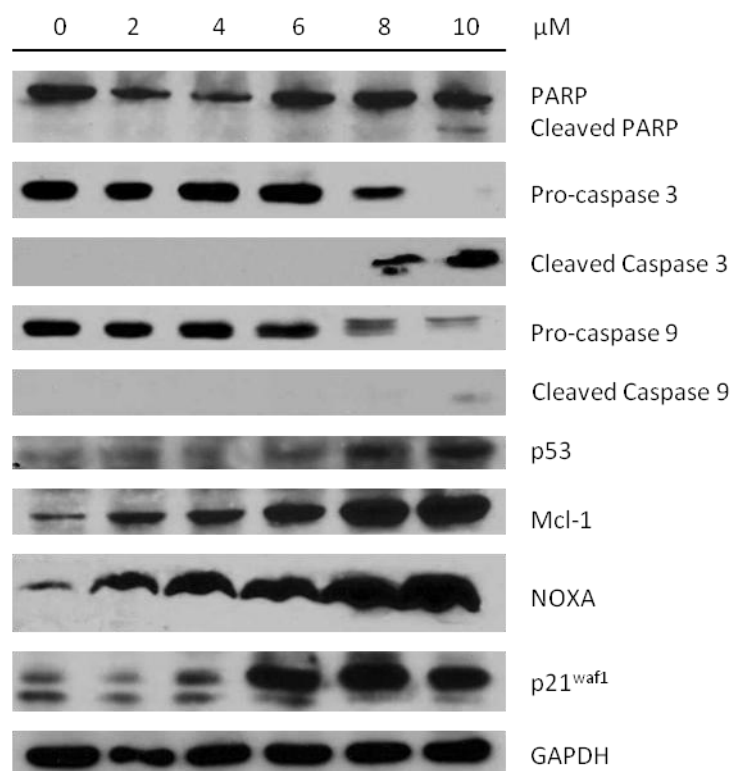


Figure 2.2.27. Compound **2.57** increased the levels of p21^{waf1}, NOXA and p53 protein in AsPC-1 cells. AsPC-1 cells were treated with compound **2.57** at the indicated concentrations for 24 h. The relative levels of indicated proteins were determined by Western blot analysis. GAPDH was used as a loading control.

2.2.3. Conclusions

In summary, this section presented a series of new *N*-alkylimidazoles, *N*-acylimidazoles and carbamate ursolic acid derivatives with the introduction of heterocyclic rings (imidazole, methylimidazole or triazole) at different positions of the ursane backbone. These new derivatives of ursolic acid **2.1** were fully characterized using NMR, MS and IR techniques.

The new semisynthetic derivatives exhibited a good antiproliferative profile against AsPC-1 cells. Compounds **2.29-2.31**, **2.43-2.45** and **2.56-2.58**, which carried a heterocyclic ring in conjugation with an α,β unsaturated ketone in ring A of the ursane skeleton, were the most active in inhibiting AsPC-1 cell growth. Compound **2.57** yielded the best results in a series of cancer cell lines, targeting NOXA, p21^{waf1} and p53 in AsPC-1 cells.

These compounds represent a new group of ursane derivatives that are a good starting point for drug discovery in cancer.

2.3. Fluorolactones and fluorine derivatives

2.3.1. Introduction

Fluorine is the least abundant halide in natural compounds, as less than 20 natural compounds have it in their structure. This is because of its low abundance on the earth's surface and because few living cells are able to metabolize it.^{446, 447} Until 1970, the presence of fluorine substituents in pharmaceutical compounds was less than 2%; currently, that percentage is around 20% and increasing.^{448, 449} This increase was possibly caused by the introduction of safer and more selective methods for fluorination reactions and of fluorinated agents that are compatible with ordinary laboratory equipment.⁴⁴⁹ Fluorinated organic compounds can be obtained from nucleophilic, electrophilic and radical forms of fluorine reagents (Figure 2.3.1).⁴⁴⁹⁻⁴⁵¹ Nucleophilic reagents, such as diethylaminosulfur trifluoride (DAST) and bis(2-methoxyethyl) aminosulfur trifluoride (Deoxofluor), are used to prepare mono and difluoroalkyl compounds from alcohols, ketones and aldehydes.^{450, 452, 453} Electrophilic reagents use an "F⁺", usually in an N-F reagent, such as 1-chloromethyl-4-fluoro-1,4-diazoniabicyclo[2.2.2]octane bis(tetrafluoroborate) (Selectfluor) and *N*-fluorobenzenesulfonimide (Accfluor), to fluorinate the carboanion present in ketones, aldehydes, esters and heterocycles.^{450, 452, 454}

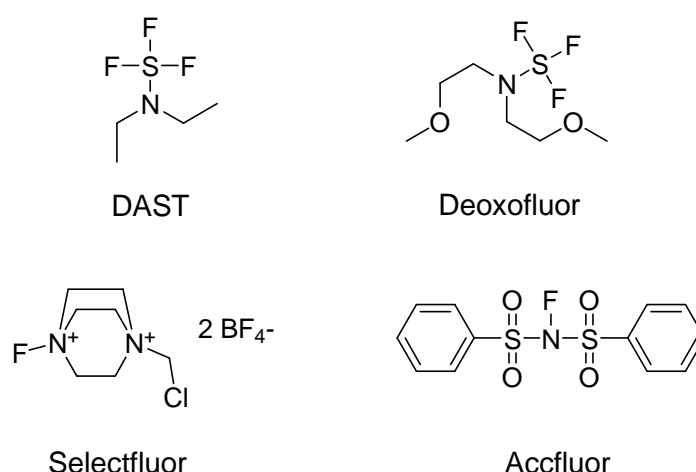


Figure 2.3.1. Examples of nucleophilic (DAST and Deoxofluor) and electrophilic (Selectfluor and Accfluor) fluorine reagents.

Fluorinated compounds are very attractive, because a single fluorine atom located in a key position of a molecule can result in a profound pharmacological effect. Fluorine is a small and highly electronegative atom, and its presence in key positions of a biologically active molecule can improve metabolic and chemical stability, membrane permeability and binding affinity.^{448, 455-457} The C–F bond is one of the strongest chemical bonds and compounds with this functional group have a high thermal and oxidative stability, low polarity and a small surface tension, making them less likely to undergo enzymatic liver degradation, especially by the P450 cytochrome enzymes.^{446, 449, 455, 456} The presence of fluorine in bioactive molecules changes the basicity of nearby functional groups, thus changing the pKa of the molecule and having a strong effect on both the pharmacokinetic properties and binding affinity.⁴⁵⁵ Fluorine is oriented toward electropositive sites; thus, fluorophilic environments in peptides, interactions such as the C–F---H–N, C–F---C=O and C–F---H–C, have been identified.⁴⁵⁶

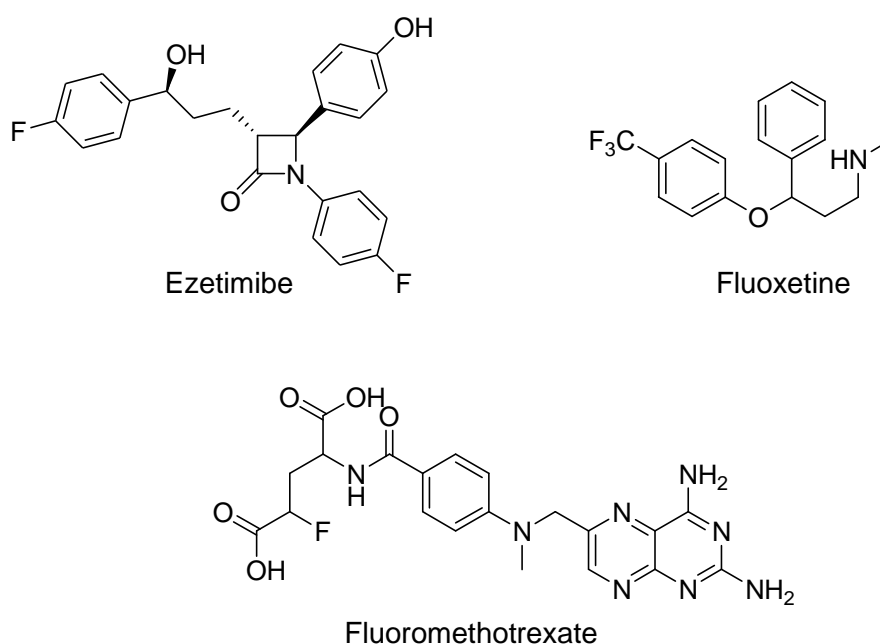


Figure 2.3.2. Some examples of fluorinated drugs used in medical settings.

5-Fluorouracil, which was synthesized by Charles Heidelberger in 1957, was the first synthetic fluorinated compound used in clinical settings as an anticancer therapeutic agent.^{448, 458, 459} Synthetic and semisynthetic fluorinated compounds used in clinical

settings have a broad range of action, such as anti-inflammatory (fluoromethotrexate or celecoxib), antibacterial (fluoroquinolones), antidepressive (fluoxetine), anti-HIV (indinavir), anticholesterol (ezetimibe), antithrombotic (7,7-difluoro-thromboxane), noninvasive monitoring therapeutic (2-deoxy-2-fluor-D-glucosyl) and antitumorigenic (gemcitabine) (Figure 2.3.2).⁴⁵⁵

Anticancer fluorinated compounds are very common in clinical practice and can be classified into different categories depending on their mechanism of action: thymidylate synthase inhibitor (5-fluorouracil), topoisomerase inhibitor (gemcitabine), multidrug efflux protein resistance inhibitor (zosuquidar), antiestrogenic (panomifene), protein kinase inhibitor (gefitinib) and antiandrogenic (flutamide) (Figure 2.3.3).⁴⁴⁷

Fluorinated ursolic acid **2.1** derivatives were developed in an attempt to improve the antitumor activity of the parental compounds.

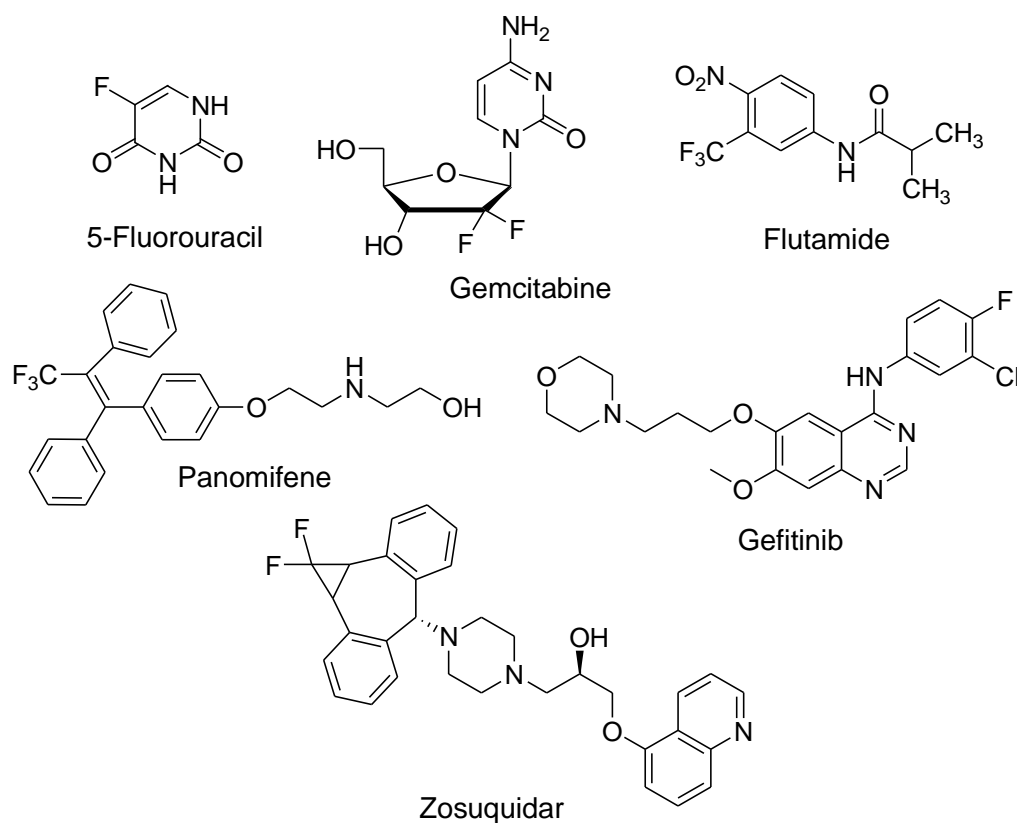


Figure 2.3.3. Anticancer fluorinated drugs.

2.3.2. Results and Discussion

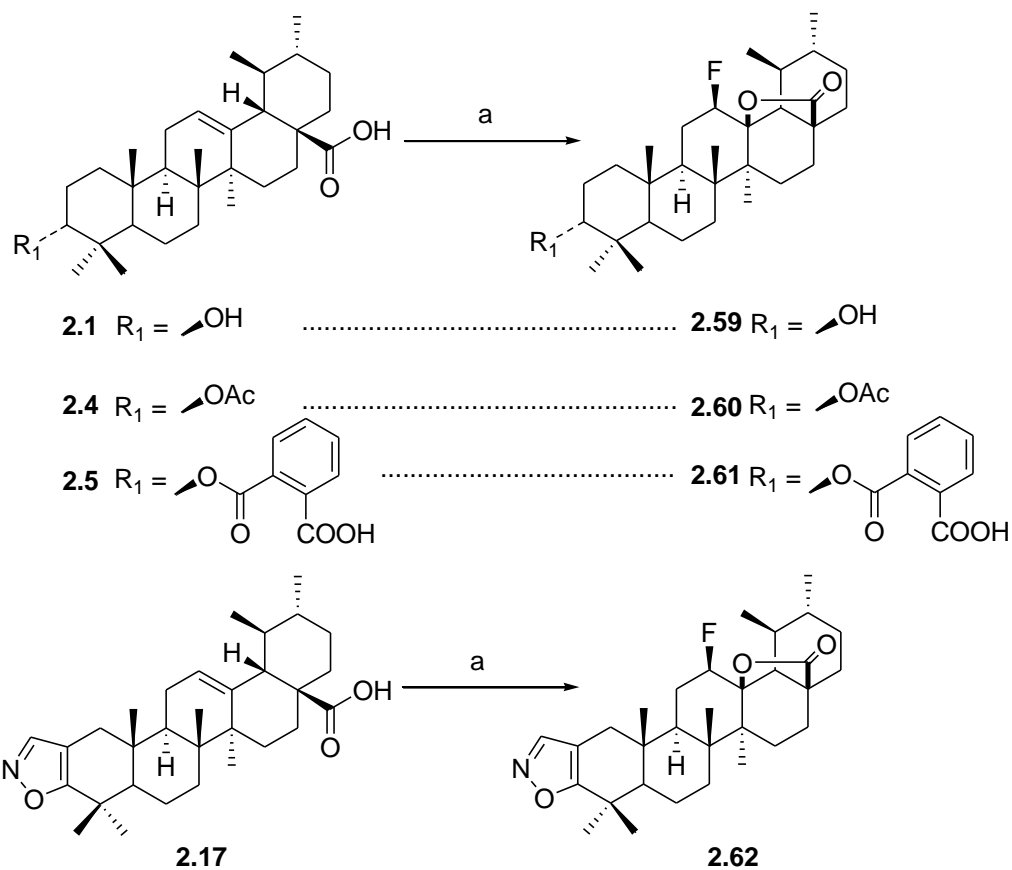
2.3.2.1. Chemistry

2.3.2.1.1. Fluorolactones

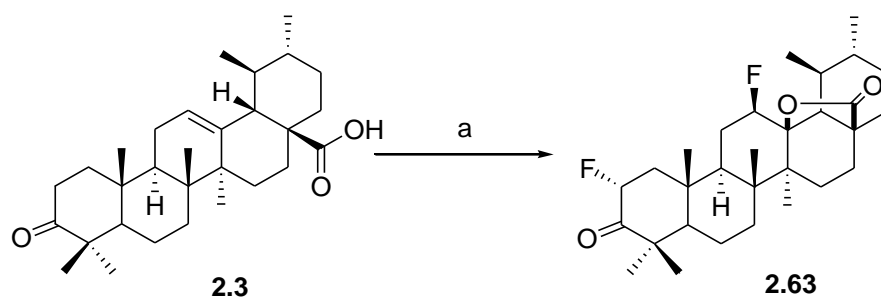
Selectfluor was used as the electrophilic fluorination reagent to introduce fluorine into ursolic acid **2.1** and derivatives. Selectfluor is a crystalline white solid and is stable at high temperatures. It is easy to work with this compound, as the byproducts are usually easily removed by an aqueous workup.^{460, 461} Several papers have described the reaction of alkenes with selectfluor, usually in the presence of a nucleophilic donor.⁴⁶²⁻⁴⁶⁶ The solvent, the temperature, and the nucleophilic donor can influence the efficiency and the outcome (number of isomers and byproducts) of this reaction. The optimal conditions for the performance of fluorination in several ursane-type substrates using selectfluor were achieved by using a mixture of two inert solvents, dioxane and nitromethane, at 80°C.

The fluorination of ursane-type triterpenoids, if performed in a reaction medium without a nucleophilic donor, allows the synthesis of a fluorolactone. The free acid behaves as a nucleophilic donor, leading to loss of the proton and promotion of cyclization at carbon C13 in the ursane skeleton. This reaction is not possible in ursane-type compounds in which the acid is protected; however, the free acid by itself does not react with selectfluor.⁴⁶⁰

Compounds **2.59-2.63** were synthesized via the reaction of compounds **2.1**, **2.3-2.5** and **2.17** with selectfluor at 80°C in a mixture of nitromethane and dioxane, affording a β -fluorine at C12 and a 13,28- β -lactone, with yields above 36% (Schemes 2.3.1 and 2.3.2). The fluorination of compound **2.3** by selectfluor results in the formation of a fluorolactone, and in an additional fluorination at carbon C2, adjacent to the carbonyl group. Fluorination of positions adjacent to a carbonyl group are described in the literature, with the α isomer being the major product (Scheme 2.3.2).^{454, 461, 465, 467}

Scheme 2.3.1.^a Synthesis of derivatives 2.59-2.62.

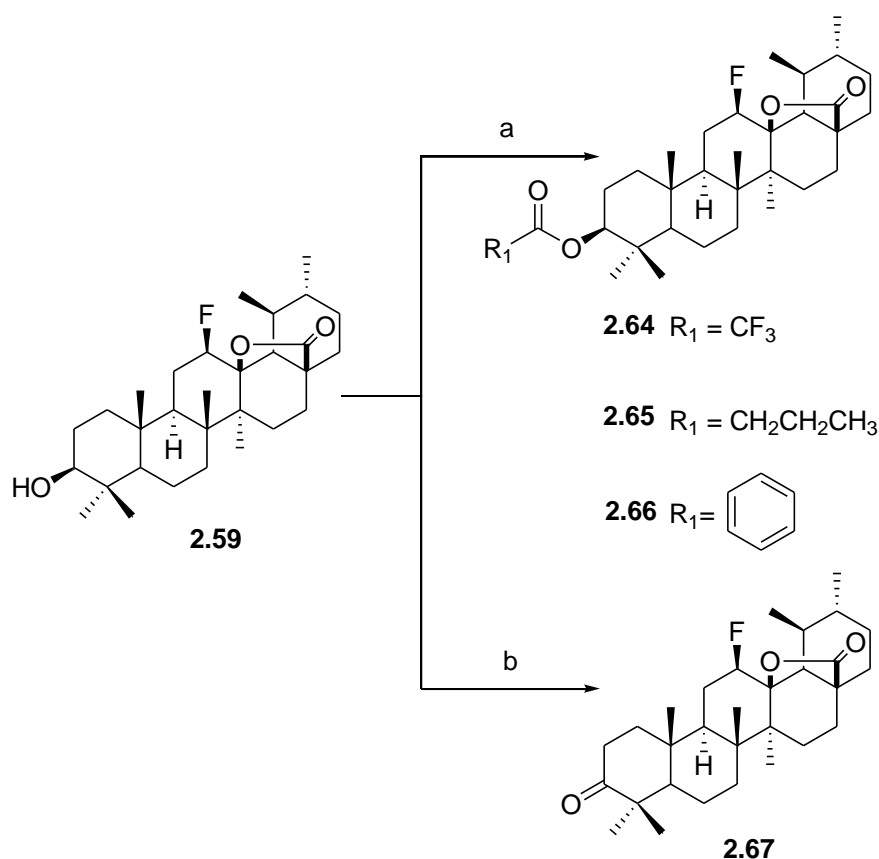
^aReagents: (a) Selectfluor, dioxane, nitromethane, 80 °C.

Scheme 2.3.2.^a Synthesis of derivative 2.63.

^aReagents: (a) Selectfluor, dioxane, nitromethane, 80 °C.

The choice of performing fluorination before esterification and Jones oxidation in compounds **2.64-2.66** and **2.67**, respectively, was based on the fact that some of these functionalities can also be fluorinated, giving a complex mixture of diverse fluorinated compounds (Scheme 2.3.3). Compounds **2.60** and **2.61** were fluorinated after esterification, as this synthetic route generates better yields. The new fluorolactones achieved are chemically stable and allow the performance of several post-fluorination modifications using acidic and basic conditions.

Scheme 2.3.3.^a Synthesis of derivatives **2.64-2.67**.

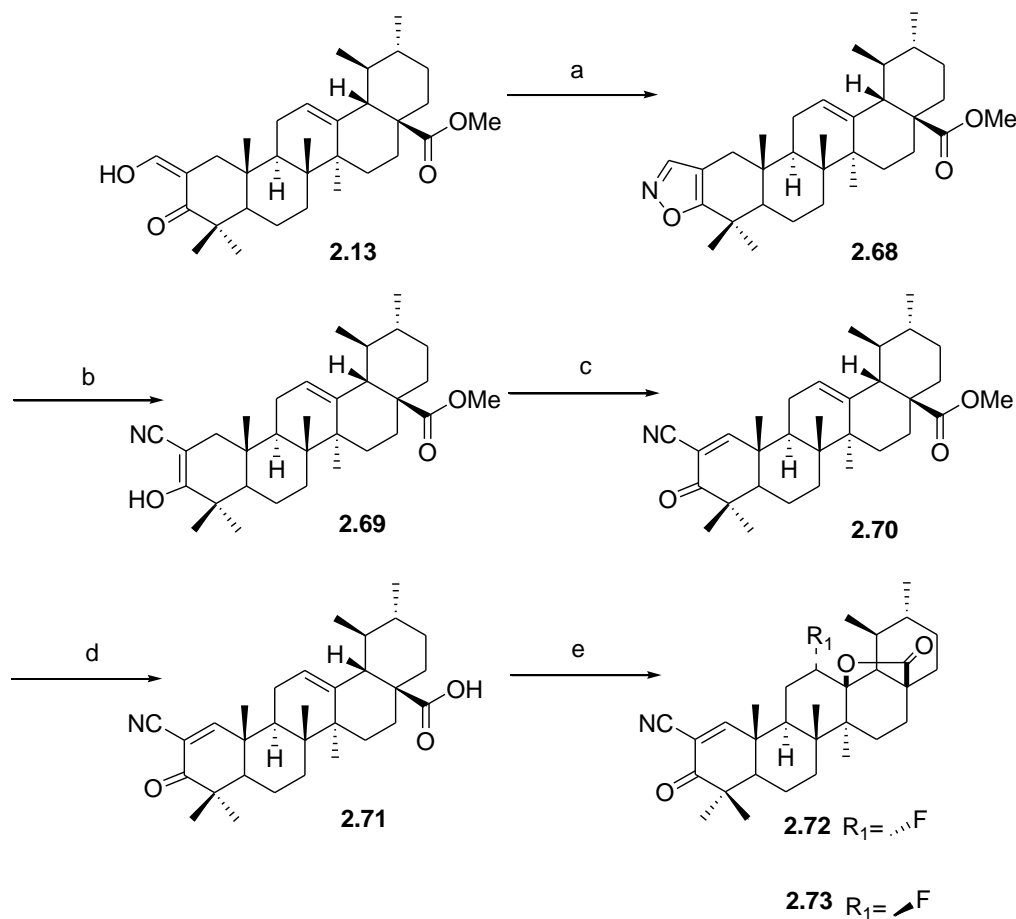


^aReagents: (a) Anhydride, DMAP, THF, r.t.; (b) Jones reagent, acetone, ice.

Honda *et al* first described the introduction of a cyano group at the C2 carbon of ursolic acid **2.1**.²⁹⁵ Herein, we reproduced a similar reactional sequence for ursolic acid **2.1**, with the introduction of the fluorolactone as the last modification of the ursane backbone (Scheme 2.3.4). Despite the optimization of the process, this reaction yielded a

mixture of fluorolactone α - and β -isomers, among which compound **2.73**, the β -isomer, was the major reaction product.

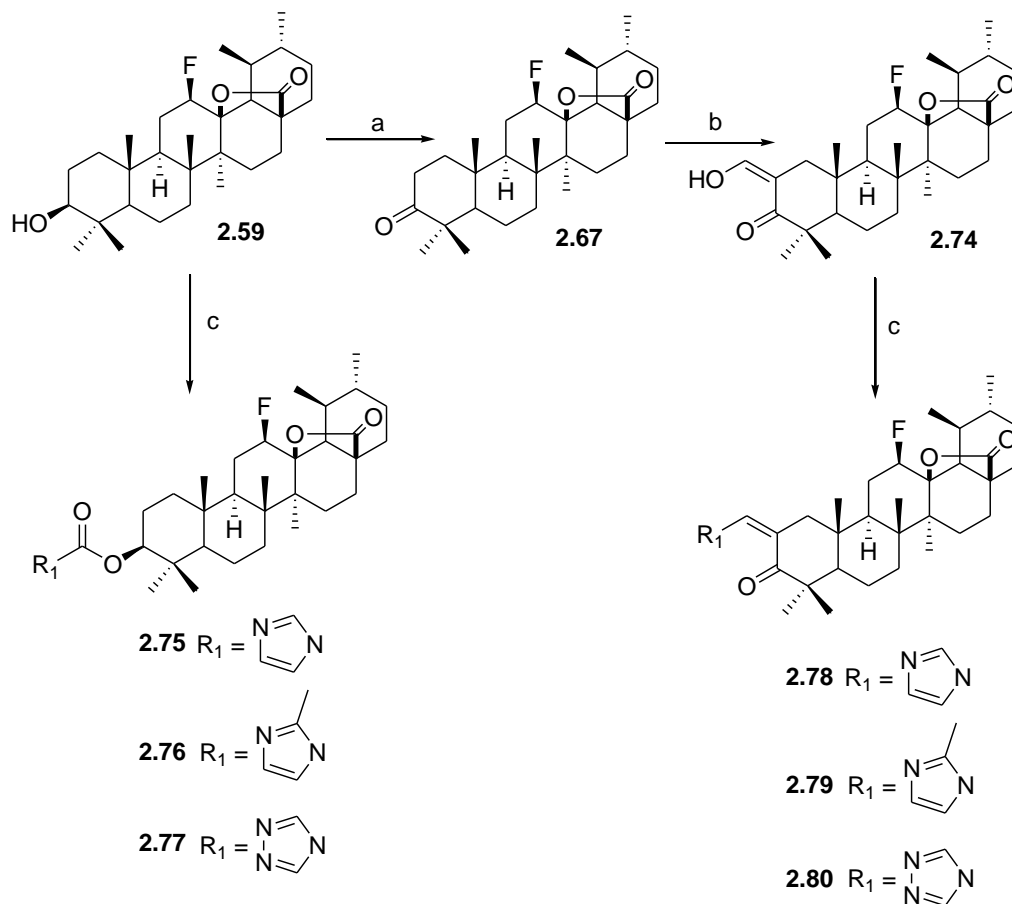
Scheme 2.3.4.^a Synthesis of derivatives **2.72** and **2.73**.



^aReagents: (a) $\text{NH}_2\text{OH}\cdot\text{HCl}$, H_2O , EtOH , reflux; (b) NaOMe , Et_2O , MeOH , $0\text{ }^\circ\text{C}$ -r.t.; (c) DDQ , benzene, reflux; (d) LiI , DMF , reflux; (e) Selectfluor , dioxane, nitromethane, $80\text{ }^\circ\text{C}$.

Previously, our group found that the introduction of heterocyclic rings into betulin and betulinic acid increased the cytotoxic activity of the parental compounds.^{433, 434, 437}

Ursolic acid **2.1** has several points in its structure that are accessible for these types of chemical modifications. The introduction of a heterocyclic ring in ursolic acid fluorine derivatives can be achieved, with good yields (Scheme 2.3.5).

Scheme 2.3.5.^a Synthesis of derivatives **2.74-2.80**.

^aReagents: (a) Jones reagent, acetone, ice; (b) Ethyl formate, NaOMe, benzene, r.t.; (c) CDI or CBMI or CDT, THF, N₂, reflux.

The preparation of the new derivatives with fluorolactone and a heterocyclic ring (compounds **2.75-2.80**) was achieved via the dissolution of the respective fluorolactone, compounds **2.59** or **2.74**, in THF, heating until reflux under an inert atmosphere and by the addition of CDI, CBMI or CDT, to give imidazole, methylimidazole and triazole derivatives, respectively (Scheme 2.3.5). The reaction of alcohols with these reagents, CDI, CBMI and CDT, gave *N*-alkylimidazoles^{438, 440} or imidazole carboxylic esters (carbamates),^{433, 434, 441} depending on the alcohol and reaction conditions used. Compound **2.59**, with a secondary alcohol at position C3, afforded carbamates **2.75-2.77**. Compound **2.74**, with a vinyl alcohol at position C2, gave the *N*-alkylimidazoles **2.78-2.80**.

Full structural elucidation of the fluorolactones was achieved using IR, 1D and 2D NMR and MS.

Usually, the band in IR corresponding to the C–F stretching vibration appeared between $1000\text{--}1400\text{ cm}^{-1}$, which in these compounds coincided with other bands, such as C–O and C–H (Figure 2.3.4).

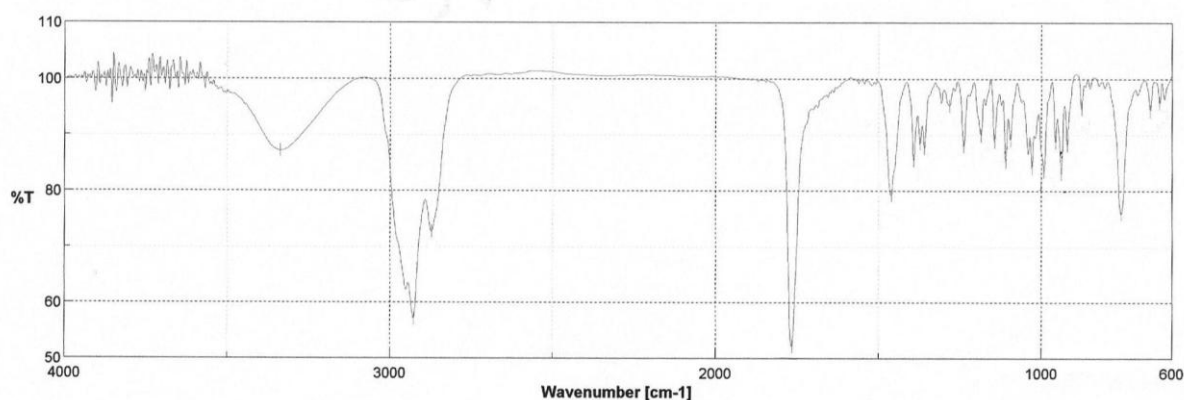


Figure 2.3.4. IR spectrum of compound **2.59**.

The nature of the isomers α and β was determined using 1D and 2D NMR and was confirmed via X-ray crystallography of compound **2.66**.

The geminal proton of the β -fluorine on carbon C12 gave a double triplet or a double quartet, with a δ signal at $5.0\text{--}4.8$ ppm and a coupling constant around 62 Hz (Figure 2.3.5). The α -isomer also gave a double triplet at δ $4.42\text{--}4.51$ ppm, a signal that was slightly lower than that of the β -isomer, and a coupling constant around 67 Hz (Figure 2.3.6), which was higher than that of the β -isomer, in the ^1H NMR spectrum.^{468, 469}

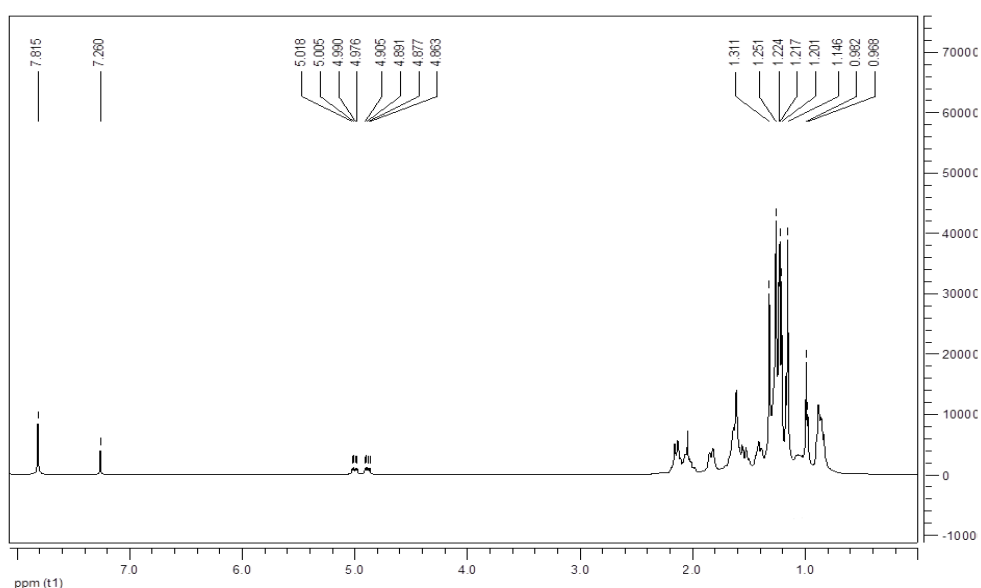


Figure 2.3.5. ^1H NMR spectrum of compound **2.73**.

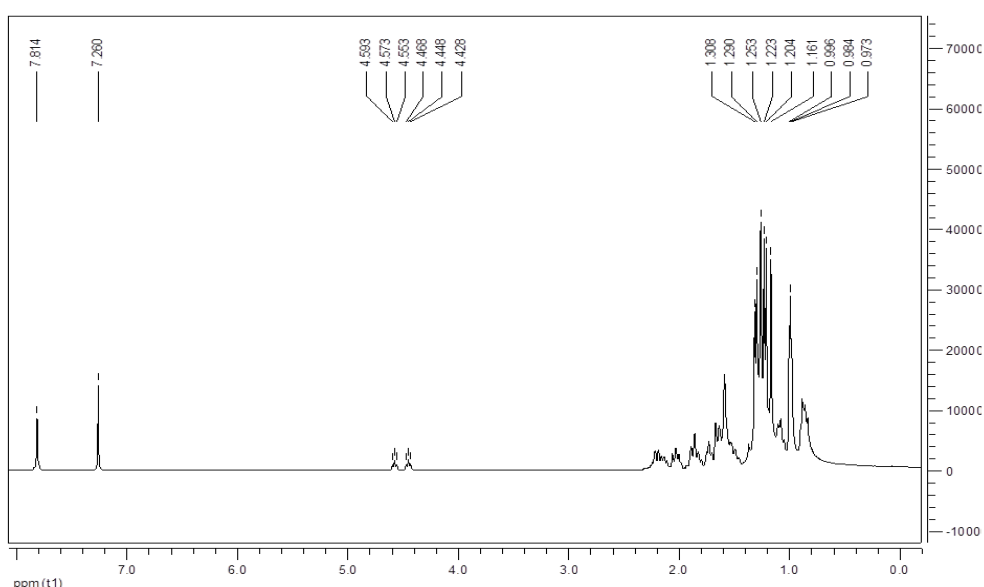


Figure 2.3.6. ^1H NMR spectrum of compound **2.72**.

In the ^{13}C NMR spectrum of compounds bearing the β -fluorolactone modification, carbon C12 appeared as a doublet, with δ values between 88.5 and 89.6 ppm and a coupling constant around 180 Hz. Carbon C13 also appeared as a doublet, with values of δ 91.5-91.9 ppm with a lower coupling constant, around 14 Hz.^{469, 470} Carbons C18, C14, C11 and C9 on the ursane β -fluorolactone also have doublet δ signals in the ^{13}C NMR

spectrum (Figure 2.3.7). In the ^{13}C NMR spectrum, compound **2.72** presented some differences from compounds with a β -fluorolactone: carbon C12 appeared at higher values, a δ signal at 96 ppm, with a coupling constant of 189 Hz, and carbon C13 was present as a singlet at δ 90 ppm.^{469, 470}

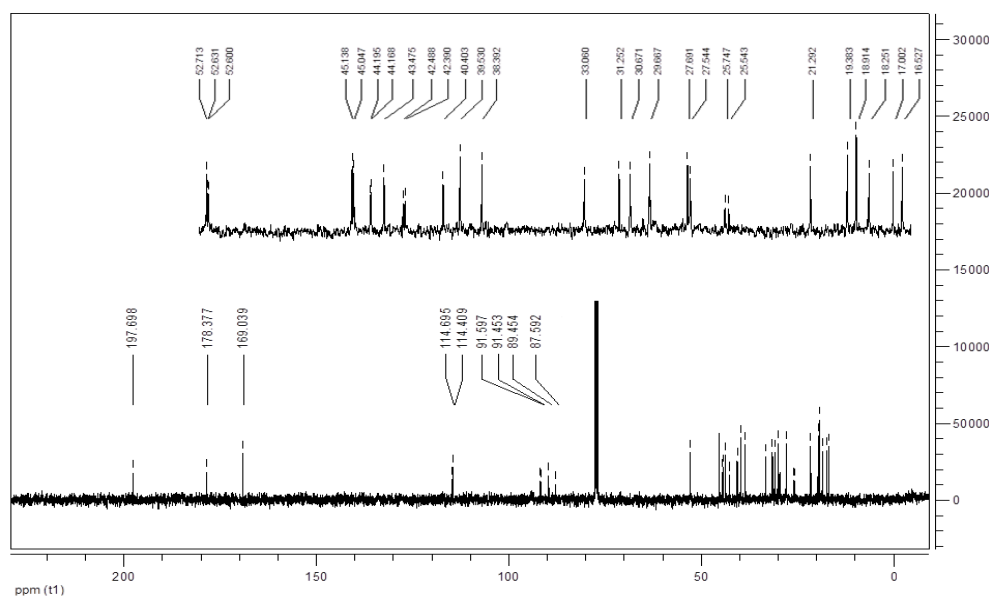


Figure 2.3.7. ^{13}C NMR of compound **2.73**.

The correlations in the HMBC and HMQC spectra of compound **2.73** allowed the identification of several δ signals in the ^1H and ^{13}C NMR spectra (Figure 2.3.8). The modifications in ring A of this compound had been described previously, which permitted the identification of the δ signals for carbons C1, C2, C3 and CN.²⁹⁴ In the ^1H NMR spectrum, compounds **2.72** and **2.73** presented a signal at δ 7.81 ppm, corresponding to proton H1. In the ^{13}C NMR spectrum, this signal corresponded to a δ signal at 169.04 ppm. Carbon C1 correlated with the methyl group at C25 and with proton H9; carbons C10 and C8 also correlated with proton H9. Carbons C13 and C17 correlated with proton H18, which allowed the identification of the δ signal observed at 52.61 ppm as C18 in the ^{13}C NMR spectrum (Table 2.3.1).

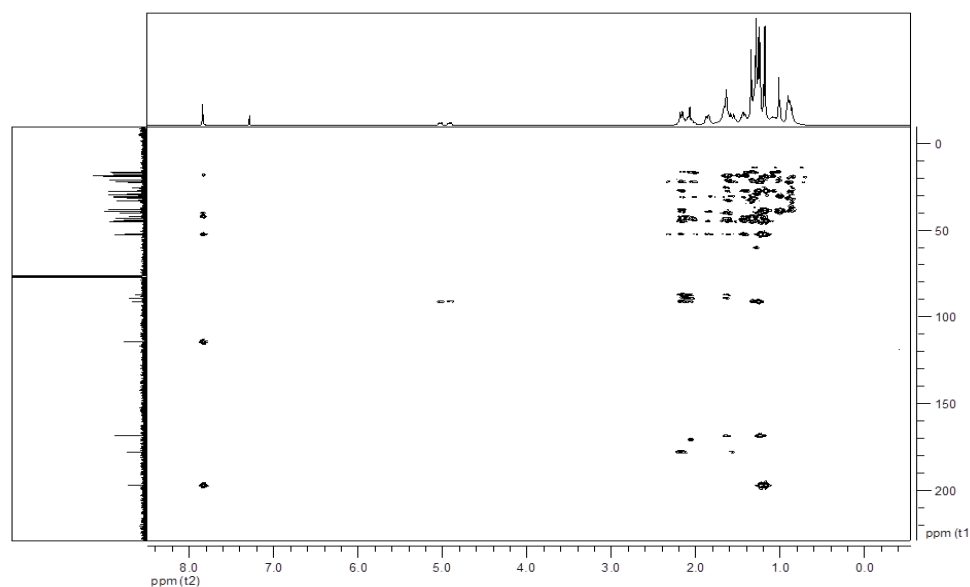


Figure 2.3.8. HMBC of compound **2.73**.

NOESY experiments correlate protons that are close to each other in space, allowing the identification of protons with the same space orientation. In the fluorolactones synthesized, NOESY spectra allowed the identification of proton H12 as presenting an α configuration in compounds **2.59-2.71** and **2.73-2.80** (Figure 2.3.9). Proton H12 in NOESY spectra correlated with the methyl group at C27 and with proton H9, both of which exhibited an α configuration (Figure 2.3.10).

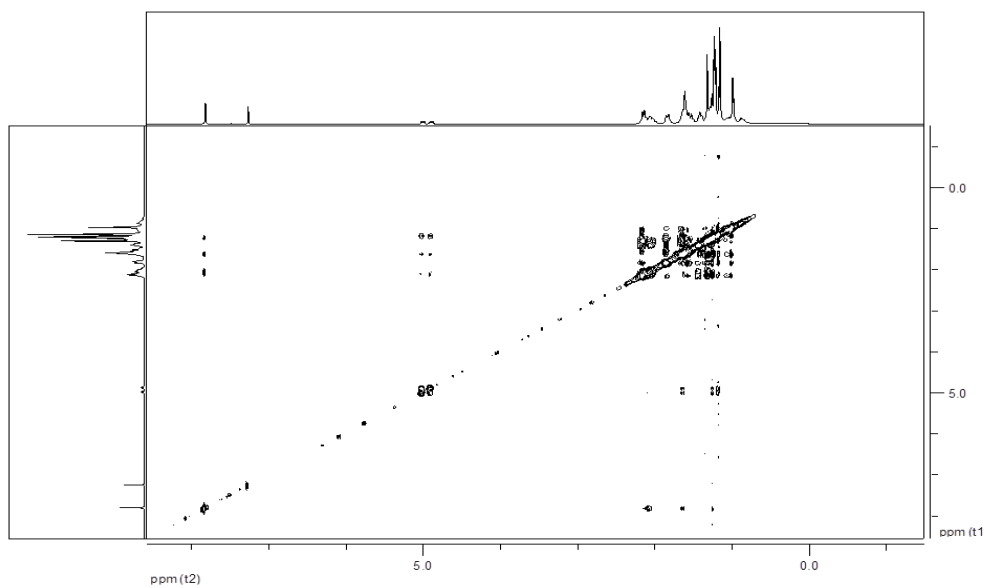


Figure 2.3.9. NOESY spectrum of compound **2.73**.

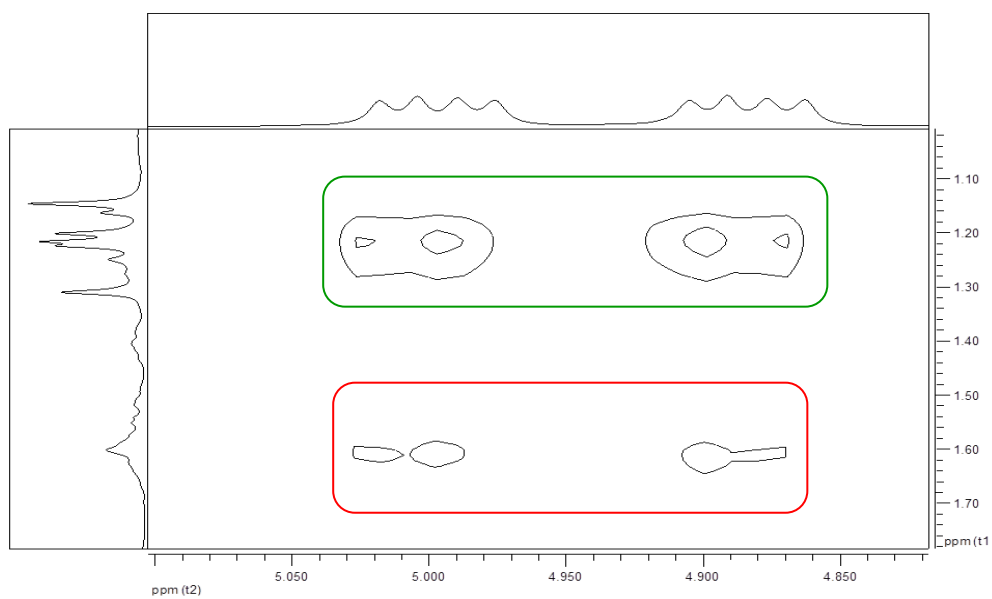


Figure 2.3.10. Detail of the NOESY spectrum of compound **2.73**. Correlation of proton H12 with the methyl group at C27 (green) and correlation of proton H12 with proton H9 (red).

The configuration 12 β -fluoro-13,28 β -lactone was confirmed in the ORTEP of compound **2.66**, which was crystallized in acetonitrile (Figure 2.3.11).

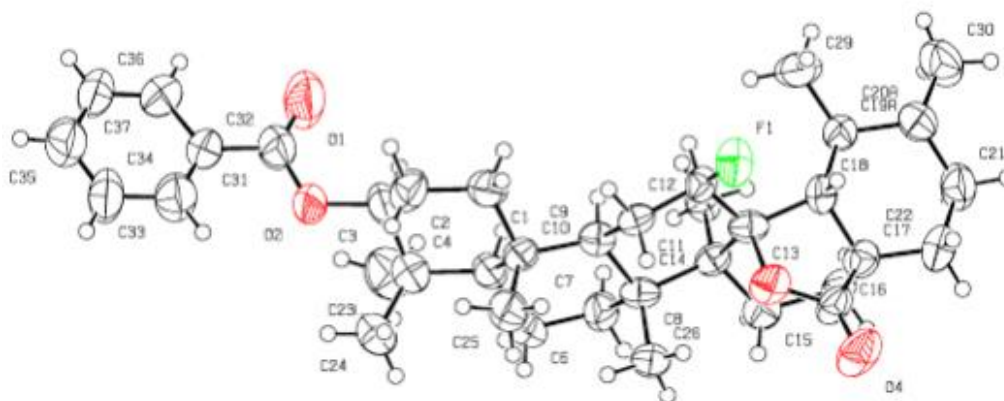


Figure 2.3.11. ORTEP diagram of compound **2.66** (50% probability level, H atoms of arbitrary sizes).

Fluorolactone **2.63**, with one additional fluorine substituent at carbon C2, presented additional duplicated δ signals in the ^1H and ^{13}C NMR spectra. The analysis of the ^1H , ^{13}C , DEPT, HMBC, HMQC and NOESY spectra permitted the identification of various δ signals in ^1H and ^{13}C NMR spectra (Table 2.3.1).

Table 2.3.1. Selected ^1H and ^{13}C NMR data from the backbone of compounds **2.63** and **2.73**.

| Entry | Position | 2.63 | | 2.73 | |
|-----------|-----------|----------------|-----------------|----------------|-----------------|
| | | δ H | δ C | δ H | δ C |
| 1 | 1 | 2.58 | 47.23 | 7.82 | 169.04 |
| | | ($J= 26.25$) | ($J= 17.17$) | | |
| 2 | 2 | 5.30 | 89.05 | - | 114.41 |
| | | ($J= 66.18$) | ($J= 186.30$) | | |
| 3 | 3 | - | 209.63 | - | 197.70 |
| 4 | 4 | - | 48.49 | - | 45.05 |
| 5 | 5 | - | 56.41 | - | 52.71 |
| 6 | 7 | - | 33.47 | - | - |
| 7 | 8 | - | 42.63 | - | 43.48 |
| | | - | 48.71 | - | 42.43 |
| 8 | 9 | - | ($J= 48.71$) | - | ($J= 9.85$) |
| | | - | 38.04 | - | 40.40 |
| 9 | 10 | - | ($J= 9.40$) | - | - |
| | | - | 25.72 | - | - |
| 10 | 11 | - | ($J= 20.16$) | - | - |
| | | 4.88 | 88.75 | 4.94 | 88.54 |
| 11 | 12 | ($J= 62.48$) | ($J= 186.09$) | ($J= 62.15$) | ($J= 183.62$) |
| | | - | 91.63 | - | 91.52 |
| 12 | 13 | - | ($J= 14.40$) | - | ($J= 14.49$) |
| | | - | 43.97 | - | - |
| 13 | 14 | - | ($J= 2.97$) | - | - |
| | | - | 27.60 | - | - |
| 14 | 15 | - | - | - | 44.17 |
| | | - | 45.13 | - | ($J= 2.72$) |
| 15 | 17 | - | - | - | 52.61 |
| | | - | 52.54 | - | ($J= 3.16$) |
| 16 | 18 | - | ($J= 3.34$) | - | - |
| | | 1.23 | 17.48 | 1.20 | 27.69 |
| 17 | 25 | 1.26 | 18.63 | 1.31 | 18.91 |
| 18 | 26 | 1.19 | 17.16 | 1.22 | 17.00 |
| | | - | - | ($J= 3.13$) | - |
| 19 | 27 | - | 178.68 | - | 178.38 |
| 20 | 28 | - | - | 1.25 | 18.91 |
| 21 | 29 | - | - | 0.98 | 19.38 |
| 22 | 30 | - | - | ($J= 5.71$) | - |
| | | - | - | - | 114.70 |
| 23 | CN | - | - | - | - |

Compounds **2.74-2.80** also exhibited the 12 β -fluor-13,28 β -lactone functionality, in which proton H12 was present in the ^1H NMR spectrum as a δ signal around 4.98 ppm. Moreover, in the ^{13}C NMR spectrum, the δ signals for carbons C12 and C13 appeared as doublets around 88 and 91 ppm, respectively. The proton of the exocyclic double bond at C2 of compounds **2.74** and **2.78-2.80** was observed on the ^1H NMR spectrum at δ signals between 8.62 and 7.66 ppm, depending on the substituent group present. The imidazole group on compounds **2.75** and **2.78** had three specific protons that appeared in the ^1H NMR spectrum at a δ signal higher than 7 ppm. Compounds **2.76** and **2.79**, with a methylimidazole group, had only two protons in the ^1H NMR spectrum, between δ 6.7 and 7.4 ppm. The triazole group in compounds **2.77** and **2.80** was identified by the presence of two δ signals higher than 8 ppm.

The HMBC, HMQC and NOESY spectra correlations allowed the identification of several δ signals (Figure 2.3.12). Table 2.3.2 presents some ^1H and ^{13}C NMR δ signals for compounds **2.75** and **2.79**.

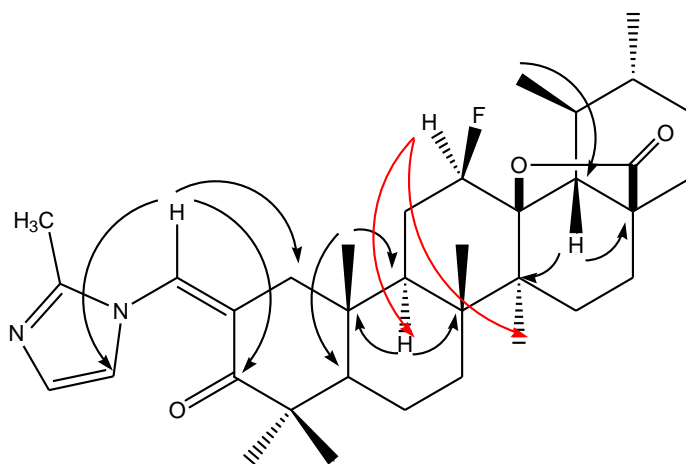


Figure 2.3.12. Some HMBC (black) and NOESY (red) correlations for compound **2.79**.

Table 2.3.2. Selected ^1H and ^{13}C NMR data from the backbone of compounds **2.75** and **2.79**.

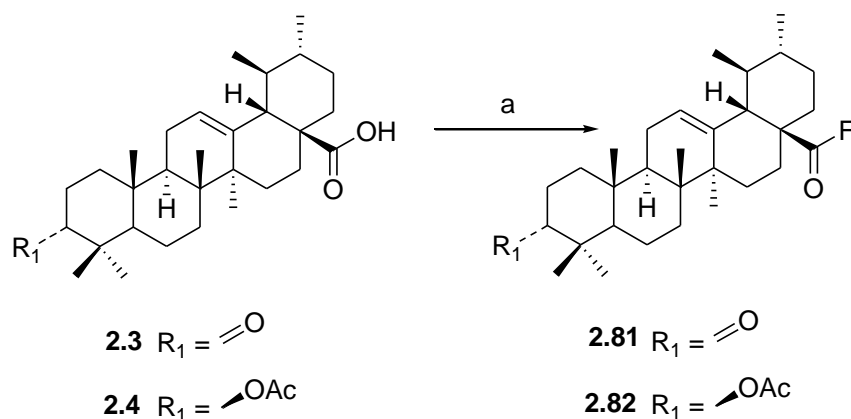
| Entry | Position | 2.75 | | 2.79 | |
|-------|------------------------------|------------------------|--------------------------|------------------------|--------------------------|
| | | δ H | δ C | δ H | δ C |
| 1 | 1 | - | - | - | 422.87 |
| 2 | 2 | - | - | - | 123.05 |
| 3 | 3 | 4.68 ($J= 15.87$) | 85.84 | - | 206.08 |
| 4 | 4 | - | 38.19 | - | 45.16 |
| 5 | 5 | 0.86 ($J= 8.75$) | 55.32 | - | 52.40 |
| 6 | 8 | - | 42.54 | - | 42.21 |
| 7 | 9 | - | 49.06 ($J= 9.38$) | - | 47.08 ($J= 9.41$) |
| 8 | 10 | - | 37.03 | - | 36.32 |
| 9 | 12 | 4.87 ($J= 62.65$) | 89.49 ($J= 185.86$) | 4.93 ($J= 62.33$) | 89.33 ($J= 186.24$) |
| 10 | 13 | - | 91.80 ($J= 14.31$) | - | 91.74 ($J= 14.41$) |
| 11 | 14 | - | 43.94 | - | 44.06 ($J= 2.74$) |
| 12 | 15 | - | 27.63 | - | - |
| 13 | 17 | - | 45.17 | - | 45.24 |
| 14 | 18 | - | 52.55 ($J= 3.34$) | - | 52.57 ($J= 3.34$) |
| 15 | 19 | - | 38.40 | - | 38.57 |
| 16 | 20 | - | 39.53 | - | 39.51 |
| 17 | 25 | 0.98 | 19.39 | 0.90 | 16.41 |
| 18 | 26 | 1.22 | 18.53 | 1.26 | 17.69 |
| 19 | 27 | 1.21 | 17.21 | 1.24 | 16.48 |
| 20 | 28 | - | 178.75 | - | 178.59 |
| 21 | 29 | 1.14 ($J= 6.20$) | 16.50 | 1.16 | 16.48 |
| 22 | 30 | - | - | 0.97 | 19.36 |
| 23 | OCO | - | 148.46 | - | - |
| 24 | C2CH | - | - | 7.66 | 130.67 |
| 25 | C2' | - | - | - | 147.37 |
| 26 | CH ₃ imidazole | - | - | 2.48 | 13.66 |
| 27 | C4' | - | - | 7.16 | 117.97 |
| 28 | C5' | - | - | 7.03 | 128.76 |

2.3.2.1.2. Acyl fluorides

Nucleophilic fluorination reactions using DAST or deoxofluor are methodologies that are widely used for the preparation of fluorinated organic compounds. Deoxofluor is thermally more stable than DAST and, in some cases, can have a better reactivity and selectivity.^{471, 472} Deoxofluor can easily convert alcohols to alkyl fluorides, aldehydes and ketones to gem-difluorides, and carboxylic acids to acid fluorides or trifluoromethyl derivatives.^{453, 473, 474}

Nucleophilic fluorination of lupane triterpenoids has been reported using DAST;⁴⁷⁵ however, the reaction conditions require the use of extremely low temperatures. The use of deoxofluor as a nucleophilic reagent in ursane derivatives allowed the synthesis of acyl fluorides of the correspondent carboxylic acid, in good yields (Scheme 2.3.6).

Scheme 2.3.6.^a Synthesis of derivatives **2.81** and **2.82**.



^aReagents: (a) Deoxofluor, THF, ice.

Acid halides have a carbonyl group with a stretching vibration near 1800 cm^{-1} . Compounds **2.81** and **2.82** presented a stretching vibration around 1827 cm^{-1} , corresponding to the carbonyl stretching vibration. The C–F stretching vibration was merged with other absorption regions of the ursane backbone (Figure 2.3.13).

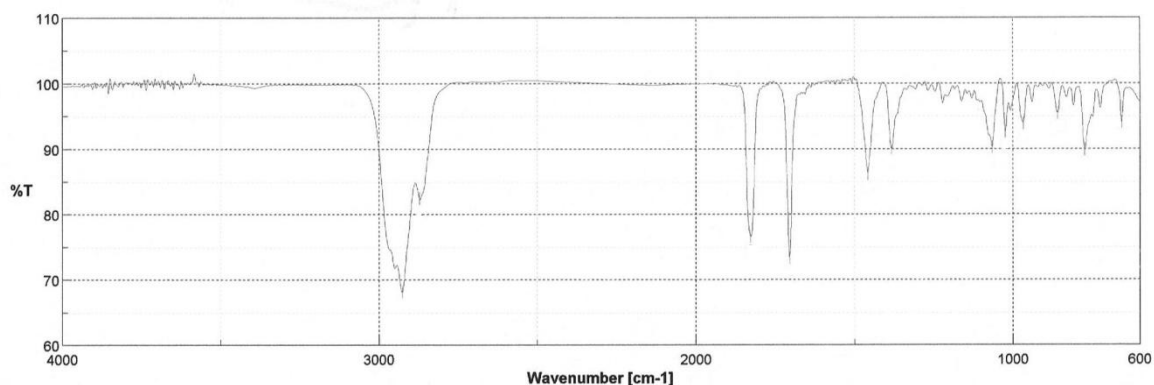


Figure 2.3.13. IR spectrum of compound **2.81**.

On the ¹H NMR spectrum, acyl fluorides with an ursane backbone presented a spectrum that was identical to that of the intermediate. On the ¹³C NMR spectrum, the only difference relative to the intermediate was the signal of the carbonyl group of the acyl halide. In compounds **2.81** and **2.82**, carbon C28 appears as a doublet with a δ signal of 167.06 ppm and a coupling constant of 376 Hz (Figure 2.3.14).

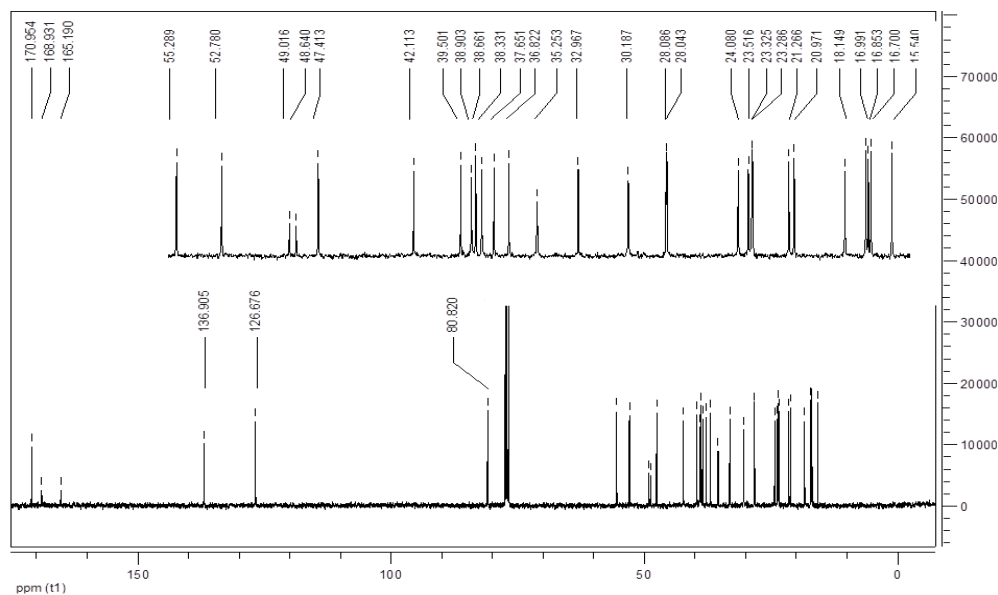


Figure 2.3.14. ¹³C NMR spectrum of compound **2.82**.

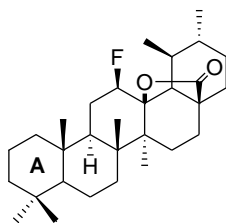
2.3.2.2. Biological evaluation

The fluorolactone of ursolic acid **2.1**, compound **2.59**, exhibited a similar antiproliferative activity against AsPC-1 cells compared with ursolic acid **2.1**. However, compounds **2.60** and **2.61**, which have a fluorolactone moiety, showed increased antiproliferative activities compared with compounds **2.4** and **2.5**, respectively (Figure 2.3.15; Tables 2.3.3 and 2.3.4). Several additional modifications were performed at C3 of the ursane fluorolactone, to yield compounds **2.64-2.67** and **2.75-2.77**. Oxidation of the hydroxyl function was reported to increase the biological activity of the triterpenoid compounds;²⁹³ however, compound **2.64** exhibited only a slight increase in the antiproliferative activity compared with compound **2.59**. In addition, the introduction of a fluorine at C2, compound **2.63**, did not increase the antiproliferative activity. Carbamates **2.75** and **2.76** exhibited an increase of 2- and 3-fold in antiproliferative activity against AsPC-1 cancer cells compared with ursolic acid fluorolactone **2.59** (Table 2.3.4). Compounds **2.65** and **2.66** were prepared by esterification with butyric and benzoic anhydrides, respectively. This process generated some of the most active compounds, with 8- and 15-fold increase in antiproliferative activity compared with compound **2.59** (Table 2.3.4).

Table 2.3.3. The IC₅₀ (μM) of ursolic acid intermediates in the inhibition of AsPC-1 cell growth.

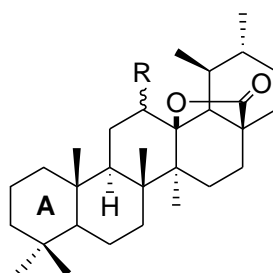
| Entry | Compd | AsPC-1 |
|-------|-------|-----------|
| 1 | 2.1 | 12.6±0.03 |
| 2 | 2.3 | 24.5±0.12 |
| 3 | 2.4 | 71.0±0.1 |
| 4 | 2.5 | 42.3±0.02 |
| 5 | 2.13 | 7.2±0.02 |
| 6 | 2.70 | 2.0±0.1 |
| 7 | 2.71 | 15.9±0.2 |

AsPC-1 cells were treated with the indicated compounds at varying concentrations for 72 h. The antiproliferative effects were determined using a MTT assay and the IC₅₀ was calculated. The results shown are means ± SE of three independent experiments.

Table 2.3.4. The IC₅₀ (μM) of ursolic acid fluorolactone derivatives in the inhibition of AsPC-1 cell growth.

| Entry | Compd | Ring A | AsPC-1 |
|-------|-------|--------|-----------|
| 1 | 2.59 | | 18.4±0.09 |
| 2 | 2.60 | | 13.4±0.10 |
| 3 | 2.61 | | 18.0±0.06 |
| 4 | 2.62 | | 10.9±0.02 |
| 5 | 2.63 | | 14.1±0.15 |
| 6 | 2.64 | | 10.0±0.07 |
| 7 | 2.65 | | 2.2±0.1 |
| 8 | 2.66 | | 1.2±0.01 |
| 9 | 2.67 | | 6.0±0.07 |
| 10 | 2.75 | | 9.5±0.1 |
| 11 | 2.76 | | 6.1±0.04 |
| 12 | 2.77 | | 26.6±0.12 |

AsPC-1 cells were treated with the indicated compounds at varying concentrations for 72 h. The antiproliferative effects were determined using a MTT assay and the IC₅₀ was calculated. The results shown are means ± SE of three independent experiments.

Table 2.3.5. The IC₅₀ (μM) of ursolic acid fluorolactones in the inhibition of the growth of three pancreatic cancer cell lines.

| Entry | Compd | Ring A | R | AsPC-1 | MIA PaCa 2 | PANC-1 |
|-------|-------|--------|---|-----------|------------|-----------|
| 1 | 2.72 | | | 0.7±0.05 | 0.9±0.01 | 1.8±0.04 |
| 2 | 2.73 | | | 0.5±0.08 | 2.1±0.1 | 14.3±0.03 |
| 3 | 2.74 | | | 11.0±0.05 | ND | ND |
| 4 | 2.78 | | | 1.1±0.02 | 6.0±0.03 | 4.6±0.03 |
| 5 | 2.79 | | | 1.0±0.05 | 28.1±0.02 | 21.4±0.06 |
| 6 | 2.80 | | | 7.5±0.07 | 10.2±0.02 | 10.1±0.02 |

AsPC-1, MIA PaCa 2 and PANC-1 cells were treated with the indicated compounds at varying concentrations for 72 h. The antiproliferative effects were determined using a MTT assay and the IC₅₀ was calculated. The results shown are means ± SE of three independent experiments. ND, not determined.

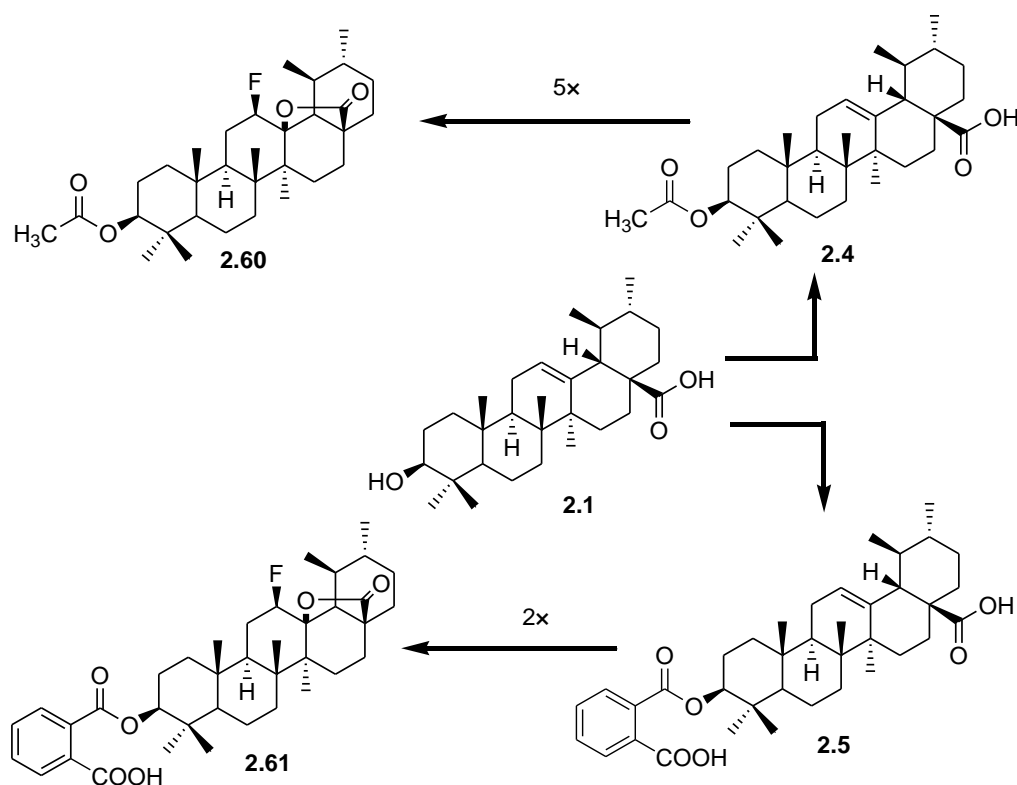


Figure 2.3.15. Structure activity relationships (SAR) among several synthetic derivatives of ursolic acid **2.1**. The comparison was made based on their IC_{50} s in the inhibition of AsPC-1 cell growth. Compound **2.60** was 5-fold more potent than compound **2.4**, and compound **2.61** was 2-fold more potent than compound **2.5**.

Previously, it was shown that the introduction of a cyano group at C2 and of a carbonyl group at C11 improved significantly the cytotoxicity of ursolic acid **2.1**.³⁰² We applied a similar chemical procedure at ring A, as described previously,²⁹⁵ and synthesized compounds **2.72** and **2.73** (Scheme 2.3.4). Compounds **2.72** and **2.73** were more effective than compounds **2.70** and **2.71** synthesized previously in the antiproliferative assay using AsPC-1 cells (Tables 2.3.3 and 2.3.5), as they exhibited an increase of 19-fold in antiproliferative activity compared with ursolic acid **2.1** (Figure 2.3.16). The intermediates of compounds **2.72** and **2.73**, compounds **2.70** and **2.71**, were less active (Table 2.3.3, entries 5 and 6), suggesting that the addition of a fluorolactone contributes to the improvement of the antiproliferative activity of compounds **2.72** and **2.73** (Table 2.3.5, entries 1 and 2).

Table 2.3.6. The IC₅₀ (μM) of ursolic acid fluorolactones in the inhibition of the growth of breast (MCF-7), prostate (PC-3), hepatic (Hep G2) and lung (A549) cancer cell lines.

| Entry | Compd | MCF-7 | PC-3 | Hep G2 | A549 |
|----------|-------------|----------|----------|-----------|-----------|
| <i>1</i> | 2.72 | 0.7±0.20 | 0.9±0.01 | 0.5±0.12 | 0.9±0.05 |
| <i>2</i> | 2.73 | 2.2±0.11 | 2.0±0.03 | 3.0±0.11 | 10.0±0.05 |
| <i>3</i> | 2.78 | 2.8±0.04 | 4.0±0.03 | 6.8±0.07 | 9.5±0.08 |
| <i>4</i> | 2.80 | 7.0±0.05 | 5.6±0.02 | 10.6±0.14 | 16.2±0.03 |

MCF-7, PC-3, Hep G2 and A549 cells were treated with the indicated compounds at varying concentrations for 72 h. The antiproliferative effects were determined using an MTT assay and the IC₅₀ was calculated. The results shown are means ± SE of three independent experiments.

Compound **2.74** was synthesized with the intent of exploring the effect of the introduction of different substituents at C2 of the fluorolactone structure, as it contains a vinyl alcohol at that position. The substitution of the alcohol group of compound **2.74** with a heterocyclic ring, imidazole or methylimidazole, afforded compounds **2.78** and **2.79**, respectively, with improved antiproliferative effects in AsPC-1 cells, reaching an increase of 17-fold compared with compound **2.59** (Figure 2.3.16). Compounds **2.78** and **2.79**, *N*-alkylimidazoles, exhibited activities similar to those of **2.72** and **2.73** in the inhibition of AsPC-1 cell growth (Table 2.3.5). The antiproliferative effects of compounds **2.72**, **2.73** and **2.78-2.80** were determined in two additional pancreatic cancer cell lines. MIA PaCa 2 and PANC-1 cells were less sensitive than AsPC-1 cells to these compounds, with higher IC_{50s} (Table 2.3.5).

The antiproliferative effects of compounds **2.72**, **2.73**, **2.78** and **2.80** were also tested against MCF-7, PC-3, Hep G2 and A549 cell lines. Among the compounds tested, compound **2.72** was the most active in all cell lines, with IC_{50s} lower than 1 μM (Table 2.3.6).

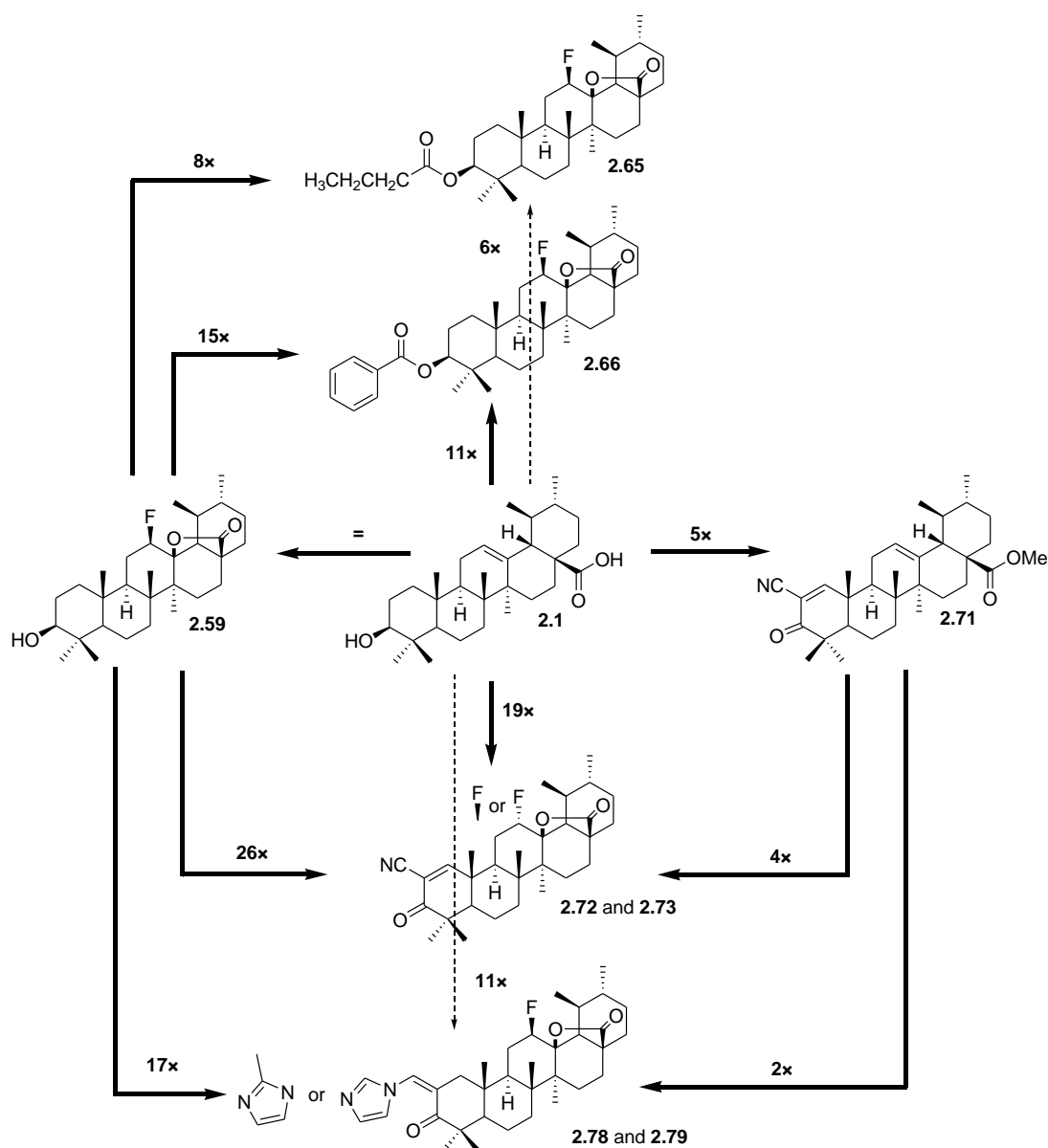


Figure 2.3.16. Structure activity relationships (SAR) among several synthetic derivatives of ursolic acid **2.1**. The comparison was made based on their IC_{50} s in the inhibition of AsPC-1 cell growth. Compound **2.71** was 5-fold more potent than ursolic acid **2.1**. Compounds **2.72** and **2.73** were 19-fold more potent than ursolic acid **2.1**, 4-fold more potent than compound **2.71** and 26-fold more potent than compound **2.59**. Compounds **2.78** and **2.79** were 11-fold more potent than ursolic acid **2.1**, 2-fold more potent than compound **2.71**, and 17-fold more potent than compound **2.59**. Compound **2.66** was 11-fold more potent than ursolic acid **2.1** and 15-fold more potent than compound **2.59**. Compound **2.65** was 6-fold more potent than ursolic acid **2.1** and 8-fold more potent than compound **2.59**.

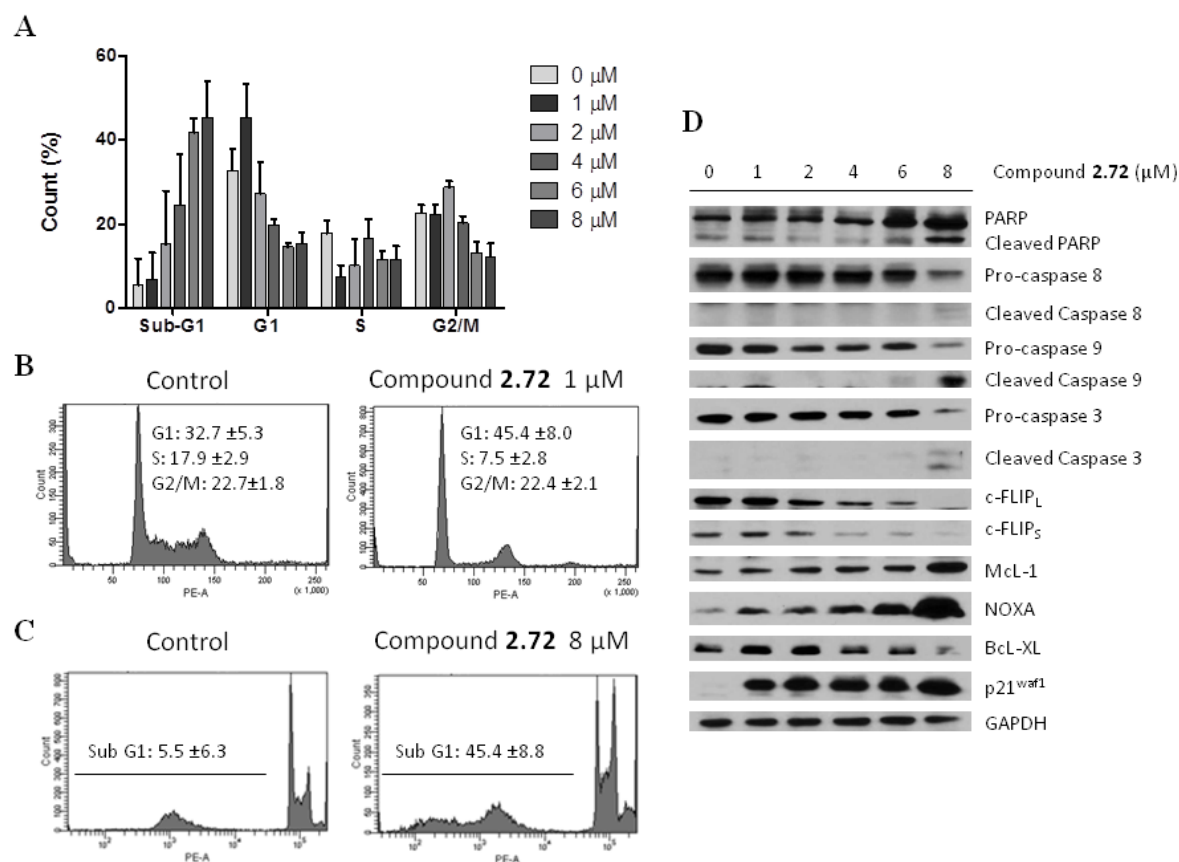


Figure 2.3.17. Cell cycle arrest and apoptosis induction by compound **2.72** in AsPC-1 cells. (A) Cell cycle analysis of AsPC-1 cells treated with compound **2.72**. (B) Representative FACS analyses of G1 phase arrest in AsPC-1 cells treated with compound **2.72** at 1 μM for 24 h. (C) Representative FACS analyses of induction of sub-G1 phase (apoptotic cells) in AsPC-1 cells treated with compound **2.72** at 8 μM for 24 h. (D) Relative levels of apoptosis- and cycle-related proteins in AsPC-1 cells treated with a variety of concentrations of compound **2.72** for 24 h. The cell cycle was determined by FACS after staining with PI. The relative protein levels were determined by Western blot analysis. GAPDH was used as a loading control.

The introduction of an electron-withdrawing group at C2 of the ursolic acid **2.1** (compounds **2.72** and **2.73**) amplified the antitumor activity of these compounds, allowing the nucleophilic attack by thiol or other nucleophiles at C1, which in turn acquired an increased electrophilic nature because of the substituent at C2.^{414, 444} The presence of a fluorolactone moiety may increase the ability of these compounds to interact with potential targets. Overall, the modification by introduction of a fluorolactone (compounds **2.72** and **2.73**) instead of a methoxyl group at C28 improved the

antiproliferative activity of these compounds by more than 4-fold compared with that of compound **2.71** (with a cyano group at C2) and by more than 19-fold compared with that of ursolic acid **2.1** (without a cyano group at C2) in AsPC-1 cells (Figure 2.3.16).

Fluoro acyl derivatives **2.81** and **2.82** had an IC_{50} of 11.8 and 33.4 μ M, respectively, which represented an improvement of 0.5- and 2-fold relative to the intermediates **2.3** and **2.4**. These compounds did not exhibit an improvement in antiproliferative activity when compared with ursolic acid **2.1**.

Because compound **2.72** was the most active, it was selected to study the mechanism by which antiproliferative activity is mediated in AsPC-1 cells. As shown in Figure 2.3.17 A-C, compound **2.72** arrested the cell cycle at the G1 phase at 1 μ M and increased the population of cells in the sub-G1 phase at higher concentrations (8 μ M). These data suggest that this compound has a dual effect: it arrests cell cycle progression and induces apoptosis. The effects of compound **2.72** were tested at the level of cell cycle-regulating and apoptosis-related proteins at concentrations of 1-8 μ M. Compound **2.72** significantly increased the levels of p21^{waf1} at 1 μ M, which correlated with cell cycle arrest in the G1 phase (Figure 2.3.17 D). The observation that other proteins were not significantly regulated by compound **2.72** at 1 μ M suggests that p21^{waf1} is a primary target of compound **2.72**. Increased concentrations of compound **2.72** did not increase the levels of p21^{waf1} further, but decreased the levels of c-FLIP (Figure 2.3.17 D). Ursolic acid **2.1** has been shown to decrease the levels of c-FLIP as a mechanism to potentiate TRAIL-induced apoptosis in the HCT116 human colon adenocarcinoma cell line.²⁰⁸ These data suggest that the downregulation of c-FLIP may lead to apoptotic effects. We observed evident apoptotic induction ability at 8 μ M, which was not only correlated with the downregulation of c-FLIP, but also correlated with the upregulation of NOXA. NOXA is a BH3 protein that blocks the anti-apoptotic protein Mcl-1. Unlike other triterpenoid derivatives, compound **2.72** did not decrease the levels of Mcl-1, suggesting a different mechanism of action for this new compound.²⁸⁰ The upregulation of p21^{waf1} and NOXA and the downregulation of c-FLIP after treatment with compound **2.72** were also observed in MIA Paca 2 and PANC-1 cells (Figure 2.3.18). This data suggest that the p21^{waf1}, NOXA and c-FLIP proteins are targets of these new fluorolactone derivatives.

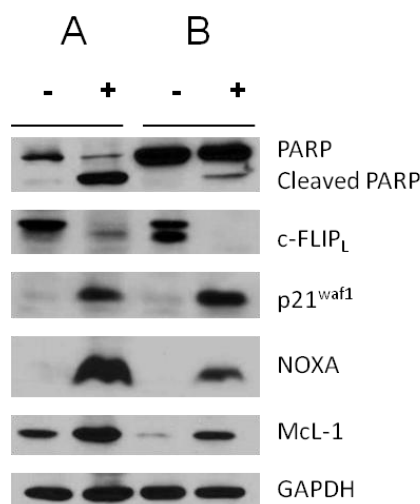


Figure 2.3.18. Relative levels of apoptosis- and cycle-related proteins in (A) MIA PaCa 2 and (B) PANC-1 cells. Cells were treated with compound **2.72** at 8 μ M for 24 h. Relative protein levels were assessed by Western blot analysis. GAPDH was used as a loading control.

2.3.3. Conclusions

In conclusion, a new procedure for the preparation of fluorolactones and fluorine acyl derivatives of ursolic acid was achieved via the preparation of a novel panel of fluorine derivatives, compounds **2.59-2.82**. Some of these compounds exhibited a better antiproliferative activity against AsPC-1 cells compared with ursolic acid **2.1**.

Compound **2.72** was the most active in inhibiting cancer cell growth, with IC_{50} values lower than 1 μ M. This compound arrested the cell cycle in the G1 phase and induced apoptosis with upregulation of NOXA and p21^{waf1} and downregulation of c-FLIP. The mechanisms underlying the increase of NOXA and p21^{waf1} levels and the decrease of c-FLIP levels are worthy of further investigation.

These results show that ursolic acid fluorolactone derivatives, such as compound **2.72**, are good starting points for drug discovery in cancer.

2.4. Experimental section

2.4.1. Chemical

IR spectra were recorded in JASCO FT/IR-420. ^1H , ^{13}C , DEPT-135, HMQC, HMBC, COESY and NOESY spectra were recorded in a Bruker Avance III 400 MHz spectrometer. The chemical shifts were recorded in δ (ppm) using the δ 7.26 of CHCl_3 (^1H NMR) and the δ 77.00 (^{13}C NMR) as internal standards. Chemical shifts measures were given in ppm and coupling constants (J) in hertz (Hz). Low resolution mass spectrometry was obtained in a Finnigan Polaris QGC/MS Benchtop Ion Trap spectrometer with a direct insertion probe and the elemental analysis was obtained in an Analyzer Elemental Carlo Erba 1108 by chromatographic combustion. Melting points were determined using a BUCHI melting point B-540 apparatus and were uncorrected. For thin layer chromatography (TLC) analysis Kiesel gel 60HF254/kiesel gel 60G was used and FCC was performed using Kieselgel 60 (230-400 mesh, Merck). Ursolic acid **2.1**, CDI, CBMI, CDT, Selectfluor, Deoxofluor, DMAP, fluoroacetic anhydride, benzoic anhydride, butyric anhydride, acetic anhydride, phthalic anhydride, ethyl formate, 2,3-dichloro-5,6-dicyanobenzoquinone (DDQ), sodium methoxide (NaOMe), lithium iodide, THF, dioxane, nitromethane, dimethylformamide (DMF) and benzene were purchased from Sigma Aldrich Co. The solvents used in the workups were purchase from VWR Portugal, and were of analytical grade. Potassium bicarbonate, sodium chloride, sodium bicarbonate, sodium sulfite, potassium permanganate, and hidroxyamine chlorhydrate were purchased from Merck Co. All the solvents used in the reactions were previously purified and dried according to the literature procedures.

3 β -Trifluoroacetoxy-urs-12-en-28-oic acid (2.2): To a stirred mixture of **2.1** (50 mg 0.11 mmol) in THF (1 mL) at room temperature, was added DMAP (10% of the mass of **2.1**) and trifluoroacetic anhydride (0.15 mL 1.1 mmol). After 30 minutes the reaction mixture was acidified with HCl 10% (40 mL) and the aqueous phase extracted with ether (3 \times 25 mL). The organic phase was washed with NaHCO_3 (3 \times 25 mL) and water (3 \times 25 mL), dried over Na_2SO_4 , filtered and evaporated to the dryness, to afford a solid (98%). mp 176.1-177.8 °C. IR (film CHCl_3): 2975.6, 2940.9, 2878.2, 1778.1, 1690.3, 1462.7, 1412.6,

1386.6, 1371.1, 1357.6, 1316.2, 1280.5, 1256.4, 1224.6 cm^{-1} . ^1H NMR (400 MHz CDCl_3): δ 5.22 (1H t $J=6.84$), 4.68 (1H dd $J=15.98$), 1.08 (3H s), 0.98 (3H s), 0.94 (3H d $J=6.23$), 0.90 (3H s), 0.85 (3H d $J=6.45$), 0.77 (3H s). ^{13}C NMR (100 MHz CDCl_3): δ 184.23, 157.36 ($J=41.80$), 137.98, 125.50, 114.66 ($J=286.19$), 86.22, 55.14, 52.42, 47.95, 47.42, 41.87, 39.45, 38.98, 38.79, 38.05, 37.93, 36.86, 36.66, 32.72, 30.55, 27.94, 27.86, 23.96, 23.59, 23.24, 23.11, 21.15, 18.05, 17.03, 16.97, 16.41, 15.48. EI-MS m/z : 550.56 (1) M^+ , 247.53 (26), 202.56 (55), 188.65 (20), 132.83 (100), 118.82 (26), 106.76 (14), 104.78 (23), 94.74 (11), 92.69 (13), 90.73 (20), 78.62 (11). Anal. Calcd for $\text{C}_{32}\text{H}_{47}\text{F}_3\text{O}_4$ C 69.54, H 8.57, found C 69.92, H 8.52.

3-Oxours-12-en-28-oic acid (2.3): **2.3** was prepared according to the literature,²⁴¹ from **2.1** (100 mg 0.218 mmol) to give a solid (99%). mp 281.5-286.8 °C. IR (film CHCl_3): 2972.7, 2929.3, 2872.4, 1690.3, 1457.9, 1385.6, 1316.2, 1276.7, 1255.4, 1235.2, 1214.0 cm^{-1} . ^1H NMR (400 MHz CDCl_3): δ 5.26 (1H t), 1.08 (3H s), 1.08 (3H s), 1.05 (3H s), 1.02 (3H s), 0.95 (3H s), 0.87 (3H s), 0.82 (3H s). ^{13}C NMR (100 MHz CDCl_3): δ 217.89 (C3), 183.92 (C28), 137.98 (C13), 125.53 (C12). EI-MS m/z : 455.3 (2) M^+ , 249.3 (20), 248.3 (100), 219.4 (22), 205.5 (20), 204.5 (22), 203.5 (55), 134.3 (22), 133.3 (44). Anal. Calcd for $\text{C}_{30}\text{H}_{46}\text{O}_3$ C 79.25, H 10.20, found C 78.98, H 10.34.

3 β -Acetoxy-urs-12-en-28-oic acid (2.4): Preparation of **2.4** was made according to previously described method from **2.1** (100 mg 0.218 mmol),¹⁸³ providing a solid (92%): mp 287.4-290.8 °C. IR (film CHCl_3): 2926.5, 1735.6, 1691.3, 1460.8 cm^{-1} . ^1H NMR (400 MHz CDCl_3): δ 5.21 (1H t $J=6.54$), 4.47 (1H dd $J=15.99$), 2.16 (1H d $J=11.51$), 2.02 (3H s), 1.05 (3H s), 0.94 (3H s), 0.84 (6H s), 0.83 (3H s), 0.74 (3H s). ^{13}C NMR (100 MHz CDCl_3): δ 183.84 (C28), 171.03 (OCOCH_3), 137.92 (C13), 125.71 (C12), 80.92 (C3). EI-MS m/z : 497.82 (1) M^+ , 437.89 (23), 93.76 (37), 91.78 (50), 89.79 (100), 81.87 (22), 79.88 (83), 77.9 (73), 75.89 (34), 67.87 (23), 65.86 (62). Anal. Calcd for $\text{C}_{32}\text{H}_{50}\text{O}_4$: C 77.06, H 10.10, found C 77.46, H 10.05.

3 β -Phthaloxy-urs-12-en-28-oic-acid (2.5): To a stirred mixture of **2.1** (200 mg 0.44 mmol) in pyridine (5 mL) at 115°C, was added DMAP (53.77 mg 1 mmol) and phthalic anhydride (651.73 mg 0.25 mmol). After 23.5 hours the reaction mixture was diluted with

ice (50 mL) and the aqueous phase extracted with chloroform (3×40 mL). The organic phase was washed with water (3×40 mL), dried over Na₂SO₄, filtered and evaporated to the dryness, to afford a solid (90%). mp 198.3-205.1 °C. IR (film CHCl₃): 3064.3, 2926.5, 1716.3, 1691.3, 1457.0 cm⁻¹. ¹H NMR (400 MHz CDCl₃): δ 7.89 (1H d *J*=6.92), 7.72 (1H d *J*=6.85), 7.59 (2H m *J*=26.69), 5.24 (1H s H12), 4.75 (1H dd *J*=14.88 H3), 1.09 (3H s), 0.94 (6H s), 0.93 (3H s), 0.88 (3H s), 0.85 (3H s), 0.78 (3H s). ¹³C NMR (100 MHz CDCl₃): δ 183.93 (C28), 171.62 (OCOC), 167.93 (COOH), 137.95 (C13), 131.59, 131.53, 131.02, 130.65, 129.61, 128.83, 125.68 (C12), 82.902 (C3). EI-MS *m/z*: 604.97 (1) M⁺, 247.72 (52), 202.77 (50), 188.87 (20), 148.90 (27), 133.19 (100), 118.96 (24), 105.10 (30), 90.94 (23). Anal. Calcd for C₃₈H₅₂O₆·H₂O: C 73.28, H 8.74, found C 73.68, H 8.52.

Methyl 3β-hydroxy-urs-12-en-28-oate (2.6): **2.6** was prepared according to the literature^{429, 434} from **2.1** (45.6 mg 0.1 mmol) to give a solid (93%). mp 170.7-172.0 °C. IR (film CHCl₃): 3434.6, 2926.5, 1718.3, 1645.9, 1457.0 cm⁻¹. ¹H NMR (400 MHz CDCl₃): δ 5.23 (1H t *J*=7.32 H12), 3.59 (3H s COOCH₃), 3.20 (1H dd *J*=15.83 H3), 1.07 (3H s), 0.98 (3H s), 0.93 (3H s), 0.91 (3H s), 0.85 (3H d *J*=6.48), 0.77 (3H s), 0.73 (3H s). ¹³C NMR (100 MHz CDCl₃): δ 178.05 (C28), 138.12 (C13), 125.55 (C12), 79.03 (C3). EI-MS *m/z*: 471.04 (7) M⁺, 261.99 (53), 207.08 (21), 203.07 (89), 202.15 (20), 189.19 (28), 134.11 (38), 133.21 (100), 119.13 (26), 91.22 (21). Anal. Calcd for C₃₁H₅₀O₃·0.25 hexane: C 79.30, H 10.95, found C 79.68, H 11.31.

3β-Trifluoroacetoxy-11-oxours-12-en-28-oic acid (2.7): To a stirred solution of **2.2** (1.3 g 2.35 mmol) in dichloromethane (25 mL) at room temperature was added a mixture of KMnO₄ (4.7 g) and Fe₂(SO₄)₃·nH₂O (2.35 g), previous reduced to fine powder, water (0.235 mL) and *t*-butanol (1.1 mL). After 27 hours the reaction mixture was diluted with ether (60 mL) and mixed for 30 minutes. The resulting mixture was filtered through a celite plate, which is washed with ether (200 ml). The resulting organic phase was washed with NaHCO₃ (2×75 mL) and water (2×75 mL), dried over Na₂SO₄, filtered and evaporated to the dryness, to afford a slight yellow powder (82%). mp 270.0-271.9 °C. IR (film CHCl₃): 2875.3, 1780.0, 1691.3, 1657.5, 1460.8, 1384.6, 1217.8, 1167.7 cm⁻¹. ¹H NMR (400 MHz CDCl₃): δ 5.60 (1H s H12), 4.68 (1H d *J*=11.38), 2.87 (1H d *J*=13.61),

2.38 (1H d $J=11.51$), 2.31 (1H s), 1.29 (3H s), 1.15 (3H s), 0.97 (3H s), 0.96 (3H s), 0.90 (12H s). ^{13}C NMR (100 MHz CDCl_3): δ 199.71, 183.05, 163.10, 157.56 ($J=7.02$), 130.63, 114.63 ($J=285.80$), 85.86, 61.16, 54.86, 52.42, 47.47, 44.64, 43.66, 38.53, 38.23, 38.21, 38.07, 36.94, 35.96, 32.75, 31.10, 30.18, 28.33, 27.86, 23.52, 23.07, 21.05, 20.90, 19.08, 17.13, 16.99, 16.35, 16.30. EI-MS m/z : 567.18 (18) M^+ , 303.04 (24), 262 (26), 257.07 (32), 234.04 (40), 189.02 (63), 175.08 (27), 161.06 (69), 159.09 (24), 133.07 (27), 119.06 (100), 107.06 (29), 105.05 (49), 95.05 (29), 93.03 (29), 91.04 (64), 79.01 (41), 76.99 (29), 66.98 (32).

3,11-Dioxours-12-en-28-oic acid (2.8): **2.8** was prepared according to the same method as for **2.7**, starting with **2.3** (100 mg 0.22 mmol). After 23.5 hours the workup is executed to afford a white powder (71%). mp 285.8-300.4 °C. IR (film CHCl_3): 2945.7, 2873.4, 1700.9, 1691.3, 1661.4, 1460.8, 1385.6, 1312.3, 1276.7, 1255.4, 1231.3, 1212.0 cm^{-1} . ^1H NMR (400 MHz CDCl_3): δ 5.62 (1H s), 1.30 (3H s), 1.24 (3H s), 1.08 (3H s), 1.02 (3H s), 0.97 (3H d $J=6.14$), 0.94 (3H s), 0.86 (3H d $J=6.25$). ^{13}C NMR (100 MHz CDCl_3): δ 217.11 (C3), 199.26 (C11), 182.65 (C28), 163.12 (C13), 130.66 (C12), 60.67, 55.31, 52.49, 47.66, 47.48, 44.50, 43.79, 39.70, 38.55, 38.52, 36.72, 35.97, 34.14, 32.34, 30.21, 28.42, 26.44, 23.59, 21.32, 20.99, 20.91, 18.92, 18.65, 16.99, 15.57. EI-MS m/z : 469.13 (14) M^+ , 303.04 (49), 262.08 (37), 257.13 (66), 134.04 (56), 190.09 (31), 189.06 (84), 175.14 (33), 161.13 (100), 119.19 (79), 105.14 (43), 95.19 (34), 91.04 (45), 79.11 (40), 67.07 (34), 55.04 (32).

3 β -Acetoxy-11-oxours-12-en-28-oic acid (2.9): Compound **2.9** was prepared using the same method as for the preparation of **2.7**, starting with **2.4** (1.3 g 2.61 mmol). After 25 hours the workup is executed to afford a white powder (83%). mp 315.7-318.1 °C. IR (film CHCl_3): 2941.9, 2873.4, 1725.0, 1690.3, 1661.4, 1459.9, 1367.3, 1318.1, 1252.5, 1214.0, 1167.7, 1141.7 cm^{-1} . EI-MS m/z : 513.30 (15) M^+ , 303.1 (73), 262.09 (63), 257.17 (68), 134.19 (80), 189.27 (100), 175.3 (63), 174.33 (63), 162.29 (46), 161.28 (99), 120.08 (47), 119.21 (87), 105.28 (53), 91.17 (45), 79.27 (45).

Methyl 3-oxours-12-en-28-oate (2.10): **2.10** was prepared according to the literature,²⁴¹ from **2.6** (2.69 g 5.7 mmol) to give a solid (93%). mp 196.3-197.2 °C. IR

(film CHCl₃): 2946.7, 2872.5, 1725.0, 1704.8, 1456.0, 1384.6, 1309.4, 1271.8, 1230.4, 1198.5, 1143.6, 1111.8 cm⁻¹. ¹H NMR (400 MHz CDCl₃): δ 5.26 (1H s), 3.61 (3H s), 1.08 (6H s), 1.04 (6H s), 0.94 (3H d *J*=5.73), 0.86 (3H d *J*=6.33), 0.79 (3H s). ¹³C NMR (100 MHz CDCl₃): δ 217.70 (C3), 177.99 (C28), 138.29 (C13), 125.33 (C12). EI-MS *m/z*: 470.48 (27) M⁺, 469.47 (94), 264.09 (51), 262.48 (100), 248.92 (16), 205.74 (18), 204.63 (19), 203.81 (25), 203.2 (16), 202.52 (26), 201.52 (23), 200.44 (18), 189.08 (16), 134.34 (25), 133.12 (64), 131.3 (16).

Methyl 3,11-dioxours-12-en-28-oate (2.11): **2.11** was prepared using the same method as for the preparation of **2.7**, starting with **2.10** (100 mg 0.22 mmol). After 23 hours the workup is executed to afford a white powder (97%). mp 128.5-130.7 °C. IR (film CHCl₃): 2948.6, 2872.5, 1725.0, 1704.8, 1660.4, 1457.0, 1386.6, 1273.8 cm⁻¹. ¹H NMR (400 MHz CDCl₃): δ 5.63 (1H s), 3.60 (3H s), 1.29 (3H s), 1.24 (3H s), 1.08 (3H s), 1.04 (3H s), 0.96 (3H d *J*=6.53), 0.93 (3H s), 0.86 (3H d *J*=5.82). ¹³C NMR (100 MHz CDCl₃): δ 217.12 (C3), 199.06 (C11), 177.13 (C28), 163.26 (C13), 130.55 (C12). EI-MS *m/z*: 483.38 (28) M⁺, 482.35 (28), 467.36 (37), 454.38 (27), 317.32 (99), 276.37 (34), 258.45 (31), 257.4 (100), 248.49 (60), 233.5 (38), 190.47 (34), 189.42 (78), 162.45 (41), 161.36 (58), 119.33 (46).

Methyl 2-hydroxymethylene-3,11-dioxours-12-en-28-oate (2.12): Preparation of **2.12** was made according to previously described method^{330, 431} from **2.11** (947.7 mg 1.96 mmol) to give a solid (98%). mp 134.7-138.1 °C. IR (film CHCl₃): 3436.5, 2949.6, 2870.5, 1726.0, 1656.6, 1588.1, 1457.0, 1387.5, 1320.0, 1272.8 cm⁻¹. ¹H NMR (400 MHz CDCl₃): δ 14.86 (1H s), 8.62 (1H s), 5.67 (1H s), 3.62 (3H s), 3.45 (1H d *J*=14.76), 2.45 (1H d *J*=11.19), 1.31 (3H s), 1.19 (3H s), 1.13 (3H s), 1.11 (3H s), 0.97 (6H d *J*=8.98), 0.88 (3H d *J*=6.40). ¹³C NMR (100 MHz CDCl₃): δ 199.20 (C3), 189.57 (C11), 188.82 (C2CH), 177.15 (C28), 163.48 (C13), 130.68 (C12), 105.79 (C2). EI-MS *m/z*: 510.28 (11) M⁺, 495.32 (18), 317.15 (52), 258.17 (20), 257.14 (100), 189.16 (22), 187.19 (22), 175.18 (16), 173.19 (18), 161.18 (96), 135.2 (25), 119.2 (25), 105.18 (18), 91.15 (21). Anal. Calcd for C₃₂H₄₆O₅·0.5H₂O C 73.95, H 9.12, found C 74.1, H 9.52.

Methyl 2-hydroxymethylene-3-oxours-12-en-28-oate (2.13): **2.13** was prepared using the same method as for the preparation of **2.12**, starting with **2.10** (100 mg 2.2mmol). After 1 hours the workup is executed to afford a solid (97%). mp 127.9-131.7 °C. IR (film CHCl₃): 3441.3, 2924.5, 2872.5, 1725.0, 1634.4, 1586.2, 1456.0, 1377.9, 1307.5, 1271.8, 1229.4, 1200.5, 1143.6 cm⁻¹. ¹H NMR (400 MHz CDCl₃): δ 14.90 (1H s), 8.57 (1H s), 5.30 (1H s), 3.61 (3H s), 1.19 (3H s), 1.11 (3H s), 1.09 (3H s), 0.94 (3H d *J*=5.98), 0.91 (3H s), 0.87 (3H d *J*=6.39), 0.81 (3H s). ¹³C NMR (100 MHz CDCl₃): δ 190.84 (C3), 188.17 (C2 \underline{C} H), 178.00 (C28), 138.23 (C13), 125.35 (C12), 105.79 (C2). EI-MS *m/z*: 497.40 (30) M⁺, 263.63 (40), 262.47 (99), 233.44 (52), 204.71 (31), 203.41 (95), 189.41 (45), 187.33 (25), 134.35 (48), 133.23 (100), 119.23 (27). Anal. Calcd for C₃₂H₄₈O₄·0.25H₂O C 76.68, H 9.75, found C 76.63, H 10.20

3β-Hydroxy-11-oxours-12-en-28-oic acid (2.14): **2.14** was prepared according to the literature,³⁶⁷ from **2.9** (1.12 g 2.01 mmol) to give a solid (79%). mp 236.7-238.6 °C. IR (film CHCl₃): 3421.1, 2930.3, 2866.7, 1687.4, 1655.6, 1457.0, 1386.6, 1038.5 cm⁻¹. EI-MS *m/z*: 471.30 (10) M⁺, 303.09 (48), 262.06 (48), 257.10 (66), 234.09 (54), 189.09 (81), 175.14 (67), 161.13 (100), 119.15 (91), 107.13 (42), 105.14 (56), 91.13 (61), 79.09 (44).

Methyl 3-hydroxy-11-oxours-12-en-28-oate (2.15): **2.15** was prepared using the same method as for the preparation of **2.6**, starting with **2.14** (794.1mg 1.7mmol). After 3 hours the workup is executed to afford a solid (98%). mp 128.2-130.2 °C. IR (film CHCl₃): 3482.8, 2947.7, 2870.5, 1725.0, 1654.6, 1457.0, 1386.6, 1386.6, 1201.4 cm⁻¹. ¹H NMR (400 MHz CDCl₃): δ 5.59 (1H s), 3.59 (3H s), 3.21 (1H dd *J*=16.35), 2.77 (1H dt *J*=20.56), 1.28 (3H s), 1.10 (3H s), 0.97 (3H s), 0.95 (3H d *J*=6.28), 0.89 (3H s), 0.85 (3H d *J*=6.47), 0.78 (3H s). ¹³C NMR (100 MHz CDCl₃): δ 199.92 (C11), 177.19 (C28), 162.89 (C13), 130.61 (C12), 78.78 (C3). EI-MS *m/z*: 484.51 (36) M⁺, 174.43 (26), 160.46 (55), 134.54 (35), 132.56 (36), 120.58 (31), 118.6 (100), 106.58 (38), 104.59 (51), 94.55 (39), 92.53 (29), 90.54 (46), 78.47 (26).

2-Hydroxymethylene-3-oxours-12-en-28-oic acid (2.16): **2.16** was prepared using the same method as for the preparation of **2.12**, starting with **2.3** (500mg 1.1mmol). After

72 hours the workup is executed to afford a solid (96%): mp 148.0-150.4 °C. IR (film CHCl₃): 3440.4, 2925.5, 2872.5, 1694.2, 1640.2, 1580.4, 1456.0, 1379.8, 1314.3, 1234.2 cm⁻¹. ¹H NMR (400 MHz CDCl₃): δ 14.89 (1H s), 8.58 (1H s), 5.29 (1H s), 1.18 (3H s), 1.09 (3H s), 1.08 (3H s), 0.95 (3H d *J*=5.93), 0.91 (3H), 0.86 (3H t *J*=12.40), 0.82 (3H s). ¹³C NMR (100 MHz CDCl₃): δ 190.60 (C3), 188.43 (C2CH), 184.01 (C28), 137.94 (C13), 125.56 (C12), 105.72 (C2). EI-MS *m/z*: 482.57 (7) M⁺, 202.50 (25), 172.57 (12), 146.63 (13), 144.66 (13), 133.72 (12), 132.72 (100), 130.76 (13), 120.70 (13), 118.75 (29), 116.72 (11), 106.69 (17), 104.71 (28), 94.65 (14), 92.62 (28). Anal. Calcd for C₃₁H₄₆O₄·0.25 H₂O C 76.42, H 9.62, found C 76.18, H 10.02.

Isoxazolo[4,5-b]urs-12-en-28-oic acid (2.17): Preparation of **2.17** was made according to previously described method,²⁹⁵ from **2.16** (250 mg 0.52 mmol) to give a solid (98%): mp 172.8-175.0 °C IR (film CHCl₃): 2970.8, 2925.5, 2870.5, 1694.2, 1456.8, 1382.7, 1275.7 cm⁻¹. ¹H NMR (400 MHz CDCl₃): δ 7.98 (1H s), 5.30 (1H s), 1.30 (3H s), 1.18 (3H s), 1.10 (3H s), 0.95 (3H s), 0.87 (3H d *J*=6.11), 0.85 (3H s), 0.83 (3H s). ¹³C NMR (100 MHz CDCl₃): δ 183.92 (C28), 173.03, 150.16 (C2CH), 137.96 (C13), 125.49 (C12), 108.84, 53.49, 52.60, 48.03, 46.05, 42.08, 39.53, 39.07, 38.79, 38.63, 36.65, 35.58, 34.69, 32.19, 30.59, 28.83, 28.01, 24.04, 23.46, 23.27, 21.32, 21.12, 18.78, 16.95, 16.76, 15.43. EI-MS *m/z*: 479.75 (7) M⁺, 202.52 (40), 132.82 (100), 118.77 (24), 106.74 (25), 94.70 (11), 90.69 (27).

3β-(1H-Imidazol-1-carboxyloxy)-urs-12-en-28-oic (2.18) and **28-(1H-imidazol-1-yl)-28-oxours-12-en-3β-yl-1H-imidazole-1-carboxylate (2.19)**: To a stirred solution of **2.1** (300 mg 0.66 mmol) in THF (4 mL), under N₂ atmosphere, at 70 °C, was added CDI (321.1 mg 1.98 mmol). After 5 hours the reaction mixture was diluted with water (60 mL), the aqueous phase was extracted with ethyl acetate (3×50 mL). The resulting organic phases were washed with NaCl 10% (3×50 mL), dried over Na₂SO₄, filtered and evaporated to the dryness, to afford a yellow residue. The residue was subjected to flash column chromatography [hexanes-ethyl acetate from (65:35) to (55:45)], to afford **2.18** (7%) and **2.19** (76%). **2.18**: mp 295.8-297.4 °C IR (film CHCl₃): 3133.8, 2926.5, 2875.3, 1803.1, 1758.8, 1467.6, 1388.5, 1318.1, 1287.3, 1239.0. ¹H NMR (400 MHz CDCl₃): δ 8.14 (1H s), 7.42 (1H s), 7.08 (1H s), 5.32 (1H s), 4.71 (1H dd *J*=16.19), 1.25 (3H s), 1.11

(3H s), 0.98 (9H s), 0.88 (3H d $J=5.97$), 0.85 (3H s). EI-MS m/z : 550.97 (2) M^+ , 202.93 (55.86), 189.96 (53.8), 188.96 (100), 186.98 (54.53), 132.91 (54.26). **2.19**: mp 228.7-231.3 °C. IR (film $CHCl_3$): 3128.0, 2927.4, 2872.5, 1756.8, 1719.2, 1468.5, 1388.5, 1318.1, 1287.3 cm^{-1} . 1H NMR (400 MHz $CDCl_3$): δ 8.23 (1H s), 8.12 (1H s), 7.52 (1H s), 7.39 (1H s), 7.05 (1H s), 7.03 (1H s), 5.23 (1H s), 4.67 (1H dd $J=16.12$), 1.10 (3H s), 0.99 (3H d $J=6.17$), 0.95 (3H s), 0.94 (6H s), 0.91 (3H d $J=6.31$), 0.68 (3H s). ^{13}C NMR (100 MHz $CDCl_3$): δ 174.65, 148.48, 137.02, 137.00, 136.94, 130.48, 129.55, 126.33, 117.44, 116.98, 86.17, 55.19, 54.11, 50.88, 47.33, 42.07, 39.40, 39.21, 38.65, 38.01, 36.75, 35.53, 32.63, 30.34, 28.13, 27.70, 24.97, 23.56, 23.37, 23.26, 20.99, 19.38, 17.99, 17.06, 16.83, 16.70, 15.45. EI-MS m/z : 600.93 (14) M^+ , 203.03 (68), 201.99 (40), 189.04 (59), 1887.05 (55), 147.05 (56), 145.06 (48), 133.03 (81), 131.03 (45), 121.03 (46), 119.04 (85), 109.06 (43), 107.02 (77), 105.02 (100). Anal. Calcd for $C_{37}H_{52}N_4O_3$ C 73.96, H 8.72, N 9.32, found C 74.25, H 9.03, N 9.27.

3 β -Trifluoroacetoxy-urs-12-en-28-yl-1H-imidazole-1-carboxylate (2.20): 2.20 was prepared using the same method as for **2.18**, using **2.2** (300 mg 0.54 mmol) as a starting material and CDI (175.12 mg 1.08 mmol). The workup was performed after 7 hours. The solid was subjected to flash column chromatography [hexanes-ethyl acetate from (75:25) to (65:35)], to afford **2.20** (84%). mp 187.9-192.9 °C. IR (film $CHCl_3$): 3128.0, 2951.5, 2875.3, 1778.1, 1720.2, 1466.6, 1382.7, 1279.5, 1222.7, 1165.8 cm^{-1} . 1H NMR (400 MHz $CDCl_3$): δ 8.24 (1H s), 7.52 (1H s), 7.04 (1H s), 5.23 (1H s H12), 4.67 (1H dd $J=15.50$ H3), 2.45 (1H d $J=11.03$ H18), 1.51 (1H s H5), 1.10 (3H s C27), 1.00 (3H d $J=6.15$ C30), 0.94 (3H s C25), 0.91 (3H d $J=6.54$ C29), 0.89 (6H s C23 and C24), 0.82 (1H d $J=11.24$ H5), 0.68 (3H s C26). ^{13}C NMR (100 MHz $CDCl_3$): δ 174.70 (C28), 157.34 ($OCOCF_3$ $J=41.77$), 137.05 (Cimidazole), 137.01 (C13), 129.63 (Cimidazole), 126.30 (C12), 117.45 (Cimidazole), 114.62 (CF_3 $J=286.24$), 86.14 (C3), 55.12 (C5), 54.10 (C18), 50.87 (C17), 47.33 (C9), 42.06 (C14), 39.39 (C8), 39.22 (C19), 38.66 (C20), 38.05 (C1), 37.88 (C4), 36.75 (C10), 35.54, 32.62 (C7), 30.35 (C21), 27.83 (C23 or C24), 27.70 (C15), 24.97, 23.56 (C27), 23.25, 23.05, 21.02 (C30), 17.97, 17.08 (C29), 16.70 (C26), 16.41 (C23 or C24), 15.47 (C25). EI-MS m/z : 602.94 (8) M^+ , 302.95 (99), 203.03 (84), 189.04 (60), 175.07 (59), 133.09 (62), 119.10 (61), 107.09 (63), 105.11 (65),

95.14 (63), 91.15 (67), 79.09 (55), 69.04 (100). Anal. Calcd for C₃₅H₄₉F₃N₂O₃ C 69.74, H 8.19, N 4.65, found C 69.91, H 8.52, N 4.58.

3-Oxours-12-en-28-yl-1H-imidazole-1-carboxylate (2.21): **2.21** was prepared using the same method as for **2.18**, using **2.3** (300 mg 0.6 mmol) as a starting material and CDI (194.58 mg 1.2 mmol). The workup was performed after 18.5 hours. The solid was subjected to flash column chromatography [hexanes-ethyl acetate from (70:30) to (60:40)], to afford **2.21** (84%). mp 141.0-147.3 °C. IR (film CHCl₃): 3128.0, 2927.4, 1703.8, 1459.0, 1381.8, 1362.5, 1277.6, 1225.5, 1204.3 cm⁻¹. ¹H NMR (400 MHz CDCl₃): δ 8.46 (1H s), 7.56 (1H s), 7.11 (1H s), 5.25 (1H t *J*=7.32 Hz), 1.10 (3H s C27), 1.06 (3H s C23 or C24), 1.03 (3H s C23 or C24), 1.02 (3H s C25), 1.00 (3H d *J*=6.32 Hz C30), 0.91 (3H d *J*=6.46 Hz C29), 0.72 (3H s C26). ¹³C NMR (100 MHz CDCl₃): δ 217.61 (C3), 174.26 (C28), 136.88 (C13), 136.69 (Cimidazole), 127.97 (Cimidazole), 126.55 (C12), 117.79 (Cimidazole), 55.23 (C5), 54.22 (C18), 51.16 (C17), 47.38 (C4), 46.62 (C9), 42.20 (C14), 39.38 (C8), 39.26, 39.22 (C19), 38.62 (C20), 36.60 (C10), 35.48, 34.11, 32.29 (C7), 30.30 (C21), 27.72 (C15), 26.41 (C23 or C24), 24.95, 23.50 (C27), 23.41, 21.45, 20.97, 19.33, 17.04 (C29), 16.73 (C26), 15.17 (C25). EI-MS *m/z*: 504.99 (11) M⁺, 205 (44), 201.01 (77), 175.06 (40), 133.04 (54), 119.04 (48), 107.03 (52), 105.04 (51), 95.04 (51), 91.03 (51), 79 (43), 68.97 (100). Anal. Calcd for C₃₃H₄₈N₂O₂ C 78.53, H 9.59, N 5.55, found C 78.93, H 9.89, N 5.67.

3β-Acetoxy-urs-12-en-28-yl-1H-imidazole-1-carboxylate (2.22): **2.22** was prepared using the same method as for **2.18**, using **2.4** (300 mg 0.60 mmol) as a starting material and CDI (194.58 mg 1.2 mmol). The workup was performed after 10 hours. The solid was subjected to flash column chromatography [hexanes-ethyl acetate from (75:25) to (70:30)], to afford **2.22** (88%). mp 204.0-207.5 °C. IR (film CHCl₃): 3151.1, 2927.4, 2873.4, 1725.0, 1466.6, 1368.3, 1275.7, 1246.8, 1205.3, 1101.2 cm⁻¹. ¹H NMR (400 MHz CDCl₃): δ 8.22 (1H s), 7.51 (1H s), 7.01 (1H s), 5.20 (1H s), 4.46 (1H t *J*=15.70), 2.43 (1H d *J*=11.03), 2.02 (3H s), 1.07 (3H s), 0.98 (3H d *J*=6.17), 0.90 (6H s), 0.82 (3H s), 0.81 (3H s), 0.65 (3H s). ¹³C NMR (100 MHz CDCl₃): δ 174.67, 170.88, 137.02, 136.92, 129.57, 126.48, 117.41, 80.74, 55.22, 54.10, 50.86, 47.33, 42.03, 39.39, 39.19, 38.64, 38.23, 37.57, 36.75, 35.54, 32.68, 30.33, 27.97, 27.68, 24.98, 23.52, 23.44, 23.24, 21.22,

20.98, 18.01, 17.06, 16.69, 16.63, 15.44. EI-MS m/z : 548.91 (14) M^+ , 248.95 (30), 203.01 (45), 189.06 (55), 187.09 (22), 147.1 (23), 133.11 (36), 119.12 (32), 107.12 (34), 105.15 (34), 95.16 (29), 91.15 (33), 79.14 (32), 69.15 (100). Anal. Calcd for $C_{35}H_{52}N_2O_3$ C 76.60, H 9.55, N 5.10, found C 76.38, H 9.74, N 5.09.

Methyl 3 β -(1H-imidazole-1-carboxyloxy)-urs-12-en-28-oate (2.23): **2.23** was prepared using the same method as for **2.18**, using **2.6** (300 mg 0.64 mmol) as a starting material and CDI (207.552 mg 1.28 mmol). The workup was performed after 4 hours. The solid was subjected to flash column chromatography [hexanes-ethyl acetate from (75:25) to (70:30)], to afford **2.23** (90%). mp 119.0-125.1 °C. IR (film $CHCl_3$): 3133.8, 2947.7, 2872.5, 1757.8, 1724.1, 1469.5, 1388.5, 1319.1, 1288.2, 1240.0, 1199.5 cm^{-1} . 1H NMR (400 MHz $CDCl_3$): δ 8.13 (1H s), 7.41 (1H s), 7.07 (1H s), 5.25 (1H s), 4.70 (1H dd $J=16.32$), 3.61 (3H s), 2.24 (1H d $J=11.24$), 1.09 (3H s), 0.99 (3H s), 0.97 (3H s), 0.97 (3H s), 0.94 (3H d $J=5.77$), 0.86 (3H d $J=6.39$), 0.76 (3H s). ^{13}C NMR (100 MHz $CDCl_3$): δ 178.01, 148.48, 138.26, 136.96, 130.42, 125.27, 117.05, 86.39, 55.25, 52.84, 51.44, 48.06, 47.47, 42.00, 39.49, 39.03, 38.85, 38.13, 38.08, 36.84, 36.60, 32.82, 30.62, 28.20, 28.00, 24.18, 23.58, 23.45, 23.29, 21.16, 18.16, 17.04, 16.89 (2C), 15.46. EI-MS m/z : 564.92 (3) M^+ , 261.99 (40), 202.97 (80), 189.03 (32), 133.01 (100), 119.02 (30), 107.02 (15), 105.02 (23), 94.99 (21), 90.99 (24), 78.96 (19), 68.93 (75), 66.95 (14). Anal. Calcd for $C_{35}H_{52}N_2O_4$ C 74.43, H 9.28, N 4.96, found C 74.06, H 9.60, N 4.86.

28-(1H-Imidazol-1-yl)-11,28-dioxours-12-en-3 β -yl-1H-imidazole-1-carboxylate (2.24): **2.24** was prepared using the same method as for **2.18**, using **2.14** (290 mg 0.62 mmol) as a starting material and CDI (301.60 mg 1.86 mmol). The workup was performed after 8 hours. The workup was performed after 4 hours. The solid was subjected to flash column chromatography [hexanes-ethyl acetate from (60:40) to (35:65)], to afford **2.24** (44%). mp 167.5-173.1 °C. IR (film $CHCl_3$): 3135.7, 2971.8, 2872.5, 1754.9, 1718.3, 1656.6, 1469.5, 1388.5, 1322.0, 1286.3, 1241.0, 1209.2 cm^{-1} . 1H NMR (400 MHz $CDCl_3$): δ 8.25 (1H s), 8.10 (1H s), 7.52 (1H s), 7.39 (1H s), 7.05 (2H s), 5.66 (1H s H12), 4.68 (1H dd $J=14.76$ H3), 2.88 (1H d $J=13.33$ H1), 2.61 (1H t $J=9.88$ H18), 2.31 (1H s H9) 1.32 (3H s C27), 1.16 (3H s C25), 1.01 (3H d $J=5.79$ C30), 0.94 (9H s C23 or C24 and C29), 0.86 (3H s C26), 0.83 (1H s H5). ^{13}C NMR (100 MHz

CDCl₃): δ 198.84 (C11), 173.77 (C28), 161.19 (C13), 148.47 (OCO), 136.95 (Cimidazole), 136.89 (Cimidazole), 131.19 (C12), 130.48 (Cimidazole), 130.11 (Cimidazole), 117.25 (Cimidazole), 116.98 (Cimidazole), 85.91 (C3), 61.17 (C9), 54.99 (C5), 54.01 (C18), 50.61 (C17), 44.59 (C8), 43.75 (C14), 38.72 (C20), 38.60 (C1), 38.33 (2C C4 and C29), 36.90 (C10), 34.82, 32.77 (C7), 30.08 (C21), 28.21 (C15), 28.11 (C23 or C24), 24.47, 23.38, 20.88 (C27), 20.78 (C30), 18.46 (C26), 17.17 (2C C29), 16.79 (C23 or C24), 16.30 (C25). EI-MS *m/z*: 615.00 (2) M⁺, 217.06 (38.), 189.06 (80), 175.12 (29), 147.11 (45), 119.13 (28), 107.1 (21), 105.09 (27), 95.08 (28), 91.11 (35), 79.07 (20), 69.02 (100). Anal. Calcd for C₃₇H₅₀N₄O₄·0.5hexane·0.5EtOAc C 71.86, H 8.76, N 7.98 found C 71.72, H 9.16, N 8.1.

3 β -Trifluoroacetoxy-11-oxours-12-en-28-yl-1*H*-imidazol-1-carboxylate (2.25):

2.25 was prepared using the same method as for **2.18**, using **2.7** (300 mg 0.53 mmol) as a starting material and CDI (171.88 mg 1.06 mmol). The workup was performed after 2 hours. The solid was subjected to flash column chromatography [hexanes-ethyl acetate from (70:30) to (60:40)], to afford **2.25** (57%). mp 129.6-134.5 °C. IR (film CHCl₃): 3138.6, 2928.4, 2874.4, 1777.1, 1719.2, 1657.5, 1466.6, 1384.6, 1365.4, 1380.5, 1259.3, 1213.0, 1167.7, 1139.7 cm⁻¹. ¹H NMR (400 MHz CDCl₃): δ 8.26 (1H s), 7.53 (1H s), 7.06 (1H s), 5.66 (1H s H12), 4.68 (1H dd *J*=16.08 H3), 2.87 (1H d *J*=13.68 H1), 2.61 (1H d *J*=11.10 H18), 2.30 (1H s H9), 1.32 (3H s C27), 1.15 (3H s C25), 1.01 (3H d *J*=6.09 C30), 0.93 (3H d *J*=6.22 C29), 0.90 (3H s C23 or C24), 0.88 (3H s C23 or C24), 0.86 (3H s C26), 0.77 (1H d *J*=11.51 H5). ¹³C NMR (100 MHz CDCl₃): δ 198.91 (C11), 173.79 (C28), 161.29 (C13), 157.31 (OCOCF₃ *J*=41.52), 136.88 (Cimidazole), 131.17 (C12), 130.11 (Cimidazole), 117.26 (Cimidazole), 114.60 (CF₃ *J*=286.29), 85.85 (C3), 61.15 (C9), 54.88 (C9), 53.99 (C18), 50.59 (C17), 44.59 (C8), 43.74 (C14), 38.72 (C19), 38.54 (C1), 38.34 (C20), 38.18 (C4), 36.88 (C10), 34.82, 32.74 (C7), 30.08 (C21), 28.19 (C15), 27.82 (C23 or C24), 24.46, 23.04, 20.87 (C30), 20.82 (C27), 18.43 (C26), 17.20 (C29), 17.13, 16.37 (C23 or C24), 16.35 (C25). EI-MS *m/z*: 616.94 (6) M⁺, 199.00 (25), 188.97 (100), 175.03 (24), 147.03 (52), 119.04 (28), 105.03 (25), 95.03 (29), 91.02 (24), 68.96 (34).

3,11-Dioxours-12-en-28-yl-1H-imidazole-1-carboxylate (2.26): **2.26** was prepared using the same method as for **2.18**, using **2.8** (300 mg 0.64 mmol) as a starting material and CDI (207.55 mg 1.28 mmol). The workup was performed after 4.5 hours. The solid was subjected to flash column chromatography [hexanes-ethyl acetate from (65:35) to (50:50)], to afford **2.26** (52%). mp 211.9-218.8 °C. IR (film CHCl₃): 3133.8, 2927.4, 2871.5, 1703.8, 1658.5, 1460.8, 1386.6, 1364.4, 1278.6, 1224.6, 1208.2 cm⁻¹. ¹H NMR (400 MHz CDCl₃): δ 8.27 (1H s Himidazole), 7.53 (1H s Himidazole), 7.06 (1H s Himidazole), 5.68 (1H s H12), 1.32 (3H s C27), 1.24 (3H s C25), 1.06 (3H s C23 or C24), 1.02 (6H d *J*=7.81 C23 or C24 or C30), 0.93 (3H d *J*=6.20 C29), 0.89 (3H s C26). ¹³C NMR (100 MHz CDCl₃): δ 216.91 (C3), 198.55 (C11), 173.82 (C28), 161.40 (C13), 136.89 (Cimidazole), 131.21 (C12), 130.14 (Cimidazole), 117.28 (Cimidazole), 60.68 (C9), 55.44 (C5), 54.06 (C18), 50.65 (C17), 47.69 (C4), 44.47 (C8), 43.86 (C14), 39.76 (C1), 38.78 (C20), 38.37 (C21), 36.73 (C10), 34.86, 34.14, 32.33 (C7), 30.11, 28.29 (C15), 26.34 (C23 or C24), 24.50, 21.36 (C23 or C24 or C30), 20.87 (C23 or C24 or C30), 20.80 (C27), 18.61, 18.36 (C26), 17.18 (C29), 15.57 (C25). EI-MS *m/z*: 519.00 (5) M⁺, 216.98 (29), 188.98 (100), 147.03 (62), 133.05 (22), 119.03 (33), 107.03 (23), 105.02 (32), 95.02 (43), 91.01 (37), 81.01 (30), 79.00 (25), 68.96 (55), 66.97 (33), 54.95 (26). Anal. Calcd for C₃₃H₄₆N₂O₃·0.5EtOAc C 74.70, H 8.95, N 4.98, found C 74.76, H 9.35, N 4.84.

3β-Acetoxy-11-oxours-12-en-28-yl-1H-imidazole-1-carboxylate (2.27): **2.27** was prepared using the same method as for **2.18**, using **2.9** (290 mg 0.57 mmol) as a starting material and CDI (184.85 mg 1.14 mmol). The workup was performed after 2.5 hours. The solid was subjected to flash column chromatography [hexanes-ethyl acetate from (65:35) to (55:45)], to afford **2.27** (56%). mp 145.7-152.4 °C. IR (film CHCl₃): 3139.5, 2969.8, 1872.5, 1721.2, 1656.6, 1465.6, 1365.4, 1245.8, 1208.2 cm⁻¹. ¹H NMR (400 MHz CDCl₃): δ 8.28 (1H s Himidazole), 7.52 (1H s Himidazole), 7.05 (1H s Himidazole), 5.64 (1H s H12), 4.48 (1H dd *J*=15.98 H3), 2.77 (1H d *J*=13.55), 2.60 (1H d *J*=11.11), 2.02 (3H s OCOCH₃), 1.30 (3H s), 1.12 (3H s), 1.01 (3H d *J*=6.17), 0.92 (3H d *J*=6.24), 0.84 (9H s). ¹³C NMR (100 MHz CDCl₃): δ 199.15, 173.78, 170.94, 161.02, 136.87, 131.24, 130.04, 117.27, 80.48, 61.28, 55.00, 53.99, 50.60, 44.61, 43.71, 38.78, 38.69, 38.34, 37.94, 36.94, 34.84, 32.83, 30.08, 28.17, 27.98, 24.47, 23.47, 21.24, 20.84, 20.80, 18.44,

17.19 (2C), 16.62, 16.33. EI-MS m/z : 563.00 (14) M^+ , 217.02 (73), 189.04 (100), 175.05 (78), 161.05 (33), 147.06 (74), 133.07 (34), 119.07 (52), 107.06 (33), 105.06 (53), 95.06 (54), 91.06 (49), 79.03 (32), 68.99 (78). Anal. Calcd for $C_{35}H_{50}N_2O_4$ C 74.70, H 8.95, N 4.98, found C 74.30, H 9.35, N 4.58.

Methyl 3 β -(1H-imidazole-1-carboxyloxy)-11-oxours-12-en-28-oate (2.28): 2.28 was prepared using the same method as for **2.18**, using **2.15** (270 mg 0.56 mmol) as a starting material and CDI (181.6 mg 1.12 mmol). The workup was performed after 6 hours. The solid was subjected to flash column chromatography [hexanes-ethyl acetate from (70:30) to (60:40)], to afford **2.28** (62%). mp 158.0-164.0 °C. IR (film $CHCl_3$): 3133.8, 2949.6, 2872.5, 1757.8, 1726.9, 1660.4, 1457.0, 1387.5, 1321.0, 1287.3, 1240.0 cm^{-1} . 1H NMR (400 MHz $CDCl_3$): δ 8.14 (1H s), 7.41 (1H s), 7.07 (1H s), 5.61 (1H s), 4.70 (1H dd $J=16.47$), 3.60 (3H s), 2.89 (1H d $J=13.70$), 2.42 (1H d $J=11.23$), 1.30 (3H s), 1.17 (3H s), 0.97 (9H s), 0.92 (3H s), 0.87 (3H d $J=6.41$). ^{13}C NMR (100 MHz $CDCl_3$): δ 199.42, 177.14, 163.10, 148.41, 136.91, 130.54, 130.26, 117.06, 86.12, 61.20, 54.98, 52.69, 51.84, 47.62, 44.60, 43.72, 38.57 (3C), 38.36, 36.91, 35.91, 32.83, 30.25, 28.35, 28.18, 23.87, 23.42, 21.04, 20.95, 18.81, 17.27, 17.08, 16.86, 16.20. EI-MS m/z : 578.95 (11) M^+ , 2447.99 (49), 188.98 (78), 174.04 (38), 161.06 (46), 119.08 (100), 107.08 (44), 105.09 (51), 95.08 (38), 93.07 (31), 91.09 (58), 79.06 (41), 69.02 (97). Anal. Calcd for $C_{35}H_{50}N_2O_5$ C 72.63, H 8.71, N 4.84 found C 72.3, H 9.1, N 7.05.

Methyl 2-(1H-imidazol-1-yl)-methylene-3,11-dioxours-12-en-28-oate (2.29): 2.29 was prepared using the same method as for **2.18**, using **2.12** (300 mg 0.59 mmol) as a starting material and CDI (191.34 mg 1.18 mmol). The workup was performed after 5.5 hours. The solid was subjected to flash column chromatography [hexanes-ethyl acetate from (65:35) to (50:50)], to afford **2.29** (56%). mp 137.3-141.0 °C. IR (film $CHCl_3$): 3116.4, 2949.6, 1866.7, 1725.0, 1686.4, 1652.7, 1613.2, 1517.7, 1486.9, 1383.7, 1302.7, 1272.8, 1212.0 cm^{-1} . 1H NMR (400 MHz $CDCl_3$): δ 7.84 (1H s), 7.65 (1H s), 7.35 (1H s), 7.14 (1H s), 5.68 (1H s), 4.16 (1H d $J=16.47$), 3.61 (3H s), 2.46 (2H s), 2.25 (1H d $J=16.45$), 1.33 (3H s), 1.18 (3H s), 1.12 (6H s), 0.97 (3H d $J=6.23$), 0.94 (3H s), 0.90 (3H d $J=6.33$). ^{13}C NMR (100 MHz $CDCl_3$): δ 206.25, 198.67, 177.11, 164.05, 138.85, 130.51, 130.26, 130.11, 122.70, 119.21, 58.91, 52.85, 52.79, 51.86, 47.63, 45.28, 44.15,

43.85, 43.17, 38.72, 38.58, 35.97, 35.88, 31.59, 30.24, 29.71, 28.45, 23.81, 22.34, 20.97, 20.93, 19.45, 18.19, 17.17, 15.44. EI-MS m/z : 561.20 (24) M^+ , 229.01 (30), 216.99 (32), 215.98 (100), 201.08 (48), 188.10 (42), 174.13 (42), 105.14 (21), 91.17 (27), 69.13 (36). Anal. Calcd for $C_{35}H_{48}N_2O_4 \cdot 0.25H_2O$ C 74.37, H 8.65, N 4.96, found C 74.29, H 9.05, N 4.83.

Methyl 2-(1*H*-imidazol-1-yl)-methylene-3-oxours-12-en-28-oate (2.30): **2.30** was prepared using the same method as for **2.18**, using **2.13** (300 mg 0.60 mmol) as a starting material and CDI (194.58 mg 1.2 mmol). The workup was performed after 4 hours. The solid was subjected to flash column chromatography [hexanes-ethyl acetate from (80:20) to (60:40)], to afford **2.30** (63%). mp 134.0-137.5 °C. IR (film $CHCl_3$): 3116.4, 2948.6, 2872.5, 1774.2, 1722.1, 1685.5, 1607.3, 1519.6, 1457.0, 1380.8, 1306.5, 1225.5 cm^{-1} . 1H NMR (400 MHz $CDCl_3$): δ 7.81 (1H s), 7.70 (1H s), 7.23 (1H s), 7.16 (1H s), 5.30 (1H s), 3.60 (3H s), 2.89 (1H d $J=15.97$), 1.17 (3H s), 1.12 (6H s), 0.95 (3H d $J=5.90$), 0.89 (6H s), 0.80 (3H s). ^{13}C NMR (100 MHz $CDCl_3$): δ 206.58, 177.93, 138.46 (2C), 130.70, 130.41, 124.94, 123.08, 119.41, 53.03, 52.62, 51.45, 48.16, 45.31, 45.18, 43.14, 42.23, 39.36, 39.15, 38.84, 36.55, 36.01, 31.98, 30.65, 29.76, 27.96, 24.18, 23.59, 23.41, 22.42, 21.11, 20.25, 17.07, 16.57, 15.59. EI-MS m/z : 546.13 (35) M^+ , 285.07 (48), 202.97 (56), 187.04 (22), 133.02 (100), 119.03 (33), 105.02 (29), 91.00 (31), 78.97 (21), 68.94 (36). Anal. Calcd for $C_{35}H_{50}N_2O_3 \cdot 0.5H_2O \cdot 0.5EtOAc$ C 74.09, H 9.24, N 4.67, found C 74.36, H 9.54, N 4.63.

28-(1*H*-Imidazol-1-yl)-3,28-dioxours-12-en-2-(1*H*-imidazol-1-yl)-methylene (2.31): **2.31** was prepared using the same method as for **2.18**, using **2.16** (323 mg 0.67 mmol) as a starting material and CDI (326 mg 2.06 mmol). The workup was performed after 5 hours. The solid was subjected to flash column chromatography [hexanes-ethyl acetate from (45:55) to (20:80)], to afford **2.31** (46%). mp 281.7-285.0 °C. IR (film $CHCl_3$): 3116.4, 2967.0, 2924.5, 2870.5, 1719.2, 1685.5, 1606.4, 1486.9, 1381.8, 1303.6, 1224.6 cm^{-1} . 1H NMR (400 MHz $CDCl_3$): δ 8.22 (1H s), 7.78 (1H s), 7.68 (1H s), 7.51 (1H s), 7.21 (1H s), 7.14 (3H s), 7.02 (1H s), 5.27 (1H s), 2.86 (1H d $J=15.90$), 2.48 (1H d $J=11.04$), 1.13 (6H s), 1.09 (3H s), 0.99 (3H d $J=5.78$), 0.95 (3H d $J=5.85$), 0.86 (3H s), 0.71 (3H s). ^{13}C NMR (100 MHz $CDCl_3$): δ 206.40, 174.59, 138.37, 137.15, 136.95,

130.76, 130.42, 129.61, 125.94, 122.67, 119.36, 117.37, 54.21, 52.42, 50.89, 45.09, 45.05, 43.06, 42.25, 39.26, 39.20, 38.57, 35.87, 35.42, 31.73, 30.32, 29.67, 27.61, 24.88, 23.51, 23.35, 22.33, 20.94, 20.03, 17.08, 16.36, 15.55. EI-MS m/z : 582.97 (7) M^+ , 488.19 (35), 487.18 (100), 486.13 (27), 297.10 (31), 145.10 (30), 133.09 (39), 131.11 (32), 119.10 (46), 117.11 (32), 107.11 (41), 105.11 (56), 95.11 (33), 91.14 (64), 79.10 (48), 69.08 (73). Anal. Calcd for $C_{37}H_{50}N_4O_2 \cdot 0.5EtOAc$ C 74.72, H 8.68, N 8.94, found C 74.93, H 9.08, N 9.16.

3 β -(2'-Methyl-1*H*-imidazol-1-carboxyloxy)-urs-12-en-28-oic (2.32): To a stirred solution of **2.1** (300 mg 0.66 mmol) in THF (4 mL), under N_2 atmosphere, at 70 °C, was added CBMI (376.6 mg 1.98 mmol). After 26 hours the reaction mixture was diluted with water (60 mL), the aqueous phase was extracted with ethyl acetate (3×50 mL). The resulting organic phases were washed with NaCl 10% (3×50 mL), dried over Na_2SO_4 , filtered and evaporated to the dryness, to afford a yellow residue. The residue was subjected to flash column chromatography [hexanes-ethyl acetate from (60:40) to (25:75)], to afford **2.32** (18%). mp 287.5-291.6 °C IR (film $CHCl_3$): 3162.7, 3122.2, 2928.4, 2872.5, 1803.1, 1753.0, 1550.5, 1510.0, 1457.0, 1395.3, 1373.1, 1321.0, 1294.0, 1214.0. 1H NMR (400 MHz $CDCl_3$): δ 7.34 (1H s), 6.86 (1H s), 5.32 (1H s), 4.67 (1H dd $J=15.97$), 2.65 (3H s), 2.21 (1H d $J=11.08$), 1.11 (3H s), 0.98 (6H s), 0.97 (6H s), 0.88 (3H d $J=5.98$), 0.85 (3H s). EI-MS m/z : 564.87 (1) M^+ , 393.08 (45), 202.98 (63), 189.94 (61), 188.97 (100), 187.04 (77), 175.03 (44), 159.01 (57), 133 (70), 118.97 (61), 105 (50), 94.96 (41).

28-(2'-Methyl-1*H*-imidazol-1-yl)-28-oxours-12-en-3 β -yl-2'-methyl-1*H*-imidazole-1-carboxylate (2.33): **2.33** was prepared using the same method as for **2.32**, using **2.1** (300 mg 0.66 mmol) as a starting material and CBMI (627.69 mg 3.3 mmol). The workup was performed after 24 hours. The solid was subjected to flash column chromatography [hexanes-ethyl acetate from (55:45) to (30:70)], to afford **2.33** (84%). mp 253.4-256.5 °C. IR (film $CHCl_3$): 3162.7, 3119.3, 2928.4, 2872.5, 1753.0, 1719.2, 1509.0, 1457.0, 1391.4, 1294.0, 1246.8 cm^{-1} . 1H NMR (400 MHz $CDCl_3$): δ 7.54 (1H s), 7.33 (1H d $J=0.92$), 6.87 (1H s), 6.85 (1H s), 5.24 (1H s), 4.66 (1H dd $J=16.27$), 2.64 (3H s), 2.56 (3H s), 1.12 (3H s), 1.00 (3H d $J=6.28$), 0.96 (6H s), 0.95 (3H s), 0.92 (3H d

$J=6.33$), 0.74 (3H s). ^{13}C NMR (100 MHz CDCl_3): δ 176.63, 149.45, 149.39, 147.85, 137.22, 127.75, 127.27, 126.24, 118.0, 117.36, 85.87, 55.26, 54.05, 51.83, 47.39, 42.23, 39.56, 39.51, 38.65, 38.21, 37.98, 36.82, 35.54, 32.65, 30.45, 28.19, 27.78, 24.87, 23.46 (2C), 23.28, 21.10, 18.06, 17.86, 17.26, 17.19, 17.04, 16.89, 15.51. EI-MS m/z : 628.91 (6) M^+ , 202.96 (13), 190.98 (10), 188.97 (13), 186.98 (11), 132.98 (11), 126.93 (18), 119.00 (15), 108.99 (12), 106.99 (12), 105.02 (15), 95.01 (15), 91.01 (14), 83.00 (100), 81.01 (17).

3 β -Trifluoroacetoxy-urs-12-en-28-yl-2'-methyl-1*H*-imidazole-1-carboxylate

(**2.34**): **2.34** was prepared using the same method as for **2.32**, using **2.2** (300 mg 0.54 mmol) as a starting material and CBMI (205.43 mg 1.08 mmol). The workup was performed after 53 hours. The solid was subjected to flash column chromatography [hexanes-ethyl acetate from (75:25) to (65:35)], to afford **2.34** (68%). mp 235.5-237.6 °C. IR (film CHCl_3): 3122.2, 2928.4, 2872.5, 1779.0, 1718.3, 1509.0, 1457.0, 1384.6, 1268.9, 1218.8, 1165.8 cm^{-1} . ^1H NMR (400 MHz CDCl_3): δ 7.53 (1H s), 6.86 (1H s), 5.23 (1H s), 4.67 (1H dd $J=15.29$), 2.55 (3H s), 1.10 (3H s), 0.99 (3H d $J=6.17$), 0.95 (3H s), 0.89 (9H s), 0.72 (3H s). ^{13}C NMR (100 MHz CDCl_3): δ 176.60, 157.34 ($J=41.54$), 149.37, 137.19, 127.28, 126.15, 117.35, 114.62 ($J=286.12$), 86.13, 55.10, 54.00, 51.77, 47.35, 42.18, 39.50, 39.47, 38.61, 38.06, 37.89, 36.75, 35.50, 32.59, 30.42, 27.84, 27.73, 24.81, 23.41, 23.23, 23.04, 21.09, 17.98, 17.90, 17.19, 17.16, 16.41, 15.49. EI-MS m/z : 616.88 (23) M^+ , 506.97 (42), 302.91 (100), 203.04 (55), 189.03 (57), 175.07 (57), 119.09 (44), 107.11 (44), 105.11 (44), 95.15 (57), 91.15 (45), 81.12 (40). Anal. Calcd for $\text{C}_{36}\text{H}_{51}\text{F}_3\text{N}_2\text{O}_3$ C 70.10, H 8.33, N 4.54, found C 69.91, H 8.73, N 4.64.

3-Oxours-12-en-28-yl-2'-methyl-1*H*-imidazole-1-carboxylate (**2.35**): **2.35** was prepared using the same method as for **2.32**, using **2.3** (300 mg 0.66 mmol) as a starting material and CBMI (251.1 mg 1.32 mmol). The workup was performed after 24 hours. The workup was performed after 53 hours. The solid was subjected to flash column chromatography [hexanes-ethyl acetate from (65:35) to (50:50)], to afford **2.35** (36%). mp 196.0-199.7 °C. IR (film CHCl_3): 3735.4, 2927.4, 2872.5, 1703.8, 1508.1, 1457.9, 1385.6, 1268.9, 1247.7 cm^{-1} . ^1H NMR (400 MHz CDCl_3): δ 7.53 (1H s Himidazole), 6.87 (1H s Himidazole), 5.24 (1H s H12), 2.56 (3H s CH_3 imidazole), 1.10 (3H s), 1.06 (3H s),

1.03 (3H s), 1.01 (3H s), 0.98 (3H d $J=6.25$), 0.90 (3H d $J=6.32$), 0.76 (3H s). ^{13}C NMR (100 MHz CDCl_3): δ 217.53, 176.55, 149.34, 137.20, 127.04, 126.25, 117.37, 55.24, 54.08, 51.86, 47.37, 46.66, 42.30, 39.50 (2C), 39.28, 38.61, 36.60, 35.48, 34.10, 32.27, 30.42, 27.74, 26.42, 24.83, 23.39, 23.36, 21.44, 21.06, 19.41, 17.76, 17.20, 17.13, 15.18. EI-MS m/z : 518.91 (13) M^+ , 408.98 (96), 244.96 (44), 204.95 (73), 203.00 (100), 89.02 (50), 175.06 (58), 121.07 (44), 119.07 (42), 107.08 (42), 105.10 (40), 95.11 (48). Anal. Calcd for $\text{C}_{34}\text{H}_{50}\text{N}_2\text{O}_2$ C 78.72, H 9.71, N 5.40, found C 78.96, H 9.91, N 5.56.

3 β -Acetoxy-urs-12-en-28-yl-2'-methyl-1H-imidazole-1-carboxylate (2.36): 2.36 was prepared using the same method as for **2.32**, using **2.4** (300 mg 0.60 mmol) as a starting material and CBMI (228.25 mg 1.2 mmol). The workup was performed after 88 hours. The solid was subjected to flash column chromatography [hexanes-ethyl acetate from (75:25) to (65:35)], to afford **2.36** (66%). mp 216.1-219.7 °C. IR (film CHCl_3): 3180.0, 3116.4, 2926.5, 2872.5, 1720.2, 1509.0, 1457.9, 1366.3, 1245.8 cm^{-1} . ^1H NMR (400 MHz CDCl_3): δ 7.53 (1H s), 6.86 (1H s), 5.22 (1H s), 4.47 (1H t $J=14.86$), 2.55 (3H s), 2.03 (3H s), 1.09 (3H s), 0.99 (3H d $J=6.00$), 0.92 (6H s), 0.84 (3H s), 0.83 (3H s), 0.71 (3H s). ^{13}C NMR (100 MHz CDCl_3): δ 176.65, 170.96, 149.35, 137.13, 127.24, 126.39, 117.35, 80.79, 55.25, 54.04, 51.83, 47.39, 42.19, 39.55, 39.49, 38.64, 38.29, 37.64, 36.80, 35.55, 32.70, 30.45, 28.01, 27.75, 24.88, 23.49, 23.41, 23.26. 21.27, 21.09, 18.06, 17.84, 17.25, 17.18, 16.67, 15.51. EI-MS m/z : 562.94 (20) M^+ , 248.94 (61), 203.06 (47), 191.08 (25), 189.07 (100), 187.13 (28), 119.14 (38), 107.14 (36), 105.16 (35), 95.19 (41), 91.18 (35), 81.15 (31), 79.14 (29). Anal. Calcd for $\text{C}_{36}\text{H}_{54}\text{N}_2\text{O}_3$ C 76.82, H 9.67, N 4.98, found C 77.04, H 9.34, N 5.03.

Methyl 3 β -(2'-methyl-1H-imidazole-1-carboxyloxy)-urs-12-en-28-oate (2.37): 2.37 was prepared using the same method as for **2.32**, using **2.6** (300 mg 0.64 mmol) as a starting material and CBMI (243.5 mg 1.28 mmol). The workup was performed after 78 hours. The solid was subjected to flash column chromatography [hexanes-ethyl acetate from (75:25) to (70:30)], to afford **2.37** (98%). mp 123.4-125.2 °C. IR (film CHCl_3): 3184.5, 3122.2, 2947.7, 2872.5, 1753.9, 1725.0, 1510.0, 1456.0, 1395.3, 1373.1, 1294.0, 1199.5 cm^{-1} . ^1H NMR (400 MHz CDCl_3): δ 7.34 (1H s), 6.85 (1H s), 5.25 (1H s), 4.67 (1H dd $J=16.32$), 3.60 (3H s), 2.65 (3H s), 1.09 (3H s), 0.98 (3H s), 0.97 (3H s), 0.96 (3H

s), 0.94 (3H d $J=5.88$), 0.86 (3H d $J=6.19$), 0.76 (3H s). ^{13}C NMR (100 MHz CDCl_3): δ 178.00, 149.41, 147.85, 138.24, 127.64, 125.28, 118.01, 86.02, 55.28, 52.84, 51.43, 48.05, 47.46, 41.99, 39.48, 39.03, 38.84, 38.18, 37.99, 36.85, 36.60, 32.82, 30.62, 28.22, 28.00, 24.18, 23.58, 23.51, 23.29, 21.16, 18.17, 17.06 (2C), 16.88 (2C), 15.45. EI-MS m/z : 578.96 (12) M^+ , 261.97 (32), 203 (67), 189.08 (32), 134.05 (21), 133.16 (100), 127.11 (20), 119.14 (29), 107.12 (17), 105.15 (21), 95.19 (22), 91.19 (26), 83.28 (86), 81.17 (23), 79.15 (19).

28-(2'-Methyl-1*H*-imidazol-1-yl)-11,28-dioxours-12-en-3 β -yl-2'-methyl-1*H* imidazole-1-carboxylate (2.38): **2.38** was prepared using the same method as for **2.32**, using **2.14** (280 mg 0.595 mmol) as a starting material and CBMI (339.50 mg 1.785 mmol). The workup was performed after 5.5 hours. The solid was subjected to flash column chromatography [hexanes-ethyl acetate from (55:45) to (25:75)], to afford **2.38** (27%). mp 237.2-240.5 °C. IR (film CHCl_3): 3166.5, 3122.2, 2971.8, 2872.5, 1753.0, 1717.3, 1659.5, 1549.5, 1511.0, 1457.0, 1391.4, 1324.9, 1294.0, 1248.7, 1215.9 cm^{-1} . ^1H NMR (400 MHz CDCl_3): δ 7.52 (1H s), 7.32 (1H s), 6.89 (1H s), 6.84 (1H s), 5.66 (1H s), 4.66 (1H dd $J=15.67$), 2.87 (1H d $J=13.45$), 2.63 (3H s), 2.53 (3H s), 1.33 (3H s), 1.17 (3H s), 1.01 (3H d $J=6.00$), 0.95 (6H s), 0.90 (3H s), 0.84 (3H d $J=7.31$). ^{13}C NMR (100 MHz CDCl_3): δ 198.97, 175.43, 161.41, 149.69, 149.38, 147.83, 131.14, 127.88, 127.64, 117.96, 116.94, 85.60, 61.16, 55.03, 54.21, 51.55, 44.65, 43.89, 38.94, 38.68, 38.35, 38.27, 36.93, 34.68, 32.77, 30.11, 28.25, 28.16, 24.14, 23.46, 20.85, 20.79, 18.87, 18.17, 17.29, 17.20, 17.00, 16.80, 16.33. EI-MS m/z : 643.21 (3) M^+ , 217.03 (27), 189.04 (100), 175.15 (22), 161.14 (22), 147.08 (50), 133.09 (22), 119.07 (30), 107.07 (22), 105.06 (35), 95.05 (31), 91.06 (37). Anal. Calcd for $\text{C}_{39}\text{H}_{54}\text{N}_4\text{O}_4 \cdot 0.5\text{hexane} \cdot 0.5\text{EtOAc}$ C 72.39, H 8.97, N 7.67, found C 72.17, H 9.37, N 7.91.

3 β -Trifluoroacetoxy-11-oxours-12-en-28-yl-2'-methyl-1*H*-imidazole-1-carboxylate (2.39): **2.39** was prepared using the same method as for **2.32**, using **2.7** (300 mg 0.53 mmol) as a starting material and CBMI (201.62 mg 1.06 mmol). The workup was performed after 7 hours. The solid was subjected to flash column chromatography [hexanes-ethyl acetate from (70:30) to (55:45)], to afford **2.39** (23%). mp 132.7-137.5 °C. IR (film CHCl_3): 3180.0, 3122.2, 2953.5, 2928.4, 2873.4, 1778.1, 1717.3, 1659.5, 1512.9,

1457.9, 1384.6, 1270.9, 1248.7, 1215.9, 1166.7 cm^{-1} . ^1H NMR (400 MHz CDCl_3): δ 7.52 (1H s), 6.90 (1H s), 5.66 (1H s), 4.68 (1H dd $J=16.10$), 2.87 (1H d $J=13.68$), 2.66 (1H d $J=11.14$), 2.53 (3H s), 1.32 (3H s), 1.15 (3H s), 1.01 (3H d $J=6.18$), 0.93 (3H d $J=6.51$), 0.90 (3H s), 0.89 (3H s), 0.89 (3H s). ^{13}C NMR (100 MHz CDCl_3): δ 199.01, 175.41, 161.51, 157.32 ($J=41.41$), 149.72, 131.10, 127.81, 116.98, 114.61 ($J=285.97$), 85.85, 61.13, 54.88, 54.19, 51.53, 44.63, 43.86, 38.92, 38.54, 38.33, 38.18, 36.87, 34.64, 32.73, 30.10, 28.22, 27.83, 24.09, 23.03, 20.88, 20.77, 18.83, 18.22, 17.30, 17.14, 16.38 (2C). EI-MS m/z : 630.94 (5) M^+ , 216.91 (27), 198.97 (21), 189.96 (16), 188.94 (100), 175.01 (17), 147.03 (39), 119.05 (18), 105.04 (17), 95.04 (22), 91.03 (17), 83.02 (24), 81.01 (20). Anal. Calcd for $\text{C}_{36}\text{H}_{49}\text{F}_3\text{N}_2\text{O}_4$ C 68.55, H 7.83, N 4.44, found C 68.16, H 7.62, N 4.26.

3,11-Dioxours-12-en-28-yl-2'-methyl-1H-imidazole-1-carboxylate (2.40): **2.40** was prepared using the same method as for **2.32** (300 mg 0.64 mmol), using **2.8** as a starting material and CBMI (243.47 mg 1.28 mmol). The workup was performed after 6 hours. The solid was subjected to flash column chromatography [hexanes-ethyl acetate from (65:35) to (50:50)], to afford **2.40** (34%). mp 279.4-285.3 $^\circ\text{C}$. IR (film CHCl_3): 3182.9, 3120.3, 2927.4, 1871.5, 1704.8, 1659.5, 1549.5, 1511.9, 1460.8, 1384.6, 1365.4, 1270.9, 1248.7, 1232.3, 1215.9 cm^{-1} . ^1H NMR (400 MHz CDCl_3): δ 7.53 (1H s), 6.91 (1H s), 5.69 (1H s), 2.55 (3H s), 1.33 (3H s), 1.25 (3H s), 1.07 (3H s), 1.03 (3H s), 1.01 (3H d $J=6.18$), 0.92 (6H s). ^{13}C NMR (100 MHz CDCl_3): δ 216.94, 198.65, 175.42, 161.60, 149.73, 131.14, 127.69, 116.99, 60.65, 55.43, 54.24, 51.60, 47.71, 44.52, 43.98, 39.75, 38.98, 38.35, 36.72, 34.67, 34.15, 32.32, 30.11, 28.32, 26.33, 24.13, 21.38, 20.87, 20.76, 18.76, 18.61, 18.13, 17.28, 15.61. EI-MS m/z : 532.95 (7) M^+ , 423.01 (12), 216.89 (18), 190.96 (16), 189.96 (16), 188.96 (100), 173.09 (12), 147.10 (38), 119.09 (14), 105.10 (12), 95.15 (23), 91.12 (13), 83.14 (24), 81.10 (14). Anal. Calcd for $\text{C}_{34}\text{H}_{48}\text{N}_2\text{O}_3$ C 76.65, H 9.08, N 5.26, found C 76.26, H 9.42, N 4.86.

3 β -Acetoxy-11-oxours-12-en-28-yl-2'-methyl-1H-imidazole-1-carboxylate (2.41): **2.41** was prepared using the same method as for **2.32**, using **2.9** (290 mg 0.57 mmol) as a starting material and CBMI (216.84 mg 1.14 mmol). The workup was performed after 7 hours. The solid was subjected to flash column chromatography [hexanes-ethyl acetate

from (60:40) to (50:50)], to afford **2.41** (39%). mp 170.0-171.0 °C. IR (film CHCl₃): 2950.6, 2872.5, 1722.1, 1656.6, 1458.9, 1365.4, 1247.7 cm⁻¹. ¹H NMR (400 MHz CDCl₃): δ 7.52 (1H s Himidazole), 6.89 (1H s Himidazole), 5.65 (1H s H12), 4.48 (1H dd *J*=15.82 H3), 2.77 (1H d *J*=13.47), 2.65 (1H d *J*=10.98), 2.53 (3H s), 2.03 (3H s), 1.31 (3H s), 1.13 (3H s), 1.00 (3H d *J*=6.19), 0.92 (3H d *J*=6.28), 0.88 (3H s), 0.84 (6H s). ¹³C NMR (100 MHz CDCl₃): δ 199.26, 175.43, 170.97, 161.22, 149.70, 131.19, 127.72, 116.99, 80.50, 61.28, 55.01, 54.18, 51.56, 44.68, 43.85, 38.91, 38.80, 38.34, 37.96, 36.95, 34.69, 32.84, 30.11, 28.21, 28.00, 24.13, 23.48, 21.26, 20.87, 20.74, 18.86, 18.15, 17.30, 17.19, 16.64, 16.36. EI-MS *m/z*: 577.02 (5) M⁺, 216.94 (31), 199.02 (12), 189.99 (17), 188.97 (100), 176.05 (11), 175.04 (40), 173.07 (11), 161.06 (10), 147.07 (34), 133.07 (10), 119.05 (13), 105.07 (12), 95.07 (17), 91.06 (10), 83.04 (20), 80.99 (14). Anal. Calcd for C₃₆H₅₂N₂O₄ C 74.96, H 9.09, N 4.86, found C 74.7, H 9.48, N 4.48.

Methyl 3β-(2'-methyl-1*H*-imidazole-1-carboxyloxy)-11-oxours-12-en-28-oate (2.42): **2.42** was prepared using the same method as for **2.32**, using **2.15** (270 mg 0.56 mmol) as a starting material and CBMI (213.03 mg 1.12 mmol). The workup was performed after 21 hours. The solid was subjected to flash column chromatography [hexanes-ethyl acetate from (70:30) to (60:40)], to afford **2.42** (66%). mp 243.1-247.0 °C. IR (film CHCl₃): 3168.5, 3122.2, 2949.6, 2872.5, 1753.0, 1727.9, 1660.4, 1457.0, 1396.2, 1324.9, 1294.0 cm⁻¹. ¹H NMR (400 MHz CDCl₃): δ 7.33 (1H d *J*=0.85), 6.85 (1H s), 5.61 (1H s H12), 4.67 (1H dd *J*=16.39 H3), 3.60 (3H s COOCH₃), 2.88 (1H dt *J*=13.68), 2.65 (3H s CH₃ imidazole), 2.42 (1H d *J*=11.21 H18), 1.30 (3H s C27), 1.17 (3H s C25), 0.97 (9H s C23, C24 and C30), 0.91 (3H s C26), 0.87 (3H d *J*=6.36 C29). ¹³C NMR (100 MHz CDCl₃): δ 199.44 (C11), 177.14 (C28), 163.09 (C13), 149.34 (OCO), 147.87 (C2'), 130.54 (C12), 127.48, 118.0, 85.76 (C3), 61.20 (C9), 55.01 (C5), 52.69 (C18), 51.83 (COOCH₃), 47.62 (C17), 44.60 (C8), 43.72 (C14), 38.64 (C1), 38.59 (C19 or C20), 38.56 (C19 or C20), 38.28 (C4), 36.93 (C10), 35.91, 32.83 (C7), 30.25, 28.35 (C15), 28.20 (C23 or C24 or C30), 23.87, 23.49, 21.04 (C27), 20.95 (C23 or C24 or C30), 18.81 (C26), 17.28, 17.08 (C23 or C24 or C30), 17.02 (C29), 16.80 (CH₃ imidazole), 16.19 (C25). EI-MS *m/z*: 593.04 (6) M⁺, 467.14 (100), 407.15 (44), 217.02 (44), 189 (61), 161.03 (51), 119.06 (61), 107.05 (42), 105.05 (43), 91.03 (41), 83.01 (53), 81.01 (43). Anal. Calcd for C₃₆H₅₂N₂O₅ C 72.94, H 8.84, N 4.73, found C 72.98, H 9.21, N 4.80.

Methyl 2-(2'-methyl-1*H*-imidazol-1-yl)-methylene-3,11-dioxours-12-en-28-oate (2.43): **2.43** was prepared using the same method as for **2.32**, using **2.12** (300 mg 0.59 mmol) as a starting material and CBMI (224.45 mg 1.18 mmol). The workup was performed after 5.5 hours. The solid was subjected to flash column chromatography [hexanes-ethyl acetate from (65:35) to (50:50)], to afford **2.43** (39%). mp 263.4-266.1 °C. IR (film CHCl₃): 3119.3, 2949.6, 2867.6, 1726.0, 1684.5, 1654.6, 1604.5, 1540.8, 1504.2, 1456.0, 1410.7, 1382.7, 1320.0, 1273.8, 1244.8 cm⁻¹. ¹H NMR (400 MHz CDCl₃): δ 7.62 (1H s C2CH), 7.32 (1H s H4'), 6.99 (1H s H5'), 5.67 (1H s H12), 4.14 (1H d *J*=16.36 H1), 3.61 (3H s COOMe), 2.49 (3H s CH₃ imidazole), 2.45 (2H H18 and H9), 2.18 (1H d *J*=16.46 H1), 1.33 (3H s C27), 1.18 (3H s C23 or C24), 1.13 (3H s C23 or C24), 1.12 (3H s C25), 0.97 (3H d *J*=6.28 C30), 0.94 (3H s C26), 0.89 (3H d *J*=6.22 C29). ¹³C NMR (100 MHz CDCl₃): δ 206.36 (C3), 198.71 (C11), 177.11 (C28), 163.99 (C13), 147.23 (C2'), 130.53 (C12), 129.69 (C2CH), 128.38 (C4'), 122.98 (C2), 118.24 (C5'), 58.90 (C9), 53.02 (C5), 52.80 (C18), 51.87 (COOMe), 47.64 (C17), 45.39 (C4), 44.19 (C8), 43.86 (C14), 42.51 (C1), 38.72 (C20), 38.59 (C19), 36.07 (C10), 35.90, 31.65 (C7), 30.25, 29.67 (C23 or C24), 28.47 (C15), 23.82, 22.47 (C23 or C24), 21.00 (C27), 20.94 (C30), 19.44, 18.26 (C26), 17.19 (C29), 15.39 (C25), 13.66 (CH₃ imidazole). EI-MS *m/z*: 575.20 (17) M⁺, 243.01 (44), 231.00 (23), 229.98 (100), 229.07 (19), 215.1 (54), 202.11 (36), 189.12 (18), 188.14 (50), 83.14 (25). Anal. Calcd for C₃₆H₅₀N₂O₄ C 75.22, H 8.77, N 4.87, found C 74.88, H 9.12, N 4.86.

Methyl 2-(2'-methyl-1*H*-imidazol-1-yl)-methylene-3-oxours-12-en-28-oate (2.44): **2.44** was prepared using the same method as for **2.32**, using **2.13** (300 mg 0.60 mmol) as a starting material and CBMI (228.25 mg 1.2 mmol). The workup was performed after 7 hours. The solid was subjected to flash column chromatography [hexanes-ethyl acetate from (75:25) to (60:40)], to afford **2.44** (55%). mp 229.5-231.7 °C. IR (film CHCl₃): 2948.6, 2872.5, 1724.1, 1685.5, 1603.5, 1540.9, 1500.4, 1456.0, 1411.6, 1274.7, 1242.9 cm⁻¹. ¹H NMR (400 MHz CDCl₃): δ 7.66 (1H s C2CH), 7.16 (1H s C5'), 7.01 (1H s C4'), 5.29 (1H s C12), 3.60 (3H s COOMe), 2.89 (1H d *J*=15.84 C1), 2.47 (3H s CH₃ imidazole), 2.26 (1H d *J*=11.27 C18), 2.17 (1H d *J*= 15.49 C1), 1.16 (3H s C23 or C24), 1.14 (3H s C23 or C24), 1.12 (3H s C27), 0.95 (3H d *J*=5.85 C30), 0.89 (6H s C29 and C25), 0.79 (3H s C26). ¹³C NMR (100 MHz CDCl₃): δ 206.63 (C3), 177.92

(C28), 147.31 (C2'), 138.45 (C13), 130.38 (C2CH), 128.57 (C4' imidazole), 124.98 (C12), 123.60 (C2), 118.19 (C5' imidazole), 53.01 (C18), 52.78 (C5), 51.45 (COOMe), 48.14 (C17), 45.31 (C4), 45.28 (C9), 42.37 (C1), 42.21 (C14), 39.38 (C8), 39.12 (C20), 38.83 (C19), 36.55, 36.12 (C10), 32.01 (C7), 30.63 (C21), 29.67 (C23 or C24), 27.97 (C15), 24.17, 23.54, 23.43 (C27), 22.57 (C23 or C24), 21.11 (C30), 20.23, 17.07 (C29), 16.62 (C26), 15.46 (C25), 13.68 (CH₃ imidazole). EI-MS m/z: 561.17 (12) M⁺, 300.07 (17), 299.06 (75), 297.08 (18), 243.06 (16), 203.03 (47), 134.01 (26), 133.15 (100), 131.1 (16), 119.07 (26), 117.09 (16), 107.05 (16), 105.09 (23), 91.13 (29), 83.18 (39), 79.08 (18).). Anal. Calcd for C₃₆H₅₂N₂O₃ C 77.10, H 9.35, N 5.00, found C 76.70, H 9.56, N 5.02.

28-(2'-Methyl-1*H*-imidazol-1-yl)-3,28-dioxours-12-en-2-(2'-methyl-1*H*-imidazol-1-yl)-methylene (2.45): **2.45** was prepared using the same method as for **2.32**, using **2.16** (300 mg 0.62 mmol) as a starting material and CBMI (353.79 mg 1.86 mmol). The workup was performed after 24.5 hours. The solid was subjected to flash column chromatography [hexanes-ethyl acetate from (40:60) to (10:90)], to afford **2.45** (36%). mp 283.3-286.1 °C. IR (film CHCl₃): 3116.4, 2952.5, 2870.5, 1717.3, 1684.5, 1603.5, 1540.9, 1411.6, 1383.7, 1247.7 cm⁻¹. ¹H NMR (400 MHz CDCl₃): δ 7.67 (1H s C2CH), 7.53 (1H s H4'' or H5''), 7.16 (1H s H5'), 7.00 (1H s H4'), 6.87 (1H s H4'' or H5''), 5.28 (1H s H12), 2.86 (1H d *J*=15.80 H1), 2.54 (4H s CH₃ C2'' and H18), 2.47 (3H s CH₃ C2'), 1.15 (6H s C27 or C23 or C24), 1.12 (3H s C23 or C24), 1.00 (3H d *J*=6.13 C30), 0.95 (3H d *J*=6.13 C29), 0.87 (3H s C25), 0.77 (3H s C26). ¹³C NMR (100 MHz CDCl₃): δ 206.50 (C3), 176.51 (C28), 149.35 (C2''), 147.39 (C2'), 137.37 (C13), 130.50 (C2CH), 128.68 (C4'), 127.37, 125.87 (C12), 123.07 (C2), 118.11 (C5'), 117.31, 54.16 (C18), 52.64 (C5), 51.84 (C17), 45.20 (C4), 45.15 (C9), 42.40 (C14), 42.36 (C1), 39.55 (C19), 39.39 (C8), 38.59 (C20), 36.03 (C10), 35.43 (C11), 31.78 (C7), 30.42 (C21), 29.66 (C3 or C24), 27.72 (C15), 24.75, 23.49, 23.28 (C27), 22.52 (C23 or C24), 21.07 (C30), 20.08 (C6), 17.93 (CH₃ C2''), 17.24 (C29), 16.90 (C26), 15.51 (C25), 13.75 (CH₃ C2'). EI-MS m/z: 611.12 (5) M⁺, 502.17 (38), 501.20 (100), 311.14 (14), 197.16 (25), 119.11 (10), 105.13 (11), 91.17 (12), 83.17 (14), 81.10 (9), 79.10 (8). Anal. Calcd for C₃₉H₅₄N₄O₂ C 76.68, H 8.91, N 9.17, found C 76.28, H 9.31, N 8.89.

28-(4H-Triazol-4-yl)-28-oxo-urs-12-en-3 β -yl-4H-triazole-4-carboxylate (2.46):

To a stirred solution of **2.1** (300 mg 0.66 mmol) in THF (4 mL), under N₂ atmosphere, at 70 °C, was added CDT (433.3 mg 2.64 mmol). After 6.5 hours the reaction mixture was diluted with water (60 mL), the aqueous phase was extracted with ethyl acetate (3×50 mL). The resulting organic phases were washed with NaCl 10% (3×50 mL), dried over Na₂SO₄, filtered and evaporated to the dryness, to afford a yellow residue. The residue was subjected to flash column chromatography [hexanes-ethyl acetate from (70:30) to (65:35)], to afford **2.46** (62%). mp 143.7-150.1 °C. IR (film CHCl₃): 3133.8, 2951.5, 2872.5, 1761.7, 1734.7, 1511.0, 1457.0, 1405.9, 1279.5, 1226.5 cm⁻¹. ¹H NMR (400 MHz CDCl₃): δ 8.82 (1H s C3'' or C5''), 8.77 (1H s C3' or C5'), 8.06 (1H s C3' or C5'), 7.99 (1H s C3'' or C5''), 5.24 (1H s H12), 4.79 (1H t $J=16.50$ H3), 1.11 (3H s C27), 0.99 (3H s C23 or C24), 0.97 (6H C30 and C23 or C24), 0.97 (3H s C25), 0.91 (3H d $J=6.35$ C29), 0.68 (3H s C26). ¹³C NMR (100 MHz CDCl₃): δ 174.82 (C28), 153.57 (C3' or C5'), 152.21 (C3'' or C5''), 147.28 (OCOC), 145.29 (2C), 137.60 (C13), 125.86 (C12), 87.69 (C3), 55.20 (C5), 51.26 (C17), 47.40 (C9), 42.14 (C14), 39.45 (2C C8), 39.09 (C19 or C20), 38.51 (C19 or C20), 38.17 (C4), 38.14, 36.78 (C10), 34.39, 32.67 (C7), 30.42, 28.13 (2C C23 or C24), 23.56 (2C C27), 23.40, 23.27, 21.05 (C30), 18.04, 17.03 (C29), 16.81 (C23 or C24), 16.71 (C26), 15.49 (C25). EI-MS m/z : 602.64 (1) M⁺, 505.07 (71), 392.15 (44), 202.02 (85), 190.00 (100), 189.04 (74), 145.10 (40), 132.05 (94), 119.09 (51), 117.13 (73), 91.16 (46), 70.04 (44).

3 β -Trifluoroacetoxy-urs-12-en-28-yl-4H-triazole-4-carboxylate (2.47): **2.47** was prepared using the same method as for **2.46**, using **2.2** (300 mg 0.54 mmol) as a starting material and CDT (265.89 mg 1.62 mmol). The workup was performed after 5 hours. The residue was subjected to flash column chromatography [hexanes-ethyl acetate from (85:15) to (80:20)], to afford **2.47** (34%). mp 189.6-191.0 °C. IR (film CHCl₃): 3142.4, 2953.5, 2927.4, 2878.2, 1780.0, 1734.7, 1511.9, 1457.0, 1347.0, 1275.9, 1219.8, 1166.7 cm⁻¹. ¹H NMR (400 MHz CDCl₃): δ 8.82 (1H s), 7.99 (1H s), 5.23 (1H s), 4.68 (1H dd $J=15.51$), 1.10 (3H s), 0.98 (3H d $J=6.26$), 0.94 (3H s), 0.91 (3H d $J=6.84$), 0.89 (6H s), 0.67 (3H s). ¹³C NMR (100 MHz CDCl₃): δ 174.82, 157.34 ($J=41.64$), 152.21, 145.29, 137.58, 125.85, 114.63 ($J=286.06$), 86.16, 55.12, 52.91, 51.25, 47.38, 42.13, 39.42, 39.08, 38.50, 38.06, 37.89, 36.76, 34.38, 32.65, 30.41, 28.12, 27.85, 23.55, 23.43, 23.25,

23.06, 21.05, 18.00, 17.02, 16.69, 16.42, 15.47. EI-MS m/z : 603.80 (1) M^+ , 505.97 (44), 201.88 (95), 200.96 (41), 189.98 (100), 188.96 (80), 145.03 (40), 133.01 (43), 131.96 (89), 131.10 (51), 119.05 (61), 117.03 (82), 105.06 (47), 91.00 (43). Anal. Calcd for $C_{34}H_{48}F_3N_3O_3$ C 67.64, H 8.01, N 6.96, found C 67.61, H 8.87, N 6.98.

3-Oxours-12-en-28-yl-4H-triazole-4-carboxylate (2.48): **2.48** was prepared using the same method as for **2.46**, using **2.3** (200 mg 0.44 mmol) as a starting material and CDT (216.65 mg 1.32 mmol). The workup was performed after 5 hours. The residue was subjected to flash column chromatography [hexanes-ethyl acetate from (75:25) to (70:30)], to afford **2.48** (98%). mp 129.4-133.9 °C. IR (film $CHCl_3$): 3133.8, 2925.5, 2870.5, 1733.7, 1703.8, 1510.0, 1457.0, 1384.6, 1348.0, 1275.7, 1181.1 cm^{-1} . 1H NMR (400 MHz $CDCl_3$): δ 8.82 (1H s Htriazole), 7.98 (1H s Htriazole), 5.24 (1H s H12), 1.10 (3H s), 1.06 (3H s), 1.02 (3H s), 1.01 (3H s), 0.97 (3H d $J=6.31$), 0.90 (3H d $J=6.37$), 0.71 (3H s). ^{13}C NMR (100 MHz $CDCl_3$): δ 217.58, 174.80, 152.20, 145.28, 137.60, 125.92, 55.24, 53.0, 51.30, 47.36, 46.69, 42.25, 39.41, 39.27, 39.10, 38.49, 36.60, 34.37, 34.11, 32.33, 30.42, 28.12, 26.44, 23.49, 23.44, 23.40, 21.44, 21.02, 19.44, 16.99, 16.69, 15.17. EI-MS m/z : 505.84 (1) M^+ , 409.02 (38), 408.01 (100), 202.98 (18), 201.94 (47), 201.01 (28), 190.00 (58), 189.02 (42), 145.09 (24), 133.04 (26), 132.03 (62), 131.05 (23), 119.08 (32), 117.10 (48), 105.10 (23), 91.12 (24). Anal. Calcd for $C_{32}H_{47}N_3O_2$ C 76.00, H 9.37, N 8.31, found C 75.66, H 9.45, N 8.70.

3 β -Acetoxy-urs-12-en-28-yl-4H-triazole-1-carboxylate (2.49): **2.49** was prepared using the same method as for **2.46**, using **2.4** (300 mg 0.60 mmol) as a starting material and CDT (295.43 mg 1.8 mmol). The workup was performed after 2 hours. The residue was subjected to flash column chromatography [hexanes-ethyl acetate from (85:15) to (80:20)], to afford **2.49** (94%). mp 124.0-128.8 °C. IR (film $CHCl_3$): 3139.5, 2950.6, 2924.5, 2872.5, 1732.7, 1511.9, 1456.0, 1348.0, 1275.7, 1246.7, 1183.1 cm^{-1} . 1H NMR (400 MHz $CDCl_3$): δ 8.81 (1H s), 7.98 (1H s), 5.23 (1H s), 4.48 (1H t $J=15.77$), 2.04 (3H s), 1.10 (3H s), 0.98 (3H d $J=6.29$), 0.92 (6H s), 0.85 (3H s), 0.84 (3H s), 0.66 (3H s). ^{13}C NMR (100 MHz $CDCl_3$): δ 174.87, 170.99, 152.20, 145.30, 137.54, 126.09, 80.84, 55.28, 52.96, 51.30, 47.43, 42.14, 39.47, 39.11, 38.54, 38.29, 37.66, 36.82, 34.44, 32.76, 30.45, 28.15, 28.03, 23.56, 23.51 (2C), 23.29, 21.29, 21.06, 18.09, 17.05, 16.74, 16.69, 15.51.

EI-MS m/z : 548.86 (1) M^+ , 452.08 (23), 202.96 (32), 201.92 (100), 201.03 (25), 190.04 (85), 189 (53), 188.05 (26), 145.02 (21), 133.05 (31), 131.93 (97), 119.02 (39), 117.04 (53), 104.98 (28), 91.00 (30), 78.96 (22). Anal. Calcd for $C_{34}H_{51}N_3O_3$ C 74.28, H 9.35, N 7.64, found C 74.56, H 9.21, N 8.00.

Methyl 3 β -(4*H*-triazole-1-carboxyloxy)-urs-12-en-28-oate (2.50): **2.50** was prepared using the same method as for **2.46**, using **2.6** (300 mg 0.64 mmol) as a starting material and CDT (315.13 mg 1.92 mmol). The workup was performed after 2.5 hours. The residue was subjected to flash column chromatography [hexanes-ethyl acetate from (85:15) to (80:20)], to afford **2.50** (93%). mp 121.6-126.8 °C. IR (film $CHCl_3$): 3133.8, 2947.7, 2872.5, 1762.6, 1723.1, 1510.0, 1456.0, 1405.9, 1280.5, 1226.5, 1200.5, 1169.6 cm^{-1} . 1H NMR (400 MHz $CDCl_3$): δ 8.78 (1H s), 8.06 (1H s), 5.25 (1H s), 4.80 (1H t $J=16.55$), 3.60 (3H s), 1.08 (3H s), 1.00 (3H s), 0.99 (6H s), 0.94 (3H d $J=5.77$), 0.86 (3H d $J=6.33$), 0.76 (3H s). ^{13}C NMR (100 MHz $CDCl_3$): δ 177.99, 153.57, 147.29, 145.30, 138.25, 125.23, 87.79, 55.23, 52.83, 51.43, 48.04, 47.47, 41.99, 39.47, 39.02, 38.83, 38.19, 38.14, 36.83, 36.58, 32.81, 30.61, 28.17, 27.99, 24.16, 23.56, 23.44, 23.27, 21.15, 18.15, 17.03, 16.87, 16.84, 15.46. EI-MS m/z : 565.68 (1) M^+ , 262.00 (66), 204.03 (18), 202.94 (100), 201.95 (27), 190.01 (19), 89.01 (36), 133.05 (89), 119.08 (24), 105.05 (19), 91.01 (21).

28-(4*H*-Triazol-4-yl)-11,28-dioxours-12-en-3 β -yl-4*H*-triazole-4-carboxylate (2.51): **2.51** was prepared using the same method as for **2.46**, using **2.14** (262.8 mg 0.56 mmol) as a starting material and CDT (459.56 mg 2.8 mmol). The workup was performed after 7 hours. The residue was subjected to flash column chromatography [hexanes-ethyl acetate from (70:30) to (60:40)], to afford **2.51** (76%). mp 162.1-165.4 °C. IR (film $CHCl_3$): 3137.6, 2955.4, 2874.4, 1763.6, 1733.7, 1658.5, 1512.9, 1457.0, 1405.9, 1362.5, 1350.9, 1279.5, 1226.5 cm^{-1} . 1H NMR (400 MHz $CDCl_3$): δ 8.80 (1H s), 8.74 (1H s), 8.02 (1H s), 7.97 (1H s), 5.61 (1H s), 4.76 (1H dd $J=16.33$ H3), 2.87 (1H d $J=13.74$), 2.45 (1H d $J=11.14$), 1.30 (3H s), 1.13 (3H s), 0.96 (6H s), 0.93 (3H s), 0.89 (3H d $J=6.31$), 0.81 (3H s). ^{13}C NMR (100 MHz $CDCl_3$): δ 198.87, 174.00, 161.84, 153.45, 152.56, 147.16, 145.27, 145.23, 130.84, 87.25, 61.09, 54.85, 53.01, 50.87, 44.50, 43.74, 38.53, 38.50, 38.35, 38.20, 36.78, 33.59, 32.66, 30.01, 28.51, 28.02, 23.29, 22.83, 20.82,

20.76, 18.42, 17.10, 17.03, 16.67, 16.22. EI-MS m/z : 616.80 (1) M^+ , 406.00 (30), 256.96 (100), 217.03 (88), 216.04 (65), 161.02 (33), 70.03 (42). Anal. Calcd for $C_{35}H_{48}N_6O_4 \cdot 0.5EtOAc$ C 67.25, H 7.93, N 12.72, found C 66.90, H 8.33, N 12.56.

3 β -Trifluoroacetoxy-11-oxours-12-en-28-yl-4H-triazole-4-carboxylate (2.52): **2.52** was prepared using the same method as for **2.46**, using **2.7** (300 mg 0.53 mmol) as a starting material and CDT (260.96 mg 1.59 mmol). The workup was performed after 2 hours. The residue was subjected to flash column chromatography [hexanes-ethyl acetate from (80:20) to (75:25)], to afford **2.52** (51%). mp 127.3-132.4. IR (film $CHCl_3$): 3139.5, 2955.4, 2930.3, 2875.3, 1778.1, 1732.7, 1660.4, 1513.9, 1457.9, 1384.6, 1348.0, 1276.7, 1214.0, 1166.7, 1139.7 cm^{-1} . 1H NMR (400 MHz $CDCl_3$): δ 8.84 (1H s), 8.01 (1H s), 5.65 (1H s), 4.68 (1H dd $J=16.35$), 2.87 (1H d $J=13.75$), 2.49 (1H d $J=12.63$), 2.32 (1H s), 1.33 (3H s), 1.14 (3H s), 1.00 (3H d $J=6.26$), 0.93 (3H d $J=6.37$), 0.90 (3H s), 0.88 (3H s), 0.84 (3H s). ^{13}C NMR (100 MHz $CDCl_3$): δ 199.07, 174.11, 161.98, 157.32 ($J=41.55$), 152.65, 145.36, 130.95, 114.61 ($J=286.26$), 85.87, 61.19, 54.88, 53.10, 50.96, 44.59, 43.82, 38.64, 38.53, 38.30, 38.19, 36.87, 33.68, 32.74, 30.11, 28.59, 27.84, 23.05, 22.91, 20.90, 20.86, 18.50, 17.16, 17.13, 16.39, 16.33. EI-MS m/z : 617.84 (4) M^+ , 258.01 (21), 257.02 (100), 255.18 (18), 217.08 (60), 216.08 (45), 176.15 (23), 161.16 (28), 146.13 (24), 119.04 (17), 105.11 (18), 91.14 (21), 79.22 (17). Anal. Calcd for $C_{34}H_{46}F_3N_3O_4$ C 66.11, H 7.51, N 6.80, found C 65.88, H 7.90, N 7.13.

3,11-Dioxours-12-en-28-yl-4H-triazole-4-carboxylate (2.53): **2.53** was prepared using the same method as for **2.46**, using **2.8** (300 mg 0.64 mmol) as a starting material and CDT (315.13 mg 1.92 mmol). The workup was performed after 4 hours. The residue was subjected to flash column chromatography [hexanes-ethyl acetate from (80:20) to (70:30)], to afford **2.53** (43%). mp 169.3-172.7 $^{\circ}C$. IR (film $CHCl_3$): 3128.0, 2955.4, 2872.5, 1732.7, 1702.8, 1659.5, 1513.9, 1458.9, 1385.6, 1349.9, 1275.7 cm^{-1} . 1H NMR (400 MHz $CDCl_3$): δ 8.84 (1H s), 8.01 (1H s), 5.67 (1H s), 1.33 (3H s), 1.23 (3H s), 1.06 (3H s), 1.02 (3H s), 1.00 (3H d $J=6.34$), 0.92 (3H d $J=6.38$), 0.87 (3H s). ^{13}C NMR (100 MHz $CDCl_3$): δ 216.98, 198.71, 174.14, 162.11, 152.65, 145.37, 130.97, 60.70, 55.41, 53.13, 51.00, 47.69, 44.46, 43.92, 39.73, 38.69, 38.30, 36.70, 34.15, 33.71, 32.31, 30.12, 28.67, 26.33, 22.94, 21.37, 20.89, 20.85, 18.62, 18.41, 17.10, 15.56. EI-MS m/z : 519.84

(8) M^+ , 421.97 (46), 407.03 (43), 256.99 (100), 217.04 (73), 216.04 (71), 161.11 (45), 147.07 (32), 146.05 (42), 105.14 (31), 91.2 (39). Anal. Calcd for $C_{32}H_{45}N_3O_3 \cdot 0.5H_2O$ C 72.69, H 8.77, N 7.95, found C 73.08, H 8.85, N 7.61.

3 β -Acetoxy-11-oxours-12-en-28-yl-4H-triazole-4-carboxylate (2.54): **2.54** was prepared using the same method as for **2.46**, using **2.9** (290 mg 0.57 mmol) as a starting material and CDT (280.66 mg 1.71 mmol). The workup was performed after 2 hours. The residue was subjected to flash column chromatography [hexanes-ethyl acetate from (80:20) to (75:25)], to afford **2.54** (46%). mp 151.8-156.5 °C. IR (film $CHCl_3$): 3133.8, 2951.5, 2872.5, 1730.8, 1661.4, 1459.9, 1349.9, 1246.8 cm^{-1} . 1H NMR (400 MHz $CDCl_3$): δ 8.83 (1H s Htriazole), 8.00 (1H s Htriazole), 5.64 (1H s H12), 4.49 (1H dd $J=16.28$ H3), 2.79 (3H d $J=2.77$), 2.48 (1H d $J=12.60$), 2.31 (1H s H9), 2.03 (3H s CH_3), 1.32 (3H s C27), 1.12 (3H s C25), 1.00 (3H d $J=6.29$ C30), 0.93 (3H d $J=6.36$ C29), 0.84 (6H s C23 or C24), 0.83 (3H s C26), 0.75 (1H d $J=11.55$ H5). ^{13}C NMR (100 MHz $CDCl_3$): δ 199.33 (C11), 174.12 (C28), 170.97 ($O\text{C}OCH_3$), 161.72 (C13), 152.61 (Ctriazole), 145.36 (Ctriazole), 131.05 (C12), 80.53 (C3), 61.34 (C9), 55.02 (C5), 53.10 (C18), 50.99 (C17), 44.65 (C8), 43.81 (C14), 38.80 (C1), 38.65 (C19 or C20), 38.32 (C19 or C20), 37.97 (C4), 36.96 (C10), 33.73, 32.86 (C7), 30.13 (C21), 28.60 (C15), 28.01 (C23 or C24), 23.51, 22.96, 21.27 ($O\text{C}OCH_3$), 20.89 (C27), 20.87 (C30), 18.53 (C26), 17.22, 17.14 (C29), 16.66 (C23 or C24), 16.33 (C25). EI-MS m/z : 563.78 (4) M^+ , 465.94 (16), 353.84 (21), 257.99 (23), 256.95 (100), 217.01 (60), 216.01 (49), 176.08 (19), 175.08 (20), 174.06 (18), 161.08 (28), 159.10 (17), 147.05 (16), 146.03 (20), 91.12 (17). Anal. Calcd for $C_{34}H_{49}N_3O_4$ C 72.43, H 8.76, N 7.45, found C 72.2, H 9.16, N 7.05.

Methyl 3 β -(4H-triazole-4-carboxyloxy)-11-oxo-urs-12-en-28-oate (2.55): **2.55** was prepared using the same method as for **2.46**, using **2.15** (270 mg 0.56 mmol) as a starting material and CDT (275.74 mg 1.68 mmol). The workup was performed after 5 hours. The residue was subjected to flash column chromatography [hexanes-ethyl acetate from (80:20) to (70:30)], to afford **2.55** (65%). mp 216.3-218.7 °C. IR (film $CHCl_3$): 2179.0, 2949.6, 2872.5, 1762.6, 1726.0, 1656.6, 1457.9, 1405.9, 1280.5, 1225.5, 1202.4 cm^{-1} . 1H NMR (400 MHz $CDCl_3$): δ 8.77 (1H s), 8.06 (1H s), 5.61 (1H s), 4.81 (1H dd $J=16.48$), 3.60 (3H s), 2.91 (1H d $J=13.67$), 2.42 (1H d $J=11.21$), 1.30 (3H s), 1.18 (3H

s), 1.01 (3H s), 0.98 (3H s), 0.96 (3H d $J=6.22$), 0.91 (3H s), 0.87 (3H d $J=6.39$). ^{13}C NMR (100 MHz CDCl_3): δ 199.36, 177.12, 163.09, 153.54, 147.27, 145.29, 130.53, 87.47, 61.19, 54.97, 52.70, 51.83, 47.62, 44.59, 43.72, 38.60 (2C), 38.56, 38.47, 36.91, 35.91, 32.83, 30.25, 28.35, 28.16, 23.87, 23.42, 21.03, 20.94, 18.81, 17.27, 17.08, 16.80, 16.21. EI-MS m/z : 580.13 (6) M^+ , 317.00 (91), 275.97 (53), 257.03 (95), 248.02 (82), 189.06 (100), 175.13 (36), 174.12 (36), 161.14 (74), 119.16 (77), 105.15 (34), 91.16 (35). Anal. Calcd for $\text{C}_{34}\text{H}_{49}\text{N}_3\text{O}_5$ C 70.44, H 8.52, N 7.25, found C 70.48, H 8.25, N 6.87.

Methyl 2-(4*H*-triazol-4-yl)-methylene-3,11-dioxours-12-en-28-oate (2.56): 2.56 was prepared using the same method as for **2.46**, using **2.12** (280 mg 0.55 mmol) as a starting material and CDT (180.54 mg 1.1 mmol). The workup was performed after 23.5 hours. The residue was subjected to flash column chromatography [hexanes-ethyl acetate from (65:35) to (55:45)], to afford **2.56** (46%). mp 250.2-251.2 °C. IR (film CHCl_3): 3122.2, 2949.6, 2869.6, 1725.0, 1688.4, 1654.6, 1617.0, 1508.1, 1457.0, 1383.7, 1275.7, 1202.4 cm^{-1} . ^1H NMR (400 MHz CDCl_3): δ 8.46 (1H s), 8.08 (1H s), 7.79 (1H s), 5.68 (1H s), 4.39 (1H d $J=17.42$), 3.61 (3H s), 1.33 (3H s), 1.19 (3H s), 1.12 (6H s), 0.97 (3H d $J=6.150$), 0.94 (3H s), 0.91 (3H d $J=6.26$). ^{13}C NMR (100 MHz CDCl_3): δ 206.32, 198.51, 177.13, 163.66, 152.49, 145.23, 130.61, 128.77, 125.27, 58.71, 53.01, 52.80, 51.87, 47.66, 45.38, 44.19, 43.86, 43.56, 38.74, 38.61, 35.93, 35.81, 31.64, 30.27, 29.73, 28.48, 23.85, 22.34, 20.97, 20.95, 19.50, 18.21, 17.19, 15.45. EI-MS m/z : 562.08 (12) M^+ , 317.91 (24), 316.93 (86), 285.03 (25), 258.03 (23), 256.97 (100), 217.01 (37), 216.04 (28), 202.03 (14), 189.05 (19), 187.10 (23), 173.12 (21), 162.07 (20), 161.16 (91), 135.18 (22), 119.16 (26). Anal. Calcd for $\text{C}_{34}\text{H}_{47}\text{N}_3\text{O}_4 \cdot 0.25\text{EtOAc}$ C 72.01, H 8.46, N 7.20, found C 71.72, H 8.85, N 6.88.

Methyl 2-(4*H*-triazol-4-yl)-methylene-3-oxours-12-en-28-oate (2.57): 2.57 was prepared using the same method as for **2.46**, using **2.13** (300 mg 0.60 mmol) as a starting material and CDT (295.43 mg 1.8 mmol). The workup was performed after 23 hours. The residue was subjected to flash column chromatography [hexanes-ethyl acetate from (80:20) to (70:30)], to afford **2.57** (40%). mp 202.1-206.3 °C. IR (film CHCl_3): 3116.4, 2947.7, 1721.2, 1688.4, 1618.0, 1509.0, 1454.1, 1381.8, 1281.5, 1226.5 cm^{-1} . ^1H NMR (400 MHz CDCl_3): δ 8.37 (1H s), 8.10 (1H s), 7.80 (1H s), 5.32 (1H s), 3.60 (3H s), 3.40

(1H d $J=17.43$), 1.18 (3H s), 1.13 (3H s), 1.12 (3H s), 0.95 (3H d $J=5.92$), 0.90 (6H s), 0.80 (3H s). ^{13}C NMR (100 MHz CDCl_3): δ 207.06, 177.97, 152.82, 145.84, 138.26, 128.35, 125.53, 125.26, 53.05, 52.80, 51.45, 48.17, 45.31, 45.07, 43.20, 42.22, 39.33, 39.13, 38.86, 36.58, 35.79, 32.00, 30.65, 29.68, 27.98, 24.20, 23.59, 23.42, 22.49, 21.13, 20.29, 17.08, 16.60, 15.67. EI-MS m/z : 584.05 (8) M^+ , 298.95 (25), 261.96 (44), 204.04 (17), 203.05 (83), 202.08 (22), 189.12 (26), 187.13 (15), 134.05 (40), 133.13 (100), 119.06 (24), 91.14 (17). Anal. Calcd for $\text{C}_{34}\text{H}_{49}\text{N}_3\text{O}_3$ C 74.55, H 9.02, N 7.67, found C 74.15, H 9.42, N 7.62.

28-(4H-Triazol-4-yl)-3,28-dioxours-12-en-2-(4H-triazol-4-yl)-methylene (2.58): **2.58** was prepared using the same method as for **2.46**, using **2.16** (300 mg 0.62 mmol) as a starting material and CDT (407 mg 2.48 mmol). The workup was performed after 7.5 hours. The residue was subjected to flash column chromatography [hexanes-ethyl acetate from (80:20) to (70:30)], to afford **2.58** (21%). mp 245.5-251.1 °C. IR (film CHCl_3): 3134.1, 2953.5, 2924.5, 2869.6, 1733.7, 1689.3, 1616.1, 1510.0, 1457.0, 1382.7, 1349.0, 1276.7, 1222.7, 1184.1 cm^{-1} . ^1H NMR (400 MHz CDCl_3): δ 8.82 (1H s), 8.37 (1H s), 8.10 (1H s), 7.99 (1H s), 7.80 (1H s), 5.31 (1H s), 3.41 (1H d $J=17.27$), 1.25 (2H), 1.16 (3H s), 1.15 (3H s), 1.11 (3H s), 0.99 (3H d $J=6.26$), 0.96 (3H d $J=6.38$), 0.88 (3H s), 0.72 (3H s). ^{13}C NMR (100 MHz CDCl_3): δ 206.95, 174.81, 152.96, 152.24, 145.30, 137.60, 137.03, 128.37, 125.92, 125.29, 52.75, 51.39, 45.28 (2C), 44.99, 43.18, 42.40, 39.30, 39.21, 38.53, 35.74, 34.39, 31.87, 30.46, 29.66, 28.13, 23.59, 23.42 (2C), 22.48, 21.02, 20.16, 17.08, 16.43, 15.68. EI-MS m/z : 584.94 (4) M^+ , 488.01 (31), 487.00 (70), 202.01 (42), 190.07 (52), 189.09 (100), 187.13 (38), 133.03 (31), 132.03 (51), 119.05 (45), 117.08 (48). Anal. Calcd for $\text{C}_{35}\text{H}_{48}\text{N}_6\text{O}_2 \cdot 0.5\text{hexane} \cdot 0.5\text{EtOAc}$ C 71.5, H 8.85, N 12.51, found C 71.26, H 9.03, N 12.42.

3 β -O1-12 β -fluor-urs-13,28 β -olide (2.59): To a stirred solution of ursolic acid **2.1** (300 mg 0.66 mmol) in NO_2Me (6 mL) and dioxane (4 mL) at 80°C was added selectfluor (701.43 mg 1.98 mmol). After 24 hours the reaction mixture was diluted with water (60 mL), the aqueous phase was extracted with ether (3 \times 55 mL). The resulting organic phases were washed with NaCl 10% (3 \times 60 mL), dried over Na_2SO_4 , filtered and evaporated to the dryness, to afford a solid. The solid was subjected to flash column

chromatography [hexanes-ethyl acetate from (90:10) to (30:70)], to afford **2.59** (88%). mp 316.8-317.6 °C. IR (film CHCl₃): 3337.2, 2927.4, 2872.5, 1765.5, 1459.8 cm⁻¹. ¹H NMR (400 MHz CDCl₃): δ 4.85 (1H dt *J*=62.84 H12), 3.19 (1H dd *J*=16.18 H3), 1.20 (3H s), 1.19 (3H s), 1.13 (3H d *J*=6.26), 0.97 (6H s), 0.91 (3H s), 0.76 (3H s). ¹³C NMR (100 MHz CDCl₃): δ 178.88 (C28), 91.97 (*J*=14.24 C13), 88.70 (*J*=185.75 C12), 78.68 (C3), 55.32, 52.55 (*J*=3.58), 49.18 (*J*=9.078), 45.19, 43.90 (*J*=2.83), 42.53, 39.53, 39.03, 38.84, 38.40, 37.12, 33.95, 31.34, 30.71, 27.92, 27.62, 27.22, 25.37 (*J*=19.72), 22.39, 19.39, 18.50, 17.65, 17.22, 16.65, 16.46, 15.26. EI-MS *m/z*: 475.12 (8) M⁺, 455.3 (93), 246.24 (89), 207.32 (66), 189.36 (100), 187.37 (77), 119.22 (76). Anal. Calcd for C₃₀H₄₇FO₃ C 75.91, H 9.98, found C 75.52, H 10.18.

3β-Acetoxy-12β-fluor-urs-13,28β-olide (2.60): To a stirred solution of **2.4** (150 mg 0.3 mmol) in NO₂Me (3 mL) and dioxane (2 mL) at 80°C was added selectfluor (318.8 mg 0.9 mmol). The workup was performed according to the same method as for **2.59** after 24 hours. The solid obtained was subjected to flash column chromatography [hexanes-ethyl acetate from (90:10) to (75:25)], to afford **2.60** (43%). mp 280.2-281.6 °C. IR (film CHCl₃): 2928.4, 1767.4, 1729.8, 1457.9 cm⁻¹. ¹H NMR (400 MHz CDCl₃): δ 4.86 (1H dt *J*=62.76 H12), 4.48 (1H dd *J*=16.35 H3), 2.05 (3H s), 1.25 (3H s), 1.21 (3H s), 1.20 (3H s), 1.14 (3H d *J*=6.26), 0.96 (3H d *J*=12.52), 0.85 (6H s). ¹³C NMR (100 MHz CDCl₃): δ 178.88 (C28), 170.98 (OC₂O), 91.93 (*J*=14.19 C13), 89.64 (*J*=185.74 C12), 80.48 (C3), 55.42, 52.57 (*J*=3.39), 49.12 (*J*=9.22), 45.20, 43.91 (*J*=2.26), 42.56, 39.55, 38.73, 38.42, 37.80, 37.06, 33.89, 31.36, 30.73, 27.89, 27.64, 25.42 (*J*=19.20), 23.54, 22.41, 21.26, 19.42, 18.54, 17.56, 17.21, 16.74, 16.53, 16.41. EI-MS *m/z*: 516.91 (5) M⁺, 497.04 (66), 190.12 (51), 189.14 (100), 187.19 (72), 119.13 (64), 107.11 (62), 105.35 (55), 93.36 (55), 91.03 (57), 79.13 (67). Anal. Calcd for C₃₂H₄₉FO₄ C 74.38, H 9.56, found C 74.78, H 9.40.

3β-Phthaloxy-12β-fluor-urs-13,28β-olide (2.61): To a stirred solution of **2.5** (304.8 mg 0.5 mmol) in nitromethane (3 mL) and dioxane (2 mL) at 80°C was added selectfluor (531.39 mg 1.5 mmol). The workup was performed according to the same method as for **2.59** after 23 hours. The solid was subjected to flash column chromatography [hexanes-ethyl acetate from (50:50) to (35:65)], to afford **2.61** (62%). mp 241.9-243.6 °C. IR (film

CHCl₃): 2929.3, 1770.3, 1723.1, 1457.9 cm⁻¹. ¹H NMR (400 MHz CDCl₃): δ 7.89 (1H d *J*=6.92), 7.72 (1H d *J*=6.85), 7.59 (2H quintet *J*=26.69), 4.88 (1H dt *J*=62.80 H12), 4.76 (1H dd *J*=16.04 H3), 1.21 (6H s), 1.15 (3H d *J*=6.24), 0.97 (6H d *J*=8.35), 0.93 (3H s), 0.89 (3H s). ¹³C NMR (100 MHz CDCl₃): δ 178.96 (C28), 171.75, 167.77, 133.35, 131.99, 130.89, 130.27, 129.85, 128.94, 91.98 (*J*=14.25 C13), 89.62 (*J*=185.85 C12), 82.59 (C3), 55.53, 52.58 (*J*=2.74), 49.09 (*J*=9.03), 45.21, 43.91 (*J*=2.56), 42.56, 39.55, 38.75, 38.42, 38.05, 37.07, 33.88, 31.35, 30.72, 27.98, 27.64, 25.44 (*J*=19.48), 22.94, 22.40, 19.42, 18.53, 17.54, 17.23, 16.68, 16.55 (2C). EI-MS *m/z*: 623.12 (2) M⁺, 245.87 (100), 201 (50), 188.96 (93), 187.02 (64), 148.95 (57), 118.96 (55). Anal. Calcd for C₃₈H₅₁FO₆ C 73.28, H 8.25, found C 73.19, H 8.34.

Methyl isoxazolo[4,5-b]-12β-fluor-13,28β-olide (2.62): To a stirred solution of **2.17** (100 mg 0.21 mmol) in nitromethane (1.5 mL) and dioxane (1 mL) at 80°C was added selectfluor (223.18 mg 0.63 mmol). The workup was performed according to the same method as for **2.59** after 25 hours. The solid was subjected to flash column chromatography [hexanes-ethyl acetate from (80:20) to (70:30)], to afford **2.62** (38%). mp 292.6-293.9 °C. IR (film CHCl₃): 2929.3, 1875.3, 1771.3, 1458.9, 1388.5, 1277.6, 1236.2 cm⁻¹. ¹H NMR (400 MHz CDCl₃): δ 8.01 (1H s), 4.90 (1H dq *J*=62.36), 2.60 (1H d *J*=14.88), 1.31 (3H s), 1.27 (3H s), 1.23 (3H s), 1.21 (3H s), 1.15 (3H d *J*=6.09), 0.98 (3H s), 0.91 (3H s). ¹³C NMR (100 MHz CDCl₃): δ 178.75, 172.82, 150.14, 108.36, 91.87 (*J*=14.17), 89.49 (*J*=186.44) 53.51, 52.58, 47.79 (*J*=9.41), 45.22, 42.45, 39.55, 38.88, 38.57, 36.23, 34.90, 33.12, 31.32, 30.73, 29.66, 28.67, 27.72, 25.76 (*J*=19.60), 22.38, 21.13, 19.39, 18.10, 17.99, 17.08, 16.70, 16.43. EI-MS *m/z*: 498.13 (12) M⁺, 245.96 (97), 232.01 (56), 230.03 (57), 201.09 (94), 189.1 (51), 187.13 (100), 145.15 (51), 120.04 (53), 119.14 (94), 107.1 (55), 105.13 (53), 91.2 (69), 79.14 (63).

3-Oxo-2α,12β-difluor-urs-13,28β-olide (2.63): To a stirred solution of **2.3** (100 mg 0.22 mmol) in nitromethane (3 mL) and dioxane (2 mL) at 80°C was added selectfluor (233.8 mg 0.66 mmol). The workup was performed according to the same method as for **2.59** after 24 hours. The solid was subjected to flash column chromatography [hexanes-ethyl acetate from (80:20) to (65:35)], to afford **2.63** (36%). mp 347.3-348.8 °C IR (film CHCl₃): 2928.4, 2875.3, 1766.5, 1720.2, 1461.8, 1389.5, 1236.2 cm⁻¹. ¹H NMR (400

MHz CDCl₃): δ 5.30 (1H dq $J=66.18$ H2), 4.88 (1H dq $J=62.48$ H12), 1.26 (3H s C26), 1.23 (3H s C25), 1.19 (3H s C27), 1.15 (3H s C23 or C24), 1.13 (3H d $J=6.41$ C29), 1.09 (3H s C23 or C24), 0.96 (3H d $J=5.58$ C30). ¹³C NMR (100 MHz CDCl₃): δ 209.63 (C3), 178.68 (C28), 91.63 ($J=14.40$ C13), 89.83 ($J=30.850$ C2), 87.98 ($J=30.65$ C12), 56.41 (C5), 52.54 ($J=3.34$ C18), 48.71 ($J=9.69$ C9), 48.49 (C4), 47.23 ($J=17.17$ C1), 45.13 (C17), 43.97 ($J=2.97$ C14), 42.63 (C8), 39.52 (C20), 38.36 (C19), 38.04 ($J=9.69$ C10), 33.47 (C7), 31.29, 30.68, 27.60 (C15), 25.72 ($J=20.16$ C11), 24.81 (C23 or C24), 22.35, 21.05 (C23 or C24), 19.40 (C30), 18.63 (C26), 18.42, 17.48 (C25), 17.16 (C27), 16.51 (C29). EI-MS m/z : 490.84 (5) M⁺, 200.69 (70), 199.96 (52), 186.99 (81), 145.02 (52), 133.03 (40), 131.03 (46), 119.04 (100), 107.04 (56), 105.05 (52), 93.03 (44), 91.04 (66), 79.01 (59), 77 (37), 66.69 (41).

3 β -Trifluoroacetoxy-12 β -fluor-urs-13,28 β -olide (2.64): To a stirred mixture of **2.59** (200 mg 0.42 mmol) in THF (5 mL) at room temperature, was added DMAP (10% of the mass of **2.59**) and trifluoroacetic anhydride (0.58 mL 4.2 mmol). After 1 hour the reaction mixture was acidified with HCl 10% (50 mL) and the aqueous phase extracted with ether (3 \times 40 mL). The organic phase is washed with NaHCO₃ (3 \times 40 mL) and water (3 \times 40 mL), dried over Na₂SO₄, filtered and evaporated to the dryness, to afford a solid. The residue was subjected to flash column chromatography [hexanes-ethyl acetate from (95:5) to (75:25)], to afford **2.64** (31%). mp 280.2-282.2 °C. IR (film CHCl₃): 2953.5, 2927.4, 2873.4, 1777.1, 1459.8 cm⁻¹. ¹H NMR (400 MHz CDCl₃): δ 4.87 (1H dd $J=62.64$ H12), 4.68 (1H dd $J=16.16$ H3), 1.26 (3H s), 1.23 (3H s), 1.21 (3H s), 1.15 (3H d $J=6.19$), 0.97 (3H s), 0.91 (3H s), 0.91 (3H s). ¹³C NMR (100 MHz CDCl₃): δ 178.82 (C28), 91.84 ($J=14.52$ C13), 89.53 ($J=185.90$ C12), 85.78 (C3), 55.30, 52.58, 49.10 ($J=9.24$), 45.21, 43.95 ($J=3.16$), 42.58, 39.57, 38.57, 38.46, 38.09, 37.06, 33.85, 31.37, 30.75, 29.70, 27.77, 27.68, 25.47 ($J=19.59$), 23.15, 22.41, 19.44, 18.56, 17.52, 17.24, 16.75, 16.54, 16.19. EI-MS m/z : 570.84 (2) M⁺, 245.98 (54), 201.05 (65), 189.08 (71), 187.1 (87), 145.16 (51), 119.16 (100), 107.15 (69), 105.15 (61), 93.16 (62), 91.23 (92), 79.17 (81), 77.16 (53), 67.14 (54). Anal. Calcd for C₃₁H₄₃F₄O₄ C 67.35, H 8.12, found C 67.74, H 8.46.

3 β -Butyroxoy-12 β -fluor-urs-13,28 β -olide (2.65): To a stirred mixture of **2.59** (200 mg 0.42 mmol) in THF (5 mL) at room temperature, was added DMAP (10% of the mass of **2.59**) and butyric anhydride (0.34 mL 2.1 mmol). The workup was performed according to the same method as for **2.64** after 1 hour. The solid obtained was subjected to a flash column chromatography [hexanes-ethyl acetate from (85:15) to (80:20)], to afford **2.65** (28%). mp 251.4-255 °C. IR (film CHCl₃): 2964.1, 2933.2, 2874.4, 1772.3, 1729.8, 1458.9 cm⁻¹. ¹H NMR (400 MHz CDCl₃): δ 4.86 (1H dt $J=62.73$ H12), 4.49 (1H dd $J=16.28$ H3), 1.21 (3H s), 1.20 (3H s), 1.14 (3H d $J=6.22$), 0.97 (3H s), 0.94 (6H d $J=3.49$), 0.85 (6H s). ¹³C NMR (100 MHz CDCl₃): δ 178.87 (C28), 173.49 (OCO), 91.94 ($J=14.16$ C13), 89.64 ($J=185.88$ C12), 80.13 (C3), 55.41, 52.56 ($J=3.47$), 49.10 ($J=9.28$), 45.19, 43.90 ($J=2.90$), 42.55, 39.55, 38.71, 38.42, 37.83, 37.06, 36.69, 33.89, 31.36, 30.73, 27.91, 27.64, 25.41 ($J=19.09$), 23.59, 22.41, 19.42, 18.59, 18.53, 17.55, 17.22, 16.72, 16.53, 16.47, 13.70. EI-MS m/z: 544.25 (1) M⁺, 201.04 (43), 190.08 (53), 189.12 (100), 187.14 (56), 120.01 (36), 119.11 (51), 93.18 (38), 91.2 (44), 79.35 (42). Anal. Calcd for C₃₄H₅₃FO₄ C, 74.96, H 9.81, found C 75.36, H 9.70.

3 β -Benzoxy-12 β -fluor-urs-13,28 β -olide (2.66): To a stirred mixture of **2.59** (200 mg 0.42 mmol) in THF (5 mL) at room temperature, was added DMAP (10% of the mass of **2.59**) and benzoic anhydride (475.08 mg 2.1 mmol). The workup was performed according to the same method as for **2.64** after 8 hours. The solid obtained was subjected to a flash column chromatography [hexanes-ethyl acetate from (85:15) to (75:25)], to afford **2.66** (50%). mp 319.2-322.6 °C. IR (film CHCl₃): 3064.3, 2030.3, 2872.5, 1785.8, 1715.4, 1599.7, 1452.1 cm⁻¹. ¹H NMR (400 MHz CDCl₃): δ 8.04 (2H d $J=7.53$), 7.55 (1H t $J=14.59$), 7.44 (2H t $J=15.16$), 4.89 (1H dt $J=62.70$ H12), 4.73 (1H dd $J=15.80$ H3), 1.24 (3H s), 1.22 (3H s), 1.16 (3H d $J=6.18$), 1.02 (3H s), 0.99 (6H d $J=5.33$), 0.94 (3H s). ¹³C NMR (100 MHz CDCl₃): δ 178.88 (C28), 166.25 (OCO), 132.80, 130.78, 129.50 (2C), 128.33 (2C), 91.95 ($J=14.25$ C13), 89.64 ($J=185.93$ C12), 81.09 (C3), 55.48, 52.58 ($J=3.33$), 49.12 ($J=9.08$), 45.20, 43.93 ($J=2.77$), 42.58, 39.55, 38.74, 38.43, 38.20, 37.11, 33.90, 31.36, 30.73, 28.06, 27.65, 25.45 ($J=19.18$), 23.61, 22.42, 19.43, 18.56, 17.58, 17.24, 16.75, 16.71, 16.54. EI-MS m/z: 578.87 (1) M⁺, 245.90 (32), 201.97 (23), 201.01 (25), 190.04 (35), 189.07 (60), 187.12 (33), 119.07 (29), 106.98 (27), 105.21 (100), 91.14

(22), 79.07 (21), 77.1 (49). Anal. Calcd for C₃₇H₅₁FO₄ C, 76.78, H 8.88, found C 76.92, H 9.09.

3-Oxo-12 β -fluor-urs-13,28 β -olide (2.67): **2.67** was prepared according to the literature²⁹⁵ from **2.59** (1.7755 g 3.74 mmol) to give a solid. The residue was subjected to flash column chromatography [hexanes-ethyl acetate from (80:20) to (65:35)], to afford **2.67** (26%). mp 327.3-329.2 °C. IR (film CHCl₃): 2928.4, 1771.3, 1704.8, 1457.9 cm⁻¹. ¹H NMR (400 MHz CDCl₃): δ 4.87 (1H dq $J=62.47$), 1.25 (3H s), 1.21 (3H s), 1.14 (3H d $J=6.31$), 1.08 (3H s), 1.04 (3H s), 1.02 (3H s), 0.96 (3H d $J=5.56$). ¹³C NMR (100 MHz CDCl₃): δ 216.97 (C3), 178.75 (C28), 91.91 ($J=14.27$ C13), 89.49 ($J=185.77$ C12), 54.83, 52.57, 48.48 ($J=9.33$), 47.28, 45.19, 44.02 ($J=3.09$), 42.40, 39.79, 39.55, 38.51, 36.85, 33.89, 33.37, 31.33, 30.73, 27.64, 26.58, 25.75 ($J=19.71$), 22.39, 20.97, 19.40, 18.99, 18.17, 17.09, 16.47, 16.42. EI-MS m/z: 473.03 (1) M⁺, 245.97 (67), 205.02 (65), 210.03 (79), 187.03 (82), 163.04 (62), 119.03 (100), 107.02 (64), 105.03 (58), 91 (71), 78.98 (75). Anal. Calcd for C₃₀H₄₅FO₃.0.5 EtOAc C 74.38, H 9.56, found C 74.16, H 9.61.

Methyl isoxazolo[4,5-b]urs-12-en-28-oate (2.68): Preparation of **2.68** was made according to previously described method,²⁹⁵ from **2.13** (325.4 mg 0.655 mmol) to afford a solid (96%). mp 119.9-120.0 °C. IR (film CHCl₃): 2925.5, 2869.6, 1723.1, 1483.0, 1457.0 cm⁻¹. ¹H NMR (400 MHz CDCl₃): δ 7.97 (1H s), 5.30 (1H s H12), 3.61 (3H s), 1.30 (3H s), 1.21 (3H s), 1.10 (3H s), 0.94 (3H d $J=5.95$), 0.89 (3H s), 0.87 (3H d $J=6.52$), 0.80 (3H s). ¹³C NMR (100 MHz CDCl₃): δ 177.08 (C28), 173.03 (C3), 150.15 (C_{HNO}), 138.23 (C13), 125.25 (C12), 108.83 (C2). EI-MS m/z: 494.22 (14) M⁺, 262.03 (32), 203.09 (67), 189.07 (41), 133.13 (100), 119.15 (34), 105.17 (24), 91.16 (26).

Methyl 2-cyano-3-hydroxy-urs-2,12-dien-28-oate (2.69): **2.69** was prepared according to the literature²⁹⁵ from **2.68** (257.6 mg 0.52 mmol) to give a solid (86%). mp 136.4-140.3 °C. IR (film CHCl₃): 2947.7, 1869.6, 1719.2, 1457.9 cm⁻¹. EI-MS m/z: 494.2 (9) M⁺, 262.0 (34), 249.1 (23), 203.02 (62), 189.05 (54), 133.1 (100), 119.13 (32), 105.09 (22), 91.13 (27).

Methyl 2-cyano-3-oxours-1,12-dien-28-oate (2.70): Preparation of **2.70** was made according to previously described method,²⁹⁵ from **2.69** (195.4mg 0.396mmol) to afford a solid (88%). mp 134.7-137.5 °C. IR (film CHCl₃): 2947.7, 2872.5, 1721.2, 1685.5, 1457.0 cm⁻¹. ¹H NMR (400 MHz CDCl₃): δ 7.75 (1H s H1), 5.33 (1H s H12), 3.62 (3H s), 1.22 (3H s), 1.20 (3H s), 1.14 (3H s), 1.10 (3H s), 0.95 (3H d *J*=5.87), 0.87 (3H d *J*=6.43), 0.85 (3H s). EI-MS *m/z*: 492.17 (7) M⁺, 203.05 (35), 189.08 (58), 187.12 (20), 133.11 (100), 119.13 (46), 117.13 (20), 105.13 (28), 91.11 (33). Anal. Calcd for C₃₂H₄₅NO₃ C 78.17, H 9.22, N 2.85, found C 77.82, H 9.23, N 2.86.

2-Cyano-3-oxours-1,12-dien-28-oic acid (2.71): **2.71** was prepared according to the literature²⁹⁵ from **2.70** (155.2 mg 0.316 mmol) to give a solid (64%). mp 213.7-217.6 °C. IR (film CHCl₃): 2926.5, 2870.5, 1652.2, 1609.3, 1456.0 cm⁻¹. ¹H NMR (400 MHz CDCl₃): δ 7.76 (1H s), 5.32 (1H s), 1.22 (3H s), 1.20 (3H s), 1.12 (3H s), 1.11 (3H s), 0.96 (3H d *J*=5.90), 0.88 (6H s). ¹³C NMR (100 MHz CDCl₃): δ 198.02 (C3), 183.07 (C28), 169.98 (C1), 138.87 (C13), 124.27 (C12), 114.91, 113.91. EI-MS *m/z*: 477.84 (1) M⁺, 247.85 (64), 218.84 (25), 202.86 (70), 188.92 (27), 186.92 (22), 132.93 (100), 118.94 (33), 104.95 (29), 90.91 (31). Anal. Calcd for C₃₁H₄₃NO₃ C 77.95, H 9.07, N 2.93, found C 77.89, H 9.47, N 2.94.

2-Cyano-3-oxo-12 α -fluor-urs-1-en-13,28 β -olide (2.72) and **2-Cyano-3-oxo-12 β -fluor-urs-1-en-13,28 β -olide (2.73):** To a stirred solution of **2.71** (178.6 mg 0.38 mmol) in nitromethane (6 mL) and dioxane (4 mL) at 80°C was added selectfluor (404.24 mg 1.14 mmol). The workup was performed according to the same method has for **2.59** after 2.5 hours. The obtained solid was subjected to flash column chromatography [hexanes-ethyl acetate from (80:20) to (60:40)], to afford **2.73** (21%), and two mixture fractions. The mixture fractions were subjected to a new flash column chromatography [hexanes-ethyl acetate from (75:25) to (60:40)], to afford **2.73** (16%) and a mixture fraction. The mixture fraction was subjected to a flash column chromatography [hexanes-ethyl acetate from (75:25) to (65:35)], to afford **2.72** (13%). **2.72:** mp 264.9-268.6 °C. IR (film CHCl₃): 2926.5, 1740.4, 1685.5, 1457.9 cm⁻¹. ¹H NMR (400 MHz CDCl₃): δ 7.81 (1H s H1), 4.51 (1H dt *J*=66.17 H12), 1.30 (3H d *J*=7.26), 1.25 (3H s), 1.22 (3H s), 1.20 (3H s), 1.16 (3H s), 0.98 (6H t *J*=9.45). ¹³C NMR (100 MHz CDCl₃): δ 197.72 (C3), 177.51

(C28), 168.79 (C1), 114.69, 114.61, 96.11 ($J=189.19$ C12), 90.38 (C13), 53.00, 45.264 45.08 ($J=9.305$), 44.68, 43.46 ($J=17.41$), 42.35 ($J=9.78$), 41.04, 40.93, 39.04, 37.34, 34.87, 31.67, 29.10, 27.396, 25.94 ($J=25.20$), 25.74, 22.73 ($J=3.35$), 21.81, 20.94, 20.49, 20.34, 20.07, 19.46, 19.11. EI-MS m/z : 495.91 (4) M^+ , 123.06 (70), 122.04 (92), 121.06 (45), 119.1 (48), 107.09 (100), 105.1 (46), 91.13 (60), 81.11 (57), 79.09 (66), 67.05 (46). Anal. Calcd for $C_{31}H_{42}FNO_3$ C, 75.12, H 8.54, N 2.83, found C 74.77, H 8.94, N 2.94. **2.73**: mp 365.5-366.8 °C. IR (film $CHCl_3$): 2926.5, 1767.4, 1684.5, 1457.9 cm^{-1} . 1H NMR (400 MHz $CDCl_3$): δ 7.82 (1H s), 4.94 (1H dq $J=62.15$ H12), 1.31 (3H s C26), 1.25 (3H s C29), 1.22 (3H d $J=3.13$ C27), 1.20 (3H s C25), 1.15 (6H s C23 and C24), 0.98 (3H d $J=5.71$ C30). ^{13}C NMR (100 MHz $CDCl_3$): δ 197.70 (C3), 178.38 (C28), 169.04 (C1), 114.70 (CN), 114.41 (C2), 91.52 ($J=14.49$ C13), 88.52 ($J=187.42$ C12), 52.71 (C5), 52.61 ($J=3.16$ C18), 45.14, 45.05 (C4), 44.17 ($J=2.72$ C17), 43.48 (C8), 42.43 ($J=9.85$ C9) 40.40 (C10), 39.53, 38.39, 33.06, 31.25, 30.67, 29.67, 27.69 (C25), 27.64, 25.64 ($J=20.53$), 21.29, 19.38 (C30), 18.91 (C26 and C29), 18.25, 17.00 (C27), 16.53 (C23 or C24). EI-MS m/z : 496.15 (6) M^{+1} , 189.11 (42), 187.17 (56), 163.2 (53), 119.2 (100), 107.18 (51), 91.21 (53), 79.2 (49). Anal. Calcd for $C_{31}H_{42}FNO_3$ C 75.12, H 8.54, N 2.83, found C 75.04, H 8.93, N 2.95.

2-Hydroxymethylene-3-oxo-12 β -fluor-urs-13,28 β -olide (2.74): **2.74** was prepared according to the literature²⁹⁵ from **2.67** (154.5 mg 0.33 mmol) to give a solid. The solid was subjected to flash column chromatography [hexanes-ethyl acetate from (80:20) to (70:30)], to afford **2.74** (67%). IR (film $CHCl_3$): 344.2, 2930.3, 1771.3, 1636.3, 1587.1, 1457.9 cm^{-1} . 1H NMR (400 MHz $CDCl_3$): δ 14.89 (1H s), 8.62 (1H s), 4.89 (1H dq $J=62.70$ H12), 1.27 (3H s), 1.22 (3H s), 1.19 (3H s), 1.14 (3H d $J=6.30$), 1.11 (3H s), 0.97 (3H d $J=5.63$), 0.92 (3H s). ^{13}C NMR (100 MHz $CDCl_3$): δ 189.87 (C3), 188.84 ($\underline{C}HOH$), 178.79 (C28), 105.21 (C2), 91.93 ($J=14.19$ C13), 89.50 ($J=185.98$ C12), 52.56 ($J=3.52$), 51.98, 47.29 ($J=9.44$), 45.21, 44.04 ($J=2.83$), 42.21, 40.18, 39.97, 39.52, 38.55, 36.53, 33.06, 31.30, 30.72, 28.19, 27.61, 25.76 ($J=19.43$), 22.36, 20.55, 19.39, 18.77, 17.99, 17.03, 16.41, 15.65. EI-MS m/z : 500.79 (2) M^+ , 245.72 (79), 232.77 (73), 200.8 (68), 186.81 (100), 172.83 (60), 144.85 (56), 118.86 (82), 106.85 (67), 104.87 (58), 90.83 (64), 78.8 (60). Anal. Calcd for $C_{31}H_{45}FO_4$ C 74.36, H 9.06, found C 73.97, H 8.81.

3 β -(1*H*-Imidazole-1-carboxyloxy)-12 β -fluor-urs-13,28 β -olide (2.75): To a stirred solution of **2.59** (300 mg 0.63 mmol) in THF (6.5 mL), under N₂ atmosphere, at 70°C, was added CDI (204.31 mg 1.26 mmol). The workup was performed according to the same method as for **2.18** after 3 hours. The residue was subjected to flash column chromatography [hexanes-ethyl acetate from (70:30) to (55:45)], to afford **2.75** (47%). mp 285.9-286.8 °C. IR (film CHCl₃): 3136.7, 2976.6, 2876.3, 1767.4, 1758.8, 1524.5, 1470.5, 1395.3, 1319.1, 1288.2, 1240.0 cm⁻¹. ¹H NMR (400 MHz CDCl₃): δ 8.13 (1H s), 7.40 (1H s), 7.07 (1H s), 4.87 (1H dt $J=45.82$ H12), 4.68 (1H dd $J=15.87$ H3), 1.22 (3H s C26), 1.21 (3H s C27), 1.14 (3H d $J=6.20$ C29), 0.98 (3H s C25), 0.96 (9H s C23 or C24 or C30), 0.86 (1H d $J=8.75$ H5). ¹³C NMR (100 MHz CDCl₃): δ 178.15 (C28), 148.46 (COO), 136.93 (Cimidazole), 130.48 (Cimidazole), 117.00 (Cimidazole), 91.80 ($J=14.31$ C13), 89.49 ($J=185.86$ C12), 85.84 (C3), 55.32 (C5), 52.55 ($J=3.34$ C18), 49.06 ($J=9.38$ C9), 45.17 (C17), 43.94 (C14), 42.54 (C7), 39.53 (C20), 38.57, 38.40 (C19), 38.19 (C4), 37.03 (C10), 33.82 (C7), 31.33, 30.70, 28.02 (C23 or C24 or C30), 27.63 (C15), 25.44 ($J=19.38$), 23.45, 22.38, 19.39 (C25), 18.53 (C26), 17.50, 17.21 (C27), 16.69 (C23 or C24 or C30), 16.58 (C23 or C24 or C30), 16.50 (C29). EI-MS m/z : 569.2 (8) M⁺, 189.2 (89), 187.2 (62), 133.2 (64), 119.2 (100), 107.2 (75), 105.2 (78), 95.2 (75), 93.2 (62), 91.2 (78), 79.15 (76). Anal. Calcd for C₃₄H₄₉FN₂O₄ C 71.80, H 8.68, N 4.93, found C 72.06, H 8.58, N 4.96.

3 β -(2'-Methyl-1*H*-imidazole-carboxyloxy)-12 β -fluor-urs-13,28 β -olide (2.76): To a stirred solution of **2.59** (300 mg 0.63 mmol) in THF (4 mL), under N₂ atmosphere, at 70°C, was added CBMI (239.66 mg 1.26 mmol). The workup was performed according to the same method as for **2.32** after 8 hours. The solid was subjected to flash column chromatography [hexanes-ethyl acetate from (70:30) to (50:50)], to afford **2.76** (49%). mp 293.1-293.6 °C. IR (film CHCl₃): 2933.2, 2878.2, 1769.4, 1758.8, 1457.9, 1395.3, 1373.1, 1294.0 cm⁻¹. ¹H NMR (400 MHz CDCl₃): δ 7.33 (1H s), 6.86 (1H s), 4.87 (1H dt $J=45.78$), 4.66 (1H dd $J=15.70$), 2.65 (3H s), 1.23 (3H s), 1.21 (3H s), 1.15 (3H d $J=6.31$), 0.98 (3H s), 0.96 (9H s). ¹³C NMR (100 MHz CDCl₃): δ 178.768, 149.366, 147.881, 127.636, 117.978, 91.83 ($J=14.21$), 89.51 ($J=186.13$), 85.54, 55.37, 52.60, 52.56, 49.13, 49.04, 45.18, 43.96, 43.93, 42.56, 39.55, 38.64, 38.42, 38.14, 37.06, 33.84, 31.35, 30.72, 28.05, 27.65, 25.56, 25.36, 23.53, 22.40, 19.40, 18.54, 17.53, 17.23, 16.80,

16.79, 16.70, 16.52. EI-MS m/z : 583.2 (6) M^+ , 190.1 (53), 189.1 (99), 187.2 (55), 147.1 (57), 145.1 (48), 133.1 (65), 127.1 (54), 121.1 (60), 119.1 (100), 109.1 (74), 107.1 (84), 105.1 (77), 95.1 (79), 93.1 (64), 91.1 (78). Anal. Calcd for $C_{35}H_{51}FN_2O_4$ C 72.13, H 8.82, N 4.81, found C 71.97, H 8.56, N 4.73.

3 β -(4H-Triazole-carbonyloxy)-12 β -fluor-urs-13,28 β -olide (2.77): To a stirred solution of **2.59** (300 mg 0.63 mmol) in THF (4 mL), under N_2 atmosphere, at 70°C, was added CDT (310.2 mg 1.89 mmol). The workup was performed according to the same method as for **2.46** after 7 hours. The solid was subjected to flash column chromatography [hexanes-ethyl acetate from (80:20) to (65:35)], to afford **2.77** (36%). mp 256.1-256.4 °C. IR (film $CHCl_3$): 3133.8, 2933.2, 2872.5, 1771.3, 1510.0, 1457.9, 1405.9, 1280.5, 1226.5, 1203.4 cm^{-1} . 1H NMR (400 MHz $CDCl_3$): δ 8.77 (1H s), 8.06 (1H s), 4.86 (2H m $J=71.41$), 1.23 (3H s), 1.21 (3H s), 1.14 (3H d $J=6.28$), 1.00 (3H s), 0.99 (3H s), 0.98 (3H s), 0.97 (3H s). ^{13}C NMR (100 MHz $CDCl_3$): δ 178.74, 153.60, 147.29, 145.30, 91.79 ($J=14.44$), 89.48 ($J=185.55$), 87.23, 55.31, 52.56 ($J=3.21$), 49.07 ($J=9.11$), 45.17, 43.94, 42.55, 39.54, 38.60, 38.41, 38.32, 37.04, 33.83, 31.33, 30.71, 28.00, 27.64, 25.44 ($J=19.43$), 23.44, 22.38, 19.39, 18.53, 17.51, 17.20, 16.71, 16.52 (2C). EI-MS m/z : 570.02 (1) M^+ , 246.07 (50), 201.16 (48), 189.2 (100), 187.22 (70), 159.26 (54), 133.2 (56), 119.2 (74), 105.2 (45), 93.18 (47), 91.27 (66), 81.29 (47), 79.22 (46), 70.3 (81).

2-(1H-Imidazol-1-yl)-methylene-3-oxo-12 β -fluor-urs-13,28 β -olide (2.78): To a stirred solution of **2.74** (240 mg 0.48 mmol) in THF (3 mL), under N_2 atmosphere, at 70°C, was added CDI (155.66 mg 0.96 mmol). The workup was performed according to the same method has for **2.18** after 4 hours. The solid was subjected to flash column chromatography [hexanes-ethyl acetate from (50:50) to (30:70)], to afford **2.78** (63%). mp 316.4-321.2 °C. IR (film $CHCl_3$): 3114.5, 2929.3, 1771.3, 1685.5, 1609.3, 1518.7, 1487.8 cm^{-1} . 1H NMR (400 MHz $CDCl_3$): δ 7.86 (1H s), 7.71 (1H s), 7.24 (1H s), 7.20 (1H s), 4.96 (1H dq $J=62.31$ H12), 3.01 (1H d $J=15.83$), 2.30 (1H d $J=15.76$), 1.28 (3H s), 1.25 (3H s), 1.18 (6H s), 1.13 (3H s), 0.99 (3H s), 0.92 (3H s). ^{13}C NMR (100 MHz $CDCl_3$): δ 206.00 (C3), 178.65 (C28), 130.78, 130.02, 129.81, 123.30, 119.61, 91.81 ($J=14.26$ C13), 89.25 ($J=186.24$ C12), 52.60 ($J=2.99$), 52.22, 46.95 ($J=9.38$), 45.19,

44.09 ($J=2.57$), 43.63, 42.18, 39.53, 38.62, 36.27, 32.80, 31.30, 30.73, 29.53, 27.57, 26.02 ($J=19.68$), 22.65, 22.34, 22.04, 19.62, 19.38, 17.65, 16.93, 16.51 (2C). EI-MS m/z : 550.5 (8) M^+ , 297.1 (47), 285.09 (100), 187.01 (44), 132.97 (38), 118.97 (45), 104.94 (50), 90.94 (46), 78.9 (47), 68.95 (79). Anal. Calcd for $C_{34}H_{47}FN_2O_3$ C 74.15, H 8.60, N 5.09, found C 73.90, H 8.99, N 4.96.

2-(2'-Methyl-1*H*-imidazol-1-yl)-methylene-3-oxo-12 β -fluor-urs-13,28 β -olide

(2.79): To a stirred solution of **2.74** (240 mg 0.48 mmol) in THF (3 mL), under N_2 atmosphere, at 70°C, was added CBMI (182.6 mg 0.96 mmol). The workup was performed according to the same method as for **2.32** after 4.5 hours. The solid obtained was subjected to flash column chromatography [hexanes-ethyl acetate from (45:55) to (25:75)], to afford **2.79** (37%). mp 321.2-325.6 °C. IR (film $CHCl_3$): 3110.6, 2929.3, 1770.3, 1684.5, 1603.5, 1539.9 cm^{-1} . 1H NMR (400 MHz $CDCl_3$): δ 7.66 (1H s C2CH), 7.16 (1H s H4'), 7.03 (1H s H5'), 4.93 (1H dq $J=62.33$ H12), 2.97 (1H d $J=15.83$ H1), 2.48 (3H s CH_3 imidazole), 1.26 (3H s C26), 1.24 (3H s C27), 1.16 (6H s C23 or C24 or C29), 1.13 (3H s C23 or C24), 0.97 (3H s C30), 0.90 (3H s C25). ^{13}C NMR (100 MHz $CDCl_3$): δ 206.08 (C3), 178.59 (C28), 147.37 (C2'), 130.67 (C2CH), 128.76 (C5'), 123.05 (C2), 117.97 (C4'), 91.74 ($J=14.41$ C13), 89.33 ($J=186.24$ C12), 52.57 ($J=3.34$ C18), 52.40 (C5), 47.08 ($J=9.41$ C9), 45.24 (C17), 45.16 (C4), 44.06 ($J=2.74$ C14), 42.87 (C1), 42.21 (C8), 39.51 (C20), 38.57 (C19), 36.32 (C10), 32.83, 31.27, 30.69, 29.45 (C23 or C24), 27.56, 25.90 ($J=19.64$), 22.33, 22.15 (C23 or C24), 19.59, 19.36 (C30), 17.69 (C26), 16.94 (C27), 16.48 (C29), 16.41 (C25), 13.66 (CH_3 imidazole). EI-MS m/z : 564.06 (10) M^+ , 300.09 (21), 299.06 (100), 189.96 (81), 187.06 (21), 119.03 (20), 107.01 (22), 91 (22), 82.99 (38), 78.98 (20). Anal. Calcd for $C_{35}H_{49}FN_2O_3$ C, 74.43, H 8.74, F 3.36, N 4.96, found C 74.54, H 8.88, N 5.14.

2-(4*H* Triazol-4-yl)-methylene-3-oxo-12 β -fluor-urs-13,28 β -olide (2.80): To a stirred solution of **2.74** (250 mg 0.50 mmol) in THF (3 mL), under N_2 atmosphere, at 70°C, was added CDT (246.2 mg 1.5 mmol). The workup was performed according to the same method as for **2.46** after 5 hours. The solid was subjected to flash column chromatography [hexanes-ethyl acetate from (70:30) to (60:40)], to afford **2.80** (33%). mp 209.2-212.1 °C. IR (film $CHCl_3$): 2929.3, 2870.5, 1771.3, 1688.4, 1616.1, 1509.0,

1457.9 cm^{-1} . ^1H NMR (400 MHz CDCl_3): δ 8.39 (1H s), 8.12 (1H s), 7.81 (1H s), 4.98 (1H dq $J=62.17$), 3.59 (1H d $J=17.43$), 2.39 (1H d $J=17.26$), 1.27 (3H s), 1.24 (3H s), 1.18 (6H s), 1.13 (3H s), 0.98 (3H s), 0.90 (3H s). ^{13}C NMR (100 MHz CDCl_3): δ 206.56 (C3), 178.71 (C28), 153.03, 146.27, 128.29, 124.84, 91.92 ($J=14.37$ C13), 89.48 ($J=185.96$ C12), 52.60 ($J=3.51$), 52.48, 46.80 ($J=9.59$), 45.28, 45.20, 44.11, 43.72, 42.15, 39.54, 38.61, 35.98, 32.85, 31.31, 30.73, 29.45, 27.59, 25.92 ($J=19.45$), 22.36, 22.15, 19.65, 19.39, 17.66, 16.94, 16.50 (2C). EI-MS m/z : 552.14 (6) M^+ , 201.01 (57), 187.02 (84), 173.04 (58), 145.04 (69), 133.04 (60), 119.04 (100), 107.03 (78), 105.04 (82), 91.02 (96), 78.99 (80). Anal. Calcd for $\text{C}_{33}\text{H}_{46}\text{FN}_3\text{O}_3 \cdot 0.5\text{hexane} \cdot 0.5\text{EtOAc}$ C 71.44, H 8.99, N 6.58, found C 71.24, H 9.04, N 6.38.

Fluor 3-oxours-12-en-28-oate (2.81): To a mixture of **2.3** (200 mg 0.44 mmol) and THF (4 mL) was added deoxofluor 50% dropwise (0.64 mL 1.76 mmol), in an ice bath. The temperature was allowed to rise up until the room temperature. After 2.5 hours, was added NaHCO_3 dropwise (10 mL) to the reaction mixture. After being stirred for 30 minutes, the mixture was extracted with ether (3×50 mL). The combined extract was washed with NaHCO_3 (3×50 mL) and water (3×50 mL), dried over Na_2SO_4 , filtered and evaporated to the dryness, to afford a solid. The residue was subjected to flash column chromatography [hexanes-ethyl acetate from (95:5) to (90:10)], to afford **2.81** (84%). mp 197.9-202.0 $^\circ\text{C}$. IR (film CHCl_3): 2926.5, 2872.5, 1827.2, 1704.8, 1457.0, 1381.8 cm^{-1} . ^1H NMR (400 MHz CDCl_3): δ 5.35 (1H s), 1.25 (3H s), 1.10 (3H s), 1.09 (3H s), 1.06 (3H s), 1.05 (3H s), 0.96 (3H d $J=6.02$), 0.87 (3H d $J=5.27$). ^{13}C NMR (100 MHz CDCl_3): δ 217.64, 167.06 ($J=376.60$), 137.01, 126.56, 55.29, 52.87, 47.40, 46.71, 42.26, 39.49, 39.36, 38.95, 38.66, 36.65, 35.23, 34.15, 32.58, 30.20, 29.68, 28.11, 26.52, 24.08, 23.45, 23.29, 21.48, 20.96, 19.54, 17.00, 16.84, 15.26. EI-MS m/z : 456.99 (23) M^+ , 409.11 (30), 250.05 (100), 222.15 (39), 221.12 (49), 205.18 (44), 204.18 (23), 203.21 (52), 134.08 (34), 133.15 (67).

Flour 3 β -acetoxy-urs-12-en-28-oate (2.82): To a mixture of **2.4** (200 mg 0.4 mmol) and THF (4mL) was added deoxofluor 50% dropwise (0.6 mL 1.6 mmol), in an ice bath. The workup was performed according to the same method as for **2.81** after 1 hour. The solid was subjected to flash column chromatography [hexanes-ethyl acetate from (95:5) to

(90:10)], to afford **2.82** (98%). mp 242.7-245.7 °C. IR (film CHCl₃): 2928.4, 2878.2, 1824.3, 1734.6, 1457.0, 1370.2, 1245.8 cm⁻¹. ¹H NMR (400 MHz CDCl₃): δ 5.32 (1H s), 4.49 (1H dd *J*=15.96), 2.04 (3H s), 1.09 (3H s), 0.96 (3H s), 0.95 (3H s), 0.88 (3H s), 0.86 (3H s), 0.85 (3H s), 0.82 (3H s). ¹³C NMR (100 MHz CDCl₃): δ 170.95, 167.05 (*J*=376.37), 136.91, 126.68, 80.82, 55.29, 52.78, 48.82 (*J*=37.79), 47.41, 42.11, 39.50, 38.90, 338.66, 38.33, 37.65, 36.82, 35.25, 32.97, 30.19, 28.09, 28.04, 24.08, 23.52, 23.33, 23.29, 21.27, 20.97, 18.15, 16.99, 16.85, 16.70, 15.54. EI-MS *m/z*: 501.07 (2) M⁺, 249.91 (100), 222.02 (37), 220.96 (48), 203.01 (55), 190.05 (73), 189.11 (80), 175.13 (32), 147.15 (38), 133.14 (64), 119.14 (36), 105.26 (40).

2.4.2. Biological activity assays

1. Reagents. 3-(4,5-dimethylthiazol-2-yl)-2,5-diphenyltetrazolium bromide (MTT) powder and dimethylsulfoxide (DMSO) were obtained from Sigma Aldrich Co (St. Luis, MO). The compounds tested for biological activity were dissolved in DMSO for stock solutions, stored at -80°C. The working solutions were prepared in medium. Antibodies to poly-(ADP-ribose)-polymerase (PARP) were obtained from Boehringer Mannheim (Mannheim-Waldhof, DE), to caspases 8 and p21^{waf1} from BD Biosciences (San Jose, CA), to c-FLIP from Alexis Biochemicals (Plymouth Meeting, PA), to Mcl-1 from Santa Cruz Biotechnology Inc., (Santa Cruz, CA), to caspase 9, cleaved caspase 9, caspase 3, cleaved caspase 3 and Bcl-xL from Cell Signaling (Danvers, MA), to NOXA from Abcam (Cambridge, UK).

2. Cell culture. Cancer cells AsPC-1, MIA PaCa 2, PANC-1, PC-3, Hep G2 and A549 cells were cultured in RPMI 1640 supplemented with 10% of FBS. MCF-7 cells were cultured in DMEM supplemented with 5% FBS and 1mg/mL insulin.

3. Determination of cell growth inhibition. AsPC-1, MIA PaCa 2, PANC-1, MCF-7, PC-3, Hep G2 and A549 cells were plated with 1.0×10³ cells/well in 96-well plates in 100 μl medium. The tested compounds with variant concentrations in 100 μl were added 24 h after seeding and the cells were continued to culture for 3 days. Fifty μl of MTT (0.5 mg/ml) was added to each well and incubated for 4 h. Supernatant was removed and the

formazan precipitated was dissolved in DMSO (100 μ l). The density of absorbance was measured at 570 nm on a multiple plate reader. Concentrations that inhibited cell growth by 50% (IC_{50}) were determined by nonlinear regression with GraphPad Prism software version 5.0 (GraphPad Software, Inc., San Diego, CA).

4. Cell cycle analysis. Cell cycle was assessed by flow cytometry using a fluorescence activated cell sorter (FACS). AsPC-1 cells were treated with diverse concentrations of compounds **2.57** and **2.72** for 24 h, and then fixed with ice-cold 70% ethanol at a density of 1×10^6 cells/mL. The cells were treated with PI/RNase solution according to the manufactures protocol. DNA content was quantitated by a flow cytometry (Becton Dickinson, San Jose, CA) with an excitation wavelength of 488 nm and an emission wavelength of 625 nm.

5. Western blot analysis. Protein extracts of cells treated with compounds **2.57** and **2.72** at variant concentrations for 24 h were prepared with RIPA lysis buffer [50 mM Tris-HCl, 150 mM NaCl, 0.1% sodium dodecyl sulfate (SDS), 1% NP-40, 0.5% sodium deoxycholate, 1 mM phenylmethylsulfonyl fluoride (PMSF), 100 μ M leupeptin, and 2 μ g/mL aprotinin (pH 8.0)]. These protein extracts were separated on 8%, 10% or 12% SDS-polyacrylamide gel and transferred to nitrocellulose membranes. The membranes were stained with 0.2% Ponceau S red to assure equal protein loading and transfer. After blocking with 5% nonfat milk for 30 minutes, the membranes were incubated with a primary specific antibody over night at 4°C. The membranes were then washed with TBS-tween 1% buffer for three times and incubated for 1.5 h with the appropriate secondary antibody in 1% non fat milk. After incubation the membranes were washed with TBS-tween 1% buffer. The immunocomplexes were visualized using enhanced chemiluminescence western blotting detection reagent (Amersahm Biosciences, England, UK).

3.

**Oleanolic acid derivatives:
synthetic routes,
structural elucidation,
biological evaluation
and SAR studies**

A panel of new oleanane derivatives with heterocyclic ring(s) and fluorine in several positions of the oleanane backbone was prepared and duly characterized using MS, IR and NMR. Hydroxy-lactones and 12-oxo derivatives were synthesized using novel methodologies with good yields. These intermediates and others served as starting materials for the synthesis of the new compounds.

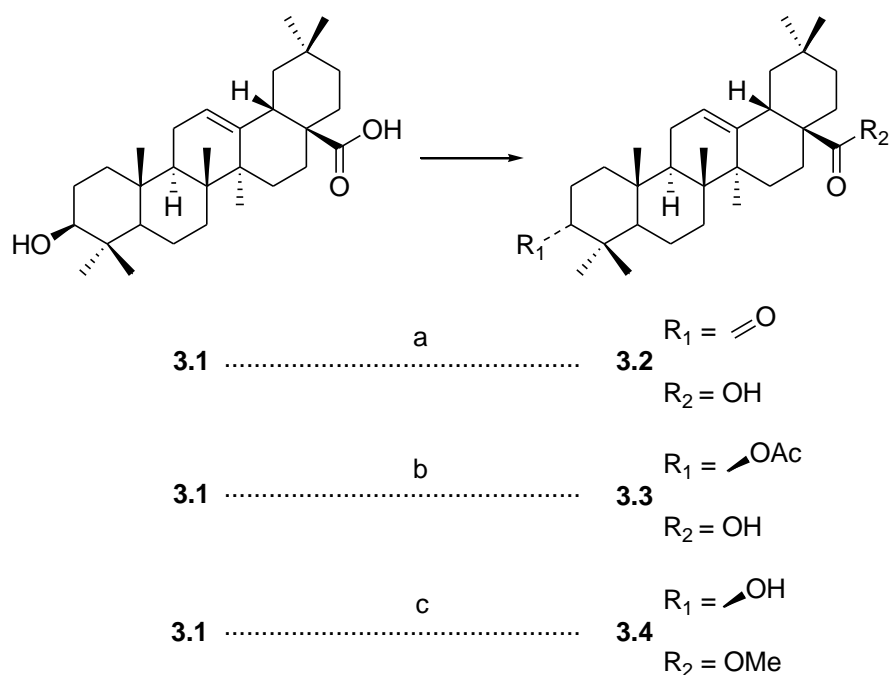
Heterocyclic derivatives were prepared via the reaction of the appropriate oleanane derivative or oleanolic acid **3.1** with commercially available reagents, such as CDI, CBMI and CDT. These modifications were performed mainly at carbons C2, C3, C12 and C28. Deoxofluor and selectfluor were used as nucleophilic and electrophilic reagents, respectively, in the synthesis of new fluorine oleanane derivatives.

The novel compounds synthesized were tested for their ability to inhibit the growth of AsPC-1 pancreatic cancer cell. Compounds **3.27**, **3.39** and **3.49** were the most active, and were studied further for their antiproliferative activity in other solid tumor cells. In addition, these compounds were found to induce apoptosis in AsPC-1 cells.

3.1. Intermediates synthesis

Most of the oleanolic acid intermediates have already been described and characterized, and some can be isolated from natural sources.^{363, 476} The reactions used to prepare the necessary oleanolic acid intermediates were performed according to previously described reactions for triterpenoids. The oxidation and acetylation of the secondary alcohol at C3 in oleanolic acid **3.1** were performed according to the literature, with good yields (Scheme 3.1.1).^{183, 241} Methylation of the carboxylic acid in oleanolic acid **3.1** was made via the reaction with methyl iodide, affording compound **3.4** with significant yields (Scheme 3.1.1).^{428, 429, 434}

Scheme 3.1.1.^a Synthesis of derivatives **3.2-3.4**.

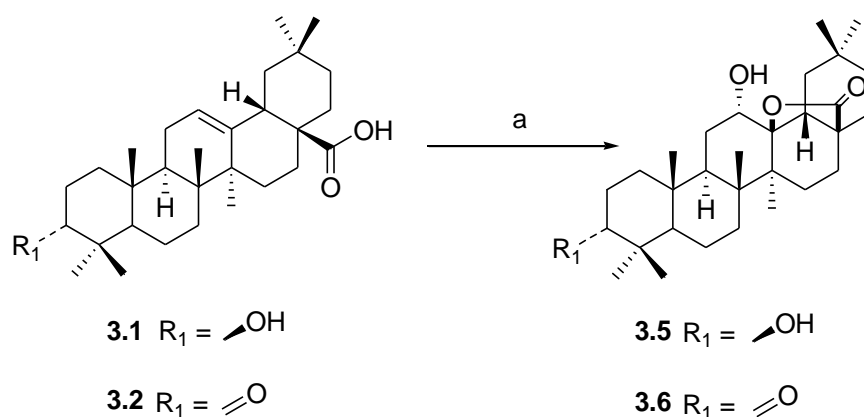


^aReagents: (a) Jones reagent, acetone, ice; (b) Acetic anhydride, DMAP, THF, r.t.; (c) CH_3I , K_2CO_3 , DMF, N_2 , r.t.

Oleanolic δ -hydroxy- γ -lactones can be obtained from Δ^{12} -oleananes by oxidative 28,13 β -lactonization. This reaction was performed under photochemical irradiation,^{477, 478} with weak selectivity and low isolated yields. Alternatively, oxidation reagents such as

oxygen peroxide in acetic acid,⁴⁷⁹ the inorganic salt mixtures $\text{KMnO}_4/\text{CuSO}_4$,³⁰⁶ ozone^{332, 480, 481} and *m*-chloroperoxybenzoic acid (*m*-CPBA)⁴⁸², resulted in low yields and poor selectivity. Herein, the β -hydroxy- γ -lactones were obtained via *m*-CPBA oxidation, with high selectivity and yields higher than 90% (Scheme 3.1.2).⁴⁸³ The formation of the δ -hydroxy- γ -lactones **3.5** and **3.6** occurs via the epoxidation of the parental compound (**3.1** or **3.2**), followed by the nucleophilic attack of the 28-carbonyl group at C13 from the β -face, with ring-opening of the 12 α , 13 α epoxide intermediate.⁴⁸⁴

Scheme 3.1.2.^a Synthesis of derivatives **3.5** and **3.6**.



^aReagents: (a) *m*-CPBA 77%, CH_2Cl_2 , r.t.

Oleanolic acid **3.1** is well characterized by NMR data, with the identification of proton H12 as a singlet at 5.49 ppm, and proton H β 18 as a double doublet at 3.30 ppm.⁴⁴³ The preparation of a δ -hydroxy- γ -lactone was confirmed in compound **3.5** by the absence of the characteristic δ signal for proton H12, which is present at 3.88 ppm in this compound. Proton H18 presents a signal at δ 2.04 ppm, this value is lower than in the substrate oleanolic acid **3.1**, which may be explained by the magnetic anisotropy induced by the lactone moiety (Figure 3.1.1). The β configuration is illustrated by the ORTEP diagram in Figure 3.1.2.

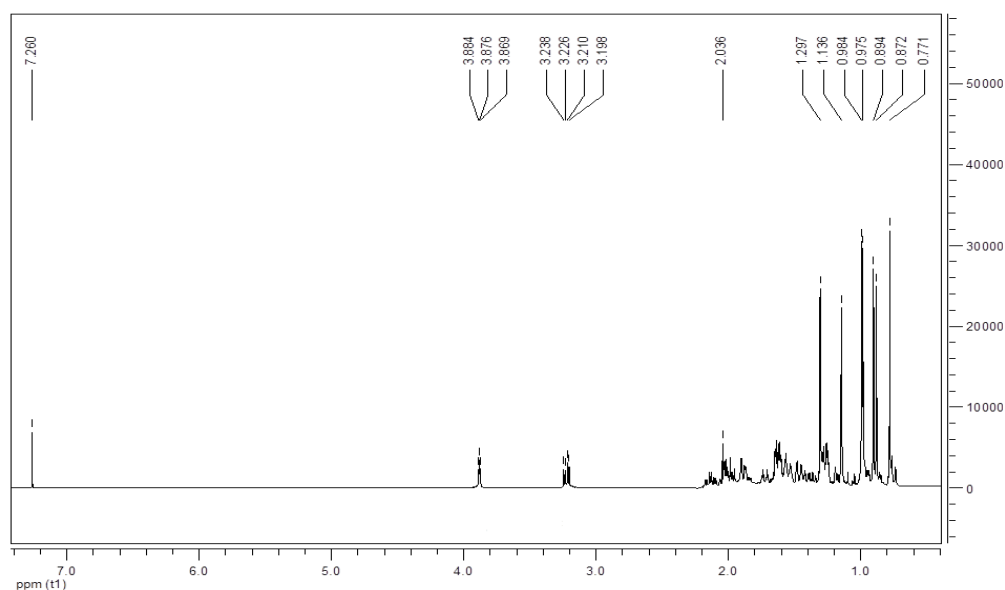


Figure 3.1.1. ^1H NMR spectrum of compound **3.5**.

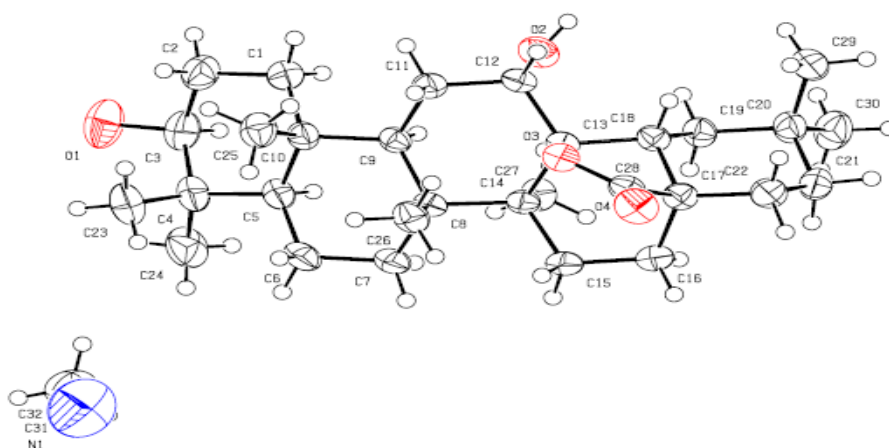
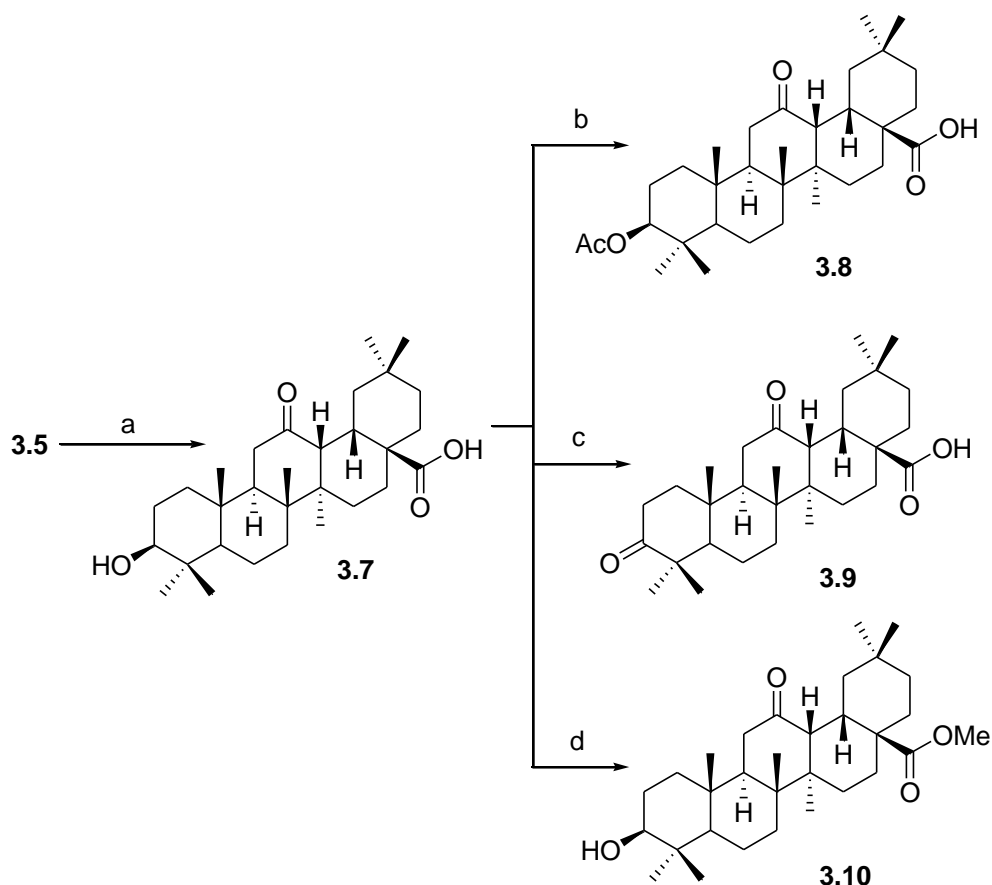


Figure 3.1.2. ORTEP diagram of compound **3.5** (50% probability level, H atoms of arbitrary sizes). The asymmetric unit also contains a molecule of acetonitrile.

In the past few years, bismuth(III) salts have emerged as convenient reagents for the development of a new chemical process for the synthesis of pharmaceutical interest molecules, under more “ecofriendly” reaction conditions.⁴⁸⁵⁻⁴⁸⁸ The reaction of compound **3.5** with 1 mol% of bismuth(III) triflate, in dichloromethane, at reflux, afforded the corresponding 12-oxo-28-carboxylic acid **3.7**, in 96% crude yield, after 3 hours (Scheme

3.1.3). Under these conditions bismuth(III) triflate is hydrolyzed, affording Brønsted acid species in situ, which promote the ring opening of the 13,28 β olide group, the formation of a carbocation at C13, and the rearrangement of the 12 α -hydroxy group to a carbonyl group.⁴⁸³

Scheme 3.1.3.^a Synthesis of derivatives **3.7-3.10**.



^aReagents: (a) Bi(OTf)₃, CH₂Cl₂, reflux; (b) Acetic anhydride, DMAP, THF, r.t.; (c) Jones reagent, acetone, ice; (d) CH₃I, K₂CO₃, DMF, N₂, r.t.

Structural elucidation of the 12-oxo-oleanane derivatives **3.7-3.10** allowed the identification of carbons C12 and C28. In compound **3.7** carbon C12 is identified as a δ signal at 211.54 ppm, and carbon C28 as a δ 183.64 ppm (Figure 3.1.3). The correlations between protons H13 and H18 signals in the NOESY spectrum allowed to assign a β stereochemistry to these protons, in compounds **3.7-3.10**, which was further confirmed by the ORTEP diagram of compound **3.9** (Figure 3.1.4).

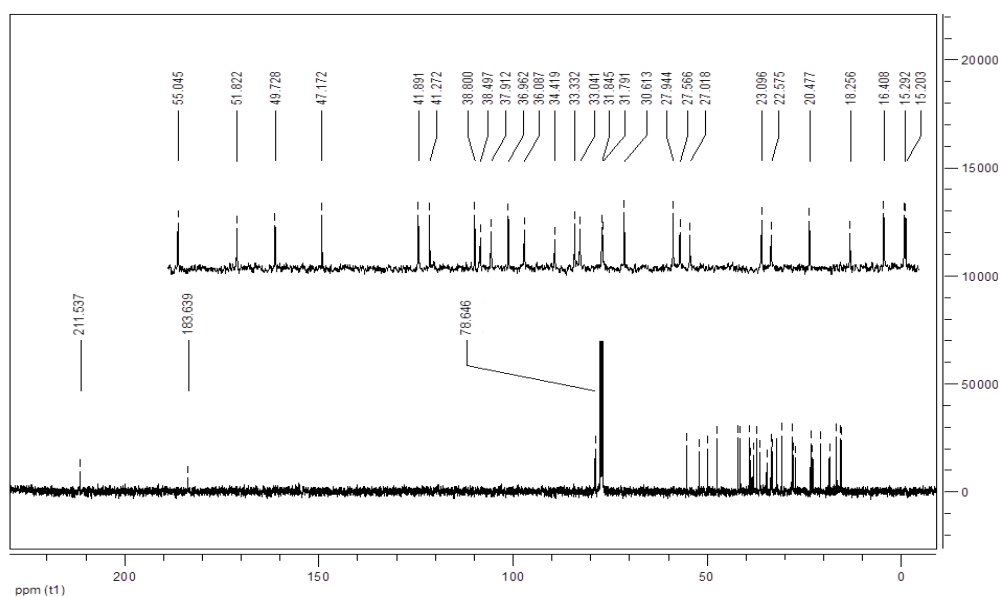


Figure 3.1.3. ^{13}C NMR spectrum of compound **3.7**.

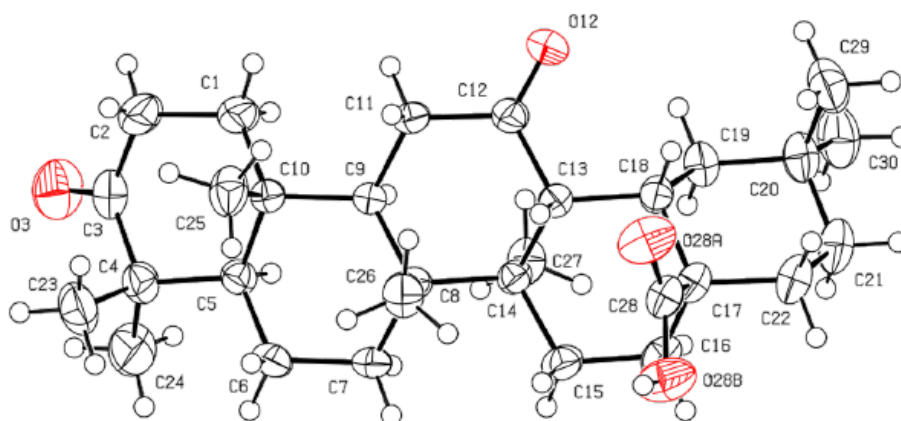
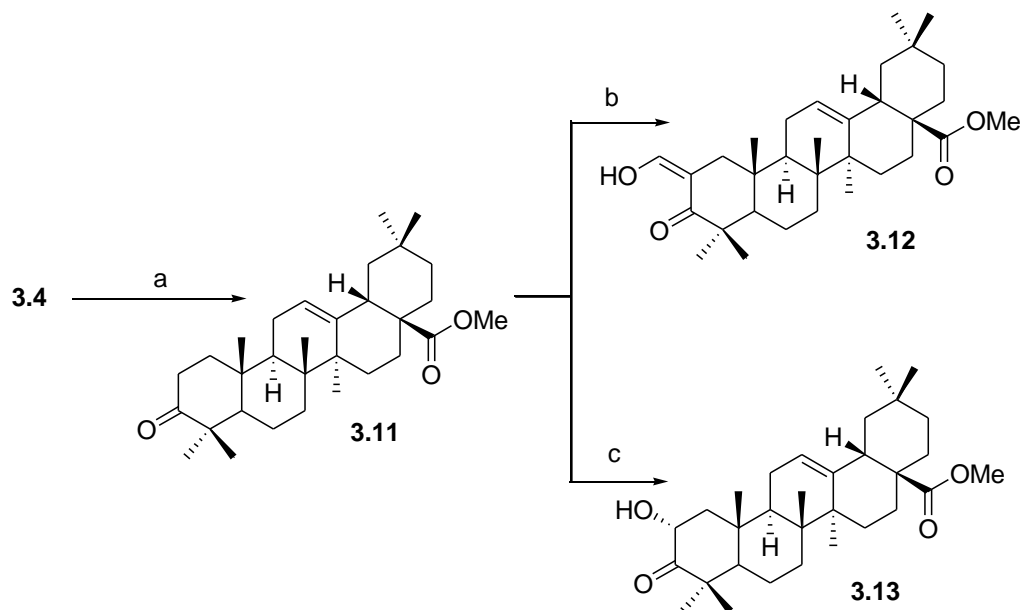


Figure 3.1.4. ORTEP diagram of compound **3.9** (50% probability level, H atoms of arbitrary sizes).

The reaction of compound **3.11** with ethyl formate and sodium methoxide allows the preparation of derivatives with an unsaturated exocyclic double bond in ring A (Scheme 3.1.4).^{330, 430, 431} In compound **3.12**, the signal at around δ 7.8 ppm corresponds to the proton in the exocyclic double bond at C2 in the ^1H NMR spectrum. In the ^{13}C NMR spectrum, the presence of this moiety is confirmed by the signal around δ 131 ppm. The signal for carbon C2 appears at around δ 123 ppm.

Scheme 3.1.4.^a Synthesis of derivatives 3.11-3.13.

^aReagents: (a) Jones reagent, acetone, ice; (b) Ethyl formate, benzene, NaOMe, r.t.; (c) *m*-CPBA 77%, H₂SO₄, CH₂Cl₂, MeOH, ice-r.t.

Compound **3.11**, in the presence of *m*-CPBA and concentrated sulfuric acid (catalyst), afforded methyl 2 α -hydroxy-3-oxoolean-12-en-28-oate **3.13** (Scheme 3.1.4).^{328, 489} The presence of the α -hydroxy group was confirmed using IR, which presented a band at 3485 cm⁻¹ corresponding to the stretching vibration of the hydroxyl group, as well as using NMR. In the ¹H NMR spectrum, proton H2 presents as a double doublet signal at δ 4.53 ppm. The signal for carbon C2 appears at δ 69.15 ppm in the ¹³C NMR spectrum. The signals for protons H12 and H18 are according to what was previously described for the oleanane compounds (Figure 3.1.5).⁴⁴³

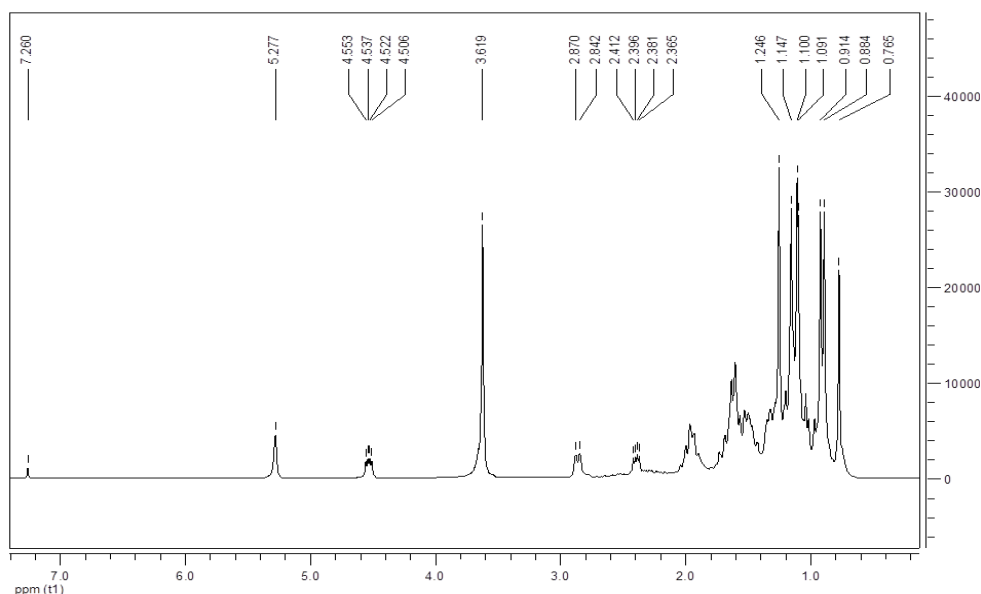
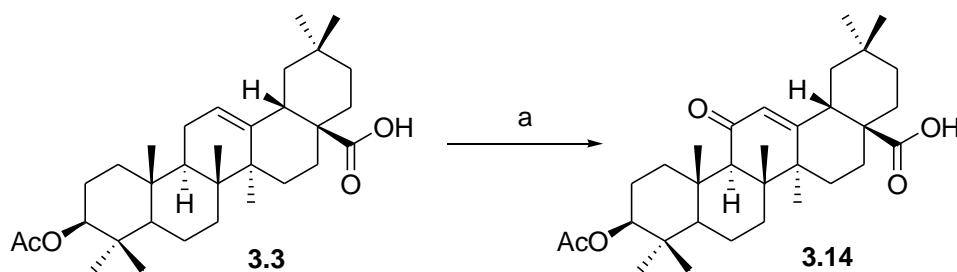


Figure 3.1.5. ^1H NMR spectrum of compound **3.13**.

Mixtures of *tert*-butyl hydroperoxide and cobalt salts have been used for the allylic oxidation of Δ^5 steroids.^{490, 491} Under these conditions, compound **3.3** affords the allylic oxidation of ring C (Scheme 3.1.5). The presence of the carbonyl group in ring C is visualized in the IR spectrum as a sharp band at 1699 cm^{-1} . The presence of the carbonyl moiety in ring C leads to the increase in the δ signals for proton H12, and for carbons C12 and C13 in the ^1H and ^{13}C NMR spectra, which is in accordance with the literature.⁴⁴³

Scheme 3.1.5.^a Synthesis of derivative **3.14**.



^aReagents: (a) *t*-BuOOH, $\text{Co}(\text{OAc})_2 \cdot 4\text{H}_2\text{O}$, MeCN, EtOAc, 77°C .

3.2. Heterocyclic and fluorine derivatives

3.2.1. Introduction

The introduction of a heterocyclic ring(s) in the structure of triterpenoids is a modification that has been performed in betulinic acid and betulin, affording several derivatives.^{433, 434, 437} The introduction of the heterocyclic ring has to be made via the reaction of an alcohol or a carboxylic acid with CDI, CBMI or CDT in THF at reflux under inert atmosphere, giving origin to *N*-alkylimidazoles,⁴³⁸⁻⁴⁴⁰ imidazole carboxylic esters (carbamates),^{433, 434, 441} or *N*-acylimidazoles.⁴⁴² The formation of *N*-acylimidazoles, carbamates or *N*-alkylimidazoles depends on the nature of the reactive alcohol or carboxylic acid and on the reaction conditions used. All products are formed by the nucleophilic attack of the alcohol to the carbonyl group of the imidazole reagent.^{438, 440, 442} A library of new *N*-acylimidazoles, carbamates and/or *N*-alkylimidazoles was synthesized via the introduction of imidazole, methylimidazole or triazole as heterocyclic rings in several positions of oleanolic acid **3.1** and derivatives, to understand the influence of the heterocyclic ring on the antiproliferative activity.

Fluorine is the least abundant halide in natural compounds and few living cells can metabolize it.^{446, 447} The introduction of a fluorine substituent in currently used pharmaceutical compounds has increased from less than 2% to around 20% since 1970.^{448, 449} Fluorinated organic compounds can be achieved using nucleophilic, electrophilic and radical forms of fluorine reagents.⁴⁵⁰ Fluorine is a small and highly electronegative atom, and its presence in key positions of biologically active molecules can improve metabolic and chemical stability, membrane permeability and binding affinity.^{448, 452, 455, 457} 5-Fluorouracil was the first synthetic fluorinated chemotherapeutic compound, and is still widely used in medicine as an anticancer agent.^{448, 458, 459} In addition, fluorinated compounds are often found in currently used anticancer drugs, including topoisomerase inhibitor gemcitabine,⁴⁹²⁻⁴⁹⁴ and anti-androgen agent flutamide.^{447, 495} This led us to develop fluorinated oleanolic acid **3.1** derivatives as an attempt to improve the antitumor activity further.

3.2.2. Results and Discussion

3.2.2.1. Chemistry

3.2.2.1.1. Imidazole derivatives

Imidazole oleanane derivatives **3.15-3.29** were prepared via the reaction of CDI with the parental compound. Compounds **3.15**, **3.16**, **3.19**, **3.20-3.23**, **3.26** and **3.28** are carbamates (Schemes 3.2.1-3.2.4); **3.17**, **3.18**, **3.24**, **3.25**, and **3.29** are *N*-acylimidazoles (Schemes 3.2.1 and 3.2.3), and **3.27** is an *N*-alkylimidazole (Scheme 3.2.4)

In the IR spectrum, carbamate **3.15** has two bands at 1760 and 1697 cm^{-1} , corresponding to the carbonyl stretching vibration of the anhydride and the carboxylic acid, respectively. The hydroxy moiety of the carboxylic acid overlaps with the C-H absorptions (Figure 3.2.1).

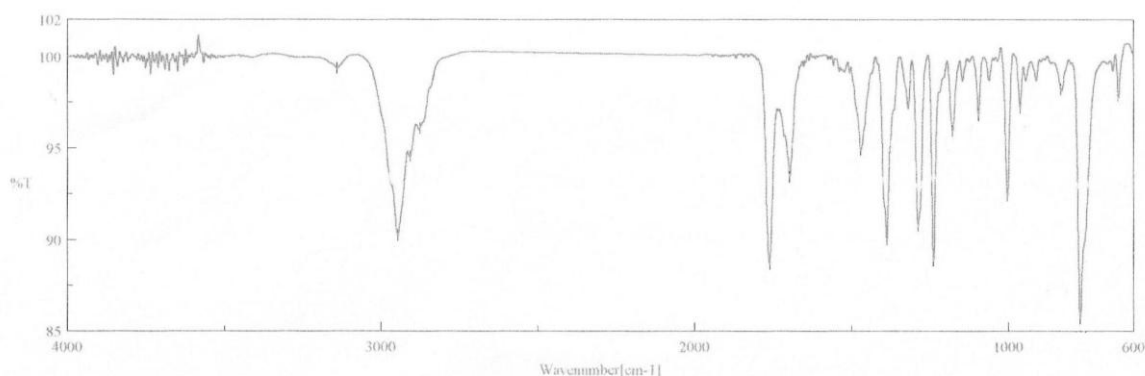
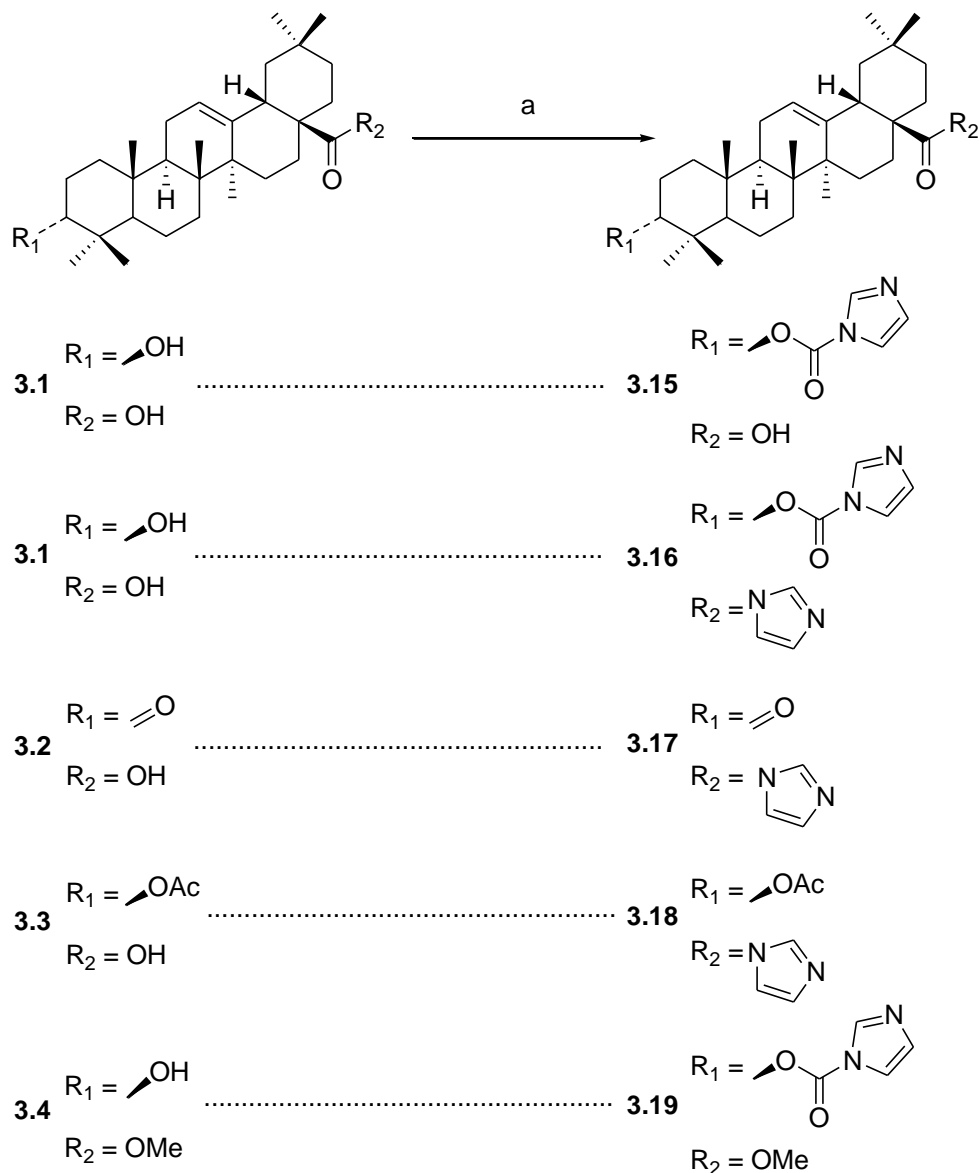


Figure 3.2.1. IR spectrum of compound **3.15**.

Scheme 3.2.1.^a Synthesis of derivatives 3.15-3.19.

^aReagents: (a) CDI, THF, N₂, reflux.

The use of 1D and 2D NMR techniques allowed the identification of several δ signals in the ¹H and ¹³C NMR spectra of compound **3.15** (Table 3.2.1). The presence of the imidazole group was confirmed by the visualization of three δ signals at 8.21, 7.44 and 7.13 ppm in the ¹H NMR spectrum, corresponding to the heterocyclic ring protons. The δ signal at 5.28 ppm corresponds to proton H12, which correlates with carbons C9 (δ 47.54 ppm) and C18 (δ 40.96 ppm), allowing the assignment of the double doublet δ signal at 3.04 ppm to proton H18 in the ¹H NMR spectrum (Figures 3.2.2 and 3.2.3).

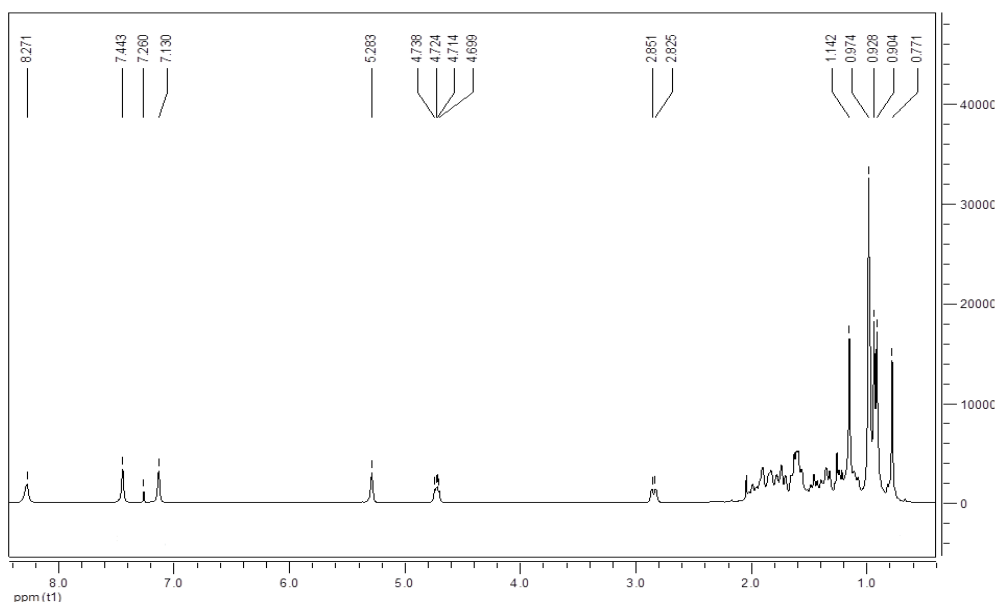


Figure 3.2.2. ^1H NMR spectrum of compound **3.15**.

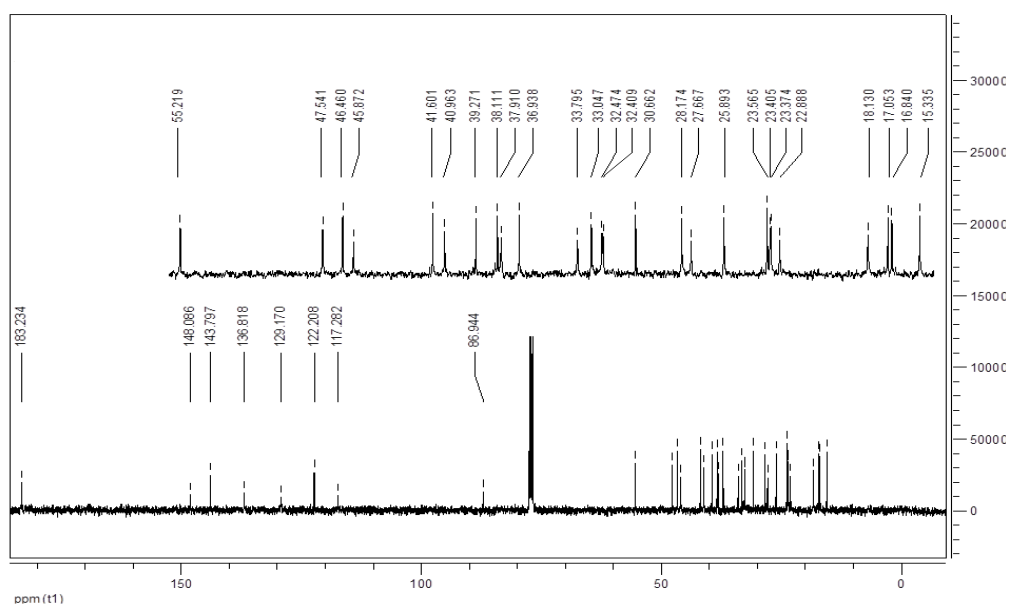


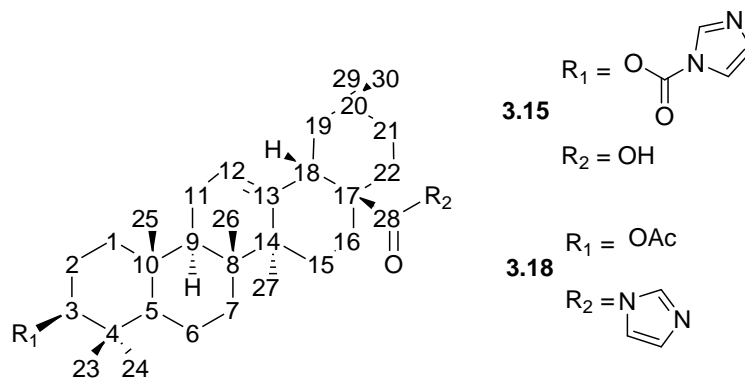
Figure 3.2.3. ^{13}C NMR spectrum of compound **3.15**.

The δ signal at 143.80 ppm corresponds to carbon C13, as proton H18 and the methyl group at C27 correlate with this signal, in compound **3.15**. Proton H18, in addition to correlating with carbon C13, correlates with carbons C12, C14, C19 and C28. Methyl groups at C25 and C26 correlate with carbon C9. Methyl groups at C23, C24 and C25 appear as a single singlet signal in the ^1H NMR spectrum at δ 0.97 ppm. Proton H3

correlates with carbon C2 and the carbon of the carbonyl group at the carbamate moiety, allowing the identification of these two signals.

Compound **3.18** was also analyzed using 1D and 2D NMR techniques which allowed the attribution of several δ signals. The results are presented in Table 3.2.1.

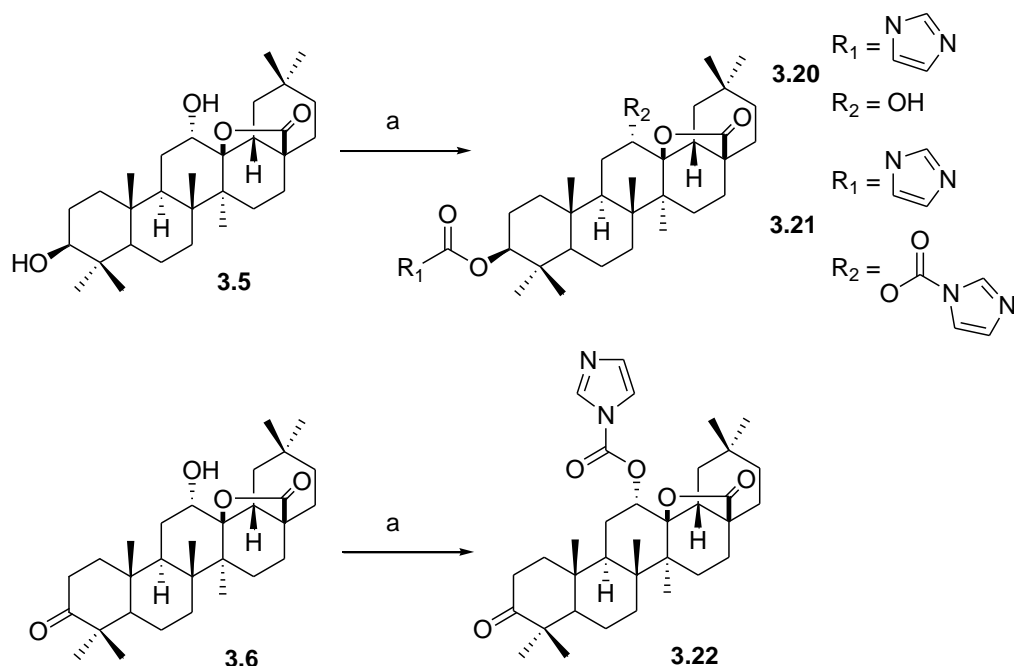
Table 3.2.1. Selected ^1H and ^{13}C NMR data from the backbone of compounds **3.15** and **3.18**.



| Entry | Position | 3.15 | | 3.18 | |
|-------|--------------------------|-----------------------|------------|-----------------------|------------|
| | | δ H | δ C | δ H | δ C |
| 1 | 3 | 4.72 ($J=15.57$) | 86.94 | 4.47 ($J=15.94$) | 80.79 |
| 2 | 4 | - | 38.11 | - | 37.63 |
| 3 | 5 | - | 55.22 | 0.79 | 55.26 |
| 4 | 8 | - | 39.27 | - | 39.17 |
| 5 | 9 | - | 47.54 | - | 47.46 |
| 6 | 10 | - | - | - | 36.86 |
| 7 | 12 | 5.28 | 122.21 | 5.34 ($J=7.16$) | 123.13 |
| 8 | 13 | - | 143.80 | - | 142.58 |
| 9 | 14 | - | 41.60 | - | 41.78 |
| 10 | 17 | - | - | - | 49.86 |
| 11 | 18 | 2.84 ($J=10.46$) | 40.96 | 3.04 ($J=18.42$) | 42.51 |
| 12 | 19 | - | 45.87 | - | - |
| 13 | 20 | - | - | - | 30.36 |
| 14 | 25 | - | - | 0.91 | 15.37 |
| 15 | 26 | 0.77 | 17.05 | 0.66 | 16.66 |
| 16 | 27 | 1.14 | 25.89 | 1.41 | 25.76 |
| 17 | 28 | - | 183.23 | - | 174.55 |
| 18 | <u>OCO</u> | - | 148.09 | - | 170.97 |
| 19 | <u>OCOCH₃</u> | - | - | 2.03 | 21.26 |

The reaction of the δ -hydroxy- γ -lactones **3.5** and **3.6** with CDI affords δ -carbamate- γ -lactones **3.21** and **3.22**, respectively. In a selective way, carbamate δ -hydroxy- γ -lactone **3.20** can also be prepared from the reaction of CDI with the δ -hydroxy- γ -lactone **3.5** (Scheme 3.2.2).

Scheme 3.2.2.^a Synthesis of derivatives **3.20-3.22**.



^aReagents: (a) CDI, THF, N₂, reflux.

The full characterization of carbamates **3.20-3.22** was made using IR, MS and 1D and 2D NMR. Compound **3.20**, which has a α -hydroxyl group at C12, exhibits a broad band in the IR at around 3400 cm⁻¹, corresponding to the hydroxyl group. The stretching vibration bands of the carbonyl groups in these compounds are present in the IR as sharp bands at around 1700 cm⁻¹. The analysis of the NMR experiments for compound **3.21** allowed the attribution of several signals in the ¹H and ¹³C NMR spectra. Figure 3.2.4 shows some of the HMBC correlations found for this derivative (Table 3.2.2).

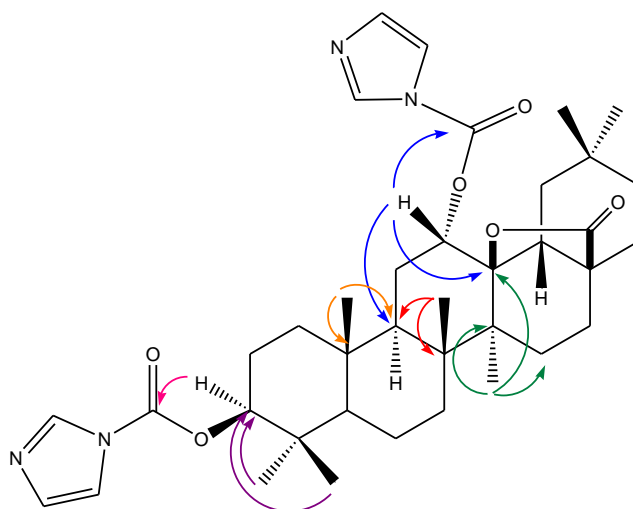


Figure 3.2.4. Selected HMBC correlations for compound **3.21**.

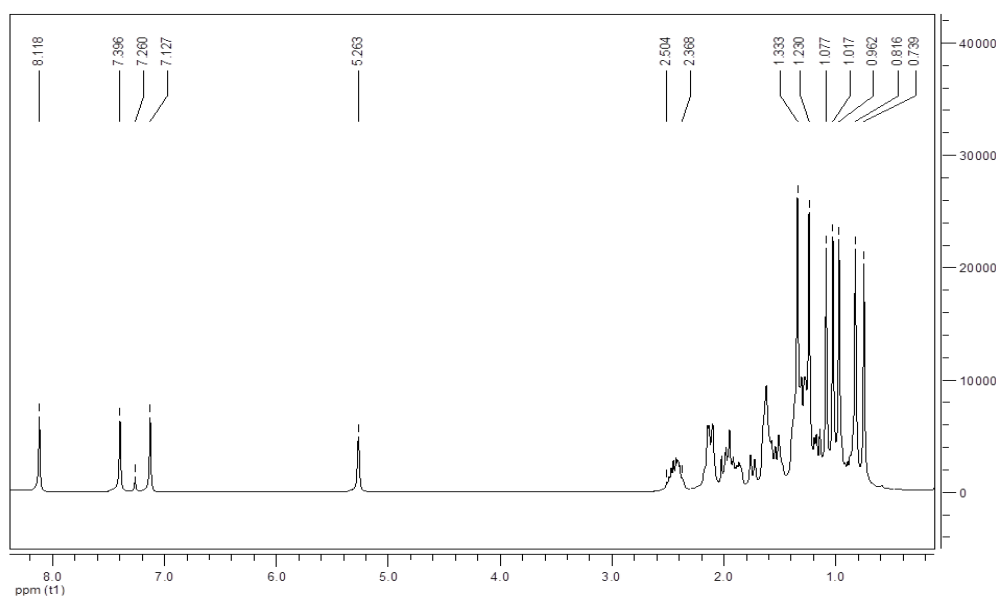


Figure 3.2.5. ^1H NMR spectrum of compound **3.22**.

The presence of the heterocyclic ring in compound **3.22** was confirmed by the presence of the δ signals at 8.12, 7.40 and 7.13 ppm in the ^1H NMR spectrum, which correspond to the δ signals at 136.80, 116.86 and 131.33 ppm, respectively, in the ^{13}C NMR spectrum (Figures 3.2.5-3.2.7). In the ^{13}C NMR spectrum, the signal for the carbonyl group of the carbamate is present at δ 147.51 ppm, and the signal for the carbonyl group at C3 appears at 216.84 ppm (Figure 3.2.6).

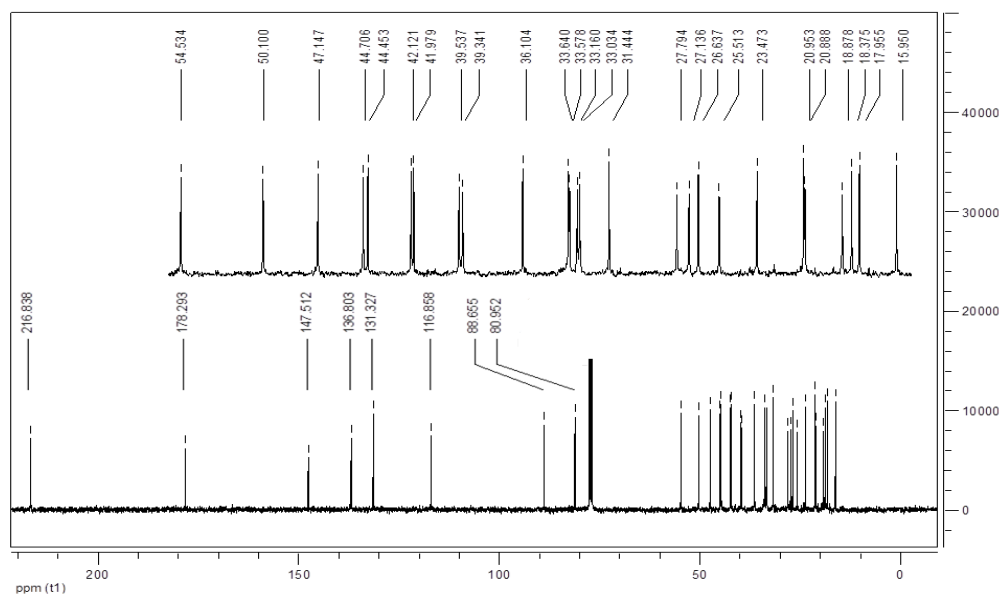


Figure 3.2.6. ^{13}C NMR spectrum of compound 3.22.

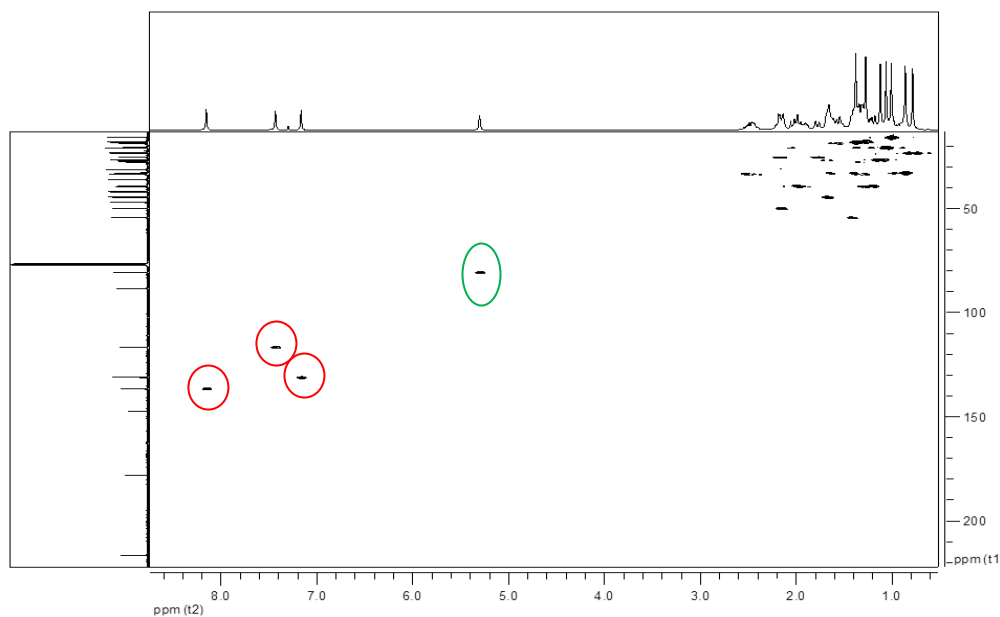


Figure 3.2.7. HMQC spectrum of compound 3.22, with the correlations between protons and carbons of imidazole ring (red) and at position C12 (green).

The identification of proton H12, with a δ signal at 5.26 ppm, allowed the visualization of the correlations with carbons C9, C11, C13 and the carbonyl group of the carbamate present at C12, with the consequent identification of these signals (Figure

3.2.8). Proton H12 has a higher δ signal than is usually seen for geminal protons of a carbamate group, due to the presence of the δ -lactone moiety (Figures 3.2.5 and 3.2.7).

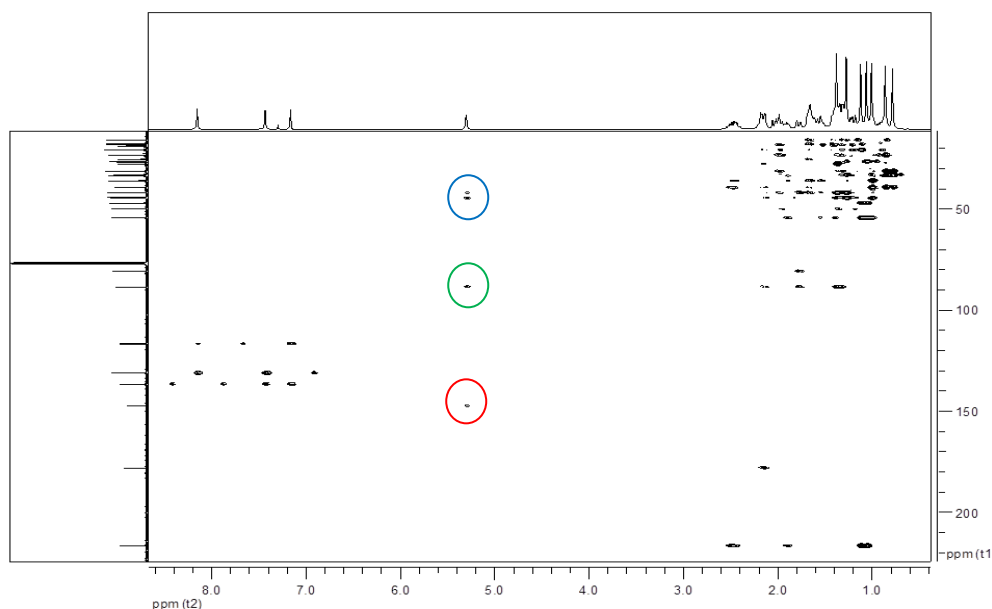


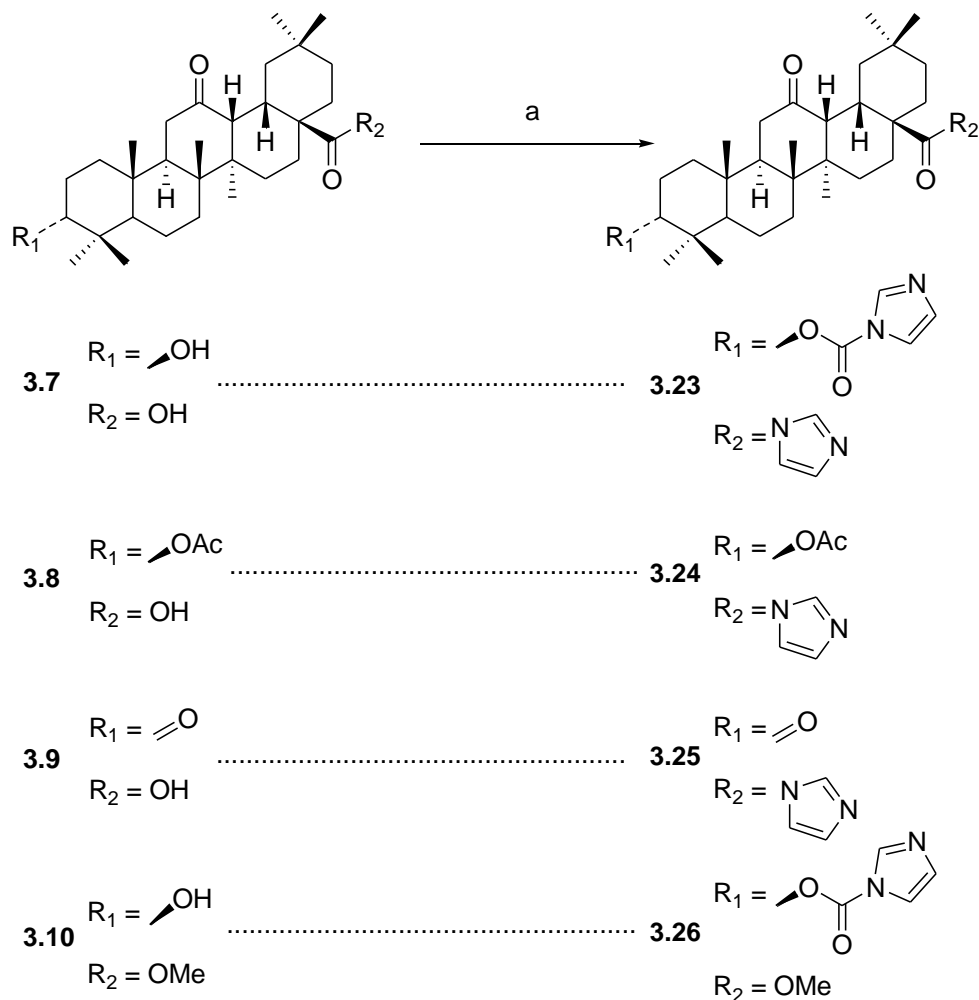
Figure 3.2.8. HMBC spectrum of compound **3.22**. Correlations between proton H12 and carbonyl carbon, carbon C13, and carbons C9 and C11, are highlighted in red, green and blue, respectively.

Other correlations were observed in the HMBC of compound **3.22**, in particular between the methyl groups and the vicinal carbons, which allowed the identification of several protons and δ carbons signals. The correlation of carbon C13 allowed the identification of the methyl group at C27. The identification of the methyl group at C27 allowed the recognition of the methyl group at C26, and consequently the identification of the methyl group at C25 (Table 3.2.2).

Table 3.2.2. Selected ^1H and ^{13}C NMR data of the backbone for compounds **3.21** and **3.22**.

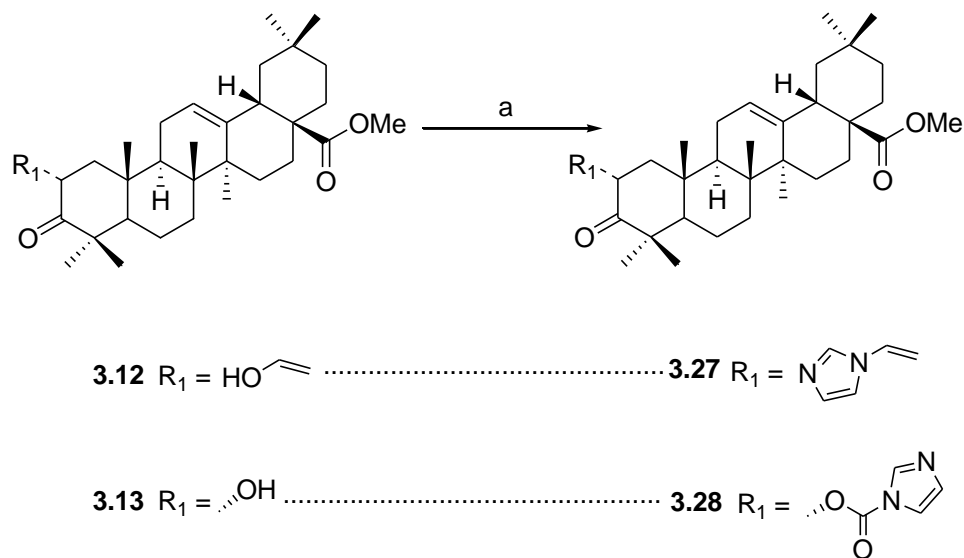
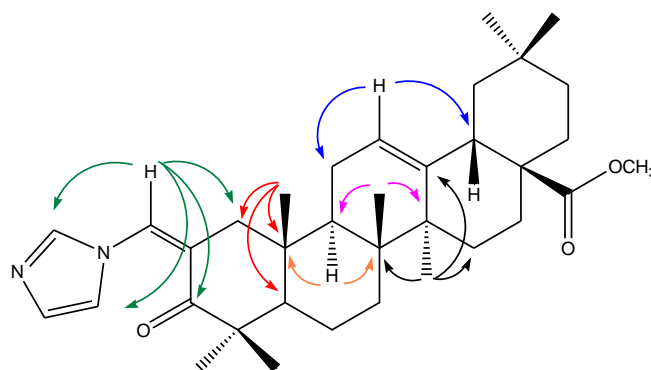
| Entry | Position | 3.21 | | 3.22 | |
|-----------|---------------------|-----------------------------|------------|------------|------------|
| | | δ H | δ C | δ H | δ C |
| <i>1</i> | 1 | - | - | - | 39.34 |
| <i>2</i> | 2 | - | - | - | 33.64 |
| <i>3</i> | 3 | 4.63 (<i>J</i> = 16.03) | 85.37 | - | 216.84 |
| <i>4</i> | 4 | - | 38.02 | - | 47.15 |
| <i>5</i> | 5 | 0.88 | 54.93 | - | 54.53 |
| <i>6</i> | 7 | - | 33.56 | - | 33.16 |
| <i>7</i> | 8 | - | 42.01 | - | 42.12 |
| <i>8</i> | 9 | - | 45.22 | - | 44.71 |
| <i>9</i> | 10 | - | 36.19 | - | 36.10 |
| <i>10</i> | 11 | - | - | - | 25.51 |
| <i>11</i> | 12 | 5.23 | 80.87 | 5.26 | 80.95 |
| <i>12</i> | 13 | - | 88.49 | - | 88.66 |
| <i>13</i> | 14 | - | 41.93 | - | 41.98 |
| <i>14</i> | 15 | - | 27.66 | - | 27.79 |
| <i>15</i> | 17 | - | 44.32 | - | 44.45 |
| <i>16</i> | 18 | - | 49.86 | - | 50.10 |
| <i>17</i> | 19 | - | 39.16 | - | 39.54 |
| <i>18</i> | 20 | - | 31.31 | - | 31.44 |
| <i>19</i> | 21 | - | - | - | 33.58 |
| <i>20</i> | 25 | - | - | 0.96 | 15.95 |
| <i>21</i> | 26 | 1.17 | 18.21 | 1.23 | 18.00 |
| <i>22</i> | 27 | 1.30 | 18.40 | 1.33 | 18.38 |
| <i>23</i> | 28 | - | 178.17 | - | 178.29 |
| <i>24</i> | C12<u>CO</u> | - | 147.45 | - | 147.51 |
| <i>25</i> | C3<u>CO</u> | - | 148.19 | - | - |

Reaction of compounds **3.7-3.10** with CDI resulted in compounds **3.23-3.26** (Scheme 3.2.3). Structural elucidation was made by the same means as for compounds **2.16-2.19**, taking into consideration the substitution of the double bond with a carbonyl group in ring C. The carbonyl group at C12 is identified by a band in the IR spectrum at around 1700 cm^{-1} and by a signal in the ^{13}C NMR spectrum at around δ 210 ppm.

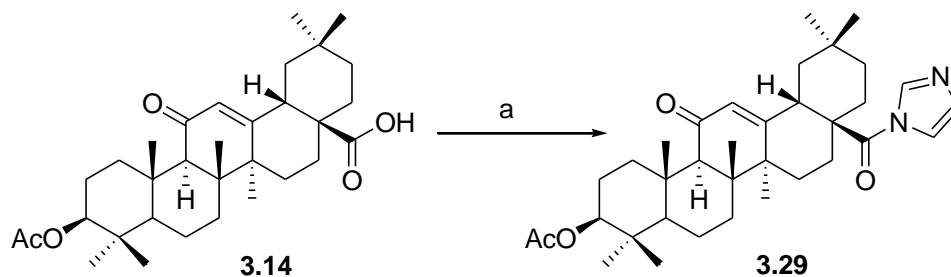
Scheme 3.2.3.^a Synthesis of derivatives 3.23-3.26.

^aReagents: (a) CDI, THF, N₂, reflux.

Compounds **3.12** and **3.13**, which have a vinyl alcohol and a secondary alcohol at C2, respectively, react with CDI to afford *N*-alkylimidazole **3.27** and carbamate **3.28** (Scheme 3.2.4). The introduction of the imidazole group was detected by the presence of three singlets in the ¹H NMR spectrum with δ signals higher than 7 ppm, corresponding to the protons in the heterocyclic ring. Both compounds (**3.27** and **3.28**) have a methoxy group at C28, which results in a lower δ signal in the ¹³C NMR spectrum than that observed in the parental oleanolic acid **3.1**. Carbamate **3.28** exhibits a signal at δ 5.70 ppm corresponding to proton H2. The signal at δ 5.27 ppm was identified as proton H12 (Table 3.2.3).

Scheme 3.2.4.^a Synthesis of derivatives **3.27** and **3.28**.^aReagents: (a) CDI, THF, N₂, reflux.**Figure 3.2.9.** Selected HMBC correlations for compound **3.27**.

N-alkylimidazole **3.27**, with an α,β unsaturated ketone in ring A, has several correlations in the HMBC spectrum that allowed the identification of various δ signals (Figure 3.2.9). In ring A, the proton of the exocyclic double bond correlates with carbons C1, C3, C2' and C5', which allows the attribution of the signal at δ 130.36 ppm to C3', as there is no interaction with this carbon. Other correlations allow the identification of methyl groups at C25, C26 and C27. Methyl groups at C23 and C24, C29 and C30 were not distinguishable as they are geminal groups.

Scheme 3.2.5.^a Synthesis of derivative **3.29**.

^aReagents: (a) CDI, THF, N₂, reflux.

Compound **3.14**, which has a carbonyl group in ring C at C11, reacts with CDI yielding amide **3.29**. The presence of the tertiary amide is confirmed by the band at 1654.6 cm⁻¹ in the IR spectrum (Figure 3.2.10). The analysis of the 1D and 2D NMR spectra permitted the identification of several δ signals (Table 3.2.3).

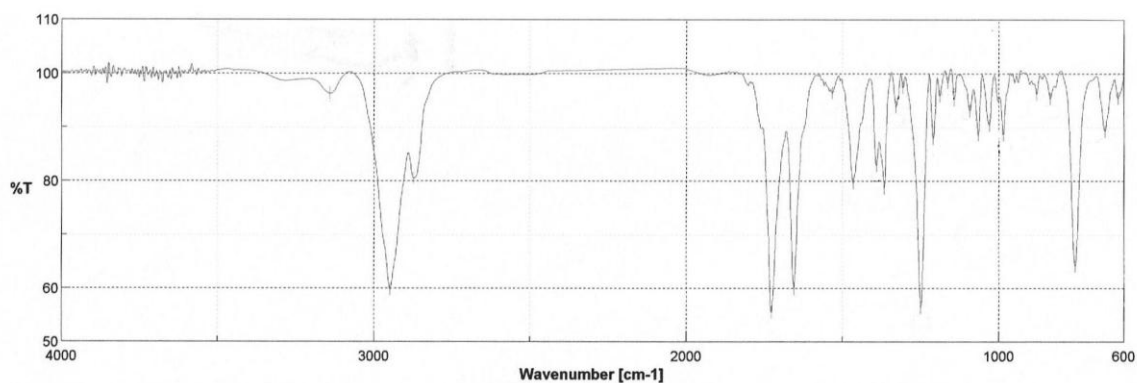


Figure 3.2.10. IR spectrum of compound **3.29**.

Carbonyl group at C11 of compound **3.29** generates a δ signal in the ¹³C NMR spectrum at 199.73 ppm, and the amide at 173.87 ppm. The correlation of proton H12 (δ signal at 5.69 ppm in the ¹H NMR spectrum) with the δ signal at 61.62 ppm allowed the identification of this signal as carbon C9. In compound **3.29**, correlations of the methyl group at C27 with carbons C13, C14 and C15 allowed the identification of the corresponding δ signals in the ¹³C NMR spectrum. Proton at H18 (signal at δ 3.15 ppm in the ¹H NMR spectrum) correlates with carbon C19. The methyl groups at C29 and C30

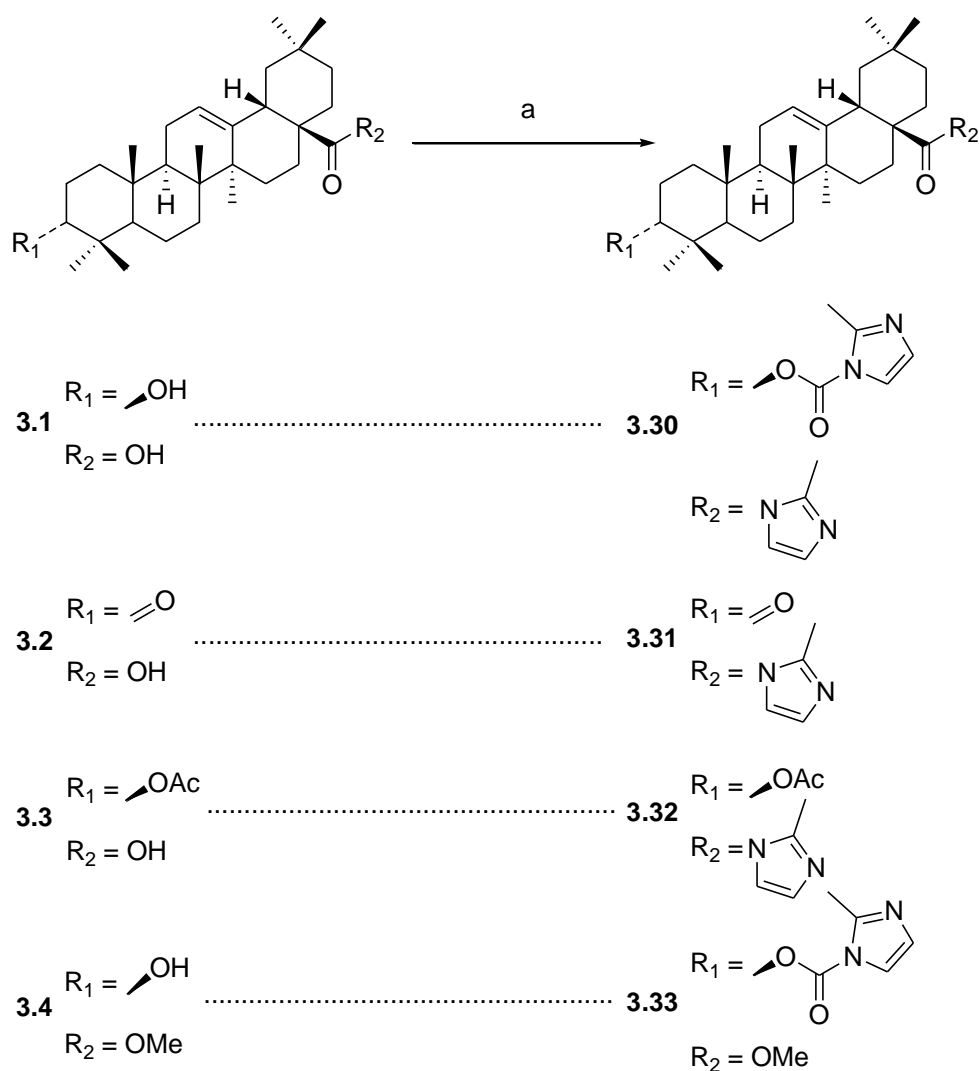
also correlate with this signal, which allows the identification of the δ signal at 44.24 ppm as carbon C19.

Table 3.2.3. Selected ^1H and ^{13}C NMR data from the backbone of compounds **3.27-3.29**.

| Entry | Position | 3.27 | | 3.28 | | 3.29 | |
|-------|--------------------------|-----------------------|------------|-----------------------|------------|-----------------------|------------|
| | | δ H | δ C | δ H | δ C | δ H | δ C |
| 1 | 1 | - | 43.01 | - | 45.07 | - | 38.71 |
| 2 | 2 | - | 122.99 | 5.70 ($J=19.27$) | 75.32 | - | - |
| 3 | 3 | - | 206.59 | - | 207.56 | 4.47 ($J=15.74$) | 80.47 |
| 4 | 4 | - | 45.19 | - | 48.68 | - | 37.95 |
| 5 | 5 | - | 52.58 | - | 5.89 | 0.75 ($J=11.40$) | 55.01 |
| 6 | 7 | - | 31.69 | - | 32.11 | - | 32.69 |
| 7 | 8 | - | 39.16 | - | 39.29 | - | 44.93 |
| 8 | 9 | - | 45.46 | - | 47.30 | 2.31 | 61.62 |
| 9 | 10 | - | 36.07 | - | 37.99 | - | 37.04 |
| 10 | 11 | - | 23.63 | - | - | - | 199.73 |
| 11 | 12 | 5.34 | 121.77 | 5.27 | 121.34 | 5.70 | 128.14 |
| 12 | 13 | - | 144.02 | - | 144.14 | - | 167.21 |
| 13 | 14 | - | 41.93 | - | 41.63 | - | 37.95 |
| 14 | 15 | - | 27.65 | - | 27.52 | - | 27.59 |
| 15 | 17 | - | 46.77 | - | 46.52 | - | 49.34 |
| 16 | 18 | 2.88 ($J=15.94$) | 41.48 | 2.85 ($J=17.20$) | 41.11 | 3.15 ($J=11.90$) | 42.79 |
| 17 | 19 | - | 45.82 | - | - | - | 44.24 |
| 18 | 20 | - | 30.69 | - | 30.59 | - | 30.32 |
| 19 | 21 | - | - | - | - | - | - |
| 20 | 25 | 0.89 | 15.39 | 1.31 | 15.86 | 1.10 | 16.28 |
| 21 | 26 | 0.79 | 16.39 | 0.77 | 16.92 | 0.85 | 18.54 |
| 22 | 27 | 1.18 | 25.65 | 1.09 | 25.81 | 1.36 | 23.30 |
| 23 | 28 | - | 178.15 | - | 178.08 | - | 173.87 |
| 24 | <u>COCH₃</u> | 3.62 | 51.54 | 3.60 | 51.50 | - | - |
| 25 | <u>OCO</u> | - | - | - | 147.93 | - | 170.94 |
| 26 | <u>C2CH</u> | 7.80 | 130.66 | - | - | - | - |
| 27 | <u>OCOCH₃</u> | - | - | - | - | 2.02 | 21.23 |
| 28 | C4' | 7.15 | 130.36 | - | - | - | - |

3.2.2.1.2. Methylimidazole derivatives

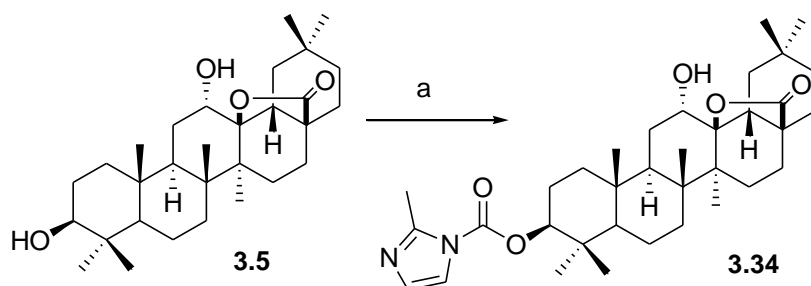
The reaction of compounds **3.1-3.5** with the commercially available reagent CBMI affords carbamates **3.30**, **3.33** and **3.34**, and *N*-acylimidazoles **3.31** and **3.32** (Schemes 3.2.6 and 3.2.7) with good yields. The methylimidazole group is characterized by the presence of two singlet signals higher than δ 6.8 ppm in the ^1H NMR spectrum, corresponding to the protons, and a signal corresponding to the methyl group in the heterocyclic ring at around 2.6 ppm.

Scheme 3.2.6.^a Synthesis of derivatives **3.30-3.33**.

^aReagents: (a) CBMI, THF, N_2 , reflux.

The characterization of compounds **3.30-3.34** was made via MS, IR and NMR experiments. Compound **3.30** was prepared via the reaction of the hydroxyl and carboxyl groups of oleanolic acid **3.1** with CBMI. The presence of the two methylimidazole groups is confirmed by the existence of four different δ signals in the ^1H NMR spectrum, corresponding to the protons of the methylimidazole ring, and by two signals of methyl groups. The δ signals in the ^1H NMR spectrum at 7.53, 6.88 and 2.57 ppm correspond to the methylimidazole ring at C3 (ring'), and the δ signals at 7.32, 6.84 and 2.63 ppm correspond to the methylimidazole ring at C28 (ring''). The previous signals correspond, respectively, to the δ signals at 117.28, 127.19, 17.78, 117.97, 127.63 and 16.83 ppm in the ^{13}C NMR spectrum. Other correlations were also found for compound **3.30** via HMBC, HMQC and COESY experiments (Table 3.2.4).

Scheme 3.2.7.^a Synthesis of derivative **3.34**.



^aReagents: (a) CBMI, THF, N_2 , reflux.

Compound **3.5**, when reacting with CBMI, only affords compound **3.34**, in which the hydroxyl group at C12 did not react with CBMI, probably because of the volume of the CBMI reagent and the sterical impairment of this position. The presence of the hydroxyl group at C12 was detected in the IR spectrum by the broad band at around 3400 cm^{-1} , which is characteristic of the hydroxyl group, and was confirmed further via NMR analysis.

Compound **3.34** exhibits a δ signal at 3.90 ppm, corresponding to proton H12. The proximity with the lactone moiety leads to the increase in the δ signal value when compared with other alcohols. The same is observed for the signal of carbon C12 (Table 3.2.4). Proton H12 and the methyl group at C27 interact with carbon C13. The methyl group at C27 has several correlations in the HMBC spectrum, for example with carbons C14 and C15. The correlation of the methyl groups at C25 and C26 with the signal at δ 44.67 ppm allowed the identification of this signal as carbon C9. The presence of the carbamate at C3 is confirmed by the correlation of methyl groups C23 and C24 with the carbonyl group of the carbamate. Proton H3 also correlates with this carbonyl group. Other correlations were observed in the 2D NMR spectra, which allowed the attribution of several δ signals (Figure 3.2.11, Table 3.2.4).

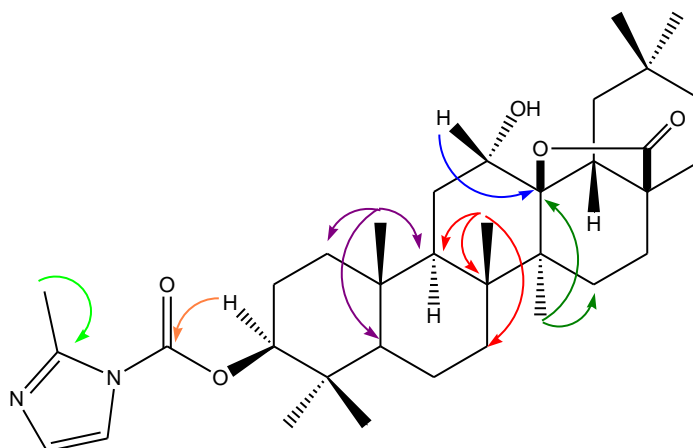


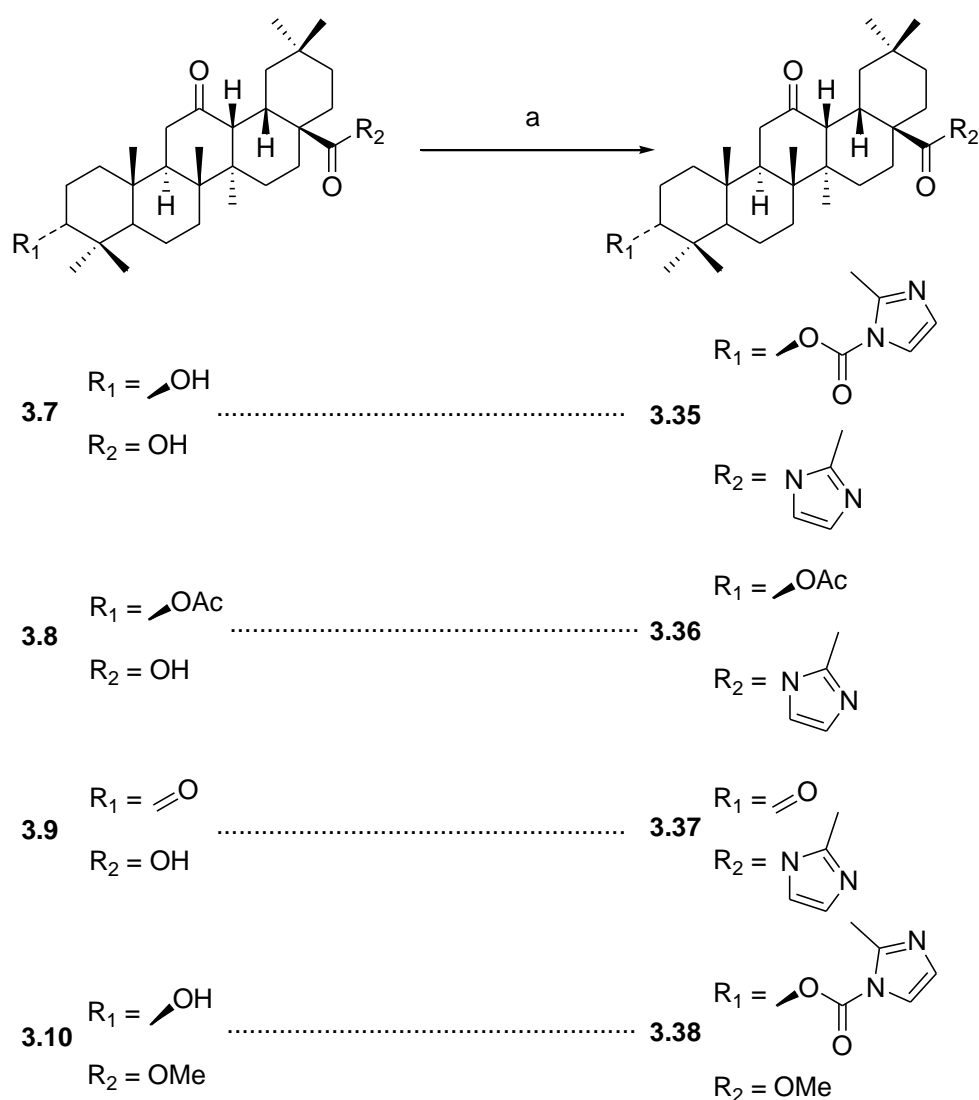
Figure 3.2.11. Selected HMBC correlations for compound **3.34**.

Table 3.2.4. Selected ^1H and ^{13}C NMR data from the backbone of compounds **3.30** and **3.34**.

| Entry | Position | 3.30 | | 3.34 | |
|-----------|----------------------------------|-----------------------------|------------|-----------------------------|------------|
| | | δ H | δ C | δ H | δ C |
| <i>1</i> | 1 | - | - | - | 38.32 |
| <i>2</i> | 3 | 4.65 (<i>J</i> = 16.32) | 85.89 | 4.67 (<i>J</i> = 16.29) | 85.77 |
| <i>3</i> | 4 | - | 37.97 | - | 38.13 |
| <i>4</i> | 5 | - | 55.26 | - | 55.23 |
| <i>5</i> | 7 | - | - | - | 34.11 |
| <i>6</i> | 8 | - | 39.31 | - | 42.26 |
| <i>7</i> | 9 | - | 47.44 | - | 44.67 |
| <i>8</i> | 10 | - | 36.87 | - | 36.34 |
| <i>9</i> | 11 | - | 23.00 | - | - |
| <i>10</i> | 12 | 5.36 (<i>J</i> = 6.97) | 122.92 | 3.90 | 76.04 |
| <i>11</i> | 13 | - | 142.96 | - | 90.59 |
| <i>12</i> | 14 | - | - | - | 42.08 |
| <i>13</i> | 15 | - | 41.89 | - | 27.99 |
| <i>14</i> | 17 | - | 50.77 | - | 44.45 |
| <i>15</i> | 18 | 3.10 (<i>J</i> = 17.28) | 42.55 | - | 51.10 |
| <i>16</i> | 19 | - | 46.10 | - | 39.34 |
| <i>17</i> | 20 | - | 30.35 | - | 31.54 |
| <i>18</i> | 25 | 0.96 | 15.37 | 0.93 | 16.33 |
| <i>19</i> | 26 | 0.73 | 17.16 | 1.16 | 18.55 |
| <i>20</i> | 27 | 1.17 | 25.74 | 1.32 | 18.55 |
| <i>21</i> | 28 | - | 176.73 | - | 179.92 |
| <i>22</i> | OCO | - | 149.40 | - | 149.37 |
| <i>23</i> | C2' | - | 149.33 | - | 147.89 |
| <i>24</i> | C2'' | - | 147.84 | - | - |
| <i>25</i> | C2'<u>CH</u>₃ | 2.57 | 17.78 | 2.65 | 16.80 |
| <i>26</i> | C2''<u>CH</u>₃ | 2.64 | 16.83 | - | - |

The reaction of compounds **3.7-3.10** with CBMI affords oleanane-type derivatives **3.35-3.38** (Scheme 3.2.8) in good yields. These compounds do not have the unsaturation in ring C, which has been replaced by a carbonyl group at C12. Therefore, the signal characteristic of proton H12 is not present in the ^1H NMR spectrum of these compounds. However, in the ^{13}C NMR spectrum, a δ signal at around 210 ppm corresponds to the signal of carbon C12, which is characteristic of a carbonyl group.

Scheme 3.2.8.^a Synthesis of derivatives **3.35-3.38**.



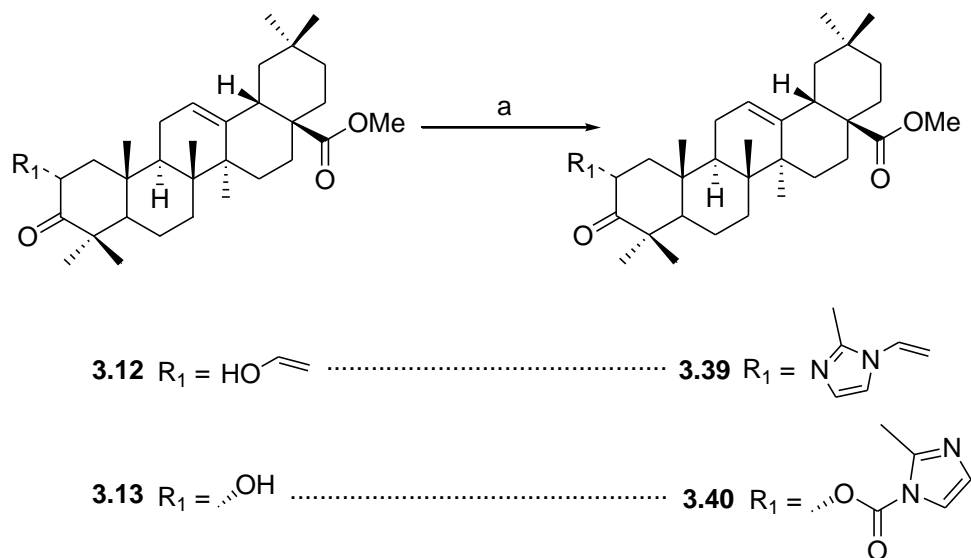
^aReagents: (a) CBMI, THF, N_2 , reflux.

Compound **3.37** presents two carbonyl groups at carbons C3 and C12, and the correlations established by them allowed their identification. Proton H13 correlates with carbon C12, which permitted the identification of the δ signal at 210 ppm as carbon C12. The methyl groups at C23 and C24 correlate with carbon C3 (δ signal at 216 ppm), although it was not possible to distinguish them. More correlations were visualized in the 2D NMR experiments that allowed the identification of other δ signals (Table 3.2.5).

Table 3.2.5. Selected ^1H and ^{13}C NMR data of the backbone of compound **3.37**.

| Entry | Position | δ ^1H NMR | δ ^{13}C NMR |
|-------|----------------------------|---------------------------|------------------------------|
| 1 | 3 | - | 216.50 |
| 2 | 5 | 1.24 | 54.89 |
| 3 | 9 | 1.69 ($J= 17.78$) | 49.13 |
| 4 | 10 | - | 36.59 |
| 5 | 12 | - | 210.14 |
| 6 | 13 | 2.70 ($J= 3.88$) | 51.24 |
| 7 | 18 | 3.01 ($J= 13.12$) | 32.96 |
| 8 | 20 | - | 30.34 |
| 9 | 25 | 0.99 | 15.99 |
| 10 | 28 | - | 177.62 |
| 11 | C2' | - | 149.01 |
| 12 | C2' <u>CH</u> ₃ | 2.60 | 17.72 |

Compounds **3.12** and **3.13** react with CBMI to afford the *N*-alkylimidazole **3.29** and the carbamate **3.40**, respectively (Scheme 3.2.9). Compound **3.39**, which has a proton in the exocyclic double bond at C2 exhibits a signal in the ^1H NMR spectrum at δ 6.65 ppm, corresponding to this proton. Compound **3.40** exhibits a different ^1H NMR spectrum, as proton H2 is present as a double doublet with a δ signal at 5.71 ppm. The δ signal is higher than that in other carbamates as the carbonyl group at C3 exercises influence over this proton (Figure 3.2.12).

Scheme 3.2.9.^a Synthesis of derivatives **3.39** and **3.40**.

^aReagents: (a) CBMI, THF, N₂, reflux.

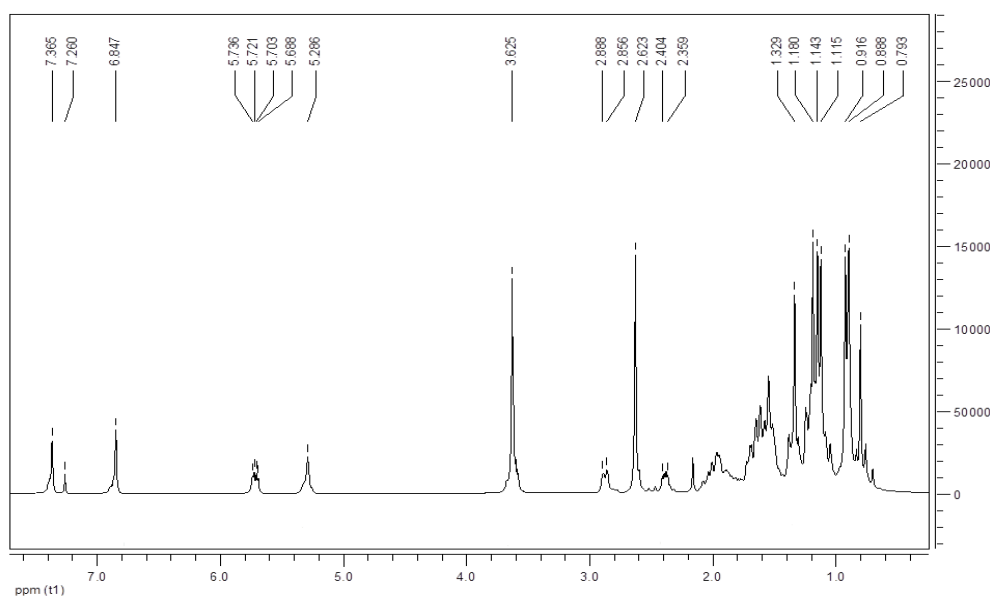


Figure 3.2.12. ¹H NMR spectrum of compound **3.40**.

In the ¹³C NMR spectrum, compound **3.40** exhibits δ signals at 207.87, 178.14 and 138.92 ppm corresponding to quaternary carbons C3, C28 and the carbonyl group of carbamate, respectively (Figure 3.2.13). The signals corresponding to the protons and the

methyl group in the methylimidazole ring were identified via HMQC experiments (Figure 3.2.14).

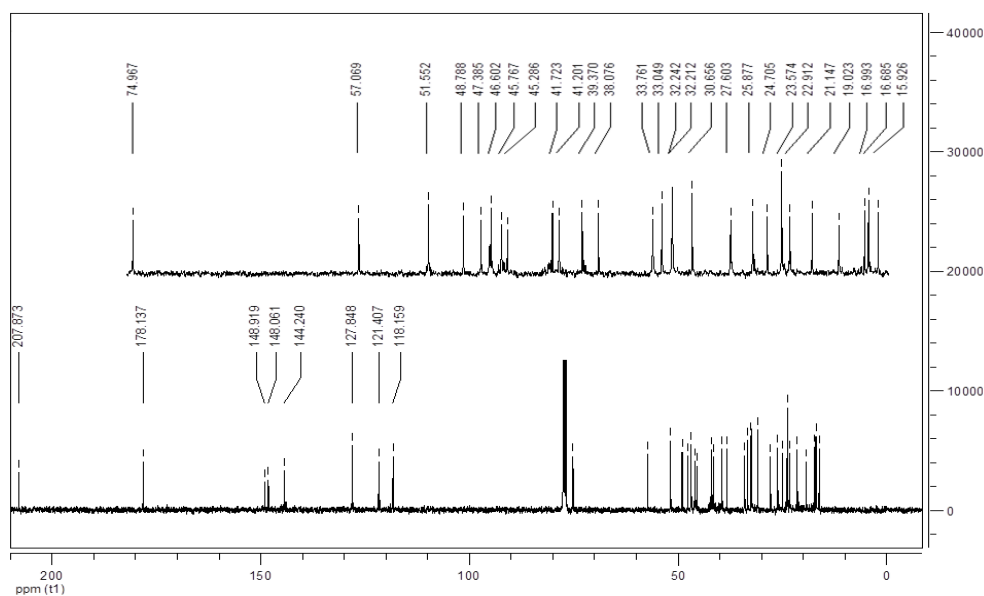


Figure 3.2.13. ^{13}C NMR spectrum of compound **3.40**.

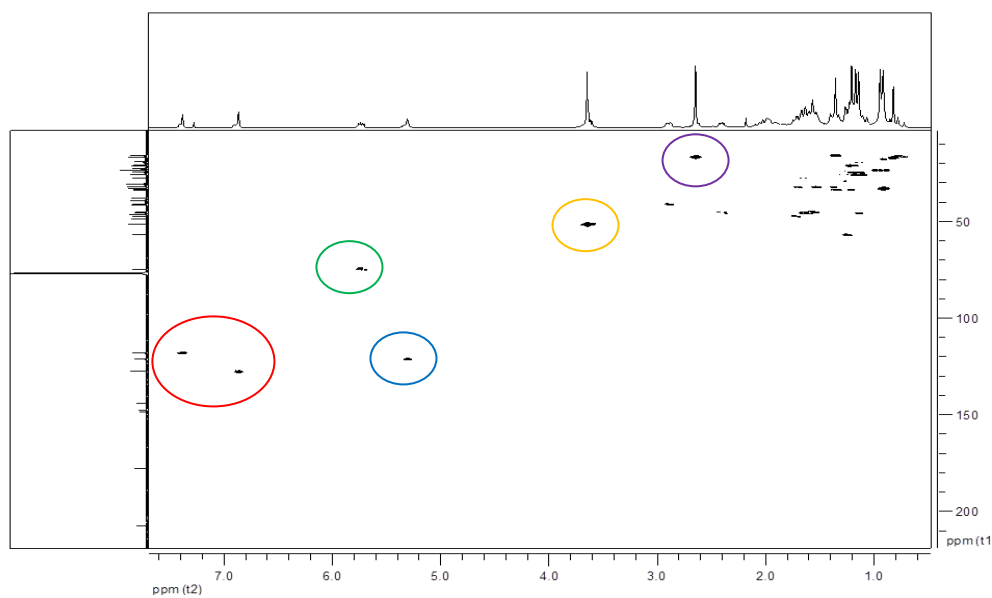


Figure 3.2.14. HMQC spectrum of compound **3.40**, with the correlations between protons and carbons of methylimidazole ring (red), C2 (green), C12 (blue), methyl group at C28 (yellow) and methyl group at the methylimidazole ring (purple).

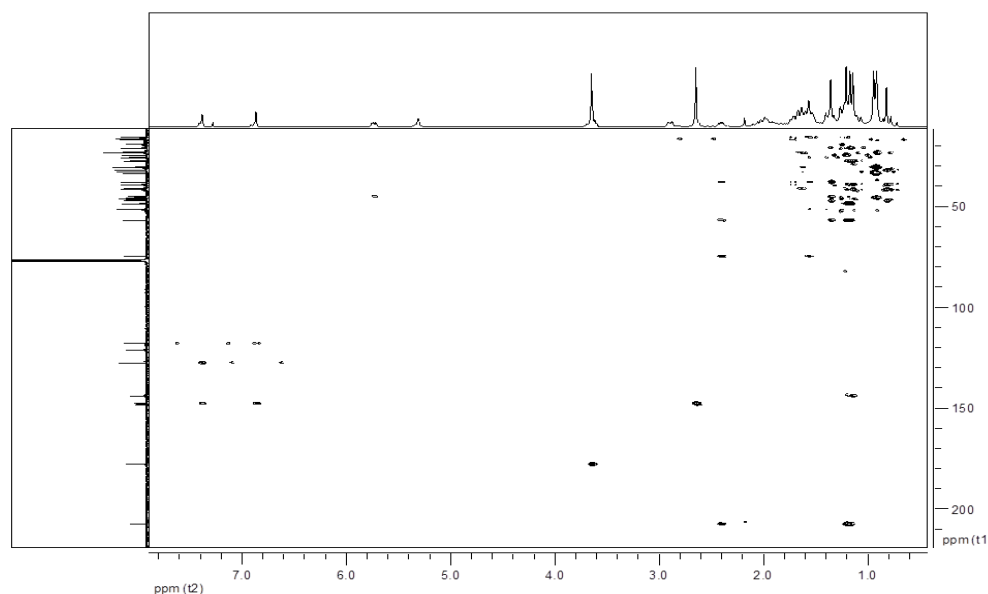
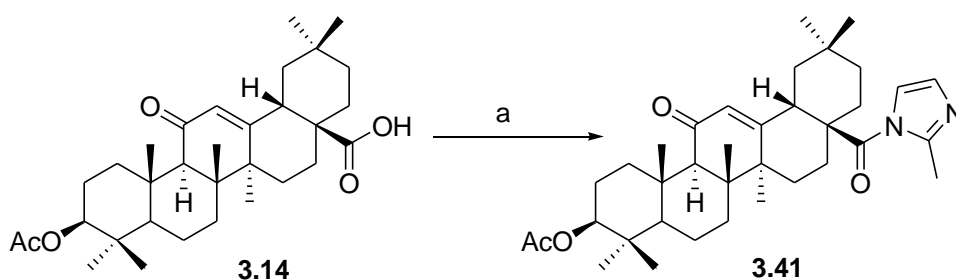


Figure 3.2.15. HMBC spectrum of compound **3.40**.

In compound **3.40**, proton H5 which exhibits a δ signal at 2.38 ppm, correlates with carbons C2, C3, C23, C24 and C25, which allows the identification of the corresponding δ signals in the ^{13}C NMR spectrum. Proton H2 correlates with the carbonyl group of the nearby carbamate (Figure 3.2.15). The methyl group at C27 correlates with carbons C13 and C14, the methyl group at C26 correlates with carbons C8 and C9, the methyl group at C25 correlates with carbons C1, C5 and C10 (Table 3.2.6). The geminal methyl groups at C23 and C24, C29 and C30 were not distinguishable as they had the same magnetic environment. The HMBC spectrum of compound **3.40** allowed the observation of more correlations.

Scheme 3.2.10.^a Synthesis of derivative **3.41**.



^aReagents: (a) CBMI, THF, N_2 , reflux.

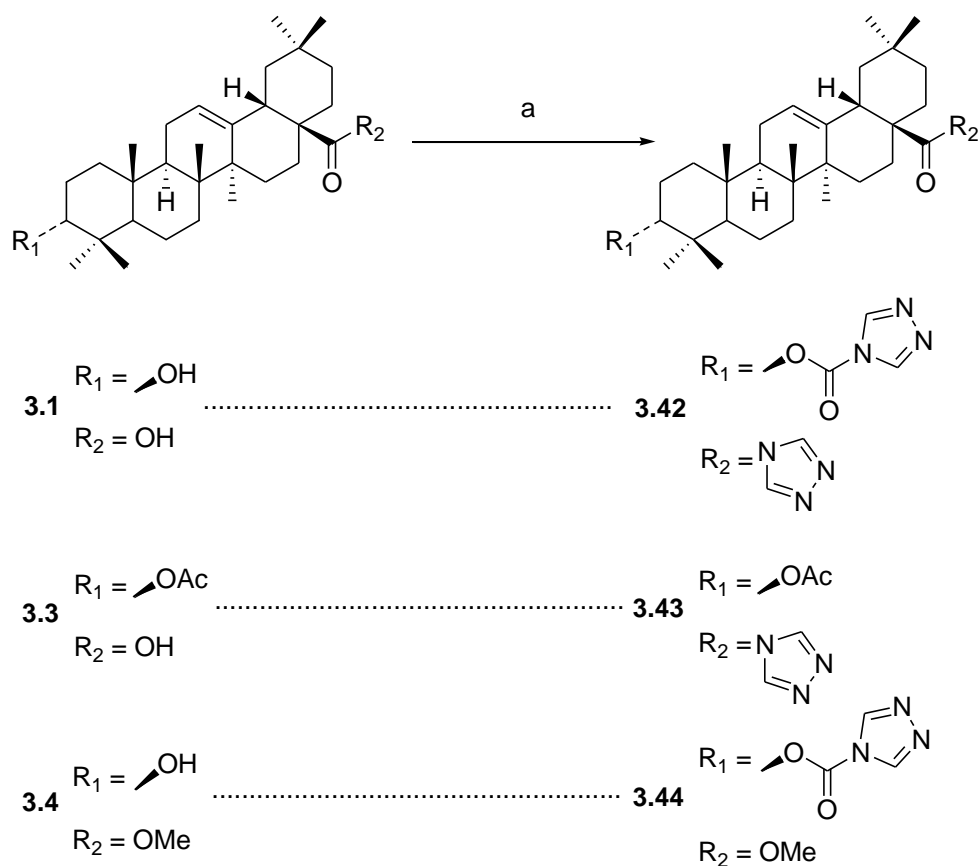
Compound **3.41** (Scheme 3.2.10) was characterized via IR, MS and 1D and 2D NMR experiments. The NMR data allowed the attribution of several δ signals (Table 3.2.6).

Table 3.2.6. Selected ^1H and ^{13}C NMR data from the backbone of compounds **3.40** and **3.41**.

| Entry | Position | 3.40 | | 3.41 | |
|-----------|--------------------------|-----------------------------|------------|-----------------------------|------------|
| | | δ H | δ C | δ H | δ C |
| <i>1</i> | 1 | - | 45.29 | 2.81 (<i>J</i> = 13.56) | 38.75 |
| <i>2</i> | 2 | 5.71 (<i>J</i> = 18.97) | 74.97 | - | - |
| <i>3</i> | 3 | - | 207.87 | 4.48 (<i>J</i> = 15.60) | 80.51 |
| <i>4</i> | 4 | - | 48.79 | - | 37.99 |
| <i>5</i> | 5 | 2.38 (<i>J</i> = 17.89) | 57.07 | - | 55.10 |
| <i>6</i> | 7 | - | - | - | 32.80 |
| <i>7</i> | 8 | - | 39.37 | - | 45.06 |
| <i>8</i> | 9 | - | 47.39 | 2.32 | 61.65 |
| <i>9</i> | 10 | - | 38.08 | - | 37.07 |
| <i>10</i> | 11 | - | - | - | 199.81 |
| <i>11</i> | 12 | 5.29 | 121.41 | 5.71 | 128.17 |
| <i>12</i> | 13 | - | 144.24 | - | 16.50 |
| <i>13</i> | 14 | - | 41.72 | - | 43.56 |
| <i>14</i> | 15 | - | 27.60 | - | 27.63 |
| <i>15</i> | 17 | - | 46.60 | - | 50.28 |
| <i>16</i> | 18 | 2.87 (<i>J</i> = 12.99) | 41.20 | 3.20 (<i>J</i> = 12.28) | 43.08 |
| <i>17</i> | 19 | - | - | - | 44.53 |
| <i>18</i> | 20 | - | 30.66 | - | 30.26 |
| <i>19</i> | 25 | 1.33 | 15.93 | 1.12 | 16.35 |
| <i>20</i> | 26 | 0.79 | 16.99 | 0.90 | 18.90 |
| <i>21</i> | 27 | 1.12 | 25.88 | 1.37 | 23.24 |
| <i>22</i> | 28 | - | 178.14 | - | 175.69 |
| <i>23</i> | COCH₃ | 3.63 | 51.55 | - | - |
| <i>24</i> | OCOCH₃ | - | - | 2.03 | 21.28 |
| <i>25</i> | OCO | - | 148.92 | - | 171.01 |
| <i>26</i> | C2' | - | 148.06 | - | 149.72 |
| <i>27</i> | C2'CH₃ | 2.62 | 16.69 | 2.55 | 18.22 |

3.2.2.1.3. Triazole derivatives

The reaction of oleanane type derivatives and oleanolic acid **3.1** with CDT affords *N*-acyltriazoles, carbamates and *N*-alkyltriazoles. Compounds **3.1**, **3.3** and **3.4** afforded carbamates **3.42** and **3.44**, and *N*-acyltriazole **3.43** with good yields (Scheme 3.2.11). The presence of the triazole ring in the oleanane structure is confirmed by the presence of two singlets in the ^1H NMR spectrum, with δ signals higher than 7.8 ppm. The attribution of the remaining δ signals was made using the same rationale as that used for the imidazole and methylimidazole derivatives.

Scheme 3.2.11.^a Synthesis of derivatives **3.42**-**3.44**.

^aReagents: (a) CDT, THF, N_2 , reflux.

Compound **3.42**, which has two triazole rings, exhibits four singlets in the ^1H NMR spectrum, with the same number of corresponding signals being present in the ^{13}C NMR

spectrum. The amide carbonyl group at C28 appears as a δ signal at 174.99 ppm, and the carbamate carbonyl group appears at 147.28 ppm, in the ^{13}C NMR spectrum. The methyl groups at C25, C26 and C27 establish several correlations with the neighboring carbons, which allows the attribution of several δ signals (Table 3.2.7).

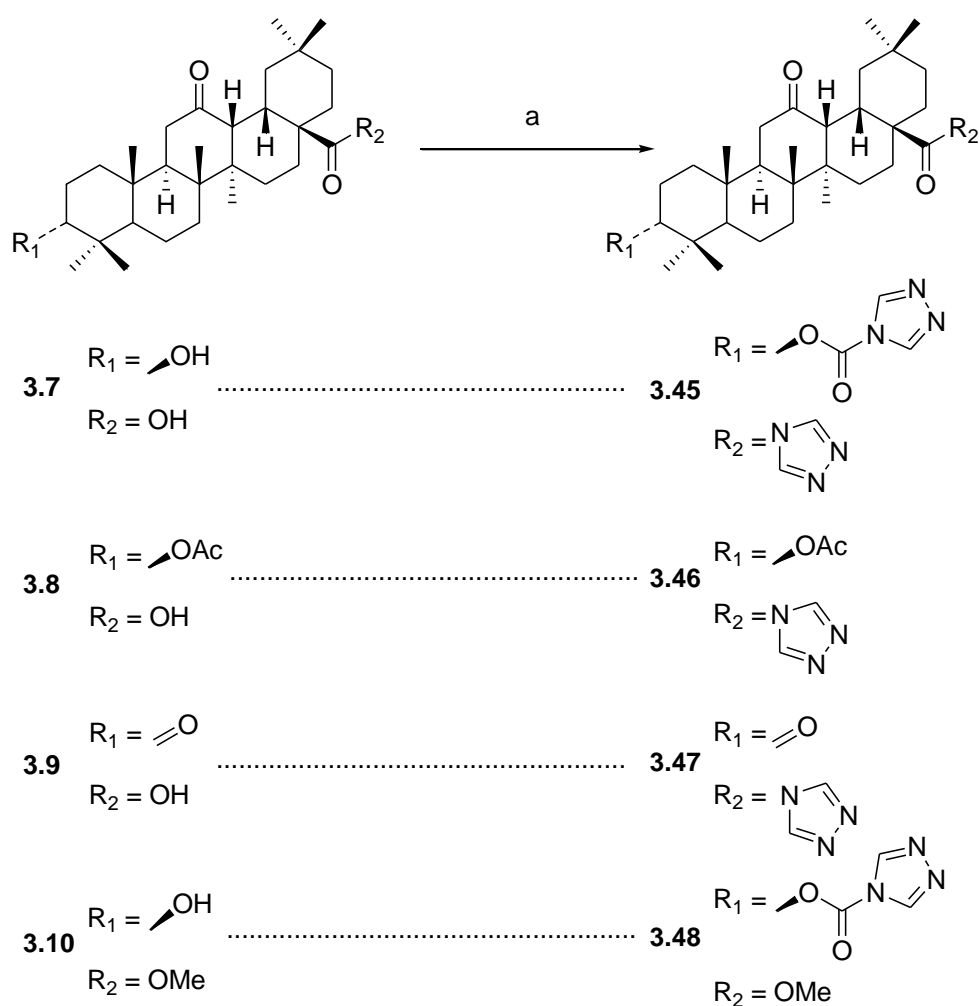
In amide **3.43** the δ signals were also attributed based on the study of the 1D and 2D NMR spectra (Table 3.2.7). The δ values of proton H3 and of carbon C3 are different from those observed for compound **3.42**, as the group at C3 changes from a carbamate to an acetoxy group.

Table 3.2.7. Selected ^1H and ^{13}C NMR data from the backbone of compounds **3.42** and **3.43**.

| Entry | Position | 3.42 | | 3.43 | |
|-------|--------------------------|-----------------------|------------|-----------------------|------------|
| | | δ H | δ C | δ H | δ C |
| 1 | 1 | - | - | - | 38.10 |
| 2 | 3 | 4.79 ($J=16.48$) | 87.68 | 4.48 ($J=15.73$) | 80.83 |
| 3 | 4 | - | 38.18 | - | 37.65 |
| 4 | 5 | 0.89 ($J=10.31$) | 55.24 | 0.80 | 55.27 |
| 5 | 7 | - | 32.40 | - | 32.47 |
| 6 | 8 | - | 39.25 | - | 39.26 |
| 7 | 9 | - | 47.49 | - | 47.50 |
| 8 | 10 | - | 36.85 | - | 36.87 |
| 9 | 12 | 5.30 | 122.60 | 5.29 | 122.80 |
| 10 | 13 | - | 143.19 | - | 143.09 |
| 11 | 14 | - | 41.79 | - | 41.68 |
| 12 | 15 | - | 27.80 | - | 27.80 |
| 13 | 17 | - | 49.97 | - | 49.99 |
| 14 | 18 | 3.20 ($J=11.41$) | 41.66 | 3.19 ($J=11.88$) | 41.78 |
| 15 | 19 | - | 45.79 | - | 45.78 |
| 16 | 20 | - | 30.50 | - | 30.49 |
| 17 | 25 | 0.96 | 15.35 | 0.91 | 15.36 |
| 18 | 26 | 0.68 | 16.70 | 0.66 | 16.63 |
| 19 | 27 | 1.17 | 25.90 | 1.15 | 25.89 |
| 20 | 28 | - | 174.99 | - | 175.02 |
| 21 | <u>OCOCH₃</u> | - | - | 2.03 | 21.28 |
| 22 | <u>OCO</u> | - | 147.28 | - | 170.98 |

Compounds **3.7-3.10** react with CDT affording compounds **3.45-3.48** (Scheme 3.2.12). Compounds that have a 12-oxo moiety present a characteristic band in the IR spectrum at around 1715 cm^{-1} , corresponding to the stretching vibration of the carbonyl group in cyclic ketones. In the ^{13}C NMR spectrum, the carbonyl group at C12 has a δ signal around 210 ppm, carbon C13 appears at around 51 ppm, and the signal for proton $\beta\text{-H13}$ appears at around 2.6 ppm in the ^1H NMR spectrum (Table 3.2.8).

Scheme 3.2.12.^a Synthesis of derivatives **3.45-3.48**.



^aReagents: (a) CDT, THF, N_2 , reflux.

Compound **3.45**, which has two triazole rings, exhibits four δ signals in the ^1H NMR spectrum corresponding to the protons of the heterocyclic rings. Other correlations are visible in the 2D NMR spectra of compound **3.45**, which allows the attribution of various

δ signals, such as the methyl groups at C25, C26 and C27. Carbonyl groups of the carbamate and amide moieties were identified by the different δ signals at 147.22 and 175.50 ppm, respectively (Table 3.2.8).

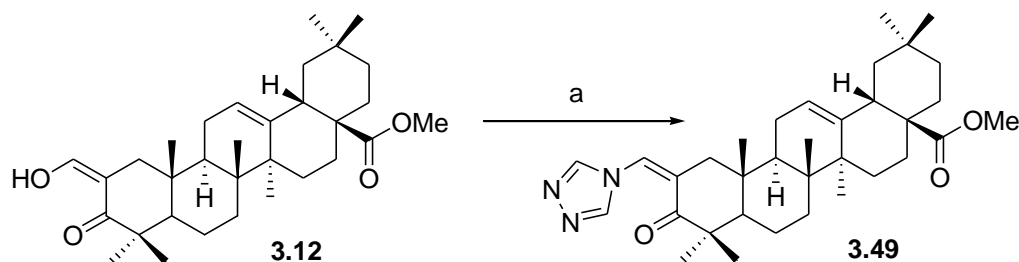
Table 3.2.8. Selected ^1H and ^{13}C NMR data from the backbone of compounds **3.45** and **3.48**.

| Entry | Position | 3.45 | | 3.48 | |
|-----------|-------------------------|-----------------------------|------------|-----------------------------|------------|
| | | δ H | δ C | δ H | δ C |
| <i>1</i> | 3 | 4.75 (<i>J</i> = 16.30) | 87.05 | 4.75 (<i>J</i> = 16.48) | 87.09 |
| <i>2</i> | 4 | - | 38.21 | - | 38.19 |
| <i>3</i> | 5 | - | 55.00 | - | 54.98 |
| <i>4</i> | 8 | - | 41.28 | - | 41.16 |
| <i>5</i> | 9 | - | 49.57 | - | 49.51 |
| <i>6</i> | 10 | - | 36.75 | - | 36.72 |
| <i>7</i> | 12 | - | 210.53 | - | 211.12 |
| <i>8</i> | 13 | 2.70 | 51.45 | 2.60 (<i>J</i> = 3.94) | 51.71 |
| <i>9</i> | 14 | - | 42.11 | - | 41.77 |
| <i>10</i> | 17 | - | 50.34 | - | 47.22 |
| <i>11</i> | 18 | 3.26 (<i>J</i> = 12.64) | 32.09 | 2.76 (<i>J</i> = 13.46) | 31.61 |
| <i>12</i> | 20 | - | 30.45 | - | 30.54 |
| <i>13</i> | 25 | 0.89 | 15.18 | 0.90 | 15.15 |
| <i>14</i> | 26 | 0.92 | 16.13 | 0.94 | 23.06 |
| <i>15</i> | 27 | 0.98 | 20.62 | 0.92 | 20.46 |
| <i>16</i> | 28 | - | 175.50 | - | 178.23 |
| <i>17</i> | COCH₃ | - | - | 3.65 | 51.71 |
| <i>18</i> | OCO | - | 147.22 | - | 147.19 |

Carbamate **3.48** has a methoxy group at C28, which was confirmed by a δ signal at 178.23 ppm, corresponding to carbon C28. The δ signal at 147.19 ppm corresponded to the carbonyl of the carbamate. Proton H3 emerged as a double doublet with a δ signal at 4.75 ppm. Carbon C3 exhibited a δ signal at 87.09 ppm in the ^{13}C NMR spectrum. Correlations between H13 and C27 allowed the identification of the latter and consequently the identification of the δ signals of carbons C26 and C25. Other

correlations of these methyl groups allowed the identifications of various δ signals (Table 3.2.8).

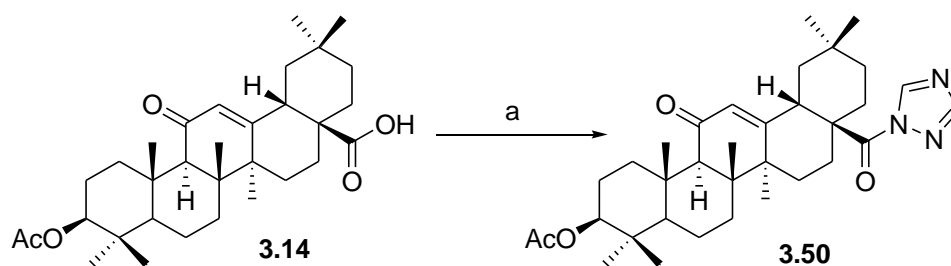
Scheme 3.2.13.^a Synthesis of derivative **3.49**.



^aReagents: (a) CDT, THF, N₂, reflux.

Compounds **3.12** and **3.14** reacted with CDT affording amine **3.49** and amide **3.50**, respectively (Schemes 3.2.13 and 3.2.14). The characterization by means of MS, IR, and 1D and 2D NMR techniques of these new compounds confirmed the introduction of a triazole ring in the parental structure.

Scheme 3.2.14.^a Synthesis of derivative **3.50**.



^aReagents: (a) CDT, THF, N₂, reflux.

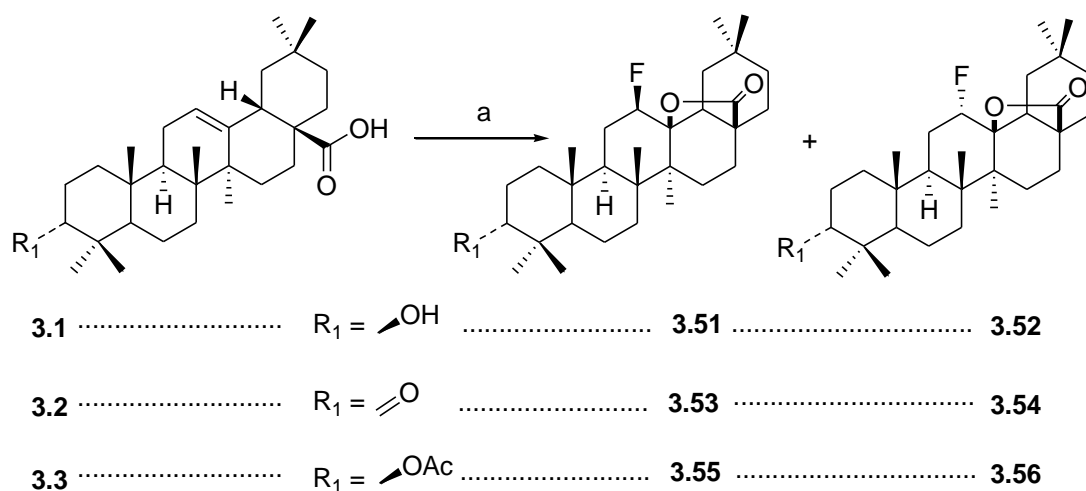
3.2.2.1.4. Fluorine derivatives

Fluorinated organic compounds can be achieved using nucleophilic, electrophilic and radical forms of fluorine reagents.⁴⁵⁰ The presence of fluorine in key positions of a biologically active molecule can improve the biological properties of the parental

molecule. Selectfluor, an electrophilic fluorination reagent, was used to introduce a fluorine atom into oleanolic acid **3.1** and derivatives. Selectfluor is a crystalline white solid that is stable at high temperatures, and is easy to work with because the byproducts are usually easily removed by an aqueous workup.⁴⁶¹ Several papers describe the reaction of alkenes with selectfluor, usually in the presence of a nucleophilic donor.^{464, 466} The solvent, the temperature, and the nucleophilic donor can influence the efficiency and the outcome (number of isomers and byproducts) of this reaction.

The reaction of oleanolic acid **3.1** and derivatives **3.2** and **3.3** with selectfluor in a mixture of two inert solvents, acetonitrile and dioxane, at 50 °C, affords a mixture of α - and β -fluorolactones, with α isomer being the major reaction product (Scheme 3.2.15). The free acid behaves like the nucleophilic donor, losing the proton and promoting cyclization to the carbon C13 in the oleanane backbone.

Scheme 3.2.15.^a Synthesis of derivatives **3.51-3.56**.



^aReagents: (a) Selectfluor, acetonitrile, dioxane, 50°C.

The fluorolactone moiety is detected as a double doublet in the ¹H NMR spectrum, corresponding to the proton H12, namely around δ 4.5 ppm for β -fluorolactones and δ 4.6 ppm for α -fluorolactones (Figure 3.2.16). In the ¹³C NMR spectrum, the signals for carbons C12 and C13 are doublets. In the β isomers their δ values are around 97 and 88 ppm, respectively, and in the α isomers they are around 100 and 90 ppm, respectively. The δ signal for carbon C28 is in the order of 179 ppm in both isomers (Figure 3.2.17).

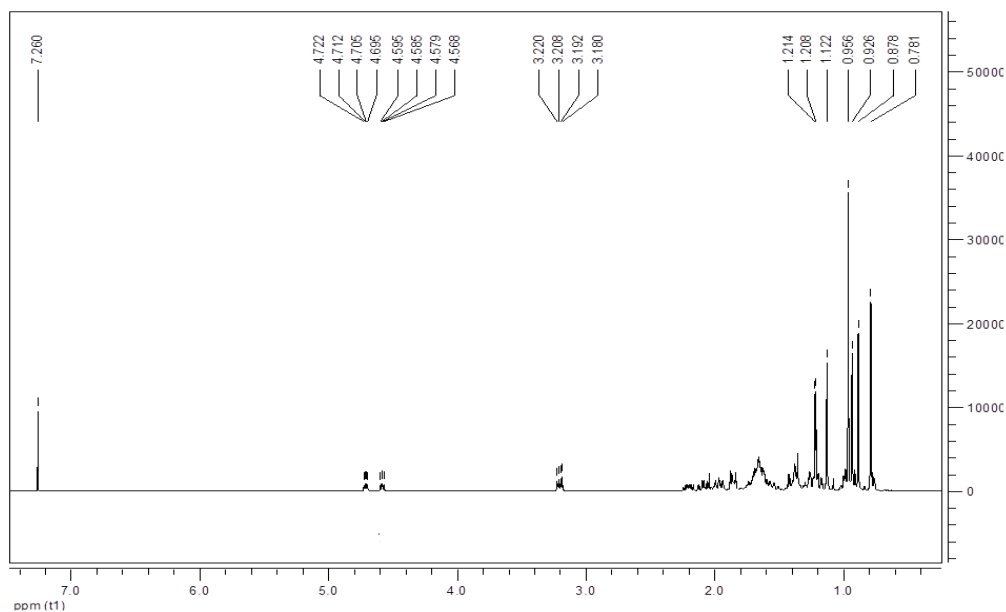


Figure 3.2.16. ^1H NMR spectrum of compound **3.52**.

The identification of the different isomers is based on the NOESY spectrum correlations of proton H12 with other groups. In fluorolactone **3.51**, proton H12 has a correlation with the methyl group at C27 and is consequently identified as the β -fluorine isomer. Proton H12 of fluorolactone **3.52** establishes a correlation with the methyl group at C26, which is therefore identified as the α -fluorine isomer (Figure 3.2.18).

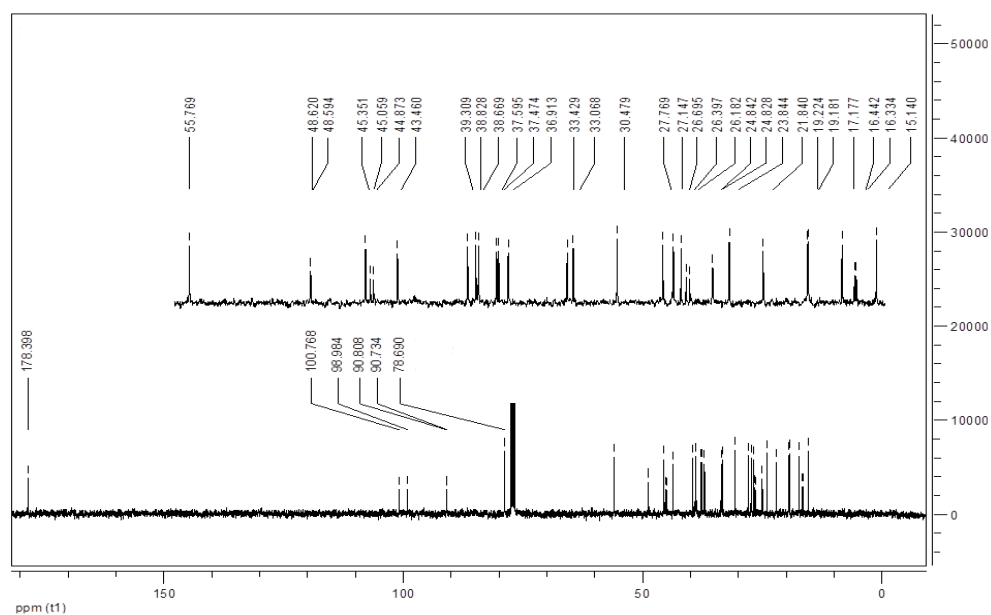


Figure 3.2.17. ^{13}C NMR spectrum of compound **3.52**.

HMBC and HMQC spectra allowed the visualization of other correlations of fluorolactones, permitting the identification of various δ signals (Figure 3.2.19). Table 3.2.9 shows selected attributions of δ signals to the isomers **3.51** and **3.52**.

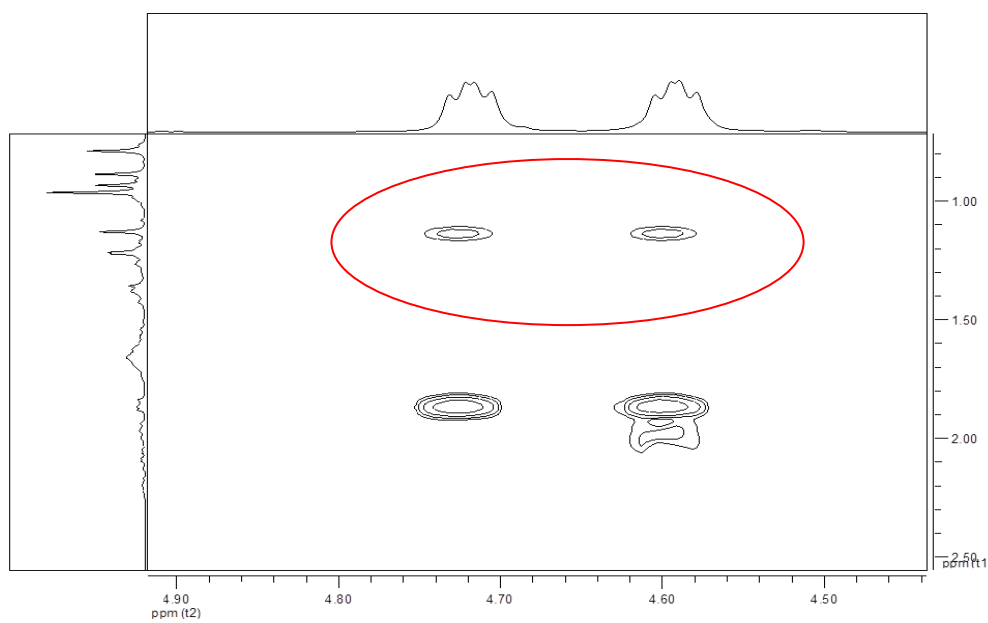


Figure 3.2.18. Detail of the NOESY spectrum of compound **3.52**. The correlation between H12 and the methyl group at C26 is marked in red.

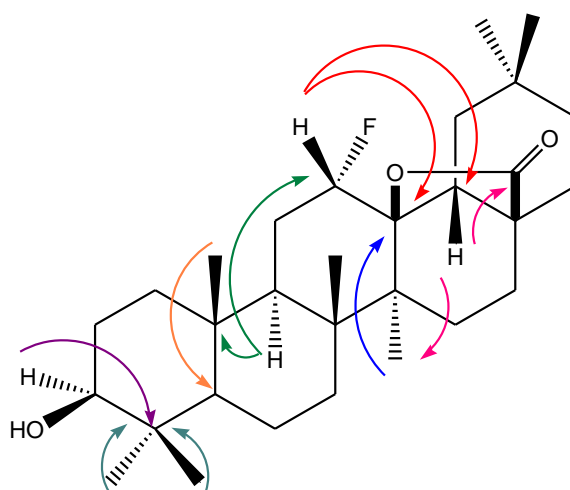
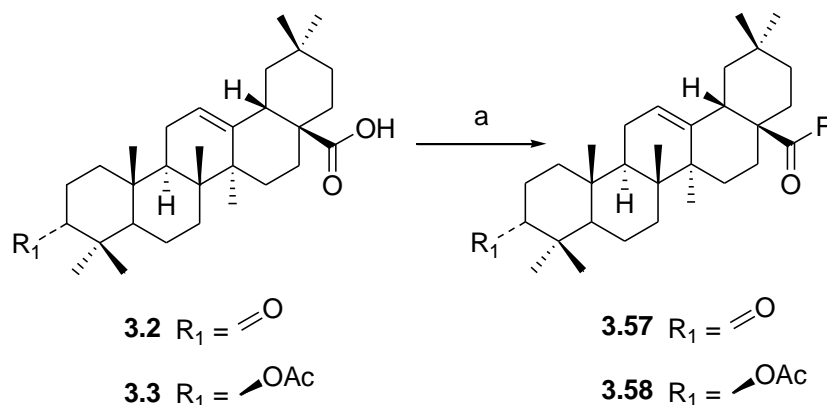


Figure 3.2.19. Selected HMBC correlations for compound **3.52**.

Table 3.2.9. Selected ^1H and ^{13}C NMR data of the backbone of compounds **3.51** and **3.52**.

| Entry | Position | 3.51 | | 3.52 | |
|-----------|-----------|-----------------------------|-------------------------------|-----------------------------|-------------------------------|
| | | δ H | δ C | δ H | δ C |
| <i>1</i> | 3 | 3.22 (<i>J</i> = 16.11) | 78.71 | 3.20 (<i>J</i> = 15.99) | 78.69 |
| <i>2</i> | 4 | - | 38.85 | - | 38.83 |
| <i>3</i> | 5 | - | 55.00 | - | 55.77 |
| <i>4</i> | 8 | - | 41.91 | - | 43.46 |
| <i>5</i> | 9 | - | 44.65 | - | 48.60 |
| <i>6</i> | 10 | - | 36.40 | - | (<i>J</i> = 2.63) 37.47 |
| <i>7</i> | 11 | - | - | - | 26.28 (<i>J</i> = 21.62) |
| <i>8</i> | 12 | 4.56 (<i>J</i> = 52.08) | 96.66 (<i>J</i> = 171.56) | 4.65 (<i>J</i> = 61.61) | 99.87 (<i>J</i> = 179.56) |
| <i>9</i> | 13 | - | 87.98 (<i>J</i> = 25.90) | - | 90.76 (<i>J</i> = 7.46) |
| <i>10</i> | 14 | - | 41.70 | - | 44.96 (<i>J</i> = 18.74) |
| <i>11</i> | 17 | - | 44.32 | - | 39.31 |
| <i>12</i> | 18 | - | 50.86 | - | 45.35 |
| <i>13</i> | 20 | - | 31.47 | - | 30.48 |
| <i>14</i> | 25 | 0.887 | 16.02 | 0.93 | 17.18 |
| <i>15</i> | 26 | 1.11 | 18.28 | 1.13 | 19.18 |
| <i>16</i> | 27 | 1.23 (<i>J</i> = 0.96) | 17.93 (<i>J</i> = 8.06) | 1.21 (<i>J</i> = 2.59) | 16.38 (<i>J</i> = 10.91) |
| <i>17</i> | 28 | - | 179.35 | - | 178.40 |
| <i>18</i> | 29 | - | - | 0.96 | 33.07 |
| <i>19</i> | 30 | - | - | 0.89 | 23.84 |

Deoxofluor, a thermodynamically stable nucleophilic reagent, is used for the fluorination of carbonyl and carboxylic functionalities.^{453, 472} The reaction of deoxofluor with oleanane derivatives **3.2** and **3.3** affords acyl fluorinated derivatives **3.57** and **3.58** (Scheme 3.2.16).

Scheme 3.2.16.^a Synthesis of derivatives **3.57** and **3.58**.

^aReagents: (a) Deoxofluor, THF, ice.

The structural elucidation of compounds **3.57** and **3.58** was made by means of MS, IR and NMR. The carbonyl band stretching vibration on the IR appears around 1820 cm^{-1} , the C-F band merges with other bands and therefore it is impossible to visualize it as an isolated band. The acid halide moiety emerges as doublet in the ^{13}C NMR spectrum, with a δ signal of 167 ppm and a coupling constant of 375 Hz.

3.2.2.2. Biological evaluation

Compounds **3.15-3.58** were evaluated for their antiproliferative activity against AsPC-1 pancreatic cell line, via a MTT assay (Tables 3.2.10 and 3.2.11).

All new derivatives tested were more potent in inhibiting cell growth than oleanolic acid **3.1** ($\text{IC}_{50} > 100$). Compounds **3.15-3.19**, **3.30-3.33** and **3.42-3.44**, with modifications only at C3 and at C28, had a moderate antiproliferative activity against AsPC-1 cells, with IC_{50} s between 8 and 26 μM , with the exception of methylimidazole derivatives **3.30-3.33**, with IC_{50} s lower than 8 μM . Compound **3.30**, the best compound found, had an IC_{50} of 3.2 μM (Table 3.2.10).

Table 3.2.10. The IC₅₀ (μM) of oleanolic acid heterocyclic derivatives to inhibit AsPC-1 cell growth.

| Imidazole-compd | | Methylimidazole-compd | | Triazole-compd | |
|-----------------|-----------------------|-----------------------|-----------------------|----------------|-----------------------|
| Compd | IC ₅₀ (μM) | Compd | IC ₅₀ (μM) | Compd | IC ₅₀ (μM) |
| | 3.1 | | | | >100 |
| 3.15 | 6.2±0.03 | - | - | - | - |
| 3.16 | 8.8±0.03 | 3.30 | 3.2±0.05 | 3.42 | 10.6±0.01 |
| 3.17 | 10.6±0.04 | 3.31 | 7.4±0.04 | - | - |
| 3.18 | 10.1±0.12 | 3.32 | 6.9±0.06 | 3.43 | 20.6±0.72 |
| 3.19 | 26.4±0.02 | 3.33 | 8.5±0.02 | 3.44 | 12.6±0.05 |
| 3.20 | 9.0±0.04 | 3.34 | 5.2±0.07 | - | - |
| 3.21 | 3.4±0.08 | - | - | - | - |
| 3.22 | 12.0±0.06 | - | - | - | - |
| 3.23 | 4.4±0.03 | 3.35 | 5.8±0.08 | 3.45 | 10.3±0.03 |
| 3.24 | 13.3±0.06 | 3.36 | 4.6±0.05 | 3.46 | 4.9±0.03 |
| 3.25 | 7.9±0.02 | 3.37 | 5.5±0.03 | 3.47 | 9.1±0.02 |
| 3.26 | 13.1±0.03 | 3.38 | 10.7±0.02 | 3.48 | 9.4±0.04 |
| 3.27 | 0.9±0.01 | 3.39 | 0.7±0.02 | 3.49 | 1.9±0.03 |
| 3.28 | 10.2±0.01 | 3.40 | 25.8±0.03 | - | - |
| 3.29 | 10.1±0.12 | 3.41 | 30.4±0.05 | 3.50 | 5.1±0.02 |

The AsPC-1 cells were treated with the indicated compounds at varying concentrations for 72 h. The antiproliferative effects were determined by MTT assay and the IC₅₀ was calculated. The results shown are means ± SE of three independent experiments.

Compounds with a carbonyl group in ring C at position C12 or C11 exhibited an improvement in the antiproliferative activity for some heterocyclic derivatives. Imidazole derivatives **3.23**, **3.25** and **3.26** exhibited better antiproliferative activity compared with compounds **3.16**, **3.18** and **3.19**, which have a double bond at C12 instead of a carbonyl group. The α,β unsaturated ketone moiety in ring C of compound **3.29** does not improve the antiproliferative activity, when compared with compound **3.18**, which does not have

this modification. The methylimidazole derivatives **3.35-3.38** did not show an improvement in the antiproliferative activity when compared with compounds **3.30-3.33**, which do not have a modification in ring C. Compound **3.41** is an exception, because the introduction of an α,β unsaturated ketone in ring C decreases the ability of this compound to inhibit cell growth.

Hydroxy-lactones **3.20-3.22** and **3.34** have the ability to inhibit the proliferation of AsPC-1 cells. Compound **3.21** was the best compound found. Lactones **3.20**, **3.21** and **3.34** were better in the inhibition of cell growth of AsPC-1 pancreatic cancer cells than were compounds **3.19**, **3.26**, **3.33** or **3.38**, which have a methoxy group at C28. The preparation of carbamates at C3 in conjugation with 13,28 β -lactones improves significantly the antiproliferative activity of oleanane compounds.

The presence of a Michael acceptor can increase the potency of the antiproliferative activity in certain compounds.^{414, 444} Oleanolic acid derivatives with modifications at C2 were prepared with the aim of creating an electron-withdrawing moiety in ring A. Compounds **3.28** and **3.40**, which have a carbamate at C2, did not exhibit an improvement of the antiproliferative activity when compared with compounds without modifications at C2. Compounds **3.27**, **3.39** and **3.49** were the best heterocyclic oleanane derivatives found in the inhibition of AsPC-1 cell growth. The conjugation of an *N*-alkylheterocyclic ring with an α,β unsaturated ketone in ring A affords a Michael acceptor moiety, which contributes to the excellent antiproliferative activity observed in these compounds.

The preparation of fluorine-13,28 β -lactones affords compounds **3.51-3.56**. These compounds were able to inhibit the growth of pancreatic cancer cells, with IC_{50s} lower than 10 μ M, with the exception of compound **3.54**. The functionality present at C3 does not seem to influence the antiproliferative activity. Acid fluorides **3.57** and **3.58** also exhibited better antiproliferative activity than that of oleanolic acid **3.1** (Table 3.2.11).

Table 3.2.11. The IC₅₀ (μM) of oleanolic acid fluorine derivatives to inhibit AsPC-1 cell growth.

| Entry | Compound | AsPC-1 |
|----------|-------------|-----------|
| 1 | 3.51 | 5.8±0.02 |
| 2 | 3.52 | 5.3±0.03 |
| 3 | 3.53 | 8.4±0.05 |
| 4 | 3.54 | 35.0±0.07 |
| 5 | 3.55 | 9.0±0.03 |
| 6 | 3.56 | 7.7±0.04 |
| 7 | 3.57 | 8.4±0.01 |
| 8 | 3.58 | 10.1±0.03 |

The AsPC-1 cells were treated with the indicated compounds with at varying of concentrations for 72 h. The antiproliferative effects were determined by MTT assay and the IC₅₀ was calculated. The results shown are means ± SE of three independent experiments.

Figure 3.2.20 represents the SAR conclusions of oleanane compounds tested for their antiproliferative activity in AsPC-1 cells. Compounds **3.30**, **3.23**, **3.21**, and **3.39** which have a Δ^{12} unsaturation in ring C, a carbonyl group at C12, 13,28 β -lactone and modifications at C2, respectively, represent the most active compounds of each group. *N*-alkylimidazoles **3.27**, **3.39** and **3.49** represent the most active compounds in the panel of newly synthesized oleanane derivatives.

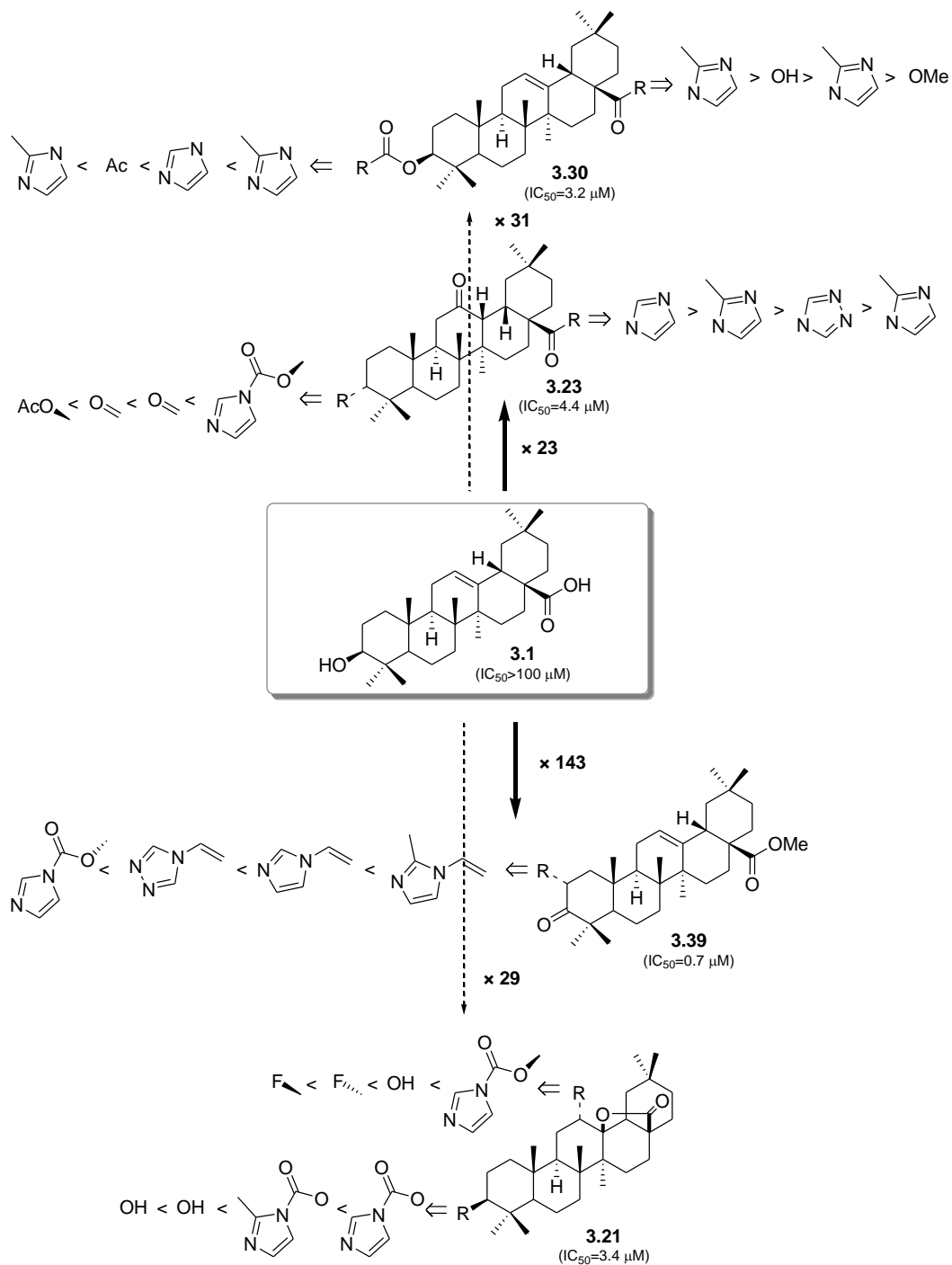


Figure 3.2.20. Structure activity relationships (SAR) among several synthetic derivatives of oleanolic acid **3.1**. The comparison was made based on their IC_{50} s in the inhibition of AsPC-1 cell growth, considering IC_{50} of oleanolic acid **3.1** as $100 \mu M$. Compound **3.30** is 31-fold more potent than oleanolic acid **3.1**. Compound **3.23** is 23-fold more potent than oleanolic acid **3.1**. Compound **3.21** is 29-fold more potent than oleanolic acid **3.1**. Compound **3.39** is 143-fold more potent than oleanolic acid **3.1**.

Compounds **3.27**, **3.39** and **3.49** showed the best antiproliferative activity against AsPC-1 cells, and were further studied for their ability to inhibit the proliferation of other solid tumor cell lines (Table 3.2.12). Compounds **3.27** and **3.39** exhibited IC_{50s} lower than 1 μ M for all cell lines tested except breast cancer cells (MCF-7). Compound **3.49** was less active, although it presented IC_{50s} lower than 3 μ M for all studied cell lines, with the exception of MCF-7 tumor cells.

Table 3.2.12. The IC_{50} (μ M) of oleanolic acid heterocyclic derivatives to inhibit growth of pancreatic (PANC-1 and MIA PaCa 2), breast (MCF-7), prostate (PC-3), hepatic (Hep G2) and lung (A549) cancer cell lines.

| Compd | PANC-1 | MIA PaCa 2 | Hep G2 | MCF-7 | A549 | PC-3 |
|-------------|----------------|----------------|-----------------|----------------|-----------------|-----------------|
| 3.27 | 0.9 \pm 0.02 | 0.9 \pm 0.01 | 0.6 \pm 0.003 | 1.1 \pm 0.04 | 0.6 \pm 0.003 | 0.8 \pm 0.02 |
| 3.39 | 1.0 \pm 0.02 | 0.9 \pm 0.01 | 0.5 \pm 0.02 | 2.0 \pm 0.03 | 0.6 \pm 0.01 | 0.7 \pm 0.003 |
| 3.49 | 3.0 \pm 0.02 | 2.8 \pm 0.01 | 2.1 \pm 0.02 | 5.6 \pm 0.03 | 2.3 \pm 0.03 | 2.3 \pm 0.01 |

The Panc-1, MiaPaCa 2, MCF-7, PC-3, HepG2 and A549 cells were treated with the indicated compounds at varying of concentrations for 72 h. The antiproliferative effects were determined by MTT assay and the IC_{50} was calculated. The results shown are means \pm SE of three independent experiments.

AsPC-1 pancreatic cancer cells were selected for the elucidation of the mechanism of action of compounds **3.27**, **3.39** and **3.49**. Cells treated with compounds **3.27** and **3.39** at 0.5 μ M had few modifications in the cell cycle, but at 1.5 μ M an increase in the number of cells in the sub-G1 phase, apoptotic cells, was observed. Compound **3.49** induced cell-cycle arrest at the G1 phase at 2 μ M, and apoptosis at 4 μ M (Table 3.2.13).

Table 3.2.13. Results of FACS analyses for AsPC-1 cells treated with compounds **3.27**, **3.39** and **3.49** for 24 h at the indicated concentrations. The results represent the percentage of the number of cells in the indicated phase of the cell cycle, mean \pm SD of three independent experiments.

| | Control | 3.27 | | 3.39 | | 3.49 | |
|---------------|----------------|----------------|----------------|----------------|----------------|----------------|----------------|
| | | 0.5 μ M | 1.5 μ M | 0.5 μ M | 1.5 μ M | 2 μ M | 4 μ M |
| Sub-G1 | 3.6 \pm 0.2 | 9.9 \pm 5.1 | 44.5 \pm 3.8 | 8.4 \pm 4.5 | 54.1 \pm 3.0 | 6.1 \pm 5.0 | 34.6 \pm 1.8 |
| G1 | 39.9 \pm 4.2 | 41.9 \pm 4.0 | 21.7 \pm 2.9 | 46.6 \pm 4.2 | 18.8 \pm 1.3 | 48.9 \pm 3.8 | 24.3 \pm 1.3 |
| S | 11.9 \pm 0.4 | 8.8 \pm 0.7 | 8.5 \pm 0.9 | 8.2 \pm 0.2 | 6.7 \pm 0.8 | 20.6 \pm 1.3 | 10.0 \pm 1.0 |
| G2/M | 25.0 \pm 1.2 | 19.6 \pm 2.0 | 11.3 \pm 2.6 | 19.1 \pm 1.9 | 8.0 \pm 1.2 | 6.1 \pm 1.8 | 15.2 \pm 2.6 |

3.2.3. Conclusions

In summary, this section presented a new procedure for the preparation of hydroxylactones and 12-oxo oleanane heterocyclic derivatives. A series of other heterocyclic *N*-acylimidazole, carbamate and *N*-alkylimidazole derivatives were also achieved. The preparation of fluorine derivatives was made via the reaction of oleanolic acid **3.1** or oleanane-type compounds with selectfluor or deoxofluor. These new derivatives of oleanolic acid **3.1** were fully characterized using NMR, MS and IR techniques

The new semisynthetic derivatives present a good antiproliferative profile against pancreatic cancer cells AsPC-1. Compounds **3.27**, **3.39** and **3.49**, in which we introduced a heterocyclic ring in conjugation with an α,β unsaturated ketone in ring A of oleanane backbone, were the most active ones in the inhibition of AsPC-1 cell growth. These compounds induce apoptosis in AsPC-1.

3.3. Experimental section

3.3.1. Chemical

IR spectra were recorded in JASCO FT/IR-420. ^1H , ^{13}C , DEPT-135, HMQC, HMBC, COESY and NOESY spectra were recorded in a Bruker Avance III 400 MHz spectrometer. The chemical shifts were recorded in δ (ppm) using the δ 7.26 of CHCl_3 (^1H NMR) and the δ 77.00 (^{13}C NMR) as internal standards. Chemical shifts measures were given in ppm and coupling constants (J) in hertz (Hz). Low resolution mass spectrometry was obtained in a Finnigan Polaris QGC/MS Benchtop Ion Trap spectrometer with a direct insertion probe and the elemental analysis was obtained in an Analyzer Elemental Carlo Erba 1108 by chromatographic combustion. Melting points were determined using a BUCHI melting point B-540 apparatus and were uncorrected. For thin layer chromatography (TLC) analysis Kiesel gel 60HF254/kiesel gel 60G was used and FCC was performed using Kieselgel 60 (230-400 mesh, Merck). Oleanolic acid **3.1**, selectfluor, deoxofluor, bismuth triflate ($\text{Bi}(\text{OTf})_3$), *m*-CPBA, DMAP, acetic anhydride, ethyl formate, sodium methoxide (NaOMe), THF, dioxane, nitromethane, DMF, benzene, cobalt acetate, *tert*-butyl hydroperoxide, CDI, CBMI and CDT were purchased from Sigma Aldrich Co. The solvents used in the workups were purchase from VWR Portugal, and were of analytical grade. Potassium bicarbonate, sodium chloride, sodium bicarbonate, and sodium sulfite were purchased from Merck Co. All the solvents used in the reactions were previously purified and dried according to the literature procedures.

3-Oxoolean-12-en-28-oic acid (3.2): **3.2** was prepared according to the literature,²⁴¹ from **3.1** (1 g 2.2 mmol) to give a solid (98%). mp 169.5-171.5 °C. IR (film CHCl_3): 2945.7, 1697.1, 1460.8, 1385.6, 1276.7, 1217.8 cm^{-1} . ^1H NMR (400 MHz CDCl_3): δ 5.29 (1H s H12), 2.84 (1H dd $J=11.37$ H18), 2.54 (1H m $J=33.61$ H2), 2.37 (1H m $J=15.30$ H2), 1.13 (3H s), 1.07 (3H s), 1.04 (6H d $J=6.93$), 0.92 (6H d $J=9.91$), 0.79 (3H s). ^{13}C NMR (100 MHz CDCl_3): δ 217.71 (C3), 184.28 (C28), 143.61 (C13), 122.35 (C12). EI-MS m/z : 455.16 (5) M^+ , 410.23 (8), 248.06 (80), 203.19 (100), 190.21 (28), 175.23 (12), 133.19 (68), 105.20 (14), 91.13 (20), 77.10 (12).

3 β -Acetoxy-olean-12-en-28-oic acid (3.3): Preparation of **3.3** was made according to a previously described method,¹⁸³ from **3.1** (100 mg 0.22 mmol), providing a solid (86%). mp 254.2-257.8 °C. IR (film CHCl₃): 2945.7, 1733.7, 1695.1, 1462.7, 1366.3, 1244.8 cm⁻¹. ¹H NMR (400 MHz CDCl₃): δ 5.26 (1H t $J=6.88$ H12), 4.49 (1H m $J=15.91$ H3); 2.81 (1H dd $J=17.64$ H18), 2.04 (3H s OCOCH₃), 1.12 (3H s), 0.99 (3H s), 0.92 (3H s), 0.90 (3H s), 0.86 (3H s), 0.84 (3H s), 0.74 (3H s). ¹³C NMR (100 MHz CDCl₃): δ 184.29 (C28), 171.03 (OCOCH₃), 143.58 (C13), 122.52 (C12), 80.90 (C3). EI-MS m/z: 498.28 (1) M⁺, 439.22 (6), 394.22 (5), 351.26 (3), 248.11 (64), 203.07 (100), 189.12 (22), 175.08 (14), 133.10 (54), 91.05 (27), 79.10 (18), 67.09 (10).

Methyl 3 β -hydroxy-olean-12-en-28-oate (3.4): **3.4** was prepared according to the literature^{429, 434} from **3.1** (100 mg 0.22 mmol) to give a solid (89%). mp 167.0-168.0 °C. IR (film CHCl₃): 3431.7, 2945.7, 1723.1, 1646.00, 1384.6, 1219.8 cm⁻¹. ¹H NMR (400 MHz CDCl₃): δ 5.27 (1H t $J=7.31$ H12), 3.61 (3H s COCH₃), 3.20 (1H m $J=15.97$ H3), 2.85 (1H dd $J=18.90$ H18), 1.12 (3H s), 0.97 (3H s), 0.91 (3H s), 0.89 (3H s), 0.88 (3H s), 0.77 (3H s), 0.71 (3H s). ¹³C NMR (100 MHz CDCl₃): δ 178.25 (C28), 143.74 (C13), 122.32 (C12), 78.99 (C3). EI-MS m/z: 470.11 (6) M⁺, 453.16 (17), 411.24 (6), 377.27 (3), 262.09 (66), 203.24 (100), 189.30 (21), 173.28 (10), 133.26 (32), 119.25 (12), 79.25 (8).

3 β ,12 α -Dihydroxyolean-28,13 β -olide (3.5): To a stirred solution of **3.1** (2 g 4.38 mmol) in chloroform (30 mL) was added *m*-CPBA 77% (1.96 g 8.76 mmol) at room temperature. After 24 hours the reaction was evaporated to dryness, the residue was dissolved in ether (100 mL), the resulting mixture was washed with sodium sulphite (200 mL) over 16 hours. The aqueous solution was extracted with ethyl acetate (3 \times 100 mL). The combined extracts were washed with HCl 10% (100 mL), NaHCO₃ sat (3 \times 100 mL), and water (3 \times 100 mL), dried over Na₂SO₄, filtered and evaporated to the dryness, and crystallized from acetonitrile, to afford **3.5** (94%).⁴⁸³ mp > 300.0 °C. IR (film CHCl₃): 3447.1, 2944.8, 1752.0, 1694.2, 1466.6, 1387.5, 1362.5, 1251.6, 1219.8 cm⁻¹. ¹H NMR (400 MHz CDCl₃): δ 3.88 (1H t $J=5.78$ H12), 3.22 (1H m $J=16.28$ H3), 1.30 (3H s), 1.14 (3H s), 0.98 (3H s), 0.98 (3H s), 0.89 (3H s), 0.87 (3H s), 0.77 (3H s). ¹³C NMR (100 MHz CDCl₃): δ 179.95 (C28), 90.60 (C13), 78.83 (C3), 76.32 (C12), 55.17, 51.10, 44.69,

44.55, 42.27, 42.03, 39.37, 38.88, 38.80, 36.42, 34.11, 33.94, 33.24, 31.54, 28.75, 28.01, 27.97, 27.45, 27.20, 23.87, 21.18, 18.60, 18.51, 17.72, 16.27, 15.34. EI-MS m/z : 472.96 (26) M^+ , 456.98 (28), 411.10 (76), 300.08 (41), 264.07 (31), 234.16 (22), 218.21 (81), 189.24 (100), 177.29 (46), 147.17 (42), 119.12 (41), 107.13 (33), 105.13 (27), 93.13 (24), 79.17 (19).

3-Oxo-12 α -hydroxyolean-28,13 β -olide (3.6): To a stirred solution of **3.2** (150 mg 0.33 mmol) in chloroform (2.5 mL), at room temperature, was added *m*-CPBA 77% (110.94 mg 0.495 mmol). The workup was performed according to the same method as for **3.5** after 24 hours, to afford **3.6** (91%). mp 283.0-285.0 °C. IR (film $CHCl_3$): 3464.5, 2950.6, 1751.1, 1701.9, 1458.9, 1386.6, 1359.6, 1218.8 cm^{-1} . 1H NMR (400 MHz $CDCl_3$): δ 3.89 (1H s H12), 1.31 (3H s), 1.17 (3H s), 1.08 (3H s), 1.03 (3H s), 0.97 (6H s), 0.89 (3H s). ^{13}C NMR (100 MHz $CDCl_3$): δ 217.79 (C3), 179.90 (C28), 90.61 (C13), 76.05 (C12), 54.72, 51.11, 47.31, 44.66, 43.74, 42.10 (2C), 39.53, 39.38, 36.13, 34.06, 33.96, 33.29, 33.22, 31.55, 29.09, 27.94, 27.39, 26.62, 23.83, 21.12, 21.01, 19.03, 18.36, 18.16, 16.23. EI-MS m/z : 470.73 (70) M^+ , 452.77 (14), 424.93 (40), 408.92 (24), 234.07 (38), 205.11 (100), 187.29 (65), 147.40 (39), 119.44 (46), 105.36 (46), 91.35 (49), 79.30 (33).

3 β -Hydroxy-12-oxoolean-28-oic acid (3.7): To a stirred solution of **3.5** (3.0271 g 6.4 mmol) at 40°C in dichloromethane (40 mL), was added $Bi(TfO)_3$ (41.99 mg 0.064 mmol). After 3 hours the reaction mixture was evaporated to the dryness, and the resulting was diluted into water (100 mL), which was extracted with ethyl acetate (3×100 mL). The organic phase was washed with $NaHCO_3$ (3×100 mL) and H_2O (3×100 mL), dried over Na_2SO_4 , filtered and evaporated to the dryness, to afford **3.7** (96%).⁴⁸³ mp 302.0-304.0 °C. IR (film $CHCl_3$): 3465.5, 2942.8, 1693.2, 1469.5, 1386.6, 1367.3, 1233.3 cm^{-1} . 1H NMR (400 MHz $CDCl_3$): δ 3.20 (1H dd $J=15.57$ H3), 2.76 (1H d $J=13.35$), 2.68 (1H d $J=3.77$), 0.99 (6H), 0.98 (3H), 0.95 (3H), 0.91 (3H), 0.86 (3H), 0.77 (3H). ^{13}C NMR (100 MHz $CDCl_3$): δ 211.54 (C12), 183.64 (C28), 78.65 (C3), 55.05, 51.82, 49.73, 47.17, 41.89, 41.27, 38.80, 38.50, 37.91, 36.96, 36.09, 34.42, 33.33, 33.04, 31.85, 31.79, 30.61, 27.94, 27.57, 27.02, 23.10, 22.58, 20.48, 18.26, 16.41, 15.29, 15.20. EI-MS m/z :

471.94 (100) M⁻, 451.86 (24), 358.30 (22), 212.42 (21), 198.29 (14), 130.05 (22), 103.48 (21), 94.11 (21), 79.97 (20), 71.62 (11), 70.44 (16), 61.40 (15).

3 β -Acetoxy-12-oxoolean-28-oic acid (3.8): Preparation of **3.8** was made according to previously described method,¹⁸³ from **3.7** (1.5 g 3.17 mmol), providing a solid (98%). mp 338.0-340.0 °C. IR (film CHCl₃): 2945.7, 2866.7, 1812.8, 1729.8, 1695.1, 1469.5, 1367.3, 1246.8 cm⁻¹. ¹H NMR (400 MHz CDCl₃): δ 4.47 (1H dd $J=15.33$ H3), 2.03 (3H s OCOCH₃), 0.98 (3H s), 0.97 (3H s), 0.94 (3H s), 0.94 (3H s), 0.90 (3H s), 0.88 (3H s), 0.86 (3H s), 0.85 (3H s). ¹³C NMR (100 MHz CDCl₃): δ 211.33 (C12), 184.01 (C28), 170.91 (OCOCH₃), 80.39 (C3), 55.10, 51.81, 49.57, 47.17, 41.80, 41.25, 38.43, 37.72, 37.58, 36.85, 36.04, 34.39, 33.31, 33.02, 31.80, 31.70, 30.59, 27.87, 27.52, 23.36, 23.08, 22.53, 21.22, 20.45, 18.14, 16.39, 15.24. EI-MS m/z: 515.38 (8) M⁺, 499.35 (33), 454.42 (41), 453.47 (100), 264.31 (38), 219.44 (23), 218.41 (67), 203.4 (26), 190.5 (30), 189.47 (49), 177.46 (32), 176.37 (22), 175.33 (29).

3,12-Dioxoolean-12-en-28-oic acid (3.9): **3.9** was prepared according to the literature,²⁴¹ from **3.7** (1.5 g 3.17 mmol) to give a solid (94%). mp 276.0-278.0 °C. IR (film CHCl₃): 2943.8, 2866.7, 1697.1, 1468.5, 1385.6, 1329.7 cm⁻¹. ¹H NMR (400 MHz CDCl₃): δ 1.09 (3H s), 1.03 (6H s), 0.98 (6H s), 0.96 (3H s), 0.91 (3H s). ¹³C NMR (100 MHz CDCl₃): δ 216.75 (C3), 210.82 (C12), 183.61 (C28), 54.84, 51.85, 49.12, 47.36, 47.14, 42.02, 41.24, 38.56 (2C), 36.65, 36.09, 34.40, 33.81, 33.30, 33.02, 31.83, 31.15, 30.61, 27.58, 26.29, 23.08, 22.58, 21.14, 20.40, 19.52, 16.06, 14.86. EI-MS m/z: 470.31 (9) M⁺, 456.3 (13), 455.33 (40), 410.44 (30), 409.51 (100), 264.35 (14), 218.4 (22), 205.4 (15), 203.44 (9).

Methyl 3 β -hydroxy-12-oxoolean-28-oate (3.10): **3.10** was prepared according to the literature^{429, 434} from **3.7** (1.5 g 3.17 mmol) to give a solid (93%). mp 188.1-191.4 °C. IR (film CHCl₃): 3511.7, 2944.8, 2866.7, 1721.2, 1698.0, 1468.5, 1386.6, 1365.4, 1304.6, 1240.0 cm⁻¹. ¹H NMR (400 MHz CDCl₃): δ 3.67 (3H s COCH₃), 3.19 (1H dd $J=15.78$ H3), 2.78 (1H dt $J=13.52$), 2.61 (1H d $J=3.96$), 0.98 (3H s), 0.97 (3H s), 0.96 (3H s), 0.93 (3H s), 0.89 (3H s), 0.84 (3H s), 0.78 (3H s). ¹³C NMR (100 MHz CDCl₃): δ 211.78 (C12), 178.37 (C28), 78.62 (C3), 55.08, 51.81, 51.77, 49.75, 47.34, 41.89, 41.23, 38.79,

38.51, 37.93, 36.92, 36.19, 34.46, 33.36, 32.94, 31.98, 31.80, 30.62, 27.94, 27.56, 27.05, 23.14, 22.73, 20.54, 18.28, 16.10, 15.32, 15.18. EI-MS m/z : 487.35 (13) M^+ , 472.47 (32), 471.48 (100), 412.70 (28), 411.68 (85), 279.63 (13), 278.39 (42), 219.66 (17), 218.5 (49), 203.41 (16).

Methyl 3-oxoolean-12-en-28-oate (3.11): **3.11** was prepared according to the literature,²⁴¹ from **3.4** (600 mg 1.3 mmol) to give a solid (96%). mp 171.8-174.4 °C. IR (film $CHCl_3$): 2946.7, 1726.9, 1704.8, 1458.9, 1434.8, 1384.6, 1363.4, 1261.2 cm^{-1} . 1H NMR (400 MHz $CDCl_3$): δ 5.30 (1H s H12), 3.62 (3H s $COCH_3$), 2.87 (1H dd $J=17.19$ H18), 2.54 (1H m $J=34.26$), 2.34 (1H m $J=25.88$), 1.13 (3H s), 1.08 (3H s), 1.04 (6H s), 0.92 (3H s), 0.89 (3H s), 0.77 (3H s). ^{13}C NMR (100 MHz $CDCl_3$): δ 217.67 (C3), 178.22 (C28), 143.86 (C13), 122.12 (C12). EI-MS m/z : 469.12 (96) M^+ , 451.23 (33), 262.17 (40), 248.21 (32), 203.32 (100), 189.33 (56), 187.35 (22), 133.26 (59), 119.25 (23), 105.25 (18).

Methyl 2-hydroxymethylene-3-oxoolean-12-en-28-oate (3.12): Preparation of **3.12** was made according to previously described method,^{330, 431} from **3.11** (500 mg 1.1 mmol), providing a solid (92%). mp 199.1-201.2 °C. IR (film $CHCl_3$): 2947.7, 1866.7, 1726.0, 1634.4, 1585.2, 1456.0, 1386.6, 1362.5, 1256.4, 1231.3 cm^{-1} . 1H NMR (400 MHz $CDCl_3$): δ 14.09 (1H $C2CHOH$), 8.57 (1H $C2CHOH$), 5.33 (1H), 3.63 (3H), 2.89 (1H dd $J=16.70$), 2.27 (1H d $J=14.36$), 1.18 (3H s), 1.14 (3H s), 1.11 (3H s), 0.93 (3H s), 0.90 (6H s), 0.78 (3H s). ^{13}C NMR (100 MHz $CDCl_3$): δ 190.80 (C3), 188.24 ($C2CHOH$), 178.21 (C28), 143.79 (C13), 122.15 (C12), 105.73 (C2). EI-MS m/z : 496.01 (17) M^- , 471.95 (44), 423.35 (39), 400.67 (27), 384.14 (63), 354.76 (20), 329.69 (33), 306.67 (33), 248.68 (100), 215.26 (18), 194.22 (35), 63.86 (22), 61.06 (19).

Methyl 2 α -hydroxy-3-oxoolean-12-en-28-oate (3.13): **3.13** was prepared according to the literature^{328, 489} from **3.11** (100 mg 0.213 mmol) to give a solid (90%). mp 116.8-123.0 °C. IR (film $CHCl_3$): 3485.7, 2947.7, 1726.0, 1703.8, 1459.9, 1434.8, 1386.6, 1363.4, 1261.2 cm^{-1} . 1H NMR (400 MHz $CDCl_3$): δ 5.28 (1H s H12), 4.53 (1H m $J=18.93$ H2), 3.62 (3H s $COCH_3$), 2.86 (1H dd $J=11.16$ H18), 1.25 (3H s), 1.15 (3H s), 1.10 (3H s), 1.09 (3H s), 0.91 (3H s), 0.88 (3H s), 0.77 (3H s). ^{13}C NMR (100 MHz

CDCl₃): δ 216.58 (C3), 178.21 (C28), 143.92 (C13), 121.84 (C12), 69.15 (C2). EI-MS m/z : 484.86 (60) M⁺, 468.98 (22), 425.09 (16), 262.16 (35), 249.16 (17), 218.19 (13), 203.20 (100), 189.18 (54), 173.17 (19), 133.08 (55), 119.02 (19), 105.03 (14), 91.03 (11).

3 β -Acetoxy-11-oxoolean-12-en-28-oic acid (3.14): To a stirred solution of **3.3** (1 g 2 mmol) in a mixture of acetonitrile (10 mL) and ethyl acetate (5 mL) at 77 °C, was added *t*-butyl hydroperoxide (0.0675 mmol 7.5 mL) and the catalyst cobalt acetate tetra hydrate (0.72 mmol 179.208 mg). After 77 hours was added to the reaction mixture an aqueous solution containing Na₂SO₃ (200 mL), and the resulting mixture was stirred 18.5 hours. The mixture was extracted with ethyl acetate (3 \times 100 mL). The combined extracts were washed with HCl 10% (2 \times 100 mL) and water (3 \times 100 mL), dried over Na₂SO₄, filtered, and concentrated to afford an oil. The residue was subjected to flash column chromatography [hexanes-ethyl acetate from (70:30) to (40:60)] to afford **3.14** (36%). mp 275.0-277.4 °C. IR (film CHCl₃): 2947.7, 1730.8, 1699.9, 1655.6, 1460.8, 1388.5, 1364.4, 1245.8, 1219.8 cm⁻¹. ¹H NMR (400 MHz CDCl₃): δ 5.61 (1H s H12), 4.51 (1H dd $J=15.85$ H3), 2.97 (1H d $J=11.52$ H18), 2.83 (1H d $J=13.60$), 2.03 (3H s COCH₃), 1.34 (3H s), 1.11 (3H s), 0.94 (3H s), 0.92 (3H s), 0.89 (3H s), 0.86 (6H s). ¹³C NMR (100 MHz CDCl₃): δ 200.29 (C11), 182.85, 171.02, 168.49, 127.96, 80.57, 61.61, 55.00, 45.00, 44.04, 43.58, 43.38, 41.33, 38.70, 37.99, 37.10, 33.59, 32.79, 32.75, 31.56, 30.61, 28.02, 27.68, 23.53, 23.49, 23.35, 22.56, 21.25, 19.16, 17.18, 16.61, 16.24. EI-MS m/z : 512.73 (40) M⁺, 302.68 (46), 261.73 (100), 256.87 (86), 216.91 (56), 188.93 (55), 174.93 (49), 118.89 (25), 104.92 (14), 80.90 (8).

3 β -(1H-Imidazol-1-carbonyloxy)-olean-12-en-28-oic acid (3.15) and **28-(1H-Imidazol-1-yl)-28-oxoolean-12-en-3 β -yl-1H-imidazole-1-carboxylate (3.16)**: To a stirred solution of **3.1** (1 g 2.2 mmol) in THF (10 mL), under N₂ atmosphere, at 70°C, was added CDI (356.73 mg 2.2 mmol). After 41 hours the reaction mixture was diluted with water (60 mL), the aqueous phase was extracted with ethyl acetate (3 \times 50 mL). The resulting organic phases were washed with NaCl 10% (3 \times 50 mL), dried over Na₂SO₄, filtered and evaporated to the dryness, to afford a yellow residue. The residue was subjected to flash column chromatography [hexanes-ethyl acetate from (90:10) to (20:80)], to afford **3.16** (29%) and **3.15** (17%). **3.15**: mp 216.2-218.3 °C. IR (film

CHCl₃): 3140.5, 2946.7, 1760.7, 1697.1, 1471.4, 1387.5, 1288.2, 1239.0 cm⁻¹. ¹H NMR (400 MHz CDCl₃): 8.72 (1H s Himidazole), 7.44 (1H s Himidazole), 7.13 (1H s Himidazole), 5.28 (1H s H12), 4.72 (1H dd *J*=15.57 H3), 2.84 (1H dd *J*=10.46 H18), 1.14 (3H s), 0.97 (9H s), 0.93 (3H s), 0.90 (3H s), 0.77 (3H s). ¹³C NMR (100 MHz CDCl₃): δ 183.24 (C28), 148.09 (OCO), 143.80 (C13), 136.82, 129.17, 122.21 (C12), 117.28, 86.94 (C3), 55.22 (C5), 47.54 (C9), 46.46, 45.87 (C19), 41.60 (C14), 40.96 (C18), 39.27 (C8), 38.11 (C4), 37.91, 36.94, 33.80, 33.05, 32.47, 32.41, 30.66, 28.17, 27.67, 25.89 (C27), 23.57, 23.41, 23.37, 22.89, 18.13, 17.05 (C26), 16.84, 15.34. EI-MS *m/z*: 549.84 (1) M⁻, 302.80 (6), 247.98 (55), 202.97 (97), 190.01 (31), 175.04 (18), 133.02 (60), 105.08 (32), 68.96 (100). **3.16**: mp 237.4-241.8 °C. IR (film CHCl₃): 3134.7, 2950.6, 1757.8, 1721.2 1525.4, 1469.5, 1388.5, 1364.4, 1319.1, 1281.5, 1240.0, 1204.3 cm⁻¹. ¹H NMR (400 MHz CDCl₃): δ 8.36 (1H s Himidazole), 8.14 (1H s Himidazole), 7.57 (1H s Himidazole), 7.41 (1H s Himidazole), 7.07 (2H s Himidazole), 5.36 (1H s H12), 4.69 (1H dd *J*=16.21 H3), 3.06 (1H dd *J*=11.36), 1.17 (3H s), 0.95 (15H s), 0.69 (3H s). ¹³C NMR (100 MHz CDCl₃): δ 174.55, 148.47, 142.69, 136.96, 130.37, 129.26, 123.01 (2C), 117.54, 117.06, 86.30, 55.26, 49.89, 47.49, 45.82, 42.54, 41.84, 39.21, 38.08, 37.99, 36.88, 33.87, 32.82, 32.44, 31.31, 30.39, 28.13, 27.61, 25.81, 23.79, 23.48, 23.40 (2C), 18.05, 16.82, 16.69, 15.37. EI-MS *m/z*: 600.86 (4) M⁺, 488.93 (16), 393.12 (11), 298.01 (12), 255.13 (9), 203.18 (22), 187.22 (14), 173.21 (9), 91.20 (8), 69.35 (100).

3-Oxoolean-12-en-28-yl-1H-imidazole-1-carboxylate (3.17): To a stirred solution of **3.2** (500 mg 1.1 mmol) in THF (10 mL), under N₂ atmosphere, at 70°C, was added CDI (356.73 mg 2.2 mmol). The workup was performed according to the same method as for **3.15** after 25.5 hours. The solid was subjected to flash column chromatography [hexanes-ethyl acetate from (70:30) to (40:60)], to afford **3.17** (71%). mp 129.6-132.9 °C. IR (film CHCl₃): 2947.7, 1716.3, 1702.8, 1462.7, 1388.5, 1363.4, 1268.0, 1226.5, 1205.3 cm⁻¹. ¹H NMR (400 MHz CDCl₃): δ 8.28 (1H s Himidazole), 7.55 (1H s Himidazole), 7.05 (1H d *J*=0.93 Himidazole), 5.37 (1H t *J*=7.07 H12), 3.06 (1H dd *J*=16.90 H18), 2.32 (1H m *J*=34.43 C2), 1.16 (3H s C27), 1.06 (3H s C23 or C24), 1.03 (3H s C26), 1.02 (3H s C23 ou C24), 0.96 (3H C29 or C30), 0.95 (3H s C29 or C30), 0.72 (3H s C25). ¹³C NMR (100 MHz CDCl₃): δ 217.50 (C3), 174.64 (C28), 142.71 (C13), 137.01 (Cimidazole), 129.66 (Cimidazole), 122.95 (C12), 117.44 (Cimidazole), 55.34 (C5),

49.83 (C17), 47.41 (C4), 46.82 (C9), 45.79 (C19), 42.59 (C18), 41.92 (C14), 39.16 (C8), 39.13 (C1), 36.71 (C10), 34.10 (C2), 33.86, 32.81 (C29 or C30), 32.08, 31.55 (C6), 31.27, 30.37 (C20), 27.60 (C15), 26.32 (C23 or C24), 25.72 (C27), 23.76 (C29 or C30), 23.47 (C11), 21.42 (C23 or C24), 19.42, 16.59 (C26), 14.98 (C25). EI-MS m/z : 505.09 (40) M^+ , 409.22 (69), 298.12 (21), 203.18 (87), 190.20 (30), 163.23 (22), 133.22 (33), 119.22 (36), 105.20 (39), 91.21 (47), 69.17 (100).

3 β -Acetoxy-olean-12-en-28-yl-1H-imidazole-1-carboxylate (3.18): To a stirred solution of **3.3** (200 mg 0.4 mmol) in THF (4 mL), under N_2 atmosphere, at 70°C, was added CDI (129.72 mg 0.8 mmol). The workup was performed according to the same method as for **3.15** after 26 hours. The solid was subjected to flash column chromatography [hexanes-ethyl acetate from (80:20) to (60:40)], to afford **3.18** (89%). mp 122.8-127.3 °C. IR (film $CHCl_3$): 2949.6, 1728.9, 1467.6, 1363.4, 1243.9, 1222.7, 1202.4 cm^{-1} . 1H NMR (400 MHz $CDCl_3$): δ 8.34 (1H s Himidazole), 7.56 (1H s Himidazole), 7.06 (1H s Himidazole), 5.34 (1H t $J=7.16$ H12), 4.47 (1H dd $J=15.94$ H3), 3.04 (1H dd $J=18.42$ H18), 2.03 (3H s $OCOCH_3$), 1.14 (3H s C27), 0.95 (3H s C29 or C30), 0.94 (3H s C29 or C30), 0.91 (3H C25), 0.83 (3H s C23 or C24), 0.83 (3H s C23 or C24), 0.66 (3H s C26). ^{13}C NMR (100 MHz $CDCl_3$): δ 174.55 (C28), 170.97 ($OCOCH_3$), 142.58 (C13), 136.962 (Cimidazole), 129.22 (Cimidazole), 123.13 (C12), 117.53 (Cimidazole), 80.79 (C3), 55.26 (C5), 49.86 (C17), 47.46 (C9), 45.76 (C19), 42.51 (C18), 41.78 (C14), 39.17 (C8), 38.09 (C1), 37.63 (C4), 36.86 (C10), 33.84, 32.80 (C29 or C30), 32.47, 31.54, 31.28, 30.36 (C20), 27.95 (C23 or 24), 27.57, 25.76 (C27), 23.76 (C29 or C30), 23.45, 23.37, 21.26 (C32), 18.05, 16.66 (C26), 16.60 (C23 or C24), 15.37 (C25). EI-MS m/z : 549.09 (7) M^+ , 453.19 (7), 393.23 (9), 298.09 (11), 215.16 (7), 203.11 (41), 189.12 (30), 147.11 (19), 119.09 (33), 105.08 (40), 91.06 (47), 69.02 (100).

Methyl 3 β -(1H-imidazole-1-carboxyloxy)-olean-12-en-28-oate (3.19): To a stirred solution of **3.4** (300 mg 0.64 mmol) in THF (5 mL), under N_2 atmosphere, at 70°C, was added CDI (207.55 mg 1.28 mmol). The workup was performed according to the same method as for **3.15** after 22 hours. The solid was subjected to flash column chromatography [hexanes-ethyl acetate from (80:20) to (55:45)], to afford **3.19** (82%). mp 220.2-221.1 °C. IR (film $CHCl_3$): 2947.7, 1757.8, 1726.0, 1468.5, 1388.5, 1319.1, 1288.2, 1240.0 cm^{-1} . 1H NMR (400 MHz $CDCl_3$): δ 8.22 (1H s Himidazole), 7.43 (1H s

Himidazole), 7.11 (1H d $J=0.79$ Himidazol), 5.28 (1H t $J=6.97$ H12), 4.70 (1H dd $J=16.54$ H3), 3.61 (3H s COOCH_3), 2.86 (1H dd $J=17.87$ H18), 1.13 (3H s), 0.96 (6H s), 0.95 (3H s), 0.92 (3H s), 0.89 (3H s), 0.73 (3H s). ^{13}C NMR (100 MHz CDCl_3): δ 178.18 (C28), 148.10 (OCO), 143.85 (C13), 136.68 (Cimidazole), 129.37 (Cimidazole), 122.03 (C12), 117.23 (Cimidazole), 86.88 (C3), 55.21 (C5), 51.49 (COOCH_3), 47.51 (C9), 46.65 (C17), 45.81 (C19), 41.60 (C14), 41.23 (C18), 39.24 (C8), 38.08 (C4), 37.91, 36.87 (C10), 33.80 (C21), 33.06 (C29 or C30), 32.48, 32.31, 30.65 (C20), 28.15 (C23 or C24 or C26), 27.64, 25.87 (C27), 23.59 (C29 or C30), 23.39 (C11), 23.36 (C2), 22.99 (C22), 18.13, 16.83 (C23 or C24 or C26), 16.78 (C26), 15.29 (C23 or C24 or C25). EI-MS m/z : 565.02 (5) M^+ , 452.18 (6), 393.23, 262.06 (13), 248.05 (5), 203.09 (60), 189.12 (28), 173.15 (12), 133.12 (50), 91.09 (26), 69.05 (100).

3 β -(1H-Imidazole-1-carboxyloxy)-12 α -hydroxyolean-28,13 β -olide (3.20): To a stirred solution of **3.5** (500 mg 1.06 mmol) in THF (5 mL), under N_2 atmosphere, at 70°C, was added CDI (343.76 mg 2.12 mmol). The workup was performed according to the same method as for **3.15** after 6 hours. The solid was subjected to flash column chromatography [hexanes-ethyl acetate from (60:40) to (0:100)], to afford **3.20** (13%). mp 278.6-280.6 °C. IR (film CHCl_3): 3480.9, 3133.8, 2951.5, 2872.5, 1759.7, 1470.5, 1388.5, 1319.1, 1288.2, 1241.0 cm^{-1} . ^1H NMR (400 MHz CDCl_3): δ 8.12 (1H s Himidazole), 7.40 (1H s Himidazole), 7.06 (1H s Himidazole), 4.70 (1H dd $J=16.33$), 3.90 (1H s), 1.32 (3H s), 1.16 (3H s), 0.98 (6H s), 0.96 (3H s), 0.94 (3H s), 0.89 (3H s). ^{13}C NMR (100 MHz CDCl_3): δ 179.93, 148.48, 136.98, 130.48, 117.03, 90.59, 86.10, 55.18, 51.08, 44.67, 44.44, 42.26, 42.07, 39.33, 38.28, 38.20, 36.33, 34.10, 33.81, 33.23, 31.54, 28.83, 28.04, 27.97, 27.44, 23.85, 23.44, 21.15, 18.54 (3C), 17.56, 16.64, 16.33. EI-MS m/z : 566.26 (40) M^+ , 476.92 (12), 391.22 (100).

3 β ,12 α -Di-(1H-imidazole-1-carboxyloxy)-olean-28,13 β -olide (3.21): To a stirred solution of **3.5** (500 mg 1.06 mmol) in THF (5 mL), under N_2 atmosphere, at 70°C, was added CDI (687.52 mg 4.24 mmol). The workup was performed according to the same method as for **3.15** after 24 hours. The solid was subjected to flash column chromatography [hexanes-ethyl acetate from (60:40) to (15:85)], to afford **3.21** (56%). mp 166.9-173.4 °C. IR (film CHCl_3): 3401.8, 3128.0, 2951.5, 2878.2, 1758.8, 1470.5,

1390.4, 1317.1, 1289.2, 1240.0 cm^{-1} . ^1H NMR (400 MHz CDCl_3): δ 8.11 (1H s Himidazole), 8.05 (1H s Himidazole), 7.74 (1H s Himidazole), 7.34 (1H s Himidazole), 7.12 (1H s Himidazole), 7.00 (1H s Himidazole), 5.23 (1H s H12), 4.63 (1H dd $J=16.03$ H3), 1.30 (3H s), 1.17 (3H s), 0.93 (3H s), 0.91 (3H s), 0.90 (3H s), 0.78 (3H s), 0.70 (3H s). ^{13}C NMR (100 MHz CDCl_3): δ 178.17 (C28), 148.190 (C3OCO), 147.45 (C12OCO), 136.77 (2C Cimidazole), 131.20 (Cimidazole), 130.26 (Cimidazole), 116.86 (Cimidazole), 116.75 (Cimidazole), 88.49 (C13), 85.37 (C3), 80.87 (C12), 54.93 (C5), 49.86 (C18), 45.22 (C9), 44.32 (C17), 42.01 (C8), 41.93 (C14), 39.16 (C19), 38.244, 38.02 (C4), 36.19 (C10), 33.56 (C7), 33.47, 32.92 (C29 or C30), 31.31 (C20), 27.82 (C23 or C24 or C25), 27.66 (C15), 27.04, 25.09, 23.39 (C29 or C30), 23.10, 20.77, 18.40 (C27), 18.21 (C26), 17.27, 16.48 (C23 or C24 or C25), 15.94 (C23 or C24 or C25). EI-MS m/z : 660.43 (5) M^+ , 436.39 (65), 391.44 (43), 255.32 (40), 202.27 (43), 201.31 (63), 199.28 (40), 189.3 (100), 188.28 (44), 187.33 (85), 175.38 (41), 173.36 (57), 133.33 (41), 119.31 (50), 107.23 (40).

3-Oxo-12 α -(1H-imidazole-1-carbonyloxy)-olean-28,13 β -olide (3.22): To a stirred solution of **3.6** (300 mg 0.64 mmol) in THF (4 mL), under N_2 atmosphere, at 70°C , was added CDI (207.55 mg 1.28 mmol). The workup was performed according to the same method as for **3.15** after 6.5 hours. The solid was subjected to flash column chromatography [hexanes-ethyl acetate from (80:20) to (40:60)], to afford **3.22** (33 %). mp $263.3\text{-}269.3^\circ\text{C}$. IR (film CHCl_3): 3128.0, 2951.5, 1776.1, 1765.5, 1702.8, 1467.6, 1390.4, 1315.2, 1289.2, 1240.0, 1218.8 cm^{-1} . ^1H NMR (400 MHz CDCl_3): δ 8.12 (1H s Himidazole), 7.40 (1H s Himidazole), 7.13 (1H s Himidazole), 5.26 (1H s H12), 1.33 (3H s C27), 1.23 (3H s C26), 1.08 (3H s C23 or C24), 1.02 (3H s C23 or C24), 0.96 (3H s C25), 0.82 (3H s C29 or C30), 0.74 (3H s C29 or C30). ^{13}C NMR (100 MHz CDCl_3): δ 216.84 (C3), 178.29 (C28), 147.51 (OCO), 136.80 (Cimidazole), 131.33 (Cimidazole), 116.86 (Cimidazole), 88.66 (C13), 80.95 (C12), 54.53 (C5), 50.10 (C18), 47.15 (C4), 44.71 (C9), 44.45 (C17), 42.12 (C8), 41.98 (C14), 39.54 (C19), 39.34 (C1), 36.10 (C10), 33.64 (C2), 33.58 (C21), 33.16 (C7), 31.44 (C20), 27.79 (C15), 27.14, 26.64 (C23 or C24), 25.51 (C11), 23.47 (C29 or C30), 20.95 (C23 or C24), 20.89, 18.88, 18.38 (C27), 17.96 (C26), 15.95 (C25). EI-MS m/z : 564.75 (50) M^+ , 539.52 (37), 457.99 (28), 424.40 (100), 314.97 (33), 272.54 (47), 146.17 (12).

28-(1*H*-Imidazol-1-yl)-12,28-dioxolean-3 β -yl-1*H*-imidazole-1-carboxylate

(3.23): To a stirred solution of **3.7** (300 mg 0.63 mmol) in THF (6 mL), under N₂ atmosphere, at 70°C, was added CDI (616.2 mg 3.8 mmol). The workup was performed according to the same method as for **3.15** after 19 hours. The solid was subjected to flash column chromatography [hexanes-ethyl acetate from (60:40) to (10:90)], to afford **3.23** (97%). mp 165.4-166.2 °C. IR (film CHCl₃): 3132.8, 2950.6, 2866.7, 1757.8, 1699.9, 1526.4, 1470.5, 1389.5, 1319.1, 1289.2, 1240.0 cm⁻¹. ¹H NMR (400 MHz CDCl₃): δ 8.30 (1H s), 8.11 (1H s), 7.59 (1H s), 7.39 (1H s), 7.06 (2H s), 4.66 (1H dd $J=11.28$), 2.96 (1H dd $J=12.45$), 2.86 (1H s), 1.02 (3H s), 0.98 (3H s), 0.96 (9H s), 0.94 (3H s), 0.91 (3H s). ¹³C NMR (100 MHz CDCl₃): δ 210.46, 175.42, 148.44, 137.25, 136.96, 130.59, 130.11, 117.51, 117.00, 85.64, 55.08, 50.91, 50.11, 49.67, 42.09, 41.29, 38.40, 38.13, 37.49, 36.80, 36.04, 34.26, 33.03, 32.09, 31.60, 30.32, 29.25, 27.99, 27.64, 23.72, 23.63, 23.27, 20.44, 18.04, 16.59, 16.14, 15.22. EI-MS m/z : 617.34 (4) M⁺, 521.44 (72), 409.45 (76), 205.37 (100), 189.43 (75).

3 β -Acetoxy-12-oxoolean-28-yl-1*H*-imidazole-1-carboxylate (3.24): To a stirred solution of **3.8** (300 mg 0.58 mmol) in THF (5 mL), under N₂ atmosphere, at 70°C, was added CDI (188.1 mg 1.16 mmol). The workup was performed according to the same method as for **3.15** after 7 hours. The solid was subjected to flash column chromatography [hexanes-ethyl acetate from (65:35) to (50:50)], to afford **3.24** (42%). mp 181.4-183.8 °C. IR (film CHCl₃): 3139.5, 2947.7, 2872.5, 1717.3, 1468.5, 1366.3, 1244.8 cm⁻¹. ¹H NMR (400 MHz CDCl₃): δ 8.29 (1H s), 7.57 (1H s), 7.05 (1H s), 4.44 (1H dd $J=15.75$), 2.94 (1H dt $J=13.08$), 2.82 (1H d $J=3.67$), 2.01 (3H s), 1.00 (3H s), 0.95 (3H s), 0.94 (3H s), 0.90 (3H s), 0.85 (3H s), 0.83 (6H s). ¹³C NMR (100 MHz CDCl₃): δ 210.72, 175.40, 170.82, 137.20, 129.97, 117.49, 80.29, 55.11, 50.88, 50.09, 49.65, 42.02, 41.24, 38.36, 37.67, 37.58, 36.77, 35.98, 34.22, 32.99, 32.98, 32.05, 31.61, 30.26, 27.81, 27.59, 23.68, 23.60, 23.30, 21.18, 20.38, 18.03, 16.36, 16.08, 15.19. EI-MS m/z : 565.24 (8) M⁺, 469.3 (32), 205.15 (100), 189.19 (68), 187.2 (36), 107.13 (25), 69.07 (36).

3,12-Dioxolean-28-yl-1*H*-imidazole-1-carboxylate (3.25): To a stirred solution of **3.9** (250 mg 0.53 mmol) in THF (5 mL), under N₂ atmosphere, at 70°C, was added CDI (171.9 mg 1.06 mmol). The workup was performed according to the same method as for

3.15 after 4 hours. The solid was subjected to flash column chromatography [hexanes-ethyl acetate from (60:40) to (45:55)], to afford **3.25** (56%). mp 144.1-149.1 °C. IR (film CHCl₃): 3138.6, 2947.7, 2865.7, 1701.9, 1468.5, 1386.6, 1364.4, 1266.0, 1231.3 cm⁻¹. ¹H NMR (400 MHz CDCl₃): δ 8.31 (1H s), 7.58 (1H s), 7.07 (1H s), 1.06 (3H s), 1.02 (3H s), 1.01 (3H s), 0.97 (6H s), 0.96 (3H s), 0.94 (3H s). ¹³C NMR (100 MHz CDCl₃): δ 216.55, 210.29, 175.37, 137.22, 129.98, 117.51, 54.92, 50.90, 50.08, 49.20, 47.35, 42.21, 41.23, 38.56, 38.52, 36.61, 36.03, 34.23, 33.79, 33.01 (2C), 32.05, 31.07, 30.29, 27.66, 26.17, 23.71, 23.61, 21.15, 20.32, 19.43, 15.88, 14.80. EI-MS m/z: 521.25 (5) M⁺, 425.3 (62), 407.34 (51), 205.19 (100), 187.29 (34).

Methyl 3β-(1H-imidazole-1-carboxyloxy)-12-oxoolean-28-oate (3.26): To a stirred solution of **3.10** (250 mg 0.514 mmol) in THF (4 mL), under N₂ atmosphere, at 70°C, was added CDI (166.69 mg 1.028 mmol). The workup was performed according to the same method as for **3.15** after 5.5 hours. The solid was subjected to flash column chromatography [hexanes-ethyl acetate from (60:40) to (55:45)], to afford **3.26** (61%). mp 233.4-236.3 °C. IR (film CHCl₃): 3133.8, 2947.7, 2863.8, 1757.8, 1721.2, 1698.0, 1468.5, 1388.5, 1318.1, 1288.2, 1240.0 cm⁻¹. ¹H NMR (400 MHz CDCl₃): δ 8.10 (1H s), 7.39 (1H s), 7.05 (1H s), 4.66 (1H dd *J*=16.26 Hz), 3.67 (3H s COOCH₃), 2.78 (1H dt *J*=13.44 Hz), 2.61 (1H d *J*=3.72), 0.96 (12H s), 0.94 (3H s), 0.91 (3H s), 0.89 (3H s). ¹³C NMR (100 MHz CDCl₃): δ 211.24, 178.30, 148.39, 136.92, 130.50, 117.00, 85.72, 55.04, 51.77 (2C), 49.55, 47.28, 41.82, 41.20, 38.42, 38.10, 37.44, 36.76, 36.14, 34.41, 33.33, 32.87, 31.92, 31.64, 30.59, 27.99, 27.50, 23.26, 23.10, 22.67, 20.51, 18.08, 16.59, 16.08, 15.18. EI-MS m/z: 581.02 (8) M⁺, 218.04 (60), 175.07 (72), 119.05 (62), 107.03 (60), 105.03 (100), 95.03 (75), 93.02 (56), 91.02 (87), 81.02 (60), 79.01 (77).

Methyl 2-(1H-imidazol-1-yl)-methylene-3-oxoolean-12-en-28-oate (3.27): To a stirred solution of **3.12** (300 mg 0.60 mmol) in THF (5 mL), under N₂ atmosphere, at 70°C, was added CDI (194.58 mg 1.2 mmol). The workup was performed according to the same method as for **3.15** after 6 hours. The solid was subjected to flash column chromatography [hexanes-ethyl acetate from (70:30) to (55:45)], to afford **3.27** (71%). mp 217.2-220.0 °C. IR (film CHCl₃): 3116.4, 2948.6, 2866.7, 1725.0, 1686.4, 1607.4, 1517.7, 1486.9, 1383.7, 1363.4, 1303.6, 1262.2, 1226.5, 1213.0 cm⁻¹. ¹H NMR (400 MHz

CDCl₃): δ 7.79 (1H s H2' or H5'), 7.70 (1H s C2CH), 7.22 (1H s H2' or H5'), 7.15 (1H s H4'), 5.34 (1H s H12), 3.62 (3H s COOCH₃), 2.88 (2H H18 and H1), 1.18 (3H s C27), 1.172 (3H s C23 or C24), 1.128 (3H s C23 or C24), 0.935 (3H s C29 or C30), 0.907 (3H s C29 or C30), 0.887 (3H s C25), 0.791 (3H s C26). ¹³C NMR (100 MHz CDCl₃): δ 206.59 (C3), 178.15 (C28), 144.02 (C13), 138.47 (C2' or C5'), 130.658 (C2CH), 130.36 (C4'), 122.99 (C2), 121.77 (C12), 119.32 (C2' or C5'), 52.58 (C5), 51.54 (COOCH₃), 46.77 (C17), 45.82 (C19), 45.46 (C9), 45.19 (C4), 43.01 (C1), 41.93 (C14), 41.48 (C18), 39.16 (C8), 36.07 (C10), 33.86, 33.09 (C29 or C30), 32.28, 31.69 (C7), 30.69 (C20), 29.76 (C23 or C24), 27.65 (C15), 25.65 (C27), 23.63 (C11), 23.58 (C29 or C30), 23.07, 22.40 (C23 or C24), 20.29, 16.39 (C26), 15.39 (C25). EI-MS m/z: 547.4 (40) M⁺, 487.45 (51), 298.24 (48), 285.34 (69), 203.3 (94), 133.3 (100), 69.35 (77).

Methyl 2 α -(1H-imidazole-1-carboxyloxy)-3-oxoolean-12-en-28-oate (3.28): To a stirred solution of **3.13** (300 mg 0.62 mmol) in THF (4 mL), under N₂ atmosphere, at 70°C, was added CDI (201.1 mg 1.24 mmol). The workup was performed according to the same method has for **3.15** after 4 hours. The solid was subjected to flash column chromatography [hexanes-ethyl acetate from (80:20) to (70:30)], to afford **2.28** (26%). mp 127.0-128.5 °C. IR (film CHCl₃): 3133.8, 2947.7, 2878.2, 1769.6, 1724.1, 1465.6, 1394.3, 1318.1, 1290.1, 1240.0 cm⁻¹. ¹H NMR (400 MHz CDCl₃): δ 8.12 (1H s Himidazole), 7.40 (1H s Himidazole), 7.04 (1H s Himidazole), 5.70 (1H dd $J=19.27$ H2), 5.27 (1H s H12), 3.60 (3H s), 2.85 (1H dd $J=17.20$ H18), 2.37 (1H dd $J=18.22$), 1.31 (3H s), 1.15 (3H s); 1.12 (3H s), 1.09 (3H s), 0.89 (3H s), 0.87 (3H s), 0.77 (3H s). ¹³C NMR (100 MHz CDCl₃): δ 207.56 (C3), 178.08 (C28), 147.93 (OCO), 144.14 (C13), 137.12 (Cimidazole), 130.42 (Cimidazole), 121.34 (C12), 117.13 (Cimidazole), 75.32 (C2), 56.89 (C5), 51.50 (COOCH₃), 48.68 (C4), 47.30 (C9), 46.52 (C17), 45.67 (C19 or C21 or C22), 45.07 (C1), 41.63 (C14), 41.11 (C18), 39.29 (C8), 37.99 (C10), 33.69 (C19 or C21 or C22), 32.99 (C29 or C30), 32.17, 32.11 (C7), 30.59 (C20), 27.52 (C15), 25.81 (C27), 24.65 (C23 or C24). 23.51 (C29 or C30), 23.48 (C19 or C21 or C22), 22.83, 21.09 (C23 or C24), 18.95, 16.92 (C26), 15.86 (C25). EI-MS m/z: 578.6 (1) M⁺, 577.99 (100), 247.25 (30), 136.78 (37), 126.95 (33).

3 β -Acetoxy-11-oxoolean-12-en-28-yl-1H-imidazole-1-carboxylate (3.29): To a stirred solution of **3.14** (145.6 mg 0.284 mmol) in THF (5 mL), under N₂ atmosphere, at 70 °C, was added CDI (92.1 mg 0.568 mmol). The workup was performed according to the same method as for **3.15** after 7 hours. The solid was subjected to flash column chromatography [hexanes-ethyl acetate from (60:40) to (20:80)], to afford **3.29** (40%). mp 156.6-163.0 °C. IR (film CHCl₃): 3140.5, 2948.6, 2873.4, 1727.9, 1654.6, 1532.2, 1465.6, 1390.4, 1365.4, 1327.8, 1305.6, 1248.7, 1209.2 cm⁻¹. ¹H NMR (400 MHz CDCl₃): δ 8.29 (1H s Himidazole), 7.55 (1H s Himidazole), 7.05 (1H s Himidazole), 5.69 (1H s H12), 4.47 (1H dd $J=15.74$ H3), 3.15 (1H d $J=11.90$ H18), 2.81 (1H d $J=13.54$), 2.02 (3H s OCOCH₃), 1.36 (3H s C27), 1.10 (3H s C25), 0.96 (3H s C29 or C23), 0.94 (3H s C29 or C23), 0.85 (3H s C26), 0.83 (6H s C23 and C24), 0.75 (1H d $J=11.40$ H5). ¹³C NMR (100 MHz CDCl₃): δ 199.73 (C11), 173.87 (C28), 170.94 (OCOCH₃), 167.21 (C13), 136.91 (Cimidazole), 129.90 (Cimidazole), 128.14 (C12), 117.30 (Cimidazole), 80.47 (C3), 61.62 (C9), 55.01 (C5), 49.34 (C17), 44.93 (C8), 44.24 (C19), 43.45 (C14), 42.79 (C18), 38.71 (C1), 37.95 (C4), 37.04 (C10), 33.77, 32.69 (C7), 32.52 (C29 or C30), 30.39, 30.32 (C20), 27.95 (C23 or C24), 27.59 (C15), 23.45 (2C C29 or C30), 23.30 (C27), 23.14, 21.23 (OCOCH₃), 18.54 (C26), 17.13, 16.57 (C23 or C24), 16.28 (C25). EI-MS m/z: 562.28 (28) M⁺, 524.55 (13), 386.82 (13), 298.10 (22), 256.64 (56), 216.63 (100), 188.63 (77), 174.65 (73), 146.72 (72), 132.62 (33), 104.58 (45), 94.83 (38), 68.80 (54).

28-(2'Methyl-1H-imidazol-1-yl)-28-oxoolean-12-en-3 β -yl-2'methyl-1H-imidazole-1-carboxylate (3.30): To a stirred solution of **3.1** (500 mg 1.1 mmol) in THF (10 mL), under N₂ atmosphere, at 70°C, was added CBMI (627.69 mg 3.3 mmol). After 94 hours the reaction mixture was diluted with water (60 mL), the aqueous phase was extracted with ethyl acetate (3 \times 60 mL). The resulting organic phases were washed with NaCl 10% (3 \times 60 mL), dried over Na₂SO₄, filtered and evaporated to the dryness, to afford a yellow residue. The residue was subjected to flash column chromatography [hexanes-ethyl acetate from (80:20) to (30:70)], to afford **3.30** (21%). mp 155.7-158.4 °C. IR (film CHCl₃): 3165.6, 3120.3, 2949.6, 1752.0, 1718.3, 1509.0, 1467.6, 1393.3, 1372.1, 1294.0, 1260.3, 1214.0 cm⁻¹. ¹H NMR (400 MHz CDCl₃): δ 7.53 (1H d $J=1.58$ H4' or H5'), 7.32 (1H d $J=1.73$ H4'' or H5''), 6.88 (1H s H4' or H5'), 6.84 (1H d $J=1.58$ H4'')

or H5''), 5.36 (1H t $J=6.97$ H12), 4.65 (1H dd $J=16.32$ H3), 3.10 (1H dd $J=16.66$ H18), 2.64 (3H s C2''CH₃), 2.569 (3H s C2'CH₃), 1.17 (3H s C27), 0.96 (3H s C25), 0.95 (6H s C23 or C24), 0.94 (6H s C29 or C30), 0.73 (3H s C26). ¹³C NMR (100 MHz CDCl₃): δ 176.73 (C28), 149.40 (OCO), 149.33 (C2'), 147.84 (C2''), 142.96 (C13), 127.63 (C4'' or C5''), 127.19 (C4' or C5'), 122.92 (C12), 117.97 (C4'' or C5''), 117.28 (C4' or C5'), 85.89 (C3), 55.26 (C5), 50.77 (C17), 47.44 (C9), 46.10 (C19), 42.55 (C18), 41.89 (C14), 39.31 (C8), 38.03, 37.97 (C4), 36.87 (C10), 33.86, 32.77 (C30 or C29), 32.44, 31.23, 30.35 (C30), 28.12, 27.57 (C15), 25.74 (C27), 23.83 (C23 or C24), 23.43, 23.35, 23.00 (C11), 18.04, 17.78 (C2'CH₃), 17.16 (C26), 16.96 (C29 or C30), 16.83 (C2''CH₃), 15.37 (C25). EI-MS m/z : 629.08 (3) M⁺, 393.21 (4), 269.14 (2), 215.13 (5), 187.12 (12), 127.05 (13), 119.11 (17), 91.08 (23), 83.09 (100).

3-Oxoolean-12-en-28-yl-2'-methyl-1H-imidazole-1-carboxylate (3.31): To a stirred solution of **3.2** (150 mg 0.33 mmol) in THF (2 mL), under N₂ atmosphere, at 70°C, was added CBMI (125.54 mg 0.66 mmol). The workup was performed according to the same method as for **3.30** after 5 hours. The solid was subjected to flash column chromatography [hexanes-ethyl acetate from (90:10) to (40:60)], to afford **3.31** (63%). mp 131.9-141.4 °C. IR (film CHCl₃): 2948.6, 1703.8, 1546.6, 1510.0, 1461.8, 1384.6, 1365.4, 1260.3, 1216.9 cm⁻¹. ¹H NMR (400 MHz CDCl₃): δ 7.53 (1H d $J=1.70$ Himidazole), 6.88 (1H d $J=1.63$ Himidazole), 5.37 (1H t $J=7.01$ H12), 3.10 (1H dd $J=16.50$ H18), 2.57 (3H s CH₃imidazole), 1.16 (3H s C27), 1.10 (3H s C23 or C24), 1.04 (3H s C26), 1.02 (3H s C23 or C24), 0.95 (3H s C29 or C30), 0.94 (3H s C29 or C30), 0.77 (3H s C25). ¹³C NMR (100 MHz CDCl₃): δ 217.48 (C3), 176.74 (C28), 149.34 (C2'), 142.96 (C13), 127.24 (C5'), 122.92 (C12), 117.267 (C4'), 55.32 (C5), 50.78 (C17), 47.41 (C4), 46.79 (C9), 46.09 (C19), 42.63 (C18), 42.00 (C14), 39.30 (C8), 39.14 (C15), 36.71 (C10), 34.09 (C2), 33.87 (C6), 32.76 (C29 or C30), 32.09 (C1), 31.21 (C22 or C16), 30.35 (C20), 27.59, 26.33 (C23 or C24), 25.65 (C27), 23.83 (C29 or C30), 23.45 (C11), 23.02 (C22 or C16), 21.42 (C23 or C24), 19.42, 17.79 (CH₃imidazole), 17.09 (C26), 15.02 (C25). EI-MS m/z : 519.17(20) M⁺, 409.18 (89), 231.14 (25), 203.18 (70), 175.10 (42), 145.10 (38), 119.08 (53), 105.14 (61), 95.10 (67), 91.07 (100), 81.13 (57), 67.11 (67).

3 β -Acetoxy-olean-12-en-28-yl-2'-methyl-1H-imidazole-1-carboxylate (3.32): To a stirred solution of **3.3** (500 mg 1.0 mmol) in THF (10 mL), under N₂ atmosphere, at 70°C, was added CBMI (324.3 mg 1.7 mmol). The workup was performed according to the same method as for **3.30** after 47 hours. The solid was subjected to flash column chromatography [hexanes-ethyl acetate from (80:20) to (40:60)], to afford **3.32** (40%). mp 256.8-259.4 °C. IR (film CHCl₃): 2948.6, 1729.8, 1468.5, 1384.6, 1365.4, 1243.9 1218.8 cm⁻¹. ¹H NMR (400 MHz CDCl₃): δ 7.53 (1H s Himidazole), 6.87 (1H s Himidazole), 5.35 (1H s H12), 4.47 (1H dd $J=15.72$ H3), 3.09 (1H dd $J=17.32$ H18), 2.57 (3H s OCOCH₃), 2.03 (3H s CH₃imidazole), 1.15 (3H s C27), 0.95 (3H s C29 or C30), 0.94 (3H s C29 or C30), 0.92 (3H s C25), 0.84 (3H s C23 or C24), 0.83 (3H s C23 or C24), 0.711 (3H s C26). ¹³C NMR (400 MHz CDCl₃): δ 176.79 (C28), 170.98 (OCOCH₃), 149.34 (C2'), 142.90 (C13), 127.22 (Cimidazole), 123.09 (C12), 117.29 (Cimidazole), 80.80 (C3), 55.28 (C5), 50.79 (C17), 47.46 (C9), 46.10 (C19), 42.57 (C18), 41.89 (C14), 39.33 (C8), 38.12 (C1 or C2), 37.65 (C4), 36.88 (C10), 33.88, 32.79 (C29 or C30), 32.52 (C7), 31.28, 30.36 (C20), 27.97 (C23 or C24), 27.57 (C1 or C2), 25.73 (CH₃imidazol), 23.85 (C29 or C30), 23.46, 23.36 (C11), 23.04 (C22 or C16), 21.27 (C27), 18.07, 17.80 (OCOCH₃), 17.18 (C26), 16.62 (C23 or C24), 15.41 (C25). EI-MS m/z: 563.17 (30) M⁺, 452.20 (34), 393.23 (41), 249.04 (26), 203.12 (100), 189.18 (66), 175.18 (19), 133.17 (27), 119.21 (36), 95.20 (34).

Methyl 3 β -(2'-methyl-1H-imidazole-1-carboxyloxy)-olean-12-en-28-oate (3.33): To a stirred solution of **3.4** (500 mg 1.06 mmol) in THF (7.5 mL), under N₂ atmosphere, at 70°C, was added CBMI (343.76 mg 1.8 mmol). The workup was performed according to the same method as for **3.30** after 27 hours. The solid was subjected to flash column chromatography [hexanes-ethyl acetate from (80:20) to (55:45)], to afford **3.33** (81%). mp 267.2-269.8 °C. IR (film CHCl₃): 2947.7, 1753.9, 1725.0, 1462.7, 1395.3, 1373.1 1294.0 cm⁻¹. ¹H NMR (400 MHz CDCl₃): δ 7.35 (1H d $J=1.78$ Himidazole), 6.89 (1H d $J=1.70$ Himidazole), 5.27 (1H t $J=7.09$ H12), 4.67 (1H dd $J=16.40$ H3), 3.61 (3H s COOCH₃), 2.85 (1H dd $J=18.13$ H18), 2.68 (3H s CH₃imidazole), 1.13 (3H s C27), 0.96 (3H s C26), 0.95 (3H s C23 or C24), 0.95 (3H s C23 or C24), 0.91 (3H s C29 or C30), 0.88 (3H s C29 or C30), 0.72 (3H s C25). ¹³C NMR (100 MHz CDCl₃): δ 178.20 (C28), 149.05 (OCO), 147.91 (C2'), 143.82 (C13), 126.60 (Cimidazole), 122.02 (C12), 118.09

(Cimidazole), 86.45 (C3), 55.20 (C5), 51.51 (COOCH₃), 47.47 (C9), 46.62 (C17), 45.78 (C19), 41.57 (C14 or C10), 41.19 (C18), 39.19 (C14 or C10), 37.94, 37.76 (C4), 36.85 (C8), 33.76, 33.05 (C29 or C30), 32.44 (C1), 32.28, 30.64 (C20), 28.14 (C26), 27.61 (C2), 25.86 (C25), 23.58 (C29 or C30), 23.43, 23.33 (C11), 22.96, 18.12, 16.99 (C23 or C24), 16.76 (C25), 16.56 (CH₃imidazole), 15.28 (C23 or C24). EI-MS m/z: 579.14 (6) M⁺, 452.23 (7), 317.03 (7), 262.08 (25), 215.16 (8), 203.10 (100), 189.13 (44), 173.16 (18), 133.12 (68), 91.09 (36), 83.08 (97).

3β-(2'Methyl-1*H*-imidazole-1-carboxyloxy)-12α-hydroxyolean-28,13β-olide

(3.34): To a stirred solution of **3.5** (500 mg 1.06 mmol) in THF (5 mL), under N₂ atmosphere, at 70°C, was added CBMI (302.45 mg 1.59 mmol). The workup was performed according to the same method as for **3.30** after 24 hours. The solid was subjected to flash column chromatography [hexanes-ethyl acetate from (60:40) to (30:70)], to afford **3.34** (49%). mp 269.2-273.1 °C. IR (film CHCl₃): 3518.5, 3172.3, 3128.0, 2948.6, 2872.5, 1754.9, 1748.2, 1552.4, 1512.9, 1469.5, 1396.2, 1296.9, 1215.9 cm⁻¹. ¹H NMR (400 MHz CDCl₃): δ 7.33 (1H s Himidazole), 6.84 (1H s Himidazole), 4.67 (1H dd *J*=16.29 Hz), 3.90 (1H s H12), 2.65 (3H s CH₃imidazole), 1.32 (3H s C27), 1.16 (3H s C26), 0.98 (6H s C23 or C24 or C29 or C30), 0.96 (3H s C23 or C24), 0.93 (3H s C25), 0.89 (3H s C29 or C30). ¹³C NMR (100 MHz CDCl₃): δ 179.92 (C28), 149.37 (OCO), 147.89 (C2'), 127.63 (Cimidazole), 118.01 (Cimidazole), 90.59 (C13), 85.77 (C3), 76.04 (C12), 55.23 (C5), 51.10 (C18), 44.67 (C9), 44.45 (C17), 42.26 (C8), 42.08 (C14), 39.34 (C19), 38.32 (C1), 38.13 (C4), 36.34 (C10), 34.11 (C7), 33.82, 33.24 (C29 or C30), 31.54 (C20), 28.85, 28.06 (C23 or C24), 27.99 (C15), 27.45, 23.86 (C29 or C30), 23.53, 21.16, 18.55 (2C C26), 17.58, 16.86 (C23 or C24), 16.80 (CH₃imidazole), 16.33 (C25). EI-MS m/z: 581.31 (8) M⁺, 205.19 (73), 204.17 (41), 189.23 (100), 187.24 (54), 177.24 (57), 175.24 (50), 161.24 (42), 147.23 (53), 133.23 (40), 127.17 (48), 121.21 (51), 119.22 (60), 109.2 (40), 107.2 (53), 105.2 (50).

28-(2'Methyl-1*H*-imidazol-1-yl)-12,28-dioxoolean-3β-yl-2'methyl-1*H*-imidazole-1-carboxylate (3.35): To a stirred solution of **3.7** (300 mg 0.63 mmol) in THF (5 mL), under N₂ atmosphere, at 70°C, was added CBMI (359.5 mg 1.89 mmol). The workup was performed according to the same method as for **3.30** after 8 hours. The solid was

subjected to flash column chromatography [hexanes-ethyl acetate from (50:50) to (10:90)], to afford **3.35** (58%). mp 170.4-179.1 °C. IR (film CHCl₃): 3168.5, 2949.6, 2866.7, 1752.0, 1699.9, 1549.5, 1509.0, 1472.4, 1395.3, 1371.1, 1295.0, 1248.7, 1214.0 cm⁻¹. ¹H NMR (400 MHz CDCl₃): δ 7.48 (1H s), 7.29 (1H s), 6.86 (1H s), 6.81 (1H s), 4.60 (1H dd *J*=16.06), 2.99 (1H dd *J*=12.95), 2.60 (3H s), 2.57 (3H s), 1.00 (3H s), 0.95 (3H s), 0.93 (6H s), 0.92 (6H s), 0.88 (3H s). ¹³C NMR (100 MHz CDCl₃): δ 210.28, 177.58, 149.26, 148.93, 147.79, 127.66, 127.54, 117.85, 117.21, 85.24, 55.00, 51.16, 50.86, 49.51, 41.96, 41.29, 38.32, 37.96, 37.48, 36.71, 36.14, 34.17, 32.93, 32.88, 31.94, 31.50, 30.28, 27.91, 27.56, 23.68, 23.27, 23.24, 20.31, 17.95, 17.63, 16.74, 16.65, 16.17, 15.17. EI-MS *m/z*: 645.29 (1) M⁺, 205.13 (59), 189.17 (41), 187.19 (30), 127.1 (22), 95.14 (20), 83.11 (100), 81.13 (36).

3β-Acetoxy-12-oxoolean-28-yl-2'methyl-1*H*-imidazole-1-carboxylate (3.36): To a stirred solution of **3.8** (300 mg 0.58 mmol) in THF (4 mL), under N₂ atmosphere, at 70°C, was added CBMI (220.6 mg 1.16 mmol). The workup was performed according to the same method has for **3.30** after 16.5 hours. The solid was subjected to flash column chromatography [hexanes-ethyl acetate from (60:40) to (55:45)], to afford **3.36** (65%). mp 157.5-164.6 °C. IR (film CHCl₃): 2946.7, 2866.7, 1724.1, 1715.4, 1706.7, 1471.4, 1384.6, 1366.3, 1246.8 cm⁻¹. ¹H NMR (400 MHz CDCl₃): δ 7.48 (1H s), 6.87 (1H s), 4.43 (1H dd *J*=15.79), 3.00 (1H d *J*=13.08), 2.65 (1H d *J*=3.83), 2.58 (3H s), 2.01 (3H s), 1.01 (3H s), 0.94 (3H s), 0.93 (6H s), 0.85 (3H s), 0.82 (6H s). ¹³C NMR (100 MHz CDCl₃): δ 210.58, 177.65, 170.81, 148.95, 127.59, 117.24, 80.25, 55.07, 51.21, 50.90, 49.56, 41.95, 41.31, 38.36, 37.66, 37.59, 36.74, 36.16, 34.21, 32.97, 32.90, 31.99, 31.58, 30.31, 27.79, 27.57, 23.71, 23.29 (2C), 21.18, 20.32, 18.00, 17.68, 16.34, 16.18, 15.22. EI-MS *m/z*: 579.05 (3) M⁺, 205.01 (100), 189.05 (67), 187.07 (37), 107.02 (20), 82.99 (24), 80.99 (24).

3,12-Diooxoolean-12-en-28-yl-2'methyl-1*H*-imidazole-1-carboxylate (3.37): To a stirred solution of **3.9** (350 mg 0.74 mmol) in THF (5 mL), under N₂ atmosphere, at 70°C, was added CBMI (416.6 mg 1.48 mmol). The workup was performed according to the same method as for **3.30** after 4 hours. The solid was subjected to flash column chromatography [hexanes-ethyl acetate from (60:40) to (40:60)], to afford **3.37** (44%).

mp 164.5-165.0 °C. IR (film CHCl₃): 3122.2, 2947.7, 2866.7, 1702.8, 1509.0, 1471.4, 1384.6, 1365.4, 1284.4, 1248.7, 1212.0 cm⁻¹. ¹H NMR (400 MHz CDCl₃): δ 7.49 (1H s), 6.89 (1H d *J*=0.72), 3.01 (1H dd *J*=13.12 H18), 2.70 (1H d *J*=3.88), 2.60 (3H s CH₃imidazole), 1.06 (3H s C23 or C24), 1.02 (6H s C23 or C24, C29 or C30), 0.99 (3H s C25), 0.99 (6H s C26 and C27), 0.93 (3H s C29 or C30). ¹³C NMR (100 MHz CDCl₃): δ 216.50 (C3), 210.14 (C11), 177.62 (C28), 149.01 (Cimidazole), 127.64 (Cimidazole), 117.26 (Cimidazole), 54.89 (C5), 51.24 (C13), 50.90, 49.13 (C9), 47.35, 42.16 (C14 or C8), 41.31 (C14 or C8), 38.59, 38.54, 36.59 (C10), 36.22, 34.22, 33.78, 32.96 (2C C29 or C30 and C18), 31.99, 31.05, 30.34 (C20), 27.67, 26.16 (C23 or C24), 23.73 (C23 or C24 or C29 or C30), 23.36, 21.14 (C23 or C24 or C29 or C30), 20.26 (C27 or C26), 19.40, 17.72 (CH₃imidazole), 15.99 (C25), 14.83 (C26 or C27). EI-MS *m/z*: 535.29 (8) M⁺, 426.33 (28), 425.35 (86), 407.42 (58), 205.34 (100), 187.43 (30).

Methyl 3β-(2'-methyl-1*H*-imidazole-1-carboxyloxy)-12-oxoolean-28-oate (3.38):

To a stirred solution of **3.10** (325 mg 0.67 mmol) in THF (5 mL), under N₂ atmosphere, at 70°C, was added CBMI (254.88 mg 1.34 mmol). The workup was performed according to the same method as for **3.30** after 8 hours. The solid was subjected to flash column chromatography [hexanes-ethyl acetate from (60:40) to (45:55)], to afford **3.38** (48%). mp 215.6-217.6 °C. IR (film CHCl₃): 3116.4, 2946.7, 2878.2, 1753.0, 1721.2, 1698.0, 1509.0, 1466.6, 1397.2, 1372.1, 1295.0, 1239.0 cm⁻¹. ¹H NMR (400 MHz CDCl₃): δ 7.31 (1H d *J*=0.85 Himidazole), 6.84 (1H s Himidazole), 4.63 (1H dd *J*=16.26 H3), 3.67 (3H s), 2.78 (1H dd *J*=13.24), 2.63 (3H s), 0.96 (12H s), 0.94 (3H s), 0.90 (3H s), 0.89 (3H s). ¹³C NMR (100 MHz CDCl₃): δ 211.25, 178.31, 149.31, 147.86, 127.67, 117.93, 85.43, 55.10, 51.78, 51.77, 49.57, 47.29, 41.84, 41.21, 38.43, 38.04, 37.52, 36.79, 36.16, 34.42, 33.33, 32.88, 31.94, 31.66, 30.60, 28.01, 27.52, 23.34, 23.11, 22.69, 20.52, 18.11, 16.81, 16.75, 16.09, 15.18. EI-MS *m/z*: 595.30 (7) M⁺, 579.33 (32), 519.37 (33), 218.2 (46), 175.21 (66), 105.19 (36), 95.19 (36), 83.16 (100), 81.17 (41).

Methyl 2-(2'-methyl-1*H*-imidazol-1-yl)-methylene-3-oxoolean-12-en-28-oate (3.39):

To a stirred solution of **3.12** (300 mg 0.60 mmol) in THF (4 mL), under N₂ atmosphere, at 70°C, was added CBMI (228.25 mg 1.2 mmol). The workup was performed according to the same method as for **3.30** after 6.5 hours. The solid was

subjected to flash column chromatography [hexanes-ethyl acetate from (60:40) to (50:50)], to afford **3.39** (75%). mp 212.1-215.3 °C. IR (film CHCl₃): 3162.7, 3122.2, 2948.6, 2866.7, 1724.1, 1685.5, 1605.5, 1540.9, 1504.2, 1461.8, 1411.6, 1383.7, 1244.8 cm⁻¹. ¹H NMR (400 MHz CDCl₃): δ 7.65 (1H s), 7.12 (1H s), 6.98 (1H s), 5.33 (1H s), 3.62 (3H s), 2.46 (3H s), 1.17 (3H s), 1.16 (3H s), 1.14 (3H s), 0.92 (3H s), 0.90 (3H s), 0.87 (3H s), 0.78 (3H s). ¹³C NMR (100 MHz CDCl₃): δ 206.63, 178.15, 147.31, 144.01, 130.25, 128.29, 123.68, 121.81, 118.12, 52.73, 51.54, 46.76, 45.84, 45.44, 45.28, 42.34, 41.92, 41.47, 39.16, 36.13, 33.83, 33.06, 32.26, 31.73, 30.67, 29.66, 27.64, 25.64, 23.57 (2C), 23.06, 22.52, 20.24, 16.42, 15.25, 13.57. EI-MS m/z: 561.48 (40) M⁺, 560.34 (44), 545.44 (45), 501.51 (42), 312.17 (47), 299.35 (67), 203.18 (98), 133.19 (100), 119.18 (59), 105.2 (62), 91.13 (47), 83.16 (95), 81.13 (41), 79.12 (43).

Methyl 2α-(2'-methyl-1H-imidazole-1-carboxyloxy)-3-oxoolean-12-en-28-oate (3.40): To a stirred solution of **3.13** (400 mg 0.825 mmol) in THF (10 mL), under N₂ atmosphere, at 70°C, was added CBMI (313.85 mg 1.65 mmol). The workup was performed according to the same method as for **3.30** after 6 hours. The solid was subjected to flash column chromatography [hexanes-ethyl acetate from (80:20) to (45:55)], to afford **3.40** (58%). mp 170.4-179.1 °C. IR (film CHCl₃): 2947.7, 2878.2, 1761.7, 1724.1, 1554.3, 1508.1, 1457.0, 1395.3, 1297.9 cm⁻¹. ¹H NMR (400 MHz CDCl₃): δ 6.85 (1H s Himidazole), 5.71 (1H dd *J*=18.97 H2), 5.29 (1H s H12), 3.63 (3H s), 2.87 (1H dd *J*=12.99), 2.62 (3H s), 2.38 (1H dd *J*=17.89), 1.33 (3H s), 1.18 (3H s), 1.14 (3H s), 1.12 (3H s), 0.92 (3H s), 0.89 (3H s), 0.93 (3H s). ¹³C NMR (100 MHz CDCl₃): δ 207.87 (C3), 178.14 (C28), 148.92 (C2OCO), 148.06 (C2'), 144.24 (C13), 127.41 (Cimidazole), 118.16 (Cimidazole), 74.97 (C2), 57.07 (C5), 51.55 (COOCH₃), 48.79 (C4), 47.39 (C9), 46.60 (C17), 45.77, 45.29 (C1), 41.72 (C14), 41.20 (C18), 39.37 (C8), 38.08 (C10), 33.76, 33.05 (C29 or C30), 32.24, 32.21 (C7), 30.66 (C20), 27.60 (C15), 25.88 (C27), 24.71 (C23 or C24), 23.57 (2C C29 or C30), 22.91, 21.15 (C23 or C24), 19.02, 16.99 (C26); 16.69 (CH₃imidazole), 15.93 (C25). EI-MS m/z: 592.31 (7) M⁺, 547.50 (5), 330.73 (6), 282.50 (8), 268.66 (23), 24.7 (17), 214.72 (100), 188.82 (71), 14.90 (27), 132.87 (67), 118.90 (52), 90.86 (62).

3 β -Acetoxy-11-oxoolean-12-en-28-yl-2'-methyl-1H-imidazole-1-carboxylate

(**3.41**): To a stirred solution of **3.14** (148.8 mg 0.29 mmol) in THF (2.5 mL), under N₂ atmosphere, at 70°C, was added CBMI (110.32 mg 0.58 mmol). The workup was performed according to the same method as for **3.30** after 5 hours. The solid was subjected to flash column chromatography [hexanes-ethyl acetate from (70:30) to (35:65)], to afford **3.41** (30%). mp 244.3-247.6 °C. IR (film CHCl₃): 3175.2, 2948.6, 1805.1, 1727.9, 1656.6, 1551.5, 1466.6, 1389.5, 1366.3, 1321.0, 1248.7 cm⁻¹. ¹H NMR (400 MHz CDCl₃): δ 7.52 (1H s Himidazole), 6.90 (1H s Himidazole), 5.71 (1H s H12), 4.48 (1H dd $J=15.60$ H3), 3.20 (1H dd $J=12.28$), 2.81 (1H dd $J=13.57$), 2.55 (3H s), 2.03 (3H s), 1.37 (3H s), 1.12 (3H s), 0.96 (6H d $J=2.09$), 0.90 (3H s), 0.84 (6H s). ¹³C NMR (100 MHz CDCl₃): δ 199.81 (C11), 175.69 (C28), 171.00 (OCOCH₃), 167.50 (C13), 149.72 (C2'), 128.17 (C12), 127.78 (Cimidazole), 117.03 (Cimidazole), 80.51 (C3), 61.61 (C9), 55.06 (C5), 50.28 (C17), 45.06 (C8), 44.53 (C19), 43.56 (C14), 43.08 (C18), 38.75 (C1), 37.99 (C4), 37.07 (C10), 33.83 (C21 or C22), 32.80 (C7), 32.54 (C29 or C30), 30.33, 30.26 (C20), 27.99 (C23 or C24), 27.63 (C15), 23.59 (C29 or C30), 23.49 (C21 or C22), 23.24 (C27), 22.64, 21.28 (OCOCH₃), 18.90 (C26), 18.22 (CH₃imidazole), 17.16, 16.61 (C23 or C24), 16.35 (C25). EI-MS m/z : 576.70 (4) M⁺, 496.59 (5), 466.79 (7), 406.79 (12), 362.73 (5), 298.97 (5), 280.99 (100), 257.34 (5), 217.24 (14), 189.35 (17), 175.36 (13), 105.32 (10), 91.43 (16), 83.39 (100).

28-(4H-Triazol-4-yl)-28-oxoolean-12-en-3 β -yl-4H-triazole-4-carboxylate (3.42**):**

To a stirred solution of **3.1** (350 mg 0.77 mmol) in THF (4 mL), under N₂ atmosphere, at 70°C, was added CDT (758.28 mg 4.62 mmol). After 7 hours the reaction mixture was diluted with water (60 mL), the aqueous phase was extracted with ethyl acetate (3 \times 50 mL). The resulting organic phases were washed with NaCl 10% (3 \times 50 mL), dried over Na₂SO₄, filtered and evaporated to the dryness, to afford a yellow residue. The residue was subjected to flash column chromatography [hexanes-ethyl acetate from (80:20) to (55:45)], to afford **3.42** (86%). mp 158.8-167.9 °C. IR (film CHCl₃): 3133.8, 2949.6, 1782.9, 1762.6, 1735.6, 1511.0, 1466.6, 1405.9, 1359.6, 1349.9, 1279.5, 1226.5 cm⁻¹. ¹H NMR (400 MHz CDCl₃): δ 8.85 (1H s Htriazole), 8.77 (1H s Htriazole), 8.06 (1H s Htriazole), 7.99 (1H s Htriazol), 5.30 (1H s H12), 4.79 (1H t $J=16.48$ H3), 3.20 (1H d $J=11.41$ H18), 2.51 (1H d $J=13.49$), 1.17 (3H s C27), 0.99 (6H s C23 or C24), 0.97 (3H s

C29 or C30), 0.96 (3H s C25), 0.94 (3H s C29 or C30), 0.89 (1H d $J=10.32$ H5), 0.68 (3H s C26). ^{13}C NMR (100 MHz CDCl_3): δ 174.99 (C28), 153.57 (Ctriazole), 152.28 (Ctriazole), 147.28 (OCO), 145.29 (2C Ctriazole), 143.19 (C13), 122.60 (C12), 87.68 (C3), 55.20 (C5), 49.97 (C17), 47.49 (C9), 45.79 (C19), 41.79 (C14), 41.66 (C18), 39.25 (C8), 38.18 (C4), 37.97, 36.85 (C10), 33.76, 32.93 (C29 or C30), 32.40 (C7), 30.50 (C20), 30.02, 28.11 (C29 or C30), 27.80 (C15), 25.90 (C27), 23.73 (C23 or C24), 23.38 (2C), 21.86, 18.07, 16.77 (C23 or C24), 16.70 (C26), 15.35 (C25). EI-MS m/z : 602.36 (24) M^- , 589.36 (47), 588.21 (47), 486.83 (56), 312.49 (48), 282.43 (26), 270 (100), 248.06 (42), 186.25 (49), 156.89 (91), 87.94 (54), 58.16 (51).

3β -Acetoxy-olean-12-en-28-yl-4*H*-triazole-4-carboxylate (3.43): To a stirred solution of **3.3** (200 mg 0.4 mmol) in THF (4 mL), under N_2 atmosphere, at 70°C , was added CDT (196.96 mg 1.2 mmol). The workup was performed according to the same method as for **3.42** after 6 hours. The solid was subjected to flash column chromatography [hexanes-ethyl acetate from (80:20) to (75:25)], to afford **3.43** (90%). mp $195.2\text{--}198.7^\circ\text{C}$. IR (film CHCl_3): 3133.8, 2948.6, 1732.7, 1511.0, 1465.6, 1361.5, 1246.8 cm^{-1} . ^1H NMR (400 MHz CDCl_3): δ 8.84 (1H s Htriazole), 7.97 (1H s Htriazole), 5.29 (1H s H12), 4.48 (1H t $J=15.73$ H3), 3.19 (1H d $J=11.88$ H18), 2.50 (1H d $J=13.51$), 2.03 (3H s), 1.15 (3H s), 0.98 (3H s), 0.94 (3H s), 0.91 (3H s), 0.84 (3H s), 0.83 (3H s), 0.80 (1H s H5), 0.66 (3H s). ^{13}C NMR (100 MHz CDCl_3): δ 175.02 (C28), 170.98 (OCOCH_3), 152.25 (Ctriazole), 145.28 (Ctriazole), 143.09 (C13), 122.80 (C12), 80.83 (C3), 55.27 (C5), 49.99 (C18), 47.50 (C9), 45.78 (C19), 41.78 (C18), 41.68 (C14), 39.26 (C8), 38.10 (C1), 37.65 (C4), 36.87 (C10), 33.78, 32.93 (C29 or C30), 32.47 (C7), 30.49 (C20), 30.04, 27.99 (C24 or C23), 27.80 (C15), 25.89 (C27), 23.74 (C29 or C30), 23.47, 23.38, 21.89, 21.28 (OCOCH_3), 18.11, 16.71 (C23 or C24), 16.63 (C26), 15.36 (C25). EI-MS m/z : 549.01 (72) M^+ , 507.26 (32), 487.65 (77), 486.61 (53), 431.43 (43), 375.45 (23), 294.67 (37), 172.68 (100), 84.56 (46).

Methyl 3β -(4*H*-triazole-4-carboxyloxy)-olean-12-en-28-oate (3.44): To a stirred solution of **3.4** (500 mg 1.062 mmol) in THF (5 mL), under N_2 atmosphere, at 70°C , was added CDT (348.6 mg 2.124 mmol). The workup was performed according to the same method as for **3.42** after 5 hours. The solid was subjected to flash column

chromatography [hexanes-ethyl acetate from (80:20) to (60:40)], to afford **3.44** (84%). mp 259.4-260.4 °C. IR (film CHCl₃): 3118.3, 2946.7, 1758.8, 1725.0, 1514.8, 1469.5, 1407.8, 1384.6, 1281.5, 1267.0, 1228.5, 1202.4 cm⁻¹. ¹H NMR (400 MHz CDCl₃): δ 8.77 (1H s Htriazole), 8.06 (1H s Htriazole), 5.28 (1H s H12), 4.80 (1H t *J*=16.38 Hz), 3.62 (3H s), 2.86 (1H dd *J*=10.92 Hz), 1.13 (3H s), 1.0 (3H s), 0.98 (3H s), 0.97 (3H s), 0.89 (3H s), 0.73 (3H s). ¹³C NMR (100 MHz CDCl₃): δ 178.20, 153.56, 147.27, 145.29, 143.85, 122.04, 87.76, 55.21, 51.50, 47.52, 46.66, 45.82, 41.61, 41.24, 39.25, 38.19, 37.95, 36.88, 33.81, 33.07, 32.49, 32.31, 30.66, 28.12, 27.64, 25.87, 23.60, 23.39, 23.37, 23.00, 18.15, 16.78 (2C), 15.32. EI-MS *m/z*: 567.21 (49) M⁺, 565.09 (98), 557.85 (50), 492.9 (60), 198.98 (53), 194.61 (52), 186.57 (100), 174.59 (50), 166.34 (48), 144.78 (46), 101.54 (51), 92.7 (48), 60.51 (48), 56.93 (58).

28-(4*H*-Triazol-4-yl)-12,28-dioxolean-3β-yl-4*H*-triazole-4-carboxylate (3.45):

To a stirred solution of **3.7** (500 mg 1.1 mmol) in THF (5 mL), under N₂ atmosphere, at 70°C, was added CDT (722.17 mg 4.4 mmol). The workup was performed according to the same method as for **3.42** after 7 hours. The solid was subjected to flash column chromatography [hexanes-ethyl acetate from (60:40) to (45:55)], to afford **3.45** (75%). mp 169.2-180.7 °C. IR (film CHCl₃): 3138.6, 2947.7, 2865.7, 1762.6, 1725.0, 1698.0, 1512.9, 1471.4, 1406.8, 1360.5, 1346.1, 1279.5, 1222.7, 1202.4 cm⁻¹. ¹H NMR (400 MHz CDCl₃): δ 8.91 (1H s), 8.76 (1H s), 8.04 (1H s), 7.99 (1H s), 4.76 (1H dd *J*=16.30 Hz), 3.26 (1H dd *J*=12.64 Hz), 2.70 (1H d *J*=2.49 Hz) 1.04 (3H s C29 or C30), 0.98 (6H s C23 or C24 and C27), 0.97 (3H s C23 or C24), 0.92 (6H s C29 or C30 and C26), 0.89 (3H s C25). ¹³C NMR (100 MHz CDCl₃): δ 210.53 (C12), 175.50 (C28), 153.55 (Ctriazole), 152.48 (Ctriazole), 147.22 (OCO), 145.48 (Ctriazole), 145.30 (Ctriazole), 87.05 (C3), 55.00 (C5), 51.45 (C13), 50.34 (C17), 49.57 (C9), 42.11 (C14), 41.28 (C8), 38.36, 38.21 (C4), 37.44, 36.75 (C10), 36.09, 34.28, 33.17 (C29 or C30), 32.09 (C18), 31.55, 30.85, 30.45 (C20), 27.94 (C23 or C24), 27.65, 23.33 (C29 or C30), 23.21, 22.07, 20.62 (C27), 18.02, 16.50 (C23 or C24), 16.13 (C26), 15.18 (C25). EI-MS *m/z*: 618.59 (1) M⁺, 521.34 (45), 408.39 (50), 218.19 (100), 205.22 (75), 204.22 (84), 189.33 (57).

3β-Acetoxy-12-oxolean-28-yl-4*H*-triazole-4-carboxylate (3.46): To a stirred solution of **3.8** (300 mg 0.58 mmol) in THF (5 mL), under N₂ atmosphere, at 70°C, was

added CDT (285.6 mg 1.74 mmol). The workup was performed according to the same method as for **3.42** after 8 hours. The solid was subjected to flash column chromatography [hexanes-ethyl acetate from (70:30) to (60:40)], to afford **3.46** (68%). mp 171.5-177.4 °C. IR (film CHCl₃): 3133.8, 2945.7, 2872.5, 1726.9, 1699.0, 1511.0, 1466.6, 1359.6, 1274.7, 1245.8 cm⁻¹. ¹H NMR (400 MHz CDCl₃): δ 8.91 (1H s Htriazole), 8.00 (1H s Htriazole), 4.45 (1H dd *J*=15.81 H3), 3.26 (1H d *J*=12.84 H18), 2.69 (1H d *J*=2.85), 2.02 (3H s), 1.05 (3H s), 0.97 (3H s), 0.93 (3H s), 0.90 (3H s), 0.84 (3H s), 0.83 (6H s). ¹³C NMR (100 MHz CDCl₃): δ 210.89, 175.56, 170.83, 153.48, 145.50, 80.33, 55.12, 51.49, 50.39, 49.62, 42.12, 41.30, 38.41, 37.70, 37.59, 36.79, 36.10, 34.32, 33.19, 32.11, 31.64, 30.89, 30.47, 27.84, 27.67, 23.37, 23.33, 22.12, 21.20, 20.64, 18.08, 16.39, 16.14, 15.20. EI-MS *m/z*: 566.09 (1) M⁺, 218.25 (76), 205.35 (100), 204.4 (97), 190.44 (35), 189.31 (58), 176.39 (28), 121.57 (30), 107.18 (27), 105.3 (26).

3,12-Dioxolean-28-yl-1H-triazole-1-carboxylate (3.47): To a stirred solution of **3.9** (250 mg 0.53 mmol) in THF (5 mL), under N₂ atmosphere, at 70°C, was added CDT (261 mg 1.59 mmol). The workup was performed according to the same method as for **3.42** after 8 hours. The solid was subjected to flash column chromatography [hexanes-ethyl acetate from (70:30) to (60:40)], to afford **3.47** (66%). mp 113.4-114.0 °C. IR (film CHCl₃): 3128.0, 2944.8, 2866.7, 1724.1, 1700.9, 1511.0, 1457.9, 1385.6, 1345.1, 1274.7 cm⁻¹. ¹H NMR (400 MHz CDCl₃): δ 8.92 (1H s), 8.00 (1H s), 3.28 (1H dd *J*=13.00), 2.73 (1H d *J*=3.31), 1.06 (3H s), 1.05 (3H s), 1.02 (3H s), 0.98 (3H s), 0.96 (6H s), 0.93 (3H s). ¹³C NMR (100 MHz CDCl₃): δ 216.54, 210.39, 175.52, 152.52, 145.51, 54.89, 51.50, 50.35, 49.16, 47.34, 42.28, 41.27, 38.54 (2C), 36.59, 36.13, 34.30, 33.79, 33.18, 32.13, 31.06, 30.87, 30.47, 27.72, 26.19, 23.35, 22.11, 21.15, 20.55, 19.45, 15.90, 14.78. EI-MS *m/z*: 522.16 (3) M⁺, 218.18 (92), 205.25 (100), 204.29, (85), 189.32 (32), 105.27 (30).

Methyl 3β-(4H-triazole-4-carboxyloxy)-12-oxolean-28-oate (3.48): To a stirred solution of **3.10** (300 mg 0.62 mmol) in THF (5 mL), under N₂ atmosphere, at 70°C, was added CDT (305.28 mg 1.86 mmol). The workup was performed according to the same method as for **3.42** after 6 hours. The solid was subjected to flash column chromatography [hexanes-ethyl acetate from (70:30) to (55:45)], to afford **3.48** (72%). mp 162.6-164.2 °C. IR (film CHCl₃): 3133.8, 2948.6, 2866.7, 1763.6, 1720.2, 1698.0,

1510.0, 1468.5, 1405.9, 1299.8, 1281.5, 1222.7, 1202.4 cm^{-1} . ^1H NMR (400 MHz CDCl_3): δ 8.76 (1H s), 8.03 (1H s), 4.75 (1H s $J=16.48$ H3), 3.65 (3H s COOCH_3), 2.76 (1H dt $J=13.46$ H18), 2.60 (1H d $J=3.94$ H13), 0.99 (3H s C23 or C24), 0.97 (3H s C23 or C24), 0.95 (3H s C29 or C30), 0.94 (3H s C26), 0.92 (3H s C27), 0.90 (3H s C25), 0.87 (3H s C29 or C30). ^{13}C NMR (100 MHz CDCl_3): δ 211.12 (C12), 178.23 (C28), 153.51 (Ctriazole), 147.19 (OCO), 145.28 (Ctriazole), 87.09 (C3), 54.98 (C5), 51.71 (C13 and COOCH_3), 49.51 (C9), 47.22 (C17), 41.77 (C14), 41.16 (C8), 38.36, 38.19 (C4), 37.42, 36.72 (C10), 36.10, 34.36, 33.29 (C29 or C30), 32.82, 31.88, 31.61 (C18), 30.54 (C20), 27.93 (C23 or C24), 27.46, 23.21, 23.06 (C26), 22.63, 20.46 (C27), 18.04, 16.49 (C23 or C24), 16.04 (C29 or C30), 15.15 (C25). EI-MS m/z : 582.29 (4) M^+ , 278.25 (45), 219.38 (31), 218.39 (100), 203.36 (35), 176.38 (31), 175.33 (34), 70.51 (33).

Methyl 2-(4*H*-triazol-4-yl)-methylene-3-oxoolean-12-en-28-oate (3.49): To a stirred solution of **3.12** (300 mg 0.60 mmol) in THF (5 mL), under N_2 atmosphere, at 70°C , was added CDT (295.47 mg 1.8 mmol). The workup was performed according to the same method as for **3.42** after 24 hours. The solid was subjected to flash column chromatography [hexanes-ethyl acetate from (70:30) to (60:40)], to afford **3.49** (56%). mp $151.7\text{-}159.4^\circ\text{C}$. IR (film CHCl_3): 3122.2, 2948.6, 1863.8, 1722.1, 1686.4, 1616.1, 1510.0, 1458.9, 1410.7, 1382.7, 1362.5, 1299.8, 1281.5 cm^{-1} . ^1H NMR (400 MHz CDCl_3): δ 8.34 (1H s), 8.06 (1H s), 7.77 (1H s), 5.36 (1H s H12), 3.621 (3H s COOCH_3), 3.36 (1H d $J=17.60$), 2.90 (1H dd $J=16.86$), 2.37 (1H d $J=17.67$), 1.18 (6H s), 1.12 (3H s), 0.93 (3H s), 0.90 (3H s), 0.88 (3H s), 0.79 (3H s). ^{13}C NMR (100 MHz CDCl_3): δ 207.17, 178.18, 152.81, 145.82, 143.76, 128.22, 125.51, 122.12, 52.73, 51.53, 46.79, 45.84, 45.29, 45.21, 43.24, 41.93, 41.51, 39.12, 35.78, 33.86, 33.07, 32.29, 31.72, 30.67, 29.70, 27.66, 25.63, 23.64, 23.58, 23.10, 22.41, 20.31, 16.40, 15.49. EI-MS m/z : 548.40 (12) M^+ , 299.25 (21), 203.23 (100), 202.28 (23), 19.33 (34), 173.3 (20), 134.21 (26), 133.29 (63), 119.23 (23), 105.35 (22).

3β -Acetoxy-11-oxoolean-12-en-28-yl-4*H*-triazole-1-carboxylate (3.50): To a stirred solution of **3.14** (210.6 mg 0.41 mmol) in THF (4 mL), under N_2 atmosphere, at 70°C , was added CDT (134.6 mg 0.82 mmol). The workup was performed according to the same method as for **3.42** after 8 hours. The solid was subjected to flash column

chromatography [hexanes-ethyl acetate from (80:20) to (65:35)], to afford **3.50** (25%). mp 138.9-145.5 °C. IR (film CHCl₃): 3141.5, 2950.6, 2875.3, 1730.8, 1659.5, 1513.9, 1466.6, 1389.5, 1362.5, 1349.9, 1275.7, 1247.7, 1210.1 cm⁻¹. ¹H NMR (400 MHz CDCl₃): δ 8.87 (1H s Htriazole), 8.02 (1H s Htriazole), 5.68 (1H s H12), 4.50 (1H dd *J*=16.16), 3.26 (1H d *J*=11.74), 2.82 (1H d *J*=13.65), 2.70 (1H d *J*=14.14), 2.04 (3H s OCOCH₃), 1.39 (3H s), 1.12 (3H s), 0.97 (6H s), 0.85 (9H s). ¹³C NMR (100 MHz CDCl₃): δ 199.88, 174.39, 170.98, 167.63, 152.66, 128.15, 80.57, 61.74, 55.09, 49.64, 45.02, 44.29, 43.59, 42.13, 38.79, 38.03, 37.12, 33.71, 32.77, 32.70, 30.43, 29.25, 28.03, 27.97, 23.54 (2C), 23.49, 23.47, 21.53, 21.27, 18.74, 17.24, 16.64, 16.28. EI-MS *m/z*: 563.22 (75) M⁺, 507.95 (44), 465.45 (100), 400.79 (78), 364.26 (34), 246.05 (26), 148.31 (34), 129.76 (40), 92.67 (26).

3β-OI-12β-fluor-olean-13,28β-olide (3.51) and **3β-ol-12α-fluor-olean-13,28β-olide (3.52)**: To a stirred solution of **3.1** (100 mg 0.22 mmol) in acetonitrile (3 mL) and dioxane (3 mL) at 50°C was added selectfluor (155.9 mg 0.44 mmol). After 4 hours the reaction mixture was diluted with water (50 mL), the aqueous phase was extracted with ether (3×50 mL). The resulting organic phases were washed with NaCl 10% (3×50 mL), dried over Na₂SO₄, filtered and evaporated to the dryness, to afford a solid. The solid was subjected to flash column chromatography [hexanes-ethyl acetate from (90:10) to (65:35)], to afford **3.51** (25%) and **3.52** (33%). **3.51**: mp 280.8-285.0 °C. IR (film CHCl₃): 3323.7, 2945.7, 1772.3, 1467.6, 1390.4, 1222.7 cm⁻¹. ¹H NMR (400 MHz CDCl₃): δ 4.56 (1H dt *J*=52.08 H12), 3.22 (1H dd *J*=16.11 H3), 1.23 (3H d *J*=0.96 C27), 1.11 (1H s C26), 0.99 (3H s C23 or C24 or C29 or C30), 0.98 (3H s C23 or C24 or C29 or C30), 0.89 (3H s C29 or C30), 0.87 (3H s C25), 0.77 (3H s C23 or C24). ¹³C NMR (100 MHz CDCl₃): δ 179.35 (C28), 96.66 (*J*=171.56 C12), 87.98 (*J*=25.90 C13), 78.71 (C3), 55.00 (C5), 50.86 (C18), 44.65 (C9), 44.32 (C17), 41.91 (C8), 41.70 (C14), 38.85 (C4), 38.53 (2C), 36.40 (C10), 34.07, 33.51, 33.18 (C29 or C30 or C24 or C23), 31.47 (C20), 27.96 (C23 or C24 or C29 or C30), 27.45, 27.35, 27.15, 25.68 (*J*=21.39), 23.75 (C29 or C30), 21.05, 18.28 (C26), 17.93 (*J*=8.06 C27), 17.66, 16.02 (C25), 15.33 (C23 or C24). EI-MS *m/z*: 475.20 (5) M⁺, 457.20 (8), 437.17 (12), 231.10 (22), 207.13 (30), 201.14 (56), 145.20 (32), 133.19 (45), 119.20 (100), 91.19 (52), 79.19 (45), 67.15 (31). **3.52**: mp 278.9-279.6 °C. IR (film CHCl₃): 3323.7, 2945.7, 1734.7, 1467.6, 1387.5,

1362.5, 1260.3 cm^{-1} . ^1H NMR (400 MHz CDCl_3): δ 4.65 (1H dq $J=61.61$ H12), 3.20 (1H dd $J=15.99$ H3), 1.21 (3H d $J=2.59$ C27), 1.122 (3H s C26), 0.96 (6H s), 0.93 (3H s C29 or C30), 0.88 (3H s C25), 0.78 (3H s C23 or C24). ^{13}C NMR (100 MHz CDCl_3): δ 178.40 (C28), 99.89 ($J=179.56$ C12), 90.76 ($J=7.46$ C13), 78.69 (C3), 55.769 (C5), 48.60 ($J=2.63$ C9), 45.351 (C18), 44.96 ($J=18.74$ C14), 43.46 (C8), 39.31 (C17), 38.83 (C4), 38.68, 37.60, 37.47 (C10), 36.91, 33.43, 33.07 (C29), 30.48 (C20), 27.77 (C23 or C24), 27.15, 26.70, 26.28 ($J=21.62$), 24.83, 23.84 (C30), 21.84, 19.22, 19.18 (C26), 17.18 (C25), 16.38 ($J=10.91$ C27), 15.14 (C23 or C24). EI-MS m/z : 475.21 (6) M^+ , 455.19 (9), 203.18 (22), 201.17 (34), 189.20 (100), 187.22 (60), 159.24 (32), 145.24 (43), 119.22 (52), 107.20 (44), 91.23 (39), 79.21 (33), 67.22 (25).

3-Oxo-12 β -fluor-urs-13,28 β -olide (3.53) and **3-oxo-12 α -fluor-urs-13,28 β -olide (3.54)**: To a stirred solution of **3.2** (100 mg 0.22 mmol) in acetonitrile (3 mL) and dioxane (1 mL) at 50°C was added selectfluor (155.9 mg 0.44 mmol). The workup was performed according to the same method as for **3.51** and **3.52** after 2.5 hours. The obtained solid was subjected to flash column chromatography [hexanes-ethyl acetate from (90:10) to (70:30)], to afford **3.53** (21%) and **3.54** (35%). **3.53**: mp 264.9-269.9 °C. IR (film CHCl_3): 2933.2, 1782.9, 1699.9, 1455.0, 1384.6, 1363.4 cm^{-1} . ^1H NMR (400 MHz CDCl_3): δ 4.57 (1H dt $J=46.51$ H12), 2.48 (2H m $J=65.47$ H2), 1.24 (3H s C27), 1.16 (3H s C26), 1.09 (3H s C23 or C24), 1.04 (3H s C23 or C24), 0.98 (6H s C25 and C29 or C30), 0.90 (3H s C29 or C30). ^{13}C NMR (100 MHz CDCl_3): δ 217.28 (C3), 179.18 (C28), 96.40 ($J=171.78$ C12), 87.90 ($J=26.01$ C13), 54.68 (C5), 50.94 (C18), 47.30 (C4), 44.31 (C17), 43.96 (C9), 41.83 (C14 and C8), 39.29, 38.58 ($J=3.54$), 36.14 (C10), 34.07, 33.90, 33.17 (C25 or C29 or C30), 32.92, 31.49 (C20), 27.48, 27.34, 26.60 (C23 or C24), 26.05 ($J=21.28$), 23.72 (C29 or C30), 21.07, 21.04, 18.99, 17.95 (C26), 17.77 ($J=8,024$ C27), 15.95 (C25 or C29 or C30). EI-MS m/z : 473.17 (24) M^+ , 453.14 (20), 231.11 (22), 205.11 (45), 201.15 (62), 187.15 (66), 163.18 (47), 145.19 (43), 119.19 (100), 105.18 (48), 91.18 (59), 79.15 (41), 77.14 (34). **3.54**: mp 264.8-270.1 °C. IR (film CHCl_3): 2945.7, 1737.6, 1703.8, 1458.9, 1384.6, 1256.4 cm^{-1} . ^1H NMR (400 MHz CDCl_3): δ 4.63 (1H dq $J=60.64$ H12), 2.49 (2H m $J=62.71$ H2), 1.21 (3H d $J=3.08$ C27), 1.15 (3H s C26), 1.07 (3H s C23 or C24), 1.04 (3H s C23 or C24), 1.00 (3H d $J=0.45$ C25), 0.96 (3H s C29 or C30), 0.88 (3H s C29 or C30). ^{13}C NMR (100 MHz CDCl_3): δ

216.92 (C3), 178.19 (C28), 100.12 ($J=180.18$ C12), 90.54 ($J=6.92$ C13), 54.77, 47.75 ($J=1.62$), 47.17 (C4), 45.97, 44.99 ($J=19.05$ C14), 43.29 (C8), 39.35 (C17), 39.20, 37.04 (C10), 36.84, 36.74, 33.63, 33.33, 33.09 (C29 or C30), 30.52 (C20), 26.71, 26.60 (C23 or C24), 26.53 ($J=21.02$), 24.46, 23.82 (C29 or C30), 21.52, 20.60 (C23 or C24), 20.52, 18.48 (C26), 16.71 (C25), 16.37 ($J=12.31$ C27). EI-MS m/z : 473.17 (16) M^+ , 453.14 (22), 247.10 (9), 187.20 (20), 165.18 (24), 145.21 (37), 133.17 (36), 120.20 (100), 105.22 (39), 91.15 (37), 79.14 (29), 67.13 (23).

3 β -Acetoxy-12 β -fluor-olean-13,28 β -olide (3.55) and 3 β -acetoxy-12 α -fluor-olean-13,28 β -olide (3.56): To a stirred solution of **3.3** (200 mg 0.4 mmol) in nitromethane (3 mL) and dioxane (2 mL) at 50°C was added selectfluor (283.41 mg 0.8 mmol). The workup was performed according to the same method as for **3.51** and **3.52** after 4 hours. The obtained solid was subjected to flash column chromatography [hexanes-ethyl acetate from (90:10) to (70:30)], to afford **3.55** (26%) and **3.56** (20%). **3.55**: mp 327.1-329.5 °C. IR (film $CHCl_3$): 2946.7, 1776.1, 1227.9, 1467.6, 1388.5, 1368.3, 1246.8 cm^{-1} . 1H NMR (400 MHz $CDCl_3$): δ 4.54 (2H m $J=56.95$ H12 and H3), 2.04 (3H s $OCOCH_3$), 1.22 (3H d $J=0.90$), 1.11 (3H s), 0.98 (3H s), 0.89 (6H s), 0.86 (3H s), 0.85 (3H s). ^{13}C NMR (100 MHz $CDCl_3$): δ 179.30 (C28), 170.90 ($OCOCH_3$), 96.52 ($J=171.84$ C12), 87.94 ($J=25.89$ C13), 80.54 (C3), 55.08 (C5), 50.84 (C18), 44.58 (C9), 44.29 (C17), 41.92, 41.69 (C14), 38.51 ($J=3.51$), 38.22, 37.77, 36.31, 34.07, 33.45, 33.16 (C29 or C30), 31.46, 27.88 (C23 or C24), 27.43, 27.35, 25.70 ($J=21.45$), 23.74, 23.46, 21.25 ($OCOCH_3$), 21.04, 18.29 (C26), 17.90 ($J=8.16$ C27), 17.53, 16.43 (C29 or C30), 16.08 (C25). EI-MS m/z : 517.21 (3) M^+ , 496.23 (10), 246.11 (58), 201.27 (76), 189.29 (100), 159.23 (35), 119.17 (58), 107.17 (31), 91.20 (27), 79.21 (22). **3.56**: mp 309.4-309.9 °C. IR (film $CHCl_3$): 2942.8, 1741.4, 1726.9, 1467.6, 1388.5, 1363.4, 1249.7 cm^{-1} . 1H NMR (400 MHz $CDCl_3$): δ 4.65 (1H dq $J=61.02$ H12), 4.47 (1H dd $J=16.03$ H3), 2.04 (3H s $OCOCH_3$), 1.21 (3H d $J=1.63$), 1.13 (3H s), 0.96 (6H s), 0.88 (3H s), 0.86 (3H s), 0.84 (3H s). ^{13}C NMR (100 MHz $CDCl_3$): δ 178.39 (C28), 170.93 ($OCOCH_3$), 99.63 ($J=179.65$ C12), 90.71 ($J=7.54$ C13), 80.45, 55.89, 48.57 ($J=2.46$), 45.24, 44.97 ($J=18.69$ C14), 43.47 (C8), 39.31 (C17), 38.37, 37.77, 37.42 (C10), 37.56, 36.93, 33.44, 33.06 (C25 or C29 or C30), 30.47 (C20), 27.72 (C23 or C24), 26.70, 26.27 ($J=21.58$), 24.92 ($J=1.31$), 23.84 (C29 or C30), 23.42, 21.89, 21.25 ($OCOCH_3$), 19.20 (C26), 19.08, 17.26 (C25 or C29 C30), 16.36 ($J=10.73$

C27), 16.24 (C23 or C24). EI-MS *m/z*: 517.18 (11) M^+ , 497.11 (19), 437.17 (43), 247.09 (19), 203.17 (24), 201.17 (44), 189.18 (100), 187.20 (82), 145.25 (62), 119.24 (76), 107.22 (65), 91.23 (57), 79.24 (47), 67.24 (35).

Fluor-3oxoolean-28-oate (3.57): To a mixture of **3.2** (200 mg 0.44 mmol) and THF (2 mL) was added deoxofluor 50% dropwise (0.39 mL 0.88 mmol), in an ice bath. The temperature was allowed to rise up until the room temperature. After 0.5 hours was added dropwise, to the reaction mixture, NaHCO_3 (10 mL). After been stirred for 30 minutes the mixture was extracted with ether (3×50 mL). The combined extract was washed with NaHCO_3 (3×60 mL) and water (3×60 mL), dried over Na_2SO_4 , filtered and evaporated to the dryness, to afford a yellow solid. The residue was subjected to flash column chromatography [hexanes-ethyl acetate from (95:5) to (85:15)], to afford **3.57** (73%). mp 245.7-249.7 °C. IR (film CHCl_3): 2948.6, 1828.2, 1703.8, 1460.8, 1385.6, 1365.4, 1224.6 cm^{-1} . ^1H NMR (400 MHz CDCl_3): δ 5.37 (1H s H12), 2.77 (1H dd $J=16.97$ H18), 2.55 (1H m $J=34.31$), 2.36 (1H m $J=25.84$), 1.16 (3H), 1.08 (3H), 1.06 (3H), 1.04 (3H), 0.94 (3H), 0.92 (3H), 0.85 (3H). ^{13}C NMR (100 MHz CDCl_3): δ 217.491 (C3), 167.32 ($J=375.78$ C28), 142.27 (C13), 123.46 (C12), 55.37, 47.43, 46.81, 45.43, 41.94, 41.49, 39.31, 39.20, 36.74, 34.13, 33.39, 32.88, 32.28, 30.98, 30.56, 27.83, 26.42, 25.58, 23.51, 23.41, 22.85, 21.47, 19.56, 16.82, 15.04. EI-MS *m/z*: 455.44 (38) M^+ , 437.48 (60), 407.51 (80), 248.66 (35), 105.86 (53), 103.85 (84), 89.85 (100), 77.89 (55).

Fluor-3 β -acetoxy-olean-28-oate (3.58): To a stirred solution of **3.3** (100 mg 0.2 mmol) in THF (2 mL) deoxofluor 50% dropwise (0.3 mL 0.8 mmol), in an ice bath. The temperature was allowed to rise up until the room temperature. The workup was performed according to the same method as for **57** after 0.5 hours. The obtained solid was subjected to flash column chromatography [hexanes-ethyl acetate from (95:5) to (90:10)], to afford **3.58** (89%). mp 248.7-252.8 °C. IR (film CHCl_3): 2946.7, 1829.2, 1733.7, 1463.7, 1368.3, 1245.8, 1219.8 cm^{-1} . ^1H NMR (400 MHz CDCl_3): δ 5.35 (1H t $J=7.33$ H12), 4.49 (1H dd $J=16.02$ H3), 2.76 (1H dd $J=18.53$ H18), 2.04 (3H s), 1.14 (3H s), 0.94 (3H d $J=0.40$), 0.93 (3H s), 0.92 (3H s), 0.87 (3H s), 0.80 (3H s). ^{13}C NMR (100 MHz CDCl_3): δ 170.99 (OCOCH_3), 167.37 ($J=375.91$ C28), 142.21 (C13), 123.60 (C12), 80.86 (C3), 55.31, 47.57, 47.48, 47.19, 45.44, 41.80, 41.41, 39.32, 38.17, 37.68, 36.91,

33.39, 32.88, 32.68, 31.01, 30.56, 28.03, 27.82, 23.51, 23.43, 22.85, 21.28, 18.19, 16.88, 16.66, 15.41. EI-MS m/z: 498.57 (9) M⁻², 440.68 (73), 391.86 (97), 249.78 (100), 221.87 (89), 189.89 (85), 174.81 (43), 146.69 (33), 132.65 (40), 118.62 (25).

3.3.2. Biological activity assays

1. Reagents. MTT powder and DMSO were obtained from Sigma Aldrich Co (St. Luis, MO). The compounds tested for biological activity were dissolved in DMSO for stock solutions, stored at -80°C. The working solutions were prepared in medium.

2. Cell culture. Cancer cells AsPC-1, MIA PaCa 2, PANC-1, PC-3, Hep G2 and A549 were cultured in RPMI 1640 supplemented with 10% of FBS. MCF-7 cells were cultured in DMEM supplemented with 5% FBS and 1mg/mL insulin.

3. Determination of cell growth inhibition. AsPC-1, MIA PaCa 2, PANC-1, MCF-7, PC-3, Hep G2 and A549 cells were plated with 1.0×10^3 cells/well in 96-well plates in 100 μ l medium. The tested compounds with variant concentrations in 100 μ l were added after 24 h after seeding and the cells were continued to culture for 3 days. Fifty μ l of MTT (0.5 mg/ml) was added to each well and incubated for 4 h. Supernatant was removed and the formazan precipitated was dissolved in DMSO (100 μ l). The density of absorbance was measured at 570 nm on a multiple plate reader. Concentrations that inhibited cell growth by 50% (IC₅₀) were determined by nonlinear regression with GraphPad Prism software version 5.0 (GraphPad Software, Inc., San Diego, CA).

4. Cell cycle analysis. Cell cycle was assessed by flow cytometry using a fluorescence activated cell sorter (FACS). AsPC-1 cells were treated with diverse concentrations of compounds **3.27**, **3.39** and **3.49** for 24 h, and then fixed with ice-cold 70% ethanol at a density of 1×10^6 cells/mL. The cells were treated with PI/RNase solution according to the manufactures protocol. DNA content was quantitated by a flow cytometry (Becton Dickinson, San Jose, CA) with an excitation wavelength of 488 nm and an emission wavelength of 625 nm.

4.

Concluding remarks

Cancer is still a disease with poor prognosis and for which few chemotherapeutic options are available. In addition, most of the drugs currently in clinical use have severe side effects. Natural products have been and still are the most reliable source of antitumoral drugs. Triterpenoids are natural products widely explored for their biological activities. Ursolic and oleanolic acids, two pentacyclic triterpenoids, are well known for their anticancer properties; however, their use in clinical settings is restricted, mainly due to pharmacokinetic problems. Therefore, new semisynthetic derivatives are needed to overcome the present problems.

The literature is abundant with examples of semisynthetic derivatives of ursolic and oleanolic acids. Oleanolic acid derivative CDDO-Me **1.108** entered clinical trials, but these were suspended because of the cytotoxicity of this compound. Despite all the new ursolic and oleanolic acid derivatives already produced, new derivatives are still needed to overcome the flaws of the previously synthesized molecules.

In this work we accomplished the synthesis and structural elucidation of several ursane and oleanane derivatives. Most of them had a better antiproliferative profile than the parental compound. In addition, we unveiled some of the mechanisms responsible for the anticancer activity of these novel compounds.

Chapter 2 describes the successful synthesis of new ursolic acid derivatives with heterocyclic ring(s) placed in carbons C2, C3 and C28, or/and a fluorolactone moiety. These compounds were characterized efficiently, with the identification of characteristic bands in the IR and δ signals in the NMR. The presence of a heterocyclic ring was visualized by the presence of δ signals at around 7 ppm in the ^1H NMR spectrum. The presence of the β -fluorolactone moiety is characterized by the double doublet of proton H12 with a δ signal between 4-6 ppm, and by doublets of carbons C12 and C13 in the ^{13}C NMR spectrum.

The new ursane compounds were tested for their ability to inhibit the proliferation of AsPC-1 cancer cells, and several compounds were found to have a better antiproliferative activity than the parental compound (ursolic acid **2.1**). Based on SAR, compounds with

modifications in ring A, by the presence of an α,β unsaturated ketone, were the best compounds found to inhibit cell growth.

The anticancer mechanism of *N*-alkyltriazole **2.57** and fluorolactone **2.72**, the best antiproliferative ursane compounds found, was tested. Compound **2.57** induced apoptosis in AsPC-1 cells via the upregulation of NOXA and p21^{waf1} as a consequence of the induction of p53. Compound **2.72** induces cell-cycle arrest at the G1 phase with an increase of p21^{waf1}, and at higher concentrations it induces apoptosis with upregulation of NOXA and downregulation of c-FLIP.

These findings shed new light on the mechanism of action of these novel ursane derivatives, which are new prototypes for exploring the ursane backbone as a starting point for better chemotherapeutic drugs.

Chapter 3 explores new chemical modifications of oleanolic acid **3.1** and derivatives; the new compounds were fully characterized by IR, MS and NMR. The modifications performed in the oleanane-type compounds were mainly in carbons C2, C3, C12 and C28, with the synthesis of new heterocyclic and fluorine derivatives, the identification of the chemical modifications was made in the same way as for ursane derivatives.

The novel oleanane compounds were tested for their antiproliferative activity in the AsPC-1 pancreatic cancer cell line and the SAR designed. Through the SAR findings oleanane compounds with a α,β unsaturated ketone moiety in ring A were established to be the most active, and were also studied for their inhibitory activity against other solid tumor cell lines, as demonstrated to have IC_{50s} lower than 5 μ M.

Compounds **3.27** and **3.39** induced apoptosis at 1.5 μ M in AsPC-1 cells treated for 24 hours. Compound **3.49** was less active than compounds **3.27** and **3.39** in the induction of apoptosis, although it induced cell cycle arrest at the G1 phase at 2 μ M in AsPC-1 pancreatic cancer cells.

New oleanane derivatives represent a novel series of compounds with the ability to inhibit cell growth via the induction of apoptosis, and represent new starting points for the development of new chemotherapeutic drugs for the treatment of solid tumors.

In summary the use of novel synthetic procedures in this work led to the synthesis of new ursane and oleanane heterocyclic and fluorine derivatives, which were successfully characterized using IR, MS and 1D and 2D NMR.

The antiproliferative activity was determined for these new compounds, as well as SAR. The best compounds were the ones bearing an α,β unsaturated ketone moiety in ring A. The antitumor mechanisms of action of the best compounds were determined via the study of the cell cycle alterations, as well as cell cycle and apoptosis-related protein modifications. Some of the new semisynthetic compounds induced cell cycle arrest at the G1 phase, and all tested compounds induced apoptosis. These alterations were related with alterations at the level of proteins that regulate cell cycle and apoptosis.

Ursane and oleanane-type triterpenoids look promising as leads for the development of new drugs and there is still much to learn from the production of novel semisynthetic derivatives, as well as the continuous study of their anticancer activities.

5.



References

1. Weinberg, RA, *The Biology of Cancer*. Garland Science: New York, 2007.
2. Pecorino, L, *Molecular Biology of Cancer: Mechanisms, Targets, and Therapeutics*. 2nd ed.; Oxford: New York, 2008.
3. Jemal, A; Siegel, R; Xu, JQ; Ward, E. Cancer Statistics, 2010. *Ca-Cancer J Clin.*, **2010**, 60, 277-300.
4. Ferlay, J; Autier, P; Boniol, M; Heanue, M; Colombet, M; Boyle, P. Estimates of the cancer incidence and mortality in Europe in 2006. *Ann. Oncol.*, **2007**, 18, 581-592.
5. Siegel, R; Ward, E; Brawley, O; Jemal, A. The Impact of Eliminating Socioeconomic and Racial Disparities on Premature Cancer Deaths. *Ca-Cancer J Clin.*, **2011**, 61, 212-236.
6. Hanahan, D; Weinberg, RA. Hallmarks of Cancer: The Next Generation. *Cell*, **2011**, 144, 646-674.
7. Albini, A; Sporn, MB. The tumour microenvironment as a target for chemoprevention. *Nat. Rev. Cancer*, **2007**, 7, 139-147.
8. Hanahan, D; Weinberg, RA. The hallmarks of cancer. *Cell*, **2000**, 100, 57-70.
9. Mantovani, A; Allavena, P; Sica, A; Balkwill, F. Cancer-related inflammation. *Nature*, **2008**, 454, 436-444.
10. Schafer, KA. The cell cycle: A review. *Vet. Pathol.*, **1998**, 35, 461-478.
11. Williams, GH; Stoeber, K. The cell cycle and cancer. *J. Pathol.*, **2012**, 226, 352-364.
12. Michalides, RJAM. Cell cycle regulators: mechanisms and their role in aetiology, prognosis, and treatment of cancer. *J. Clin. Pathol.*, **1999**, 52, 555-568.
13. Shapiro, GI; Harper, JW. Anticancer drug targets: cell cycle and checkpoint control. *J. Clin. Invest.*, **1999**, 104, 1645-1653.
14. Kastan, MB; Bartek, J. Cell-cycle checkpoints and cancer. *Nature*, **2004**, 432, 316-323.
15. Bartek, J; Lukas, J; Bartkova, J. Perspective: Defects in cell cycle control and cancer. *J. Pathol.*, **1999**, 187, 95-99.
16. Hengartner, MO. The biochemistry of apoptosis. *Nature*, **2000**, 407, 770-776.
17. Ghavami, S; Hashemi, M; Ande, SR; Yeganeh, B; Xiao, W; Eshraghi, M; Bus, CJ; Kadkhoda, K; Wiechec, E; Halayko, AJ; Los, M. Apoptosis and cancer: mutations within caspase genes. *J. Med. Genet.*, **2009**, 46, 497-510.
18. Rastogi, RP; Richa; Sinha, RP. Apoptosis: Molecular Mechanisms and Pathogenicity. *Excli J.*, **2009**, 8, 155-181.
19. Kerr, JFR; Winterford, CM; Harmon, BV. Apoptosis - Its Significance in Cancer and Cancer-Therapy. *Cancer*, **1994**, 73, 2013-2026.
20. Lowe, SW; Lin, AW. Apoptosis in cancer. *Carcinogenesis*, **2000**, 21, 485-495.
21. Ferreira, CG; Epping, M; Kruyt, FAE; Giaccone, G. Apoptosis: Target of cancer therapy. *Clin. Cancer Res.*, **2002**, 8, 2024-2034.

22. Vermeulen, K; Van Bockstaele, DR; Berneman, ZN. Apoptosis: mechanisms and relevance in cancer. *Ann. Hematol.*, **2005**, 84, 627-639.
23. Reed, JC. Apoptosis-targeted therapies for cancer. *Cancer Cell*, **2003**, 3, 17-22.
24. Sun, SY; Hail, N; Lotan, R. Apoptosis as a novel target for cancer chemoprevention. *J. Natl. Cancer I.*, **2004**, 96, 662-672.
25. Ghobrial, IM; Witzig, TE; Adjei, AA. Targeting apoptosis pathways in cancer therapy. *Ca-Cancer J Clin.*, **2005**, 55, 178-194.
26. Hunter, AM; LaCasse, EC; Korneluk, RG. The inhibitors of apoptosis (IAPs) as cancer targets. *Apoptosis*, **2007**, 12, 1543-1568.
27. Lowe, SW; Cepero, E; Evan, G. Intrinsic tumour suppression. *Nature*, **2004**, 432, 307-315.
28. Sellers, WR; Fisher, DE. Apoptosis and cancer drug targeting. *J. Clin. Invest.*, **1999**, 104, 1655-1661.
29. Reed, JC. Dysregulation of apoptosis in cancer. *J. Clin. Oncol.*, **1999**, 17, 2941-2953.
30. Johnstone, RW; Ruefli, AA; Lowe, SW. Apoptosis: A link between cancer genetics and chemotherapy. *Cell*, **2002**, 108, 153-164.
31. Potterat, O; Hamburger, M, *Drug Discovery and development with plant-derived compounds*. Birkhauser Verlag: Basel, 2008; Vol. 65.
32. Mukherjee, AK; Basu, S; Sarkar, N; Ghosh, AC. Advances in cancer therapy with plant based natural products. *Curr. Med. Chem.*, **2001**, 8, 1467-1486.
33. Newman, DJ; Cragg, GM; Snader, KM. The influence of natural products upon drug discovery. *Nat. Prod. Rep.*, **2000**, 17, 215-234.
34. McChesney, JD; Venkataraman, SK; Henri, JT. Plant natural products: Back to the future or into extinction? *Phytochemistry*, **2007**, 68, 2015-2022.
35. Mishra, BB; Tiwari, VK. Natural Products: An evolving role in future drug discovery. *Eur. J. Med. Chem.*, **2011** 46, 4769-44807.
36. Clardy, J; Walsh, C. Lessons from natural molecules. *Nature*, **2004**, 432, 829-837.
37. Newman, DJ. Natural products as leads to potential drugs: An old process or the new hope for drug discovery? *J. Med. Chem.*, **2008**, 51, 2589-2599.
38. Newman, DJ; Cragg, GM. Natural products as sources of new drugs over the last 25 years. *J. Nat. Prod.*, **2007**, 70, 461-477.
39. Newman, DJ; Cragg, GM; Snader, KM. Natural products as sources of new drugs over the period 1981-2002. *J. Nat. Prod.*, **2003**, 66, 1022-1037.
40. Chin, YW; Balunas, MJ; Chai, HB; Kinghorn, AD. Drug discovery from natural sources. *Aaps Journal*, **2006**, 8, E239-E253.
41. Butler, MS. Natural products to drugs: natural product derived compounds in clinical trials. *Nat. Prod. Rep.*, **2005**, 22, 162-195.

42. Butler, MS. Natural products to drugs: natural product-derived compounds in clinical trials. *Nat. Prod. Rep.*, **2008**, 25, 475-516.
43. Harvey, AL. Natural products in drug discovery. *Drug Discov. Today*, **2008**, 13, 894-901.
44. Ganesan, A. The impact of natural products upon modern drug discovery. *Curr. Opin. Chem. Biol.*, **2008**, 12, 306-317.
45. Butler, MS. The role of natural product chemistry in drug discovery. *J. Nat. Prod.*, **2004**, 67, 2141-2153.
46. Paterson, I; Anderson, EA. The renaissance of natural products as drug candidates. *Science*, **2005**, 310, 451-453.
47. Lam, KS. New aspects of natural products in drug discovery. *Trends Microbiol.*, **2007**, 15, 279-289.
48. Gullo, VP; McAlpine, J; Lam, KS; Baker, D; Petersen, F. Drug discovery from natural products. *J. Ind. Microbiol. Biot.*, **2006**, 33, 523-531.
49. Koehn, FE; Carter, GT. The evolving role of natural products in drug discovery. *Nat. Rev. Drug Discov.*, **2005**, 4, 206-220.
50. Harvey, AL. Natural products as a screening resource. *Curr. Opin. Chem. Biol.*, **2007**, 11, 480-484.
51. Harvey, A. Strategies for discovering drugs from previously unexplored natural products. *Drug Discov. Today*, **2000**, 5, 294-300.
52. Jones, WP; Chin, YW; Kinghorn, AD. The role of pharmacognosy in modern medicine and pharmacy. *Curr. Drug Targets*, **2006**, 7, 247-264.
53. Baker, DD; Chu, M; Oza, U; Rajgarhia, V. The value of natural products to future pharmaceutical discovery. *Nat. Prod. Rep.*, **2007**, 24, 1225-1244.
54. Li, JWH; Vederas, JC. Drug Discovery and Natural Products: End of an Era or an Endless Frontier? *Science*, **2009**, 325, 161-165.
55. Balunas, MJ; Kinghorn, AD. Drug discovery from medicinal plants. *Life Sci.*, **2005**, 78, 431-441.
56. Galm, U; Shen, B. Natural product drug discovery: the times have never been better. *Chem. Biol.*, **2007**, 14, 1098-1104.
57. Gordaliza, M. Natural products as leads to anticancer drugs. *Clin. Transl. Oncol.*, **2007**, 9, 767-776.
58. Pfisterer, PH; Wolber, G; Efferth, T; Rollinger, JM; Stuppner, H. Natural Products in Structure-Assisted Design of Molecular Cancer Therapeutics. *Curr. Pharm. Design*, **2010**, 16, 1718-1741.
59. Kingston, DGI; Newman, DJ. The search for novel drug leads for predominately antitumor therapies by utilizing mother nature's pharmacophoric libraries. *Curr. Opin. Drug Dev.*, **2005**, 8, 207-227.
60. Braguer, D; Barret, J-M; McDaid, H; Kruczynski, A. Antitumor Activity of Vinflunine: Effector Pathways and Potential for Synergies. *Semin. Oncol.*, **2008**, 35, Supplement 3, S13-S21.

61. Brana, MF; Sanchez-Migallon, A. Anticancer drug discovery and pharmaceutical chemistry: a history. *Clinical & translational oncology : official publication of the Federation of Spanish Oncology Societies and of the National Cancer Institute of Mexico*, **2006**, 8, 717-728.
62. Hong, WK; Sporn, MB. Recent advances in chemoprevention of cancer. *Science*, **1997**, 278, 1073-1077.
63. Sporn, MB; Dunlop, NM; Newton, DL; Smith, JM. Prevention of Chemical Carcinogenesis by Vitamin-a and Its Synthetic Analogs (Retinoids). *Fed. Proc.*, **1976**, 35, 1332-1338.
64. Kelloff, GJ; Crowell, JA; Steele, VE; Lubet, RA; Malone, WA; Boone, CW; Kopelovich, L; Hawk, ET; Lieberman, R; Lawrence, JA; Ali, I; Viner, JL; Sigman, CC. Progress in cancer chemoprevention: Development of diet-derived chemopreventive agents. *J. Nutr.*, **2000**, 130, 467S-471S.
65. Kinghorn, AD; Su, BN; Jang, DS; Chang, LC; Lee, D; Gu, JQ; Carcache-Blanco, EJ; Powlus, AD; Lee, SK; Park, EJ; Cuendet, M; Gills, JJ; Bhat, K; Park, HS; Mata-Greenwood, E; Song, LL; Jong, MH; Pezzuto, JM. Natural inhibitors of carcinogenesis. *Planta Med.*, **2004**, 70, 691-705.
66. Mehta, RG; Pezzuto, JM. Discovery of cancer preventive agents from natural products: from plants to prevention. *Current oncology reports*, **2002**, 4, 478-486.
67. Singh, S; Khar, A. Biological effects of curcumin and its role in cancer chemoprevention and therapy. *Anti-cancer agents in medicinal chemistry*, **2006**, 6, 259-270.
68. Maheshwari, RK; Singh, AK; Gaddipati, J; Srimal, RC. Multiple biological activities of curcumin: A short review. *Life Sci.*, **2006**, 78, 2081-2087.
69. Signorelli, P; Ghidoni, R. Resveratrol as an anticancer nutrient: molecular basis, open questions and promises. *J. Nutr. Biochem.*, **2005**, 16, 449-466.
70. Phillips, DR; Rasbery, JM; Bartel, B; Matsuda, SPT. Biosynthetic diversity in plant triterpene cyclization. *Curr. Opin. Plant Biol.*, **2006**, 9, 305-314.
71. Eisenreich, W; Bacher, A; Arigoni, D; Rohdich, F. Biosynthesis of isoprenoids via the non-mevalonate pathway. *Cell Mol. Life Sci.*, **2004**, 61, 1401-1426.
72. Xu, R; Fazio, GC; Matsuda, SPT. On the origins of triterpenoid skeletal diversity. *Phytochemistry*, **2004**, 65, 261-291.
73. Shibuya, M; Xiang, T; Katsube, Y; Otsuka, M; Zhang, H; Ebizuka, Y. Origin of structural diversity in natural triterpenes: Direct synthesis of seco-triterpene skeletons by oxidosqualene cyclase. *J. Am. Chem. Soc.*, **2007**, 129, 1450-1455.
74. Kushiro, T; Shibuya, M; Ebizuka, Y. Chimeric triterpene synthase. A possible model for multifunctional triterpene synthase. *J. Am. Chem. Soc.*, **1999**, 121, 1208-1216.
75. Abe, I. Enzymatic synthesis of cyclic triterpenes. *Nat. Prod. Rep.*, **2007**, 24, 1311-1331.
76. Dzubak, P; Hajduch, M; Vydra, D; Hustova, A; Kvasnica, M; Biedermann, D; Markova, L; Urban, M; Sarek, J. Pharmacological activities of natural triterpenoids and their therapeutic implications. *Nat. Prod. Rep.*, **2006**, 23, 394-411.
77. Liu, J. Pharmacology of oleanolic acid and ursolic acid. *J. Ethnopharmacol.*, **1995**, 49, 57-68.
78. Aggarwal, BB; Shishodia, S. Molecular targets of dietary agents for prevention and therapy of cancer. *Biochem. Pharmacol.*, **2006**, 71, 1397-1421.

79. Ren, DC; Zuo, RJ; Barrios, AFG; Bedzyk, LA; Eldridge, GR; Pasmore, ME; Wood, TK. Differential gene expression for investigation of *Escherichia coli* biofilm inhibition by plant extract ursolic acid. *Appl. Environ. Microb.*, **2005**, 71, 4022-4034.
80. Gu, JQ; Wang, YH; Franzblau, SG; Montenegro, G; Timmermann, BN. Constituents of *Quinchamalium majus* with potential antitubercular activity. *Z. Naturforsch. C*, **2004**, 59, 797-802.
81. Abe, F; Yamauchi, T; Nagao, T; Kinjo, J; Okabe, H; Higo, H; Akahane, H. Ursolic acid as a trypanocidal constituent in rosemary. *Biol. Pharm. Bull.*, **2002**, 25, 1485-1487.
82. Suksamrarn, A; Tanachatchairatana, T; Kanokmedhakul, S. Antiplasmodial triterpenes from twigs of *Gardenia saxatilis*. *J. Ethnopharmacol.*, **2003**, 88, 275-277.
83. Torres-Santos, EC; Lopes, D; Oliveira, RR; Carauta, JPP; Falcao, CAB; Kaplan, AAC; Rossi-Bergmann, B. Antileishmanial activity of isolated triterpenoids from *Pourouma guianensis*. *Phytomedicine*, **2004**, 11, 114-120.
84. Xu, HX; Zeng, FQ; Wan, M; Sim, KY. Anti-HIV triterpene acids from *Geum japonicum*. *J. Nat. Prod.*, **1996**, 59, 643-645.
85. Kim, J; Jang, DS; Kim, H; Kim, JS. Anti-lipase and lipolytic activities of ursolic acid isolated from the roots of *Actinidia arguta*. *Arch. Pharm. Res.*, **2009**, 32, 983-987.
86. Lee, WS; Im, KR; Park, YD; Sung, ND; Jeong, TS. Human ACAT-1 and ACAT-2 inhibitory activities of pentacyclic triterpenes from the leaves of *Lycopus lucidus* Turcz. *Biol. Pharm. Bull.*, **2006**, 29, 382-384.
87. Heo, HJ; Cho, HY; Hong, B; Kim, HK; Heo, TR; Kim, EK; Kim, SK; Kim, CJ; Shin, DH. Ursolic acid of *Origanum majorana* L. reduces A beta-induced oxidative injury. *Mol. Cells*, **2002**, 13, 5-11.
88. Chung, YK; Heo, HJ; Kim, EK; Kim, HK; Huh, TL; Lim, Y; Kim, SK; Shin, DH. Inhibitory effect of ursolic acid purified from *Origanum majorana* L. on the acetylcholinesterase. *Mol. Cells*, **2001**, 11, 137-143.
89. Saraswat, B; Visen, PKS; Agarwal, DP. Ursolic acid isolated from *Eucalyptus tereticornis* protects against ethanol toxicity in isolated rat hepatocytes. *Phytother. Res.*, **2000**, 14, 163-166.
90. Taviano, MF; Miceli, N; Monforte, MT; Tzakou, O; Galati, EM. Ursolic acid plays a role in *Nepeta sibthorpii* Benthams CNS depressing effects. *Phytother. Res.*, **2007**, 21, 382-385.
91. Baricevic, D; Sosa, S; Della Loggia, R; Tubaro, A; Simonovska, B; Krasna, A; Zupancic, A. Topical anti-inflammatory activity of *Salvia officinalis* L. leaves: the relevance of ursolic acid. *J. Ethnopharmacol.*, **2001**, 75, 125-132.
92. Horiuchi, K; Shiota, S; Hatano, T; Yoshida, T; Kuroda, T; Tsuchiya, T. Antimicrobial activity of oleanolic acid from *Salvia officinalis* and related compounds on vancomycin-resistant enterococci (VRIE). *Biol. Pharm. Bull.*, **2007**, 30, 1147-1149.
93. Banno, N; Akihisa, T; Tokuda, H; Yasukawa, K; Higashihara, H; Ukiya, M; Watanabe, K; Kimura, Y; Hasegawa, J; Nishino, H. Triterpene acids from the leaves of *Perilla frutescens* and their anti-inflammatory and antitumor-promoting effects. *Biosci. Biotech. Bioch.*, **2004**, 68, 85-90.
94. Ryu, SY; Oak, MH; Yoon, SK; Cho, DI; Yoo, GS; Kim, TS; Kim, KM. Anti-allergic and anti-inflammatory triterpenes from the herb of *Prunella vulgaris*. *Planta Med.*, **2000**, 66, 358-360.

95. Ringbom, T; Segura, L; Noreen, Y; Perera, P; Bohlin, L. Ursolic acid from *Plantago major*, a selective inhibitor of cyclooxygenase-2 catalyzed prostaglandin biosynthesis. *J. Nat. Prod.*, **1998**, 61, 1212-1215.
96. Aguirre, MC; Delporte, C; Backhouse, N; Erazo, S; Letelier, ME; Cassels, BK; Silva, X; Alegria, S; Negrete, R. Topical anti-inflammatory activity of 2 alpha-hydroxy pentacyclic triterpene acids from the leaves of *Ugni molinae*. *Bioorg. Med. Chem.*, **2006**, 14, 5673-5677.
97. Tapondjou, LA; Lontsi, D; Sondengam, BL; Choi, JW; Lee, KT; Jung, HJ; Park, HJ. In vivo anti-nociceptive and anti-inflammatory effect of the two triterpenes, ursolic acid and 23-hydroxyursolic acid, from *Cussonia bancoensis*. *Arch. Pharm. Res.*, **2003**, 26, 143-146.
98. Huang, Y; Nikolic, D; Pendland, S; Doyle, BJ; Locklear, TD; Mahady, GB. Effects of cranberry extracts and ursolic acid derivatives on P-fimbriated *Escherichia coli*, COX-2 activity, pro-inflammatory cytokine release and the NF-kappa beta transcriptional response in vitro. *Pharm. Biol.*, **2009**, 47, 18-25.
99. Essaady, D; Najid, A; Simon, A; Denizot, Y; Chulia, AJ; Delage, C. Effects of Ursolic Acid and Its Analogs on Soybean 15-Lipoxygenase Activity and the Proliferation Rate of a Human Gastric Tumor-Cell Line. *Mediat. Inflamm.*, **1994**, 3, 181-184.
100. Yamai, H; Sawada, N; Yoshida, T; Seike, J; Takizawa, H; Kenzaki, K; Miyoshi, T; Kondo, K; Bando, Y; Ohnishi, Y; Tangoku, A. Triterpenes augment the inhibitory effects of anticancer drugs on growth of human esophageal carcinoma cells in vitro and suppress experimental metastasis in vivo. *Int. J. Cancer*, **2009**, 125, 952-960.
101. Tanachatchairatana, T; Bremner, JB; Chokchaisiri, R; Suksamrarn, A. Antimycobacterial activity of cinnamate-based esters of the triterpenes betulinic, oleanolic and ursolic acids. *Chem. Pharm. Bull.*, **2008**, 56, 194-198.
102. Fontanay, S; Grare, M; Mayer, J; Finance, C; Duval, RE. Ursolic, oleanolic and betulinic acids: Antibacterial spectra and selectivity indexes. *J. Ethnopharmacol.*, **2008**, 120, 272-276.
103. Reguera, RM; Redondo, CM; de Prado, RG; Perez-Pertejo, Y; Balana-Fouce, R. DNA topoisomerase I from parasitic protozoa: A potential target for chemotherapy. *BBA-Gene Struct. Expr.*, **2006**, 1759, 117-131.
104. Mullie, C; Jonet, A; Dassonville-Klimpt, A; Gosmann, G; Sonnet, P. Inhibitory effect of ursolic acid derivatives on hydrogen peroxide- and glutathione-mediated degradation of hemin: A possible additional mechanism of action for antimalarial activity. *Exp- Parasitol.*, **2010**, 125, 202-207.
105. Amusan, OOG. Antimalarial active principles of *Spathodea campanulata* stem bark. *Phytother. Res.*, **1996**, 10, 692-693.
106. Traore-Keita, F; Gasquet, M; Di Giorgio, C; Ollivier, E; Delmas, F; Keita, A; Doumbo, O; Balansard, G; Timon-David, P. Antimalarial activity of four plants used in traditional medicine in Mali. *Phytother. Res.*, **2000**, 14, 45-47.
107. Gnoatto, SCB; Dalla Vecchia, L; Lencina, CL; Dassonville-Klimpt, A; Da Nascimento, S; Mossalayi, D; Guillon, J; Gosmann, G; Sonnet, P. Synthesis and preliminary evaluation of new ursolic and oleanolic acids derivatives as antileishmanial agents. *J. Enzym. Inhib. Med. Chem.*, **2008**, 23, 604-610.
108. Kashiwada, Y; Hashimoto, F; Cosentino, LM; Chen, CH; Garrett, PE; Lee, KH. Betulinic acid and dihydrobetulinic acid derivatives as potent anti-HIV agents. *J. Med. Chem.*, **1996**, 39, 1016-1017.

109. Yogeeswari, P; Sriram, D. Betulinic acid and its derivatives: A review on their biological properties. *Curr. Med. Chem.*, **2005**, 12, 657-666.
110. Kashiwada, Y; Nagao, T; Hashimoto, A; Ikeshiro, Y; Okabe, H; Cosentino, LM; Lee, KH. Anti-AIDS agents 38. Anti-HIV activity of 3-O-acyl ursolic acid derivatives. *J. Nat. Prod.*, **2000**, 63, 1619-1622.
111. Quere, L; Wenger, T; Schramm, HJ. Triterpenes as potential dimerization inhibitors of HIV-1 protease. *Biochem. Bioph. Res. Co.*, **1996**, 227, 484-488.
112. Mizushina, Y; Iida, A; Ohta, K; Sugawara, F; Sakaguchi, K. Novel triterpenoids inhibit both DNA polymerase and DNA topoisomerase. *Biochem. J.*, **2000**, 350, 757-763.
113. Deng, SL; Baglin, I; Nour, M; Flekhter, O; Vita, C; Cave, C. Synthesis of ursolic phosphonate derivatives as potential Anti-HIV agents. *Phosphorus Sulfur*, **2007**, 182, 951-967.
114. Horowitz, MC; Xi, YG; Wilson, K; Kacena, MA. Control of osteoclastogenesis and bone resorption by members of the TNF family of receptors and ligands. *Cytokine Growth F. R.*, **2001**, 12, 9-18.
115. Martin, TJ; Ng, KW. Mechanisms by Which Cells of the Osteoblast Lineage Control Osteoclast Formation and Activity. *J. Cell. Biochem.*, **1994**, 56, 357-366.
116. Bilic-Curcic, I; Milas-Ahic, J; Smolic, M; Smolic, R; Mihaljevic, I; Tucak-Zoric, S. Urolithiasis and Osteoporosis: Clinical Relevance and Therapeutic Implications. *Collegium Antropol.*, **2009**, 33, 189-192.
117. Lee, SU; Park, SJ; Kwak, HB; Oh, J; Min, YK; Kim, SH. Anabolic activity of ursolic acid in bone: Stimulating osteoblast differentiation in vitro and inducing new bone formation in vivo. *Pharmacol. Res.*, **2008**, 58, 290-296.
118. Heron, M. Deaths: leading causes for 2007. *National vital statistics reports : from the Centers for Disease Control and Prevention, National Center for Health Statistics, National Vital Statistics System*, 59, 1-95.
119. Somova, LO; Nadar, A; Rammanan, P; Shode, FO. Cardiovascular, antihyperlipidemic and antioxidant effects of oleanolic and ursolic acids in experimental hypertension. *Phytomedicine*, **2003**, 10, 115-121.
120. Somova, LI; Shode, FO; Mipando, M. Cardiotoxic and antidysrhythmic effects of oleanolic and ursolic acids, methyl maslinate and uvaol. *Phytomedicine*, **2004**, 11, 121-129.
121. Saravanan, R; Pugalendi, V. Impact of ursolic acid on chronic ethanol-induced oxidative stress in the rat heart. *Pharmacol. Rep.*, **2006**, 58, 41-47.
122. Senthil, S; Chandramohan, G; Pugalendi, KV. Isomers (oleanolic and ursolic acids) differ in their protective effect against isoproterenol-induced myocardial ischemia in rats. *Int. J. Cardiol.*, **2007**, 119, 131-133.
123. Liobikas, J; Bernatoniene, J; Majiene, D; Kursvietiene, L; Masteikova, R; Kopustinskiene, D; Trumbeckaite, S; Savickas, A. Direct effects of ursolic acid on oxidative phosphorylation of rat heart mitochondria. *Biomedicine & Preventive Nutrition*.
124. Radhiga, T; Rajamanickam, C; Sundaresan, A; Ezhumalai, M; Pugalendi, KV. Effect of ursolic acid treatment on apoptosis and DNA damage in isoproterenol-induced myocardial infarction. *Biochimie*, **2012**, 94, 1135-1142.

125. Kopelman, PG. Obesity as a medical problem. *Nature*, **2000**, 404, 635-643.
126. Larsson, B; Bjorntorp, P; Tibblin, G. The Health Consequences of Moderate Obesity. *Int. J. Obesity*, **1981**, 5, 97-116.
127. Jang, DS; Lee, GY; Kim, J; Lee, YM; Kim, JM; Kim, YS; Kim, JS. A new pancreatic lipase inhibitor isolated from the roots of *Actinidia arguta*. *Arch. Pharm. Res.*, **2008**, 31, 666-670.
128. Jang, SM; Kim, MJ; Choi, MS; Kwon, EY; Lee, MK. Inhibitory effects of ursolic acid on hepatic polyol pathway and glucose production in streptozotocin-induced diabetic mice. *Metabolism*, **2010**, 59, 512-519.
129. Liu, Y; Tian, WX; Ma, XF; Ding, WJ. Evaluation of inhibition of fatty acid synthase by ursolic acid: Positive cooperation mechanism. *Biochem. Bioph. Res. Co.*, **2010**, 392, 386-390.
130. Jia, Y; Bhuiyan, MJH; Jun, HJ; Lee, JH; Hoang, MH; Lee, HJ; Kim, N; Lee, D; Hwang, KY; Hwang, BY; Choi, DW; Lee, SJ. Ursolic acid is a PPAR-alpha agonist that regulates hepatic lipid metabolism. *Bioorg. Med. Chem. Lett.*, **2011**, 21, 5876-5880.
131. Libby, P. Inflammation in atherosclerosis. *Nature*, **2002**, 420, 868-874.
132. Ross, R. Mechanisms of disease - Atherosclerosis - An inflammatory disease. *New Engl. J. Med.*, **1999**, 340, 115-126.
133. Pozo, M; Castilla, V; Gutierrez, C; de Nicolas, R; Egido, J; Gonzalez-Cabrero, J. Ursolic acid inhibits neointima formation in the rat carotid artery injury model. *Atherosclerosis*, **2006**, 184, 53-62.
134. Mortensen, RF. C-reactive protein, inflammation, and innate immunity. *Immunol. Res.*, **2001**, 24, 163-176.
135. Pasceri, V; Willerson, JT; Yeh, ETH. Direct proinflammatory effect of C-reactive protein on human endothelial cells. *Circulation*, **2000**, 102, 2165-2168.
136. Torzewski, M; Rist, C; Mortensen, RF; Zwaka, TP; Bienek, M; Waltenberger, J; Koenig, W; Schmitz, G; Hombach, V; Torzewski, J. C-reactive protein in the arterial intima - Role of C-reactive protein receptor-dependent monocyte recruitment in atherogenesis. *Arteriosclerosis Thrombosis and Vascular Biology*, **2000**, 20, 2094-2099.
137. Lv, Y-Y; Jin, Y; Han, G-Z; Liu, Y-X; Wu, T; Liu, P; Zhou, Q; Liu, K-X; Sun, H-J. Ursolic acid suppresses IL-6 induced C-reactive protein expression in HepG2 and protects HUVECs from injury induced by CRP. *Eur. J. Pharm. Sci.*, 45, 190-194.
138. Huang, ES; Liu, JY; Moffet, HH; John, PM; Karter, AJ. Glycemic Control, Complications, and Death in Older Diabetic Patients The Diabetes and Aging Study. *Diabetes Care*, 34, 1329-1336.
139. Zhang, W; Hong, D; Zhou, Y; Zhang, Y; Shen, Q; Li, JY; Hu, LH; Li, J. Ursolic acid and its derivative inhibit protein tyrosine phosphatase 1B, enhancing insulin receptor phosphorylation and stimulating glucose uptake. *BBA- Gen. Subjects*, **2006**, 1760, 1505-1512.
140. Jung, SH; Ha, YJ; Shim, EK; Choi, SY; Jin, JL; Yun-Choi, HS; Lee, JR. Insulin-mimetic and insulin-sensitizing activities of a pentacyclic triterpenoid insulin receptor activator. *Biochem. J.*, **2007**, 403, 243-250.
141. Jang, SM; Yee, ST; Choi, J; Choi, MS; Do, GM; Jeon, SM; Yeo, J; Kim, MJ; Seo, KI; Lee, MK. Ursolic acid enhances the cellular immune system and pancreatic beta-cell function in streptozotocin-induced diabetic mice fed a high-fat diet. *Int. Immunopharm.*, **2009**, 9, 113-119.

142. Wang, ZH; Hsu, CC; Huang, CN; Yin, MC. Anti-glycative effects of oleanolic acid and ursolic acid in kidney of diabetic mice. *Eur. J. Pharmacol.*, **2010**, 628, 255-260.
143. Roberts, RO; Geda, YE; Knopman, DS; Christianson, TJH; Pankratz, VS; Boeve, BF; Vella, A; Rocca, WA; Petersen, RC. Association of duration and severity of diabetes mellitus with mild cognitive impairment. *Ach. Neurol.*, **2008**, 65, 1066-1073.
144. Zhang, XQ; Zhang, G; Zhang, H; Karin, M; Bai, H; Cai, DS. Hypothalamic IKK beta/NF-kappa B and ER stress link overnutrition to energy imbalance and obesity. *Cell*, **2008**, 135, 61-73.
145. Nakamura, T; Furuhashi, M; Li, P; Cao, HM; Tuncman, G; Sonenberg, N; Gorgun, CZ; Hotamisligil, GS. Double-Stranded RNA-Dependent Protein Kinase Links Pathogen Sensing with Stress and Metabolic Homeostasis. *Cell*, **2010**, 140, 338-U341.
146. Lu, J; Wu, DM; Zheng, YL; Hu, B; Cheng, W; Zhang, ZF; Shan, Q. Ursolic acid improves high fat diet-induced cognitive impairments by blocking endoplasmic reticulum stress and I kappa B kinase beta/nuclear factor-kappa B-mediated inflammatory pathways in mice. *Brain Behav. Immun.*, **2011**, 25, 1658-1667.
147. Dennis, C. A2M is associated with late-onset Alzheimer disease. *Nat. Med.*, **1998**, 4, 888-888.
148. Brufani, M; Marta, M; Pomponi, M. Anticholinesterase Activity of a New Carbamate, Heptylphysostigmine, in View of Its Use in Patients with Alzheimer-Type Dementia. *Eur. J. Biochem.*, **1986**, 157, 115-120.
149. Raphael, TJ; Kuttan, G. Effect of naturally occurring triterpenoids glycyrrhizic acid, ursolic acid, oleanolic acid and nomilin on the immune system. *Phytomedicine*, **2003**, 10, 483-489.
150. Saravanan, R; Viswanathan, P; Pugalendi, KV. Protective effect of ursolic acid on ethanol-mediated experimental liver damage in rats. *Life Sci.*, **2006**, 78, 713-718.
151. Martin-Aragon, S; de las Heras, B; Sanchez-Reus, MI; Benedi, J. Pharmacological modification of endogenous antioxidant enzymes by ursolic acid on tetrachloride-induced liver damage in rats and primary cultures of rat hepatocytes. *Exp. Toxicol. Pathol.*, **2001**, 53, 199-206.
152. Agarwal, D; Patnaik, G; Visen, PKS; Dayal, R; Binduja, S. Protective action of ursolic acid against chemical induced hepato-toxicity in rats. *Indian J. Pharmacol.*, **1996**, 28, 232-239.
153. Coyle, P; Philcox, JC; Carey, LC; Rofe, AM. Metallothionein: The multipurpose protein. *Cell Mol. Life Sci.*, **2002**, 59, 627-647.
154. Jeong, HG; Kim, HG; Hwang, YP. Involvement of cytokines in the hepatic expression of metallothionein by ursolic acid. *Toxicol. Lett.*, **2005**, 155, 369-376.
155. Friedman, SL. Molecular regulation of hepatic fibrosis, an integrated cellular response to tissue injury. *J. Biol. Chem.*, **2000**, 275, 2247-2250.
156. Iredale, JP; Benyon, RC; Pickering, J; McCullen, M; Northrop, M; Pawley, S; Hovell, C; Arthur, MJP. Mechanisms of spontaneous resolution of rat liver fibrosis - Hepatic stellate cell apoptosis and reduced hepatic expression of metalloproteinase inhibitors. *J. Clin. Invest.*, **1998**, 102, 538-549.
157. Wang, X; Ikejima, K; Kon, K; Arai, K; Aoyama, T; Okumura, K; Abe, W; Sato, N; Watanabe, S. Ursolic acid ameliorates hepatic fibrosis in the rat by specific induction of apoptosis in hepatic stellate cells. *J. Hepatol.*, **2011**, 55, 379-387.

158. Ikejima, K; Wang, X; Kon, K; Arai, K; Fukuhara, K; Hosoya, S; Yamashina, S; Watanabe, S. Ursolic Acid Ameliorates Hepatic Fibrogenesis through Induction of Apoptosis in Hepatic Stellate Cells. *J. Hepatol.*, **2011**, 54, S53-S54.
159. Najid, A; Simon, A; Cook, J; Chablerabinovitch, H; Delage, C; Chulia, AJ; Rigaud, M. Characterization of Ursolic Acid as a Lipoxygenase and Cyclooxygenase Inhibitor Using Macrophages, Platelets and Differentiated HL-60 Leukemic-Cells. *Febs Lett.*, **1992**, 299, 213-217.
160. Simon, A; Najid, A; Chulia, AJ; Delage, C; Rigaud, M. Inhibition of Lipoxygenase Activity and HL-60 Leukemic-Cell Proliferation by Ursolic Acid Isolated from Heather Flowers (*Calluna-Vulgaris*). *Biochim. Biophys. Acts*, **1992**, 1125, 68-72.
161. Subbaramaiah, K; Michaluart, P; Sporn, MB; Dannenberg, AJ. Ursolic acid inhibits cyclooxygenase-2 transcription in human mammary epithelial cells. *Cancer Res.*, **2000**, 60, 2399-2404.
162. Cha, HJ; Park, MT; Chung, HY; Kim, ND; Sato, H; Seiki, M; Kim, KW. Ursolic acid-induced down-regulation of MMP-9 gene is mediated through the nuclear translocation of glucocorticoid receptor in HT1080 human fibrosarcoma cells. *Oncogene*, **1998**, 16, 771-778.
163. Cha, HJ; Bae, SK; Lee, HY; Lee, OH; Sato, H; Seiki, M; Park, BC; Kim, KW. Anti-invasive activity of ursolic acid correlates with the reduced expression of matrix metalloproteinase-9 (MMP-9) in HT1080 human fibrosarcoma cells. *Cancer Res.*, **1996**, 56, 2281-2284.
164. Suh, N; Honda, T; Finlay, HJ; Barchowsky, A; Williams, C; Benoit, NE; Xie, QW; Nathan, C; Gribble, GW; Sporn, MB. Novel triterpenoids suppress inducible nitric oxide synthase (iNOS) and inducible cyclooxygenase (COX-2) in mouse macrophages. *Cancer Res.*, **1998**, 58, 717-723.
165. Shishodia, S; Majumdar, S; Banerjee, S; Aggarwal, BB. Ursolic acid inhibits nuclear factor-kappa B activation induced by carcinogenic agents through suppression of I kappa B alpha kinase and p65 phosphorylation: Correlation with down-regulation of cyclooxygenase 2, matrix metalloproteinase 9, and cyclin D1. *Cancer Res.*, **2003**, 63, 4375-4383.
166. You, HJ; Choi, CY; Kim, JY; Park, SJ; Hahm, KS; Jeong, HG. Ursolic acid enhances nitric oxide and tumor necrosis factor-alpha production via nuclear factor-kappa B activation in the resting macrophages. *Febs Lett.*, **2001**, 509, 156-160.
167. Ikeda, Y; Murakami, A; Ohigashi, H. Ursolic acid: An anti- and pro-inflammatory, triterpenoid. *Mol. Nutr. Food Res.*, **2008**, 52, 26-42.
168. Takada, K; Nakane, T; Masuda, K; Ishii, H. Ursolic acid and oleanolic acid, members of pentacyclic triterpenoid acids, suppress TNF-alpha-induced E-selectin expression by cultured umbilical vein endothelial cells. *Phytomedicine*, **2010**, 17, 1114-1119.
169. Ikeda, Y; Murakami, A; Ohigashi, H. Ursolic acid promotes the release of macrophage migration inhibitory factor via ERK2 activation in resting mouse macrophages. *Biochem. Pharmacol.*, **2005**, 70, 1497-1505.
170. Heo, HJ; Kim, C; Lee, HJ; Kim, YS; Kang, SS; Seo, UK; Kim, YH; Park, YC; Seok, JH; Lee, CJ. Carbenoxolone and triterpenoids inhibited mucin secretion from airway epithelial cells. *Phytother. Res.*, **2007**, 21, 462-465.
171. Ikeda, Y; Murakami, A; Nishizawa, T; Ohigashi, H. Ursolic acid enhances cyclooxygenases and tumor necrosis factor-alpha expression in mouse skin. *Biosci. Biotech. Bioch.*, **2006**, 70, 1033-1037.

172. Salvador, JAR, Ed., *Pentacyclic Triterpenes as Promising Agents in Cancer*. Nova Science Publishers Inc.: New York, 2010.
173. Novotny, L; Vachalkova, A; Biggs, D. Ursolic acid: An anti-tumorigenic and chemopreventive activity. *Neoplasma*, **2001**, 48, 241-246.
174. Liu, H. Oleanolic acid and ursolic acid: Research perspectives. *J. Ethnopharmacol.*, **2005**, 100, 92-94.
175. Ovesna, Z; Vachalkova, A; Horvathova, K; Tothova, D. Pentacyclic triterpenoic acids: new chemoprotective compounds. *Neoplasma*, **2004**, 51, 327-333.
176. Baglin, I; Mitaine-Offer, AC; Nour, M; Tan, K; Cave, C; Lacaille-Dubois, MA. A Review of Natural and Modified Betulinic, Ursolic and Echinocystic Acid Derivatives as Potential Antitumor and Anti-HIV Agents. *Mini Rev. Med. Chem.*, **2003**, 3, 525-539.
177. Kuo, RY; Qian, KD; Morris-Natschke, SL; Lee, KH. Plant-derived triterpenoids and analogues as antitumor and anti-HIV agents. *Nat. Prod. Rep.*, **2009**, 26, 1321-1344.
178. Laszczyk, MN. Pentacyclic Triterpenes of the Lupane, Oleanane and Ursane Group as Tools in Cancer Therapy. *Planta Med.*, **2009**, 75, 1549-1560.
179. Taniguchi, S; Imayoshi, Y; Kobayashi, E; Takamatsu, Y; Ito, H; Hatano, T; Sakagami, H; Tokuda, H; Nishino, H; Sugita, D; Shimura, S; Yoshida, T. Production of bioactive triterpenes by *Eriobotrya japonica* calli. *Phytochemistry*, **2002**, 59, 315-323.
180. Chiang, YM; Chang, JY; Kuo, CC; Chang, CY; Kuo, YH. Cytotoxic triterpenes from the aerial roots of *Ficus microcarpa*. *Phytochemistry*, **2005**, 66, 495-501.
181. Chen, IH; Lu, MC; Du, YC; Yen, MH; Wu, CC; Chen, YH; Hung, CS; Chen, SL; Chang, FR; Wu, YC. Cytotoxic Triterpenoids from the Stems of *Microtropis japonica*. *J. Nat. Prod.*, **2009**, 72, 1231-1236.
182. Ma, CM; Cai, SQ; Cui, JR; Wang, RQ; Tu, PF; Hattori, M; Daneshtalab, M. The cytotoxic activity of ursolic acid derivatives. *Eur. J. Med. Chem.*, **2005**, 40, 582-589.
183. Meng, YQ; Liu, D; Cai, LL; Chen, H; Cao, B; Wang, YZ. The synthesis of ursolic acid derivatives with cytotoxic activity and the investigation of their preliminary mechanism of action. *Bioorg. Med. Chem.*, **2009**, 17, 848-854.
184. Shao, JW; Dai, YC; Xue, JP; Wang, JC; Lin, FP; Guo, YH. In vitro and in vivo anticancer activity evaluation of ursolic acid derivatives. *Eur. J. Med. Chem.*, **2011**, 46, 2652-2661.
185. Meng, YQ; Song, YL; Yan, ZK; Xia, Y. Synthesis and in vitro Cytotoxicity of Novel Ursolic Acid Derivatives. *Molecules*, **2010**, 15, 4033-4040.
186. Bai, KK; Chen, FL; Yu, Z; Zheng, YQ; Li, YN; Guo, YH. Synthesis of [3 beta-acetoxy-urs-12-en-28-oyl]-1-monoglyceride and investigation on its anti tumor effects against BGC-823. *Bioorg. Med. Chem.*, **2011**, 19, 4043-4050.
187. Chen, GQ; Yao, ZW; Zheng, WP; Chen, L; Duan, H; Shen, Y. Combined antitumor effect of ursolic acid and 5-fluorouracil on human esophageal carcinoma cell Eca-109 in vitro. *Chin. J. Canc. Res.*, **2010**, 22, 62-67.
188. Chen, GQ; Shen, Y; Duan, H. Anti-tumor effect and its mechanisms of ursolic acid on human esophageal carcinoma cell Eca-109 in vivo. *Chin. J. Canc. Res.*, **2008**, 20, 205-210.

189. Andersson, D; Cheng, YJ; Duan, RD. Ursolic acid inhibits the formation of aberrant crypt foci and affects colonic sphingomyelin hydrolyzing enzymes in azoxymethane-treated rats. *J. Cancer Res. Clin.*, **2008**, 134, 101-107.
190. Furtado, RA; Rodrigues, EP; Araujo, FRR; Oliveira, WL; Furtado, MA; Castro, MB; Cunha, WR; Tavares, DC. Ursolic Acid and Oleanolic Acid Suppress Preneoplastic Lesions Induced by 1,2-Dimethylhydrazine in Rat Colon. *Toxicol. Pathol.*, **2008**, 36, 576-580.
191. Andersson, D; Liu, JJ; Nilsson, A; Duan, RD. Ursolic acid inhibits proliferation and stimulates apoptosis in HT29 cells following activation of alkaline sphingomyelinase. *Anticancer Res.*, **2003**, 23, 3317-3322.
192. Andersson, D; Nilsson, A; Duan, RD. Ursolic acid and other pentacyclic triterpenoids stimulate intestinal alkaline sphingomyelinase in vitro. *Eur. J. Lipid Sci. Technol.*, **2006**, 108, 103-108.
193. Shan, JZ; Xuan, YY; Zheng, S; Dong, Q; Zhang, SZ. Ursolic acid inhibits proliferation and induces apoptosis of HT-29 colon cancer cells by inhibiting the EGFR/MAPK pathway. *J. Zhejiang Univ.-Sc B*, **2009**, 10, 668-674.
194. Eberhart, CE; Coffey, RJ; Radhika, A; Giardiello, FM; Ferrenbach, S; Dubois, RN. Up-Regulation of Cyclooxygenase-2 Gene-Expression in Human Colorectal Adenomas and Adenocarcinomas. *Gastroenterology*, **1994**, 107, 1183-1188.
195. Sun, YJ; Tang, XM; Half, E; Kuo, MT; Sinicrope, FA. Cyclooxygenase-2 overexpression reduces apoptotic susceptibility by inhibiting the cytochrome c-dependent apoptotic pathway in human colon cancer cells. *Cancer Res.*, **2002**, 62, 6323-6328.
196. Limami, Y; Pinon, A; Leger, DY; Mousseau, Y; Cook-Moreau, J; Beneytout, JL; Delage, C; Liagre, B; Simon, A. HT-29 colorectal cancer cells undergoing apoptosis overexpress COX-2 to delay ursolic acid-induced cell death. *Biochimie*, **2011**, 93, 749-757.
197. Baglin, I; Poumaroux, A; Nour, M; Tan, K; Mitaine-Offer, AC; Lacaille-Dubois, MA; Chauffert, B; Cave, C. New ursolic and betulinic derivatives as potential cytotoxic agents. *J. Enzym. Inhib. Med. Chem.*, **2003**, 18, 111-117.
198. Li, J; Guo, WJ; Yang, QY. Effects of ursolic acid and oleanolic acid on human colon carcinoma cell line HCT15. *World J. Gastroentero.*, **2002**, 8, 493-495.
199. Xavier, CPR; Lima, CF; Preto, A; Seruca, R; Fernandes-Ferreira, M; Pereira-Wilson, C. Luteolin, quercetin and ursolic acid are potent inhibitors of proliferation and inducers of apoptosis in both KRAS and BRAF mutated human colorectal cancer cells. *Cancer Lett.*, **2009**, 281, 162-170.
200. Kim, SH; Ahn, BZ; Ryu, SY. Antitumour effects of ursolic acid isolated from *Oldenlandia diffusa*. *Phytother. Res.*, **1998**, 12, 553-556.
201. Rios, MY; Gonzalez-Morales, A; Villarreal, ML. Sterols, triterpenes and biflavonoids of *Viburnum jucundum* and cytotoxic activity of ursolic acid. *Planta Med.*, **2001**, 67, 683-684.
202. Chavez, IO; Apan, TR; Martinez-Vazquez, M. Cytotoxic activity and effect on nitric oxide production of tirucallane-type triterpenes. *J. Pharm. Pharmacol.*, **2005**, 57, 1087-1091.
203. Kim, YK; Yoon, SK; Ryu, SY. Cytotoxic triterpenes from stem bark of *Physocarpus intermedius*. *Planta Med.*, **2000**, 66, 485-486.

204. Ramos, AA; Pereira-Wilson, C; Collins, AR. Protective effects of Ursolic acid and Luteolin against oxidative DNA damage include enhancement of DNA repair in Caco-2 cells. *Mutat. Res.-Fund. Mol. M.*, **2010**, 692, 6-11.
205. He, XJ; Liu, RH. Triterpenoids isolated from apple peels have potent antiproliferative activity and may be partially responsible for apple's anticancer activity. *J. Agr. Food Chem.*, **2007**, 55, 4366-4370.
206. Shan, JZ; Xuan, YY; Ruan, SQ; Sun, M. Proliferation-inhibiting and apoptosis-inducing effects of ursolic acid and oleanolic acid on multi-drug resistance cancer cells in vitro. *Chin. J. Integr. Med.*, **2011**, 17, 607-611.
207. Aggarwal, BB. Signalling pathways of the TNF superfamily: A double-edged sword. *Nat. Rev. Immunol.*, **2003**, 3, 745-756.
208. Prasad, S; Yadav, VR; Kannappan, R; Aggarwal, BB. Ursolic Acid, a Pentacyclin Triterpene, Potentiates TRAIL-induced Apoptosis through p53-independent Up-regulation of Death Receptors. Evidence for the role of reactive oxygen species and JNK. *J. Biol. Chem.*, **2011**, 286, 5546-5557.
209. Xavier, CPR; Lima, CF; Preto, A; Seruca, R; Fernandes-Ferreira, M; Pereira-Wilson, C. Quercetin, luteolin and ursolic acid are potent inhibitors of proliferation in colorectal carcinoma cells: new therapeutic tools? *Ejc Supplements*, **2008**, 6, 140-140.
210. Xavier, CPR; Lima, C; Rohde, M; Pereira-Wilson, C. Autophagy triggered by ursolic acid synergistically enhances 5-fluorouracil induced cell death in HCT15 (MSI p53 mutant) colorectal cancer cells. *Ejc Supplements*, **2010**, 8, 66-67.
211. Bosch, FX; Ribes, J; Diaz, M; Cleries, R. Primary liver cancer: Worldwide incidence and trends. *Gastroenterology*, **2004**, 127, S5-S16.
212. Yan, SL; Huang, CY; Wu, ST; Yin, MC. Oleanolic acid and ursolic acid induce apoptosis in four human liver cancer cell lines. *Toxicol. in Vitro*, **2010**, 24, 842-848.
213. Tang, C; Lu, YH; Xie, JH; Wang, F; Zou, JN; Yang, JS; Xing, YY; Xi, T. Downregulation of survivin and activation of caspase-3 through the PI3K/Akt pathway in ursolic acid-induced HepG2 cell apoptosis. *Anti-Cancer Drugs*, **2009**, 20, 249-258.
214. Kim, DK; Baek, JH; Kang, CM; Yoo, MA; Sung, JW; Kim, DK; Chung, HY; Kim, ND; Choi, YH; Lee, SH; Kim, KW. Apoptotic activity of ursolic acid may correlate with the inhibition of initiation of DNA replication. *Int. J. Cancer*, **2000**, 87, 629-636.
215. Satomi, Y; Nishino, H; Shibata, S. Glycyrrhetic acid and related compounds induce G1 arrest and apoptosis in human hepatocellular carcinoma HepG2. *Anticancer Res.*, **2005**, 25, 4043-4047.
216. Ramos, AA; Lima, CF; Pereira, ML; Fernandes-Ferreira, M; Pereira-Wilson, C. Antigenotoxic effects of quercetin, rutin and ursolic acid on HepG2 cells: Evaluation by the comet assay. *Toxicol. Lett.*, **2008**, 177, 66-73.
217. Petraccia, L; Onori, P; Sferra, R; Lucchetta, MC; Liberati, G; Grassi, M; Gaudio, E. [MDR (multidrug resistance) in hepatocarcinoma clinical-therapeutic implications]. *La Clinica terapeutica*, **2003**, 154, 325-335.
218. Zhang, DM; Tang, PMK; Chan, JYW; Lam, HM; Au, SWN; Kong, SK; Tsui, SKW; Waye, MMY; Mak, TCW; Fung, KP. Anti-proliferative effect of ursolic acid on multidrug, resistant hepatoma cells R-HepG2 by apoptosis induction. *Cancer Biol. Ther.*, **2007**, 6, 1381-1389.

219. Yang, L; Liu, XZ; Lu, ZB; Chan, JYW; Zhou, LL; Fung, KP; Wu, P; Wu, SH. Ursolic acid induces doxorubicin-resistant HepG2 cell death via the release of apoptosis-inducing factor. *Cancer Lett.*, **2010**, 298, 128-138.
220. Chen, L; Qiu, W; Tang, J; Wang, ZF; He, SY. Synthesis and bioactivity of novel nitric oxide-releasing ursolic acid derivatives. *Chinese Chem. Lett.*, **2011**, 22, 413-416.
221. He, XJ; Liu, RH. Cranberry phytochemicals: Isolation, structure elucidation, and their antiproliferative and antioxidant activities. *J. Agr. Food Chem.*, **2006**, 54, 7069-7074.
222. Yu, YX; Gu, ZL; Yin, JL; Chou, WH; Kwok, CY; Qin, ZH; Liang, ZQ. Ursolic acid induces human hepatoma cell line SMMC-7721 apoptosis via p53-dependent pathway. *Chinese Med. J.*, **2010**, 123, 1915-1923.
223. Shyu, MH; Kao, TC; Yen, GC. Oleanolic Acid and Ursolic Acid Induce Apoptosis in HuH7 Human Hepatocellular Carcinoma Cells through a Mitochondrial-Dependent Pathway and Downregulation of XIAP. *J. Agr. Food Chem.*, **2010**, 58, 6110-6118.
224. Gayathri, R; Priya, DKD; Gunassekaran, GR; Sakthisekaran, D. Ursolic Acid Attenuates Oxidative Stress-mediated Hepatocellular Carcinoma Induction by Diethylnitrosamine in Male Wistar Rats. *Asian Pac. J. Cancer P.*, **2009**, 10, 933-938.
225. Yim, EK; Lee, KH; Namkoong, SE; Um, SJ; Park, JS. Proteomic analysis of ursolic acid-induced apoptosis in cervical carcinoma cells. *Cancer Lett.*, **2006**, 235, 209-220.
226. Kanamori, Y; Kigawa, J; Itamochi, H; Shimada, M; Takahashi, M; Kamazawa, S; Sato, S; Akeshima, R; Terakawa, N. Correlation between loss of PTEN expression and Akt phosphorylation in endometrial carcinoma. *Clin. Cancer Res.*, **2001**, 7, 892-895.
227. Vivanco, I; Sawyers, CL. The phosphatidylinositol 3-kinase-AKT pathway in human cancer. *Nat. Rev. Cancer*, **2002**, 2, 489-501.
228. Achiwa, Y; Hasegawa, K; Udagawa, Y. Regulation of the phosphatidylinositol 3-Kinase-Akt and the mitogen-activated protein kinase pathways by ursolic acid in human endometrial cancer cells. *Biosci. Biotech. Bioch.*, **2007**, 71, 31-37.
229. Wang, XH; Li, LL; Wang, B; Xiang, JY. Effects of ursolic acid on the proliferation and apoptosis of human ovarian cancer cells. *J. Huazhong Univ. Sci. Technol*, **2009**, 29, 761-764.
230. Slamon, DJ; Clark, GM; Wong, SG; Levin, WJ; Ullrich, A; McGuire, WL. Human-Breast Cancer - Correlation of Relapse and Survival with Amplification of the Her-2 Neu Oncogene. *Science*, **1987**, 235, 177-182.
231. Bishayee, A; Ahmed, S; Brankov, N; Perloff, M. Triterpenoids as potential agents for the chemoprevention and therapy of breast cancer. *Frontiers in Bioscience-Landmark*, **2011**, 16, 980-996.
232. Singletary, K; MacDonald, C; Wallig, M. Inhibition by rosemary and carnosol of 7,12 dimethylbenz[alpha]anthracene (DMBA)-induced rat mammary tumorigenesis and in vivo DMBA-DNA adduct formation. *Cancer Lett.*, **1996**, 104, 43-48.
233. Topcu, G; Yapar, G; Turkmen, Z; Goren, AC; Oksuz, S; Schilling, JK; Kingston, DGI. Ovarian antiproliferative activity directed isolation of triterpenoids from fruits of *Eucalyptus camaldulensis* Dehnh. *Phytochemistry Lett.*, **2011**, 4, 421-425.
234. Lee, I; Lee, J; Lee, YH; Leonard, J. Ursolic acid-induced changes in tumor growth, O-2 consumption, and tumor interstitial fluid pressure. *Anticancer Res.*, **2001**, 21, 2827-2833.

235. Kassi, E; Sourlingas, TG; Spiliotaki, M; Papoutsis, Z; Pratsinis, H; Aligiannis, N; Moutsatsou, P. Ursolic Acid Triggers Apoptosis and Bcl-2 Downregulation in MCF-7 Breast Cancer Cells. *Cancer Invest.*, **2009**, 27, 723-733.
236. Amico, V; Barresi, V; Condorelli, D; Spatafora, C; Tringali, C. Antiproliferative terpenoids from almond hulls (*Prunus dulcis*): Identification and structure-activity relationships. *J. Agr. Food Chem.*, **2006**, 54, 810-814.
237. Chen, YH; Chang, FR; Wu, CC; Yen, MH; Liaw, CC; Huang, HC; Kuo, YH; Wu, YC. New cytotoxic 6-oxygenated 8,9-dihydrofurocoumarins, hedyotiscone A-C, from *Hedyotis biflora*. *Planta Med.*, **2006**, 72, 75-78.
238. Kim, KH; Seo, HS; Choi, HS; Choi, I; Shin, YC; Ko, SG. Induction of Apoptotic Cell Death by Ursolic Acid through Mitochondrial Death Pathway and Extrinsic Death Receptor Pathway in MDA-MB-231 Cells. *Arch. Pharm. Res.*, **2011**, 34, 1363-1372.
239. Yeh, CT; Wu, CH; Yen, GC. Ursolic acid, a naturally occurring triterpenoid, suppresses migration and invasion of human breast cancer cells by modulating c-Jun N-terminal kinase, Akt and mammalian target of rapamycin signaling. *Mol. Nutr. Food Res.*, **2010**, 54, 1285-1295.
240. Yang, HJ; Dou, QP. Targeting Apoptosis Pathway with Natural Terpenoids: Implications for Treatment of Breast and Prostate Cancer. *Curr. Drug Targets*, **2010**, 11, 733-744.
241. Gnoatto, SCB; Dassonville-Klimpt, A; Da Nascimento, S; Galera, P; Boumediene, K; Gosmann, G; Sonnet, P; Moslemi, S. Evaluation of ursolic acid isolated from *Ilex paraguariensis* and derivatives on aromatase inhibition. *Eur. J. Med. Chem.*, **2008**, 43, 1865-1877.
242. Gittes, RF. Carcinoma of the Prostate. *New Engl. J. Med.*, **1991**, 324, 236-245.
243. Kassi, E; Papoutsis, Z; Pratsinis, H; Aligiannis, N; Manoussakis, M; Moutsatsou, P. Ursolic acid, a naturally occurring triterpenoid, demonstrates anticancer activity on human prostate cancer cells. *J. Cancer Res. Clin.*, **2007**, 133, 493-500.
244. Zhang, YX; Kong, CZ; Wang, LH; Li, JY; Liu, XK; Xu, B; Xu, CL; Sun, YH. Ursolic Acid Overcomes Bcl-2-Mediated Resistance to Apoptosis in Prostate Cancer Cells Involving Activation of JNK-Induced Bcl-2 Phosphorylation and Degradation. *J. Cell. Biochem.*, **2010**, 109, 764-773.
245. Shanmugam, MK; Rajendran, P; Li, F; Nema, T; Vali, S; Abbasi, T; Kapoor, S; Sharma, A; Kumar, AP; Ho, PC; Hui, KM; Sethi, G. Ursolic acid inhibits multiple cell survival pathways leading to suppression of growth of prostate cancer xenograft in nude mice. *J. Mol. Med.-Jmm*, **2011**, 89, 713-727.
246. Zhang, YX; Kong, CZ; Zeng, Y; Wang, LH; Li, ZH; Wang, HQ; Xu, CL; Sun, YH. Ursolic Acid Induces PC-3 Cell Apoptosis via Activation of JNK and Inhibition of Akt Pathways In Vitro. *Mol. Carcinogen.*, **2010**, 49, 374-385.
247. Shin, SW; Kim, SY; Park, J-W. Autophagy inhibition enhances ursolic acid-induced apoptosis in PC3 cells. *Biochim. Biophys. Acts*, **2012**, 1823, 451-457.
248. Shanmugam, MK; Manu, KA; Ong, TH; Ramachandran, L; Surana, R; Bist, P; Lim, LHK; Kumar, AP; Hui, KM; Sethi, G. Inhibition of CXCR4/CXCL12 signaling axis by ursolic acid leads to suppression of metastasis in transgenic adenocarcinoma of mouse prostate model. *Int. J. Cancer*, **2011**, 129, 1552-1563.
249. Zhang, YX; Kong, CZ; Wang, HQ; Wang, LH; Xu, CL; Sun, YH. Phosphorylation of Bcl-2 and activation of caspase-3 via the c-Jun N-terminal kinase pathway in ursolic acid-induced DU145 cells apoptosis. *Biochimie*, **2009**, 91, 1173-1179.

250. Kwon, SH; Park, HY; Kim, JY; Jeong, IY; Lee, MK; Seo, KI. Apoptotic action of ursolic acid isolated from Corni fructus in RC-58T/h/SA#4 primary human prostate cancer cells. *Bioorg. Med. Chem. Lett.*, **2010**, 20, 6435-6438.
251. Hsu, YL; Kuo, PL; Lin, CC. Proliferative inhibition, cell-cycle dysregulation, and induction of apoptosis by ursolic acid in human non-small cell lung cancer A549 cells. *Life Sci.*, **2004**, 75, 2303-2316.
252. Huang, CY; Lin, CY; Tsai, CW; Yin, MC. Inhibition of cell proliferation, invasion and migration by ursolic acid in human lung cancer cell lines. *Toxicol. in Vitro*, **2011**, 25, 1274-1280.
253. Li, YL; Xing, D; Chen, Q; Chen, WR. Enhancement of chemotherapeutic agent-induced apoptosis by inhibition of NF-kappa B using ursolic acid. *Int. J. Cancer*, **2010**, 127, 462-473.
254. Lai, MY; Leung, HWC; Yang, WH; Chen, WH; Lee, HZ. Up-regulation of matrix metalloproteinase family gene involvement in ursolic acid-induced human lung non-small carcinoma cell apoptosis. *Anticancer Res.*, **2007**, 27, 145-153.
255. Lens, MB; Dawes, M. Global perspectives of contemporary epidemiological trends of cutaneous malignant melanoma. *Brit. J. Dermatol.*, **2004**, 150, 179-185.
256. Huang, MT; Ho, CT; Wang, ZY; Ferraro, T; Lou, YR; Stauber, K; Ma, W; Georgiadis, C; Laskin, JD; Conney, AH. Inhibition of Skin Tumorigenesis by Rosemary and Its Constituents Carnosol and Ursolic Acid. *Cancer Res.*, **1994**, 54, 701-708.
257. Tokuda, H; Ohigashi, H; Koshimizu, K; Ito, Y. Inhibitory Effects of Ursolic and Oleanolic Acid on Skin Tumor Promotion by 12-O-Tetradecanoylphorbol-13-Acetate. *Cancer Lett.*, **1986**, 33, 279-285.
258. Ohigashi, H; Takamura, H; Koshimizu, K; Tokuda, H; Ito, Y. Search for Possible Antitumor Promoters by Inhibition of 12-O-Tetradecanoylphorbol-13-Acetate-Induced Epstein-Barr Virus-Activation - Ursolic Acid and Oleanolic Acid from an Antiinflammatory Chinese Medicinal Plant, Glechoma-Hederaceae L. *Cancer Lett.*, **1986**, 30, 143-151.
259. Hata, K; Hori, K; Takahashi, S. Differentiation- and Apoptosis-Inducing Activities by Pentacyclic Triterpenes on a Mouse Melanoma Cell Line. *J. Nat. Prod.*, **2002**, 65, 645-648.
260. Pinon, A; Limami, Y; Micallef, L; Cook-Moreau, J; Liagre, B; Delage, C; Duval, RE; Simon, A. A novel form of melanoma apoptosis resistance: Melanogenesis up-regulation in apoptotic B16-F0 cells delays ursolic acid-triggered cell death. *Exp. Cell Res.*, **2011**, 317, 1669-1676.
261. Manu, KA; Kuttan, G. Ursolic acid induces apoptosis by activating p53 and caspase-3 gene expressions and suppressing NF-kappa B mediated activation of bcl-2 in B16F-10 melanoma cells. *Int. Immunopharm.*, **2008**, 8, 974-981.
262. Essaady, D; Simon, A; Ollier, M; Maurizis, JC; Chulia, AJ; Delage, C. Inhibitory effect of ursolic acid on B16 proliferation through cell cycle arrest. *Cancer Lett.*, **1996**, 106, 193-197.
263. Harmand, PO; Duval, R; Delage, C; Simon, A. Ursolic acid induces apoptosis through mitochondrial intrinsic pathway and caspase-3 activation in M4Beu melanoma cells. *Int. J. Cancer*, **2005**, 114, 1-11.
264. Hollosy, F; Idei, M; Csorba, G; Szabo, E; Bokonyi, G; Seprodi, A; Meszaros, G; Szende, B; Keri, G. Activation of caspase-3 protease during the process of ursolic acid and its derivative-induced apoptosis. *Anticancer Res.*, **2001**, 21, 3485-3491.

265. Bonaccorsi, I; Altieri, F; Sciamanna, I; Oricchio, E; Grillo, C; Contartese, G; Galati, EM. Endogenous reverse transcriptase as a mediator of ursolic acid's anti-proliferative and differentiating effects in human cancer cell lines. *Cancer Lett.*, **2008**, 263, 130-139.
266. Duval, RE; Harmand, PO; Jayat-Vignoles, C; Cook-Moreau, J; Pinon, A; Delage, C; Simon, A. Differential involvement of mitochondria during ursolic acid-induced apoptotic process in HaCaT and M4Beu cells. *Oncol. Rep.*, **2008**, 19, 145-149.
267. Harmand, PO; Duval, R; Liagre, B; Jayat-Vignoles, C; Beneytout, JL; Delage, C; Simon, A. Ursolic acid induces apoptosis through caspase-3 activation and cell cycle arrest in HaCat cells. *Int. J. Oncol.*, **2003**, 23, 105-112.
268. Pinon, A; Duval, RE; Micallef, L; Jayat-Vignoles, C; Delage, C; Simon, A. Exploring ursolic acid-triggered transduction pathways in B16-F0 mouse melanoma cells: evidences for concomitant apoptosis and melanogenesis, but without tyrosinase activity. *B. Cancer*, **2007**, 94, 537-538.
269. Jedinak, A; Maliar, T. Inhibitors of proteases as anticancer drugs - Minireview. *Neoplasma*, **2005**, 52, 185-192.
270. Jedinak, A; Muckova, M; Kost'alova, D; Maliar, T; Materova, I. Antiprotease and antimetastatic activity of ursolic acid isolated from *Salvia officinalis*. *Z. Naturforsch. C*, **2006**, 61, 777-782.
271. Raphael, TJ; Kuttan, G. Effect of naturally occurring triterpenoids ursolic acid and glycyrrhizic acid on the cell-mediated immune responses of metastatic tumor-bearing animals. *Immunopharm. Immunot.*, **2008**, 30, 243-255.
272. Baek, JH; Lee, YS; Kang, CM; Kim, JA; Kwon, KS; Son, HC; Kim, KW. Intracellular Ca²⁺ release mediates ursolic acid-induced apoptosis in human leukemic HL-60 cells. *Int. J. Cancer*, **1997**, 73, 725-728.
273. Choi, BM; Park, R; Pae, HO; Yoo, JC; Kim, YC; Jun, CD; Jung, BH; Oh, GS; So, HS; Kim, YM; Chung, HT. Cyclic adenosine monophosphate inhibits ursolic acid-induced apoptosis via activation of protein kinase A in human leukaemic HL-60 cells. *Pharmacol. Toxicol.*, **2000**, 86, 53-58.
274. Zhang, T; He, YM; Wang, JS; Shen, J; Xing, YY; Xi, T. Ursolic acid induces HL60 monocytic differentiation and upregulates C/EBP beta expression by ERK pathway activation. *Anti-Cancer Drugs*, **2011**, 22, 158-165.
275. Liu, XS; Jiang, JK. Induction of apoptosis and regulation of the MAPK pathway by ursolic acid in human leukemia K562 cells. *Planta Med.*, **2007**, 73, 1192-1194.
276. Ovesna, Z; Kozics, K; Slamenova, D. Protective effects of ursolic acid and oleanolic acid in leukemic cells. *Mutat. Res.-Fund. Mol. M.*, **2006**, 600, 131-137.
277. Cipak, L; Grausova, L; Miadokova, E; Novotny, L; Rauko, P. Dual activity of triterpenoids: apoptotic versus antidifferentiation effects. *Arch. Toxicol.*, **2006**, 80, 429-435.
278. Noda, Y; Kaiya, T; Kohda, K; Kawazoe, Y. Enhanced cytotoxicity of some triterpenes toward leukemia L1210 cells cultured in low pH media: Possibility of a new mode of cell killing. *Chem. Pharm. Bull.*, **1997**, 45, 1665-1670.
279. Chiang, LC; Chiang, W; Chang, MY; Ng, LT; Lin, CC. Antileukemic activity of selected natural products in Taiwan. *Am. J. Chinese Med.*, **2003**, 31, 37-46.

280. Pathak, AK; Bhutani, M; Nair, AS; Ahn, KS; Chakraborty, A; Kadara, H; Guha, S; Sethi, G; Aggarwal, BB. Ursolic acid inhibits STAT3 activation pathway leading to suppression of proliferation and chemosensitization of human multiple myeloma cells. *Mol. Canc. Res.*, **2007**, 5, 943-955.
281. Huang, HC; Huang, CY; Lin-Shiau, SY; Lin, JK. Ursolic Acid Inhibits IL-1 beta or TNF-alpha-Induced C6 Glioma Invasion Through Suppressing the Association ZIP/p62 With PKC-zeta and Downregulating the MMP-9 Expression. *Mol. Carcinogen.*, **2009**, 48, 517-531.
282. Tu, HY; Huang, AM; Wei, BL; Gan, KH; Hour, TC; Yang, SC; Pu, YS; Lin, CN. Ursolic acid derivatives induce cell cycle arrest and apoptosis in NTUB1 cells associated with reactive oxygen species. *Bioorg. Med. Chem.*, **2009**, 17, 7265-7274.
283. Carmeliet, P. Mechanisms of angiogenesis and arteriogenesis. *Nat. Med.*, **2000**, 6, 389-395.
284. Shon, KH; Lee, HY; Chung, HY; Young, HS; Yi, SY; Kim, KW. Anti-Angiogenic Activity of Triterpene Acids. *Cancer Lett.*, **1995**, 94, 213-218.
285. Cardenas, C; Quesada, AR; Medina, MA. Effects of ursolic acid on different steps of the angiogenic process. *Biochem. Bioph. Res. Co.*, **2004**, 320, 402-408.
286. Kiran, MS; Viji, RI; Kumar, VBS; Sudhakaran, PR. Modulation of angiogenic factors by ursolic acid. *Biochem. Bioph. Res. Co.*, **2008**, 371, 556-560.
287. Kanjoormana, M; Kuttan, G. Antiangiogenic Activity of Ursolic Acid. *Integr. Cancer Ther.*, **2010**, 9, 224-235.
288. Ulrich, S; Stein, J. Ursolic Acid Inhibits Pro-Angiogenic Factors in Colorectal Cancer Cells Independently of PPAR gamma. *Gastroenterology*, **2009**, 136, A227-a227.
289. Lin, CC; Huang, CY; Mong, MC; Chan, CY; Yin, MC. Antiangiogenic Potential of Three Triterpenic Acids in Human Liver Cancer Cells. *J. Agr. Food Chem.*, **2011**, 59, 755-762.
290. Resende, FA; Mattos de Andrade Barcala, CA; da Silva Faria, MC; Kato, FH; Cunha, WR; Tavares, DC. Antimutagenicity of ursolic acid and oleanolic acid against doxorubicin-induced clastogenesis in Balb/c mice. *Life Sci.*, **2006**, 79, 1268-1273.
291. Hsu, HY; Yang, JJ; Lin, CC. Effects of oleanolic acid and ursolic acid on inhibiting tumor growth and enhancing the recovery of hematopoietic system postirradiation in mice. *Cancer Lett.*, **1997**, 111, 7-13.
292. Ramachandran, S; Prasad, NR. Effect of ursolic acid, a triterpenoid antioxidant, on ultraviolet-B radiation-induced cytotoxicity, lipid peroxidation and DNA damage in human lymphocytes. *Chem. Biol. Interact.*, **2008**, 176, 99-107.
293. Honda, T; Finlay, HJ; Gribble, GW; Suh, N; Sporn, MB. New enone derivatives of oleanolic acid and ursolic acid as inhibitors of nitric oxide production in mouse macrophages. *Bioorg. Med. Chem. Lett.*, **1997**, 7, 1623-1628.
294. Honda, T; Gribble, GW; Suh, N; Finlay, HJ; Rounds, BV; Bore, L; Favalaro, FG; Wang, YP; Sporn, MB. Novel synthetic oleanane and ursane triterpenoids with various enone functionalities in ring A as inhibitors of nitric oxide production in mouse macrophages. *J. Med. Chem.*, **2000**, 43, 1866-1877.
295. Honda, T; Rounds, BV; Bore, L; Finlay, HJ; Favalaro, FG; Suh, N; Wang, YP; Sporn, MB; Gribble, GW. Synthetic oleanane and ursane triterpenoids with modified rings A and C: A series of highly active inhibitors of nitric oxide production in mouse macrophages. *J. Med. Chem.*, **2000**, 43, 4233-4246.

296. Kwon, TH; Lee, B; Chung, SH; Kim, DH; Lee, YS. Synthesis and NO Production Inhibitory Activities of Ursolic Acid and Oleanolic Acid Derivatives. *B. Kor. Chem. Soc.*, **2009**, 30, 119-123.
297. Kerwin, JF; Heller, M. The Arginine-Nitric Oxide Pathway - a Target for New Drugs. *Med. Res. Rev.*, **1994**, 14, 23-74.
298. Jia, QA; Janczuk, AJ; Cai, TW; Xian, M; Wen, Z; Wang, PG. NO donors with anticancer activity. *Expert. Opin. Ther. Pat.*, **2002**, 12, 819-826.
299. Hou, YC; Janczuk, A; Wang, PG. Current trends in the development of nitric oxide donors. *Curr. Pharm. Design*, **1999**, 5, 417-441.
300. Wang, PG; Xian, M; Tang, XP; Wu, XJ; Wen, Z; Cai, TW; Janczuk, AJ. Nitric oxide donors: Chemical activities and biological applications. *Chem. Rev.*, **2002**, 102, 1091-1134.
301. Biedermann, D; Eigenerova, B; Hajduch, M; Sarek, J. Synthesis and Evaluation of Biological Activity of the Quaternary Ammonium Salts of Lupane-, Oleanane-, and Ursane-Type Acids. *Synthesis-Stuttgart*, **2010**, 3839-3848.
302. Chadalapaka, G; Jutooru, I; McAlees, A; Stefanac, T; Safe, S. Structure-dependent inhibition of bladder and pancreatic cancer cell growth by 2-substituted glycyrrhetic and ursolic acid derivatives. *Bioorg. Med. Chem. Lett.*, **2008**, 18, 2633-2639.
303. Finlay, HJ; Honda, T; Gribble, GW; Danielpour, D; Benoit, NE; Suh, N; Williams, C; Sporn, MB. Novel A-ring cleaved analogs of oleanolic and ursolic acids which affect growth regulation in NRP.152 prostate cells. *Bioorg. Med. Chem. Lett.*, **1997**, 7, 1769-1772.
304. Amr, AEGE; Ali, KA; Abdalla, MM. Cytotoxic, antioxidant activities and structure activity relationship of some newly synthesized terpenoidal oxaliplatin analogs. *Eur. J. Med. Chem.*, **2009**, 44, 901-907.
305. Singh, GB; Singh, S; Bani, S; Gupta, BD; Banerjee, SK. Antiinflammatory Activity of Oleanolic Acid in Rats and Mice. *J. Pharm. Pharmacol.*, **1992**, 44, 456-458.
306. Hichri, F; Ben Jannet, H; Cheriaa, J; Jegham, S; Mighri, Z. Antibacterial activities of a few prepared derivatives of oleanolic acid and of other natural triterpenic compounds. *Compt. Rendus Chem.*, **2003**, 6, 473-483.
307. Rivero-Cruz, JF; Zhu, M; Kinghorn, AD; Wu, CD. Antimicrobial constituents of Thompson seedless raisins (*Vitis vinifera*) against selected oral pathogens. *Phytochemistry Lett.*, **2008**, 1, 151-154.
308. Pungitore, CR; Garcia, M; Gianello, JC; Sosa, ME; Tonn, CE. Insecticidal and antifeedant effects of *Junellia aspera* (Verbenaceae) triterpenes and derivatives on *Sitophilus oryzae* (Coleoptera : Curculionidae). *J. Stored Prod. Res.*, **2005**, 41, 433-443.
309. Zhu, YM; Shen, JK; Wang, HK; Cosentino, LM; Lee, KH. Synthesis and anti-HIV activity of oleanolic acid derivatives. *Bioorg. Med. Chem. Lett.*, **2001**, 11, 3115-3118.
310. Kashiwada, Y; Wang, HK; Nagao, T; Kitanaka, S; Yasuda, I; Fujioka, T; Yamagishi, T; Cosentino, LM; Kozuka, M; Okabe, K; Ikeshiro, Y; Hu, CQ; Yeh, E; Lee, KH. Anti-AIDS agents. 30. Anti-HIV activity of oleanolic acid, pomolic acid, and structurally related triterpenoids. *J. Nat. Prod.*, **1998**, 61, 1090-1095.
311. Ma, CM; Nakamura, N; Hattori, M; Kakuda, H; Qiao, JC; Yu, HL. Inhibitory effects on HIV-1 protease of constituents from the wood of *Xanthoceras sorbifolia*. *J. Nat. Prod.*, **2000**, 63, 238-242.

312. Ma, CM; Wu, XH; Masao, H; Wang, XJ; Kano, Y. HCV Protease Inhibitory, Cytotoxic and Apoptosis-Inducing Effects of Oleanolic Acid Derivatives. *J. Pharm. Pharm. Sci.*, **2009**, 12, 243-248.
313. Stauber, RE; Stadlbauer, V. Novel approaches for therapy of chronic hepatitis C. *J. Clin. Virol.*, **2006**, 36, 87-94.
314. Zhang, Y; Li, JX; Zhao, JW; Wang, SZ; Pan, Y; Tanaka, K; Kadota, S. Synthesis and activity of oleanolic acid derivatives, a novel class of inhibitors of osteoclast formation. *Bioorg. Med. Chem. Lett.*, **2005**, 15, 1629-1632.
315. Rajasekaran, M; Bapna, JS; Lakshmanan, S; Nair, AGR; Veliath, AJ; Panchanadam, M. Antifertility Effect in Male-Rats of Oleanolic Acid, a Triterpene from Eugenia-Jambolana Flowers. *J. Ethnopharmacol.*, **1988**, 24, 115-121.
316. Astudillo, L; Rodriguez, JA; Schmeda-Hirschmann, G. Gastroprotective activity of oleanolic acid derivatives on experimentally induced gastric lesions in rats and mice. *J. Pharm. Pharmacol.*, **2002**, 54, 583-588.
317. Rodriguez, JA; Astudillo, L; Schmeda-Hirschmann, G. Oleanolic acid promotes healing of chronic gastric lesions acetic acid-induced in rats. *Pharmacol. Res.*, **2003**, 48, 291-294.
318. Matsuda, H; Li, YH; Murakami, T; Yamahara, J; Yoshikawa, M. Protective effects of oleanolic acid oligoglycosides on ethanol- or indomethacin-induced gastric mucosal lesions in rats. *Life Sci.*, **1998**, 63, P1245-P1250.
319. Sanchez, M; Theoduloz, C; Schmeda-Hitschmann, G; Razmilic, I; Yanez, T; Rodriguez, JA. Gastroprotective and ulcer-healing activity of oleanolic acid derivatives: In vitro-in vivo relationships. *Life Sci.*, **2006**, 79, 1349-1356.
320. Martinez-Gonzalez, J; Rodriguez-Rodriguez, R; Gonzalez-Diez, M; Rodriguez, C; Herrera, MD; Ruiz-Gutierrez, V; Badimon, L. Oleanolic acid induces prostacyclin release in human vascular smooth muscle cells through a cyclooxygenase-2-dependent mechanism. *J. Nutr.*, **2008**, 138, 443-448.
321. Alvarez, ME; Maria, AOM; Saad, JR. Diuretic activity of Fabiana patagonica in rats. *Phytother. Res.*, **2002**, 16, 71-73.
322. Rodriguez-Rodriguez, R; Stankevicius, E; Herrera, MD; Ostergaard, L; Andersen, MR; Ruiz-Gutierrez, V; Simonsen, U. Oleanolic acid induces relaxation and calcium-independent release of endothelium-derived nitric oxide. *Brit. J. Pharmacol.*, **2008**, 155, 535-546.
323. Kobayashi, A; Watanabe, H; Ozawa, K; Hayashi, H; Yamazaki, N. Oxygen-Derived Free-Radicals Related Injury in the Heart during Ischemia and Reperfusion. *Jpn. Circ. J.*, **1989**, 53, 1122-1131.
324. Du, Y; Ko, KM. Oleanolic acid protects against myocardial ischemia-reperfusion injury by enhancing mitochondrial antioxidant mechanism mediated by glutathione and alpha-tocopherol in rats. *Planta Med.*, **2006**, 72, 222-227.
325. Feng, J; Zhang, P; Chen, XX; He, GX. PI3K and ERK/Nrf2 Pathways Are Involved in Oleanolic Acid-Induced Heme Oxygenase-1 Expression in Rat Vascular Smooth Muscle Cells. *J. Cell. Biochem.*, **2011**, 112, 1524-1531.
326. Simonsen, U; Hansson, N; Rodriguez-Rodriguez, R; Andersen, MR; Stankevicius, E; Buus, NH; Eskildsen-Helmond, Y. Anti-Atherogenic Effect of Oleanolic Acid Appears Unrelated to Endothelial Release of Nitric Oxide. *J. Vasc. Res.*, **2009**, 46, 89-89.

327. Buus, NH; Hansson, NC; Rodriguez-Rodriguez, R; Stankevicius, E; Andersen, MR; Simonsen, U. Antiatherogenic effects of oleanolic acid in apolipoprotein E knockout mice. *Eur. J. Pharmacol.*, **2011**, 670, 519-526.
328. Wen, XA; Sun, HB; Liu, J; Cheng, KG; Zhang, P; Zhang, LY; Hao, J; Zhang, LY; Ni, PZ; Zographos, SE; Leonidas, DD; Alexacou, KM; Gimisis, T; Hayes, JM; Oikonomakos, NG. Naturally occurring pentacyclic triterpenes as inhibitors of glycogen phosphorylase: Synthesis, structure-activity relationships, and X-ray crystallographic studies. *J. Med. Chem.*, **2008**, 51, 3540-3554.
329. Chen, J; Liu, J; Zhang, LY; Wu, GZ; Hua, WY; Wu, XM; Sun, HB. Pentacyclic triterpenes. Part 3: Synthesis and biological evaluation of oleanolic acid derivatives as novel inhibitors of glycogen phosphorylase. *Bioorg. Med. Chem. Lett.*, **2006**, 16, 2915-2919.
330. Chen, J; Gong, YC; Liu, J; Hua, WY; Zhang, LY; Sun, HB. Synthesis and biological evaluation of novel pyrazolo[4,3-b]oleanane derivatives as inhibitors of glycogen phosphorylase. *Chem. Biodivers.*, **2008**, 5, 1304-1312.
331. Zhang, YN; Zhang, W; Hong, D; Shi, L; Shen, Q; Li, JY; Li, J; Hu, LH. Oleanolic acid and its derivatives: New inhibitor of protein tyrosine phosphatase 1B with cellular activities. *Bioorg. Med. Chem.*, **2008**, 16, 8697-8705.
332. Ali, MS; Jahangir, M; ul Hussan, SS; Choudhary, MI. Inhibition of alpha-glucosidase by oleanolic acid and its synthetic derivatives. *Phytochemistry*, **2002**, 60, 295-299.
333. Gao, DW; Li, QW; Li, Y; Liu, ZH; Fan, YS; Liu, ZW; Zhao, HW; Li, J; Han, ZS. Antidiabetic and Antioxidant Effects of Oleanolic Acid from *Ligustrum lucidum* Ait in Alloxan-induced Diabetic Rats. *Phytother. Res.*, **2009**, 23, 1257-1262.
334. Gao, DW; Li, QW; Li, Y; Liu, ZH; Liu, ZW; Fan, YS; Han, ZS; Li, J; Li, K. Antidiabetic potential of oleanolic acid from *Ligustrum lucidum* Ait. *Can. J. Physiol. Pharm.*, **2007**, 85, 1076-1083.
335. Musabayane, CT; Mahlalela, N; Shode, FO; Ojewole, JAO. Effects of *Syzygium cordatum* (Hochst.) [Myrtaceae] leaf extract on plasma glucose and hepatic glycogen in streptozotocin-induced diabetic rats. *J. Ethnopharmacol.*, **2005**, 97, 485-490.
336. Mapanga, RF; Tufts, MA; Shode, FO; Musabayane, CT. Renal Effects of Plant-Derived Oleanolic Acid in Streptozotocin-Induced Diabetic Rats. *Renal Failure*, **2009**, 31, 481-491.
337. Nataraju, A; Saini, D; Ramachandran, S; Benshoff, N; Liu, W; Chapman, W; Mohanakumar, T. Oleanolic Acid, a Plant Triterpenoid, Significantly Improves Survival and Function of Islet Allograft. *Transplantation*, **2009**, 88, 987-994.
338. de Melo, CL; Queiroz, MGR; Fonseca, SGC; Bizerra, AMC; Lemos, TLG; Melo, TS; Santos, FA; Rao, VS. Oleanolic acid, a natural triterpenoid improves blood glucose tolerance in normal mice and ameliorates visceral obesity in mice fed a high-fat diet. *Chem. Biol. Interact.*, **2010**, 185, 59-65.
339. Sato, H; Genet, C; Strehle, A; Thomas, C; Lobstein, A; Wagner, A; Mioskowski, C; Auwerx, J; Saladin, R. Anti-hyperglycemic activity of a TGR5 agonist isolated from *Olea europaea*. *Biochem. Biophys. Res. Co.*, **2007**, 362, 793-798.
340. Dirnagl, U; Iadecola, C; Moskowitz, MA. Pathobiology of ischaemic stroke: an integrated view. *Trends Neurosci.*, **1999**, 22, 391-397.
341. Chan, PH. Reactive oxygen radicals in signaling and damage in the ischemic brain. *J. Cerebr. Blood F. Met.*, **2001**, 21, 2-14.

342. Cho, SO; Ban, JY; Kim, JY; Ju, HS; Lee, IS; Song, KS; Bae, K; Seong, YH. Anti-ischemic activities of *Aralia cordata* and its active component, oleanolic acid. *Arch. Pharm. Res.*, **2009**, 32, 923-932.
343. Rong, ZT; Gong, XJ; Sun, HB; Li, YM; Ji, H. Protective effects of oleanolic acid on cerebral ischemic damage in vivo and H₂O₂-induced injury in vitro. *Pharm. Biol.*, **2011**, 49, 78-85.
344. Hemmer, B; Archelos, JJ; Hartung, HP. New concepts in the immunopathogenesis of multiple sclerosis. *Nat. Rev. Neurosci.*, **2002**, 3, 291-301.
345. Martin, R; Carvalho-Tavares, J; Hernandez, M; Arnes, M; Ruiz-Gutierrez, V; Nieto, ML. Beneficial actions of oleanolic acid in an experimental model of multiple sclerosis: A potential therapeutic role. *Biochem. Pharmacol.*, **2010**, 79, 198-208.
346. Winter, G; Harris, WJ. Humanized Antibodies (Reprinted from Trends in Pharmacological Sciences, Vol 14, Pg 139-143, 1993). *Immunol. Today*, **1993**, 14, 243-246.
347. Dat, NT; Lee, IS; Cai, XF; Shen, G; Kim, YH. Oleanane triterpenoids with inhibitory activity against NFAT transcription factor from *Liquidambar formosana*. *Biol. Pharm. Bull.*, **2004**, 27, 426-428.
348. Maia, JL; Lima-Junior, RCP; David, JP; David, JM; Santos, FA; Rao, VS. Oleanolic acid, a pentacyclic triterpene attenuates the mustard oil-induced colonic nociception in mice. *Biological & Pharmaceutical Bulletin*, **2006**, 29, 82-85.
349. Maia, JL; Lima-Junior, RCP; Melo, CM; David, JP; David, JM; Campos, AR; Santos, FA; Rao, VSN. Oleanolic acid, a pentacyclic triterpene attenuates capsaicin-induced nociception in mice: Possible mechanisms. *Pharmacol. Res.*, **2006**, 54, 282-286.
350. Liu, J; Liu, YP; Klaassen, CD. Protective Effect of Oleanolic Acid against Chemical-Induced Acute Necrotic Liver-Injury in Mice. *Acta Pharm. Sin.*, **1995**, 16, 97-102.
351. Liu, YP; Hartley, DP; Liu, J. Protection against carbon tetrachloride hepatotoxicity by oleanolic acid is not mediated through metallothionein. *Toxicol. Lett.*, **1998**, 95, 77-85.
352. Liu, J; Wu, Q; Lu, YF; Pi, JB. New insights into generalized hepatoprotective effects of oleanolic acid: Key roles of metallothionein and Nrf2 induction. *Biochem. Pharmacol.*, **2008**, 76, 922-928.
353. Yim, TK; Wu, WK; Pak, WF; Ko, KM. Hepatoprotective action of an oleanolic acid-enriched extract of *Ligustrum lucidum* fruits is mediated through an enhancement on hepatic glutathione regeneration capacity in mice. *Phytother. Res.*, **2001**, 15, 589-592.
354. Jeong, HG. Inhibition of cytochrome P450 2E1 expression by oleanolic acid: hepatoprotective effects against carbon tetrachloride-induced hepatic injury. *Toxicol. Lett.*, **1999**, 105, 215-222.
355. Kim, NY; Lee, MK; Park, MJ; Kim, SJ; Park, HJ; Choi, JW; Kim, SH; Cho, SY; Lee, JS. Momordin Ic and oleanolic acid from *Kochia fructus* reduce carbon tetrachloride-induced hepatotoxicity in rats. *J. Med. Food*, **2005**, 8, 177-183.
356. Liu, J; Liu, YP; Madhu, C; Klaassen, CD. Protective Effects of Oleanolic Acid on Acetaminophen-Induced Hepatotoxicity in Mice. *J. Pharmacol. Exp. Ther.*, **1993**, 266, 1607-1613.
357. Reisman, SA; Aleksunes, LM; Klaassen, CD. Oleanolic acid activates Nrf2 and protects from acetaminophen hepatotoxicity via Nrf2-dependent and Nrf2-independent processes. *Biochem. Pharmacol.*, **2009**, 77, 1273-1282.

358. Liu, YP; Kreppel, H; Liu, J; Choudhuri, S; Klaassen, CD. Oleanolic Acid Protects against Cadmium Hepatotoxicity by Inducing Metallothionein. *J. Pharmacol. Exp. Ther.*, **1993**, 266, 400-406.
359. Wang, X; Ye, XL; Liu, R; Chen, HL; Bai, H; Liang, X; Zhang, XD; Wang, Z; Li, WL; Hai, CX. Antioxidant activities of oleanolic acid in vitro: Possible role of Nrf2 and MAP kinases. *Chem. Biol. Interact.*, **2010**, 184, 328-337.
360. Liu, J; Liu, YP; Parkinson, A; Klaassen, CD. Effect of Oleanolic Acid on Hepatic Toxicant-Activating and Detoxifying Systems in Mice. *J. Pharmacol. Exp. Ther.*, **1995**, 275, 768-774.
361. Takagi, K; Park, EH; Kato, H. Anti-Inflammatory Activities of Hederagenin and Crude Saponin Isolated from *Sapindus-Mukorossi* Gaertn. *Chem. Pharm. Bull.*, **1980**, 28, 1183-1188.
362. Vasconcelos, MAL; Royo, VA; Ferreira, DS; Crotti, AEM; Silva, MLAE; Carvalho, JCT; Bastos, JK; Cunha, WR. In vivo analgesic and anti-inflammatory activities of ursolic acid and oleanolic acid from *Miconia albicans* (Melastomataceae). *Z. Naturforsch. C*, **2006**, 61, 477-482.
363. Giner-Larza, EM; Manez, S; Recio, MC; Giner, RM; Prieto, JM; Cerda-Nicolas, M; Rios, JL. Oleanonic acid, a 3-oxotriterpene from *Pistacia*, inhibits leukotriene synthesis and has anti-inflammatory activity. *Eur. J. Pharmacol.*, **2001**, 428, 137-143.
364. Dharmappa, KK; Kumar, RV; Nataraju, A; Mohamed, R; Shivaprasad, HV; Vishwanath, BS. Anti-inflammatory Activity of Oleanolic Acid by Inhibition of Secretory Phospholipase A(2). *Planta Med.*, **2009**, 75, 211-215.
365. Wang, HH; Yang, H; Czura, CJ; Sama, AE; Tracey, KJ. HMGB1 as a late mediator of lethal systemic inflammation. *Am. J. Resp. Crit. Care*, **2001**, 164, 1768-1773.
366. Yang, E-J; Lee, W; Ku, S-K; Song, K-S; Bae, J-S. Anti-inflammatory activities of oleanolic acid on HMGB1 activated HUVECs. *Food and Chemical Toxicology*, **2012**, 50, 1288-1294.
367. Assefa, H; Nimrod, A; Walker, L; Sindelar, R. Synthesis and evaluation of potential complement inhibitory semisynthetic analogs of oleanolic acid. *Bioorg. Med. Chem. Lett.*, **1999**, 9, 1889-1894.
368. Assefa, H; Nimrod, A; Walker, L; Sindelar, R. Enantioselective synthesis and complement inhibitory assay of A/B-ring partial analogues of oleanolic acid. *Bioorg. Med. Chem. Lett.*, **2001**, 11, 1619-1623.
369. Kapil, A; Sharma, S. Anti-Complement Activity of Oleanolic Acid - an Inhibitor of C-3-Convertase of the Classical Complement Pathway. *J. Pharm. Pharmacol.*, **1994**, 46, 922-923.
370. Muto, Y; Ninomiya, M; Fujiki, H. Present Status of Research on Cancer Chemoprevention in Japan. *Jpn J. Clin. Oncol.*, **1990**, 20, 219-224.
371. Janakiram, NB; Indranie, C; Malisetty, SV; Jagan, P; Steele, VE; Rao, CV. Chemoprevention of Colon Carcinogenesis by Oleanolic Acid and Its Analog in Male F344 Rats and Modulation of COX-2 and Apoptosis in Human Colon HT-29 Cancer Cells. *Pharmaceut. Res.*, **2008**, 25, 2151-2157.
372. Kawamori, T; Tanaka, T; Hara, A; Yamahara, J; Mori, H. Modifying Effects of Naturally-Occurring Products on the Development of Colonic Aberrant Crypt Foci Induced by Azoxymethane in F344 Rats. *Cancer Res.*, **1995**, 55, 1277-1282.
373. Juan, ME; Planas, JM; Ruiz-Gutierrez, V; Daniel, H; Wenzel, U. Antiproliferative and apoptosis-inducing effects of maslinic and oleanolic acids, two pentacyclic triterpenes from olives, on HT-29 colon cancer cells. *Brit. J. Nutr.*, **2008**, 100, 36-43.

374. Juan, ME; Wenzel, U; Ruiz-Gutierrez, V; Daniel, H; Planas, JM. Olive fruit extracts inhibit proliferation and induce apoptosis in HT-29 human colon cancer cells. *J. Nutr.*, **2006**, 136, 2553-2557.
375. Cao, DL; Fan, ST; Chung, SSM. Identification and characterization of a novel human aldose reductase-like gene. *J. Biol. Chem.*, **1998**, 273, 11429-11435.
376. Satow, R; Shitashige, M; Kanai, Y; Takeshita, F; Ojima, H; Jigami, T; Honda, K; Kosuge, T; Ochiya, T; Hirohashi, S; Yamada, T. Combined Functional Genome Survey of Therapeutic Targets for Hepatocellular Carcinoma. *Clin. Cancer Res.*, **2010**, 16, 2518-2528.
377. Liu, JH; Wen, GB; Cao, DL. Aldo-Keto Reductase Family 1 Member B1 Inhibitors: Old Drugs with New Perspectives. *Recent Pat. Anti-Canc.*, **2009**, 4, 246-253.
378. Takemura, M; Endo, S; Matsunaga, T; Soda, M; Zhao, HT; El-Kabbani, O; Tajima, K; Inuma, M; Hara, A. Selective Inhibition of the Tumor Marker Aldo-keto Reductase Family Member 1B10 by Oleanolic Acid. *J. Nat. Prod.*, **2011**, 74, 1201-1206.
379. Allouche, Y; Warleta, F; Campos, M; Sanchez-Quesada, C; Uceda, M; Beltran, G; Gaforio, JJ. Antioxidant, Antiproliferative, and Pro-apoptotic Capacities of Pentacyclic Triterpenes Found in the Skin of Olives on MCF-7 Human Breast Cancer Cells and Their Effects on DNA Damage. *J. Agr. Food Chem.*, **2011**, 59, 121-130.
380. Amico, V; Barresi, V; Chillemi, R; Condorelli, DF; Sciuto, S; Spatafora, C; Tringali, C. Bioassay-Guided Isolation of Antiproliferative Compounds from Grape (*Vitis vinifera*) Stems. *Nat. Prod. Comm.*, **2009**, 4, 27-34.
381. Paszel, A; Hofmann, J; Zaprutko, L; Bednarczyk-Cwynar, B; Bock, G; Rybczynska, M. Antitumor activity and reversal of multidrug resistance by the newly synthesised oleanolic acid derivative - methyl-3,11-dioxolean-12en-28-oate. *Ejc Supplements*, **2007**, 5, 115-115.
382. Chu, R; Zhao, XY; Griffin, C; Staub, RE; Shoemaker, M; Climent, J; Leitman, D; Cohen, I; Shtivelman, E; Fong, S. Selective concomitant inhibition of mTORC1 and mTORC2 activity in estrogen receptor negative breast cancer cells by BN107 and oleanolic acid. *Int. J. Cancer*, **2010**, 127, 1209-1219.
383. Zhou, RP; Zhang, ZM; Zhao, L; Jia, CH; Xu, S; Mai, QG; Lu, M; Huang, MJ; Wang, L; Wang, XK; Jin, DD; Bai, XC. Inhibition of mTOR Signaling by Oleanolic Acid Contributes to Its Anti-Tumor Activity in Osteosarcoma Cells. *J. Orthopaed. Res.*, **2011**, 29, 846-852.
384. Feng, L; Au-yeung, W; Xu, YH; Wang, SS; Zhu, Q; Xiang, P. Oleanolic Acid from *Prunella Vulgaris* L. Induces SPC-A-1 Cell Line Apoptosis Via Regulation of Bax, Bad and Bcl-2 Expression. *Asian Pac. J. Cancer P.*, **2011**, 12, 403-408.
385. Giaccone, G; vanArkOtte, J; Rubio, GJ; Gazdar, AF; Broxterman, HJ; Dingemans, AMC; Flens, MJ; Scheper, RJ; Pinedo, HM. MRP is frequently expressed in human lung-cancer cell lines, in non-small-cell lung cancer and in normal lung. *Int. J. Cancer*, **1996**, 66, 760-767.
386. Young, LC; Campling, BG; Voskoglou-Nomikos, T; Cole, SPC; Deeley, RG; Gerlach, JH. Expression of multidrug resistance protein-related genes in lung cancer: Correlation with drug response. *Clin. Cancer Res.*, **1999**, 5, 673-680.
387. Lucio, KA; Rocha, GD; Moncao-Ribeiro, LC; Fernandes, J; Takiya, CM; Gattass, CR. Oleanolic Acid Initiates Apoptosis in Non-Small Cell Lung Cancer Cell Lines and Reduces Metastasis of a B16F10 Melanoma Model In Vivo. *PLoS ONE*, **2011**, 6.

388. Hua, YQ; Zhang, ZY; Li, JX; Li, QA; Hu, SO; Li, JA; Sun, MX; Cai, ZD. Oleanolic acid derivative Dex-OA has potent anti-tumor and anti-metastatic activity on osteosarcoma cells in vitro and in vivo. *Invest. New Drug.*, **2011**, 29, 258-265.
389. Gao, Z; Maloney, DJ; Dedkova, LM; Hecht, SM. Inhibitors of DNA polymerase beta: Activity and mechanism. *Bioorg. Med. Chem.*, **2008**, 16, 4331-4340.
390. Pratheeshkumar, P; Kuttan, G. Oleanolic Acid Induces Apoptosis by Modulating p53, BAX, Bcl-2, and Caspase-3 Gene Expression, and Regulates the Activation of Transcription Factors and Cytokine Profile in B16F-10 Melanoma Cells. *J. Environ. Pathol.Tox.*, **2011**, 30, 21-31.
391. Oguro, T; Liu, J; Klaassen, CD; Yoshida, T. Inhibitory effect of oleanolic acid on 12-O-tetradecanoylphorbol-13-acetate-induced gene expression in mouse skin. *Toxicol. Sci.*, **1998**, 45, 88-93.
392. Fukuda, Y; Sakai, K; Matsunaga, S; Tokuda, H; Tanaka, R. Cancer chemopreventive activity of lupane- and oleanane-type triterpenoids from the cones of *Liquidamber styraciflua*. *Chem. Biodivers.*, **2005**, 2, 421-428.
393. Lu, XM; Yi, HW; Xu, JL; Sun, Y; Li, JX; Cao, SX; Xu, Q. A novel synthetic oleanolic acid derivative with amino acid conjugate suppresses tumour growth by inducing cell cycle arrest. *J. Pharm. Pharmacol.*, **2007**, 59, 1087-1093.
394. Wang, F; Hua, HM; Pei, YH; Chen, D; Jing, YK. Triterpenoids from the resin of *Styrax tonkinensis* and their antiproliferative and differentiation effects in human leukemia HL-60 cells. *J. Nat. Prod.*, **2006**, 69, 807-810.
395. Martin, R; Carvalho, J; Ilbeas, E; Hernandez, M; Ruiz-Gutierrez, V; Nieto, ML. Acidic triterpenes compromise growth and survival of astrocytoma cell lines by regulating reactive oxygen species accumulation. *Cancer Res.*, **2007**, 67, 3741-3751.
396. Zhang, PX; Li, HM; Chen, D; Ni, JH; Kang, YM; Wang, SQ. Oleanolic acid induces apoptosis in human leukemia cells through caspase activation and Poly(ADP-ribose) polymerase cleavage. *Acta Bioch. Bioph. Sin.*, **2007**, 39, 803-809.
397. Umehara, K; Takagi, R; Kuroyanagi, M; Ueno, A; Taki, T; Chen, YJ. Studies on Differentiation-Inducing Activities of Triterpenes. *Chem. Pharm. Bull.*, **1992**, 40, 401-405.
398. Fernandes, J; Castilho, RO; da Costa, MR; Wagner-Souza, K; Kaplan, MAC; Gattass, CR. Pentacyclic triterpenes from *Chrysobalanaceae* species: cytotoxicity on multidrug resistant and sensitive leukemia cell lines. *Cancer Lett.*, **2003**, 190, 165-169.
399. Braga, F; Ayres-Saraiva, D; Gattass, CR; Capella, MAM. Oleanolic acid inhibits the activity of the multidrug resistance protein ABCC1 (MRP1) but not of the ABCB1 (P-glycoprotein): Possible use in cancer chemotherapy. *Cancer Lett.*, **2007**, 248, 147-152.
400. Fujiwara, Y; Komohara, Y; Kudo, R; Tsurushima, K; Ohnishi, K; Ikeda, T; Takeya, M. Oleanolic acid inhibits macrophage differentiation into the M2 phenotype and glioblastoma cell proliferation by suppressing the activation of STAT3. *Oncol. Rep.*, **2011**, 26, 1533-1537.
401. Chaney, SG; Sancar, A. DNA repair: Enzymatic mechanisms and relevance to drug response. *J. Natl. Cancer I.*, **1996**, 88, 1346-1360.
402. Canitrot, Y; Cazaux, C; Frechet, M; Bouayadi, K; Lesca, C; Salles, B; Hoffmann, JS. Overexpression of DNA polymerase beta in cell results in a mutator phenotype and a decreased sensitivity to anticancer drugs. *P. Natl. Acad. Sci. USA*, **1998**, 95, 12586-12590.

403. Deng, JZ; Starck, SR; Hecht, SM. DNA polymerase beta inhibitors from *Baeckea gunniana*. *J. Nat. Prod.*, **1999**, 62, 1624-1626.
404. Deng, JZ; Starck, SR; Hecht, SM. Pentacyclic triterpenoids from *Freziera* sp that inhibit DNA polymerase beta. *Bioorg. Med. Chem.*, **2000**, 8, 247-250.
405. Johnston, LH; Nasmyth, KA. *Saccharomyces-Cerevisiae* Cell-Cycle Mutant Cdc9 Is Defective in DNA-Ligase. *Nature*, **1978**, 274, 891-893.
406. Fabre, F; Roman, H. Evidence That a Single DNA-Ligase Is Involved in Replication and Recombination in Yeast. *P. Natl. Acad. Sci. USA*, **1979**, 76, 4586-4588.
407. Tan, GT; Lee, SK; Lee, IS; Chen, JW; Leitner, P; Besterman, JM; Kinghorn, AD; Pezzuto, JM. Natural-product inhibitors of human DNA ligase I. *Biochem. J.*, **1996**, 314, 993-1000.
408. Yin, MC; Chan, KC. Nonenzymatic antioxidative and antiglycative effects of oleanolic acid and ursolic acid. *J. Agr. Food Chem.*, **2007**, 55, 7177-7181.
409. Honda, T; Rounds, BV; Gribble, GW; Suh, NJ; Wang, YP; Sporn, MB. Design and synthesis of 2-cyano-3,12-dioxolean-1,9-dien-28-oic acid, a novel and highly active inhibitor of nitric oxide production in mouse macrophages. *Bioorg. Med. Chem. Lett.*, **1998**, 8, 2711-2714.
410. Honda, T; Rounds, BV; Bore, L; Favalaro, FG; Gribble, GW; Suh, N; Wang, YP; Sporn, MB. Novel synthetic oleanane triterpenoids: A series of highly active inhibitors of nitric oxide production in mouse macrophages. *Bioorg. Med. Chem. Lett.*, **1999**, 9, 3429-3434.
411. Xu, WM; Liu, LZ; Loizidou, M; Ahmed, M; Charles, IG. The role of nitric oxide in cancer. *Cell Res.*, **2002**, 12, 311-320.
412. Mocellin, S; Bronte, V; Nitti, D. Nitric oxide, a double edged sword in cancer biology: Searching for therapeutic opportunities. *Med. Res. Rev.*, **2007**, 27, 317-352.
413. Honda, T; Honda, Y; Favalaro, FG; Gribble, GW; Suh, N; Place, AE; Rendi, MH; Sporn, MB. A novel dicyanotriterpenoid, 2-cyano-3,12-dioxooleana-1,9(11)-dien-28-onitrile, active at picomolar concentrations for inhibition of nitric oxide production. *Bioorg. Med. Chem. Lett.*, **2002**, 12, 1027-1030.
414. Sporn, MB; Liby, KT; Yore, MM; Fu, LF; Lopchuk, JM; Gribble, GW. New Synthetic Triterpenoids: Potent Agents for Prevention and Treatment of Tissue Injury Caused by Inflammatory and Oxidative Stress. *J. Nat. Prod.*, **2011**, 74, 537-545.
415. Liby, KT; Yore, MM; Sporn, MB. Triterpenoids and rexinoids as multifunctional agents for the prevention and treatment of cancer. *Nat. Rev. Cancer*, **2007**, 7, 357-369.
416. Van Laecke, S; Vanholder, R. Bardoxolone Methyl, Chronic Kidney Disease, and Type 2 Diabetes. *New Engl. J. Med.*, **2011**, 365, 1745-1745.
417. Huang, D; Ding, Y; Li, Y; Zhang, WM; Fang, WS; Chen, XG. Anti-tumor activity of a 3-oxo derivative of oleanolic acid. *Cancer Lett.*, **2006**, 233, 289-296.
418. Chen, L; Zhang, YH; Kong, XW; Peng, SX; Tian, J. Synthesis and biological evaluation of nitric oxide-releasing derivatives of oleanolic acid as inhibitors of HepG2 cell apoptosis. *Bioorg. Med. Chem. Lett.*, **2007**, 17, 2979-2982.
419. Chen, L; Zhang, YH; Kong, XW; Lan, E; Huang, ZJ; Peng, SX; Kaufman, DL; Tian, J. Design, synthesis, and antihepatocellular carcinoma activity of nitric oxide releasing derivatives of oleanolic acid. *J. Med. Chem.*, **2008**, 51, 4834-4838.

420. Huang, ZJ; Zhang, YH; Zhao, L; Jing, YW; Lai, YS; Zhang, LY; Guo, QL; Yuan, ST; Zhang, JJ; Chen, L; Peng, SX; Tian, JD. Synthesis and anti-human hepatocellular carcinoma activity of new nitric oxide-releasing glycosyl derivatives of oleanolic acid. *Org. Biomol. Chem.*, **2010**, 8, 632-639.
421. Chen, L; Zhu, Z-F; Meng, F; Xu, C-S; Zhang, Y-H. Synthesis and Cytotoxicity of Oleanolic Acid/N-aryl-N'-hydroxyguanidine Hybrids. *Chinese Journal of Natural Medicines*, **2010**, 8, 436-440.
422. Finlay, HJ; Honda, T; Gribble, GW. Synthesis of novel [3,2-b]indole fused oleanolic acids as potential inhibitors of cell proliferation. *Arkivoc*, **2002**, 38-46.
423. Deng, SL; Baglin, I; Nour, M; Cave, C. Synthesis of phosphonodipeptide conjugates of ursolic acid and their homologs. *Heteroatom Chem.*, **2008**, 19, 55-65.
424. Kvasnica, M; Sarek, J; Klinotova, E; Dzubak, P; Hajdich, M. Synthesis of phthalates of betulinic acid and betulin with cytotoxic activity. *Bioorg. Med. Chem.*, **2005**, 13, 3447-3454.
425. Farina, C; Pinza, M; Pifferi, G. Synthesis and anti-ulcer activity of new derivatives of glycyrrhetic, oleanolic and ursolic. *Farmaco*, **1998**, 53, 22-32.
426. Salvador, JAR; Melo, MLSE; Neves, ASC. Oxidations with potassium permanganate metal sulphates and nitrates. beta-selective epoxidation of Delta(5)-unsaturated steroids. *Tetrahedron Lett.*, **1996**, 37, 687-690.
427. Micheli, RA. Synthesis of Some Derivatives of Ursolic Acid. *J. Org. Chem.*, **1962**, 27, 666-&.
428. Jeong, BS; Kim, YC; Lee, ES. Modification of C2,3,23,28 functional groups on asiatic acid and evaluation of hepatoprotective effects. *B. Kor. Chem. Soc.*, **2007**, 28, 977-982.
429. Zhao, LX; Park, HG; Jew, SS; Lee, MK; Kim, YC; Thapa, P; Karki, R; Jahng, Y; Jeong, BS; Lee, ES. Modification of C11, C28, C2,3,23 or C2,23,28 functional groups on asiatic acid and evaluation of hepatoprotective effects. *B. Kor. Chem. Soc.*, **2007**, 28, 970-976.
430. Konoike, T; Takahashi, K; Kitaura, Y; Kanda, Y. Synthesis of [2-C-13]-oleanolic acid and [2-C-13]-myricerone. *Tetrahedron*, **1999**, 55, 14901-14914.
431. Qiu, WW; Shen, Q; Yang, F; Wang, B; Zou, H; Li, JY; Li, J; Tang, J. Synthesis and biological evaluation of heterocyclic ring-substituted maslinic acid derivatives as novel inhibitors of protein tyrosine phosphatase 1B. *Bioorg. Med. Chem. Lett.*, **2009**, 19, 6618-6622.
432. Moreira, VMA; Vasaitis, TS; Guo, ZY; Njar, VCO; Salvador, JAR. Synthesis of novel C17 steroidal carbamates Studies on CYP17 action, androgen receptor binding and function, and prostate cancer cell growth. *Steroids*, **2008**, 73, 1217-1227.
433. Santos, RC; Salvador, JAR; Marin, S; Cascante, M. Novel semisynthetic derivatives of betulin and betulinic acid with cytotoxic activity. *Bioorg. Med. Chem.*, **2009**, 17, 6241-6250.
434. Santos, RC; Salvador, JAR; Marin, S; Cascante, M; Moreira, JN; Dinis, TCP. Synthesis and structure-activity relationship study of novel cytotoxic carbamate and N-acylheterocyclic bearing derivatives of betulin and betulinic acid. *Bioorg. Med. Chem.*, **2010**, 18, 4385-4396.
435. Rossello, A; Bertini, S; Lapucci, A; Macchia, M; Martinelli, A; Rapposelli, S; Herreros, E; Macchia, B. Synthesis, antifungal activity, and molecular modeling studies of new inverted oxime ethers of oxiconazole. *J. Med. Chem.*, **2002**, 45, 4903-4912.

436. Botta, M; Corelli, F; Gasparri, F; Messina, F; Mugnaini, C. Chiral azole derivatives. 4. Enantiomers of bifonazole and related antifungal agents: Synthesis, configuration assignment, and biological evaluation. *J. Org. Chem.*, **2000**, 65, 4736-4739.
437. Santos, RC; Salvador, JAR; Cortes, R; Pachon, G; Marin, S; Cascante, M. New betulinic acid derivatives induce potent and selective antiproliferative activity through cell cycle arrest at the S phase and caspase dependent apoptosis in human cancer cells. *Biochimie*, **2011**, 93, 1065-1075.
438. Tottleben, MJ; Freeman, JP; Szmuszkovicz, J. Imidazole transfer from 1,1'-carbonyldimidazole and 1,1'-(thiocarbonyl)diimidazole to alcohols. A new protocol for the conversion of alcohols to alkylheterocycles. *J. Org. Chem.*, **1997**, 62, 7319-7323.
439. Tafi, A; Costi, R; Botta, M; Di Santo, R; Corelli, F; Massa, S; Ciacci, A; Manetti, F; Artico, M. Antifungal agents. 10. New derivatives of 1-[(aryl)[4-aryl-1H-pyrrol-3-yl]methyl]-1H-imidazole, synthesis, anti-Candida activity, and quantitative structure-analysis relationship studies. *J. Med. Chem.*, **2002**, 45, 2720-2732.
440. Mulvihill, MJ; Cesario, C; Smith, V; Beck, P; Nigro, A. Regio- and stereospecific syntheses of syn- and anti-1,2-imidazolylpropylamines from the reaction of 1,1'-carbonyldiimidazole with syn- and anti-1,2-amino alcohols. *J. Org. Chem.*, **2004**, 69, 5124-5127.
441. Moreira, VM; Salvador, JAR; Vasaitis, TS; Njar, VCO. CYP17 inhibitors for prostate cancer treatment - An update. *Curr. Med. Chem.*, **2008**, 15, 868-899.
442. Rannard, SP; Davis, NJ. The selective reaction of primary amines with carbonyl imidazole containing compounds: Selective amide and carbamate synthesis. *Org. Lett.*, **2000**, 2, 2117-2120.
443. Seebacher, W; Simic, N; Weis, R; Saf, R; Kunert, O. Complete assignments of H-1 and C-13 NMR resonances of oleanolic acid, 18 alpha-oleanolic acid, ursolic acid and their 11-oxo derivatives. *Magn. Reson. Chem.*, **2003**, 41, 636-638.
444. Dinkova-Kostova, AT; Massiah, MA; Bozak, RE; Hicks, RJ; Talalay, P. Potency of Michael reaction accepters as inducers of enzymes that protect against carcinogenesis depends on their reactivity with sulfhydryl groups. *P. Natl. Acad. Sci. USA*, **2001**, 98, 3404-3409.
445. Sarkar, FH; Banerjee, S; Li, YW. Pancreatic cancer: Pathogenesis, prevention and treatment. *Toxicol. Appl. Pharm.*, **2007**, 224, 326-336.
446. Thomas, CJ. Fluorinated natural products with clinical significance. *Curr. Top. Med. Chem.*, **2006**, 6, 1529-1543.
447. Isanbor, C; O'Hagan, D. Fluorine in medicinal chemistry: A review of anti-cancer agents. *J. Fluorine Chem.*, **2006**, 127, 303-319.
448. Gouverneur, V; Purser, S; Moore, PR; Swallow, S. Fluorine in medicinal chemistry. *Chem. Soc. Rev.*, **2008**, 37, 320-330.
449. Muller, K; Faeh, C; Diederich, F. Fluorine in pharmaceuticals: Looking beyond intuition. *Science*, **2007**, 317, 1881-1886.
450. Kirk, KL. Fluorination in medicinal chemistry: Methods, strategies, and recent developments. *Org. Process Res. Dev.*, **2008**, 12, 305-321.
451. Bégué, J-P; Bonnet-Delpon, D, *Bioorganic and Medicinal Chemistry of Fluorine*. 1 ed.; John Wiley and Sons, Inc.: New Jersey, 2008.

452. Hagmann, WK. The many roles for fluorine in medicinal chemistry. *J. Med. Chem.*, **2008**, 51, 4359-4369.
453. Singh, RP; Shreeve, JM. Recent advances in nucleophilic fluorination reactions of organic compounds using Deoxofluor and DAST. *Synthesis-Stuttgart*, **2002**, 2561-2578.
454. Enders, D; Huttel, MRM. Direct organocatalytic alpha-fluorination of aldehydes and ketones. *Synlett*, **2005**, 991-993.
455. Westwell, AD; Shah, P. The role of fluorine in medicinal chemistry. *J. Enzym. Inhib. Med. Chem.*, **2007**, 22, 527-540.
456. Hulliger, J; Berger, R; Resnati, G; Metrangolo, P; Weber, E. Organic fluorine compounds: a great opportunity for enhanced materials properties. *Chem. Soc. Rev.*, **2011**, 40, 3496-3508.
457. Bohm, HJ; Banner, D; Bendels, S; Kansy, M; Kuhn, B; Muller, K; Obst-Sander, U; Stahl, M. Fluorine in medicinal chemistry. *ChemBioChem*, **2004**, 5, 637-643.
458. Duschinsky, R; Plevin, E; Heidelberger, C. The Synthesis of 5-Fluoropyrimidines. *J. Am. Chem. Soc.*, **1957**, 79, 4559-4560.
459. Heidelberger, C; Chaudhuri, NK; Danneberg, P; Mooren, D; Griesbach, L; Duschinsky, R; Schnitzer, RJ; Plevin, E; Scheiner, J. Fluorinated Pyrimidines, a New Class of Tumour-Inhibitory Compounds. *Nature*, **1957**, 179, 663-666.
460. Zhang, F; Song, JZ. A novel general method for preparation of alpha-fluoro-alpha-arylcarboxylic acid. Direct fluorination of silyl ketene acetals with Selectfluor (R). *Tetrahedron Lett.*, **2006**, 47, 7641-7644.
461. Banks, RE. Selectfluor (TM) reagent F-TEDA-BF₄ in action: Tamed fluorine at your service. *J. Fluorine Chem.*, **1998**, 87, 1-17.
462. Stavber, S; Sotler, T; Zupan, M. A Mild, Selective Method for Preparation of Vicinal Fluoro Ethers Using F-Teda-Bf₄. *Tetrahedron Lett.*, **1994**, 35, 1105-1108.
463. Stavber, S; SotlerPecan, T; Zupan, M. Stereochemistry and some kinetic aspects of fluorination of phenyl-substituted alkenes with Selectfluor(TM) reagent F-TEDA-BF₄. *B. Chem. Soc. Jpn.*, **1996**, 69, 169-175.
464. Zhou, C; Li, J; Lu, B; Fu, CL; Ma, SM. An efficient approach for monofluorination via highly regioselective fluorohydroxylation reaction of 3-aryl-1,2-allenes with selectfluor. *Org. Lett.*, **2008**, 10, 581-583.
465. Lal, GS. Site-Selective Fluorination of Organic-Compounds Using 1-Alkyl-4-Fluoro-1,4-Diazabicyclo[2.2.2]Octane Salts (Selectfluor Reagents). *J. Org. Chem.*, **1993**, 58, 2791-2796.
466. Zhou, C; Ma, ZC; Gu, ZH; Fu, CL; Ma, SM. An efficient approach for monofluorination via aqueous fluorolactonization reaction of 2,3-allenoic acids with Selectfluor. *J. Org. Chem.*, **2008**, 73, 772-774.
467. Fuglseth, E; Thvedt, THK; Moll, MF; Hoff, BH. Electrophilic and nucleophilic side chain fluorination of para-substituted acetophenones. *Tetrahedron*, **2008**, 64, 7318-7323.
468. Emsley, JW; Phillips, L; Wray, V. Fluorine Coupling-Constants. *Prog. Nucl. Mag. Res. Sp.*, **1976**, 10, 83-756.

469. Dolbier, WR, *Guide to Fluorine NMR for Organic Chemists*. 1 ed.; Jonh Wiley and Sons, Inc.: New Jersey, 2009.
470. Brey, WS. Carbon-13 NMR of fluorocyclopropanes. *Magn. Reson. Chem.*, **2008**, 46, 480-492.
471. Lal, GS; Pez, GP; Pesaresi, RJ; Prozonic, FM. Bis(2-methoxyethyl)aminosulfur trifluoride: a new broad-spectrum deoxofluorinating agent with enhanced thermal stability. *Chem. Commun.*, **1999**, 215-216.
472. Lal, GS; Pez, GP; Pesaresi, RJ; Prozonic, FM; Cheng, HS. Bis(2-methoxyethyl)aminosulfur trifluoride: A new broad-spectrum deoxofluorinating agent with enhanced thermal stability. *J. Org. Chem.*, **1999**, 64, 7048-7054.
473. Singh, RP; Shreeve, JM. Nucleophilic fluorination of amino alcohols and diols using Deoxofluor. *J. Fluorine Chem.*, **2002**, 116, 23-26.
474. Lal, GS; Lobach, E; Evans, A. Fluorination of thiocarbonyl compounds with bis(2-methoxyethyl)aminosulfur trifluoride (deoxo-fluor reagent): A facile synthesis of gem-difluorides. *J. Org. Chem.*, **2000**, 65, 4830-4832.
475. Biedermann, D; Sarek, J; Klinot, J; Hajduch, M; Dzubak, P. Fluorination of betulines and other triterpenoids with DAST. *Synthesis-Stuttgart*, **2005**, 1157-1163.
476. Connolly, JD; Hill, RA. Triterpenoids. *Nat. Prod. Rep.*, **2008**, 25, 794-830.
477. Kitagawa, I; Kitazawa, K; Yosioka, I. Photochemical Transformation Leading to Eupteleogenin .1. Introduction of Epoxy-Lactone System. *Tetrahedron*, **1972**, 28, 907-&.
478. Kitagawa, I; Kitazawa, K; Yosioka, I. Photooxidation of Oleanolic Acid - Formation of 11Alpha,12Alpha-Epoxy- and 12Alpha-Hydroxy-Oleanolic Lactones. *Tetrahedron Lett.*, **1968**, 509-512.
479. Barton, DHR; Holness, NJ. Triterpenoids .5. Some Relative Configurations in Ring-C, Ring-D, and Ring-E of the Beta-Amyrin and the Lupeol Group of Triterpenoids. *J. Chem Soc.*, **1952**, 78-92.
480. Konoike, T; Takahashi, K; Araki, Y; Horibe, I. Practical partial synthesis of myriceric acid A, an endothelin receptor antagonist, from oleanolic acid. *J. Org. Chem.*, **1997**, 62, 960-966.
481. Garcia-Granados, A; Lopez, PE; Melguizo, E; Parra, A; Simeo, Y. Partial synthesis of C-ring derivatives from oleanolic and maslinic acids. Formation of several triene systems by chemical and photochemical isomerization processes. *Tetrahedron*, **2004**, 60, 1491-1503.
482. Konoike, T; Araki, Y; Kanda, Y. A novel allylic hydroxylation of sterically hindered olefins by Fe-porphyrin-catalyzed mCPBA oxidation. *Tetrahedron Lett.*, **1999**, 40, 6971-6974.
483. Salvador, JAR; Moreira, VM; Pinto, RMA; Leal, AS; Le Roux, C. Bismuth(III) Triflate-Based Catalytic Direct Opening of Oleanolic Hydroxy-gamma-lactones to Afford 12-Oxo-28-carboxylic Acids. *Advanced Synthesis & Catalysis*, **2011**, 353, 2637-2642.
484. Garcia-Granados, A; Lopez, PE; Melguizo, E; Parra, A; Simeo, Y. Oxidation of several triterpenic diene and triene systems. Oxidative cleavage to obtain chiral intermediates for drimane and phenanthrene semi-synthesis. *Tetrahedron*, **2004**, 60, 3831-3845.
485. Salvador, JAR; Pinto, RMA; Santos, RC; Le Roux, C; Beja, AM; Paixao, JA. Bismuth triflate-catalyzed Wagner-Meerwein rearrangement in terpenes. Application to the synthesis of the 18

- alpha-oleanane core and A-neo-18 alpha-oleanene compounds from lupanes. *Org. Biomol. Chem.*, **2009**, 7, 508-517.
486. Ollevier, T; Li, ZY. Bismuth Triflate-Catalyzed Addition of Allylsilanes to N-Alkoxy-carbonylamino Sulfones: Convenient Access to 3-Cbz-Protected Cyclohexenylamines. *Advanced Synthesis & Catalysis*, **2009**, 351, 3251-3259.
487. Ollevier, T; Bouchard, JE; Desyroy, V. Diastereoselective mukaiyama aldol reaction of 2-(trimethylsilyloxy)furan catalyzed by bismuth triflate. *J. Org. Chem.*, **2008**, 73, 331-334.
488. Salvador, JAR; Pinto, RMA; Silvestre, SM. Recent Advances of Bismuth(III) Salts in Organic Chemistry: Application to the Synthesis of Aliphatics, Alicyclics, Aromatics, Amino Acids and Peptides, Terpenes and Steroids of Pharmaceutical Interest. *Mini-Reviews in Organic Chemistry*, **2009**, 6, 241-274.
489. Wen, XA; Zhang, P; Liu, J; Zhang, LY; Wu, XM; Ni, PZ; Sun, HB. Pentacyclic triterpenes. Part 2: Synthesis and biological evaluation of maslinic acid derivatives as glycogen phosphorylase inhibitors. *Bioorg. Med. Chem. Lett.*, **2006**, 16, 722-726.
490. Salvador, JAR; Clark, JH. The allylic oxidation of unsaturated steroids by tert-butyl hydroperoxide using homogeneous and heterogeneous cobalt acetate. *Chem. Commun.*, **2001**, 33-34.
491. Salvador, JAR; Silvestre, SM; Moreira, VM. Catalytic oxidative processes in steroid chemistry: Allylic oxidation, beta-selective epoxidation, alcohol oxidation and remote functionalization reactions. *Curr. Org. Chem.*, **2006**, 10, 2227-2257.
492. Ljungman, M. Targeting the DNA Damage Response in Cancer. *Chem. Rev.*, **2009**, 109, 2929-2950.
493. Hertel, LW; Kroin, JS; Misner, JW; Tustin, JM. Synthesis of 2-Deoxy-2,2-Difluoro-D-Ribose and 2-Deoxy-2,2-Difluoro-D-Ribofuranosyl Nucleosides. *J. Org. Chem.*, **1988**, 53, 2406-2409.
494. Jiang, XR; Li, JF; Zhang, RX; Zhu, Y; Shen, JS. An improved preparation process for gemcitabine. *Org. Process Res. Dev.*, **2008**, 12, 888-891.
495. Kenny, B; Ballard, S; Blagg, J; Fox, D. Pharmacological options in the treatment of benign prostatic hyperplasia. *J. Med. Chem.*, **1997**, 40, 1293-1315.

